

Open Research Online

The Open University's repository of research publications
and other research outputs

The duration of volcanic eruptions: empirical probabilistic forecasting models based on historic eruption data

Thesis

How to cite:

Gunn, Leanne Sarah (2014). The duration of volcanic eruptions: empirical probabilistic forecasting models based on historic eruption data. PhD thesis The Open University.

For guidance on citations see [FAQs](#).

© 2014 Leanne Sarah Gunn

Version: Version of Record

Copyright and Moral Rights for the articles on this site are retained by the individual authors and/or other copyright owners. For more information on Open Research Online's data [policy](#) on reuse of materials please consult the policies page.

oro.open.ac.uk

The duration of volcanic eruptions: empirical probabilistic forecasting models based on historic eruption data

Leanne Sarah Gunn

MGEOL, University of Leicester (2009)

A thesis submitted for the degree of Doctor of Philosophy

Department of Environment, Earth and Ecosystems,

The Open University,

Walton Hall,

Milton Keynes,

MK7 6AA

May 2014

DATE OF SUBMISSION : 21 MAY 2014

DATE OF AWARD : 20 OCTOBER 2014

ProQuest Number: 13889383

All rights reserved

INFORMATION TO ALL USERS

The quality of this reproduction is dependent upon the quality of the copy submitted.

In the unlikely event that the author did not send a complete manuscript and there are missing pages, these will be noted. Also, if material had to be removed, a note will indicate the deletion.



ProQuest 13889383

Published by ProQuest LLC (2019). Copyright of the Dissertation is held by the Author.

All rights reserved.

This work is protected against unauthorized copying under Title 17, United States Code
Microform Edition © ProQuest LLC.

ProQuest LLC.
789 East Eisenhower Parkway
P.O. Box 1346
Ann Arbor, MI 48106 – 1346

Abstract

The ability to forecast future volcanic eruption durations would greatly benefit emergency response planning. A probabilistic model to forecast the duration of eruptions is presented here. The model relies on past eruptions being a good indicator of future activity. Datasets of historic eruptions from Mt. Etna (flank only), Kilauea, Piton de la Fournaise (PdIF) and Iceland have been compiled through a critical examination of existing literature and careful consideration of uncertainties in reported dates. The eruptions from Mt. Etna, Kilauea and PdIF are all basaltic effusive eruptions, however, the Icelandic dataset is more diverse and seven types of duration have been identified and are assessed independently. These datasets have also enabled an assessment of repose intervals (eruption end to eruption start) to be conducted.

Eruption duration and repose interval data are modelled using exponential, Weibull, log-logistic and Burr type XII distributions with parameters found by maximum likelihood estimation. Log-logistic distributions are found to often provide the best-fit to the observed data. Survivor function statistics are applied to the best-fit theoretical distribution of each dataset and used to forecast (a) the probability of an eruption exceeding a given duration, (b) the probability of an on-going eruption (having reached t days) exceeding a specified total duration and (c) the minimum duration associated with a given probability.

Eruption duration analyses at individual volcanic systems show systematic variations with time and different time periods have different duration regimes. Comparisons of the erupted volumes associated with these duration regimes show that volume is an important control on eruption duration. Average eruption rates also determine eruption duration and comparisons of data from Kilauea, PdIF and volcanic systems from

different regions of Iceland have led to the hypothesis that volcano spreading rate may have an important control on eruption rate and subsequently eruption duration.

Parts of this thesis have been published, presented and abstracted:

Publications

Gunn, L.S., Blake, S., Jones, M. C., Rymer, H. (2014) Forecasting the duration of volcanic eruptions: an empirical probabilistic model *Bulletin of Volcanology*, 76

Conference Talks

Gunn, L.S., Blake, S., Jones, M.C., Rymer, H. The duration of volcanic eruptions: Controls and forecasts. In: (*MIAVITA: International Scientific Conference on Integrated Approaches for Volcanic Risk Managements*, Stuttgart, Germany, September 2012.

Gunn, L.S., Blake, S., Jones, M.C., Rymer, H. The duration of volcanic eruptions: Controls and forecasts. In: *Volcano Magmatics Study Group Annual Meeting*, Bristol, UK, January 2013.

Gunn, L.S., Blake, S., Jones, M.C., Rymer, H. Volcanic eruption durations: Forecasts and controls. In: *IAVCEI 2013 Scientific Assembly, Forecasting Volcanic Activity*, Kagoshima, Japan, July 2013.

Conference Posters

Gunn, L.S., Blake, S., Rymer, H. Durations of volcanic eruptions. In: *Volcano Magmatics Study Group Annual Meeting*, Cambridge, UK, January 2011.

Gunn, L.S., Blake, S., Rymer, H., Einarsson, P. Forecasting the duration of volcanic eruptions. In: *BRISK Summer School, The Assessment of Risk and Uncertainty in Environmental Sciences, Bristol, UK, July 2011.*

Gunn, L.S., Blake, S., Jones, M.C., Rymer, H. The duration of Icelandic volcanic eruptions. In: *Volcano Magmatics Study Group Annual Meeting, Durham, UK, January 2012.*

Gunn, L.S., Blake, S., Jones, M.C., Rymer, H. The duration of Icelandic volcanic eruptions. In: *The Open University Poster Competition and the Midlands Hub Poster Competition, Milton Keynes and Coventry, UK, June/July 2012.*

Gunn, L.S., Blake, S., Jones, M.C., Rymer, H. A physical model of volcanic eruption durations. In: *Volcano Magmatics Study Group Annual Meeting, Edinburgh, UK, January 2014.*

Acknowledgements

In which I thank the many people who have helped me complete this thesis...

“Think, think, think”

- A.A. Milne, Winnie-the-Pooh

The first quote is for my supervisors who have guided and supported me throughout this project. To Steve, thank you for our long meetings full of interesting and insightful discussion and for never failing to have faith in me, the project or its data, even when I was unable to see their strengths. To Hazel, thank you for all the support and encouragement you have given me along the way. To Chris, thank you for guiding the statistics and proving to me that maths is not my nemesis. Additional thanks go to John Murray and Pall Einarsson who helped with the compilation of the Mt. Etna and Iceland datasets, respectively and to NERC for funding the project itself.

I would also like to thank some people who built the foundations on which this project grew; Mr Derrett who is responsible for my enthusiasm in geology, Mike Norry for teaching me how to play ‘academic volley ball’ and finally Becky Williams who was a brilliant masters supervisor teaching me essential research skills and has since become a very good friend, hopefully I will see more of you now that I have finished writing.

“Nobody can be uncheered with a balloon”

- A.A. Milne, Winnie-the-Pooh

The second quote is for everyone at the OU who I have shared a house, office, coffee or beer with me, in particular, special thanks go to; Liz, Louise and Helen for all their administrative help especially when it came to expenses; Sion and Josie for giving me copious amounts of kittie therapy; Liz, Catherine, Anne and Feargus for looking after

me when I was broken; Sonia, Chris, Alice, Kat and Mel for cheering the office up with both balloons and bubbles; and finally the other members of VDG for providing chat and tea every afternoon.

A special thanks goes to Sarah who made sure she was never forgotten by arriving and covering my house in sparkles (which we were still finding years later)! You know how to brighten up every occasion and you never fail to make me laugh.

“It is more fun to talk with someone who doesn’t use long, difficult words but rather short, easy words like “What about lunch?” ”

- A.A. Milne, Winnie-the-Pooh

This third quote is for the girls from Romford, the ones I met at school, who did not go on to do science related things or PhD’s but have ‘proper jobs’. Sophy, Angela, Kirsty and Karen, thank you for accepting my absence while writing. Lets have lunch again soon.

“A bear, however hard he tries, grows tubby without exercise”

- A.A. Milne, Winnie-the-Pooh

The fourth quote is to those responsible for getting me out of the office and doing some exercise. Thank you to RocSoc for making me play cricket and football and a special thanks to the girls at Polenastics for making exercise so much fun! I would like to also thank the Milton Keynes physiotherapy team for getting me back on my feet following my dislocated knee and two bouts of knee surgery over the last 4 years.

“You are braver than you believe, stronger than you seem and smarter than you think”

- A.A. Milne, Winnie-the-Pooh

The fifth quote relates to my Mum, Dad and the rest of the family who are always there

with words of encouragement, no matter what I decide to do. Thank you for all your support and for trying to understand my research, which I realise is totally alien to you all. Don't worry I won't make you read it!

"Some people care too much. I think its called love"

- A.A. Milne, Winnie-the-Pooh

This final quote is for Peter. Thank you for putting up with me, especially over the past few months during the frantic writing. At times I have been envious of your unrelenting enthusiasm for all things science but this combined with your support and encouragement has powered me through the writing process (along with your mums cake parcels of course!). Thank you for always believing in me, I hope that I can be an equally sturdy rock for you when you are writing up next year.



A.A. Milne

Contents

1	Introduction	1
1.1	Aims and Objectives	2
1.2	Previous studies concerned with forecasting volcanic activity	3
1.2.1	Probabilistic forecasting of volcanic eruption durations and onset times	4
1.3	An introduction to the volcanic systems investigated in this study . . .	6
1.3.1	Mt. Etna	8
1.3.2	Kilauea	11
1.3.3	Piton de la Fournaise	14
1.3.4	Iceland	16
1.4	Thesis structure	21
2	Methods	23
2.1	Dataset compilation	23
2.1.1	Defining eruption duration	23
2.1.2	Dealing with individual eruption duration uncertainty	25
2.2	Survivor function analysis	29
2.2.1	Survival analysis in volcanology	32
2.2.2	Calculating empirical survivor functions	33
2.2.3	Comparing empirical survivor functions	34
2.2.4	Example: Comparing two subsets of the repose interval dura- tion data from Soufrière Hills, Montserrat	38
2.3	Fitting theoretical distributions to the data	39
2.3.1	Goodness-of-fit	41
2.3.2	Example: Fitting theoretical distributions to the repose interval data of Soufrière Hills, Montserrat	44
2.4	An empirical probabilistic model using survival analysis	46

CONTENTS

2.4.1	Survivor function	47
2.4.2	Residual life function	47
2.4.3	Quantile function	48
2.4.4	Calculating confidence intervals	49
2.4.5	Example: Forecasting the duration of repose intervals between vulcanian explosions at Soufrière Hills, Montserrat	55
3	Dataset compilation: a critical examination of the literature	59
3.1	Available data for Mt. Etna	61
3.1.1	The eruption duration dataset of Mt. Etna	62
3.1.2	Additional information on specific eruptions from Mt. Etna	70
3.1.3	Vent location data at Mt. Etna	71
3.1.4	Volume data for flank eruptions from Mt. Etna	73
3.1.5	The completeness of the eruption record at Mt. Etna	74
3.2	Available data for Kilauea	76
3.2.1	The eruption duration dataset for Kilauea	76
3.2.2	Comments on lava lake activity at Kilauea	82
3.2.3	Additional information on specific eruptions at Kilauea	83
3.2.4	Volume data for eruptions from Kilauea	85
3.2.5	The completeness of the eruption record at Kilauea	86
3.3	Available data for Piton de la Fournaise (PdlF)	88
3.3.1	The eruption duration dataset of PdlF	88
3.3.2	Location, volume and petrological data for eruptions from PdlF	105
3.3.3	Additional information on specific eruptions from PdlF	106
3.3.4	The completeness of the eruption record at PdlF	107
3.4	Available data for Iceland	110
3.4.1	Duration types identified on Iceland	110
3.4.2	The eruption duration dataset of Iceland	112

3.4.3	Additional information on specific eruptions from Icelandic volcanic systems	119
3.4.4	The completeness of the Icelandic eruption record	124
4	Investigating the distribution of eruption durations at Mt. Etna, Kilauea, Piton de la Fournaise and Iceland	129
4.1	The effect of individual eruption duration uncertainty on the overall distribution of eruption duration	130
4.2	The overall distribution of eruption duration	133
4.2.1	Mt. Etna: 1600-2010	133
4.2.2	Kilauea: 1912-1983	134
4.2.3	PdlF: 1911-2011	135
4.2.4	Iceland: 1300-2011	137
4.3	Eruption durations from individual volcanic systems on Iceland	141
4.3.1	Mixed eruption durations from Hekla	141
4.3.2	Single basaltic eruption durations from Askja, Grímsvötn, Katla and Krafla	144
4.4	Temporal variation in the distribution of eruption duration	148
4.4.1	Temporal variation at Mt. Etna	149
4.4.2	Temporal variation at Kilauea	152
4.4.3	Temporal variation at PdlF	153
4.4.4	Temporal variation at Hekla, Iceland	157
4.5	Spatial variation in the distribution of eruption duration	159
4.5.1	Spatial variation at Mt. Etna	159
4.5.2	Spatial variation at Kilauea	162
4.5.3	Spatial variation at PdlF	164
4.5.4	Spatial variation on Iceland	166
4.6	Conclusions	169
5	An empirical probabilistic approach to forecasting the duration of vol-	

CONTENTS

canic eruptions	171
5.1 Forecasting the duration of future flank eruptions at Mt. Etna	172
5.1.1 Identifying the best fit distribution to the data of Mt. Etna . . .	173
5.1.2 Forecasting results for Mt. Etna	174
5.2 Forecasting the duration of eruptions from Kilauea	176
5.2.1 Identifying the best fit distribution to the data of Kilauea . . .	177
5.2.2 Forecasting results for Kilauea	178
5.3 Forecasting the duration of future eruptions from Piton de la Fournaise (PdlF)	181
5.3.1 Identifying the best fit distribution to the data of PdlF	181
5.3.2 Forecasting results for PdlF	185
5.4 Forecasting the duration of volcanic eruptions on Iceland	187
5.4.1 Forecasting mixed eruption durations (d_{3a} and d_4) from Hekla	187
5.4.2 Forecasting the duration of single basaltic eruptions (d_6) on Iceland	192
5.4.3 Forecasting the total duration of basaltic eruption sequences (d_7) on Iceland	200
5.5 Conclusions	202
 6 An investigation of repose intervals	 205
6.1 The definition and calculation of repose interval	206
6.2 Repose data available to this study	208
6.2.1 Repose intervals at Mt. Etna	208
6.2.2 Repose intervals at Kilauea	210
6.2.3 Repose intervals at Piton de la Fournaise (PdlF)	212
6.2.4 Repose intervals at Hekla, Iceland	215
6.3 A comparison of true and inferred repose	217
6.4 Temporal variation in repose intervals	218
6.4.1 Temporal variation in repose intervals at Mt. Etna	219

6.4.2	Temporal variation in repose at Kilauea	220
6.4.3	Temporal variation in repose at Piton de la Fournaise (PdlF)	221
6.4.4	Temporal variation in repose at Hekla, Iceland	223
6.5	Forecasting future repose intervals and the onset of future eruption	225
6.5.1	Forecasting repose intervals between flank eruptions at Mt. Etna	225
6.5.2	Forecasting repose between eruptions at Kilauea	229
6.5.3	Forecasting repose between eruptions at PdlF	233
6.5.4	Forecasting repose between mixed eruptions at Hekla, Iceland	236
6.6	Conclusions	240
7	Conclusions: possible controls on eruption duration and further work	243
7.1	A brief summary of the duration regimes identified in this thesis	244
7.2	The relationship between repose interval and eruption duration	245
7.2.1	Repose interval as a control on eruption duration	245
7.2.2	Eruption duration as a control on repose interval	247
7.3	Eruption duration as a function of erupted volume and average eruption rate	249
7.3.1	Volume data for Mt. Etna, Kilauea, PdlF and Hekla	249
7.3.2	The relationship between erupted volume and eruption duration	252
7.3.3	The role of eruption rate in controlling eruption duration	255
7.3.4	Hypothesised link between volcano spreading rate and eruption duration	257
7.4	Conclusions	261
7.5	Suggestions for further work	264
7.5.1	Possible model refinements	265
7.5.2	Possible other applications for the empirical probabilistic model	266
7.5.3	Further assessment of the factors controlling eruption duration	266
Appendix A Additional information regarding the Mt. Etna dataset		299

CONTENTS

Appendix B	Additional information regarding the Kilauea dataset	331
Appendix C	Additional information regarding the PdIF dataset	347
Appendix D	Additional information regarding the Icelandic dataset	393
D.1	Askja	399
D.2	Brennisteinfjöll	402
D.3	Eyjafjallajökull	402
D.4	Grímsvötn	404
D.5	Hekla	412
D.6	Katla	417
D.7	Krafla	420
D.8	Krýsuvík	423
D.9	Kverkfjöll	423
D.10	Öræfajökull	424
D.11	Torfajökull	425
D.12	Vestmannaeyjar	425
D.13	Miscellaneous	427
D.14	Fire Events	428

List of Figures

1.1	Sketch map of Mt. Etna	9
1.2	Sketch map of Kilauea	13
1.3	Sketch map of Piton de la Fournaise	15
1.4	Sketch map of Iceland	18
2.1	Diagram explaining eruption duration uncertainty assignment	27
2.2	Example of an empirical survivor function curve	34
2.3	Comparison of two empirical survivor function curves	38
2.4	The shape of exponential, Weibull, log-logistic and Burr type XII distributions with varying parameter values.	40
2.5	Empirical survivor function curves and best fit theoretical distributions for the data of Table 2.3)	45
3.1	Sketch map of Mt. Etna showing the position of vents and fissures . . .	72
3.2	Plots investigating the effect of reporting biases in the documentation of flank eruptions from Mt. Etna	75
3.3	Plots investigating the effect of reporting biases in the documentation of eruptions from Kilauea	87
3.4	Plots investigating the effect of reporting biases in the documentation of PdlF eruptions	107
3.5	Plots of eruption duration against eruption start year at PdlF	108
3.6	Empirical survivor function plot for eruption durations from PdlF in the periods 1644-1910, 1911-1979 and 1980-2011	109
3.7	Schematic diagram showing six different eruption types identified within the Iceland dataset and the durations which describe them	112
3.8	Plots investigating the effect of reporting biases in the documentation of Icelandic eruptions	125
3.9	Plot of Icelandic eruption duration against eruption start year	127

LIST OF FIGURES

4.1	Plots assessing the effect of individual eruption duration uncertainty on the overall distribution of eruption duration	131
4.2	Plot assessing the effect of individual eruption duration uncertainty on the distribution of eruption durations > 1 day at PdIF	132
4.3	The distribution of flank eruption durations at Mt. Etna for the period 1600-2010	133
4.4	The distribution of eruption durations at Kilauea for the period 1912-1983	135
4.5	The distribution of eruption durations at PdIF for the period 1911-2011	136
4.6	The distribution of single basaltic eruption durations (d_6) on Iceland for the period 1300-2011	139
4.7	The distribution of the total duration of basaltic eruption sequences (d_7) on Iceland	141
4.8	The distribution of mixed eruption durations at Hekla for the period 1300-2000 (d_{3a} and d_4)	143
4.9	The distribution of single basaltic eruption durations (d_6) on Iceland at individual volcanic systems	145
4.10	Empirical survivor function plot for flank eruption durations at Mt. Etna assessing any temporal variations	150
4.11	Empirical survivor function plot for eruption durations at Kilauea assessing any temporal variations	152
4.12	Plots showing the duration of each eruption from PdIF in the period 1911-2011	154
4.13	Empirical survivor function plot for eruption durations at PdIF assessing any temporal variations	155
4.14	Plots assessing temporal variation in the duration of mixed eruptions (d_4 and d_{3a}) from Hekla	158
4.15	Empirical survivor function plots for flank eruption durations from Mt. Etna assessing any spatial variations	161

4.16	Empirical survivor function plots for eruption durations from Kilauea assessing any spatial variations	163
4.17	Empirical survivor function plot for eruption durations from PdIF assessing any spatial variations	164
4.18	Plot showing the relationship between eruption location and lava type at PdIF	166
4.19	Plots assessing spatial variation in the duration of single basaltic eruptions (d_6) on Iceland	167
5.1	Empirical survivor function curves and fitted theoretical distributions for flank eruption durations at Mt. Etna	173
5.2	Empirical survivor function curves and fitted theoretical distributions for eruption durations at Kilauea	177
5.3	Empirical survivor function curves and best fit theoretical distributions for eruption durations from PdIF	182
5.4	Empirical survivor function curves and best fit theoretical distributions for the duration of mixed eruptions (d_{3a} and d_4) from Hekla, Iceland	188
5.5	Empirical survivor function curves and best fit theoretical distributions for the duration of single basaltic eruptions (d_6) on Iceland	194
5.6	Empirical survivor function curves and best fit theoretical distributions for the duration of single basaltic eruptions (d_6) from volcanic systems in different regions of Iceland	198
5.7	Empirical survivor function curves and best fit theoretical distributions for the total duration of basaltic eruption sequences (d_7) on Iceland	201
6.1	Schematic diagram highlighting the difference between a repose interval and a recurrence interval	207
6.2	Plots assessing the use of recurrence interval as a proxy for repose interval	217
6.3	Plots assessing temporal variation in repose interval at Mt. Etna	219

LIST OF FIGURES

6.4	Plots assessing temporal variation in repose interval at Kilauea	221
6.5	Plots assessing temporal variation in repose interval at PdIF	222
6.6	Plots assessing temporal variation in repose interval at Hekla	224
6.7	Empirical survivor function curves and fitted theoretical distributions for repose intervals between flank eruptions at Mt. Etna	226
6.8	Empirical survivor function curves and fitted theoretical distributions for repose intervals between eruptions at Kilauea	230
6.9	Empirical survivor function curves and fitted theoretical distributions for repose intervals between eruptions at PdIF	235
6.10	Empirical survivor function curves and fitted theoretical distributions for repose intervals between mixed eruptions at Hekla, Iceland	238
7.1	Plots assessing the effect of repose interval on succeeding eruption duration at the volcanic systems investigated	246
7.2	Plots assessing the effect of eruption duration on succeeding repose interval at the volcanic systems investigated	248
7.3	Empirical survivor function plots of erupted volumes at Mt. Etna, Ki- lauea, PdIF and Hekla	251
7.4	Plots assessing the relationship between erupted volume and eruption duration at the volcanic systems investigated	253
7.5	Empirical survivor function plot comparing of average eruption rates from Kilauea and PdIF	257
7.6	Empirical survivor function plot of eruption durations and erupted vol- umes for Kilauea and PdIF	258

List of Tables

2.1	Table of assigned dates and uncertainties	26
2.2	Table of uncertainty thresholds	29
2.3	List of the times of Vulcanian explosions at Soufrière Hills Volcano .	31
2.4	Significance test results comparing interval data for two time periods (data from Table 2.3)	39
2.5	Parameter values and goodness-of-fit test results for theoretical distri- butions fitted to the repose interval data of Soufrière Hills, Montserrat	46
2.6	Likelihood scale of the IPCC	49
2.7	Forecast results for the interval between vulcanian explosions at Soufrière Hills, Montserrat	56
3.1	Eruptions from Mt. Etna with known durations, 1300-2010	64
3.2	Eruptions from Kilauea with known durations, 1750-1983	78
3.3	Eruptions from PdlF with known durations, 1644-2011	89
3.4	Significance test results assessing the effect of reporting bias on the distribution of eruption duration at PdlF	110
3.5	Eruptions from Iceland with known durations 1300-2012	114
3.6	Icelandic fires with known durations (d_7)	120
4.1	Significance tests assessing temporal variation in the distribution of single basaltic eruption durations (d_6) on Iceland	140
4.2	Historical mixed eruptions from the Hekla volcanic system	142
4.3	Significance tests assessing variation in single basaltic eruption dura- tions (d_6) from individual volcanic systems on Iceland	147
4.4	Single basaltic eruptions from the Krafla volcanic system	148
4.5	Significance test results assessing temporal variation in eruption dura- tions from Mt. Etna	151

LIST OF TABLES

4.6	Significance test results assessing temporal variation in eruption durations from Kilauea	152
4.7	Significance test results assessing temporal variation in eruption durations from PdlF	156
4.8	Significance test results assessing temporal variation in mixed eruption durations (d_{3a} and d_4) from Hekla, Iceland	157
4.9	Significance test results assessing spatial variation in eruption durations from Mt. Etna	161
4.10	Significance test results assessing spatial variation in eruption durations from Kilauea	163
4.11	Significance test results assessing spatial variation in eruption durations from PdlF	165
4.12	Significance test results assessing spatial variation in eruption durations on Iceland	168
5.1	Parameter values and goodness-of-fit test results for theoretical distributions fitted to the flank eruption duration data of Mt. Etna	175
5.2	Forecasts for the duration of flank eruptions from Mt. Etna	176
5.3	Parameter values and goodness-of-fit test results for theoretical distributions fitted to the duration data of Kilauea	179
5.4	Forecasts for the duration of eruptions from Kilauea	180
5.5	Parameter values and goodness-of-fit test results for theoretical distributions fitted to the duration data of PdlF	183
5.6	Forecasts for the duration of eruptions from PdlF	186
5.7	Parameter values and goodness-of-fit test results for theoretical distributions fitted to the mixed eruption duration data of Hekla, Iceland	189
5.8	Forecasts for initial explosive phase durations of mixed eruptions (d_{3a}) from Hekla, Iceland	191

5.9	Forecasts for the total duration of mixed eruptions (d_4) from Hekla, Iceland	192
5.10	Parameter values and goodness-of-fit test results for theoretical distributions fitted to the single basaltic eruption duration data of Iceland	195
5.11	Parameter values and goodness-of-fit test results for theoretical distributions fitted to the single basaltic eruption duration data from different regions of Iceland	196
5.12	Forecasts for the duration of single basaltic eruptions (d_6) from volcanic systems on Iceland	199
5.13	Forecasts for the duration of single basaltic eruptions (d_6) from different regions of Iceland	200
5.14	Parameter values and goodness-of-fit test results for theoretical distributions fitted to data for basaltic eruption sequence duration on Iceland	202
5.15	Forecast results for the total duration of basaltic eruption sequences (d_7) on Iceland	203
6.1	Repose intervals following flank eruptions at Mt. Etna	209
6.2	Repose intervals following eruptions at Kilauea	211
6.3	Repose intervals following eruptions at PdlF	212
6.4	Repose intervals following eruptions at Hekla	216
6.5	Significance test results assessing temporal variation in repose intervals at Mt. Etna	220
6.6	Significance test results assessing temporal variations in repose intervals from Kilauea	221
6.7	Significance test results assessing temporal variations in repose interval at PdlF	223
6.8	Significance test results assessing temporal variations in repose intervals at Hekla, Iceland	225

LIST OF TABLES

6.9	Parameter values and goodness-of-fit test results for theoretical distributions fitted to the repose interval data of Mt. Etna	227
6.10	Forecasts for repose intervals between flank eruptions from Mt. Etna .	228
6.11	Parameter values and goodness-of-fit test results for theoretical distributions fitted to the repose interval data of Kilauea	231
6.12	Forecasts for repose intervals between eruptions from Kilauea	232
6.13	Parameter values and goodness-of-fit test results for theoretical distributions fitted to the repose interval data of PdlF	234
6.14	Forecasts for repose intervals eruptions from PdlF	236
6.15	Parameter values and goodness-of-fit test results for theoretical distributions fitted to the repose interval data for mixed eruptions of Hekla .	237
6.16	Forecasts for repose intervals eruptions from Hekla, Iceland	239
7.1	Significance test results assessing variation in erupted volume at individual volcanic systems	254
7.2	Significance test results assessing variation in average eruption rate at Kilauea and PdlF	258
7.3	Significance tests assessing variation in eruption duration and erupted volume at Kilauea and PdlF	259
A.1	Reported flank eruptions from Mt. Etna	300
A.2	Potential flank eruptions excluded from this study due to their close proximity to summit vents	302
B.1	Reported eruptions from Kilauea	332
C.1	Reported eruptions from PdlF	348
D.1	Reported eruptions from Icelandic volcanic systems	394

Chapter 1

Introduction



The anticipated duration of future or on-going volcanic eruptions is often a topic of much concern in volcanically active areas. As population density surrounding active volcanoes increases so does the demand for effective risk mitigation measures (Behncke et al., 2005; Connor et al., 2006; Marzocchi and Bebbington, 2012). The UK became acutely aware of this during the summit eruption of Eyjafjallajökull in South Iceland which started erupting on the 14 April 2010 and quickly gained notoriety by injecting large volumes of very fine volcanic ash into the atmosphere, grounding international air traffic (Gudmundsson et al., 2010, 2012). The resultant growing economic impact and the threat the eruption posed to aircraft safety led to concerns about the likely duration of the eruption, yet systematic studies of eruption duration are rare (Mulargia et al., 1985; Stieltjes and Moutou, 1989; Simkin, 1993; Sparks and Aspinall, 2004; Mastin et al., 2009).

The ability to confidently forecast future eruption durations would greatly benefit emergency response planning at times of volcanic crisis. Empirical statistical models can provide probabilistic constraints on the likely duration of future or on-going eruptions and statistical analyses of historic eruption duration data may provide useful insight into the processes driving volcanic eruptions.

1.1 Aims and Objectives

This PhD uses published information of historical eruption durations to compile reliable datasets on the duration of eruptions from Mt. Etna, Kilauea, Piton de la Fournaise (PdIF) and Iceland. By using a clearly stated definition of eruption duration and a thorough qualitative assessment on the uncertainty surrounding documented eruption start and end dates the datasets compiled within this study are both consistent and reliable.

The primary aims of this investigation are to use these newly compiled datasets to demonstrate an empirical probabilistic model developed to forecast the likely duration of future eruptions. The model itself can be used to forecast events which have not yet started by giving the probability associated with exceeding a stated duration or the minimum duration associated with a stated probability. Alternatively, the model can be refined so that it can be used to forecast the eventual duration of an eruption which is on-going. To demonstrate the versatility of the empirical forecasting model it is also applied to repose interval data for the volcanic systems being investigated.

Although probabilistic forecasts of future volcanic eruption durations are undoubtedly useful, they could be improved with increased understanding on the processes physically controlling an eruption's duration (Decker, 1986). By comparing the distributions of eruption durations, repose intervals, erupted volumes and average eruption rates

from the volcanic systems investigated within this study, this thesis begins to identify some leading controls on volcanic eruption durations.

The ultimate objective of this study is to develop new methods of forecasting the evolution of volcanic eruptions so that emergencies can be managed more effectively in the future.

1.2 Previous studies concerned with forecasting volcanic activity

The planning of effective risk mitigation of volcanic hazards relies on sensible long-term forecasts of the timing, location, size and style of future eruptions (Marzocchi and Bebbington, 2012; Bebbington, 2013). These forecasting goals are complicated due to the complex physical processes underlying volcanic eruptions and the large uncertainties involved (Decker, 1986; Marzocchi and Bebbington, 2012; Schmid et al., 2012). In general volcanic hazards are closely related to the character of their eruptions, i.e. effusive eruptions often pose less of a threat than their more explosive counterparts (Decker, 1986). As such, much can be learnt from good historical eruption records of potentially active volcanoes. Forecasting models based on historical records are effective and inexpensive, however, they have their limitations (Decker, 1986). Most importantly, eruption habits can change with time, rendering past eruptive behaviour a poor representation of future activity (Stein and Geller, 2012) and therefore the identification of fluctuations and trends in the eruptive behaviour of a volcanic system forms a fundamental part in the development of models of future activity (Decker, 1986; De la Cruz-Reyna, 1991; Behncke and Neri, 2003). Despite this precaution, unprecedented events can still occur, and estimating extreme events is a tough challenge for scientists in any field (Stein and Geller, 2012). For example the 2011 Tohoku earthquake was

considerably larger than those considered in the Japanese government's hazard map, and as a result the subsequent tsunami over-topped seawalls causing more than \$210 billion damage and 18, 000 deaths (Stein and Geller, 2012).

For short-term forecasting (hours to months) monitoring information and observed physical changes in volcanic systems are considered to provide more sensitive information about an imminent eruption than the character of the volcano's past activity (Marzocchi and Bebbington, 2012; Bebbington, 2013). Such deterministic attempts typically give limited results, that could be misleading due to the inherent uncertainties that they contain (Bonadonna, 2006; Marzocchi and Bebbington, 2012). A probabilistic approach to forecasting attempts to quantify these uncertainties using all available information (Marzocchi and Bebbington, 2012). For many years such probabilistic approaches to forecasting volcanic activity were limited to long-term problems (occurring over years to decades), where uncertainties are more readily accepted (Marzocchi and Bebbington, 2012). In many ways meteorologists have taken the lead in accepting that the lack of deterministic predictions is not a sign of scientific failure but a rational approach to the nature of the problem (Decker, 1986; Marzocchi and Bebbington, 2012; Stein and Geller, 2012). It is worth noting, however, that while probabilistic forecasts based on empirical data are useful, they do not approach the potential accuracy that may be achieved by fully understanding how volcanoes work (Decker, 1986). Marzocchi and Bebbington (2012) (and references therein) give a good over-view of probabilistic eruption forecasting at both long and short time scales.

1.2.1 Probabilistic forecasting of volcanic eruption durations and onset times

The physical properties controlling the duration of volcanic eruptions are not fully known. As such, the monitoring of on-going volcanic eruptions is currently not suffi-

cient to give information regarding how much longer the eruption will last. This study analyses datasets of historic eruption durations and makes probabilistic forecasts of future eruption durations based on them. While previous investigations into eruption durations are rare (Decker, 1986), the number of studies concerned with the period of inactivity between volcanic eruptions (repose interval) is vast (Marzocchi and Bebbington (2012), and references therein).

In a simple volcanic system (such as Kilauea) the inter-eruptive period is defined by surface quiescence while the magma reservoir fills and inflates. An intrusion or eruption occurs when the pressure within the magma reservoir exceeding the confining pressure. As such, eruption onset is most probably related to the amount of magma and/or excess pressure accumulated and the mechanical stability of the volcano, while the end of an eruption is related to the amount of pressure required to keep the conduit open or simply the volume of magma available. Although the physical processes of inter-eruptive periods and eruptive periods are different, similarities can be drawn between previous studies of repose intervals and the methods used to investigate eruption duration in this thesis. The general themes in these investigations are commented on below, however, more specific descriptions of their models and data is beyond the scope of this PhD (a good overview of these methods are included within Bebbington (2012)). Investigations which draw strong similarities with the statistical methods used in this investigation are discussed in more detail in Chapter 2.

Wickman (1966) first proposed that repose interval data could be used to forecast future eruption onsets. This early investigation demonstrated that while the timing of eruptions at some volcanic systems appear random, other volcanoes show patterns of increasing or decreasing probability of an eruption with increasing repose interval. Statistical analyses of repose intervals have since been applied to global data, for eruptions of similar sizes and characteristics (De la Cruz-Reyna, 1991; Coles and Sparks, 2006; Connor et al., 2006; Marzocchi and Zaccarelli, 2006), to regional data, for volcano

specific forecasting (Mulargia et al., 1985; Stieltjes and Moutou, 1989; De la Cruz-Reyna, 1993; Bebbington and Lai, 1996; Connor et al., 2003) or to a combination of the two (Pyle, 1998; Varley et al., 2006; Watt et al., 2007; Dzierma and Wehrmann, 2010; Passarelli et al., 2010; Thelen et al., 2010). Results from such investigations have identified patterns in historical data that can be matched to particular statistical distributions (e.g. Poisson, exponential, Weibull and log-logistic distributions). Different theoretical distributions are found to fit different volcanoes due to differences in the physical mechanisms controlling the volcanoes' output (De la Cruz-Reyna, 1991; Watt et al., 2007; Bebbington, 2013). The fact that theoretical distributions fit at all suggests that such analyses could become an important forecasting tool in the future (Connor et al., 2006; Varley et al., 2006).

Extreme value statistics have been used in volcanology to forecast rare, extreme events instead of typical eruptive behaviour. An overview of this technique along with an assessment of its potential importance is given by Coles and Sparks (2006). The duration analyses and forecasts of this study are intended to investigate typical eruption durations from the volcanoes studied. Where extreme value statistics have been applied to the volcanic systems considered here (i.e. Mulargia et al. (1985)) their results have been compared to the results of this study.

1.3 An introduction to the volcanic systems investigated in this study

The duration and repose analyses of this study are based on historic eruption data from Mt. Etna, Kilauea, Piton de la Fournaise (PdIF) and Iceland. The first three volcanoes were chosen based primarily on their highly active nature and good historical record where eruptions are often reported with both start and end dates. For similar reasons,

the eruption records of these volcanoes have often been interrogated in the past, leading to a good understanding of their underlying patterns and trends (Tanguy, 1981; Klein, 1982; Stieltjes and Moutou, 1989; Behncke and Neri, 2003; Branca and Del Carlo, 2004; Peltier et al., 2009).

These three volcanic systems show similarities in the composition and physical properties of their erupted lavas, and as such have been compared in the past. Most notably, Aki and Ferrazzini (2001) compared eruption histories from these three volcanoes by modelling their eruption durations and erupted volumes. On the surface strong similarities exist between Aki and Ferrazzini (2001) and the analyses of this thesis. However, the models involved are very different with Aki and Ferrazzini (2001) quantitatively modelling the plumbing system of the volcanoes and simulating the observed duration/volume relationships, whereas the models of this investigation are purely empirical. Furthermore, while the duration data of both investigations are based on published records, we have critically examined all available data to ensure that a single definition of eruption duration is used throughout.

Icelandic eruption durations have also been considered in response to the 2010 Eyjafjallajökull eruption and its wide reaching effects. The diverse volcanic activity displayed on Iceland and its robust historical record will be shown to provide insight into the duration of different types of eruptions and styles of activity.

The following subsections introduce each of these volcanoes and volcanic regions, providing information on their geology and tectonic setting and the general style of their volcanism. In each case previous investigations into their eruption histories are outlined.

1.3.1 Mt. Etna

Mt. Etna, situated in Eastern Sicily, is a composite volcano with a shape transitional between a stratovolcano and shield volcano (Duncan et al., 1981; Proietti et al., 2011) (Fig. 1.1). Activity at Mt. Etna is primarily effusive, consisting of slightly evolved Hawaiite lavas which are chemically rather uniform, with the fractionation of mafic phases causing only slight variations (Armienti et al., 1989; Salvi et al., 2006). Historically, two types of volcanic activity have been recognised at Mt. Etna: persistent activity from the summit vents and periodic activity from eruptive fissures on the volcano's flanks (Guest and Murray, 1979; Duncan et al., 1981; Acocella and Neri, 2003; Behncke and Neri, 2003; Branca and Del Carlo, 2005; Crisci et al., 2010). For reasons discussed in Chapter 3 only the flank eruption data for the period 1300 to 2010 are investigated here.

As the most active volcano in Europe, Mt. Etna is one of the most widely studied and documented volcanoes in the world (Andronico and Lodato, 2005). Hazard studies of Mt Etna began in the late 1970's and early 1980's focussing on patterns in historic eruptions and predicting the location of future activity (Frazzetta and Romano, 1978; Guest and Murray, 1979; Duncan et al., 1981). Since then numerous studies have built on that work by analysing catalogues of historic eruptions (Mulargia et al., 1985; Behncke and Neri, 2003; Branca and Del Carlo, 2004, 2005; Salvi et al., 2006; Neri et al., 2011; Smethurst et al., 2009; Passarelli et al., 2010; Proietti et al., 2011) and producing susceptibility and probabilistic hazard maps of surrounding areas (Andronico and Lodato, 2005; Bisson et al., 2009; Behncke et al., 2005; Crisci et al., 2010; Harris et al., 2011; Cappello et al., 2012, 2013). Such extensive historical records and wealth of previous investigations make it an ideal candidate for this type of investigation. The following two sections will outline the key findings within these previous investigations with particular emphasis on results pertaining to flank eruption durations or repose intervals between successive flank eruptions at Mt. Etna.

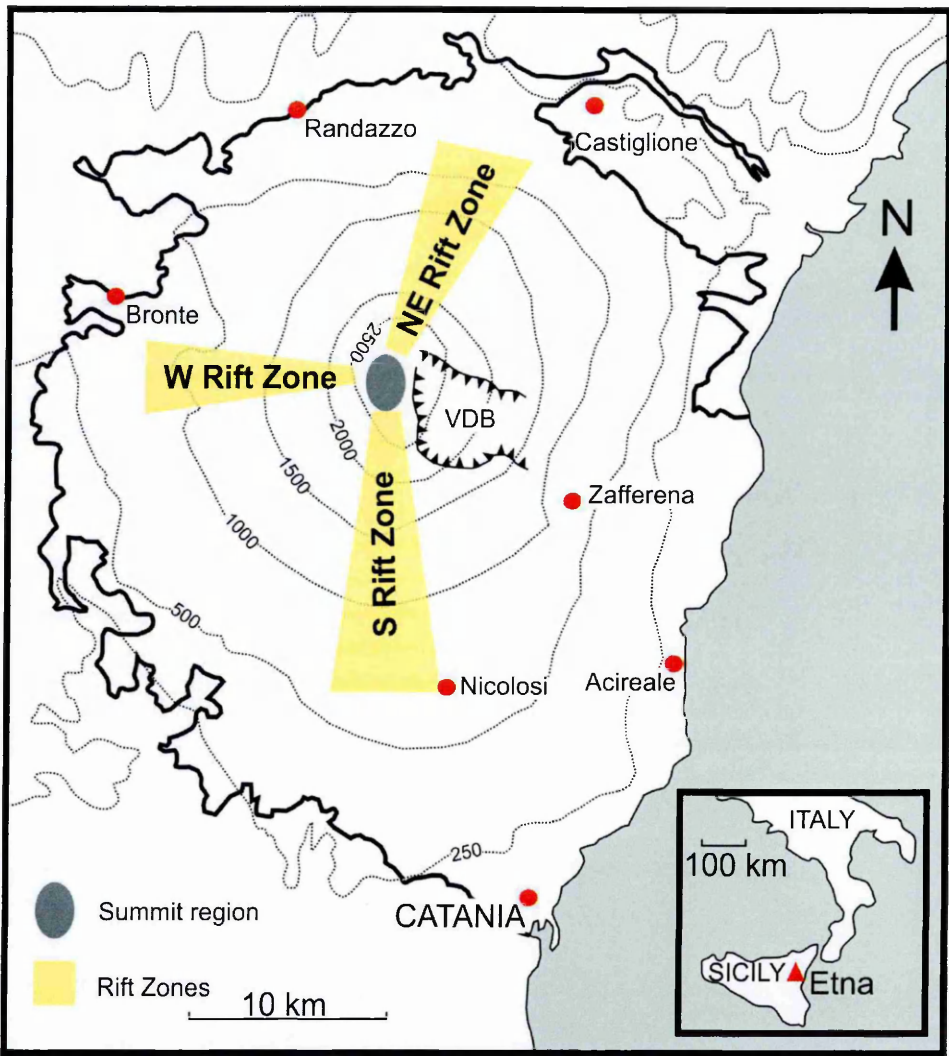


Fig. 1.1 Sketch map of Mt. Etna showing the location of Mt. Etna and its principle features including the Valle de Bove (VDB) and the approximate position of the North-East, West and South Rift Zones as indicated by vent densities in Duncan et al. (1981). Map based on that within Chester et al. (2012), contours are displayed in metres above sea level

Previously recognised patterns and trends in eruptive activity at Mt. Etna

Previous attempts have been made to suggest that Mt. Etna's activity is cyclic and both century scale and decade scale cycles have been proposed in the past. This notion was first suggested by Imbò (1928) who used apparent clusters in eruption frequency and location to define patterns in eruptive activity. Since then Behncke and Neri (2003) identified five cycles between 1865 and 2002, each starting with low-level activity, fol-

lowed by nearly continuous summit activity and ending with a series of flank eruptions of which the last is the most voluminous. However, such analyses suffer from a lack of detail regarding intra-crater Strombolian activity leading to a very subjective definition of repose period and thus an inconsistent definition of eruptive cycles in the literature (Chester et al., 1985; Branca and Del Carlo, 2005).

The evidence for longer-term, century scale cycles at Mt. Etna is stronger. A sharp drop in productivity and in lava phenocryst content following 1669 have been recognised and linked to the draining of a shallow magma chamber during the 1669 eruption (Hughes et al., 1990; Patané et al., 2003; Behncke and Neri, 2003). While a magma reservoir at Mt. Etna akin to that prior to 1669 has not been re-established since, a gradual increase in eruption frequency, output rate and magma accumulation has been identified in recent years (Behncke and Neri, 2003; Patané et al., 2003; Allard et al., 2006). This pattern has been interpreted as a century scale cycle with the large eruptions reported for the period 1600-1669 representing the culminating phase of the previous cycle (Behncke and Neri, 2003). Although the basis of this interpretation is physical evidence, the term cycle implies a repeating pattern, however, for Mt. Etna this notion is based on the recognition of a single ‘cycle’. For these reasons the current investigation does not consider eruptive activity at Mt. Etna to be cyclic, but previously recognised trends in productivity and output rate are considered along with the physical properties to which they are attributed (Wadge et al., 1975; Wadge, 1981; Hughes et al., 1990; Behncke and Neri, 2003; Branca and Del Carlo, 2004; Andronico and Lodato, 2005; Behncke et al., 2005; Branca and Del Carlo, 2005; Salvi et al., 2006; Bebbington, 2013; Cappello et al., 2013).

Previous investigations into eruption durations and repose intervals at Mt. Etna

Wickman (1966) took advantage of Mt. Etna’s extensive historical record and used it to highlight the potential use of repose data as a tool for forecasting future eruption

onsets. The results of this early investigation are compared to those derived in the current study (Chapter 6). Since then numerous studies have developed this theory. Mulargia et al. (1985) applied extreme value statistics to flank eruption data to estimate the probability of a major eruption ($> 150 \times 10^6 \text{m}^3$ or > 500 days) occurring within different time intervals.

Although rare, specific analyses of eruption durations at Mt. Etna have highlighted a strong correlation between flank eruption duration and volume at Mt. Etna (Mulargia et al., 1985; Andronico and Lodato, 2005; Proietti et al., 2011). Proietti et al. (2011) defined six classes of eruption based on this relationship and Mulargia et al. (1985) proposed that eruption duration provides a good estimate of eruption magnitude (where magnitude is volume output). Variations in both of these parameters with time have been investigated by Andronico and Lodato (2005), who identified an increase in both median duration and the volume of lava erupted during flank eruptions after 1971.

1.3.2 Kilauea

Kilauea is the south-easternmost of five large shield volcanoes whose activity has formed the island of Hawaii, in the Hawaiian Island Chain (Eaton, 1962; Moore et al., 1980; Peterson and Moore, 1987). It consists of a summit region dominated by a caldera of 3-5 km in size and elongate topographic ridges, forming the East and South-West Rift Zones (ERZ and SWRZ, respectively) (Eaton, 1962; Moore et al., 1980; Hill and Zucca, 1987; Holcomb, 1987; Peterson and Moore, 1987) (Fig. 1.2). Rift zone eruptions begin as a line of fissures that quickly become focussed on a single vent (Holcomb, 1987; Klein, 1982). Summit deflations and drops in summit lava lake levels often accompany rift zone eruptions, indicating a close association between summit and rift activity at Kilauea (Wolfe et al., 1987; Tilling and Dvorak, 1993). In terms of

an eruptive model, this relationship has been used to propose that rift eruptions derive from magma which has travelled laterally from the shallow summit reservoir (Holcomb, 1987; Tilling and Dvorak, 1993; Cayol et al., 2000). Geochemically erupted products of Kilauea are tholeiitic basalt, differing from one another in their olivine content (Eaton, 1962).

Previous analyses of Kilauea's eruptive history

The highly active nature of Kilauea and the accessibility of its eruptions has made it the basis of many volcanological investigations (Eaton, 1962). It has been intensively studied, and is an ideal candidate for further studies of magma movement and eruption dynamics driven both from its historic eruption record and monitoring information (Klein, 1982; Tilling and Dvorak, 1993).

Eruption frequency and type at Kilauea has changed through time over the interval of decades to centuries Holcomb (1987). While some changes have been repeated over long intervals others have occurred in evolutionary sequences (Holcomb, 1987). The most widely recognised pattern in eruptive behaviour at Kilauea is the sympathetic behaviour between summit and flank activity, where heightened activity in one region tends to result in decreased activity at the other (Holcomb, 1987). Statistical analyses performed by Klein (1982) also found evidence of this relationship, as well as noting that the longest periods of repose at Kilauea correlate well with heightened activity at Mauna Loa, and vice versa. Other results indicate that future eruptions at Kilauea are largely independent of the date that the last eruption occurred, with the only exception being large volume-eruptions which are often followed by long periods of repose (Klein, 1982).

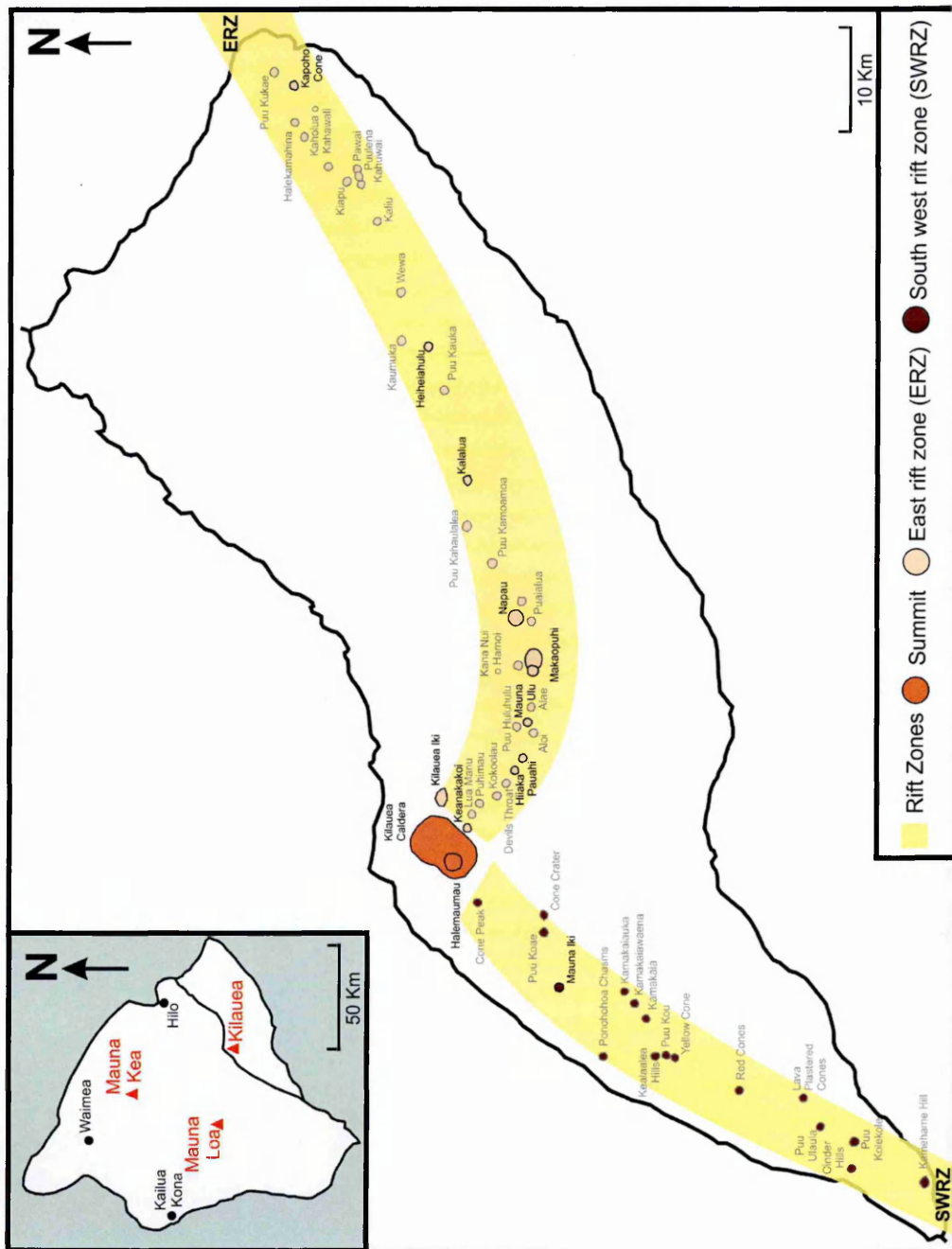


Fig. 1.2 Sketch map of Kilauea showing the location of principle vents. Vents are coloured depending on the rift zone to which they belong, those with pale outlines and names do not have eruptions with known durations in this study. Map is based on that within Holcomb (1987)

The extensive historical record of Kilauea led to Wright (2008) defining three types of eruptions. The most common of these are short duration rift eruptions which are followed by several months of quiescence before new eruptions begin on a different part of the rift zone. The second are episodic eruptions, characterised by a return to the same vent following repose of days to weeks with the entire eruptive sequence lasting weeks to years. Finally, sustained eruptions occur at Kilauea marked by uninterrupted activity at single vents lasting for months to years. Holcomb (1987) also considered eruption durations and suggested that eruptions from Kilauea's rift zones are often briefer than those from the summit caldera.

1.3.3 Piton de la Fournaise

Piton de la Fournaise (PdIF) is an intra-plate basaltic shield volcano built upon the flank of two inactive volcanoes: Piton de Neiges and Les Alizés situated on Réunion Island (Indian Ocean) (Lénat et al., 2012; Schmid et al., 2012) (Fig. 1.3). The summit caldera is an 8 km wide collapse depression (Enclos Fouqué caldera), within which the principal intra-caldera vent exists as a shield volcano with two smaller craters at its summit; Dolomieu and Bory (Stieltjes and Moutou, 1989; Peltier et al., 2009) (Fig. 1.3). The caldera is connected to a down-faulted trough to the East which extends to the coast (Stieltjes and Moutou, 1989; Peltier et al., 2009). Although the majority of historic activity occurred within the Enclos Fouqué caldera, three rift zones are identified on PdIF (Stieltjes and Moutou, 1989; Peltier et al., 2009; Schmid et al., 2012). The North-Western Rift Zone contains localised cinder ridges and cones, while the North-Eastern and South-Eastern Rift Zones form broad, tapering ridges that extend well below sea level (Stieltjes and Moutou, 1989) (Fig. 1.3).

PdIF is one of the most active volcanoes in the world, having erupted on average once per year over the past 100 years (Stieltjes and Moutou, 1989; Boivin and Bachélery,

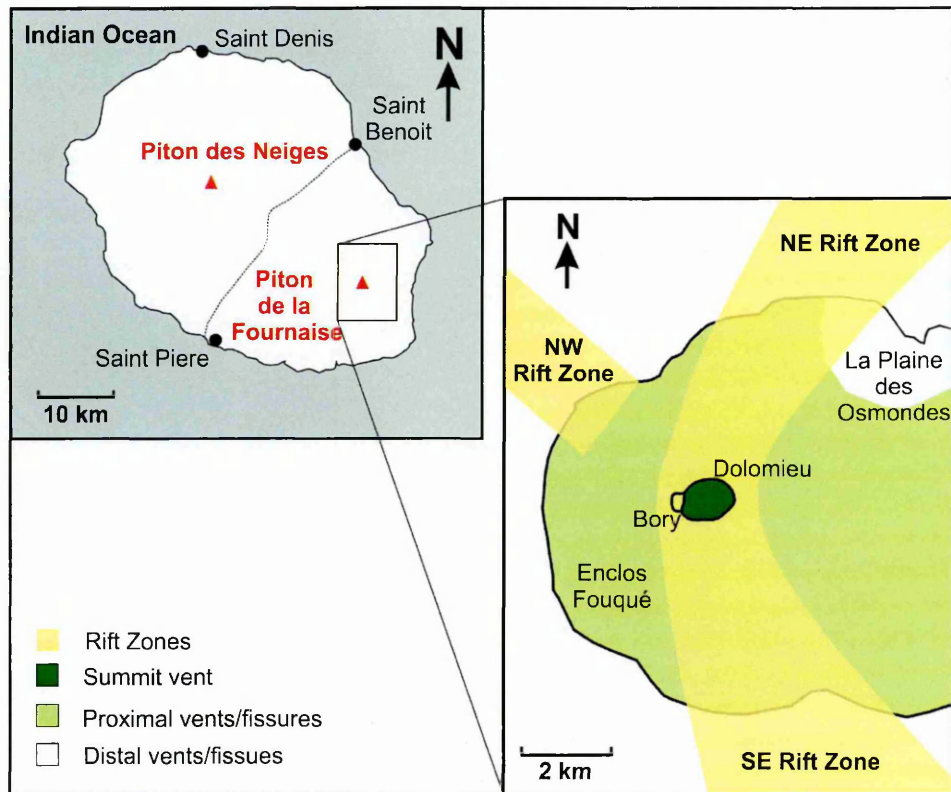


Fig. 1.3 Sketch map of PdlF showing its location (Inset) and principle features (main), including the extent of the NW, NE and SE Rift Zones. Colours are used to show the extent of regions described as summit, proximal and distal in this study. Map based on those within Albarède et al. (1997) and Peltier et al. (2009)

2009; Peltier et al., 2009). Its extensive eruptive record dates back to 1644 and contains over 200 recorded events (Stieltjes and Moutou, 1989). Geophysical and geochemical measurements accompany the eruption record for PdlF since 1980, when the Observatoire Volcanologique was established (Peltier et al., 2009; Schmid et al., 2012). Geochemically erupted lavas at PdlF are transitional between alkalic and tholeiitic basalts (Albarède et al., 1997; Lénat et al., 2012), containing 42 - 49 wt % SiO_2 with viscosities of 10^2 Pa.s (Grasso and Bachélery, 1995).

Previous analyses of PdlF's eruptive history

Stieltjes and Moutou (1989) performed statistical analyses on eruption durations from PdlF (1844-1985) and conclude that eruptions are generally short, with 88 % lasting

≤ 2 months and 25 % lasting only 1 to 2 days. They also investigated the relationship between eruption duration and repose interval, finding that with the exception of very short events, eruption duration has a direct effect on the following repose interval (with short repose intervals (< 2 months) often following eruptions of < 1 month duration) but that the duration of repose does not influence the duration of a succeeding eruption.

Previous investigations have recognised eruptive cycles at PdlF. Ludden (1977) recognised large outbursts of oceanitic lava every 20-40 years, and Stieltjes and Moutou (1989) identify 3 major cycles in the period 1931-1981, each starting with one of these eruptions (1931-1960, 1961-1976 and 1977-continuing in 1981). Stieltjes and Moutou (1989) use relationships between the volume of magma erupted and the duration of activity and inactive periods to conclude that these decade-long cycles relate to the refilling of a magma reservoir at intermediate depth (5-10 km). Peltier et al. (2009) focussed on more recent activity at PdlF (1972-2007) and noted a change in eruptive behaviour for the period 2000-2007. During this time they recognised 5 eruptive cycles each ending in a large distal eruption of oceanite lava and conclude that this change represents a switch from a period characterised by progressive draining of a shallow magma reservoir, with occasional recharge (1972-1992), to one of continuous recharge from a deeper source (2000-2007).

1.3.4 Iceland

Iceland forms the sub-aerial portion of the spreading plate boundary between the American and Eurasian plates in the North Atlantic Ocean (Thordarson and Larsen, 2007; Thordarson and Höskuldsson, 2008). The Iceland basalt plateau is a manifestation of this divergent tectonic setting and its interaction with the Iceland mantle plume (Óladóttir et al., 2008; Thordarson and Höskuldsson, 2008). The current position of

this plume is believed to be beneath the Bárðarbunga, Grímsvötn and Kverkfjöll volcanic systems in central-eastern Iceland (Björnsson, 1985; Gudmundsson, 2000; Thordarson and Larsen, 2007; Thordarson and Höskuldsson, 2008) (Fig. 1.4). As a result of this complex geological setting volcanism on Iceland is diverse and has experienced almost all known eruption types and styles on Earth (Thordarson and Larsen, 2007; Thordarson and Höskuldsson, 2008).

The superposition of the spreading plate boundary over the mantle plume causes volcanism to be distributed in discrete belts of active faulting and volcanism (Gudmundsson, 2000; Thordarson and Larsen, 2007; Óladóttir et al., 2011). The most prominent of these is the axial rift zone, which marks the loci of active spreading and follows the divergent plate boundary across Iceland (Björnsson, 1985; Thordarson and Larsen, 2007) (Fig. 1.4 shaded pink). Electrical resistivity measurements of the Icelandic crust have identified a variable crustal thickness which is thinnest beneath the axial rift zone in the north-east and south-west (8-10 km). The crust thickens with age, so that regions away from the axial rift and also with increasing distance from the mantle plume are thicker, reaching 20-30 km thick in older (Tertiary) areas (Björnsson, 1985, 2008).

Previous studies of Icelandic volcanism have used petrological and volcano-tectonic evidence to identify 30 volcanic systems, each consisting of a fissure/dyke swarm, central volcano or both (Fig. 1.4) (Jakobsson, 1979; Thordarson and Self, 1993; Larsen, 1999; Gudmundsson, 2000; Óladóttir et al., 2008; Thordarson and Larsen, 2007; Thordarson and Höskuldsson, 2008; Siebert et al., 2010). In general the central volcanoes are responsible for the more intermediate to acidic lavas on Iceland, attributed to the presence of shallow magma chambers within them (Björnsson, 1985; Gudmundsson, 2000). In contrast, eruptions from their associated fissure swarms erupt basaltic lavas only (Björnsson, 1985; Gudmundsson, 2000).

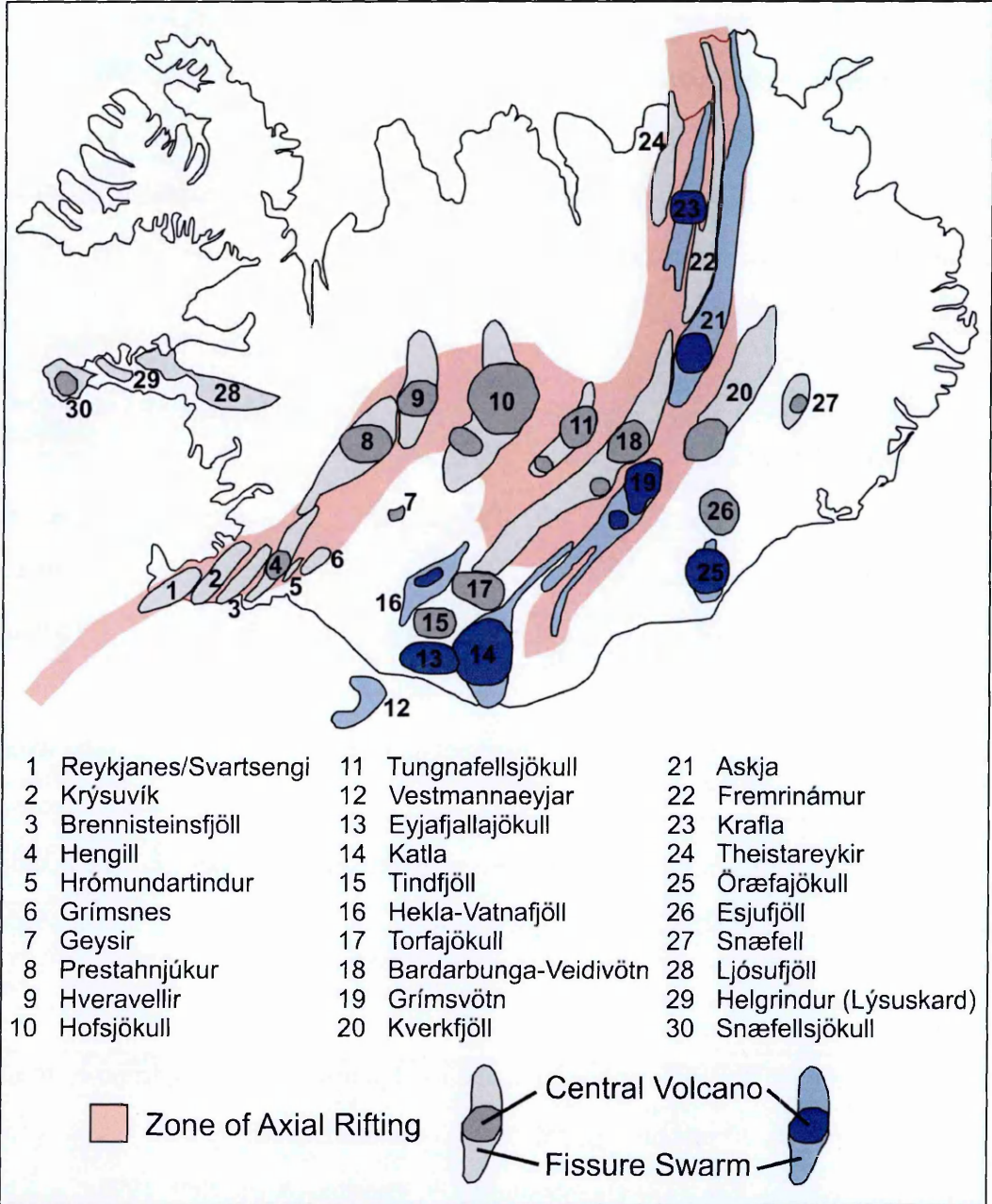


Fig. 1.4 Sketch map of Iceland showing the position of the axial rift and 30 volcanic systems (modified from Thordarson and Larsen (2007) and Thordarson and Höskuldsson (2008)). Blue volcanic systems are those with historic eruption durations used in this study

Volcanic systems on Iceland and previous investigations into their eruptive history

Written documentation and the ice-record of Iceland results in an eruption history that is robust and has been extensively studied in the past (Larsen, 2002). Thordarson and

Larsen (2007) stated that of the 205 events documented, 172 are verified by deposit analysis in the field and 159 are single eruptions with classified eruption styles. This high eruption frequency makes Iceland one of the most historically active sub-aerial volcanic regions on Earth (Thordarson and Larsen, 2007; Öladóttir et al., 2011). In terms of general volcanic activity an average of 20 eruptions per century, or an eruption every ~ 5 years has been calculated (Thorarinsson, 1979; Thordarson and Höskuldsson, 2008; Öladóttir et al., 2011). The frequency of eruptions is, however, not constant and a long term trend with a periodicity of 140 years has been noted in eruption frequency with 40-80 years of high eruption frequency followed by a similar duration of low eruption frequency (Larsen, 2002; Thordarson and Larsen, 2007).

Eight Icelandic volcanic systems have erupted historically and have reliable documented eruption durations, forming the basis of the Iceland investigations of this study (Chapter 3). These are Vestmannaeyjar, Eyjafjallajökull, Katla, Hekla, Grímsvötn, Krafla, Askja and Öräfajökull (systems 12, 13, 14, 16, 19, 21, 23 and 25, Fig. 1.4 respectively). Each volcanic system has its own volcanic architecture driving its own style of volcanism. Ideally, investigations of Icelandic volcanism should be conducted on a volcano specific level, however, some volcanic systems have a more complete historic eruption record than others. As a result a more general approach to the volcanism on Iceland is adopted for the majority of this investigation. While the intricacies of this are discussed in more detail in Chapter 3, general features of the volcanic systems and their volcanism are introduced below.

Broadly speaking Icelandic volcanic systems can be split into two groups, based on the stress regimes that they are subjected to (Björnsson, 1985). Extensional stresses dominate the active rift region of Iceland, and volcanic systems there (Askja, Krafla and Grímsvötn) tend to have well developed fissure swarms consisting of tensional fractures and normal faults (Björnsson, 1985; Gudmundsson, 2000). Spreading and rifting is not uniform in time or space, resulting in periods of intense rifting confined

to a single volcanic system (e.g. Grímsvötn: Laki 1783-1784, Krafla: 1724-1729 and 1975-1984 and Askja: 1874-1875 and 1921-1929). Björnsson (1977) investigated the historic records of Krafla and demonstrated that these periods of episodic rifting occur at the Krafla region every 100-150 years.

The off-rift volcanic systems considered in this study are Vestmannaeyjar, Eyjafjallajökull, Katla, Hekla and Öräfajökull and are responsible for some of the most notable historic eruptions on Iceland. The initially sub-marine volcanism of Vestmannaeyjar formed the basaltic island of Surtsey 1963-1967 and the dramatic eruptions of Heimaey in 1973 (Jakobsson, 1979; Thordarson and Sigmarsson, 2009), while the largest known eruption from Katla is the 934-938 AD Eldgjá flood lava which is the greatest volcanic pollution event in historical times (Thordarson and Larsen, 2007; Óladóttir et al., 2008). Most recently the 2010 eruptions of Eyjafjallajökull caused major disruption across Europe due to the large quantities of volcanic ash it generated (Gudmundsson et al., 2010, 2012).

The reduced extensional stresses acting on these regions result in systems with larger central volcanoes and smaller associated fissure swarms than those situated within the active rift (Thordarson and Larsen, 2007). Volcanism displayed by these systems shows greater variation in both eruption style and the geochemistry of erupted products. In contrast to the tholeiitic basalt eruptions of inside rift volcanoes, off-rift volcanism tends to have erupted products with higher SiO₂ content. For example, Öräfajökull erupted rhyolitic tephra during its 1362 Plinian eruption (Thorarinsson, 1958; Selbekk and Trønnes, 2007; Thordarson and Larsen, 2007). The other off-rift volcanic systems investigated here form part of the eastern volcanic zone, which represents the early stages of axial rifting. While eruptions from Vestmannaeyjar have an alkalic nature the other volcanic systems in this region are more transitional.

For Iceland the historical eruption record of Hekla is unusually complete (Grönvold et al., 1983; Thorarinsson, 1967a; Gudmundsson et al., 1992), containing 23 doc-

umented eruptions since its first historic eruption in 1104 (Thordarson and Larsen, 2007). Such detailed historical records have made Hekla the subject of numerous studies. Thordarson and Larsen (2007) described the majority of eruptions from Hekla as mixed eruptions due to their initial Plinian phase which transitions into an effusive phase with time. A decrease in the silica content of products erupted during the initial phase of these eruptions has been noted with time, so that material erupted in the initial explosive phase can have signatures indicative of rhyolites while later products have that of basaltic andesites (Pórarinnsson, 1954; Thorarinnsson, 1967a; Pórarinnsson, 1976; Sigmarsson et al., 1991; Gudmundsson et al., 1992; Ólafsdóttir et al., 2002). Further relationships between the volume and chemistry of an eruption and the length of preceding repose have been found and used to indicate evidence of a large magma chamber existing beneath the Hekla central volcano (Jakobsson, 1979).

1.4 Thesis structure

Chapter 2 introduces the methods used throughout this investigation, including important considerations when defining eruption duration and the statistics behind the analyses and forecasts of future chapters. Chapter 3 presents the eruption duration datasets compiled specifically for this study and Chapter 4 investigates temporal and spatial variations within these data. The empirical probabilistic model outlined in Chapter 2 is then used to forecast the duration of future (and on-going) eruptions at each volcanic system in Chapter 5.

Although the main aim of this investigation is to further understanding on eruption durations, the empirical probabilistic model is versatile and can be adapted to other duration types or volcanoes. Chapter 6 demonstrates this and considers the application of this model to repose interval data and, where possible, compares the results obtained to those of previous investigations.

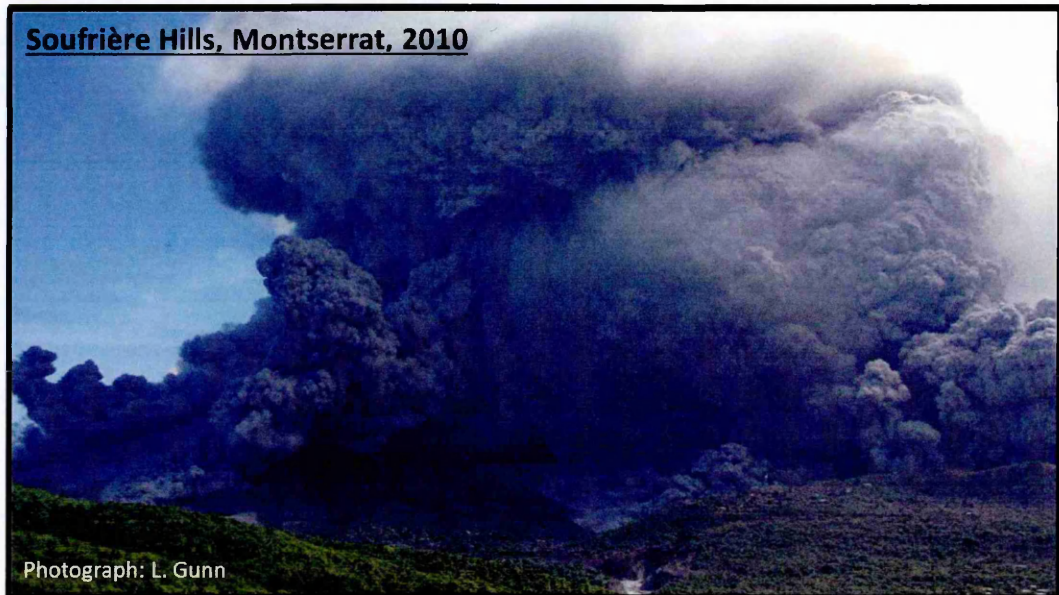
CHAPTER 1. INTRODUCTION

Finally Chapter 7 investigates possible controls on eruption duration by assessing relationships between the eruption duration regimes identified in Chapter 4 and their associated repose interval, erupted volume and average eruption rate data. This chapter concludes the work of this PhD and includes ideas for further work.

The appendices of this thesis include a brief section about each volcanic eruption considered for use in this study, including information regarding their eruption start and end dates, durations and location. These outline the reasons behind any uncertainty assignments made in Chapter 3 and should be referred to for any queries regarding the duration of individual eruptions used within this study.

Chapter 2

Methods



2.1 Dataset compilation

2.1.1 Defining eruption duration

The duration of a volcanic eruption can be defined as the period of time when fresh volcanic material is being emitted at the Earth's surface. Here we consider a period of continuous magma discharge as the basic building block of an eruption, where magma discharge included lava, and ash but not persistent degassing. The definition of eruption duration with respect to lava lake existence is complex and affects the Kilauea dataset of this investigation. It is therefore covered in detail in section 3.2.2.

The intensity of volcanic activity during an eruption is rarely constant. More often, discrete phases of heightened activity separated by periods of surface quiescence lasting hours or days can be observed (Simkin 1993; Siebert et al. 2010). An argument could be made that each phase constitutes a separate eruption, however, given the nature of historical records it is unrealistic to assume that we have information about every quiescent period that occurred during every eruption in this study.

The Smithsonian Institution's Global Volcanism Program considers eruptive phases separated by periods of quiescence of less than 3 months as the same eruption, unless there are significant reasons to treat them as distinct events (Venzke et al. 2013; Siebert et al. 2010). This is an arbitrary value, chosen as a sensible cut off for a global dataset of historic volcanic eruptions, however, in reality, the degree and duration of a quiescent pause required to warrant grouping a series of eruptive phases as one eruption, or splitting a series of eruptive phases into more than one eruption, is likely to depend on local circumstances. A three month classification could greatly increase the duration of successions of short duration eruptions making them appear as a single long duration eruption.

Furthermore, this study focusses on the duration of volcanic eruptions with the aim of making probabilistic forecasts regarding the duration of future eruptions. In terms of the model's real-life application three months is a relatively long length of time following a basaltic, effusive eruption before regarding it as finished and it is likely that surrounding populations would consider the eruption finished before three months has passed. Instead, this threshold is reduced to 10 days and we consider any non-eruptive period of ≤ 10 days during an eruption as not significant enough to warrant treating the activity either side of it as independent eruptions. This threshold is largely arbitrary, although to some extent is based on the resolution of the data available for the volcanic systems investigated in this study. It is worth noting that where sequences of eruptions are recognised separate analyses on the total duration of eruptive sequences

are performed.

2.1.2 Dealing with individual eruption duration uncertainty

An ideal dataset of historic eruption durations would contain information regarding eruption start and end date to the nearest minute or second allowing a precise duration to be calculated. However, such high resolution data requires a level of monitoring that is unrealistic, especially in remote areas and early in the historical record. As a result a means of assessing and assigning the uncertainty in the duration of an eruption is required, ensuring that all eruptions in this study are treated equally.

Two types of uncertainty have been identified: resolution-derived uncertainty and literature-derived uncertainty. In both cases uncertainty can surround both the start and end date of an eruption, therefore the assigned uncertainties are often asymmetrical. The majority of the analyses within this study use the preferred eruption duration data, considering the uncertainty negligible. Section 4.1, investigates the validity of this assumption and uses the uncertainty data which results in the largest deviation from the preferred duration of each eruption. As a result the asymmetric uncertainty, inherent to some eruptions, is not used in any analyses.

Resolution-derived uncertainty

Resolution-derived uncertainty applies to all eruptions and is especially important for eruption dates that are only reported to the nearest month or year. Here a date was assigned along with a number of days uncertainty, according to the method adopted by Bebbington and Lai (1996) and Benoit and McNutt (1996) (Table 2.1). Sometimes, despite the start and/or end date of an eruption only being known to the nearest month, slightly more qualitative information is provided indicating that it was ‘early’, ‘mid’

or ‘late’ in that month. Again the method of Benoit and McNutt (1996), summarised in Table 2.1, was applied.

Table 2.1: Table of assigned dates and uncertainties

Reporting	Start and/or End	
	Date	Uncertainty (days)
Nearest hour	-	+/- 0.02
Nearest day	-	+/- 0.5
Nearest month	15/mm/yyyy	+/- 15
Nearest year	01/07/yyyy	+/- 182.5
‘Early’ month	05/mm/yyyy	+/- 5
‘Mid’ month	15/mm/yyyy	+/- 5
‘Late’ month	25/mm/yyyy	+/- 5

mm = Reported month, *yyyy* = Reported year

The majority of eruption durations considered in this study are known to the nearest day and Fig. 2.1a uses a hypothetical eruption to demonstrate the importance of assigning a duration uncertainty to eruptions with this resolution of reporting. It is worth noting that when an eruption is reported as starting and ending on the same day its preferred eruption duration is reported as 0.5 days and is treated according to the ‘nearest hour’ category of Table 2.1.

Literature-derived uncertainty

Literature-derived uncertainty results from contradictory reporting of eruption start and/or end dates in the existing literature. This is largely a result of differing interpretations of what constitutes an eruption, and in particular whether an eruption is the continuation of a previous one or a new eruption in its own right (Bebbington, 2013; Wang and Bebbington, 2013). Furthermore, some studies only report eruption start dates and durations (e.g. Mulargia et al. (1985)) and depending on the method used to calculate eruption duration this could lead to different end dates being derived. For

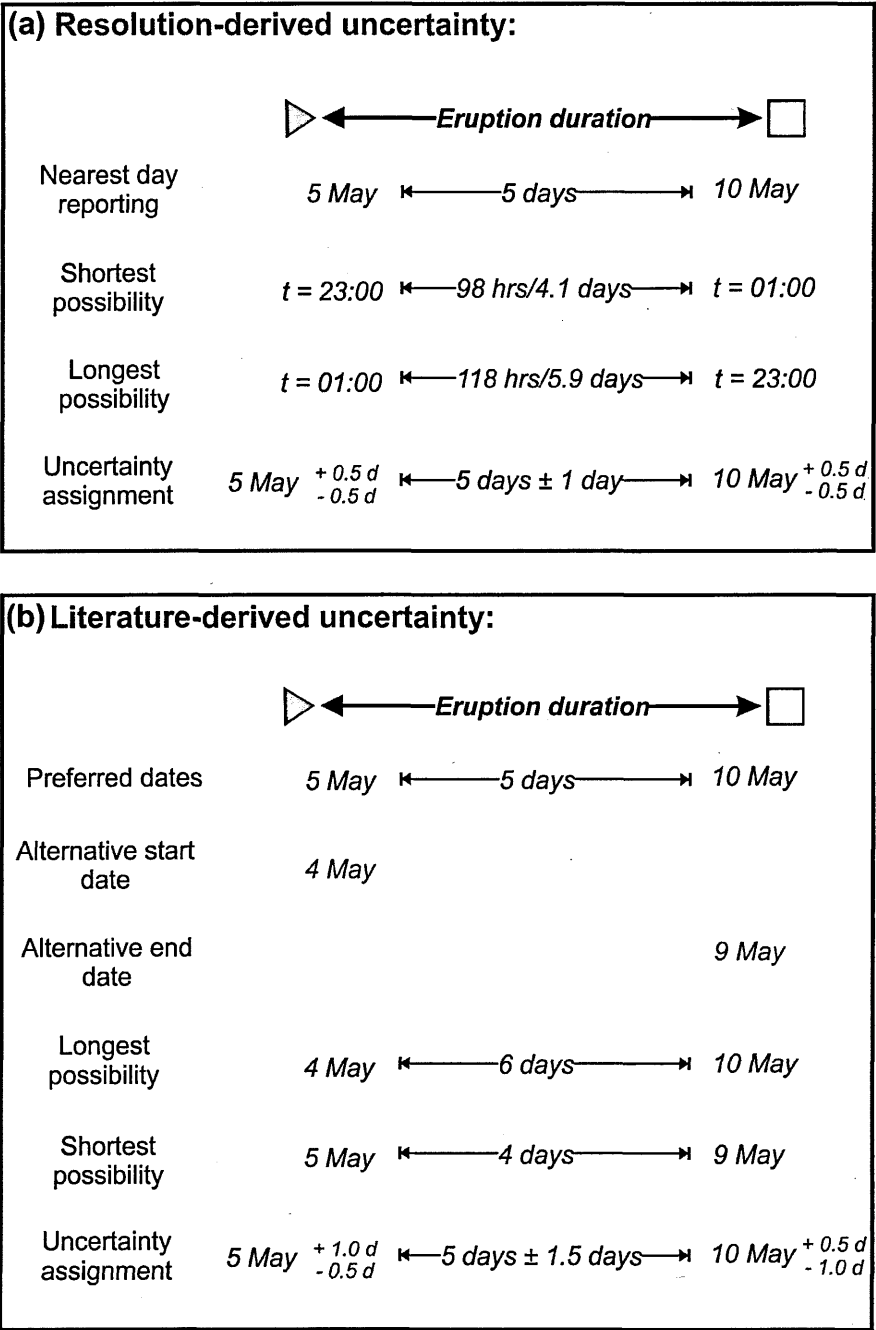


Fig. 2.1 Diagram explaining how (a) resolution-derived uncertainties and (b) literature-derived uncertainties are assigned

example an eruption starting on one day and ending on the following day could be considered to have either a 1 day duration (this study) or a 2 day duration. Regardless of how the contradictory information in the literature was generated, some degree of uncertainty needs to be applied.

Where contradictory reporting exists the eruption start and end dates that are reported most frequently or from the most reputable source are used as the eruption's preferred start and end dates. The duration between these dates is then considered the preferred eruption duration. Fig. 2.1b demonstrates how literature-derived uncertainty is applied to a hypothetical eruption which has an alternative start and an alternative end date reported. Using these alternative start and end dates the shortest and longest possible eruption duration can be calculated (in this case, 4 and 6 days respectively) and the range of durations which need to be covered by the literature-derived uncertainty are identified. Duration uncertainty values are then assigned to the dates that they apply to (e.g. + 1 day to the eruption start date and - 1 day to the eruption end date (blue values in Fig. 2.1b). The precise times of day that the eruption started and ended are still unknown and therefore resolution-derived uncertainty still exists and is assigned for the aspects of the eruption start and end dates that are not affected by the literature-derived uncertainty (red values in Fig. 2.1b). The duration of this eruption would therefore be reported as 5 days \pm 1.5 days.

Uncertainty thresholds: How uncertain is too uncertain?

Some degree of uncertainty is acceptable for all data, however an uncertainty threshold above which the eruption duration is considered too uncertain for this study needed to be decided. In general any eruption carrying a duration uncertainty of greater than 50 % of its total preferred eruption duration is excluded from the study. However, eruptions with 'nearest day' resolution data automatically carry a duration uncertainty of \pm 1 day as a result of resolution-derived uncertainty (Fig. 2.1a). Therefore eruptions with preferred durations of 1 day always carry a duration uncertainty of 100 %. In addition to this, eruptions with preferred durations of 2 days carry 50 % duration uncertainties and thus any additional literature-derived uncertainty will render the eruption too uncertain. In these circumstances the uncertainty threshold is increased and 2 day

eruptions can carry maximum duration uncertainties of 75 % (allowing either the start or end date of the eruption to carry a 1 day literature-derived uncertainty) while 1 day eruptions are included with their 100 % uncertainty. These uncertainty thresholds are summarised in Table 2.2.

Table 2.2: Table of uncertainty thresholds above which eruption durations are considered too uncertain and excluded from the study

Preferred Duration	Duration U/C as %	Hypothetical Example
1 day	100 %	1 day ± 1 day
2 days	75 %	2 days ± 1.5 days
> 2 days	50 %	5 days ± 2.5 days

U/C = Uncertainty

The uncertainties discussed above relate to individual eruptions within a dataset, however, the analyses within this study often focus on entire distributions of eruption duration. To ensure the overall distribution of eruption durations is not altered too greatly by the individual uncertainties that they contain the distribution of preferred eruption duration is compared to the distributions of maximum and minimum possible eruption duration when the uncertainties are taken into consideration. This process and the results are discussed in Chapter 4.

2.2 Survivor function analysis

Survival analysis was first employed as a method of costing insurance premiums and is now commonly used to answer medical and engineering problems (Machin et al., 2006). For example medical applications enable the user to determine the time till death following cancer tumour removal or the time a patient is pain-free following different osteoarthritis treatments. Here the ‘time’ of interest is triggered by an event (tumour removal or osteoarthritis treatment) and ended by a subsequent event (death or the return of osteoarthritis pain). The time between the two events is known as

the survival time (Machin et al., 2006). This study uses the same procedure as these medical examples, except the initial event is the eruption onset and the subsequent event is the eruption end date giving a number of days between the two which is the eruption duration, or the survival time.

A dataset of Vulcanian explosions at Soufrière Hills Volcano, Montserrat is taken from Druitt et al. (2002) and used to illustrate these methods and to familiarise the reader with graphs and tables commonly used within this thesis. The data are reproduced in Table 2.3 which includes the start date and time of 75 explosions from the period September - October 1997. From this the repose interval between the explosions has been calculated and, due to the nature of the dataset, can be considered to contain negligible uncertainties. Where these data are used in this chapter it is analogous to eruption duration or repose interval in the remainder of the thesis.

Table 2.3: List of the times of Vulcanian explosions at Soufrière Hills Volcano (Druitt et al., 2002)

Date	Local Time	Interval (hours)	Date	Local Time	Interval (hours)
22/09/1997	00:57		04/10/1997	08:33	9.72
22/09/1997	10:45	9.8	04/10/1997	18:27	9.9
22/09/1997	20:42	9.95	05/10/1997	02:53	8.43
23/09/1997	07:23	10.68	05/10/1997	10:41	7.8
24/09/1997	00:34	17.18	05/10/1997	18:41	8
24/09/1997	10:54	10.03	06/10/1997	02:44	8.05
24/09/1997	17:16	6.37	06/10/1997	10:42	7.97
25/09/1997	03:54	10.63	06/10/1997	17:50	7.13
25/09/1997	11:09	7.25	07/10/1997	04:06	10.27
25/09/1997	20:05	8.93	07/10/1997	16:02	11.93
26/09/1997	04:25	8.03	08/10/1997	03:47	11.75
26/09/1997	14:56	10.52	08/10/1997	15:10	11.38
27/09/1997	00:01	9.08	09/10/1997	03:03	11.88
27/09/1997	09:46	9.75	09/10/1997	12:32	9.48
27/09/1997	17:15	7.48	10/10/1997	04:13	15.68
28/09/1997	04:28	11.22	10/10/1997	18:40	14.45
28/09/1997	10:34	6.1	11/10/1997	17:57	23.28
28/09/1997	23:03	12.48	12/10/1997	07:55	13.97
29/09/1997	06:26	7.38	12/10/1997	22:24	14.48
29/09/1997	11:23	4.95	13/10/1997	09:32	11.13
29/09/1997	16:48	5.42	13/10/1997	15:24	5.87
29/09/1997	21:57	5.15	14/10/1997	01:36	10.2
30/09/1997	04:43	6.77	14/10/1997	13:48	12.2
30/09/1997	17:44	13.02	14/10/1997	23:16	9.47
01/10/1997	05:00	11.27	15/10/1997	05:47	6.52
01/10/1997	11:34	6.57	15/10/1997	08:33	2.77
01/10/1997	17:40	6.1	15/10/1997	14:50	6.28
02/10/1997	01:05	7.42	15/10/1997	22:20	7.05
02/10/1997	12:53	11.8	16/10/1997	02:51	4.52
02/10/1997	22:50	9.95	16/10/1997	06:35	3.73

Continued on next page...

Table 2.3 – Continued

Date	Local Time	Interval (hours)	Date	Local Time	Interval (hours)
16/10/1997	09:44	3.15	18/10/1997	15:17	8.48
16/10/1997	14:20	4.6	19/10/1997	05:13	13.93
16/10/1997	18:48	4.47	19/10/1997	21:27	16.23
17/10/1997	04:01	9.22	20/10/1997	05:04	7.62
17/10/1997	12:35	8.57	20/10/1997	15:13	10.15
17/10/1997	16:05	3.05	21/10/1997	11:39	20.43
17/10/1997	23:18	7.22	21/10/1997	19:02	7.38
18/10/1997	06:48	7.05			

2.2.1 Survival analysis in volcanology

Survival analysis is not new to volcanology and has been used to assess eruption time series data in the past. Connor et al. (2003) previously applied survival analysis style probabilistic models to the example data used in this study (Druitt et al., 2002) and more recently Connor et al. (2006) applied similar models to repose interval data on global explosive eruptions of varying sizes (VEI 4 to 7). Dzierma and Wehrmann (2010) also used survival analysis to investigate repose interval data from Villarica and Llaima volcanoes, Chile. In all three investigations exponential, Weibull and log-logistic distributions are fitted to the observed repose data and survival analysis used to make probabilistic forecasts of future events.

Strong similarities exist between the methods used in the three highlighted investigations and those of this study. A key, yet obvious, difference is the actual event being forecast. Although repose intervals are investigated in Chapter 6, the aim of this PhD is to investigate and forecast eruption duration. Furthermore, the style of activity investigated in Connor et al. (2003), Connor et al. (2006) and Dzierma and Wehrmann (2010)

are generally more explosive than the eruptions investigated in this study. As such, the analysed volcanic systems are very different. Furthermore, subtle differences include the use of maximum likelihood to estimate unknown parameter values of theoretical distributions, the additional testing of a Burr type XII distribution and the modification of the model to answer three different forecasting questions.

2.2.2 Calculating empirical survivor functions

The duration of a volcanic eruption or the duration of a period of repose between eruptions can be considered a type of survival time measurement. The empirical survivor function of the observed data can be calculated and used to illustrate the survival experience of the data (Machin et al., 2006). It is calculated by first placing the observed durations of interest (x_i) in rank order so that $x_1 \leq x_2 \leq \dots \leq x_N$ where N is the total number of observations. The empirical survivor function ($\hat{F}_n(x_i)$) is then calculated for each duration interval (x_i) using equation 2.1.

$$\hat{F}_n(x_i) = \frac{N - i}{N}, \quad i = 1, \dots, N. \quad (2.1)$$

Empirical survivor function curves are produced when the empirical survivor function is plotted against duration (x) and it provides a useful summary of the data. The estimated survival curve remains at a plateau between successive durations and it is therefore plotted as a step function and not a smooth curve (Machin et al., 2006). Typically these curves have an inverse 'S' shape when plotted, as throughout this thesis, on a log scale, with shallow gradient distribution tails representing rarer events with unusually long or short durations and a steeper central portion where the majority of the data plot. Fig. 2.2 shows the empirical survivor function curve for the data of Table 2.3.

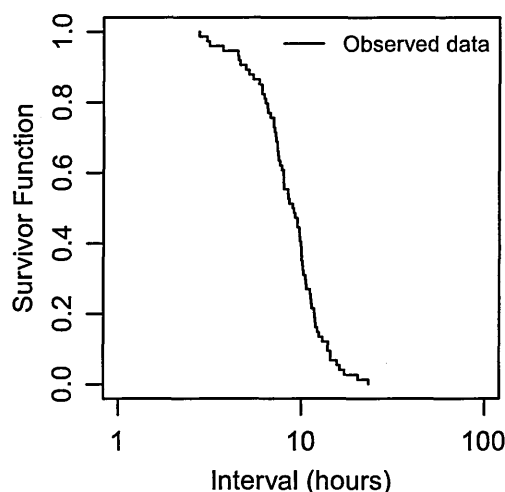


Fig. 2.2 Empirical survivor function curve for repose intervals between Vulcanian explosions at Soufrière Hills Volcano, Montserrat (data from Table 2.3)

2.2.3 Comparing empirical survivor functions

Throughout this study the distribution of eruption durations from different time periods, regions etc. are compared to investigate reporting biases or any factors that may be controlling eruption duration. Although visual differences between eruption duration distributions may be identified, significance tests are used to determine if it is conceivable that they derived from different distributions entirely. This study uses Mantel-Haenszel Logrank tests, Mann-Whitney tests and t -tests to compare sub-datasets (or 'groups') in pairs. In each case the thresholds used are similar to that of Klein (1982), whereby p -values of < 0.05 indicate significant differences between the two distributions, p -values of 0.05 - 0.1 indicate moderately significant differences between the two distributions and p -values of > 0.1 indicate that the differences between the two distributions are not significant and that it is conceivable that both datasets derive from the same over-riding distribution. Throughout this thesis \star and \bullet symbols are used in significance test result tables to indicate significant and moderately significant results respectively.

Mantel-Haenszel Logrank Test

The most widely used method of comparing two survival curves is the Logrank test (also called the Mantel-Cox test) (Machin et al., 2006) and is used throughout this study. The null hypothesis of this test is that the datasets being compared all have the same survival experience, and thus any variation between their empirical survivor functions can be attributed purely to chance (Machin et al., 2006). The method and equations outlined in this section are based on the information within Machin et al. (2006).

Firstly observed durations from both datasets are placed in rank order irrespective of their original group and the expected number of eruptions ending from each group is estimated at each duration value (i) using

$$E_{\{g_1, i\}} = \frac{r_i T_{\{g_1, i\}}}{N_i} \quad \text{and} \quad E_{\{g_2, i\}} = \frac{r_i T_{\{g_2, i\}}}{N_i}. \quad (2.2)$$

Here r_i is the total number of observed eruptions with duration i (irrespective of group), $T_{g,i}$ is the total number of eruptions in the specified group (g_1 or g_2) with durations longer than or equal to i and N_i is the total number of observations in both groups with durations longer than or equal to i . The total number of observations in each group (O_{g_1} and O_{g_2}) and the total expected number of eruptions ending in each group (E_{g_1} and E_{g_2}) are calculated (by summing the results from equation 2.2). For better treatment of tied data, where two or more observed eruptions are of equal duration, the Mantel-Haenszel version of the Logrank test is employed, involving the calculation of the hypergeometric variance V at each duration interval:

$$V_i = \frac{T_{\{g_1, i\}} T_{\{g_2, i\}} r_i s_i}{N_i^2 (N_i - 1)} \quad (2.3)$$

where s_i is the total number of observed eruptions with durations longer than i (irrespective of group) ($s_i = N_i - r_i$). The individual V_i values obtained from equation 2.3 are then summed to get V and the χ^2_{MH} Logrank statistic is calculated by either:

$$\chi^2_{MH} = \frac{(O_{g1} - E_{g1})^2}{V} \quad \text{or} \quad \chi^2_{MH} = \frac{(O_{g2} - E_{g2})^2}{V} \quad (2.4)$$

For this thesis this test is performed using the "Survdiff" function within the "survival" package of "R" (R Development Core Team, 2011) which also computes associated p -value. The null hypothesis of this test is rejected if this p -value is < 0.05 and the distribution of the data within the two groups is said to be significantly different at the 0.05 level.

A variation of this test can be used to compare three or more empirical survivor functions allowing the user to establish whether the differences are statistically significant, however, it does not provide information about where these differences occur. For this reason, we have chosen not to use this modified test, but to run the Logrank test outlined above on pairs of empirical survivor functions to assess where significant differences lie.

T-test

This study uses a two sample location t -test to test the null hypothesis that the means of two groups of data are equal. As such, if the null hypothesis is rejected, the mean values are considered sufficiently different that the two tested datasets could have derived from different over-riding distributions. Generally t -tests assume that the data being tested are normally distributed or that the sample sizes involved are sufficiently large that the central limit theorem can be applied. The duration data used within this study often does not fulfil either of these criteria, however, by applying the t -test to

the logs of the data a more normal distribution is achieved and the test can be used in conjunction with other significance tests to compare groups of data.

Due to the variances of the data often not being equal, a Welch's t -test is used here. The "t.test" function (with "var.equal = FALSE") of "R" (R Development Core Team, 2011) is used to compute the test statistic and associated p -value. The null hypothesis of this test is rejected if this p -value is < 0.05 and the distribution of the data within the two groups is said to be significantly different at the 0.05 level.

Mann-Whitney test

The Mann-Whitney test (also called the Mann-Whitney-Wilcoxon test or the Wilcoxon rank sum test) is similar to the Logrank test in that it is based on the rank order of the data within the two groups. It is often used as an alternative to the t -test and given that the datasets compared in this study are not strictly normally distributed it is used here in addition to the t test to verify results.

The "Wilcox.test" function of "R" (R Development Core Team, 2011) is used to compute the test statistic and associated p -value. The definition of this test is not unanimous and the test statistic calculated using "R" (R Development Core Team, 2011) corresponds to the sum of the ranks of the first group with the minimum value subtracted, such that it can be larger than other methods by $m(m + 1)/2$ where m is the size of the first group. The outcome of the test is the same because the sampling distribution, and hence the p -value, accounts for the difference. The null hypothesis of this test is rejected if this p -value is < 0.05 and the distribution of the data within the two groups is said to be significantly different at the 0.05 level.

2.2.4 Example: Comparing two subsets of the repose interval duration data from Soufrière Hills, Montserrat

For illustrative purposes, the repose interval data of Table 2.3 has been split into two groups: 22 September - 5 October (g_1) and 6 October - 21 October (g_2). Fig. 2.3 plots the empirical survivor function curves for both sets of data. The greater range of g_2 leads to visual differences in the distribution tails of the two datasets, however, p -values obtained from the Mantel-Haenszel Logrank test, Mann-Whitney test and t -test are all > 0.05 indicating that the two distributions are not significantly different at the 0.05 level (Table 2.4). This implies that the data from both time periods could have derived from the same overriding distribution, and that separating the data into these two groups is unnecessary. In such a situation, the entire dataset (22 September - 21 October) would be used in future analyses and, assuming additional temporal or spatial variations were not found, would form the basis any empirical forecasting models.

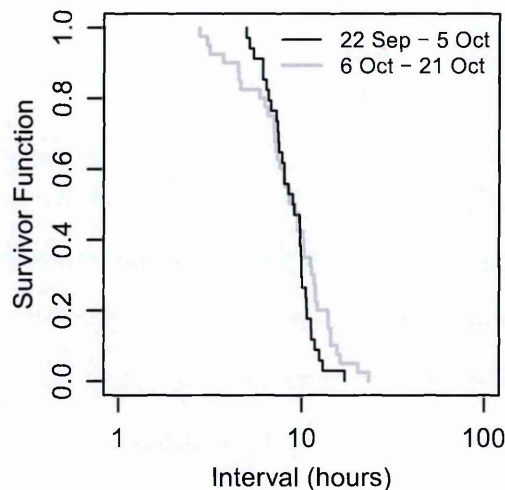


Fig. 2.3 Empirical survivor function curves for the repose interval data of Table 2.3 for the periods 22 September - 5 October 2007 ($n = 34$) and 6 October - 21 October 2007 ($n = 40$) (data from Table 2.3)

When significant differences between the groups of data being investigated are identified, it is considered unlikely that their data derive from the same over-riding distribu-

Table 2.4: Significance test results comparing the distribution of interval duration between vulcanian explosions at Soufrière Hills Volcano for the periods 22 September - 5 October 2007 and 6 October - 21 October 2007

Data	Logrank	Mann-Whitney	T-Test
g_1 ($n=34$) g_2 ($n=40$)	$p = 0.208$	$p = 0.803$	$p = 0.891$

$g_1 = 22 \text{ Sep} - 5 \text{ Oct } 2007$, $g_2 = 6 \text{ Oct} - 21 \text{ Oct } 2007$.

* = significant at a 0.05 level, • = moderate significance ($p\text{-value} = 0.05\text{-}0.1$).

t -test applied to the logs of the data.

tion and the two groups are treated independently in remaining analyses.

2.3 Fitting theoretical distributions to the data

In order to make probabilistic forecasts of future eruption durations, empirical survivor function curves are modelled using a theoretical distribution. Exponential, Weibull, log-logistic and Burr type XII distributions are tested for each dataset investigated in this study. The survivor function ($\hat{F}(x)$) equation of each distribution is presented in Eqs. 2.5 to 2.8.

$$\hat{F}(x)_{(exponential)} = \exp(-x/\mu) \quad (2.5)$$

$$\hat{F}(x)_{(Weibull)} = \exp(-(x/\mu)^\beta) \quad (2.6)$$

$$\hat{F}(x)_{(log-logistic)} = \frac{1}{1 + (x/\sigma)^\beta} \quad (2.7)$$

$$\hat{F}(x)_{(Burr\ XII)} = \frac{1}{\{1 + (x/\sigma)^\beta\}^{\alpha/\beta}} \quad (2.8)$$

For each distribution x is the only known quantity and represents the variable being investigated (i.e. duration or repose interval). The other parameters defining these distributions have been estimated using maximum likelihood (in particular, the "mle" function within the "stats4" package of "R" (R Development Core Team, 2011)).

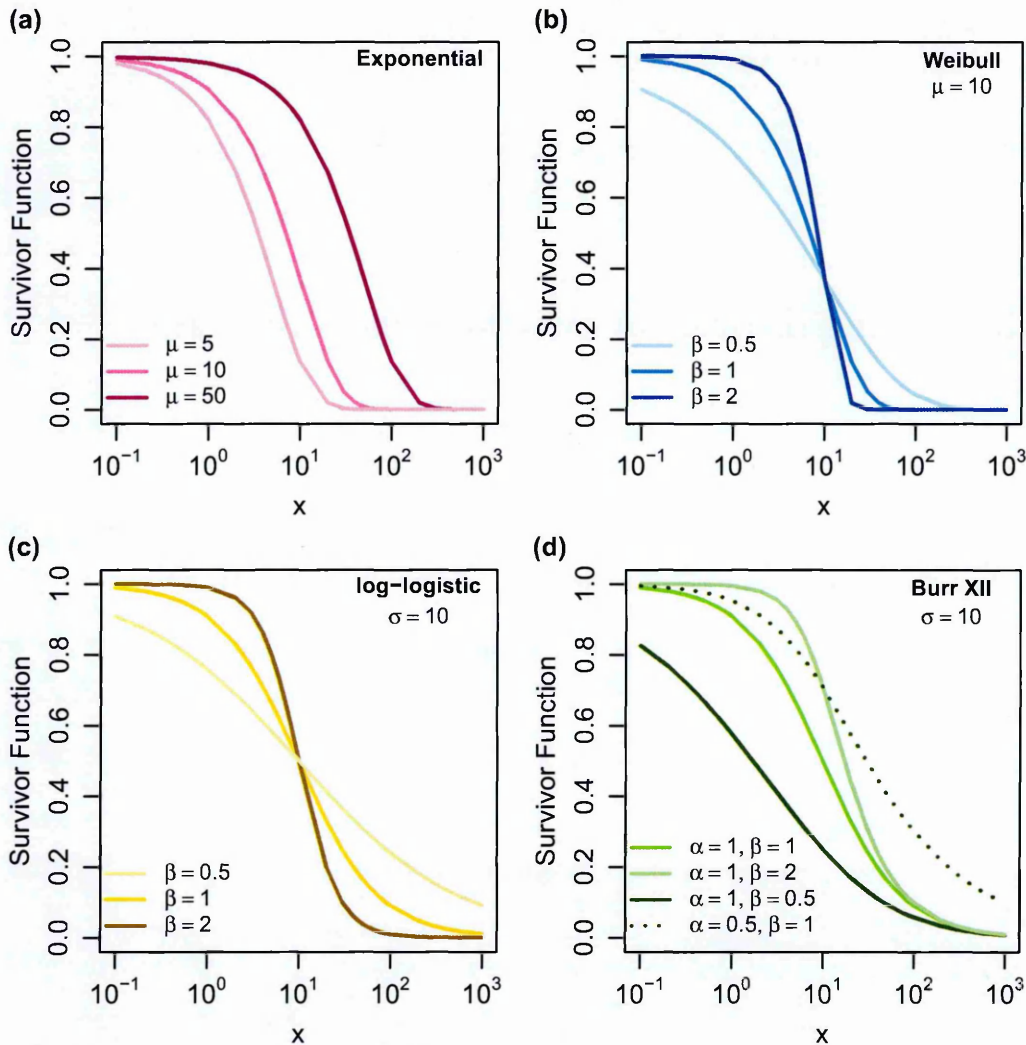


Fig. 2.4 Plot showing how the shape of (a) exponential, (b) Weibull, (c) log-logistic and (d) Burr type XII distributions changes with varying parameter values. Scale parameters of the Weibull (μ), log-logistic and Burr type XII (σ) distribution remain constant at 10 in each curve

The exponential distribution contains only one estimated parameter (μ) which is equal to the mean of the observed data. Changing this value has little effect on the shape of the survivor function curve, however, moves its position on the graph (Fig. 2.4a). Both the Weibull and log-logistic distributions contain a shape parameter (β in both)

and a scale parameter (μ and σ for Weibull and log-logistic respectively). The scale parameter controls the range that the distribution operates over, and as such determines the position of the empirical survivor function curve when displayed graphically. Figs. 2.4b and c demonstrate how the shape of these two distributions change when β is altered and the scale parameter kept constant. The Weibull distribution is related to the exponential distribution and the two distributions are identical when $\beta = 1$ (compare appropriate curves on Figs. 2.4a and b). The long duration tail of the log-logistic distribution is heavier than that of the Weibull distribution while their short duration tails are similar (Figs. 2.4b and c).

The Burr type XII distribution has three parameters; two shape parameters (α and β) and one scale parameter (σ). The additional shape parameter allows both tails of the distribution to behave independently with α controlling the long duration tail and β the short duration tail (Fig. 2.4d). Akin to the Weibull and exponential distribution, the Burr type XII distribution is related to the log-logistic distribution and when $\alpha = \beta$ it reduces to it.

Throughout this thesis graphical representations of these four distributions will have the same colours as those in Fig. 2.4, whereby exponential is pink, Weibull is blue, log-logistic is yellow and Burr type XII is green.

2.3.1 Goodness-of-fit

Goodness-of-fit tests are used to determine whether the fitted theoretical distributions adequately describe the duration data. The following section outlines the goodness-of-fit test used throughout this thesis as well as a likelihood ratio test which is used in conjunction with observed differences to decide which distribution to use when both the log-logistic and Burr type XII distributions are considered a sufficient fit to the data.

Kolmogorov-Smirnov test

Kolmogorov-Smirnov (KS) goodness-of-fit tests are used to determine whether theoretical distributions provide a good fit to observed data and have been used in volcanological investigations in the past (e.g. Mulargia et al. (1985), Salvi et al. (2006), Connor et al. (2003) and Bebbington (2013)). It is based on comparisons between the empirical distribution function (F_n) of the observed data (here this is the duration data (x)) and the cumulative distribution function (F_0) of an assumed theoretical distribution (exponential, Weibull, log-logistic or Burr type XII). These equate to one minus the empirical survivor function (Eq. 2.1) or theoretical distribution's survivor function (Eqs. 2.5- 2.8), respectively. Graphically the KS test statistic D identifies the maximum vertical displacement between F_n and F_0 and thus is obtained by computing the maximum absolute difference between F_n and F_0 at all values of x :

$$D = \max_x |F_n(x) - F_0(x)| \quad (2.9)$$

The null hypothesis of this test is that the observed sample is derived from the theoretical distribution being tested. It can be accepted when D is lower than the critical value for that sample size (N) at the appropriate significance level (0.05 for this study).

The benefit of using this method is that it works well for small sample sizes, however, some degree of approximation has been introduced to this method due to the presence of tied data and due to the parameters of theoretical distributions being estimated from the observed data. To reduce this bias the significance level of the difference between F_n and F_0 is estimated using a bootstrap re-sampling technique. This approach simulates 3000 (R) datasets from the fitted distribution, each of equal size to the observed data N . Parameters for the best fit distribution of each simulated dataset are estimated using maximum likelihood and their KS test statistic obtained (D_i for

$i = 1, \dots, R$).

This process should result in the same number of simulated test statistics as simulated datasets ($R = 3000$), however, sometimes the maximum likelihood estimator fails to provide parameter values for the best fit distribution and where this is the case a test statistic cannot be calculated. So long as 95 % of the simulated datasets (2850) complete this process a p -value can be estimated (\hat{P}) by the proportion of simulated KS test statistics that are as extreme or more extreme than the KS test statistic originally obtained (D_{obs}). Eq. 2.10 summarises this where r is the total number of simulated KS test statistics obtained.

$$\hat{P} = \frac{\sum_{i=1}^r (D_i \geq D_{obs}) + 1}{r + 1} \quad (2.10)$$

Instead of comparing the KS test statistic to the critical value and using that relationship to determine if the null hypothesis can be accepted, \hat{P} gives the significance level of the test. As such, if this value is > 0.05 the difference between the observed and fitted distribution is not significant at the 0.05 level and the null hypothesis can be accepted, the observed data could have derived from the fitted distribution. Throughout this thesis \diamond is used to indicate KS test results that are not significant at the 0.05 level.

Likelihood ratio test

In situations where the KS test indicates that both the log-logistic and Burr type XII distributions adequately describe the observed duration data, a likelihood ratio (LR) test is used to assess whether the additional parameter of the Burr type XII distribution sufficiently alters its shape, such that it is worthwhile using this more complicated distribution to model the data. The null hypothesis is that there is little benefit in

employing the Burr type XII distribution with three parameters in preference to the log-logistic distribution with only 2 parameters.

To perform this test the log-likelihood (L) corresponding to the fitted log-logistic distribution and Burr type XII distribution is found and equation 2.11 used to obtain LR . This value is compared to the appropriate quantile of the χ^2 distribution with degrees-of-freedom corresponding to the difference between the number of parameters estimated in each distribution (Burr type XII = 3 parameters, log-logistic = 2 parameters so $df = 3 - 2$, $df = 1$).

$$LR = -2(L_{(log-logistic)} - L_{(Burr)}) \quad or \quad 2(L_{(Burr)} - L_{(log-logistic)}) \quad (2.11)$$

The 5 % quantile of the χ^2 distribution with 1 degree-of-freedom has a critical value of 3.84. A $LR < 3.84$ indicates a minimal difference between L and the null hypothesis is accepted, the log-logistic distribution is adequate and there is little benefit in using the Burr type XII distribution. In contrast if $LR > 3.84$ the difference between the two models is greater and the null hypothesis is rejected.

2.3.2 Example: Fitting theoretical distributions to the repose interval data of Soufrière Hills, Montserrat

Parameter values for the best fit exponential, Weibull, log-logistic and Burr type XII distribution of the repose interval data of Soufrière Hills, Montserrat (Table 2.3) are reported in Table 2.5. Fig. 2.5 plots the survivor function of each fitted distribution alongside the empirical survivor function curve of the observed data.

Visually it is evident that the exponential distribution gives a poor fit to the data, how-

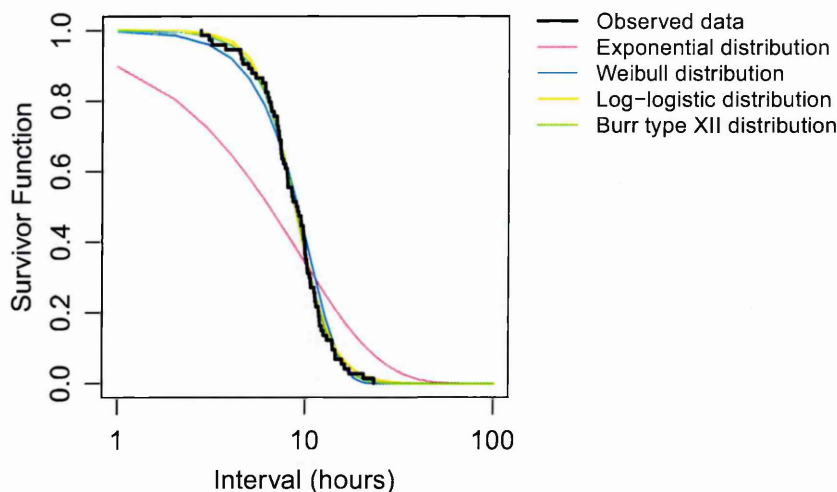


Fig. 2.5 Empirical survivor function curves and best fit distributions for the repose interval data of Soufrière Hills, Montserrat (data of Table 2.3). Parameter values can be found in Table 2.5

ever, the remaining three distributions plot with similar shapes and positions (Fig. 2.5). *KS* tests support these results with only the exponential distribution resulting in a *p*-value of < 0.05 (Table 2.5). A *LR* test performed on the log-logistic and Burr type XII distributions yields a test statistic of 1.397 indicating little variation between the log-likelihood values of the two distributions and that there is little benefit in employing the Burr type XII distribution in preference to the log-logistic distribution (Table 2.5).

In this situation either the Weibull or log-logistic distribution could be used as the basis of an empirical forecasting model for this dataset. Early stages of this investigation found that a log-logistic distribution often provides an adequate fit to eruption duration data and therefore this distribution would be used here. Furthermore, it could also be argued that visually the Weibull distribution has a poorer fit to the observed data at durations < 7 days (Fig. 2.5).

Connor et al. (2003) also fitted theoretical distributions to the data of Druitt et al. (2002) and found that found that a log-logistic distribution with $\mu = 9$ and $K = 4$ provided an excellent fit whereas a Weibull distribution was less sufficient. The log-

Table 2.5: Parameter values, Kolmogorov-Smirnov (KS) test and likelihood ratio (LR) test results for theoretical distributions fitted to the repose interval data of Soufrière Hills, Montserrat

	Exponential	Weibull	Log-logistic	Burr type XII
	$\mu = 9.3$	$\beta = 2.59$	$\beta = 4.37$	$\alpha = 6.56$
		$\mu = 10.47$	$\sigma = 8.72$	$\beta = 3.75$
				$\sigma = 10.69$
D_{obs}	0.333	0.084	0.062	0.051
\hat{p}	0.000	0.209 \diamond	0.550 \diamond	0.824 \diamond
r	3000	3000	3000	2995
LR test statistic (log-logistic and Burr type XII):				1.397

\diamond not significant at the 0.05 level (p -value > 0.05).

D_{obs} = KS statistic, \hat{p} = estimated p -value and r = final bootstrap size.

logistic parameters estimated here are $\mu = 8.72$ and $\beta = 4.37$ (Table 2.5), and although the notation is slightly different and our values are estimated by maximum likelihood, it is evident that the log-logistic distributions concluded to provide a good fit to the data are similar.

2.4 An empirical probabilistic model using survival analysis

Having decided which theoretical distribution best describes the observed duration data, survival analysis can be used to estimate the probability that a future eruption will exceed a given length of time. The following section discusses three types of forecast, each designed to answer slightly different questions that might be of interest when forecasting future eruption durations. In each case, equations are presented which result in a ‘point estimate’ for the answer to each question. Section 2.4.4 provides information about how 95 % and 80 % confidence intervals are calculated for each of these forecasts.

2.4.1 Survivor function

The simplest type of forecast made in this investigation is of the survivor function and requires the survivor function equation of the appropriate distribution. The forecast answers the question “What is the probability of a future eruption exceeding x ?”, where x is a specified duration. The durations of interest vary depending on the range of the durations within the dataset being modelled, however, for the majority of examples in this thesis forecasts are performed for the probability of exceeding 7 days (1 week), 30 days (\sim 1 month) and 365 days (1 year).

2.4.2 Residual life function

The residual life function is a variation on the survivor function (Section 2.4.1), adapted for on-going eruptions. It can be used to answer the question “What is the probability of a future eruption exceeding x , having already reached duration t ?”. Note that because x represents the total duration of the eruption, forecasts performed where $t = x$ result in an exceedance probability of 100 %. The following equations give the ‘point estimate’ forecasts for the residual life function of the stated distribution.

$$\hat{F}_t(x)_{(exponential)} = \exp\{(t - x)/\mu\} \quad (2.12)$$

$$\hat{F}_t(x)_{(Weibull)} = \exp\{(t/\mu)^\beta - (x/\mu)^\beta\} \quad (2.13)$$

$$\hat{F}_t(x)_{(log-logistic)} = \frac{\sigma^\beta + t^\beta}{\sigma^\beta + x^\beta} \quad (2.14)$$

$$\hat{F}_t(x)_{(Burr\ XII)} = \left(\frac{\sigma^\beta + t^\beta}{\sigma^\beta + x^\beta} \right)^{\alpha/\beta} \quad (2.15)$$

As with the survivor function forecasts the values of interest (x and t) are dependent on the duration range of the dataset being modelled.

2.4.3 Quantile function

The quantile function enables the user to find the duration associated with a stated quantile p , that is, the duration that has probability $1 - p$ of being exceeded. The following equations give the ‘point estimate’ forecasts for the quantile function of the stated distribution.

$$x_p \text{ (exponential)} = -\mu \log(1 - p) \quad (2.16)$$

$$x_p \text{ (Weibull)} = \mu \{-\log(1 - p)\}^{1/\beta} \quad (2.17)$$

$$x_p \text{ (log-logistic)} = \sigma \left(\frac{p}{1 - p} \right)^{1/\beta} \quad (2.18)$$

$$x_p \text{ (Burr XII)} = \sigma \left\{ \frac{1}{(1 - p)^{\beta/\alpha}} - 1 \right\}^{1/\beta} \quad (2.19)$$

In contrast to the survivor function and residual life function the quantiles of interest p are completely independent of the range of durations within the dataset being investigated. Deciding which exceedance probabilities should be forecast is a subjective

process, dependent on how the user views probabilities and in particular which probabilities they would associate with likely or unlikely events (Budescu et al., 2009).

Table 2.6: Likelihood scale of the IPCC (taken from Mastrandrea et al. (2010))

Qualitative Term	Likelihood of the Outcome
Virtually certain	99-100 % probability
Very likely	90-100 % probability
Likely	66-100 % probability
About as likely as not	33-66 % probability
Unlikely	0-33 % probability
Very unlikely	0-10 % probability
Exceptionally unlikely	0-1 % probability

For the purpose of this investigation the likelihood scale developed and used by the Intergovernmental Panel on Climate Change (IPCC) (Mastrandrea et al., 2010) is adopted here and is reproduced in Table 2.6. Here the two qualitative terms considered most useful are “likely” and “unlikely”. Values of p of 0.34 (66 %) and 0.67 (33 %) are used for all quantile functions forecasts used in this study and give the duration that is likely and unlikely to be exceeded, respectively. It is noted that in a real life application of the model the thresholds for likely and unlikely may need to be modified to suit the eruption style or volcanic region being investigated.

2.4.4 Calculating confidence intervals

As previously mentioned the equations presented thus far result in ‘point estimates’ for the specific value of interest (x or p for the survivor/residual life function and quantile functions, respectively). In each case 95 and 80 % confidence intervals are given in the form of

$$'point\ estimate' \pm 1.96 \sqrt{\hat{V}}$$

and

$$'point\ estimate' \pm 1.28 \sqrt{\hat{V}}$$

respectively, where \hat{V} is the estimated variance for the formula being used in the model. The calculation of \hat{V} is specific to the theoretical distribution and is based on standard asymptotic theory for maximum likelihood estimation. The equations involved are displayed in the following pages. It is worth noting that although both the 95 % and 80 % confidence intervals are calculated and reported in the results tables throughout this thesis, only the 80 % confidence intervals are reported when results are discussed in the text.

Confidence interval equations for the exponential distribution

The exponential distribution has one estimated parameter and therefore the general formula for \hat{V} is

$$\hat{V} = D^2 C[1, 1] \tag{2.20}$$

Here $C[1,1]$ refers to the asymptotic covariance between $\hat{\mu}$, the estimated value of which is provided by "R" (R Development Core Team, 2011) at the same time as the parameter estimate itself.

For the survivor function of the exponential distribution D is given by

$$D = (x/\mu^2) \exp(-x/\mu) \tag{2.21}$$

For the residual life function of the exponential distribution D is given by

$$D = ((x - t)/\mu^2) \exp((t - x)/\mu) \quad (2.22)$$

For the quantile function of the exponential distribution D is given by

$$D = -\log(1 - p) \quad (2.23)$$

Confidence interval equations for the Weibull distribution

The Weibull distribution has two estimated parameters and therefore the general formula for \hat{V} is

$$\hat{V} = D^2 C[1, 1] + E^2 C[2, 2] + 2DE C[1, 2] \quad (2.24)$$

Here the C 's are elements of the asymptotic covariance matrix associated with the maximum likelihood estimates $\hat{\beta}$ and $\hat{\mu}$ of β and μ , respectively; specifically, $C[1,1]$ is the asymptotic variance of $\hat{\beta}$, $C[2,2]$ that of $\hat{\mu}$ and $C[1,2]$ is the asymptotic covariance between $\hat{\beta}$ and $\hat{\mu}$. The estimated values of the C 's are provided by "R" (R Development Core Team, 2011) at the same time as the parameter estimates themselves.

For the survivor function of the Weibull distribution D and E are given by

$$D = -(x/\mu)^\beta \log(x/\mu) \exp(-(x/\mu)^\beta) \quad (2.25)$$

$$E = (\beta/\mu) (x/\mu)^\beta \exp(-(x/\mu)^\beta) \quad (2.26)$$

For the residual life function of the Weibull distribution D and E are given by

$$D = \exp\{(t/\mu)^\beta - (x/\mu)^\beta\} \{(t/\mu)^\beta \log(t/\mu) - (x/\mu)^\beta \log(x/\mu)\} \quad (2.27)$$

$$E = (\beta/\mu) \exp\{(t/\mu)^\beta - (x/\mu)^\beta\} \{(x/\mu)^\beta - (t/\mu)^\beta\} \quad (2.28)$$

For the quantile function of the Weibull distribution D and E are given by

$$D = -\frac{\mu}{\beta^2} \{-\log(1-p)\}^{1/\beta} \log\{-\log(1-p)\} \quad (2.29)$$

$$E = \{-\log(1-p)\}^{1/\beta} \quad (2.30)$$

Confidence interval equations for the log-logistic distribution

The general formula for \hat{V} of the log-logistic distribution is the same as that of the Weibull distribution (Eq. 2.24) due to also having two estimated parameters. Here the C's are elements of the asymptotic covariance matrix associated with the maximum likelihood estimates $\hat{\beta}$ and $\hat{\sigma}$ of β and σ , respectively; specifically, C[1,1] is the asymptotic variance of $\hat{\beta}$, C[2,2] that of $\hat{\sigma}$ and C[1,2] is the asymptotic covariance between $\hat{\beta}$ and $\hat{\sigma}$. The estimated values of the C's are provided by "R" (R Development Core Team, 2011) at the same time as the parameter estimates themselves.

For the survivor function of the log-logistic distribution D and E are given by

$$D = -\frac{(x/\sigma)^\beta \log(x/\sigma)}{\{1 + (x/\sigma)^\beta\}^2} \quad (2.31)$$

$$E = \frac{\beta}{\sigma} \frac{(x/\sigma)^\beta}{\{1 + (x/\sigma)^\beta\}^2} \quad (2.32)$$

For the residual life function of the log-logistic distribution D and E are given by

$$D = \frac{(xt)^\beta \log(t/x) + (\sigma t)^\beta \log(t/\sigma) - (\sigma x)^\beta \log(x/\sigma)}{(\sigma^\beta + x^\beta)^2} \quad (2.33)$$

$$E = \frac{\beta \sigma^{\beta-1} (x^\beta - t^\beta)}{(\sigma^\beta + x^\beta)^2} \quad (2.34)$$

For the quantile function of the log-logistic distribution D and E are given by

$$D = -\frac{\sigma}{\beta^2} \left(\frac{p}{1-p} \right)^{1/\beta} \log \left(\frac{p}{1-p} \right) \quad (2.35)$$

$$E = \left(\frac{p}{1-p} \right)^{1/\beta} \quad (2.36)$$

Confidence interval equations for the Burr type XII distribution

The Burr type XII distribution has three estimated parameters and therefore the general formula for \hat{V} is

$$\hat{V} = D^2 C[1, 1] + E^2 C[2, 2] + F^2 C[3, 3] + 2DE C[1, 2] + 2DF C[1, 3] + 2EF C[2, 3] \quad (2.37)$$

Here the C's are elements of the asymptotic covariance matrix associated with the maximum likelihood estimates $\hat{\alpha}$, $\hat{\beta}$ and $\hat{\sigma}$ of α , β and σ , respectively; specifically, $C[1,1]$ is the asymptotic variance of $\hat{\alpha}$, $C[2,2]$ that of $\hat{\beta}$ and $C[2,2]$ that of $\hat{\sigma}$ while $C[1,2]$ is the asymptotic covariance between $\hat{\alpha}$ and $\hat{\beta}$, $C[1,3]$ that between $\hat{\beta}$ and $\hat{\sigma}$ and $C[2,3]$ that between $\hat{\beta}$ and $\hat{\sigma}$. The estimated values of the C's are provided by "R" (R Development Core Team, 2011) at the same time as the parameter estimates themselves.

For the survivor function of the Burr type XII distribution D, E and F are given by

$$D = -\frac{1}{\beta} \frac{\log\{1 + (x/\sigma)^\beta\}}{\{1 + (x/\sigma)^\beta\}^{\alpha/\beta}} \quad (2.38)$$

$$E = \frac{\alpha}{\beta^2} \frac{[\{1 + (x/\sigma)^\beta\} \log\{1 + (x/\sigma)^\beta\} - \beta(x/\sigma)^\beta \log(x/\sigma)]}{\{1 + (x/\sigma)^\beta\}^{\alpha/\beta+1}} \quad (2.39)$$

$$F = \frac{\alpha}{\sigma} \frac{(x/\sigma)^\beta}{\{1 + (x/\sigma)^\beta\}^{(\alpha/\beta)+1}} \quad (2.40)$$

For the residual life function of the Burr type XII distribution D, E and F are given by

$$D = \frac{1}{\beta} \left(\frac{\sigma^\beta + t^\beta}{\sigma^\beta + x^\beta} \right)^{\alpha/\beta} \log \left(\frac{\sigma^\beta + t^\beta}{\sigma^\beta + x^\beta} \right) \quad (2.41)$$

$$E = \frac{\alpha}{\beta^2} \left(\frac{\sigma^\beta + t^\beta}{\sigma^\beta + x^\beta} \right)^{(\alpha/\beta)-1} \left[- \left(\frac{\sigma^\beta + t^\beta}{\sigma^\beta + x^\beta} \right) \log \left(\frac{\sigma^\beta + t^\beta}{\sigma^\beta + x^\beta} \right) + \beta \left\{ \frac{(xt)^\beta \log(t/x) + (\sigma t)^\beta \log(t/\sigma) - (\sigma x)^\beta \log(x/\sigma)}{(\sigma^\beta + x^\beta)^2} \right\} \right] \quad (2.42)$$

$$F = \alpha \sigma^{\beta-1} \left(\frac{\sigma^\beta + t^\beta}{\sigma^\beta + x^\beta} \right)^{(\alpha/\beta)-1} \frac{x^\beta - t^\beta}{(\sigma^\beta + x^\beta)^2} \quad (2.43)$$

For the quantile function of the Burr type XII distribution D, E and F are given by

$$D = \frac{\sigma}{\alpha^2} \left\{ \frac{1}{(1-p)^{\beta/\alpha}} - 1 \right\}^{(1/\beta)-1} \frac{\log(1-p)}{(1-p)^{\beta/\alpha}} \quad (2.44)$$

$$E = - \frac{\sigma}{\alpha \beta^2} \left\{ \frac{1}{(1-p)^{\beta/\alpha}} - 1 \right\}^{1/\beta-1} \times \left[\alpha \left\{ \frac{1}{(1-p)^{\beta/\alpha}} - 1 \right\} \log \left\{ \frac{1}{(1-p)^{\beta/\alpha}} - 1 \right\} + \beta \frac{\log(1-p)}{(1-p)^{\beta/\alpha}} \right] \quad (2.45)$$

$$F = \left\{ \frac{1}{(1-p)^{\beta/\alpha}} - 1 \right\}^{1/\beta} \quad (2.46)$$

2.4.5 Example: Forecasting the duration of repose intervals between vulcanian explosions at Soufrière Hills, Montserrat

Table 2.7 contains the results of ten forecasts based on the best fit log-logistic distribution of the repose interval data of Soufrière Hills, Montserrat (data of Table 2.3). Survivor function forecasts give a high probability that an explosion will follow a repose

interval in excess of 6 hours ($84 \% \pm 2 \%$) with the probability gradually decreasing as the value assigned to x increases (Table 2.7). For the residual life function $t = 6$ hours has been used and the same trend of decreasing probability with increase x can be observed (Table 2.7).

The use of the IPCC likelihood scale (Table 2.6) enables the quantile function to be used here to conclude that an explosion is likely to follow a repose interval in excess of 7.49 hours (± 0.47 hours) and unlikely to follow a repose interval in excess of 10.25 hours (± 0.63 hours).

Table 2.7: Survivor function (SF), residual life function (R_{life}) and quantile function (Q) forecast results for the interval between vulcanian explosions at Soufrière Hills, Montserrat (data of Table 2.3) (for the residual life function $t = 6$ hours)

	Input	Result	C/I	
			95 %	80 %
SF	6 h	84 %	$\pm 7 \%$	$\pm 5 \%$
	9 h	47 %	$\pm 10 \%$	$\pm 6 \%$
	12 h	20 %	$\pm 7 \%$	$\pm 5 \%$
	18 h	4 %	$\pm 3 \%$	$\pm 2 \%$
	40 h	0.001 %	$\pm 0.002 \%$	$\pm 0.001 \%$
R_{life}	9 h	56 %	$\pm 9 \%$	$\pm 6 \%$
	12 h	24 %	$\pm 9 \%$	$\pm 6 \%$
Q	0.34	7.49 h	$\pm 0.72 h$	$\pm 0.47 h$
	0.67	10.25 h	$\pm 0.97 h$	$\pm 0.63 h$
	0.998	36.14 h	$\pm 10.26 h$	$\pm 6.71 h$

h = hours, C/I = confidence interval

As discussed in section 2.3.2, Connor et al. (2003) modelled the repose interval data of Soufrière Hills with a similar log-logistic distribution. They concluded that there was a 0.002 % probability of a vulcanian explosion following a 40 hour repose interval. A survivor function performed for $x = 40$ on the best fit log-logistic distribution of the current study gives a slightly lower probability of 0.001 % ($\pm 0.001 \%$), and a quantile function reveals that a 0.002 % probability (or 0.998 value of p) corresponds with a

minimum repose interval of 36.14 hours (± 6.71 hours) (Table 2.7). These results reflect the similarity between the two log-logistic distribution used to model the Druitt et al. (2002) data. It is worth noting that the confidence intervals associated with these extreme forecasts are high, due to the limited information within the long duration tail of the data from which to constrain the theoretical model. This is perhaps a situation where extreme value statistics would have provided a more useful result than survival analyses performed to forecast typical eruptive behaviour.

Chapter 3

Dataset compilation: a critical examination of the literature



Historical eruption duration datasets were compiled for Mt. Etna, Kilauea, Piton de la Fournaise (PdlF) and Iceland. In each case, data were collated from the literature and subjected to critical examination and uncertainty assignment using the methods outlined in section 2.1. It is worth noting that although the catalogue compiled by The Smithsonian Institution's Global Volcanism Program is a thorough and detailed compilation of global volcanism (Siebert et al., 2010; Venzke et al., 2013) their definition of an eruption end (subsection 2.1.1) differs considerably from that used here and they do not always provide references to primary literature for eruption dates. For these reasons the GVP catalogue has not been used as a source of data in this study. Due to the different methods available to calculate erupted volume a single source is used for

each dataset.

This chapter introduces each dataset in turn, focussing on specific aspects that warrant further discussion and outlining the source literature used. The tables included in this chapter contain the eruptions with reported eruption durations that are considered reliable and thus used in this study. A complete list of all considered eruptions along with information regarding their reported start and end dates, clarification of any assigned uncertainties and the reasoning behind any exclusions are included in the appropriate appendices (Appendix A = eruptions from Mt. Etna, Appendix B = eruptions from Kilauea, Appendix C = eruptions from PdlF and Appendix D = eruptions from Iceland).

The completeness of the eruption record requires some consideration when investigating past eruptive activity. It is important to recognise that in addition to eruptions being excluded from the study due to insufficient information regarding their duration, some eruptions will have gone completely unnoticed, especially in the early historical record and in remote regions. With time, increased human population in volcanically active areas, technological advances in eruption detection and a greater understanding of volcanic processes has led to an apparent increase in volcanic activity which is an artefact of reporting (Siebert et al., 2010). Furthermore, local fluctuations in reporting occur in response to increased interest following large, often devastating eruptions and decreases during periods of great international instabilities such as wars (Siebert et al., 2010). To assess the effect of reporting bias each section ends with an investigation into the completeness of the eruption record to which it pertains.

3.1 Available data for Mt. Etna

Two types of volcanic activity have been recognised in the historical records of Mt. Etna: persistent activity from summit vents and periodic activity from eruptive fissures on the volcano's flanks (Guest and Murray, 1979; Duncan et al., 1981; Acocella and Neri, 2003; Behncke and Neri, 2003; Branca and Del Carlo, 2005; Crisci et al., 2010). The sustained nature of Mt. Etna's summit eruptions makes defining eruption start and end dates difficult, especially further back in the historical record. Furthermore, while the historical record of flank eruptions is considered reliable and nearly complete after 1600 AD (Mulargia et al., 1985; Behncke and Neri, 2003; Branca and Del Carlo, 2004; Behncke et al., 2005; Branca and Del Carlo, 2005; Tanguy et al., 2007), summit activity is only considered reliable after the late 19th century (Chester et al., 1985; Andronico and Lodato, 2005; Branca and Del Carlo, 2005; Proietti et al., 2011). This restricts the time period available for analysis within this study, and therefore reliable datasets of historic summit eruption duration data would be small.

Furthermore, despite the typically explosive nature of summit activity, its effects are often localised to within a few hundred/thousand metres of the eruption site and therefore its threat to property and surrounding populations is confined above 1600-1800 m above sea level. Consequently, only the tourist facilities are potentially exposed to the risk of lava invasion (Duncan et al., 1981; Proietti et al., 2011; Cappello et al., 2013). However, flank eruptions tend to produce lava flows that can extend for far greater distances and to lower elevations making them the greatest hazard on Mt. Etna (Duncan et al., 1981; Chester et al., 1985; Behncke and Neri, 2003; Andronico and Lodato, 2005; Behncke et al., 2005; Proietti et al., 2011).

The greater relevance to lava flow hazard assessment in conjunction with the difficulties in defining historical summit eruption start and end dates has led to the exclusion of summit activity from this study which focuses only on flank eruptions. The dis-

inction between summit eruptions and flank eruptions on Mt. Etna is in many ways arbitrary. The eruption data included within this study begins prior to the formation of the NE crater and SE crater (in 1911 and 1978, respectively), so while eruptions from the Voragine and Bocca Nuova are definitely summit eruptions, eruptions from fissures in the region of the NE and SE craters prior to their formation were flank eruptions. Since the formation of these craters any eruptions from these two vents have been considered summit eruptions and excluded from the study. In most instances eruptions from vents or fissures above 3000 m elevation are considered summit eruptions, however, where fissures then extend down the flanks of the volcano, and erupt in a style most similar to flank activity on Mt. Etna, they are often categorised as flank eruptions and included within this study. Where some debate existed in whether eruptions were considered summit or flank for the purpose of this study they are discussed in more detail in Section 3.1.2 and Appendix A.

3.1.1 The eruption duration dataset of Mt. Etna

A catalogue of historic flank eruptions from 1300-2010 from Mt. Etna was collated from the literature yielding an initial dataset of 80 volcanic eruptions (included in Appendix A). Where flank activity is reported during longer periods of summit activity the dates corresponding to the flank component are used (e.g. May 1780), however, sometimes the precise start and/or end date of the flank eruption is unknown and where this is the case the eruption has been excluded (e.g. May 1759). Furthermore, the September 1869, February 1999 and July 2006 eruptions were initially thought to be flank eruptions, however, investigations into their source vents/fissures indicated that they were best described as summit eruptions and have therefore been excluded from the study but still exist in the descriptions within Appendix A.

Critical assessment of the existing eruption record resulted in 62 volcanic eruptions

with reliable eruption durations carrying acceptably small duration uncertainties (section 2.1.2). These eruptions are reported in Table 3.1. The method of determining the source location of each eruption is discussed in section 3.1.3. Lava volumes are taken from Behncke et al. (2005) and specific considerations regarding the volumes used in this study are discussed in section 3.1.4.

Table 3.1: Eruptions from Mt. Etna with known durations, 1300-2010

#	Location	Start Date	End Date	Duration	Duration U/C		
					Start	End	Tot Volume
1	VDB (B)	28-06-1329	25-08-1329	1,2	+0.5 -0.5	+5 -5	+5.5 -5.5
2	S-Rift (B)	09-11-1408	21-11-1408	3	+0.5 -0.5	+0.5 -0.5	+1 -1
3	S-Rift (B)	22-03-1536	05-04-1536	1	+0.5 -0.5	+5 -5	+5.5 -5.5
4	S-Rift (B)	11-05-1537	29-05-1537	3	+1 -1	+0.5 -0.5	+1.5 -1.5
5	SW flank (B)	06-02-1610	15-08-1610	1,2,5	+0.5 -0.5	+0.5 -0.5	+1 -1
6	NE-Rift (A)	01-07-1614	01-07-1624	1,2,3,5	+0.5 -0.5	+182.5 -182.5	+183 -183
7	S-Rift (B)	19-12-1634	15-06-1636	1,2,3,5	+1 -0.5	+15 -15	+16 -16
8	NE-Rift (A)	20-02-1643	28-02-1643	2,5	+0.5 -0.5	+0.5 -0.5	+1 -1
9	NE-Rift (A)	20-11-1646	17-01-1647	1,2,3,4,5	+0.5 -0.5	+0.5 -0.5	+1 -1
10	W-Rift (C)	17-01-1651	01-07-1653	1,2,3 see Appendix A	+1 -30	+182.5 -182.5	+183.5 -212.5

Continued on next page...

Table 3.1 – Continued

#	Location	Start Date	End Date	Duration	Duration U/C				
					Start	End	Tot Volume		
11	S-Rift	(B) 11-03-1669	11-07-1669	1;2;3;4;5	122	+0.5 -0.5	+0.5 -0.5	+1 -1	997.5
12	VDB	(B) 08-03-1702	08-05-1702	1;2;3;5	61	+0.5 -0.5	+0.5 -0.5	+1 -1	16.94
13	VDB	(A) 09-03-1755	15-03-1755	1;2;3;4;5;6	6	+1 -0.5	+0.5 -0.5	+1.5 -1	4.73
14	W-Rift	(C) 06-02-1763	10-03-1763	3;5;6	32	+1 -0.5	+5 -0.5	+6 -1	18.48
15	S-Rift	(B) 18-06-1763	10-09-1763	1;2;3;5;6	84	+1 -2	+0.5 -0.5	+1.5 -2.5	99.96
16	S-Rift	(B) 28-04-1766	07-11-1766	1;2	193	+1 -0.5	+0.5 -1	+1.5 -1.5	135.45
17	S-Rift	(B) 18-05-1780	29-05-1780	3	11	+0.5 -0.5	+2 -1	+2.5 -1.5	29.34
18	S-Rift	(B) 26-05-1792	15-05-1793	1;2;3;4;5	354	+3 -17	+15 -15	+18 -32	90.03
19	VDB	(A) 15-11-1802	17-11-1802	3	2	+0.5 -0.5	+1 -1	+1.5 -1.5	
20	NE-Rift	(A) 27-03-1809	09-04-1809	1;2;3;5;6;7	13	+0.5 -1	+0.5 -0.5	+1 -1.5	36.07
21	VDB	(A) 27-10-1811	24-04-1812	1;2;3;5;6	180	+0.5 -1	+0.5 -0.5	+1 -1.5	50.9

Continued on next page...

Table 3.1 – Continued

#	Location	Start Date	End Date	Duration	Duration U/C		
					Start	End	Tot
22	VDB	(B) 27-05-1819	01-08-1819	66	+1 -0.5	+4 -0.5	+5 -1
23	W-Rift	(C) 01-11-1832	22-11-1832	21	+2 -0.5	+0.5 -0.5	+2 -1
24	W-Rift	(C) 17-11-1843	28-11-1843	11	+0.5 -0.5	+0.5 -0.5	+1 -1
25	VDB	(B) 20-08-1852	27-05-1853	280	+0.5 -0.5	+0.5 -0.5	+1 -1
26	NE flank	(A) 30-01-1865	28-06-1865	149	+0.5 -0.5	+0.5 -0.5	+1 -1
27	NE-Rift	(A) 26-05-1879	07-06-1879	12	+0.5 -0.5	+0.5 -1	+1 -1.5
28	S-Rift	(B) 22-03-1883	24-03-1883	2	+0.5 -0.5	+0.5 -0.5	+1 -1
29	S-Rift	(B) 19-05-1886	07-06-1886	19	+0.5 -0.5	+0.5 -0.5	+1 -1
30	S-Rift	(B) 09-07-1892	29-12-1892	173	+0.5 -2	+20 -1	+20.5 -3
31	VDB	(B) 29-04-1908	30-04-1908	0.75	+0.02 -0.02	+0.02 -0.02	+0.04 -0.04
32	S-Rift	(B) 23-03-1910	18-04-1910	26	+0.5 -0.5	+0.5 -0.5	+1 -1

Continued on next page...

Table 3.1 – Continued

#	Location	Start Date	End Date	Duration	Duration U/C		
					Start	End	Tot Volume
33	NE-Rift (A)	10-09-1911	22-09-1911	12	+1 -0.5	+1 -1.5	55.4
34	NE-Rift (A)	17-06-1923	18-07-1923	31	+1 -0.5	+0.5 -0.5	78
35	NE flank (A)	02-11-1928	20-11-1928	18	+0.5 -1	+0.5 -0.5	40
36	SW flank (B)	30-06-1942	30-06-1942	0.54	+0.02 -0.02	+0.02 -0.02	1.66
37	NE-Rift (A)	24-02-1947	10-03-1947	14	+3 -0.5	+0.5 -0.5	11.88
38	VDB (A)	25-11-1950	02-12-1951	372	+0.5 -0.5	+0.5 -1.5	151.36
39	VDB (A)	01-03-1956	02-03-1956	1	+0.5 -0.5	+0.5 -1	
40	VDB (A)	01-02-1964	25-02-1964	24	+0.5 -0.5	+5 -5.5	
41	VDB (B)	07-01-1968	04-05-1968	118	+0.5 -0.5	+0.5 -1	1
42	VDB (A)	05-04-1971	12-06-1971	68	+0.5 -0.5	+0.5 -0.5	45.2
43	W-Rift (C)	30-01-1974	17-02-1974	18	+0.5 -0.5	+1 -0.5	2.4

Continued on next page...

Table 3.1 – Continued

#	Location	Start Date	End Date	Duration	Duration U/C		
					Start	End	Tot
44	W-Rift (C)	11-03-1974	29-03-1974	18	+0.5 -0.5	+0.5 -0.5	+1 -1
45	NE-Rift (A)	24-02-1975	29-08-1975	186	+0.5 -0.5	+14 -0.5	+14.5 -1
46	NW flank (A)	29-11-1975	08-01-1977	406	+0.5 -0.5	+0.5 -0.5	+1 -1
47	VDB (B)	29-04-1978	05-06-1978	37	+0.5 -0.5	+0.5 -0.5	+1 -1
48	VDB (B)	24-08-1978	30-08-1978	6	+1 -1	+0.5 -1	+1.5 -2
49	VDB (B)	18-11-1978	30-11-1978	12	+0.5 -5	+0.5 -1	+1 -6
50	VDB (A)	03-08-1979	09-08-1979	6	+0.5 -0.5	+0.5 -0.5	+1 -1
51	N flank (A)	17-03-1981	23-03-1981	6	+0.5 -0.5	+0.5 -1	+1 -1.5
52	S-Rift (B)	28-03-1983	06-08-1983	131	+0.5 -0.5	+0.5 -0.5	+1 -1
53	S-Rift (B)	10-03-1985	13-07-1985	125	+0.5 -2	+0.5 -0.5	+1 -2.5
54	VDB (B)	25-12-1985	31-12-1985	6	+0.5 -0.5	+0.5 -0.5	+1 -1

Continued on next page...

Table 3.1 – Continued

#	Location	Start Date	End Date	Duration	Duration U/C		
					Start	End	Tot Volume
55	VDB (A)	30-10-1986	01-03-1987	3;5;6;9;10;11	+0.5 -0.5	+0.5 -4	+1 -4.5
56	VDL (A)	27-09-1989	09-10-1989	1;3;5;6;8;9;10 11	+0.5 -0.5	+0.5 -0.5	+1 -1
57	VDB (B)	14-12-1991	31-03-1993	1;3;5;6;8;9;10 11	+0.5 -0.5	+0.5 -1	+1 -1.5
58	S-Rift (B)	17-07-2001	09-08-2001	1;3;10;11;19 20;21	+0.5 -0.5	+0.5 -1	+1 -1.5
59	S-Rift (B)	27-10-2002	28-01-2003	1;3;5;6;11	+1 -0.5	+0.5 -0.5	+1.5 -1
60	SE flank (B)	07-09-2004	08-03-2005	5;11;21;22;23	+0.5 -0.5	+0.5 -0.5	+1 -1
61	E flank (B)	13-10-2006	15-12-2006	24	+0.5 -0.5	+0.5 -0.5	+1 -1
62	E flank (B)	13-05-2008	06-07-2009	25;26;27	+0.5 -0.5	+0.5 -2	+1 -2.5

U/C = uncertainty. Units: durations and duration uncertainties = days, volumes = $\times 10^6 \text{m}^3$.

Bracketed letters represent the sector that the eruptive fissure/vent belongs, according to Fig 3.1

Grey numbers following dates represent the following references: ¹ Tanguy et al. (2007), ² Tanguy (1981), ³ Branca and Del Carlo (2004), ⁴ Mulargia et al. (1985), ⁵ Behncke et al. (2005), ⁶ Branca and Del Carlo (2005), ⁷ Chester et al. (2012), ⁸ Behncke and Neri (2003), ⁹ Andronico and Lodato (2005), ¹⁰ Acocella and Neri (2003), ¹¹ Neri et al. (2011); ¹² Chester et al. (1999), ¹³ Wadge (1976), ¹⁴ Tanguy et al. (1973), ¹⁵ Wadge and Guest (1981), ¹⁶ Le Guern (1972), ¹⁷ Guerra et al. (1976), ¹⁸ Pinkerton and Sparks (1976), ¹⁹ Harris et al. (2000), ²⁰ Coltelli et al. (2007), ²¹ Corsaro and Miraglia (2009), ²² Burton et al. (2005), ²³ Neri and Acocella (2006), ²⁴ Behncke et al. (2009), ²⁵ Bonaccorso et al. (2011a), ²⁶ Branca et al. (2008), ²⁷ Bonaccorso et al. (2011b). Volumes are taken from Behncke et al. (2005) and represent the volume of lava erupted during the eruption (bulk deposit volumes).

3.1.2 Additional information on specific eruptions from Mt. Etna

Tanguy et al. (2007) provide the most comprehensive catalogue of historical eruptions from Mt. Etna extending from 1600 to 2003. The majority of the eruptions within this time period that are included in Table 3.1 are also reported by Tanguy et al. (2007), although sometimes, where numerous other sources give alternative dates, the dates of Tanguy et al. (2007) are not used but are covered in the eruption's assigned uncertainty. However, two of the eruptions are not included by Tanguy et al. (2007). These are the February 1643 and the January 1968 eruptions (#8 and #41, Table 3.1). The latter eruption is documented in numerous other sources, including Tanguy (1981) and its exclusion by Tanguy et al. (2007) may have been an oversight, with other eruptions between 1966 and 1970 included in Tanguy (1981) but missing from Tanguy et al. (2007). The 1968 eruption is therefore included in our dataset using information from other sources (Table 3.1). The February 1643 eruption is excluded by Tanguy et al. (2007) due to some confusion in the literature between its vent location and the location of the 1646-7 lava flows (Tanguy et al., 2007). We include this eruption here, using the dates reported by Behncke et al. (2005) and Tanguy (1981).

Information about the dates of three other eruptions differs significantly from Tanguy et al. (2007). These are the March 1536 and the February and November 1975 eruptions (#3, #45 and #46, Table 3.1). The flank eruption of March 1536 (#3, Table 3.1) was accompanied by summit activity that continued until the end of the year (Tanguy et al., 2007; Siebert et al., 2010). The flank component of this eruption is reported as ending in April (Behncke et al., 2005), whereas the information within appendix 1 of Tanguy et al. (2007) states that the eruption "probably ended on 8 April". To account for this uncertainty the precision to which the end date is known is considered to be in the 'early month' category of Table 2.1 so the 5 April is assigned with a ± 5 day duration uncertainty (Table 3.1).

The two 1975 flank eruptions also occurred during a period dominated by summit activity. Such close association between the summit and flank activity makes isolating the dates of the flank component difficult and Tanguy et al. (2007) have simply recorded these eruptions within the longer summit activity. Other workers tried to resolve this, and it is the dates and uncertainty within these alternative references that are included in Table 3.1.

3.1.3 Vent location data at Mt. Etna

Flank eruptions at Mt. Etna are often associated with multiple aligned vents or fissures radiating from the volcano's summit (Acocella and Neri, 2003). These vents and fissures are mostly concentrated in three rift zones and the Valle del Bove (Duncan et al., 1981; Acocella and Neri, 2003; Behncke et al., 2005). Table 3.1 and Fig. 3.1 contain information about the location of each eruption, derived from maps by Romano et al. (1979), Chester et al. (1985), Acocella and Neri (2003) and Branca et al. (2011).

The East flank of Mt. Etna is dominated by the two collapse features of the Valle del Bove (Guest et al., 1984) and the smaller Valle del Leone. The 19 eruptions with vents/fissures located within the Valle del Bove and the 1 eruption within the Valle del Leone are identified as "VDB" or "VDL" in the location column of Table 3.1, however for the remainder of this paper the Valle del Leone eruption (#56, Table 3.1) will be grouped with the Valle del Bove eruptions and referred to as such.

The April 1971 eruption (#42, Table 3.1) was a complex flank eruption (Tanguy et al., 2007). The activity occurred at 3 vents on the upper South flank and a series of vents on the East flank of the volcano within the Valle del Bove and extending onto the NE flank (Le Guern, 1972; Branca and Del Carlo, 2004, 2005; Tanguy et al., 2007). Despite the varying location of activity during this eruption, and its association with the early formation of the summit's South-East crater, it is included here as one event

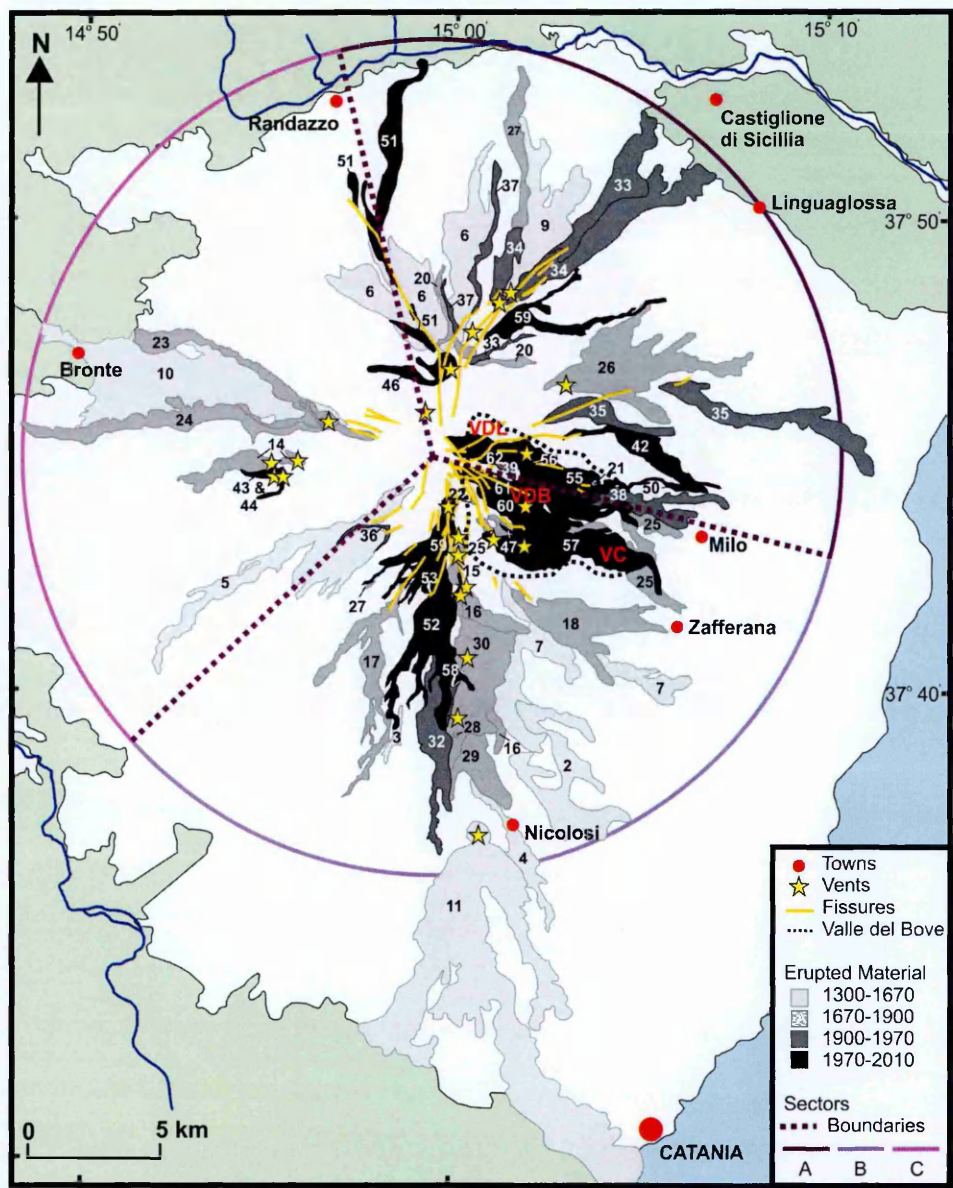


Fig. 3.1 Sketch map of Mt. Etna based on Romano et al. (1979) and Branca et al. (2011) showing the extent of erupted material and the position of their vents or fissures (yellow stars and lines respectively) for the eruptions within Table 3.1. Dashed lines represent the boundaries between sectors A, B and C (discussed in the text), VDB = Valle del Bove, VDL = Valle del Leone and VC = Val Calanna

with a duration of 68 days on the ENE flank.

The May 1879 and October 2002 eruptions (#27 and #59, Table 3.1) both involved more than one vent located on different flanks of the volcano. Here the vent which was active for each eruption's entire duration is used, although the erupted material

from both vents is shown on the map in Fig. 3.1. Precise vent locations could not be found for two of the eruptions in Table 3.1 (#8 and #45). Examination of the literature and careful location of their erupted products indicates that both eruptions affected the North-North-East region of Mt. Etna and thus an approximate location could be assigned (Sector A).

3.1.4 Volume data for flank eruptions from Mt. Etna

Lava volumes for the flank eruptions used in this investigation have been taken from Behncke et al. (2005). Their catalogue spans the period 1600 to 2005 and thus earlier or more recent eruptions in Table 3.1 do not have volumes associated with them. It is unclear what method Behncke et al. (2005) used to obtain these volume measurements, however, they are assumed to be bulk deposit volumes. Where flank eruptions included within Table 3.1 are combined with summit activity in Behncke et al. (2005) (#19, #39 and #40, Table 3.1) it is unclear what proportion of erupted lava relates to the flank activity, and therefore these eruptions do not have lava volumes associated with them.

Erupted volumes are only used in Chapter 7 of this thesis. Here relationships between eruption duration, volume and eruption rate are considered. Due to the effusive nature of flank eruptions from Mt. Etna, only lava volumes are used in this study, and any tephra component of the eruption considered negligible. Behncke et al. (2005) report that 60 % of the total volume erupted during the October 2002 eruption (#59, Table 3.1) corresponds to tephra and therefore, a volume for the October 2002 eruption is not included in Table 3.1 or used in the analyses of Chapter 7.

3.1.5 The completeness of the eruption record at Mt. Etna

The recording of Mt. Etna's eruptive activity dates back to Greek and Roman epochs (Branca and Del Carlo, 2004, 2005; Tanguy et al., 2007). However, the records are often only considered to be complete after 1600 AD (Mulargia et al., 1985; Behncke and Neri, 2003; Branca and Del Carlo, 2004; Behncke et al., 2005; Branca and Del Carlo, 2005; Tanguy et al., 2007; Cappello et al., 2013). Fig. 3.2a shows a scarcity of data prior to 1600 AD and an apparent increase in eruption frequency with time which is related to increased reporting. Fig. 3.2b shows eruption frequency at 100 year intervals and demonstrates how increased reporting since 1600 AD is accompanied by a reduction in the number of eruptions excluded due to unknown or poorly constrained durations. All reported flank eruptions after 1970 have accurately known durations.

Furthermore, an increase in the range of reported eruption durations can be observed with time (Fig. 3.2c) suggesting that the early eruption record is biased towards eruptions which made the most impact on surrounding areas (Andronico and Lodato, 2005). A shift towards more modern approaches in observing and documenting volcanic activity followed the large 1669 eruption (Branca and Del Carlo, 2004, 2005) and is most probably responsible for the reduction of this reporting bias during the 18th Century (Fig. 3.2c). The lack of short duration eruptions following 1971 is unlikely to be an artefact of reporting and the significance of this change in eruption duration is discussed in Chapter 4.

A regional bias in the quality and completeness of eruption records may also exist on Mt. Etna. The volcano's Western flank (sector C) appears to have experienced fewer flank eruptions than other areas of the volcano (Fig. 3.1 and Fig. 3.2c). Geological maps of Mt. Etna (Romano et al., 1979; Branca et al., 2011) show more lava flows on this flank than are represented in this study, however, these were either erupted prior to

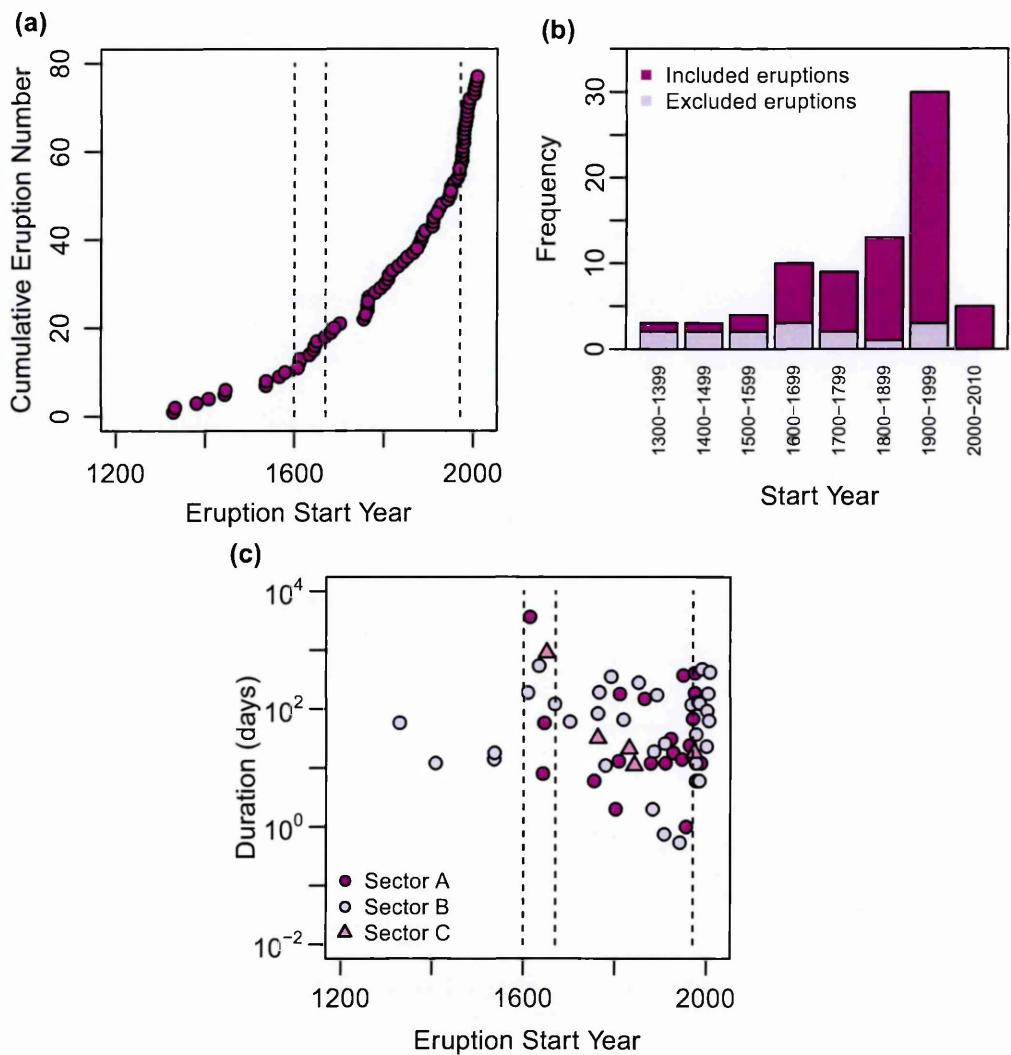


Fig. 3.2 (a) Plot of cumulative eruption number against eruption start year for the 76 flank eruptions reported between 1300 and 2010 and (b) the same data displayed as a bar plot at 100 year intervals separated into eruptions included and excluded from this study. (c) Plot of eruption duration (on a log scale) against start year for the eruptions within Table 3.1 separated into the three sectors identified in Fig. 3.1 (A = NE, B = S and C = W). Vertical dashed lines in plots a and c represent the years 1600, 1670 and 1971

1300 AD, and therefore outside the range of this investigation, or have undocumented eruption years. Although the reduced number of eruptions, especially in recent years, from vents located on Mt. Etna's West flank may reflect a preference for eruptive vents to open on other flanks, some of this may be a reporting bias due to the Western flank being the least populated region of Mt. Etna (Behncke et al., 2005). Similarly, 95 % of the reported eruptions within the uninhabited and poorly accessible Valle del Bove

post-date 1600 AD (Table 3.1), which may reflect a reporting bias here too.

Data before 1600 AD may be a poor representation of Mt. Etna's activity due to the reporting biases discussed. The analyses of this study therefore exclude this data and focus on the dataset of historic flank eruptions for Mt. Etna in the period 1600-2010. Previous studies have recognised increases in eruption frequency and output rate at Mt. Etna following 1971 (Wadge and Guest, 1981; Mulargia et al., 1985; Andronico and Lodato, 2005; Behncke et al., 2005; Branca and Del Carlo, 2005; Salvi et al., 2006; Bebbington, 2007; Smethurst et al., 2009; Cappello et al., 2013) and therefore notable reduction in short duration eruptions after 1971 observed in Fig. 3.2c is not considered a function of reporting. A more thorough discussion of the change in eruption duration across this boundary is included in Chapter 4.

3.2 Available data for Kilauea

3.2.1 The eruption duration dataset for Kilauea

A catalogue of historic eruption durations for the period 1750-1983 was collated from existing catalogues and primary literature for Kilauea yielding an initial dataset of 50 volcanic eruptions (presented in Appendix B). The dataset stops with the onset of the Pu'u'Ō'ō - Kūpaianaha eruption in January 1983 (Heliker and Mattox, 2003). This exceptionally long duration eruption was still continuing on 19 July 2013 (Venzke et al., 2013) and as such a final duration is unknown.

Due to the existence of the Hawaiian Volcano Observatory, documentation of volcanic eruptions is unusually detailed, with many eruptions containing information about the time of day that the eruption started and ended. This hourly resolution data is only used for short, less than 1 day eruptions. The eruption catalogues within Klein (1982) and

Peterson and Moore (1987) only contain eruption start dates and durations. As a result the calculated end date (using the method outlined in section 2.1) is sometimes different from that reported by other sources. Where primary sources containing sufficient descriptions about the eruption have been found this possible duration uncertainty is not accounted for in this study. Where more descriptive sources have not been found or where the descriptions suggest some ambiguity over the actual end of the eruption a duration uncertainty is assigned. Furthermore, Wadge (1981) gives the duration of actual magma discharge, excluding any periods of inactivity between them. Again here primary sources and descriptions have been used to verify that these pauses of activity are < 10 days and are therefore considered negligible in this study (section 2.1).

Critical assessment of the existing eruption record for Kilauea resulted in 41 volcanic eruptions with reliable eruption durations carrying acceptably small duration uncertainties (section 2.1.2). These are reported in Table 3.2 along with erupted volumes taken from Peterson and Moore (1987). Information is also included about the source location of each eruption with regards to whether it was from one of the summit craters (S), the east rift zone (ERZ) or the south west rift zone (SWRZ). These regions and the principle vents associated with them are shown in Fig. 1.2. Lava volumes are taken from Peterson and Moore (1987) and specific considerations regarding the volumes used in this study are discussed in section 3.2.4

Table 3.2: Eruptions from Kilauea with known durations, 1750-1983

#	Location	Start Date	End Date	Duration	Duration U/C		
					Start	End	Tot Volume
1	S	01-07-1823	01-07-1924	1,2;3	36890	+182.5 -182.5	+182.5 -365
2	ERZ	30-05-1840	25-06-1840	3;4	26	+0.5 -0.5	+1 -1
3	ERZ	22-01-1884	23-01-1884	3	1	+0.5 -0.5	+1 -1
4	SWRZ	15-12-1919	15-07-1920	see Appendix B	213	+0.5 -6	+15.5 -21
5	ERZ	28-05-1922	30-05-1922	3;5	2	+0.5 -0.5	+1 -1
6	S	07-07-1927	20-07-1927	3;4;5;6	13	+0.5 -0.5	+1 -1
7	S	20-02-1929	22-02-1929	3;5;6	2	+0.5 -0.5	+1 -1.5
8	S	25-07-1929	28-07-1929	3;4;5;6	3	+0.5 -0.5	+1.5 -1
9	S	19-11-1930	07-12-1930	3;4;5;6	18	+0.5 -0.5	+1.5 -1
10	S	23-12-1931	05-01-1932	3;4;5;6	13	+0.5 -0.5	+1.5 -1

Continued on next page...

Table 3.2 – Continued

#	Location	Start Date	End Date	Duration	Duration U/C			
					Start	End	Tot Volume	
11	S	06-09-1934	07-10-1934	4;6	+0.5 -0.5	+2 -0.5	+2.5 -1	8
12	S	27-06-1952	10-11-1952	3;4;5;6	+0.5 -0.5	+0.5 -0.5	+1 -1	51
13	S	31-05-1954	03-06-1954	3;4;5;6;7	+0.5 -0.5	+0.5 -0.5	+1 -1	7
14	ERZ	28-02-1955	07-04-1955	4	+0.5 -0.5	+1 -0.5	+1.5 -1	
15	ERZ	24-04-1955	26-05-1955	4;6	+0.5 -0.5	+0.5 -0.5	+1 -1	
16	ERZ	14-11-1959	20-12-1959	3;4;5;8;9	+0.5 -0.5	+0.5 -0.5	+1 -1	40
17	ERZ	14-01-1960	19-02-1960	3;4;5;8	+0.5 -1	+0.5 -0.5	+1 -1.5	119
18	S	24-02-1961	25-03-1961	3;4;5;10	+0.5 -0.5	+0.5 -0.5	+1 -1	0.5
19	S	10-07-1961	17-07-1961	3;4;5;10	+0.5 -0.5	+0.5 -0.5	+1 -1	13
20	ERZ	22-09-1961	25-09-1961	3;4;5	+0.5 -0.5	+0.5 -0.5	+1 -1	2.5
21	ERZ	07-12-1962	09-12-1962	3;4;5;11	+0.5 -0.5	+0.5 -0.5	+1 -1	0.3

Continued on next page...

Table 3.2 – Continued

#	Location	Start Date	End Date	Duration	Duration U/C		
					Start	End	Tot Volume
22	ERZ	21-08-1963	23-08-1963	12	+0.5 -0.5	+0.5 -0.5	+1 -1 0.8
23	ERZ	05-10-1963	06-10-1963	3;4;13	+0.5 -0.5	+0.5 -0.5	+1 -1 8
24	ERZ	05-03-1965	15-03-1965	3;4;14	+0.5 -0.5	+0.5 -0.5	+1 -1 18
25	ERZ	24-12-1965	25-12-1965	3;4;15	+0.02 -0.02	+0.02 -0.02	+0.04 -0.04 0.8
26	S	05-11-1967	13-07-1968	3;4;5;16;17	+0.5 -0.5	+0.5 -0.5	+1 -1 84
27	ERZ	22-08-1968	26-08-1968	3;4;18	+0.5 -0.5	+0.5 -0.5	+1 -1 0.01
28	ERZ	07-10-1968	22-10-1968	3;4;18	+0.5 -0.5	+0.5 -0.5	+1 -1 7
29	ERZ	22-02-1969	28-02-1969	3;4;19	+0.5 -0.5	+2 -0.5	+2.5 -1 17
30	ERZ	24-05-1969	15-10-1971	4;9;20;21	+0.5 -0.5	+0.5 -0.5	+1 -1 185
31	S	14-08-1971	14-08-1971	4	+0.02 -0.02	+0.02 -0.02	+0.04 -0.04 10
32	S	24-09-1971	29-09-1971	3;4;5;23;24	+0.5 -0.5	+0.5 -0.5	+1 -1 8

Continued on next page...

Table 3.2 – Continued

#	Location	Start Date	End Date	Duration	Duration U/C			
					Start	End	Tot Volume	
33	ERZ	05-02-1972	22-07-1974	21	900	+5 -5	+5.5 -5.5	161.5
34	S	19-07-1974	22-07-1974	3;4;5;25	3	+0.5 -0.5	+1 -1	10
35	ERZ	19-09-1974	22-09-1974	25	3	+0.5 -0.5	+1 -1	62
36	SWRZ	31-12-1974	31-12-1974	4;25	0.25	+0.02 -0.02	+0.04 -0.04	15
37	S	29-11-1975	29-11-1975	3;4;5;26 <i>see Appendix B</i>	0.7	+0.02 -0.02	+0.04 -0.04	0.2
38	ERZ	13-09-1977	01-10-1977	4;26;27	18	+1 -0.5	+2 -1	40
39	ERZ	16-11-1979	17-11-1979	3;5	0.9	+0.02 -0.02	+0.04 -0.04	0.4
40	S	30-04-1982	01-05-1982	3	0.9	+0.02 -0.02	+0.04 -0.04	
41	S	25-09-1982	26-09-1982	28	0.6	+0.02 -0.02	+0.04 -0.04	

U/C = uncertainty. Units: durations and duration uncertainties = days, volumes = $\times 10^6 \text{m}^3$.
S = summit, ERZ = east rift zone and SWRZ = south west rift zone.
Volumes are taken from Klein (1982) and represent the volume of lava erupted during the eruption (bulk deposit volumes).
Footnote continued on following page...

Footnote for Table 3.2 continued...

Grey numbers following dates represent the following references: ¹ Dzurisin et al. (1984), ² Holcomb (1987), ³ Peterson and Moore (1987), ⁴ Wadge (1981), ⁵ Klein (1982), ⁶ Fiske et al. (1987), ⁷ Macdonald and Eaton (1957), ⁸ Richter et al. (1970), ⁹ Macdonald (1962), ¹⁰ Richter et al. (1964), ¹¹ Moore and Krivoy (1964), ¹² Peck et al. (1964), ¹³ Moore and Koyanagi (1969), ¹⁴ Wright et al. (1968), ¹⁵ Fiske and Koyanagi (1968), ¹⁶ Kinoshita et al. (1969), ¹⁷ Nicholls and Stout (1988), ¹⁸ Jackson et al. (1975), ¹⁹ Swanson et al. (1976), ²⁰ Swanson et al. (1979), ²¹ Tilling et al. (1987), ²² Keller et al. (1972), ²³ Duffield et al. (1982), ²⁴ Dvorak (1990), ²⁵ Lockwood et al. (1999), ²⁶ Dzurisin et al. (1980), ²⁷ Moore et al. (1980), ²⁸ Casadevall and Hazlett (1983).

3.2.2 Comments on lava lake activity at Kilauea

Two types of lava lakes have been recognised at Kilauea: active lava lakes which are linked directly to the feeding magma column and inactive lava lakes formed by passive ponding of magma within pre-existing pit craters (Tilling et al., 1987). The presence of active lava lakes complicates the definition of eruption duration, especially when they exist for several years. Previous studies have used distinct outbreaks or major phases of increased activity in an existing lava lake as separate eruptions (Klein, 1982). However, this may generate a bias in the data toward larger eruptions, on the grounds that smaller eruptions, that would be recognised if a lava lake did not exist, would not make a sufficient impact on the lava lake so as to be defined as a distinct outbreak or increased activity. Here, the definition of an eruption remains the same even when an active lava lake is present (subsection 2.1.1) and the total duration that the active lava lake is present is used for the duration of the eruption.

3.2.3 Additional information on specific eruptions at Kilauea

The first eruption in Table 3.2 has an exceptionally long duration of 36,890 days (~101 years). This was a sustained summit eruption dominated by lava lake activity starting in 1823 and ending in 1924 (Dzurisin et al., 1984; Holcomb, 1987; Peterson and Moore, 1987). Whether eruptive activity was constant throughout this eruptive period is difficult to discern. The period 1894-1907 is described by Holcomb (1987) as ‘13 years of dormancy and very subdued episodic activity’ and Peterson and Moore (1987) attempt to break this period into distinct episodes of Halemaumau overflows and/or caldera fissure outbreaks. However, it is evident that some activity was continuing at this time and here we report a single, sustained eruption starting in 1823 and ending in 1924 (treating both according to the ‘nearest year’ category of Table 2.1). It is therefore not separated into individual episodes. As such, any separately reported summit eruptions for the time period covered by this eruption are not reported separately but are considered part of this eruption. In contrast, eruptions from either the ERZ or SWRZ that occurred during this 101 year period are reported separately and thus their durations are used in this study (# 2-5, Table 3.2).

A series of eruptions are reported for the ERZ in 1955. While Klein (1982) and Peterson and Moore (1987) report an 88 day eruption starting on 28 February 1955, Wadge (1981) separates this into three eruptions; 28 February-6 March, 6 March-7 April and 24 April-26 May. The period of quiescences between the first and second of these eruptions is < 10 days, and therefore these have been combined here as a single eruption (#14 Table 3.2), however, the break in activity between the second and third eruption is > 10 days and therefore, using the definition of eruption duration outlined in subsection 2.1.1, this eruption is considered separately (#15, Table 3.2).

The 1959 eruption of Kilauea Iki (# 16, Table 3.2) is reported to start on 14 November 1959 and end on 20 December 1959. 36 days exist between these two dates, how-

ever, Wadge (1981) reports only a 14 day period of magma effusion for this eruption. Closer inspection of the volcanic activity during this time reveals that it consisted of 17 eruptive phases (Macdonald, 1962; Richter et al., 1970; Wadge, 1981; Dzurisin et al., 1984), however, repose periods between these phases are all < 10 days (Macdonald, 1962; Richter et al., 1970). Therefore a single eruption is reported here with a preferred eruption duration of 36 days.

Similarly the 1967-1968 summit eruption (# 26, Table 3.2) is reported to start on 5 November 1959 and end on 13 July 1968. Although Wadge (1981) reports only a 204 day duration for this eruption Kinoshita et al. (1969) describe this activity as 250 days of returned lava lake activity to the Halemaumau summit crater. They recognise 31 eruptive phases within this 250 day period, however, an active lava lake at the summit was present throughout and these phases represent heightened activity or overflows (Kinoshita et al., 1969; Nicholls and Stout, 1988). Given the definition of eruption duration and the method of dealing with lava lakes this eruption is reported here as a single eruption with a preferred eruption duration of 250 days.

The precise onset of the 1972-1974 eruption (# 33, Table 3.2) was not observed but is inferred as starting in early February 1972 and ending on 22 July 1974 (Tilling et al., 1987). Detailed descriptions of this eruption indicate that although the majority of activity was from the Mauna Ulu-Alae area, there was an outburst of activity near Pauahi and Hiiaka craters on 5 May 1973 and a month long eruption at Pauahi from November to December 1973 (Wadge, 1981; Klein, 1982; Peterson and Moore, 1987; Tilling et al., 1987). These other vents are situated very close to Mauna Ulu (Fig. 1.2) and prior to the Pauahi eruption lava was observed draining from the Mauna Ulu lava lake suggesting that some connection between the plumbing system of these vents exists (Tilling et al., 1987). This eruption is therefore treated here as a single event.

A 3 day summit eruption starting on 19 July 1974 is reported by Wadge (1981), Klein (1982), Peterson and Moore (1987) and Lockwood et al. (1999). Although the dates of

this eruption overlap with the end of the 1972-1974 Mauna Ulu eruption (# 33, Table 3.2) it is included here as a separate eruption due to its different source location (# 35, Table 3.2).

The 19 September 1974 eruption (# 35, Table 3.2) is often reported with a short duration of approximately 1 day (Wadge, 1981; Klein, 1982; Peterson and Moore, 1987). While Lockwood et al. (1999) state that active fire fountaining ended in the afternoon of 19 September 1974 they also describe irregular overturning of the lava lake crust until 22 September 1974. This implies that the lava lake was still active and the later end date of 22 September 1974 is used here to give a preferred duration of 3 days.

3.2.4 Volume data for eruptions from Kilauea

Lava volumes of the eruptions of Kilauea used in this study are taken from Klein (1982). It is unclear what method Klein (1982) used to obtain these volume measurements, however, the volume data for Kilauea is largely assumed to be accurate, especially for eruptions since 1970. The sustained summit eruption of July 1823 (#1, Table 3.2) is reported here as ending in July 1924 and as such overlaps with shorter eruptions from the ERZ and SWRZ. To simplify the volume investigations of this study, volumes are reported here for eruptions which occurred after the end of the 1823 eruption, and therefore the July 1927 summit eruption (#6, Table 3.2) is the first eruption with volume information reported here.

Volumes are not provided for the two 1955 eruptions in Table 3.2 (#14 and #15) due to them being included as one eruption in Peterson and Moore (1987) (see subsection 3.2.3) and therefore the proportion of lava erupted during each phase separately is unknown and cannot be reported here.

3.2.5 The completeness of the eruption record at Kilauea

Klein (1982) states that the eruption record is ‘certainly complete’ after the establishment of the Hawaiian Volcano Observatory in 1912. Fig. 3.3a plots cumulative eruption number against eruption start year for the 50 eruptions reported for Kilauea between 1750 and 1983 and Fig. 3.3b plots this data at 50 year intervals showing the proportion of eruptions excluded from the study due to insufficient information regarding their durations. The scarcity of eruptions prior to 1912 and the sharp increase in the number of documented eruptions after it demonstrate the importance of the Hawaiian Volcano Observatory in reporting these eruptions.

Whether the eruption record can be considered complete is debatable. The near constant gradient of Fig. 3.3a and the exclusion of only 1 eruption following 1912 certainly supports this notion. However, it is unrealistic to assume that advancements in technology and monitoring equipment since 1912 have had little effect on the reporting of volcanic eruptions at Kilauea. Dzurisin et al. (1984) suggests that a more modern approach to monitoring volcanic activity began in the late 1950’s and the number of eruptions reported in the period 1950-1983 is over three times greater than that for the period 1900-1949 (Fig. 3.3b). Furthermore, Fig. 3.3c shows an increase in the number of short duration eruptions reported following the large 1959 eruption. The new monitoring techniques established in the 1950’s may have led to the better detection of small eruptions and it is therefore entirely possible that the earlier eruption record contains a reporting bias towards longer duration eruptions.

On a global scale fewer eruptions are reported during times of war, when human attention is directed elsewhere (Simkin, 1993; Siebert et al., 2010). A period of quiescence at Kilauea can be observed between 1935 and 1951 (Fig. 3.3a), which coincides with World War II and it is therefore possible that this is a reporting bias. However, this absence of reported eruptions has not been attributed to World War II in the past and

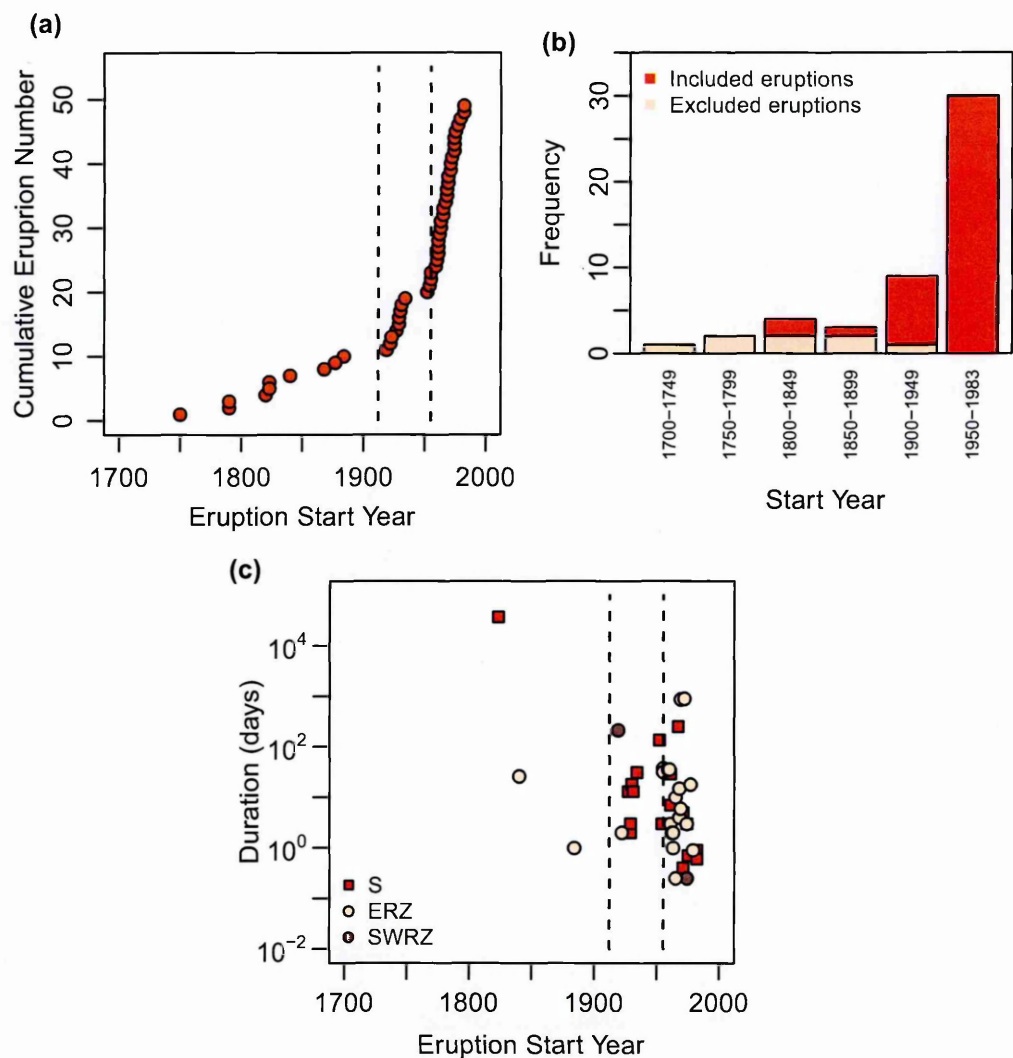


Fig. 3.3 (a) Plot of cumulative eruption number against eruption start year for the 50 eruptions reported between 1750-1983 and (b) the same data displayed as a bar plot at 50 year intervals separated into eruptions included and excluded from this study. (c) Plot of eruption duration (on a log scale) against start year for the eruptions within Table 3.2 separated into the three sectors identified in Fig. 1.2 (S = Summit, ERZ = East Rift Zone and SWRZ = South West Rift Zone). Vertical dashed lines in plots a and c represent the years 1912 and 1959

this abnormally long repose interval is included in the analyses of Klein (1982). Furthermore, it correlates with a period of increased activity at Mauna Loa and previous studies have indicated a connection between the volcanic activity of these two volcanoes such that during periods of heightened activity at one, the other shows reduced activity and fewer eruptions. This repose interval is therefore treated as a real artefact of the data and is included in the repose analyses of Kilauea in Chapter 6.

Despite the possible reporting biases prior to 1959 the evidence for a near complete record of eruptions following 1912 cannot be ignored. It is possible that the increased proportion of short duration eruptions after 1959 is not due to reporting biases but reflects some change in the physical properties of Kilauea's volcanic system. The 1912-1983 dataset of historic eruptions at Kilauea is therefore used in the remainder of this study but the distribution of eruption durations before and after 1959 is investigated thoroughly in Chapter 4.

3.3 Available data for Piton de la Fournaise (PdlF)

3.3.1 The eruption duration dataset of PdlF

A catalogue of historic eruptions from 1644 to 2011 was collated from the existing literature for PdlF. The initial dataset contained 267 volcanic eruptions (included in Appendix C) which were then critically assessed according to the methods described in section 2.1. The comprehensive catalogues of historic eruptions within Stieltjes and Moutou (1989) and Peltier et al. (2009) were relied on heavily during this critical examination and given the limited information available for the early historical record many eruptions prior to 1966 rely entirely on the information within Stieltjes and Moutou (1989). More information is available for eruptions following 1966 and as such a more thorough critical assessment has been conducted for these eruptions.

This process of critical assessment resulted in 172 eruptions with reliable durations carrying acceptably small duration uncertainties (section 2.1). These eruptions are reported in Table 3.3 and are used in the duration analyses of this study.

Table 3.3: Eruptions from PdIF with known durations, 1644-2011

#	Location	Start Date	End Date	Duration	Duration U/C			Volume	Petrology
					Start	End	Tot		
1		15-12-1760	29-12-1760	1	+0.5 -0.5	+0.5 -0.5	+1 -1		
2		14-05-1766	31-05-1766	1	+0.5 -0.5	+0.5 -0.5	+1 -1		
3		14-06-1787	01-08-1787	1	+0.5 -0.5	+0.5 -0.5	+1 -1		
4		26-06-1791	17-07-1791	1	+0.5 -0.5	+0.5 -0.5	+1 -1		
5		02-11-1800	08-11-1800	1	+0.5 -0.5	+0.5 -0.5	+1 -1		
6		17-01-1802	30-01-1802	1	+0.5 -0.5	+0.5 -0.5	+1 -1		
7		23-03-1807	27-05-1807	1	+0.5 -0.5	+0.5 -0.5	+1 -1		
8		10-06-1807	13-06-1807	1	+0.5 -0.5	+0.5 -0.5	+1 -1		
9		17-07-1809	08-08-1809	1	+0.5 -0.5	+0.5 -0.5	+1 -1		
10		20-11-1810	28-11-1810	1	+0.5 -0.5	+0.5 -0.5	+1 -1		

Continued on next page...

Table 3.3 – Continued

#	Location	Start Date	End Date	Duration	Duration U/C		
					Start	End	Petrology
11		03-09-1812	30-09-1812	1	27	+0.5 -0.5	+1 -1
12		16-09-1813	16-09-1813	1	0.5	+0.02 -0.02	+0.04 -0.04
13		18-11-1813	26-11-1813	1	8	+0.5 -0.5	+1 -1
14		10-09-1814	12-09-1814	1	2	+0.5 -0.5	+1 -1
15		13-10-1814	13-10-1814	1	0.5	+0.02 -0.02	+0.04 -0.04
16		21-01-1815	27-01-1815	1	6	+0.5 -0.5	+1 -1
17		15-08-1815	16-08-1815	1	1	+0.5 -0.5	+1 -1
18		15-12-1816	15-12-1816	1	0.5	+0.02 -0.02	+0.04 -0.04
19		27-02-1821	10-04-1821	1	42	+0.5 -0.5	+1 -1
20		19-03-1844	11-05-1844	1	53	+0.5 -0.5	+1 -1
21		03-11-1850	12-11-1850	1	9	+0.5 -0.5	+1 -1

Continued on next page...

Table 3.3 – Continued

#	Location	Start Date	End Date	Duration	Duration U/C			Volume	Petrology
					Start	End	Tot		
22		08-05-1859	08-05-1859	1	0.5	+0.02 -0.02	+0.02 -0.02	+0.04 -0.04	
23		22-01-1860	24-02-1860	1	33	+0.5 -0.5	+0.5 -0.5	+1 -1	
24		11-03-1860	20-03-1860	1	9	+0.5 -0.5	+0.5 -0.5	+1 -1	
25		19-03-1861	19-03-1861	1	0.5	+0.02 -0.02	+0.02 -0.02	+0.04 -0.04	
26		20-12-1863	29-01-1864	1	40	+0.5 -0.5	+0.5 -0.5	+1 -1	
27		05-02-1865	10-02-1865	1	5	+0.5 -0.5	+0.5 -0.5	+1 -1	
28		21-06-1871	05-07-1871	1	14	+0.5 -0.5	+0.5 -0.5	+1 -1	
29		29-06-1874	24-07-1874	1	25	+0.5 -0.5	+0.5 -0.5	+1 -1	
30		20-12-1874	20-12-1874	1	0.5	+0.02 -0.02	+0.02 -0.02	+0.04 -0.04	
31		26-11-1875	26-11-1875	1	0.5	+0.02 -0.02	+0.02 -0.02	+0.04 -0.04	
32		11-12-1875	11-12-1875	1	0.5	+0.02 -0.02	+0.02 -0.02	+0.04 -0.04	

Continued on next page...

Table 3.3 – Continued

#	Location	Start Date	End Date	Duration	Duration U/C		
					Start	End	Petrology
33		11-12-1876	11-12-1876	1	0.5	+0.02 -0.02	+0.04 -0.04
34		14-03-1878	30-03-1878	1	16	+0.5 -0.5	+1 -1
35		24-11-1880	25-11-1880	1	1	+0.5 -0.5	+1 -1
36		04-02-1884	05-02-1884	1	1	+0.5 -0.5	+1 -1
37		15-06-1889	15-08-1889	1	61	+15 -15	+30 -30
38		21-10-1890	20-11-1890	1	30	+0.5 -0.5	+1 -1
39		14-01-1898	20-01-1898	1	6	+0.5 -0.5	+1 -1
40		11-05-1900	30-05-1900	1	19	+0.5 -0.5	+1 -1
41		21-02-1901	25-02-1901	1	4	+0.5 -0.5	+1 -1
42		04-07-1901	06-07-1901	1	2	+0.5 -0.5	+1 -1
43		13-08-1902	18-08-1902	1	5	+0.5 -0.5	+1 -1

Continued on next page...

Table 3.3 – Continued

#	Location	Start Date	End Date	Duration	Duration U/C			Volume	Petrology
					Start	End	Tot		
44		19-08-1904	20-08-1904	1	+0.5 -0.5	+0.5 -0.5	+1 -1		
45		04-10-1904	17-10-1904	13	+0.5 -0.5	+0.5 -0.5	+1 -1		
46		15-02-1905	16-02-1905	1	+0.5 -0.5	+0.5 -0.5	+1 -1		
47		16-11-1910	12-12-1910	26	+0.5 -0.5	+0.5 -0.5	+1 -1		
48		10-07-1913	03-08-1913	24	+0.5 -0.5	+0.5 -0.5	+1 -1		
49		08-09-1915	08-09-1915	0.5	+0.02 -0.02	+0.02 -0.02	+0.04 -0.04		
50		08-10-1915	20-10-1915	12	+0.5 -0.5	+0.5 -0.5	+1 -1		
51		09-11-1915	21-11-1915	12	+0.5 -0.5	+0.5 -0.5	+1 -1		
52		29-04-1917	29-04-1917	0.5	+0.02 -0.02	+0.02 -0.02	+0.04 -0.04		
53		28-06-1920	04-07-1920	6	+0.5 -0.5	+0.5 -0.5	+1 -1		
54		10-10-1920	18-10-1920	8	+0.5 -0.5	+0.5 -0.5	+1 -1		

Continued on next page...

Table 3.3 – Continued

#	Location	Start Date	End Date	Duration	Duration U/C		
					Start	End	Tot
55		03-09-1924	13-09-1924	1	10	+0.5 -0.5	+1 -1
56		30-12-1925	30-12-1925	1	0.5	+0.02 -0.02	+0.04 -0.04
57		18-09-1926	19-09-1926	1	1	+0.5 -0.5	+1 -1
58		05-11-1926	08-11-1926	1	3	+0.5 -0.5	+1 -1
59		11-01-1927	20-01-1927	1	9	+0.5 -0.5	+1 -1
60		05-02-1927	20-02-1927	1	15	+5 -5	+5.5 -5.5
61		23-12-1929	31-12-1929	1	8	+0.5 -0.5	+1 -1
62		23-05-1930	24-05-1930	1	1	+0.5 -0.5	+1 -1
63		15-02-1931	15-05-1931	1	89	+15 -15	+30 -30
64		14-06-1931	25-06-1931	1	11	+0.5 -0.5	+5.5 -5.5
65		04-08-1931	25-08-1931	1	21	+0.5 -0.5	+5.5 -5.5

Continued on next page...

Table 3.3 – Continued

#	Location	Start Date	End Date	Duration	Duration U/C			Volume	Petrology
					Start	End	Tot		
66		07-06-1933	15-06-1933	1	8	+0.5 -0.5	+0.5 -0.5	+1 -1	
67		01-11-1933	01-11-1933	1	0.5	+0.02 -0.02	+0.02 -0.02	+0.04 -0.04	
68		11-11-1933	13-11-1933	1	2	+0.5 -0.5	+0.5 -0.5	+1 -1	
69		05-02-1934	23-02-1934	1	18	+0.5 -0.5	+0.5 -0.5	+1 -1	
70		30-03-1934	01-04-1934	1	2	+0.5 -0.5	+0.5 -0.5	+1 -1	
71		13-08-1937	12-09-1937	1	30	+0.5 -0.5	+0.5 -0.5	+1 -1	
72		05-11-1937	25-11-1937	1	20	+0.5 -0.5	+0.5 -0.5	+1 -1	
73		25-07-1938	29-07-1938	1	4	+0.5 -0.5	+0.5 -0.5	+1 -1	
74		07-12-1938	15-01-1939	1	39	+0.5 -0.5	+0.5 -0.5	+1 -1	
75		05-10-1942	25-10-1942	1	20	+0.5 -0.5	+0.5 -0.5	+1 -1	
76		04-04-1943	25-04-1943	1	21	+0.5 -0.5	+0.5 -0.5	+1 -1	

Continued on next page...

Table 3.3 – Continued

#	Location	Start Date	End Date	Duration	Duration U/C		
					Start	End	Petrology
77		11-04-1944	01-05-1944	1	20	+0.5 -0.5	+1 -1
78		15-04-1945	06-05-1945	1	21	+0.5 -0.5	+1 -1
79		18-06-1946	05-07-1946	1	17	+0.5 -0.5	+1 -1
80		14-02-1948	08-03-1948	1	23	+0.5 -0.5	+1 -1
81		25-02-1950	02-04-1950	1	36	+0.5 -0.5	+1 -1
82		30-08-1950	05-09-1950	1	6	+0.5 -0.5	+1 -1
83		10-09-1951	20-09-1951	1	10	+0.5 -0.5	+1 -1
84		19-05-1952	20-07-1952	1	62	+0.5 -0.5	+1 -1
85		13-03-1953	15-04-1953	1	33	+0.5 -0.5	+1 -1
86		15-06-1953	08-07-1953	1	23	+0.5 -0.5	+1 -1
87		15-01-1954	15-12-1954	1	334	+15 -15	+30 -30

Continued on next page...

Table 3.3 – Continued

#	Location	Start Date	End Date	Duration	Duration U/C			Volume	Petrology
					Start	End	Tot		
88		08-03-1956	15-04-1956	1	+0.5 -0.5	+0.5 -0.5	+1 -1		
89		22-11-1956	23-11-1956	1	+0.5 -0.5	+0.5 -0.5	+1 -1		
90		30-12-1956	16-03-1957	1	+0.5 -0.5	+0.5 -0.5	+1 -1		
91		02-09-1957	09-09-1957	1	+0.5 -0.5	+0.5 -0.5	+1 -1		
92		21-10-1957	16-11-1957	1	+0.5 -0.5	+0.5 -0.5	+1 -1		
93		30-05-1958	31-05-1958	1	+0.5 -0.5	+0.5 -0.5	+1 -1		
94		06-08-1958	20-09-1958	1	+0.5 -0.5	+0.5 -0.5	+1 -1		
95		11-03-1959	20-04-1959	1	+0.5 -0.5	+0.5 -0.5	+1 -1		
96		04-08-1959	06-08-1959	1	+0.5 -0.5	+0.5 -0.5	+1 -1		
97		11-01-1960	12-01-1960	1	+0.5 -0.5	+0.5 -0.5	+1 -1		
98		08-02-1960	10-03-1960	1	+0.5 -0.5	+0.5 -0.5	+1 -1		

Continued on next page...

Table 3.3 – Continued

#	Location	Start Date	End Date	Duration	Duration U/C				Volume	Petrology
					Start	End	Tot			
99		05-04-1961	25-04-1961	1	20	+0.5 -0.5	+0.5 -0.5	+1 -1		
100		07-11-1963	21-11-1963	1	14	+0.5 -0.5	+0.5 -0.5	+1 -1		
101		30-04-1964	08-05-1964	1	8	+0.5 -0.5	+0.5 -0.5	+1 -1		
102		21-12-1964	15-02-1965	1	56	+0.5 -0.5	+0.5 -0.5	+1 -1		
103		15-03-1966	15-05-1966	1	61	+0.5 -0.5	+0.5 -0.5	+1 -1		
104	Proximal	09-06-1972	11-06-1972	1;2	2	+0.5 -0.5	+0.5 -0.5	+1 -1	0.27	PP
105	Proximal	25-07-1972	17-08-1972	1;2	23	+0.5 -0.5	+0.5 -0.5	+1 -1	2.9	PP
106	Proximal	07-09-1972	27-09-1972	1	20	+0.5 -0.5	+0.5 -1	+1 -1.5	4	PP
107	Proximal	08-10-1972	10-12-1972	1;2	63	+0.5 -0.5	+0.5 -0.5	+1 -1	9.3	O
108		08-01-1973	16-01-1973	1	8	+0.5 -0.5	+0.5 -0.5	+1 -1		
109	Summit	10-05-1973	28-05-1973	1;2	18	+0.5 -0.5	+7 -0.5	+7.5 -1	1.6	PP

Continued on next page...

Table 3.3 – Continued

#	Location	Start Date	End Date	Duration	Duration U/C			Volume	Petrology
					Start	End	Tot		
110		04-09-1973	05-09-1973	1	+0.5 -0.5	+0.5 -0.5	+1 -1		
111	Summit	04-11-1975	18-11-1975	14	+0.5 -0.5	+0.5 -0.5	+1 -1	1.4	PP
112	Summit	18-12-1975	06-04-1976	110	+0.5 -0.5	+0.5 -0.5	+1 -1	11.6	PP
113	Proximal	02-11-1976	03-11-1976	0.63	+0.02 -0.02	+0.02 -0.02	+0.04 -0.04	0.46	PP
114	Proximal	24-03-1977	24-03-1977	0.5	+0.02 -0.02	+0.02 -0.02	+0.04 -0.04	0.06	PP
115	Distal	05-04-1977	16-04-1977	11	+0.5 -0.5	+0.5 -0.5	+1 -1	20	O
116	Proximal	24-10-1977	17-11-1977	24	+0.5 -0.5	+0.5 -0.5	+1 -1	23	OR
117	Proximal	28-05-1979	29-05-1979	1	+0.5 -0.5	+0.5 -0.5	+1 -1	0.2	PP
118	Proximal	13-07-1979	14-07-1979	0.71	+0.02 -0.02	+0.02 -0.02	+0.04 -0.04	0.3	PP
119	Proximal	03-02-1981	05-05-1981	91	+0.5 -0.5	+0.5 -0.5	+1 -1	12	PP
120	Proximal	04-12-1983	18-02-1984	76	+0.5 -0.5	+0.5 -0.5	+1 -1	17	PP

Continued on next page...

Table 3.3 – Continued

#	Location	Start Date	End Date	Duration	Duration U/C			Volume	Petrology
					Start	End	Tot		
121	Proximal	14-06-1985	15-06-1985	1;2;3 1	+0.02 -0.02	+0.02 -0.02	+0.04 -0.04	1	PP
122	Summit	05-08-1985	10-10-1985	1;2;3 66	+0.5 -0.5	+6 -0.5	+6.5 -1	21	PP
123	Proximal	02-12-1985	03-12-1985	1;2;3 1.17	+0.02 -0.02	+0.02 -0.02	+0.04 -0.04	0.7	PP
124	Summit	29-12-1985	08-02-1986	1;2;3 3 41	+0.5 -0.5	+10 -1	+10.5 -1.5	7	PP
125	Distal	19-03-1986	05-04-1986	1;2;3 2;3 17	+0.5 -0.5	+0.5 -4	+1 -4.5	14	PP
126	Summit	13-07-1986	14-07-1986	2;3 0.25	+0.02 -0.02	+0.02 -0.02	+0.04 -0.04	0.27	PP
127	Summit	12-11-1986	13-11-1986	2;3 1	+0.5 -0.5	+0.5 -0.5	+1 -1	0.27	PP
128	Summit	26-11-1986	27-11-1986	1;2;3 1	+0.5 -0.5	+0.5 -0.5	+1 -1	0.24	PP
129	Summit	06-12-1986	06-01-1987	1;2;3 2;3 31	+0.5 -0.5	+1 -0.5	+1.5 -1	2	PP
130	Summit	10-06-1987	29-06-1987	1;2;3 1;2;3 19	+0.5 -0.5	+0.5 -0.5	+1 -1	1.5	PP
131	Proximal	19-07-1987	20-07-1987	1;2;3 1;2;3 1.33	+0.02 -0.02	+0.02 -0.02	+0.04 -0.04	0.8	PP

Continued on next page...

Table 3.3 – Continued

#	Location	Start Date	End Date	Duration	Duration U/C			Volume	Petrology
					Start	End	Tot		
132	Proximal	06-11-1987	08-11-1987	1;2;3 2	+0.5 -0.5	+0.5 -0.5	+1 -1	1.6	PP
133	Proximal	30-11-1987	01-01-1988	2;3 32	+0.5 -0.5	+0.5 -0.5	+1 -1	10	PP
134	Proximal	07-02-1988	02-04-1988	2;3 55	+0.5 -0.5	+0.5 -0.5	+1 -1	8	PP
135	Proximal	18-05-1988	01-08-1988	2;3 75	+0.5 -0.5	+0.5 -0.5	+1 -1	15	PP
136	Proximal	31-08-1988	12-09-1988	2;3 2	+0.5 -0.5	+0.5 -0.5	+1 -1	7	PP
137	Proximal	14-12-1988	29-12-1988	2;3 15	+0.5 -0.5	+0.5 -0.5	+1 -1	8	PP
138	Summit	18-01-1990	19-01-1990	2;3 0.75	+0.02 -0.02	+0.02 -0.02	+0.04 -0.04	0.5	PP
139	Proximal	18-04-1990	08-05-1990	2;3 20	+0.5 -0.5	+0.5 -0.5	+1 -1	8	PP
140	Summit	19-07-1991	20-07-1991	2;3 1.17	+0.02 -0.02	+0.02 -0.02	+0.04 -0.04	2.8	PP
141	Summit	27-08-1992	23-09-1992	2;3 27	+0.5 -0.5	+0.5 -0.5	+1 -1	5.5	PP
142	Distal	09-03-1998	21-09-1998	2;3;4 196	+0.5 -0.5	+0.5 -0.5	+1 -1	60	PP

Continued on next page...

Table 3.3 – Continued

#	Location	Start Date	End Date	Duration	Duration U/C			Volume	Petrology
					Start	End	Tot		
143	Summit	19-07-1999	31-07-1999	2;5	+0.5 -0.5	+0.5 -0.5	+1 -1	1.8	PP
144	Summit	28-09-1999	23-10-1999	2;5	+0.5 -0.5	+0.5 -0.5	+1 -1	1.5	PP
145	Proximal	14-02-2000	03-03-2000	6	+1 -0.5	+1 -0.5	+2 -1	4.1	PP
146	Proximal	23-06-2000	30-07-2000	2;5	+0.5 -0.5	+0.5 -0.5	+1 -1	6	PP
147	Proximal	12-10-2000	13-11-2000	2	+0.5 -0.5	+0.5 -0.5	+1 -1	9	PP
148	Proximal	27-03-2001	04-04-2001	2	+0.5 -0.5	+0.5 -0.5	+1 -1	4.8	PP
149	Proximal	11-06-2001	07-07-2001	2	+0.5 -0.5	+0.5 -0.5	+1 -1	9.5	OR
150	Distal	05-01-2002	16-01-2002	2	+0.5 -0.5	+1 -0.5	+1.5 -1	13	O
151	Proximal	16-11-2002	03-12-2002	2	+0.5 -0.5	+1 -0.5	+1.5 -1	8	OR
152	Summit	30-05-2003	07-07-2003	2	+0.5 -0.5	+0.5 -0.5	+1 -1	1.28	PP
153	Proximal	22-08-2003	27-08-2003	2	+0.5 -1	+1 -0.5	+1.5 -1.5	6.2	OR

Continued on next page...

Table 3.3 – Continued

#	Location	Start Date	End Date	Duration	Duration U/C			Volume	Petrology
					Start	End	Tot		
154	Proximal	30-09-2003	01-10-2003	2	+0.5 -0.5	+0.5 -0.5	+1 -1	1	PP
155	Proximal	07-12-2003	25-12-2003	2	+0.5 -0.5	+0.5 -0.5	+1 -1	1.2	PP
156	Distal	08-01-2004	10-01-2004	2	+0.5 -0.5	+0.5 -0.5	+1 -1	1.9	OR
157	Proximal	02-05-2004	18-05-2004	2;8	+0.5 -0.5	+0.5 -0.5	+1 -1	16	PP
158	Summit	12-08-2004	16-10-2004	2;8	+0.5 -1	+0.5 -12	+1 -13	20	PP
159	Distal	17-02-2005	26-02-2005	2;8	+0.5 -0.5	+0.5 -0.5	+1 -1	19	O
160	Summit	04-10-2005	17-10-2005	2;8	+0.5 -0.5	+1 -0.5	+1.5 -1	1.5	PP
161	Summit	29-11-2005	29-11-2005	2;8	+0.02 -0.02	+0.02 -0.02	+0.04 -0.04	1	PP
162	Distal	26-12-2005	18-01-2006	2	+0.5 -0.5	+0.5 -1	+1 -1.5	18	O
163	Proximal	20-07-2006	14-08-2006	2	+0.5 -0.5	+1 -0.5	+1.5 -1	3	PP
164	Summit	30-08-2006	01-01-2007	2	+0.5 -0.5	+0.5 -0.5	+1 -1	20	PP

Continued on next page...

Table 3.3 – Continued

#	Location	Start Date	End Date	Duration	Duration U/C			Volume	Petrology
					Start	End	Tot		
165	Summit	18-02-2007	19-02-2007	2;9	+0.5 -0.5	+0.5 -0.5	+1 -1		PP
166	Distal	30-03-2007	01-05-2007	2;4	+0.5 -0.5	+0.5 -0.5	+1 -1	140	O
167	Summit	21-09-2008	02-10-2008	9	+0.5 -0.5	+0.5 -0.5	+1 -1		
168	Summit	27-11-2008	28-11-2008	9	+0.5 -0.5	+0.5 -0.5	+1 -1		
169	Summit	14-12-2008	04-02-2009	9	+0.5 -0.5	+0.5 -0.5	+1 -1		
170	Summit	05-11-2009	12-01-2010	GVP	+0.5 -0.5	+0.5 -0.5	+1 -1		
171	Proximal	14-10-2010	31-10-2010	GVP	+0.5 -0.5	+0.5 -0.5	+1 -1		
172	Proximal	09-12-2010	10-12-2010	GVP	+0.5 -0.5	+0.5 -0.5	+1 -1		

U/C = uncertainty, PP = Poorly Phryic, OR = Olivine Rich and O = Oceanite.

Units: durations and duration uncertainties = days, volumes = $\times 10^6 \text{m}^3$.

Location volumes and petrology are based on Peltier et al. (2009) where volumes represent the volume of lava erupted during the eruption (bulk deposit volumes).

Grey numbers following dates represent the following references: ¹ Stieltjes and Moutou (1989), ² Peltier et al. (2009), ³ Boivin and Bachélery (2009), ⁴ Coppola et al. (2009) ⁵ Fukushima et al. (2010), ⁶ Fukushima et al. (2005), ⁷ Peltier et al. (2011), ⁸ Peltier et al. (2008), ⁹ Staudacher et al. (2009), ^{GVP} Venzke et al. (2013).

3.3.2 Location, volume and petrological data for eruptions from PdIF

The information within Peltier et al. (2009) has been used to determine approximate vent/fissure location for the eruptions in the period 1972-2007. Alternative sources were used for the six more recent eruptions in the period 2008-2011. These eruptions have been separated into three spatial groups; summit eruptions (from Dolomieu Crater), proximal eruptions from within Enclos Fouqué Caldera and distal eruptions from outside the Enclos Fouqué Caldera or within the Plaines des Osmondes (Fig. 1.3).

Erupted lava volumes and types are also taken from Peltier et al. (2009). It is unclear what method Peltier et al. (2009) used to obtain these volume measurements, however, they are assumed to be bulk deposit volumes. Due to the thorough nature of Peltier et al. (2009) the eruptions of Table 3.3 are often split into smaller eruption episodes, each with their own erupted volumes. Here the appropriate volumes are combined to provide the total volume of lava erupted during the period of a single eruption in Table 3.3. In contrast, the volume reported for the October 1972 eruption (#107, Table 3.3) is that erupted during the eruption's main phases (10 October 1972 to 10 December 1972) and does not include the initial short eruption on the 8 October 1972 for which a small lava flow is reported by Stieltjes and Moutou (1989) but not included in the catalogue of Peltier et al. (2009).

Eruptions in the period 1972-2007 have been separated into three groups based on the petrology of their lavas, and the classification of Peltier et al. (2009).

Peltier et al. (2009) identified three petrological groups in the 1972-2007 historical eruption data of PdIF; poorly-phyric lavas (PP) with < 5 % phenocrysts, olivine-rich basalts (OR) with 10 - 20 % olivine crystals and oceanites (O) with > 20 % olivine

crystals. Variations in petrology have the potential to alter magma viscosity prior to and during eruption, which may have an important control effect on eruption duration. The clearly defined petrological variation at PdlF has led to the inclusion of this information in Table 3.3 and in some analyses performed on the eruption duration data for this volcanic system in this thesis.

3.3.3 Additional information on specific eruptions from PdlF

The highly active nature of PdlF often results in numerous eruptions occurring in the same year and sometimes even in the same month. Given the varying definitions of eruption duration in the existing literature this can lead to discrepancies between pre-existing catalogues and the dataset compiled for this study. The November 1810, December 1938, October 1972, December 1975, February 1981, December 1983, May 2003 and March 2007 eruptions (#10, #74, #107, #112 #119, #120, #152 and #166, Table 3.3) have all previously been documented as a series of eruptive phases, however, close inspection of the literature pertaining to them demonstrate that these phases either overlap in time or have periods of inactivity between them of < 10 days (specific information for each eruption is included within Appendix C).

Some discrepancy regarding the end date of the August 1988 eruption (#136, Table 3.3) exists in the literature. Here 12 September 1988 is used reported by Peltier et al. (2009), however, Boivin and Bachélery (2009) report this eruption ending on 26 October 1988. The Smithsonian Institution's monthly report (SEAN 13:09) describes strong degassing following the end of the eruption in September and that this degassing continued into October. Here the later date reported by Boivin and Bachélery (2009) is believed to represent the end of the degassing and not the end of the actual eruption.

3.3.4 The completeness of the eruption record at PdlF

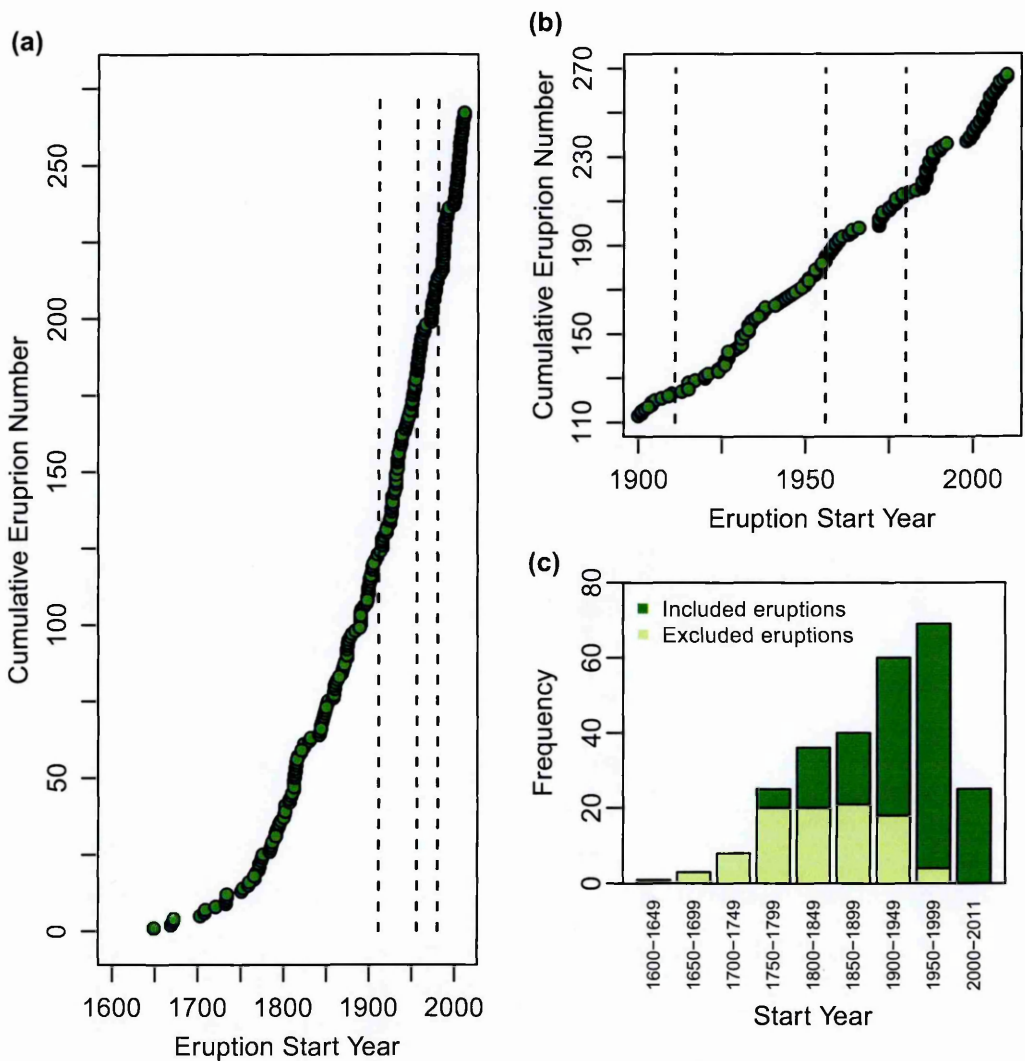


Fig. 3.4 (a) Plot of cumulative eruption number against eruption start year for the 267 eruptions reported between 1644 and 2011 and (b) a larger version of this plot for the period 1900-2011. (c) Bar plot showing the frequency of eruptions reported at 50 year intervals separated into eruptions included and excluded from the study. Vertical dashed lines in plots a and b represent the years 1911, 1956 and 1980

An extensive historical record is available for PdlF and it is the largest dataset considered in this study. A gradual increase in the number of reported eruptions with time can be observed in Fig. 3.4a with very few eruptions reported prior to 1750. A plot restricted to the period 1900-2011 identifies two 6 year periods of repose (1966-1972 and 1992-1998) that have been recognised in previous studies (Fig. 3.4b) and are believed to be a true representation of volcanic activity at PdlF and not an artefact of

reporting (Peltier et al., 2009).

Fig. 3.4c shows how this increasing eruption frequency is accompanied by an increase in the number of eruptions with known durations. This is particularly evident for the period 1950-2011, with only four eruptions being excluded due to insufficient duration data, all of which occurred in the period 1950-1956. Despite the clear evidence for an eruption record improving with time it is difficult to determine when it can be considered complete.

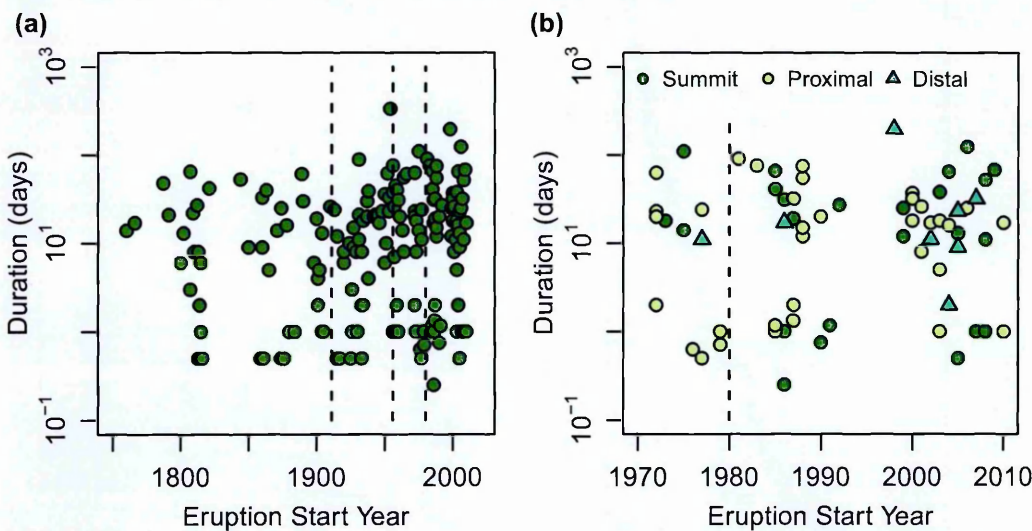


Fig. 3.5 Plots of eruption duration (on a log scale) against start year for (a) all the eruptions within Table 3.3 and (b) eruptions in the period 1972-2011 categorised by location. In (a) vertical dashed lines represent the years 1911, 1956 and 1980, in (b) vertical dashed line represents the year 1980.

In terms of reporting, two events during the 20th Century may be important; 1911 when the first geological observations at PdlF were made and 1980 when the Observatoire Volcanologique was introduced. Fig. 3.5 plots eruption start year against duration for the eruptions within Table 3.3. Although little variation in reported eruption duration can be seen following 1911, an increase in the number of eruptions with hourly resolution data can be observed following 1980 most probably due to the Observatoire Volcanologique’s increased monitoring and seismic network.

Plots of eruption duration against time at PdlF (for the entire dataset (Fig. 3.5a) and

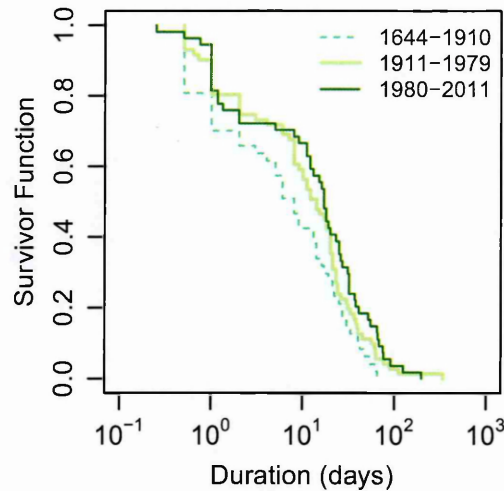


Fig. 3.6 Empirical survivor function curves for eruption durations reported at PdIF in the periods 1644-1910, 1911-1979 and 1980-2011

with data restricted to the period with location information and categorised as such (Fig. 3.5b) do not show evidence of reporting biases. To assess whether the increased interest and monitoring of volcanic activity in 1911 and 1980 have had any effect on the distribution of reported eruption durations at PdIF significance tests have been performed (Table 3.4). Empirical survivor function curves for the periods 1644-1910, 1911-1979 and 1980-2011 are displayed in Fig. 3.6. The distribution of eruption duration for the periods 1911-1979 and 1980-2011 are found to be statistically similar, suggesting that the introduction of the Observatoire Volcanologique had little effect on the overall distribution of eruption durations reported. However, when the distribution of eruption durations for the period 1911-2011 is compared to that of 1644-1910 the three significance tests all yield p-values of < 0.05 implying that they are statistically different at the 0.05 level. A dataset of historic eruptions for the period 1911-2011 from PdIF will therefore be used in the remainder of the analyses of this study.

Table 3.4: Logrank, Mann-Whitney and *t*-test results assessing the effect of reporting bias on the distribution of eruption duration at PdIF

Data		Logrank	Mann-Whitney	<i>t</i> -test
A (n=71)	B (n=54)	$p = 0.337$	$p = 0.363$	$p = 0.600$
C (n=47)	D (n=125)	$p = 0.020$ *	$p = 0.031$ *	$p = 0.040$ *

A = 1911-1979, B = 1980-2011, C = 1644-1910, D = 1911-2011.

* = significant at a 0.05 level, • = moderate significance (p -value = 0.05-0.1).

t-test applied to the logs of the data.

3.4 Available data for Iceland

Whereas the other datasets investigated in this study represent single volcanic systems with relatively consistent eruption styles, Iceland is a volcanic region with 30 identified volcanic systems erupting each varying in the chemistry of erupted products and the style of volcanic activity that they produce (subsection 1.3.4). As a result eruptions on Iceland cannot be treated equally or as a single eruption duration dataset. Instead it provides an opportunity to assess the duration of different types and styles of volcanic activity and variations on a regional scale.

3.4.1 Duration types identified on Iceland

Six broad eruption types have been identified in the historical record of Iceland based on the chemical composition of their eruptive products, style of volcanic activity and whether the eruption is temporally discrete or part of a longer eruptive sequence (Fig. 3.7). Each eruption type can be described by one or more duration leading the the classification scheme portrayed in Fig. 3.7 and used for the Icelandic eruption data throughout this thesis.

In Iceland, eruptions of intermediate and felsic magma typically start with a Plinian or sub-plinian explosive phase, which either ends abruptly or evolves into mild explosive behaviour and then into effusive behaviour. In the Icelandic volcanology litera-

ture these are known as explosive and mixed eruptions respectively (Thordarson and Larsen, 2007). We denote the duration of a single explosive eruption as d_1 (Fig. 3.7). If a series of two or more discrete explosive eruptions occur then the duration of the entire explosive sequence is denoted as d_2 (Fig. 3.7). Mixed eruptions begin with an explosive phase of duration d_{3a} leading into an effusive phase of duration d_{3b} , and have an entire duration d_4 (Fig. 3.7). Where a succession of two or more of these mixed eruptions occur then the total duration of that eruptive sequence is denoted as d_5 (Fig. 3.7).

The explosivity of eruptions of mafic magmas in Iceland (basalt *sensu lato*) is heavily influenced by the degree to which external water interacts with the magma (Vogfjörð et al., 2005). Eruptions through seawater, groundwater or ice can favour violent explosive phreatomagmatic eruptions of basaltic magma which would otherwise erupt in an effusive style or with Hawaiian fire-fountaining or Strombolian activity if the vent had been dry. This reflects a more general point that the phenomena used to classify the style of an eruption are often determined by conditions in or just below the vent, whereas the processes that determine eruption duration are likely to be associated with deeper sub-surface aspects of the system such as those controlling the rate at which over-pressure is released from a magma chamber. The duration of a single continuous eruption of basalt is designated d_6 (Fig. 3.7) irrespective of the detailed eruptive style. Sequences of basaltic eruptions ('fires') lasting several years are common on Iceland during prolonged rifting events (Thordarson and Larsen, 2007) and the total duration of a period of fires is denoted as d_7 (Fig. 3.7). It is worth noting that the duration of individual basaltic eruptions within a longer eruptive sequence are designated d_6 .

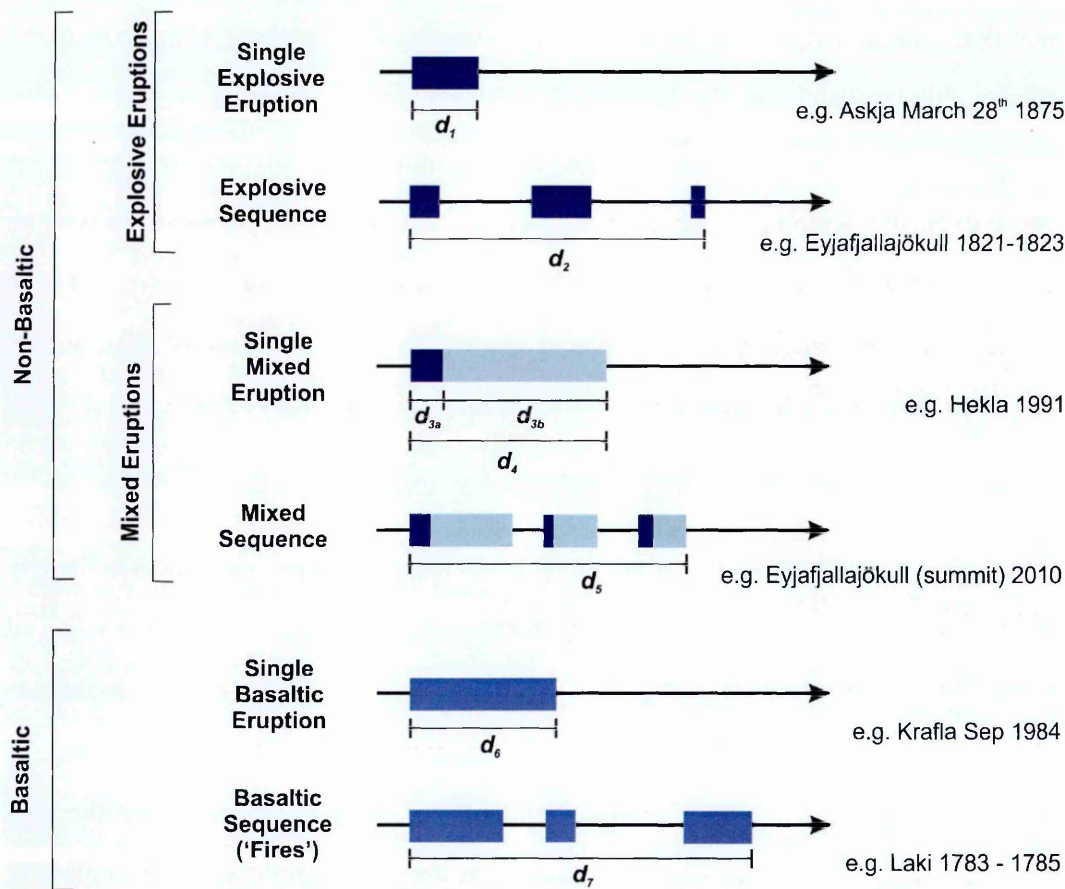


Fig. 3.7 Schematic diagram showing six different eruption types identified within the Iceland dataset and the durations which describe them. These depend on the chemical composition of the magma, the temporal resolution of the activity and its eruptive style. Non-basaltic eruptions are separated into phases of explosive and effusive activity (dark and pale shades respectively). Such segregation is considered unnecessary for basaltic eruptions. In each scenario the black arrow represents time

3.4.2 The eruption duration dataset of Iceland

A catalogue of historic eruption durations dating back to 1300 AD was collated from the primary literature for Iceland. Eruptions from the Bårðarbunga volcanic system were excluded due to uncertainties about their location, duration or status as a true eruption. The initial dataset contained 163 eruptions (listed in Appendix D) which were then critically assessed according to the methods described in subsection 2.1.2, leaving a dataset of 54 eruptions with durations that were considered reliable and carrying acceptably small duration uncertainties (subsection 2.1.2).

Table 3.5 includes eruptions from the eight volcanic systems (Askja, Eyjafjallajökull, Grímsvötn, Hekla, Katla, Krafla, Öraefajökull and Vestmannaeyjar) outlined in subsection 1.3.4 and shown in blue on Fig. 1.4. Eruptions from a further four volcanic systems (Brennisteinfjöll, Krýsuvík, Kverkfjöll and Torfajökull) have erupted historically but were excluded due to insufficient information regarding their eruption start and/or end dates.

Eruptions were classified according to the scheme in Figure 3.7 on the basis of magma composition and the way in which the eruption progressed. Thus the durations of single basaltic eruptions were equated to d_6 whereas the durations of all other eruptions were described by one or more of the parameters d_1 to d_5 depending on the descriptions of the eruptions or their deposits. The total durations of Fires (d_7) were taken from Thorarson and Larsen (2007) and in some cases refined from known eruption dates. These are displayed in Tables 3.5 (d_1 - d_6) and 3.6 (d_7). Eruptions that involved mixed or hybrid magmas between basaltic and non-basaltic compositions (Askja March 1875, Eyjafjallajökull April 2010; #19 and #53 in Table 3.5 respectively) were treated as ‘non-basaltic’. This enables the set of basaltic eruptions d_6 to only contain eruptions whose energetics were unlikely to involve the complex time-dependent changes in viscosity or gas exsolution that can be anticipated to occur during mixed magma eruptions. Appendix D contains information about the duration type of each eruption including the source used for information regarding magma composition.

Table 3.5: Eruptions from Iceland with known durations 1300-2012

#	System	Start Date	End Date	Duration	Duration U/C			d-type
					Start	End	Tot	
1	Hekla	11-07-1300	15-07-1301	1	+0.5 -0.5	+15 -15	+15.5 -15.5	d_4
2	Hekla	05-05-1554	15-06-1554	1	+5 -5	+15 -15	+20 -20	d_6
3	Hekla	03-01-1597	15-07-1597	1;2	+0.5 -0.5	+15 -15	+15.5 -15.5	d_4
4	Hekla	08-05-1636	15-05-1637	1;2	+0.5 -0.5	+15 -15	+15.5 -15.5	$(d_{3a})d_4$
5	Grímsvötn	20-12-1684	10-01-1685	3	+0.5 -0.5	+0.5 -0.5	+1 -1	d_6
6	Hekla	13-02-1693	01-11-1693	1	+0.5 -30	+45 -45	+45.5 -75	$(d_{3a})d_4$
7	Öræfajökull	05-08-1727	15-04-1728	4	+5 -5	+15 -15	+20 -20	d_4
8	Krafla	10-07-1746	10-07-1746	5	+0.02 -0.02	+0.02 -0.02	+0.04 -0.04	d_6
9	Katla	17-10-1755	13-02-1756	7	+0.5 -0.5	+0.5 -0.5	+1 -1	d_6
10	Hekla	05-04-1766	01-05-1768	1;2	+30 -30	+0.5 -0.5	+30.5 -30.5	$(d_{3a})d_4$

Continued on next page...

Table 3.5 – Continued

#	System	Start Date	End Date	Duration	Duration U/C			
					Start	End	Tot d-type	
11	Grímsvön	08-06-1783	07-02-1784	8;9;10	244	+0.5 -0.5	+1 -1	d_6
12	Eyjafjallajökull	15-12-1821	01-02-1823	11 <i>see Appendix D</i>	427	+15 -15	+30 -30	d_2
13	Katla	26-06-1823	23-07-1823	6;7	27	+0.5 -0.5	+0.5 -0.5	d_6
14	Hekla	02-09-1845	05-04-1846	1;2;4;12	(0.17) 215	+0.5 -0.5	+5 -2	$(d_{3a}) d_4$
15	Katla	08-05-1860	27-05-1860	6;7	19	+0.5 -0.5	+0.5 -0.5	d_6
16	Grímsvön	08-01-1873	25-01-1873	3	17	+0.5 -0.5	+0.5 -0.5	d_6
17	Askja	18-02-1875	25-02-1875	13;14	7	+0.5 -0.5	+0.5 -0.5	d_6
18	Askja	10-03-1875	23-03-1875	13;14;15	13	+0.5 -0.5	+1 -0.5	d_6
19	Askja	28-03-1875	29-03-1875	1;4;13;14;15 16;17;18;19	0.6	+0.02 -0.02	+0.02 -0.02	d_1
20	Askja	04-04-1875	15-04-1875	13;14 <i>see Appendix D</i>	11	+0.5 -0.5	+5 -4	d_6
21	Askja	15-08-1875	17-10-1875	20	63	+0.5 -0.5	+0.5 -0.5	d_6

Continued on next page...

Table 3.5 – Continued

#	System	Start Date	End Date	Duration	Duration U/C			d-type
					Start	End	Tot	
22	Hekla	27-02-1878 ²	15-04-1878 ²	47	+0.5 -0.5	+15 -15	+15.5 -15.5	d_6
23	Grímsvön	15-01-1883 ³	15-04-1883 ³	90	+0.5 -0.5	+5 -5	+5.5 -5.5	d_6
24	Hekla	25-04-1913 ²	18-05-1913 ²	23	+0.5 -0.5	+0.5 -0.5	+1 -1	d_6
25	Katla	12-10-1918 ^{6;7;22}	04-11-1918 ^{7;22}	23	+0.5 -0.5	+0.5 -0.5	+1 -1	d_6
26	Grímsvön	30-03-1934 ^{3;22}	11-04-1934 ^{3;22}	12	+0.5 -0.5	+4 -4	+4.5 -4.5	d_6
27	Hekla	29-03-1947 ^{1;23;24;25}	22-04-1948 ²⁷	(0.04) 390	+0.5 -0.5	+3 -1	+3.5 -1.5	$(d_{3a}) d_4$
28	Katla	25-06-1955 ²²	25-06-1955 ²²	0.5	+0.02 -0.02	+0.02 -0.02	+0.04 -0.04	d_6
29	Askja	26-10-1961 ¹⁶	17-12-1961 ¹⁶	52	+0.5 -0.5	+0.5 -12	+1 -12.5	d_6
30	Vestmannaeyjar	06-11-1963 ^{27;28}	30-04-1964 ^{27;29;30}	176	+0.5 -0.5	+0.5 -0.5	+1 -1	d_6
31	Vestmannaeyjar	09-06-1964 ^{27;30;31}	17-10-1965 ^{27;29;31;32}	495	+0.5 -0.5	+0.5 -0.5	+1 -1	d_6
32	Vestmannaeyjar	26-12-1965 ^{27;30}	05-06-1967 ^{27;30;33}	526	+0.5 -0.5	+0.5 -0.5	+1 -1	d_6

Continued on next page...

Table 3.5 – Continued

#	System	Start Date	End Date	Duration	Duration U/C			d-type
					Start	End	Tot	
33	Hekla	05-05-1970	05-07-1970	2;12;34 (0.1) 61	+0.5 -0.5	+5 -5	+5.5 -5.5	$(d_{3a}) d_4$
34	Vestmannaeyjar	23-01-1973	26-06-1973	35;36;37 38	+0.5 -0.5	+0.5 -0.5	+1 -1	d_6
35	Krafla	20-12-1975	20-12-1975	5;39;40	+0.02 -0.02	+0.02 -0.02	+0.04 -0.04	d_6
36	Krafla	27-04-1977	27-04-1977	39;40;41	+0.02 -0.02	+0.02 -0.02	+0.04 -0.04	d_6
37	Krafla	08-09-1977	08-09-1977	29;39;41;42	+0.02 -0.02	+0.02 -0.02	+0.04 -0.04	d_6
38	Krafla	16-03-1980	16-03-1980	29;43	+0.02 -0.02	+0.02 -0.02	+0.04 -0.04	d_6
39	Krafla	10-07-1980	18-07-1980	29	+0.5 -0.5	+0.5 -0.5	+1 -1	d_6
40	Hekla	17-08-1980	20-08-1980	12;34 (0.08) 3	+0.5 -0.5	+0.5 -0.5	+1 -1	$(d_{3a}) d_4$
41	Krafla	18-10-1980	23-10-1980	29;39	+0.5 -0.5	+0.5 -0.5	+1 -1	d_6
42	Krafla	30-01-1981	04-02-1981	29;39;44	+0.5 -0.5	+0.5 -0.5	+1 -1	d_6
43	Hekla	09-04-1981	16-04-1981	12;34	+0.5 -0.5	+0.5 -0.5	+1 -1	d_4

Continued on next page...

Table 3.5 – Continued

#	System	Start Date	End Date	Duration	Duration U/C				
					Start	End	Tot d-type		
44	Krafla	18-11-1981	23-11-1981	29;39	5	+0.5 -0.5	+1 -1	d_6	
45	Grímsvötn	28-05-1983	01-06-1983	45;46	4	+0.5 -1	+1 -0.5	+1.5 -1.5	d_6
46	Krafla	04-09-1984	18-09-1984	29	14	+0.5 -0.5	+0.5 -0.5	+1 -1	d_6
47	Hekla	17-01-1991	11-03-1991	34;48;50;51	(0.4) 53	+0.5 -0.5	+0.5 -0.5	+1 -1	$(d_{3a}) d_4$
48	Gjálp	30-09-1996	13-10-1996	22;52;53;54;55 56	13	+0.5 -0.5	+0.5 -0.5	+1 -1	d_6
49	Grímsvötn	18-12-1998	28-12-1998	54	10	+0.5 -0.5	+0.5 -0.5	+1 -1	d_6
50	Hekla	26-02-2000	08-03-2000	50;57;58;59	(0.2) 11	+0.5 -0.5	+0.5 -0.5	+1 -1	$(d_{3a}) d_4$
51	Grímsvötn	01-11-2004	06-11-2004	60;61;62	5	+0.5 -0.5	+0.5 -0.5	+1 -1	d_6
52	Eyjafjallajökull	20-03-2010	12-04-2010	63;64;65;66;67	23	+0.5 -0.5	+0.5 -0.5	+1 -1	d_6
53	Eyjafjallajökull	14-04-2010	22-05-2010	63;65;66;67;68 69;70;71;72	38	+0.5 -1	+2 -0.5	+2.5 -1.5	d_5
54	Grímsvötn	21-05-2011	28-05-2011	73	7	+0.5 -0.5	+0.5 -0.5	+1 -1	d_6

U/C = uncertainty. d-type = The duration type according to Fig. 3.7,

Units: durations and duration uncertainties = days,

Footnote continued on following page...

Footnote for Table 3.5 continued...

Grey numbers represent the following references: ¹ Thorarinsson (1967a), ² Thorarinsson et al. (1970), ³ Þórarinnsson (1974), ⁴ Thorarinsson (1958), ⁵ Thorarinsson (1979), ⁶ Eliasson et al. (2006), ⁷ Þórarinnsson (1975), ⁸ Thordarson and Self (1993), ⁹ Thordarson and Self (2003), ¹⁰ Thordarson et al. (2003), ¹¹ Larsen (1999), ¹² Grönvold et al. (1983), ¹³ Sigurdsson and Sparks (1978), ¹⁴ Sparks et al. (1981), ¹⁵ Sigurdsson and Sparks (1981), ¹⁶ Thorarinsson and Sigvaldason (1962), ¹⁷ Lupi et al. (2011), ¹⁸ Carey et al. (2010), ¹⁹ Hartley and Thordarson (2013), ²⁰ Thoroddsen (1925), ²¹ Grimsstaðir (1875), ²² Gudmundsson (2005), ²³ Þórarinnsson (1950), ²⁴ Þórarinnsson (1954), ²⁵ Þórarinnsson (1976), ²⁶ Einarsson (1949), ²⁷ Thorarinsson (1967c), ²⁸ Thordarson and Sigmarsson (2009), ²⁹ Sturkell et al. (2009), ³⁰ Thorarinsson (1965), ³¹ Thorarinsson (1966), ³² Thorarinsson (1967b), ³³ Thorarinsson (1968), ³⁴ Tryggvason (1994), ³⁵ Thorarinsson et al. (1973), ³⁶ Einarsson and Boucher (1974), ³⁷ Olafsson (1975), ³⁸ Jakobsson et al. (2008), ³⁹ Einarsson (1991), ⁴⁰ Harris et al. (2000), ⁴¹ Björnsson et al. (1979), ⁴² Brandsdóttir and Einarsson (1979), ⁴³ Tryggvason (1980), ⁴⁴ Tryggvason (1984), ⁴⁵ Grönvold and Jóhannesson (1984), ⁴⁶ Einarsson and Brandsdóttir (1984), ⁴⁷ Rossi (1997), ⁴⁸ Gudmundsson et al. (1992), ⁴⁹ Larsen et al. (1992), ⁵⁰ Haraldsson and Ólafsdóttir (2002), ⁵¹ Soosalu et al. (2003), ⁵² Einarsson et al. (1997), ⁵³ Gudmundsson et al. (1997), ⁵⁴ Sigmarsson et al. (2000), ⁵⁵ Steinhórnsson et al. (2000), ⁵⁶ Gudmundsson et al. (2004), ⁵⁷ Haraldsson et al. (2002), ⁵⁸ Ólafsdóttir et al. (2002), ⁵⁹ Höskuldsson et al. (2007), ⁶⁰ Vogfjörð et al. (2005), ⁶¹ Witham et al. (2007), ⁶² Jude-Eton et al. (2012), ⁶³ Sigmundsson et al. (2010), ⁶⁴ Donovan and Oppenheimer (2011), ⁶⁵ Sigmarsson et al. (2011), ⁶⁶ Edwards et al. (2012), ⁶⁷ Gudmundsson et al. (2012), ⁶⁸ Gudmundsson et al. (2010), ⁶⁹ Arason et al. (2011), ⁷⁰ Stevenson et al. (2012), ⁷¹ Karlsdóttir et al. (2012), ⁷² Woodhouse et al. (2013), ⁷³ Tesche et al. (2012).

3.4.3 Additional information on specific eruptions from Icelandic volcanic systems

Contemporary reports and tephrochronological investigations of the 1636 Hekla eruption (#4, Table 3.5) indicate that its initial phase was not particularly explosive and as such the volume of tephra produced was considerably less ($20 \times 10^6 \text{ m}^3$ as DRE) than other mixed eruptions from Hekla (Thorarinsson, 1967a). The tephra that was produced has a SiO_2 content of 58.28 wt % (Thorarinsson, 1967a). Thordarson and Larsen (2007) classify the 1636 eruption as a mixed eruption from Hekla, and this in

Table 3.6: Icelandic fires with known durations (d_7)

ID	Fire Name	Start Date		End Date		Duration		U/C
						(days)	(years)	
A	Eldjá	01-07-934	^{1;2}	01-07-940	²	2192	6.0	±365
B	Mývatnseldar	01-07-1724	¹	01-07-1729	¹	1826	5.0	±365
C	Laki	08-06-1783	³	26-05-1785	^{1;3}	718	2.0	±1
D	Tröllahraun	01-07-1862	^{1;4}	01-07-1864	^{1;4}	731	2.0	±365
E	Askja	01-01-1875	⁵	20-10-1875	⁵	292	0.8	±1
F	Askja Fires	01-07-1921	¹	01-07-1929	¹	2922	8.0	±365
G	Surtsey	06-11-1963	^{6;7}	05-06-1967	^{6;8;9}	1307	3.6	±1
H	Krafla Fires	20-12-1975	¹	18-09-1984	¹	3195	8.8	±1

U/C represents the maximum possible duration uncertainty (in days) assigned according to the method in Table 2.1.

Grey numbers following dates represent the following references: ¹ Thordarson and Larsen (2007), ² Thordarson et al. (2001), ³ Thordarson and Self (1993), ⁴ Jónsson et al. (1997), ⁵ Sparks et al. (1981), ⁶ Thorarinsson (1967c), ⁷ Thordarson and Sigmarsson (2009), ⁸ Thorarinsson (1967b), ⁹ Thorarinsson (1968).

conjunction with the non-basaltic nature of the tephra produced has led to the same classification being adopted here. A duration for the initial explosive phase of the eruption however is not provided.

The course of the basaltic 1783-1784 Laki eruption of Grímsvötn has been reconstructed from remarkable eye witness accounts and geological studies of the deposits (Thordarson and Self, 1993; Thordarson et al., 2003; Thordarson and Self, 2003). The fissure eruption occurred from migrating vents between 8 June 1783 and 7 February 1784 (#11, Table 3.5) with activity waxing and waning between periods of high lava fountaining and subdued lava effusion. This, along with descriptions of earthquake occurrences, allows the activity to be split into episodes of heightened eruptive activity (Thordarson and Self, 1993; Thordarson et al., 2003). Nonetheless, the historical accounts strongly suggest that magma discharge was continuous throughout the 244 days, albeit at highly variable rates (Thordarson et al., 2003) and we suspect that any breaks in activity lasted less than 10 days. As a result, the Laki event is considered to be a single basaltic eruption with a (d_6) duration of 244 days.

At least six eruptions from Grímsvötn central volcano occurred during the Laki fissure eruption and two followed shortly after (Thordarson et al., 2003; Thordarson and Self, 2003). We include these in a period of fires at the Grímsvötn system lasting from the start of the Laki eruption (8 June 1783) until 26 May 1785 (a total of 718 days listed as d_7 in Table 3.6).

Some uncertainty surrounds the nature of the 1821-1823 eruption of Eyjafjallajökull (#12, Table 3.5), which produced several distinct tephra fall deposits of trachytic to rhyolitic composition in three 1 to 25 day bursts (Larsen, 1999; Larsen et al., 1999; Karlsdóttir et al., 2012). This suggests that the eruption consisted of either a sequence of explosive eruptions ($d_2 = 427$ days) or was a mixed eruption, with prolonged, unrecognised effusive activity disrupted by intermittent phreatomagmatic explosions driven by the sub-glacial setting of the vent ($d_4 = 427$ days). Although both interpretations are feasible, the former interpretation is more reasonable given the apparent lack of a major opening explosive phase that characterises mixed eruptions (as defined by Thordarson and Larsen (2007)).

A period of fires is reported for Askja in 1875 and its total duration is listed as d_7 in Table 3.6. Two eruptive phases within this sequence of eruptions occurred in March 1875, the first of these produced basaltic fire fountains and lava, whereas the latter was a rhyolite and mixed basalt Plinian eruption lasting only one day (Thorarinsson, 1958; Thorarinsson and Sigvaldason, 1962; Sigurdsson and Sparks, 1978; Sparks et al., 1981; Carey et al., 2010; Lupi et al., 2011; Hartley and Thordarson, 2013). The different styles of activity of these two eruptions have led us to classify them as a single basaltic eruption with a d_6 duration of 13 days and a single explosive eruption with a d_1 duration of 0.5 days respectively. They are therefore included in Table 3.5 as two separate eruptions (#18 and #19) despite the period of quiescence between the two being less than 10 days.

Table 3.5 includes the inferred sub-glacial eruption of Katla in 1955 (#28) on the basis

of the pattern of jökulhlaup, seismic and ice-deflation activity (Gudmundsson, 2005). This is generally accepted as a definite basaltic eruption but less distinctive episodes of unrest at Katla on 18 July 1999 (Sturkell, 2003) and 9 July 2011 (Ofeigsson et al., 2011) are still a matter of debate and are therefore not included in Table 3.5 (Dugmore et al., 2013).

The 1963-1967 eruption of Vestmannaeyjar started on the ocean bottom and the vents shifted between various submarine and surface locations, with the style and vigour of eruptions changing through time (Thorarinsson, 1967b; Thordarson and Sigmarsson, 2009). Close inspection of historical records suggest that the eruption can be split into three eruptive phases; 6 November 1963 to 30 April 1964, 9 June 1964 to 17 October 1965 and 26 December 1965 to 5 June 1967. Each of these is separated by a period of quiescence of longer than 10 days and they are therefore included in Table 3.5 as three separate eruptions (#30, #31 and #32), rather than as a period of continuous magma effusion with a d_6 duration of 1307 days. An alternative view (Thordarson and Larsen, 2007) is that the activity represents a fire event with duration 1307 days, we include this in our d_7 dataset.

The 1973 (Eldfell; #34, Table 3.5) eruption of Vestmannaeyjar produced hawaiite, trachybasalt and basalt. Previous authors have proposed that this eruption belongs in the mixed eruption category due to its products containing a relatively high proportion of tephra (Thorarinsson et al., 1973; Jakobsson, 1979; Furman et al., 1991; Thordarson and Larsen, 2007). However, the eruption lacked the initial sub-Plinian or Plinian phase which characterises the archetypal mixed eruptions recognised at Hekla and displayed fire-fountaining, Strombolian and effusive behaviours (with superimposed Surtseyan activity when the vents were below sea level) typical of basaltic eruptions. This eruption is therefore assigned to the single basaltic eruption category and its duration is given a d_6 value.

The Gjálp-1996 eruption (#48, Table 3.5) occurred at a fissure under the Vatnajökull

icecap between the Grímsvötn and Bárðarbunga volcanic systems and, as a result, some debate exists over which volcanic system the eruption can be accredited to (Einarsson et al., 1997; Gudmundsson et al., 1997, 2004; Sigmarsson et al., 2000; Steinthorsson et al., 2000; Gudmundsson, 2005). All of the premonitory activity was in Bárðarbunga and there was no deflation of the Grímsvötn system during the eruption, a feature that accompanied the 1998, 2004 and 2011 Grímsvötn eruptions (Einarsson et al., 1997; Sigmarsson et al., 2000; Pagli et al., 2007). In contrast, the isotopic and trace element signature of the eruptive products are more closely related to the Grímsvötn volcanic system (Sigmarsson et al., 2000). To account for this uncertainty this eruption is referred to as Gjálp in this study and is not assigned to a specific volcanic system. Although the eruptive products had 52-53 wt% SiO₂ and were therefore not basalt *sensu stricto* (Sigmarsson et al., 2000; Steinthorsson et al., 2000) the eruption was not notably different from eruptions of magma with SiO₂ contents less than 52 wt% and therefore here this eruption is considered a single basaltic eruption and its duration is given a d_6 value.

The 2010 Eyjafjallajökull activity is comprised of two eruptions; the first from the Fimmvöruðuháls flank fissure commencing on 20 March 2010 and the second from Eyjafjallajökull's summit commencing on 14 April 2010. Despite the period of inactivity between these two eruptions being less than 2 days, they are kept as separate eruptions in this study due to their clearly very different locations, magma composition and eruption styles (#53 and #54, Table 3.5).

The summit eruption of Eyjafjallajökull (#53, Table 3.5) was intensely monitored throughout, yet some uncertainty still exists regarding its end date. Recent publications favour an end date of 22 May 2010 (Gudmundsson et al., 2010, 2012; Edwards et al., 2012; Karlsdóttir et al., 2012; Stevenson et al., 2012; Woodhouse et al., 2013) and thus indicate a duration of continuous activity of 38 days. However, less energetic explosive activity involving minimal magma and generating limited ash fall (Edwards

et al., 2012; Gudmundsson et al., 2012; Karlsdóttir et al., 2012) occurred at the vent in June and continued until 11 June 2010 when the Nordic Volcanological Institution’s activity report (Nordic Volcanological Center, 2013) stated that ‘no magma is being erupted’ and that activity at the vent was ‘confined to steaming’. If the total duration of the Eyjafjallajökull summit eruption is considered to include this longer period of activity the resultant duration would be extended to 58 days. Given the wealth of publications quoting the shorter duration and our definition that eruptions separated by periods of quiescence of longer than 10 days are classified as separate eruptions a duration of 38 days is also used here.

The 2010 Eyjafjallajökull summit eruption produced trachyandesites formed by mixing basaltic and silicic magmas (Sigmarsson et al., 2011). Gudmundsson et al. (2012) and Karlsdóttir et al. (2012) provide good descriptions of the activity throughout this eruption, and recognise four phases of differing activity. The initial four days of the eruption was characterised by explosive activity most probably augmented by ice interaction (Sammonds et al., 2010; Sigmundsson et al., 2010; Arason et al., 2011; Gudmundsson et al., 2012; Karlsdóttir et al., 2012; Stevenson et al., 2012). This was followed by a dominantly effusive phase before a second explosive phase lasting from 5 to 17 May 2010 (Gudmundsson et al., 2012; Karlsdóttir et al., 2012; Woodhouse et al., 2013). The transition of explosive to effusive activity is characteristic of mixed eruptions, however, here the presence of a second explosive phase indicates that this eruption may represent a sequence of mixed eruptions with total duration d_5 .

3.4.4 The completeness of the Icelandic eruption record

Iceland is a small country with few people, many of whom live along the coast. As a result, the interior of the country is remote and volcanic activity from volcanic systems situated there is poorly known. Furthermore, for sub-glacial volcanoes, it takes

a substantial eruption to break through the overlying ice, and often this is the necessary evidence required to be certain that an eruption occurred (Larsen, 2002; Vogfjörð et al., 2005). Even when the occurrence of a volcanic eruption is known, information regarding its duration may not have been available or recorded. Fig. 3.8a shows the population of Iceland on 1 January every 5 years for the period 1735-2010 (data from Statistics Iceland (2013)) demonstrating its increasing population especially through the 20th century.

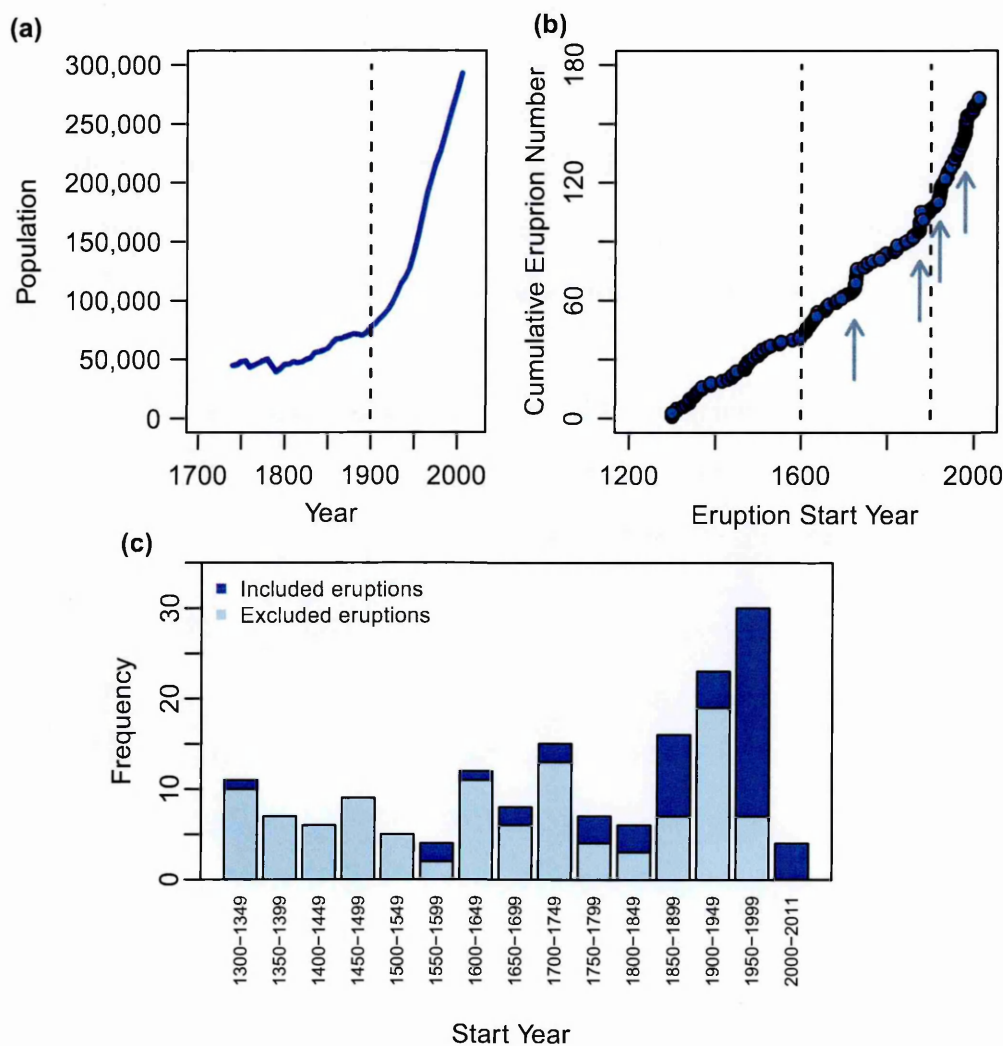


Fig. 3.8 (a) Plot of Icelandic population against Year (data from Statistics Iceland (2013)) Vertical dashed line represents the year 1900. (b) Plot of cumulative eruption number against eruption start year of all 163 eruptions reported between 1300 and 2012. Vertical dashed lines represent the years 1600 and 1900, arrows point to periods of very high eruption frequency. (c) Bar plot showing the frequency of reported eruptions in 50 year periods

Previous authors have suggested that the documentation of eruptions on Iceland began to increase after 1600 AD (Thordarson and Larsen, 2007; Thordarson and Höskuldsson, 2008). Fig. 3.8b plots cumulative eruption number against start year for the 163 eruptions considered in this study while Fig. 3.8c shows the frequency of eruptions reported at 50 year intervals and the proportion of those in each case with reliable durations and thus included in Table 3.5. Both plots demonstrate the scarcity of data in the period 1300-1599 with only 42 eruptions reported. The frequency of eruptions appears to increase through 1600-1799, however, the proportion of these eruptions with reliable durations is still low (Fig. 3.8b and c).

The period 1900-2011 is characterised by an increasing population (Fig. 3.8a) which is reflected in both the frequency of eruptions reported and the proportion of eruptions with known durations increasing from 34 % (1600-1899) to 56 % (1900-2011) (Fig. 3.8b and c). Furthermore, the excluded eruptions are mainly from the sub-glacial volcanic systems of Grímsvötn and Kverkfjöll and from Askja which is situated in a remote region of the central highlands. Despite the increasing overall population of Iceland these regions are still poorly populated.

Four periods of very high eruption frequency can be observed in Fig. 3.8b and are highlighted by arrows. These represent individual eruptive episodes within longer sequences of basaltic eruptions. In particular they refer to Mývatnseldar (Krafla, 1724-1729), Askja (1875), Askja fires (1921-1929) the end of the Krafla fires (1975-1984) (B, E, F and H, Table 3.6 respectively).

Fig. 3.9 plots eruption duration against eruption start year. It clearly shows the very poor reporting of eruption durations prior to the year 1600 and a gradual increase in the range of reported durations since then through to present day. This is particularly evident for single basaltic eruptions. Prior to 1900, short basaltic eruptions that would have made little impact on surrounding areas are under-represented (Fig. 3.9) reflecting an early reporting bias towards larger and more explosive eruptions, particularly in

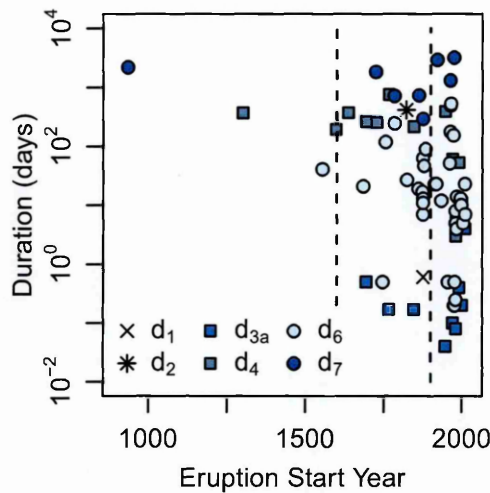


Fig. 3.9 Plot of eruption duration (on a log scale) against start year for the eruptions within Tables 3.5 and 3.6 separated into the different duration types outlined in Fig. 3.7. Vertical dashed lines represent the years 1600 and 1900

sparsely populated regions (Thordarson and Larsen, 2007).

The above analyses demonstrate that reporting bias on Iceland is volcano specific and is largely determined by the population density of the areas surrounding the volcanic system and the style of volcanic activity that it displays. Although advances in geophysical monitoring and remote sensing in recent years can be expected to have reduced the number of undetected volcanic eruptions at very remote or sub-glacial volcanic systems, we still cannot be entirely sure that very small eruptions have not gone unnoticed (For example the potential eruption at Katla in July 2011 is still a matter of debate). For the purpose of this study a single year beyond which the eruption record for Iceland as a whole can be considered complete is not defined. Instead, the entire dataset of eruptions from 1300-2011 will be used in this study and the reporting biases that they contain discussed throughout.

Chapter 4

Investigating the distribution of eruption durations at Mt. Etna, Kilauea, Piton de la Fournaise and Iceland



A fundamental assumption of any investigation using historical eruption data as an insight into future activity is that the character of past eruptions is a good indication of future activity (Chester et al., 1985; Behncke and Neri, 2003; Behncke et al., 2005; Cappello et al., 2013). This chapter considers the appropriateness of this assumption for the data introduced in Chapter 3. It begins by assessing the effect of individual eruption duration uncertainty on the general distribution of eruption duration and

then investigating any temporal or spatial variation within each dataset. To determine whether any variations are significant Log-rank tests, Mann-Whitney tests and t -tests are performed on groups of data using the methods outlined in section 2.2.

4.1 The effect of individual eruption duration uncertainty on the overall distribution of eruption duration

Every eruption considered in this study carries some duration uncertainty (subsection 2.1.2). This study often focuses on overall distributions of eruption duration and it is important to assess how sensitive these distributions are to the uncertainties associated with the individual eruption durations that they contain.

The total duration uncertainty of each eruption is reported in Tables 3.1 (Etna), 3.2 (Kilauea), 3.3 (PdlF), 3.5 (Iceland d_4 and d_6) and 3.6 (Iceland d_7) and it is these values which are used to calculate the maximum and minimum possible duration of each eruption. Due to the method of uncertainty assignment (subsection 2.1.2) eruptions with 1 day durations automatically carry duration uncertainties of ± 1 day, and thus the calculated minimum possible eruption duration is 0 days. For an eruption to have occurred it must have a positive duration, therefore where the minimum possible eruption duration calculated is 0 days a duration of 0.04 days (1 hour) is used for the purpose of this investigation.

Fig. 4.1 shows empirical survivor function plots for (a) Etna, (b) Kilauea, (c) PdlF, (d) Iceland d_4 eruptions, (e) Iceland d_6 eruptions and (f) Iceland d_7 eruptions. Each contains the empirical survivor function curve of their preferred eruption durations alongside that for their maximum and minimum possible eruption durations. For Mt.

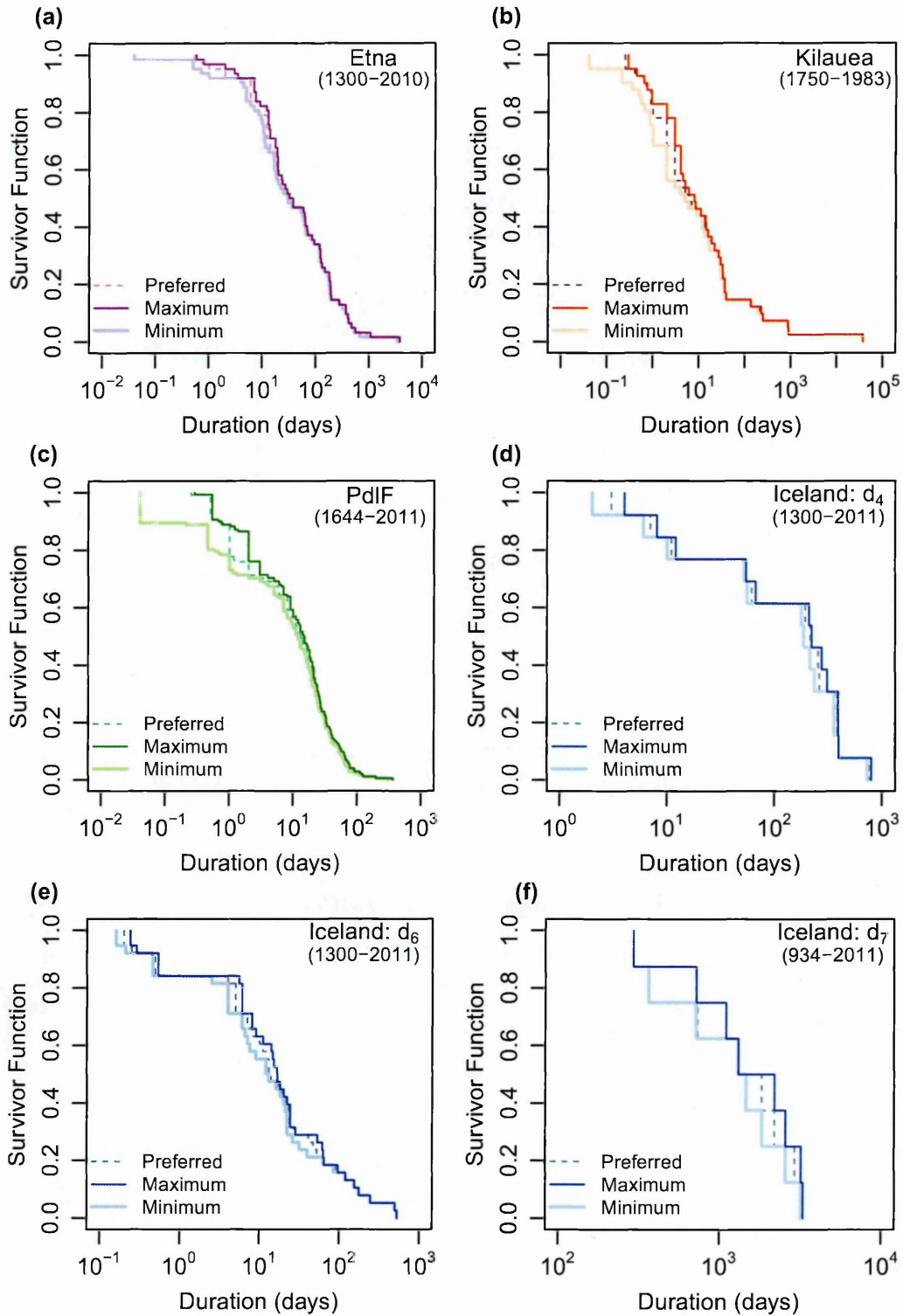


Fig. 4.1 Empirical survivor function plots comparing the distribution of preferred eruption durations from (a) Etna ($n = 62$), (b) Kilauea ($n = 41$), (c) PdIF ($n = 172$), (d) Iceland d_4 eruptions ($n = 13$), (e) Iceland d_6 eruptions ($n = 38$) and (f) Iceland d_7 eruptions ($n = 8$) with that of their maximum and minimum possible eruption durations when uncertainty is taken into account

Etna and the three Icelandic datasets the overall shapes and positions of these empirical survivor functions curves are very similar (Fig. 4.1a, d, e and f). While the same is true for the distribution of maximum and preferred eruption durations at Kilauea and PdIF (Fig. 4.1b and c), the curves for their minimum possible eruption duration data are visually offset at durations of less than a few days.

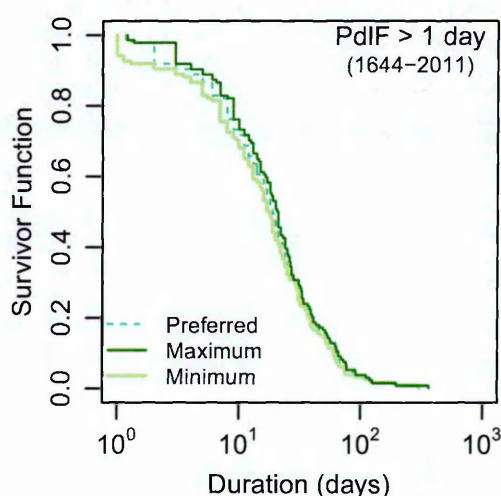


Fig. 4.2 Empirical survivor function plot comparing the distribution of preferred eruption durations > 1 day from PdIF with that of their maximum and minimum possible eruption durations

This offset is primarily due to the proportion of eruptions with durations of 1 day which are not known to the nearest hour. These eruptions carry unavoidably high duration uncertainties. The Kilauea and PdIF data contain 3 and 19 of these eruptions respectively, while Mt. Etna contains only 1 and Iceland does not contain any. The removal of eruptions with durations ≤ 1 day at PdIF results in considerably less variation between the three empirical survivor function curves (Fig. 4.2).

It is therefore concluded that individual eruption duration uncertainty has a negligible effect on the overall distribution of eruption duration. When an effect is observed it applies only to durations ≤ 10 days and is often a direct result of the conservative uncertainty assignment method adopted by this study (subsection 2.1.2). For the remainder preferred values are used for eruption durations and referred to as such.

4.2 The overall distribution of eruption duration

4.2.1 Mt. Etna: 1600-2010

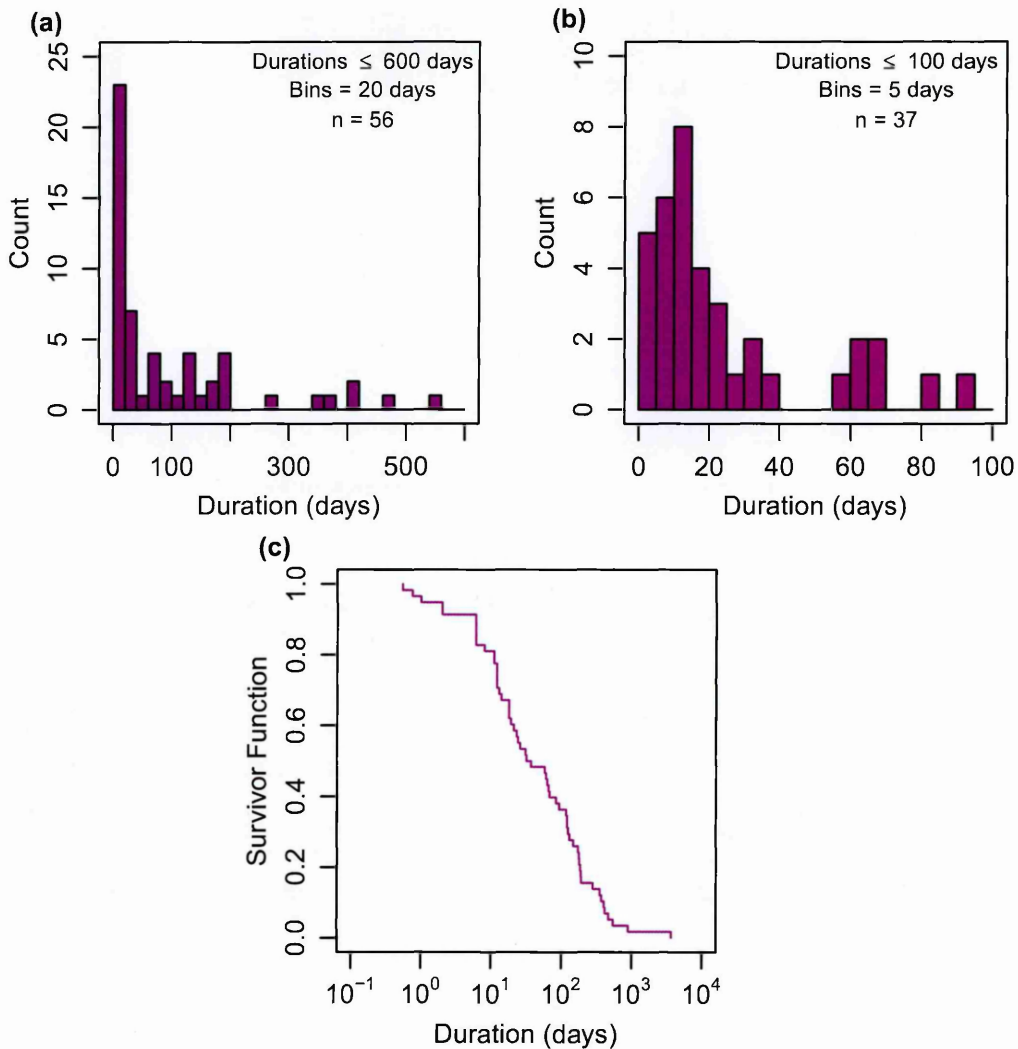


Fig. 4.3 The distribution of flank eruption durations at Mt. Etna for the period 1600-2010 displayed as histograms of (a) durations ≤ 600 days in 20 day bins and (b) durations ≤ 100 days in 5 day bins and (c) data displayed as an empirical survivor function curve (data from Table 3.1)

Reported flank eruption durations at Mt. Etna for the period 1600-2010 (#5 to #62, Table 3.1) range from 0.54 days to 3,653 days with a median duration of 34.5 days. A histogram of the data plotted with bins of 20 days identifies a long duration tail to the distribution (Fig. 4.3a) with 52 % of eruptions having durations of > 40 days. It is

worth noting that two eruptions have durations of greater than 600 days (#6 and #10, Table 3.1 with durations 3,653 and 896 days respectively). Almost 40 % of the data plot within the 0-20 day bin, and when viewed at 5 day bins a slight short duration tail to the data can be observed (Fig. 4.3b). Fig. 4.3c displays the empirical survivor function curve for this data plotted on a log scale allowing both the long and short duration tail of the distribution to be identified.

4.2.2 Kilauea: 1912-1983

Reported eruption durations at Kilauea in the period 1912-1983 (#4 to #41, Table 3.2) range from 0.25 days to 900 days with a median duration of 5.5 days. A histogram of the data plotted with bins of 20 days clearly identifies a heavy long duration tail to the distribution (Fig. 4.4a) with only five eruptions exceeding 50 days, of which two exceed 300 days and the limit of this histogram (#31 and #34, Table 3.2 with durations 874 and 900 days respectively).

A histogram plotted at 2 day bins shows that 31 % of the data have very short durations, plotting in the 0-2 day bin (Fig. 4.4b). A slight short duration tail to the distribution becomes evident at durations < 1 day when displayed as an empirical survivor function curve (Fig. 4.4c).

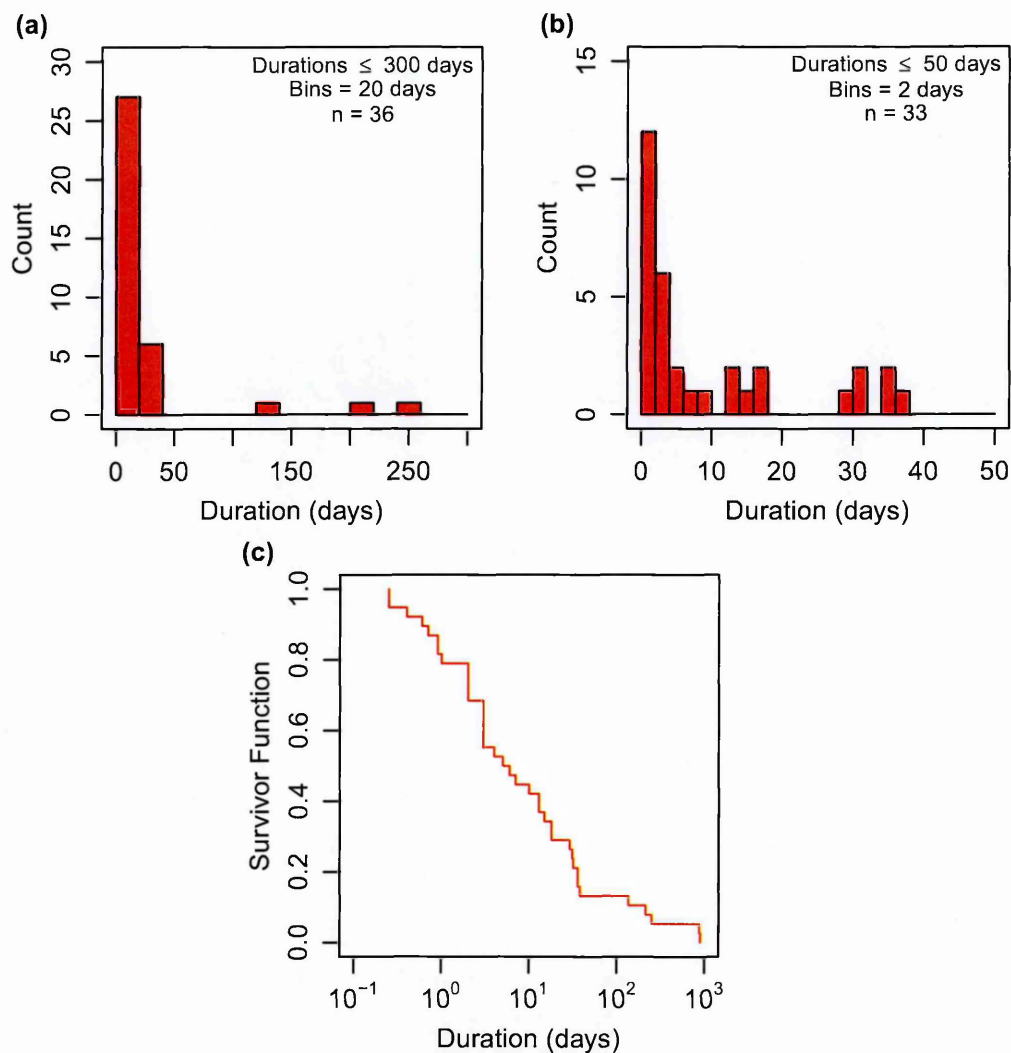


Fig. 4.4 The distribution of eruption durations at Kilauea for the period 1912-1983 displayed as histograms of (a) durations ≤ 300 days in 20 day bins and (b) durations ≤ 50 days in 2 day bins and (c) data displayed as an empirical survivor function curve (data from Table 3.2)

4.2.3 PdlF: 1911-2011

Reported eruption durations at PdlF in the period 1911-2010 (#48 to #172, Table 3.3) range from 0.25 days to 334 days with a median duration of 16 days. A histogram of the data plotted with bins of 10 days clearly identifies a heavy long duration tail to the distribution (Fig. 4.5a) with one eruption not shown on this plot due to its longer duration of 334 days (#87, Table 3.3).

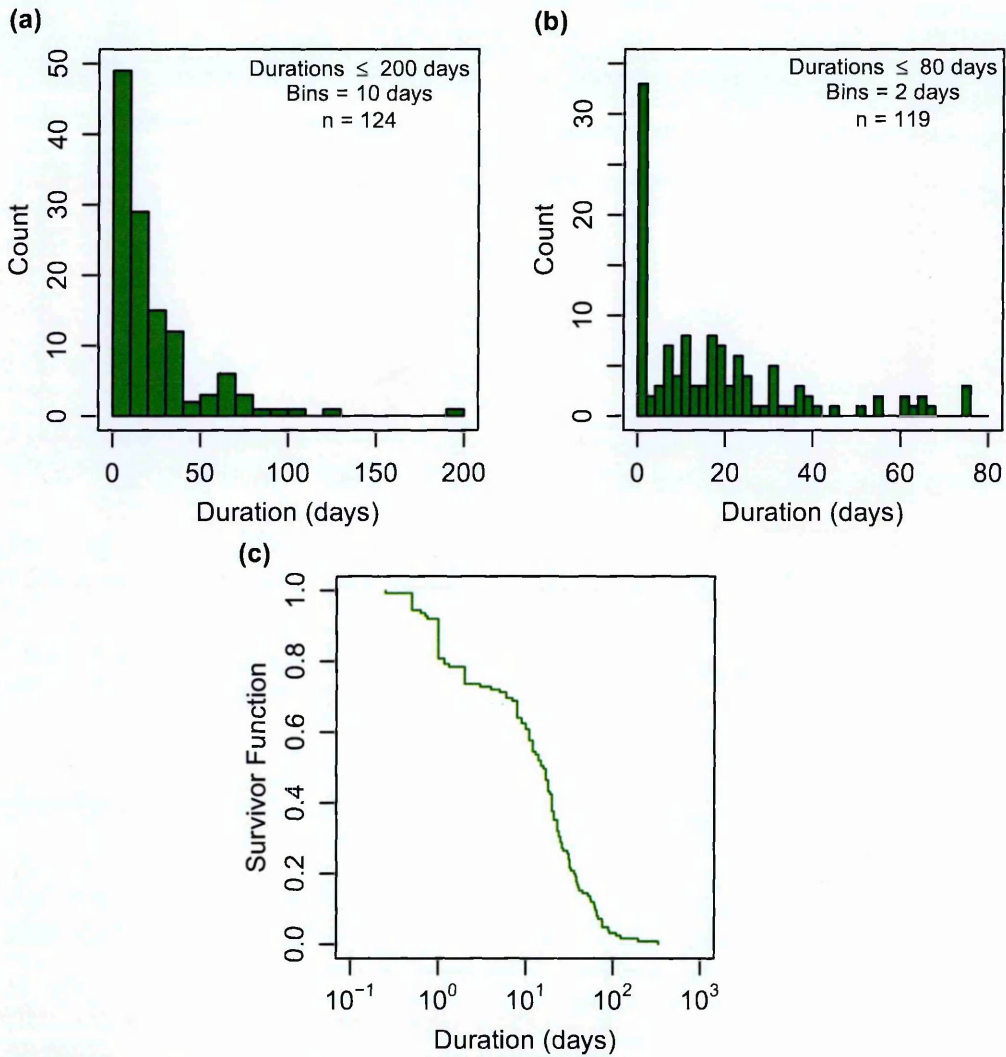


Fig. 4.5 The distribution of eruption durations at PdIF for the period 1911-2011 displayed as histograms of (a) durations ≤ 200 days in 10 day bins and (b) durations ≤ 80 days in 2 day bins and (c) data displayed as an empirical survivor function curve (data from Table 3.3)

The analyses of Stieltjes and Moutou (1989) noted that eruption durations from PdIF were generally short and our data supports this with 84 % of the data having durations of ≤ 40 days, of which 39 % plot within the 0-10 day bin (Fig. 4.5a). When the data is split into 2 day bins a short duration tail to the distribution is not clearly observed but a high proportion of the data plots in the 0-2 day bin and is followed by a broad second hump in the histogram with a peak at approximately 10-16 days (Fig. 4.5b). Fig. 4.5c displays the empirical survivor function curve for this data plotted with duration on a log scale. The shape of this curve is also atypical with an inverse 'S' shape

only being observed at durations > 2 days. This implies a bimodal distribution to the duration data at PdIF, with not only eruptions with durations around the median of the data being common but also a tendency for eruptions to have very short durations (< 2 days). It is important to determine whether these short duration eruptions relate to any patterns or specific scenarios at PdIF. For example if the very short duration eruptions all correspond to the same source region or time period it may imply that a different eruption scenario is responsible for these eruptions. If such a scenario could be identified during the early stages of an eruption, any forecasting models could be modified accordingly. These short duration eruptions will be assessed throughout the remainder of this thesis.

4.2.4 Iceland: 1300-2011

The following section takes each type of eruption duration on Iceland (identified in subsection 3.4.1) in turn and describes the available data.

The duration of explosive (non-basaltic) eruptions (d_1 and d_2) from volcanic systems on Iceland

Most explosive eruptions on Iceland ('explosive' in the sense of Thordarson and Larsen (2007)) develop into effusive eruptions with time, and are thus classified as the explosive phase of a mixed eruption (d_{3a}). Only two purely explosive Icelandic eruptions have known durations: Askja 28-29 March 1875 and Eyjafjallajökull 1821-23 (#19 and #12, Table 3.5 respectively). The first of these represents a single Plinian eruption with a d_1 duration of 0.6 days whereas the Eyjafjallajökull eruption represents a sequence of explosive eruptions with a total (d_2) duration of 427 days. Being the only examples of explosive eruption durations on Iceland further analyses of these types of eruption duration could not be performed.

The duration of mixed eruptions (d_{3a} , d_{3b} and d_4) from volcanic systems on Iceland

Mixed eruptions can be considered in terms of their total duration (d_4) or the duration of their constituent explosive (d_{3a}) and effusive (d_{3b}) phases (Fig. 3.7). 13 eruptions within Table 3.5 have total durations classified as d_4 , 12 from the Hekla volcanic system and 1 from Öräfajökull. Analyses performed on a complete dataset of all 13 mixed eruptions in Table 3.5 would be biased by eruptions from Hekla, such that results obtained would provide more information about mixed eruption durations from Hekla than mixed eruption durations in general. It is therefore considered more worthwhile to restrict datasets of d_{3a} , d_{3b} and d_4 duration types to those from Hekla and perform analyses at a volcano specific level (covered in section 4.3).

The duration of sequences of mixed eruptions (d_5) from volcanic systems on Iceland

The 2010 Eyjafjallajökull summit eruption (# 53, Table 3.5) is the only example of a sequence of mixed eruptions identified on Iceland. The total duration (d_5) of this eruption is 38 days. Surprisingly, despite this eruption being a sequence of mixed eruptions its total duration is less than the median duration of single mixed eruptions (d_4) from Hekla (204 days) and may reflect a volcano specific control, however, without additional data this is purely speculative.

The duration of single basaltic eruptions (d_6) from volcanic systems on Iceland

The period 1300-2011 contains 38 reported single basaltic eruptions from volcanic systems on Iceland with durations ranging from 0.2 days to 526 days and a median duration of 13.5 days. A histogram of the data plotted with bins of 20 days clearly

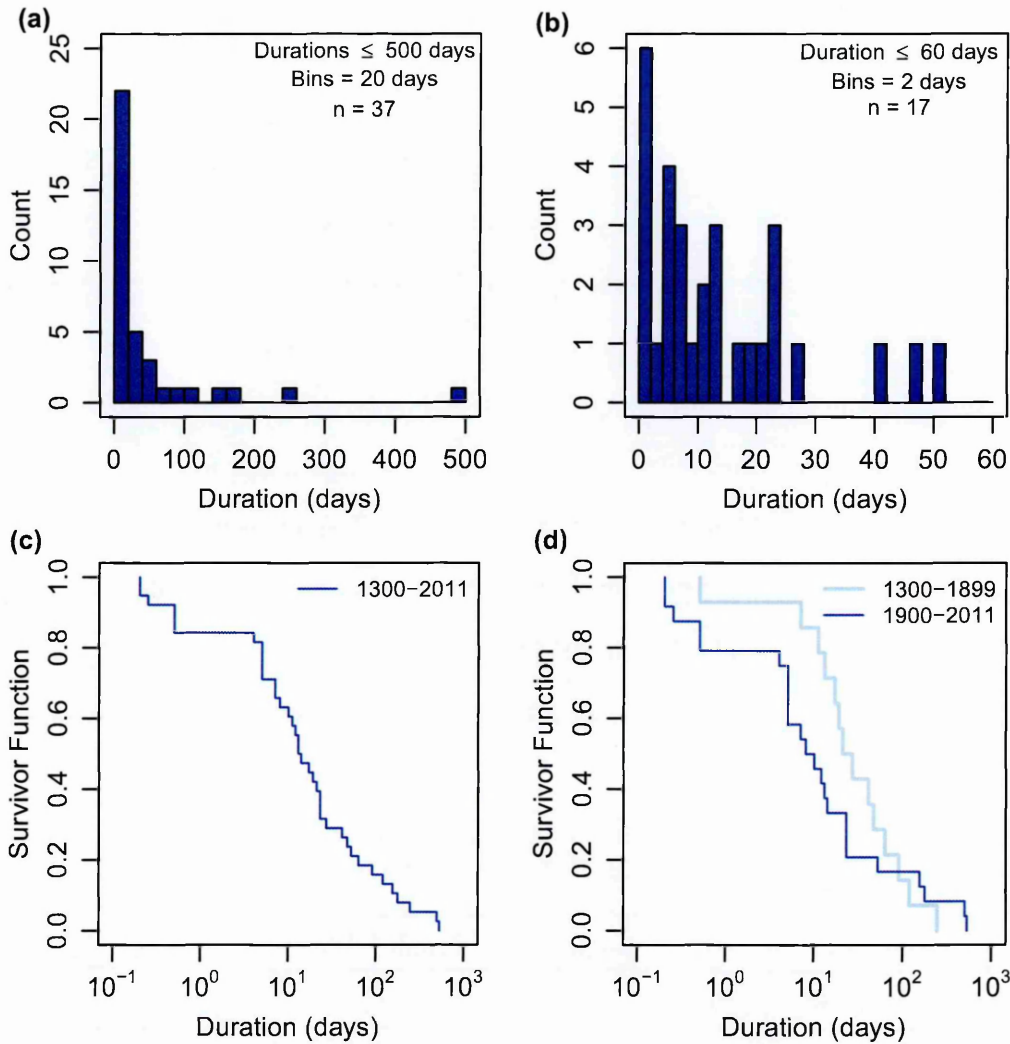


Fig. 4.6 The distribution of single basaltic eruption durations (d_6) on Iceland for the period 1300-2011 displayed as histograms of (a) durations ≤ 500 days in 20 day bins and (b) durations ≤ 60 days in 2 day bins and (c) data displayed as an empirical survivor function curve (data from Table 3.5). (d) Empirical survivor function curves for the distribution of d_6 durations in the periods 1300-1899 and 1900-2011

identifies a dominance of 0-20 day eruptions and a heavy long duration tail to the distribution (Fig. 4.6a). It is worth noting that one eruption is not shown on this plot due to its longer duration of 526 days (#32 Table 3.5). The higher resolution histogram of Fig. 4.6b, plotted with bins of 2 days, shows the gradual decline of eruption frequency into the long duration tail of the distribution. A short duration tail is only observed when the data is viewed as an empirical survivor function curve (Fig. 4.6c), however, the distribution is dominated by the gradual transition into the long

duration tail which begins around the median duration.

A reporting bias towards longer eruptions in the early historic record of Iceland was demonstrated in Chapter 3. Due to the effusive nature of basaltic eruptions this bias may have a strong effect on the d_6 duration dataset discussed here. Fig. 4.6d shows empirical survivor function curves for eruption durations in the periods 1300-1899 and 1900-2011. The increased proportion of short duration eruptions reported in more recent years has the effect of offsetting the 1900-2011 curve downwards and left of the 1300-1899 curve, however, the shape of this curve is very similar to that plotted using all available data (1300-2011, Fig. 4.6c). Table 4.1 contains the results of three significance tests performed to compare the 1300-1899 and 1900-2011 duration data. Results indicate moderately significant difference between the two distributions implying that reporting biases may exist in the single basaltic eruption duration dataset of Iceland.

Table 4.1: Significance test results comparing the distribution of single basaltic eruption durations (d_6) on Iceland for the periods 1300-1899 and 1900-2011.

Compared Data	Logrank	Mann-Whitney	<i>t</i> -test
A $(n=14)$, B $(n=24)$	$p = 0.478$	$p = 0.067$ •	$p = 0.096$ •

A = 1300-1899, B = 1900-2011.
* = significant at a 0.05 level, • = moderate significance (p -value = 0.05-0.1).
t-test applied to the logs of the data.

The duration of sequences of basaltic eruptions (d_7)

Table 3.6 contains a record of eight basaltic eruption sequences on Iceland, and their durations (d_7) range from 292 to 3,195 days with a median of 1,567 days. A crude histogram and empirical survivor function curve of their total durations are displayed in Fig. 4.7, however, due to the low sample size and long durations little can be inferred about their overall distribution and the empirical survivor function curve for these data is approximately linear when plotted on a log scale (Fig. 4.7b).

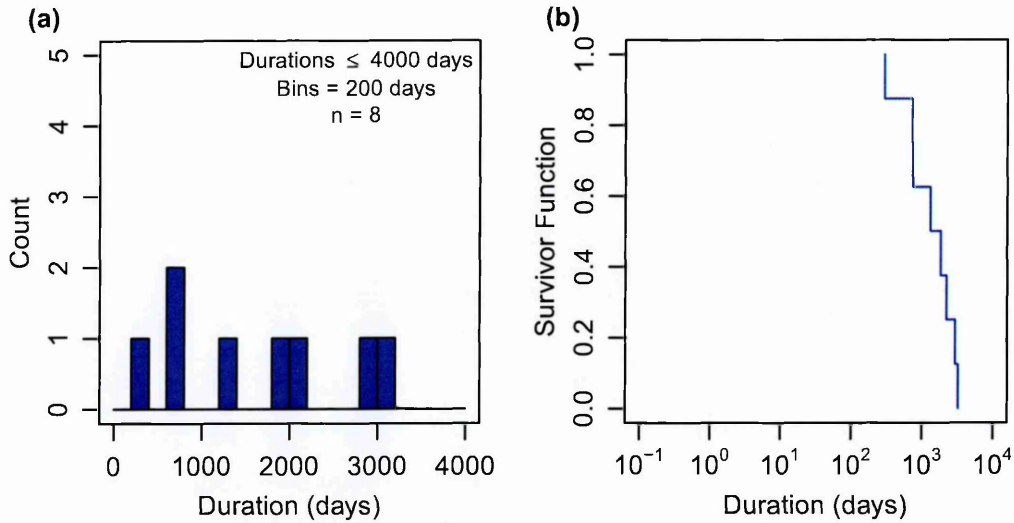


Fig. 4.7 The distribution of the total duration of basaltic eruption sequences (d_7) on Iceland (a) displayed as a histograms of durations ≤ 4000 days in 200 day bins and (b) displayed as an empirical survivor function curve (data from Table 3.6)

4.3 Eruption durations from individual volcanic systems on Iceland

4.3.1 Mixed eruption durations from Hekla

The historic record for the Hekla volcanic system is unusually complete (Thorarinsson, 1967a) and the data on the durations of its mixed eruptions can be considered to be unaffected by reporting biases. 15 mixed eruptions since 1300 AD are recorded in Table 4.2. For those with reported eruption durations, lava, tephra (DRE) and total volumes have been included based on those within Thordarson and Larsen (2007). The 1980 and 1981 eruptions of Hekla (#12 and #13, Table 4.2) are reported as a single eruption in Thordarson and Larsen (2007) and therefore the proportion of lava and tephra erupted in each eruptive phase is unknown and not included in Table 4.2 or the analyses of this study.

The total duration (d_4) is known for every eruption of this type since 1597. Including

Table 4.2: Historical mixed eruptions from the Hekla volcanic system

#	Start Date	End Date	Duration (days)		Volume ($\times 10^6 \text{m}^3$)		
			d_4	d_{3a}	Lava	Tephra	Total
1	11-07-1300	15-07-1301	369	-	1500	220	1720
2	19-05-1341	-	-	-			
3	-	-	-	-			
4	25-07-1510	-	-	-			
5	03-01-1597	15-07-1597	193	-	900	130	1030
6	08-05-1636	15-05-1637	372	-	500	80	580
7	13-02-1693	01-11-1693	261	0.5	900	130	1030
8	05-04-1766	01-05-1768	757	0.17	1300	180	1480
9	02-09-1845	05-04-1846	215	0.17	630	100	730
10	29-03-1947	22-04-1948	390	0.04	800	80	880
11	05-05-1970	05-07-1970	61	0.1	200	30	230
12	17-08-1980	20-08-1980	3	0.08	-	-	-
13	09-04-1981	16-04-1981	7	-	-	-	-
14	17-01-1991	11-03-1991	53	0.4	150	10	160
15	26-02-2000	08-03-2000	11	0.2	170	4	174

Erupted volumes are taken from Thordarson and Larsen (2007) and tephra volumes are DRE.

the 1300 eruption, this results in a dataset of 12 d_4 durations ranging from 3 to 757 days with a median duration of 204 days. A histogram plotted with 50 day bins demonstrates a large spread to the data with the highest proportion of eruptions having durations of 0-50 days and 350-400 days (Fig. 4.8a). Information regarding the duration of the initial explosive phase (d_{3a}) is known for eight of these eruptions and ranges from 0.04 to 0.5 days with a median duration of 0.17 days. A histogram plotted with bins of 0.1 days shows that the majority of these phases are very short lasting less than 5 hours (0.2 days) (Fig. 4.8b).

The different scale of the d_{3a} and d_4 duration of Hekla eruptions enables their empirical survivor function curves to be displayed on the same plot without any overlap (Fig. 4.8c). The d_{3a} data has a relatively straight empirical survivor function curve, lacking

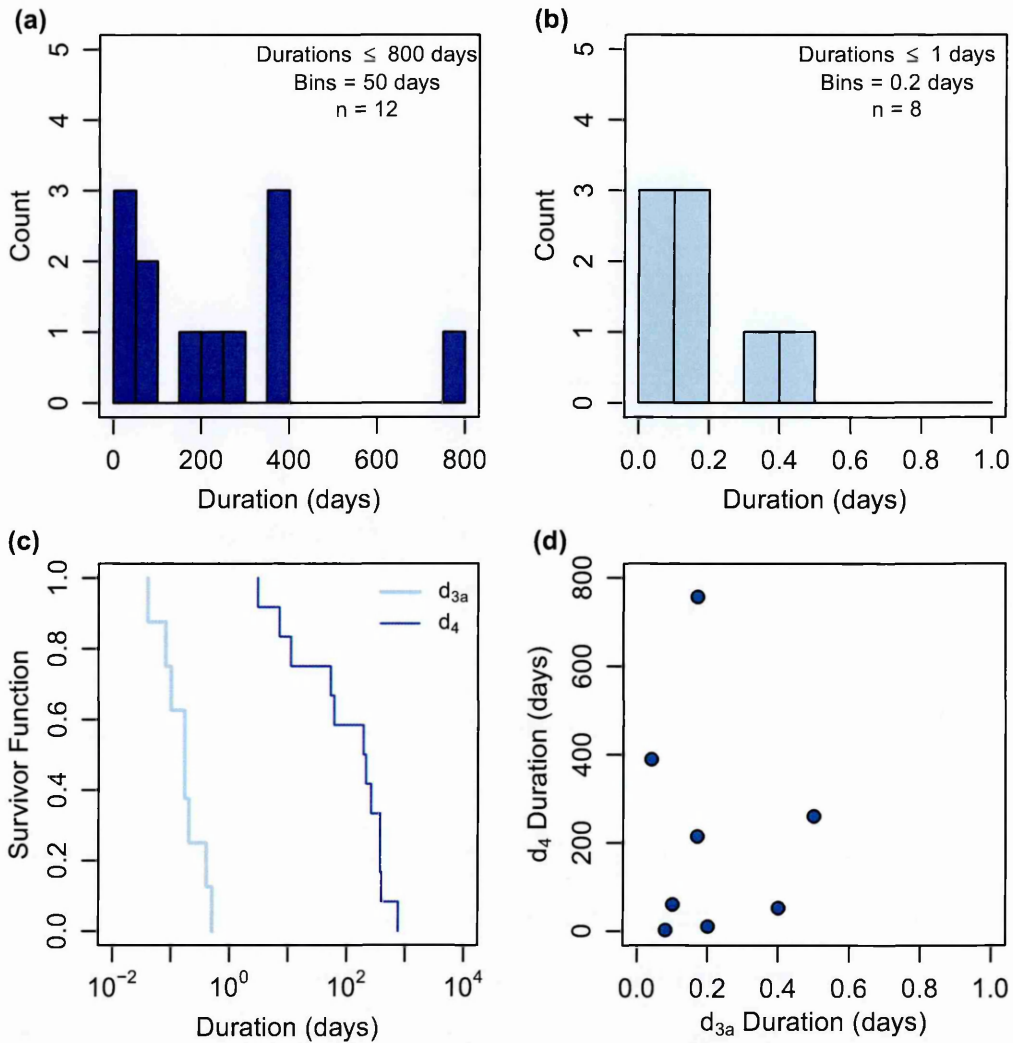


Fig. 4.8 The distribution of mixed eruption durations from Hekla for the period 1300-2000 displayed as histograms of (a) d_4 durations ≤ 800 days in 50 day bins and (b) d_{3a} durations ≤ 1 days in 0.2 day bins. (c) Data for both d_{3a} and d_4 durations displayed as empirical survivor function curves ($n = 9$ and 12 respectively). (d) Plot of d_{3a} against d_4 duration.

both long and short duration tails. In contrast, a slight short duration tail to the empirical survivor function curve of the d_4 data is observed (Fig. 4.8c) which is masked within the 0-50 day bin of Fig. 4.8a.

The initial explosive phase of mixed eruptions (d_{3a}) equates to between 0.01 and 2.67 % of the total eruption duration (d_4) and therefore the total duration of mixed eruptions are dominated by their effusive phases (i.e., $d_4 \approx d_{3b} \gg d_{3a}$). The relationship

between d_{3a} and d_4 of individual mixed eruptions from Hekla has been investigated to determine whether the duration of an initial explosive phase could be used to forecast the overall duration of the eruption (Fig. 4.8d). Results indicate that although the d_{3a} duration is always much shorter than the subsequent d_{3b} duration, the relationship is not entirely systematic and d_{3a} is at best a poor predictor of d_4 (i.e. the 1766 eruption began with 0.17 days of high-powered explosive activity yet it is the longest eruption in the dataset with a duration of 757 days).

4.3.2 Single basaltic eruption durations from Askja, Grímsvötn, Katla and Krafla

38 eruptions within Table 3.5 fall within the single basaltic eruption (d_6) category of this study. Of these, 10 are from Krafla, 9 from Grímsvötn and 5 each from Katla and Askja. An investigation into the volcano specific nature of their durations was conducted using these 4 volcanic systems. Subsection 4.2.4 demonstrated that reporting biases prior to 1900 have a moderately significant effect on the distribution of single basaltic eruptions on Iceland. Restricting the data to the period 1900-2011 would reduce the sample size such that only the Krafla and Grímsvötn datasets are sufficient to provide insight into volcanic specific investigations. The degree of reporting bias will vary for different volcanic systems (subsection 3.4.4) and therefore data from the period 1300-2011 are used in the following analyses and their specific reporting biases discussed.

Fig. 4.9 displays crude histograms plotted for each volcanic system (a-d) along with a plot containing their empirical survivor function curves (e). Despite their small sample sizes some key differences between their duration ranges and distributions can be observed. In particular, the Krafla dataset is comprised of relatively short duration eruptions (median = 2.75 days), compared to Katla, Askja and Grímsvötn with median

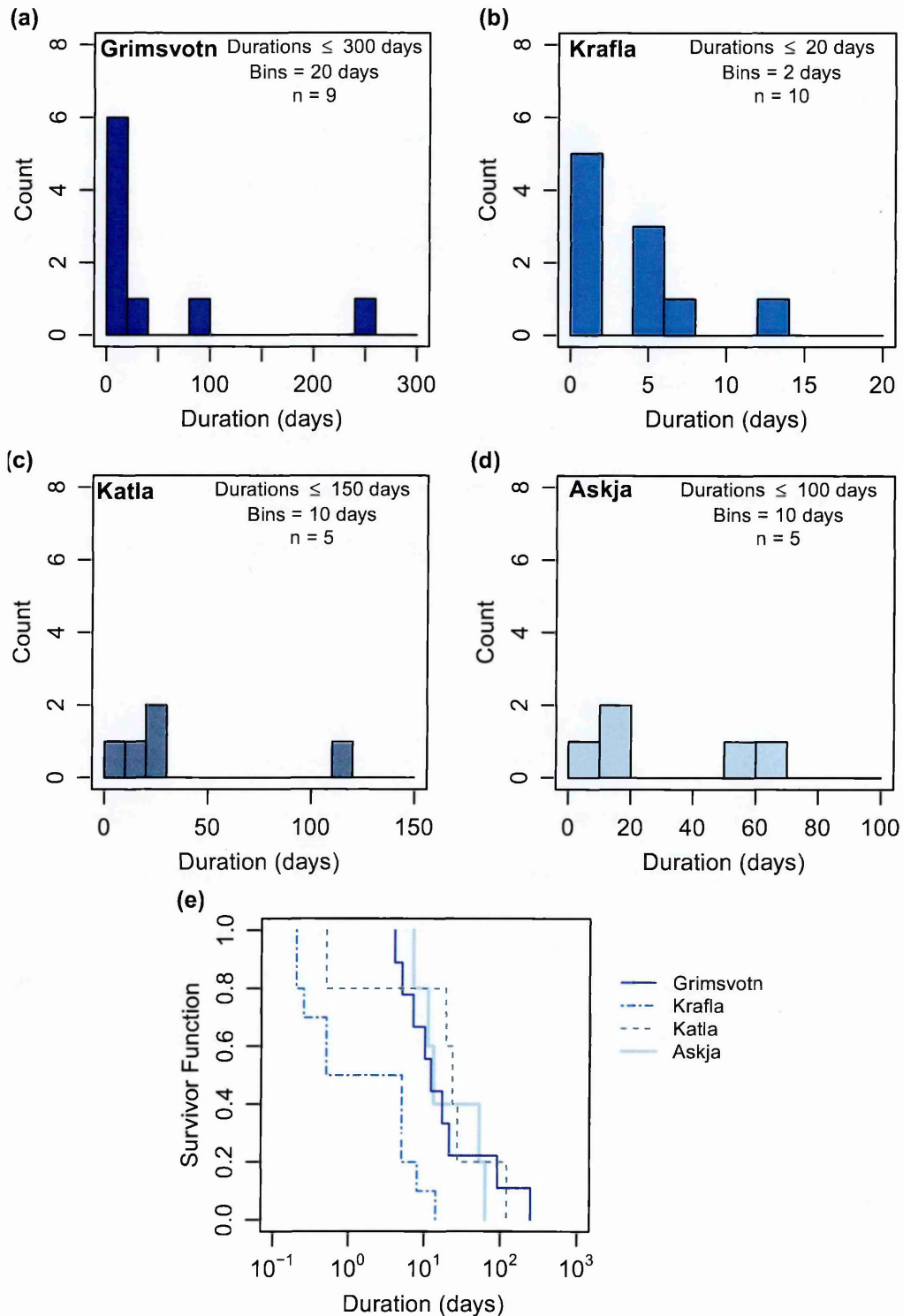


Fig. 4.9 The distribution of single basaltic eruptions (d_6) on Iceland at individual volcanic systems plotted as histograms for (a) Grímsvötn, (b) Krafla, (c) Katla and (d) Askja. (e) The data displayed as empirical survivor function curves where G = Grímsvötn, Kr = Krafla, Ka = Katla and A = Askja (data from Table 3.5)

durations of 23 days, 13 days and 12 days respectively. The empirical survivor function curve for Krafla is also completely offset from the other three curves reflecting the short duration of its eruptions (Fig. 4.9e). Significance tests performed comparing these data support these findings, with the distribution of eruption durations from Krafla being significantly different from Askja, Grímsvötn and Kata at the 0.05 level while significant difference between these latter three systems are not found (Table 4.3).

It is worth noting that the longest Grímsvötn eruption included in Table 3.5 is the 244 day long Laki fissure eruption (#11) which may be unrepresentative of this volcano's more usual behaviour. Gudmundsson (1987) and Thordarson and Self (1993) argue that the very large erupted volume (15 km^3), high discharge rate and lack of collapse at Grímsvötn caldera are inconsistent with the magma having been sourced from a shallow magma chamber beneath Grímsvötn and transported laterally, as had been argued by Sigurdsson and Sparks (1978). The alternative to this is that the Laki eruption was derived from deep-seated magma residing near the crust-mantle interface and much of the magma transport occurred vertically beneath the active fissures (Thordarson and Larsen, 2007). If this were the case then it is likely that the dynamics of the Laki system were different from those of Grímsvötn's shallow summit system, such that the factors controlling eruption duration are also different. Removing the Laki eruption from the dataset of Grímsvötn eruptions has the effect of reducing the maximum recorded duration from 244 to 90 days but only reduces the median duration from 12 to 11 days.

Volcanic systems located close to population centres are more likely to have all eruptions documented, even if they are short or small (e.g. the Krafla 1975-1984 eruptions were well monitored throughout). In contrast, volcanic systems located in more remote areas are likely to suffer poorer reporting (e.g. Askja has sparse/incomplete records of the small basaltic eruptions which occurred in the 1870's and 1920's). As men-

Table 4.3: Significance test results for single basaltic eruption durations (d_6) from individual volcanic systems on Iceland

Data		Logrank	Mann-Whitney	t -test
A ($n=5$)	G ($n=9$)	$p = 0.900$	$p = 0.739$	$p = 0.810$
A ($n=5$)	Ka ($n=5$)	$p = 0.676$	$p = 0.841$	$p = 0.776$
A ($n=5$)	Kr ($n=10$)	$p = 0.015$ *	$p = 0.012$ *	$p = 0.002$ *
G ($n=9$)	Ka ($n=5$)	$p = 0.686$	$p = 0.519$	$p = 0.885$
G ($n=9$)	Kr ($n=10$)	$p = 0.006$ *	$p = 0.009$ *	$p = 0.002$ *
Kr ($n=10$)	Ka ($n=5$)	$p = 0.006$ *	$p = 0.022$ *	$p = 0.062$ •

A = Askja, **G** = Grímsvötn, **Ka** = Katla, **Kr** = Krafla.

* = significant at a 0.05 level, • = moderate significance (p -value = 0.05-0.1).

t -test applied to the logs of the data.

tioned in subsection 3.4.4, volcanic systems covered by ice (e.g. Katla and Grímsvötn) require large eruptions to break through that ice before there is definitive evidence that an eruption occurred. This will undoubtedly result in an under-representation of short eruptions at ice-covered volcanoes. Katla is covered by a much thicker ice-cap (maximum thickness 830-700 m, (Larsen, 2002)) than Grímsvötn (300-600 m, (Gudmundsson et al., 1997)) so even larger eruptions are required to break through the ice. This may contribute to the apparently longer duration eruptions at Katla compared to Grímsvötn.

Although it is possible that better reporting at Krafla has led to less short duration eruptions being missed and thus under-represented in the dataset, the lack of Krafla eruptions longer than 14 days still suggests that its eruptions are shorter than those from the other volcanic systems investigated. The 9 volcanic eruptions at Krafla in the period 1900-2011 all represent single eruptions during the longer Krafla fire event (1975-1984, # H, Table 3.6). It is therefore unclear whether these short duration eruptions are a function of the Krafla volcanic system, or typical of fire events on a more general level. It is evident however, that the short duration tail of the overall d_6 eruption duration distribution (Fig. 4.6) is dominated by these Krafla eruptions, and thus performing forecasts based on that data could lead to biased results (i.e. a greater probability of short duration eruptions). For this reason it is considered more sensible

to analyse the Krafla data separately from the overall d_6 data in the remainder of this investigation. The 10 eruptions reported for Krafla in the period 1300-2011 are summarised in Table 4.4. Note that the 1746 eruption is the only eruptions that was not part of a longer eruptive sequence.

Table 4.4: Single basaltic eruptions from Krafla, Iceland (1300-2011)

#	Start Date	End Date	d_6 Duration (days)
1	10-07-1746	10-07-1746	0.5
2	20-12-1975	20-12-1975	0.2
3	27-04-1977	27-04-1977	0.5
4	08-09-1977	08-09-1977	0.2
5	16-03-1980	16-03-1980	0.25
6	10-07-1980	18-07-1980	8
7	18-10-1980	23-10-1980	5
8	30-01-1981	04-02-1981	5
9	18-11-1981	23-11-1981	5
10	04-09-1984	18-09-1984	14

4.4 Temporal variation in the distribution of eruption duration

Volcanic systems can change with time causing temporal variations in the nature of volcanic activity. It is important to assess if any changes in eruption duration with time are apparent or if any previously recognised changes in volcanic activity or the

volcano's plumbing system affect the duration of the eruptions produced. If so it may be sensible to restrict the data used in the forecasting models of Chapter 5 such that they contain only the most recent data that best represents the current state of the volcanic system. Furthermore, any links between the physical properties of the volcanic systems and the duration of the eruptions produced could provide useful insight into the leading controls on eruption durations (discussed in Chapter 7). The following section assesses any temporal variation in the datasets used in this study.

4.4.1 Temporal variation at Mt. Etna

The distribution of eruption duration between 1600 and 1669 at Mt. Etna is dominated by long duration eruptions, three of which are longer than any subsequent eruption (Fig. 3.2c). During this time, erupted lavas were rich in plagioclase phenocrysts and believed to have been stored in a shallow magma reservoir within the volcanic edifice prior to eruption. However, directly following the 1669 eruption Mt. Etna experienced a sharp decrease in productivity and a reduction in the phenocryst content of erupted lavas, which has been attributed to the draining of a shallow magma reservoir within the volcanic edifice during the 17th Century (Hughes et al., 1990; Behncke and Neri, 2003). It is possible that the shallow magma chamber existing at this time promoted longer duration eruptions.

After 1669 eruption durations range from 0.5 to 473 days and there has been a general increase in eruption frequency with time that is not an artefact of reporting (Behncke and Neri, 2003; Behncke et al., 2005; Branca and Del Carlo, 2005; Cappello et al., 2013). In particular, dramatic increases in eruption frequency and output rate have been recognised following 1971 (Wadge and Guest, 1981; Mulargia et al., 1985; Andronico and Lodato, 2005; Behncke et al., 2005; Branca and Del Carlo, 2005; Salvi et al., 2006; Bebbington, 2007; Smethurst et al., 2009; Cappello et al., 2013). A similar trend can

be observed in our data (Table 3.1), with 20 flank eruptions in the past 38 years (1971-2010), as opposed to only 7 in the 41 years before it (1930-1971) (Fig. 3.2, Table 3.1).

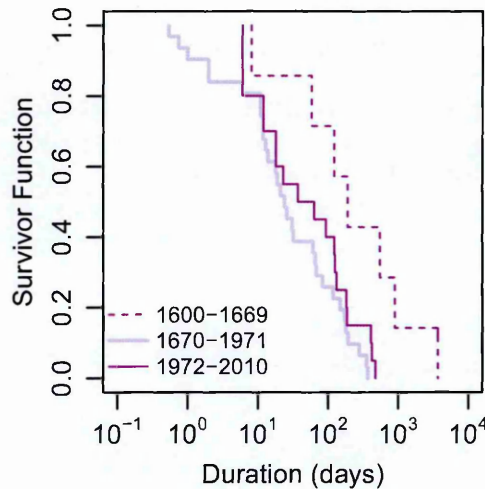


Fig. 4.10 Empirical survivor function curves for flank eruption durations at Mt. Etna for the periods 1600-1669 ($n = 7$), 1670-1971 ($n = 31$) and 1972-2010 ($n = 20$) (data from Table 3.1)

Andronico and Lodato (2005) noted that the median duration of eruptions from the period 1971-1999 was also higher than that of 1900-1971. Again this is supported here with reported eruption durations of < 6 days being absent after 1971 (Fig. 3.2c). Median durations for the periods 1600-1669, 1670-1971 and 1972-2010 are 190 days, 24 days and 50 days respectively.

Fig. 4.10 shows empirical survivor function curves for the eruption durations of these three time periods. While the 1670 to 1971 and 1972 to 2010 datasets diverge at durations < 10 days (Fig. 4.10), significance tests indicate that the curves are not statistically different at the 0.05 level and it cannot be concluded that they derive from different distributions (Table 4.5). This implies that restricting the data to eruptions in the period 1972-2010 only is currently unnecessary.

In contrast, the empirical survivor function curve for the 1600-1669 dataset is entirely offset from the 1670-1971 and 1972-2010 curves (Fig. 4.10). Significance tests in-

Table 4.5: Significance test results comparing the distribution of flank eruption durations from Mt. Etna for the periods 1600-1669, 1670-1971 and 1972-2010.

Data		Logrank	Mann-Whitney	t-test
A (n=7)	B (n=31)	p =0.008 *	p =0.024 *	p =0.029 *
A (n=7)	C (n=20)	p =0.023 *	p =0.067 •	p =0.099 •
B (n=31)	C (n=20)	p =0.161	p =0.330	p =0.194

A = 1600-1669, B = 1670-1971, C = 1972-2010.
* = significant at a 0.05 level, • = moderate significance (p-value = 0.05-0.1).
t-test applied to the logs of the data.

dicating that the difference between the duration data in the period 1600-1669 and the 1670-1971 period are significant at the 0.05 level and moderately significant differences exist between it and the 1972-2010 data (Table 4.5). This implies that the different physical properties of Mt. Etna’s volcanic system prior to 1670 were sufficient enough to generate a different eruption duration regime to that following 1669.

These results suggest that further analyses performed on the flank eruption duration data for Mt. Etna should be conducted for the 1600-1669 and 1670-2010 datasets separately. Furthermore, this combined with the evidence for a different plumbing system beneath Mt. Etna prior to 1670 may indicate that a future eruption on the scale and duration of the 1600-1669 eruptions is unlikely and therefore that we should only use eruptions after 1669 as the basis of any forecasting models. However, the 1600-1669 time period has previously been interpreted as the culminating phase of a century scale cycle, with the next cycle still continuing today (Behncke and Neri, 2003; Tanguy et al., 2007; Cappello et al., 2013). Recent investigations into the plumbing system of Mt. Etna indicate increasing magma accumulation beneath the volcano (Behncke and Neri, 2003). This, along with the trend of increasing eruption frequency and output rate, may indicate a gradual return to the style of activity that was typical in the early seventeenth century. By excluding the 1600-1669 data the model would be unable to account for the possibility that future activity at Mt. Etna could become more voluminous and potentially hazardous in the future. For this reason both the 1600-2010 and 1670-2010 datasets are used for the analyses in the remainder of this study and their

results compared.

4.4.2 Temporal variation at Kilauea

Section 3.2 noted a change in eruption durations following 1959, with a minimum duration of 2 days for the period 1912-1959 while 32 % of eruptions in the period 1960-1983 have durations less than this. Klein (1982) also identified a reduction in repose interval across this boundary and although it is possible that these observed changes may reflect an earlier bias it is considered unlikely given the detailed records of Kilauea activity.

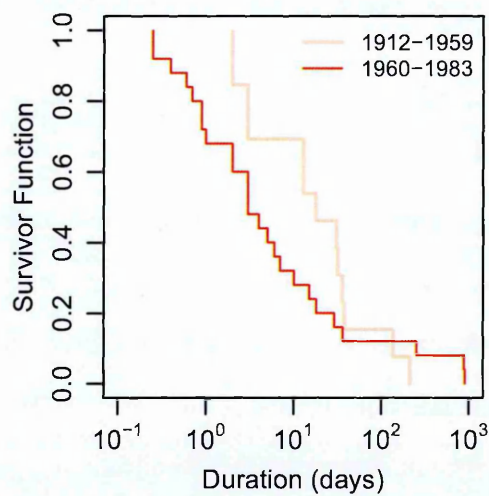


Fig. 4.11 Empirical survivor function curves for eruption durations from Kilauea for the periods 1912-1959 ($n = 13$) and 1960-1983 ($n = 25$) (data from Table 3.2)

Table 4.6: Significance test results comparing the distribution of eruption durations from Kilauea for the periods 1912-1959 and 1960-1983.

Data		Logrank	Mann-Whitney	t-test
A ($n=13$)	B ($n=25$)	$p = 0.324$	$p = 0.052$ •	$p = 0.074$ •
A = 1912-1959, B = 1960-1983.				
★ = significant at a 0.05 level, • = moderate significance (p -value = 0.05-0.1).				
t -test applied to the logs of the data.				

Fig. 4.11 plots empirical survivor function curves for eruption durations in the periods 1912-1959 and 1960-1983 at Kilauea. The median durations of these two groups are

18 days and 3 days respectively and as such the two curves are offset, only overlapping in their long duration tails. Mann-Whitney and *t*-test results indicate moderately significant differences between these distributions and a log-rank test considers them statistically similar (Table 4.6). Although the results are not strictly significant, when combined with the visual difference of the data they imply that something changed across the 1959 boundary and that short duration eruptions either became more common or were more commonly reported. Either way, this carries implications for the remaining analyses of this study and from here on both the 1912-1983 dataset and a smaller subset of the data for the period 1960-1983 will be considered and their results compared.

4.4.3 Temporal variation at PdlF

Previous studies into the eruption history of PdlF have demonstrated a relationship between the chemistry and location of eruptions (Ludden, 1977; Stieltjes and Moutou, 1989; Boivin and Bachelery, 2009; Peltier et al., 2009) and have speculated that this relationship manifests itself on decade scale cycles. Stieltjes and Moutou (1989) report three major cycles for the period 1911-1988, starting in the years 1931, 1961 and 1977 each with a high volume eruption of oceanite lava ($> 20\%$ olivine crystals). The investigations of Peltier et al. (2009) span the period 1972-2008 and thus only slightly overlap this period. They investigate the eruptive activity at PdlF either side of the 6 year repose interval (1992-1998, see subsection 3.3.4) and recognise changes in the plumbing system of PdlF following the 1998 eruption such that the volcanic system switched from one dominated by progressive drainage of a shallow reservoir to one of continuous recharge from a deeper reservoir. Following this change a return to cyclic activity is suggested, however, unlike Stieltjes and Moutou (1989), Peltier et al. (2009) define these cycles as ending with eruptions of olivine-rich or oceanite lavas from outside Enclos Fougué caldera.

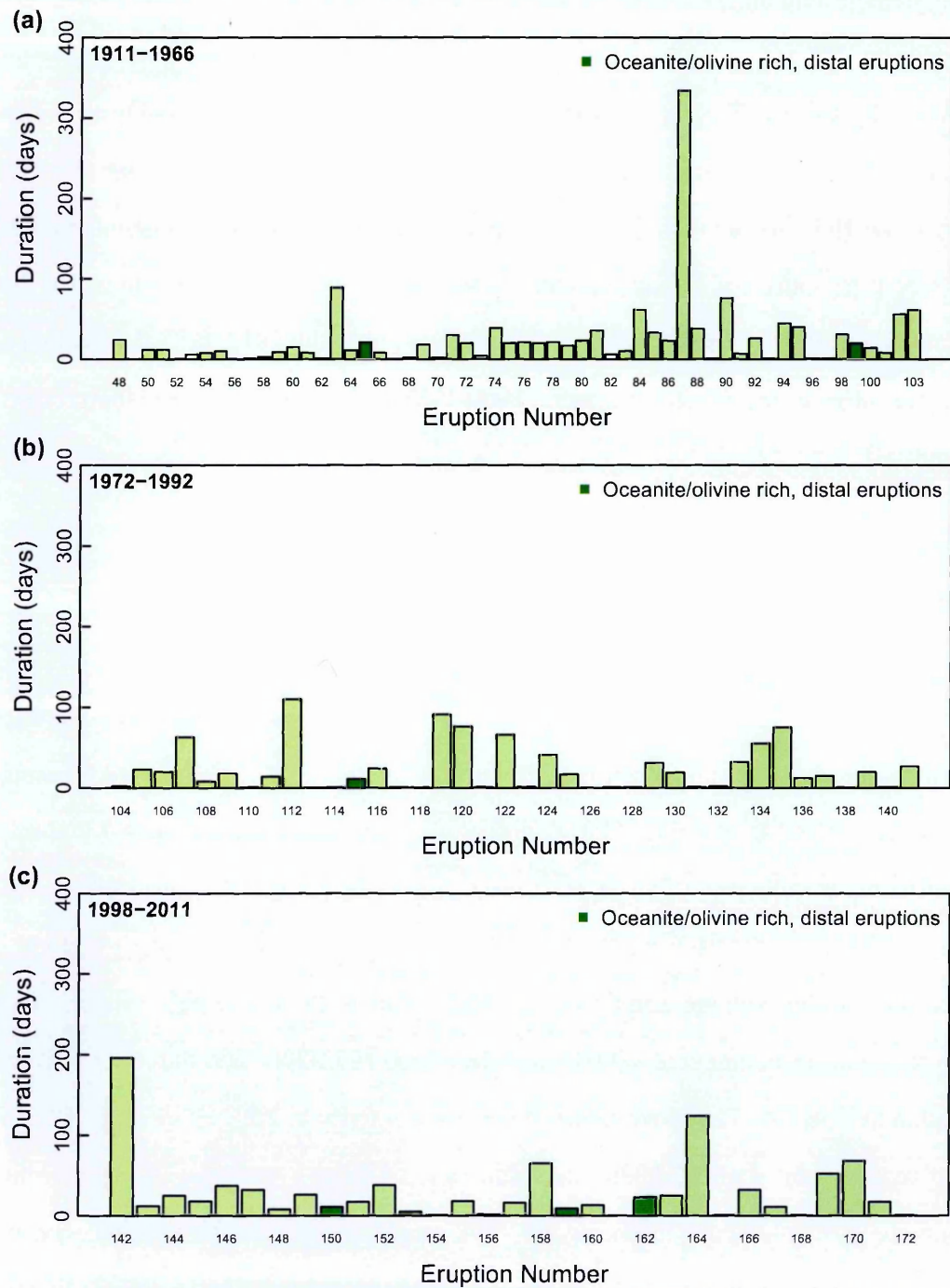


Fig. 4.12 Plots showing the duration of each eruption from PdIF in the periods (a) 1911-1966, (b) 1972-1992 and (c) 1998-2011 where eruption numbers correspond to the eruption numbers of Table 3.3 and dark bars represent distal, olivine-rich or oceanite eruptions

To assess whether eruption durations systematically vary between these distal/olivine rich eruptions Fig. 4.12 has been plotted to show the duration of each eruption in the 1911-2011 period. Dark green bars represent distal eruptions which erupted olivine rich or oceanite lavas based on the descriptions and information within Stieltjes and Moutou (1989) (1911-1971) and Peltier et al. (2009) (1972-2008). The three plots are separated temporally by the two 6 year repose intervals (1966-1972 and 1992-1998). The figure demonstrates little relationship between an eruption's position within these potential cycles and its duration.

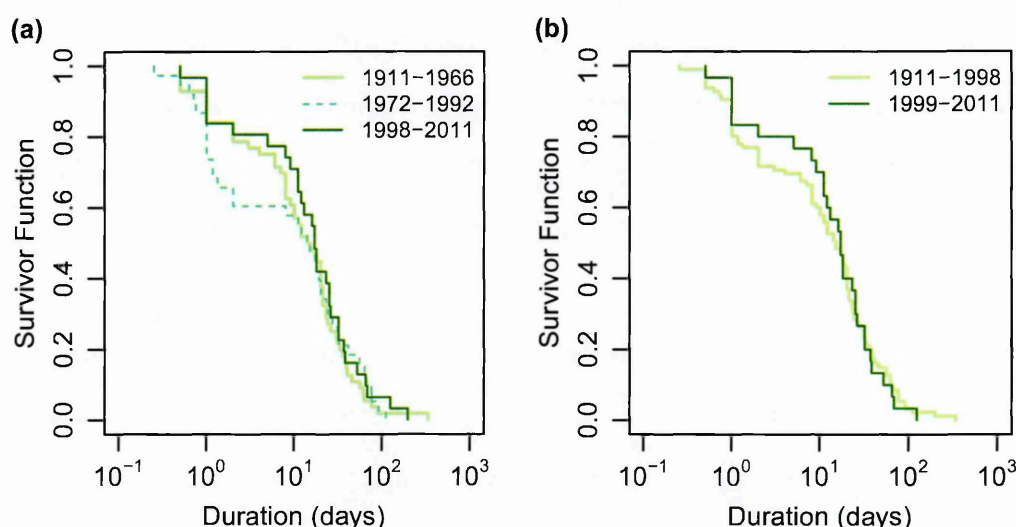


Fig. 4.13 Empirical survivor function curves for the duration of PdIF eruptions from the periods (a) 1911-1966 ($n = 56$), 1972-1992 ($n = 38$) and 1998-2011 ($n = 31$) and (b) for the periods 1911-1998 ($n = 95$) and 1999-2011 ($n = 30$) (data from Table 3.3)

This study focusses on the distribution of eruption durations separated by the 6 year repose intervals (i.e. the separate distributions within each plot of Fig. 4.12 irrespective of its source location or petrology). Fig. 4.13a shows the empirical survivor function curves for the periods 1911-1966, 1972-1992 and 1998-2011. Although the 1972-1992 distribution shows greatest divergence for durations of 1-10 days, significance tests performed on these three distributions do not show any significant differences (Table 4.7).

Additional investigations have been performed on data before and after the 1998 erup-

tion at PdIF to assess whether the potential change in PdIF’s plumbing system at this time (Peltier et al., 2009) has had any effect on eruption duration. Fig. 4.13b displays empirical survivor function curves for the 1911-1999 and 2000-2011 periods. The two distributions plot with similar shapes and positions and again significance tests do not indicate significant differences at the 0.05 level (Table 4.7).

Although significant differences have not been found between any of the time periods investigated, the different shape of the 1972-1992 curve in Fig. 4.13a cannot be disregarded entirely and may provide information about the bimodal nature of the PdIF eruption duration data demonstrated in subsection 4.2.3 (Fig. 4.5). For the three time periods investigated in Fig. 4.13a 1972-1992 contains the highest proportion of eruptions with durations < 2 days (1911-1971 = 16 %, 1971-1992 = 40 % and 1998-2011 = 6 %) implying that these short duration eruptions were more common during this time period. Given that the distribution of eruption durations were not found to be significantly different at the 0.05 level this temporal variation will not be used to restrict the data for forecasting purposes in Chapter 5. However, the tendency for shorter duration eruptions during 1971-1992 will be returned to in Chapter 7 when possible controls on eruption duration are discussed

Table 4.7: Significance test results comparing the distribution eruption durations from PdIF for the periods 1911-1966, 1972-1992 and 1998-2011 and also comparing the periods 1911-1998 and 1999-2011.

Data		Logrank	Mann-Whitney	t-test
A (n=56)	B (n=38)	p = 0.859	p = 0.666	p = 0.373
A (n=56)	C (n=31)	p = 0.301	p = 0.454	p = 0.488
B (n=38)	C (n=31)	p = 0.484	p = 0.368	p = 0.170
D (n=95)	E (n=30)	p = 0.975	p = 0.569	p = 0.443

A = 1911-1966, B = 1972-1992, C = 1998-2011, D = 1911-1998, E = 1999-2011.

★ = significant at a 0.05 level, ● = moderate significance (p-value = 0.05-0.1).

t-test applied to the logs of the data.

4.4.4 Temporal variation at Hekla, Iceland

Thordarson and Larsen (2007) recognised an increase in eruption frequency from 0.17 to 0.94 eruptions per decade at Hekla following the 1947 eruption. The five shortest mixed eruptions at Hekla also occurred after 1947 and range from 3 to 61 days (1970-2000), whereas eruptions in the period 1597-1947 (and the 1300 AD eruption) had longer durations ranging from 193-757 days (Fig. 4.14a). The median duration of these two time periods is 11 days and 369 days respectively and empirical survivor function curves for each dataset are shown in Fig. 4.14b. These two curves are offset from one another entirely and significance tests indicate that, despite the small sample sizes involved, the two distributions can be considered statistically different at a 0.05 level (Table 4.8).

Table 4.8: Significance test results comparing the distribution of total eruption durations (d_4) and initial explosive phase durations (d_{3a}) of mixed eruptions from Hekla, Iceland for the periods 1300-1969 and 1970-2000.

Data		Logrank	Mann-Whitney	<i>t</i> -test
d_4	A ($n=7$) B ($n=5$)	$p = 0.000$ *	$p = 0.003$ *	$p = 0.005$ *
d_{3a}	A ($n=4$) B ($n=4$)	$p = 0.713$	$p = 1.00$	$p = 0.969$

A = 1300-1947, B = 1948-2000.
 * = significant at a 0.05 level, • = moderate significance (p -value = 0.05-0.1).
t-test applied to the logs of the data.

Although it is possible that the shorter duration of more recent eruptions may be influenced by the reporting biases discussed in section 3.4, the explosive nature of these eruptions and the exceptionally good documentation of the eruptions from Hekla imply that this is unlikely. It is more likely that these changes in eruptive activity at Hekla reflect changes in the volcano’s plumbing system, such that it promotes more frequent, shorter duration eruptions. Possible explanations for this are discussed in Chapter 7.

In light of this temporal variation the duration of the initial explosive phase (d_{3a}) of these mixed eruptions was also investigated for the periods 1300-1947 and 1948-2000.

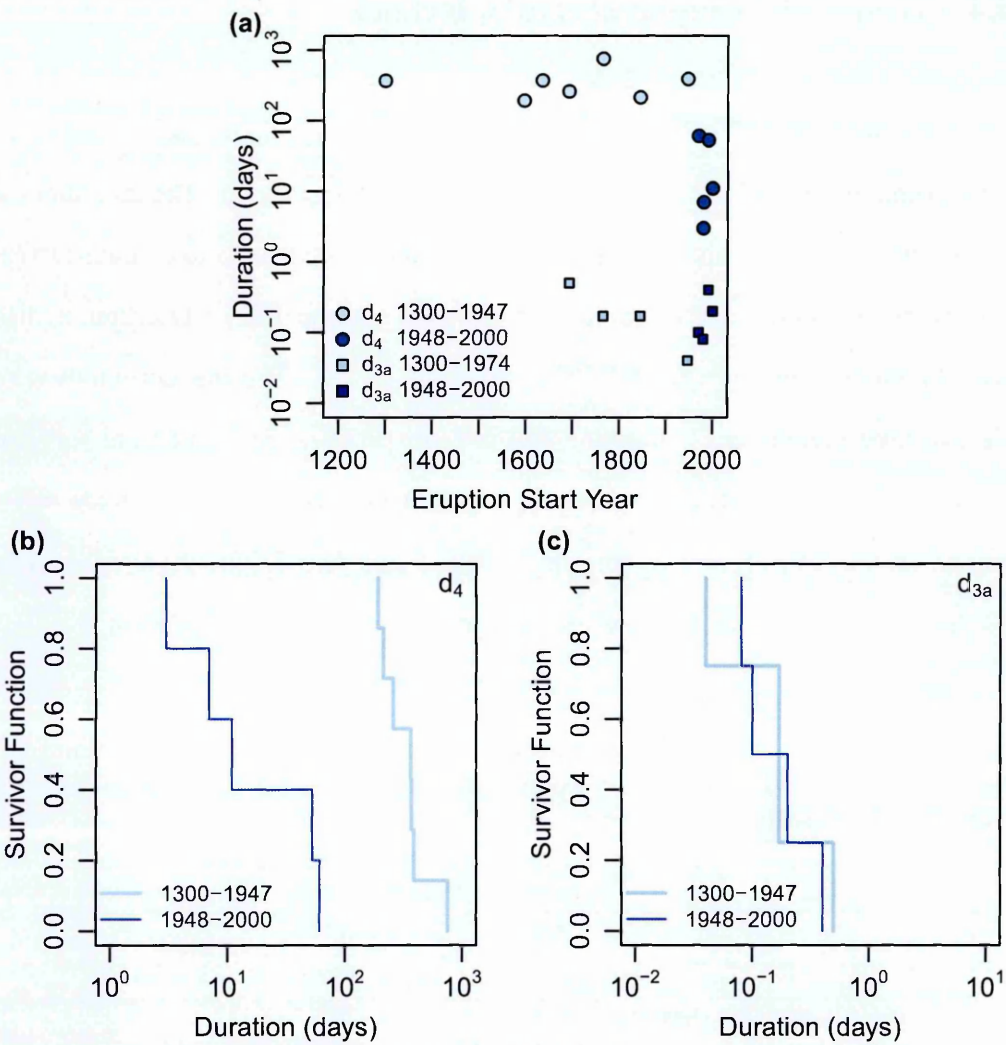


Fig. 4.14 (a) Plot of eruption start year against duration of mixed eruptions (d_4 and d_{3a}). (b) and (c) display the d_4 and d_{3a} duration data as empirical survivor function curves for the periods 1300-1947 and 1948-2000

Fig. 4.14a displays a possible trend of decreasing d_{3a} durations with time for the period 1300-1947 and increasing d_{3a} durations with time for the period 1948-2000. However, this is plotted with duration on a log scale and actually this trend occurs over a narrow duration range of 0.04-0.5 days (1 to 12 hours). Empirical survivor function curves for the d_{3a} durations plot with similar shapes and positions (Fig. 4.14c) and significance test results imply that any differences between these two distributions are not significant at the 0.05 level (Table 4.8). This further supports the lack of correlation between the duration of the initial explosive phase and the total duration of Hekla's

mixed eruptions (discussed in subsection 4.3.1, Fig. 4.8d).

4.5 Spatial variation in the distribution of eruption duration

An investigation into how eruption duration varies with vent location has been performed on each dataset used in this study. Where applicable this involves a comparison between the duration of eruptions from summit and flank vents and between different rift zones. For Iceland a comparison of single basaltic eruptions from volcanic systems situated inside and outside the axial rift zone has been performed.

The identification of any spatial variation in eruption duration may indicate the necessity to forecast different areas independently of each other, instead of treating all eruptions from one dataset as the same. Furthermore, comparison of the nature of these variations and physical properties of the different settings could provide useful insight into factors controlling eruption durations (discussed in Chapter 7).

4.5.1 Spatial variation at Mt. Etna

Previous investigations into the location of historical flank eruptions at Mt. Etna have highlighted three regions of high vent density on the North-Eastern, Southern and Western flanks of the volcano interpreted as three rift zones where eruptions are common (Duncan et al., 1981; Chester et al., 1985; Behncke et al., 2005; Neri et al., 2011; Proietti et al., 2011). To assess whether the distribution of eruption duration varies between each rift zone we have split the volcano into three sectors. Unlike Proietti et al. (2011) our sectors are not evenly distributed or positioned so that one boundary is directed North. Instead, we have used similar sectors to Behncke et al. (2005) whereby

each sector contains one of the three identified rift zones along with any vents which appear closely associated with it. Using a point centred above the summit, these are between (A) 347° and 104° , (B) 104° and 226° and (C) 226° and 347° (Fig. 3.1), and include the North-Eastern, Southern and Western rift zones respectively.

The boundary between sectors A and B cuts through the Valle del Bove. Eruptions within this area are common and, since 1971, many lava flows from the summit's South East crater enter this valley making the resurfacing rate high. This can make identifying vents and fissures within this area difficult. The precise positions of the 1755 and 1802 fissures (#13 and #19, Table 3.1) are unknown, but reported to be close to Rocca Mussarra and are therefore considered here as part of sector A (Fig. 3.1, Table 3.1). Other fissures and vents within the Valle del Bove have been located using the sources previously discussed and assigned to sector A or B accordingly.

The majority of eruptive vents and fissures outside the Valle del Bove fall clearly within one of the three sectors (Fig. 3.1). The March 1981 eruption (#51, Table 3.1) was the result of a long fissure which crosses the boundary between sectors A and C. The eruption is most probably a result of the North-East rift zone and is therefore considered part of sector A (Fig. 3.1). Similarly the eruptive fissure of the May 2008 eruption (#62, Table 3.1) crosses the boundary between sectors A and B. The lower portion of this fissure was active throughout the eruption and thus the eruption is attributed here to sector B (Fig. 3.1).

Empirical survivor function curves plotted for the 1600 to 2010 flank eruption durations of sectors A, B and C are displayed in Fig. 4.15a. The small sample size of sector C ($n = 6$) results in a crude empirical survivor function curve. Any differences between its eruption duration distribution and that of sectors A and B is difficult to discern and significance tests reveal p -values of greater than 0.05 (Table 4.9). The sample sizes of sectors A and B are higher ($n = 23$ and $n = 29$ respectively) and while the tails of their distributions overlap, the central portions diverge, with median durations

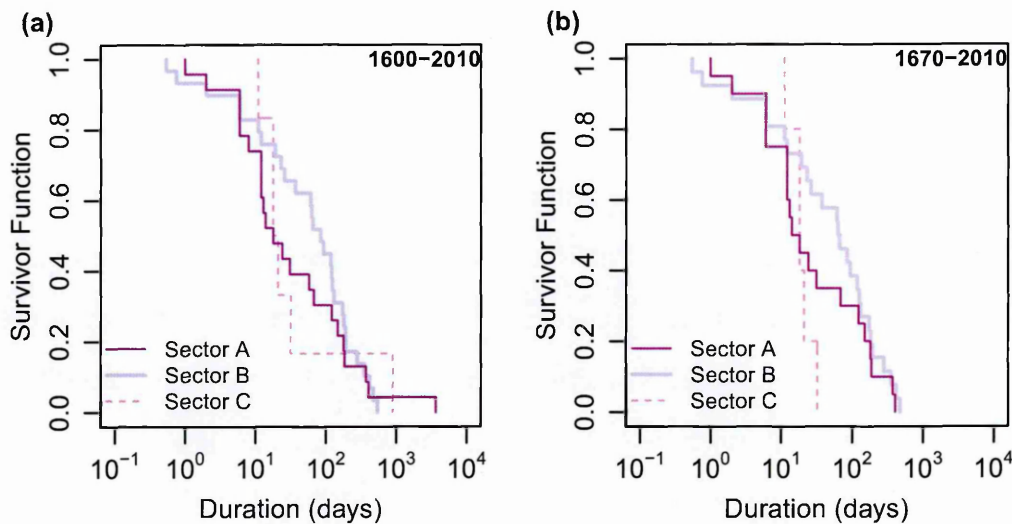


Fig. 4.15 Empirical survivor function curves for flank eruption durations from sectors A, B and C at Mt. Etna for the period (a) 1600-2010 and (b) 1670-2010 (data from Table 3.1)

of 18 days (sector A) and 84 days (sector B) (Fig. 4.15). Despite such obvious differences between the duration distributions of sector A and B significance tests yield results indicating that the two distributions cannot be considered statistically different at the 0.05 level (Table 4.9).

Table 4.9: Significance test results comparing the distribution of flank eruption durations from Sectors A, B and C at Mt. Etna for the periods 1600-2010 and 1670-2010

Data			Logrank	Mann-Whitney	t-test
1600-2010	A (n=23)	B (n=29)	p = 0.472	p = 0.227	p = 0.393
	A (n=23)	C (n=6)	p = 0.870	p = 0.686	p = 0.851
	B (n=29)	C (n=6)	p = 0.988	p = 0.381	p = 0.690
1670-2010	A (n=20)	B (n=26)	p = 0.331	p = 0.324	p = 0.371
	A (n=20)	C (n=5)	p = 0.483	p = 1.000	p = 0.491
	B (n=26)	C (n=5)	p = 0.029 *	p = 0.147	p = 0.067 •

A = Sector A, B = Sector B, C = Sector C.
* = significant at a 0.05 level, • = moderate significance (p-value = 0.05-0.1).
t-test applied to the logs of the data.

Given that the distribution of flank eruption durations at Mt. Etna is found to be different for the period 1600-1669 (section 4.4.1), empirical survivor function curves have also been plotted for sectors A, B and C excluding this data (Fig. 4.15b). The curves

are very similar to their 1600-2010 counterpart (Fig. 4.15a) and the most prominent difference is the reduction in the longest reported eruption duration in sectors B and C. This reduces the degree of overlap in the long duration tail of sector A and B, however, significance tests comparing their distributions still yield p -values of greater than 0.05 and thus they cannot be considered statistically different at the 0.05 level (Table 4.9). In contrast a Logrank test and t -test applied to the distribution of flank eruption durations from sectors B and C in the period 1670-2010 indicate significant and moderate differences at the 0.05 level respectively (Table 4.9). The very low sample size of sector C ($n = 5$) make this result unreliable and it is not considered enough evidence to exclude the sector C data from any further analyses or forecasts made on the 1670-2010 data of Mt. Etna flank eruption durations.

4.5.2 Spatial variation at Kilauea

Table 3.2 contains information about the location of each eruption in terms of the broad location of the eruptive vent (i.e. summit (S), East Rift Zone (ERZ) and South-West Rift Zone (SWRZ)). Only two eruption durations are reported for the SWRZ in the period 1750-1983 (#4 and #37, Table 3.2 with durations 213 days and 0.25 days respectively) and further analyses on eruptions from this rift zone have not been performed.

Holcomb (1987) suggested that eruptions from the rift zones at Kilauea were briefer than those from the summit, however, the summit and ERZ eruptions of the current study in the period 1912-1983 have median durations that are very similar, at 5 days and 6 days respectively. Furthermore, the duration of eruptions from the ERZ range from 0.25 to 900 days while the summit eruptions have smaller range of 0.4 to 251 days. Empirical survivor function curves reflect these differences, with the ERZ data having a slightly longer eruption duration tail than the summit eruptions but both

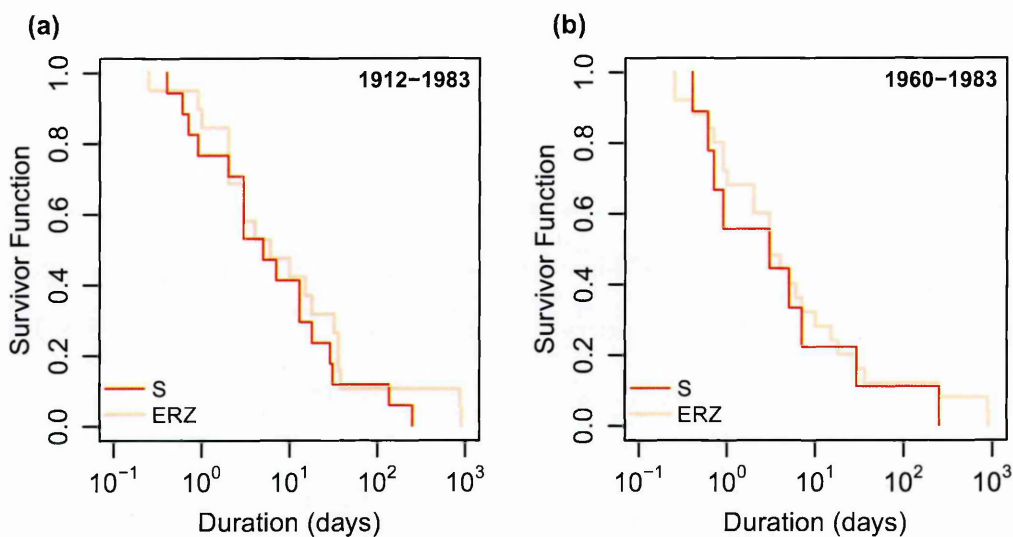


Fig. 4.16 Empirical survivor function curves from the summit (S) and east rift zone (ERZ) at Kilauea for the periods (a) 1912-1983 and (b) 1960-1983 (data from Table 3.2)

curves having similar overall shapes and positions (Fig. 4.16a). Significance tests also show that the distributions are not significantly different at the 0.05 level (Table 4.10). The same is true when the data are restricted to the period 1960-1983 (Fig. 4.16a, Table 4.10).

Table 4.10: Significance test results for eruption duration data from the summit and east rift zone (ERZ) of Kilauea for the periods 1912-1983 and 1960-1983

Data			Logrank	Mann-Whitney	t-test
1912-1983	A (n=17)	B (n=19)	p = 0.388	p = 0.578	p = 0.576
1960-1983	A (n=9)	B (n=15)	p = 0.380	p = 0.387	p = 0.441

A = Summit, B = ERZ.

★ = significant at a 0.05 level, ● = moderate significance (p-value = 0.05-0.1).

t-test applied to the logs of the data.

This implies that eruption duration does not vary with location (summit and ERZ) at Kilauea, however, little can be concluded about the duration of eruptions within the SWRZ due to limited data. The close association between summit and rift activity on Kilauea (Wolfe et al., 1987; Tilling and Dvorak, 1993) might be the reason for the similar eruption duration of these two regions.

4.5.3 Spatial variation at PdlF

Table 3.3 categorises the eruptions in the period 1972-2011 depending on their source location. Three categories have been used, summit eruptions from within Dolomieu crater, proximal eruptions from within the Enclose Fouqué caldera and distal eruptions from outside the Enclos Fouqué caldera and from the Plaines des Osmondes (Fig. 1.3) with median durations of 18 days, 17 days and 14 days respectively.

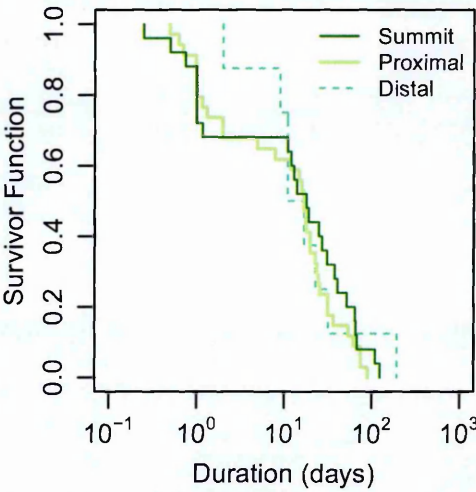


Fig. 4.17 Empirical survivor function curves for eruption durations within the summit, proximal and distal regions of PdlF (Fig. 1.3) for the period 1972-2011 (data from Table 3.3)

Fig. 4.17 displays empirical survivor function curves for these three datasets. The closeness in their median durations is reflected in their similar central portions, however, while the shapes of the summit and proximal eruption curves are very similar the curve for the distal eruption data contains fewer short duration eruptions and therefore shows greater variation. In fact, the bimodal distribution of eruption durations previously observed at PdlF and still visible in the empirical survivor function curves of summit and proximal durations is absent from the distal eruption data. This may imply that the parameters controlling eruption duration are different for distal eruptions such that very short duration eruptions are less frequent.

Despite the visual differences between the distributions of eruption durations from summit, proximal and distal vents, significance tests indicate that they are statistically similar (Table 4.11). This implies that the location of eruptions at PdlF has a negligible effect on the final duration of an eruption, however, the observations discussed above cannot be ignored and the implication they have on forecasting the duration of future eruptions at PdlF are discussed in Chapter 5.

Table 4.11: Significance test results comparing the distribution eruption durations from summit, proximal and distal eruptions of PdlF.

Data		Logrank	Mann-Whitney	t-test
A (n=25)	B (n=34)	p = 0.348	p = 0.718	p = 0.827
A (n=25)	C (n=8)	p = 0.824	p = 0.983	p = 0.399
B (n=34)	C (n=8)	p = 0.531	p = 0.676	p = 0.269

A = Summit, B = Proximal, C = Distal.
★ = significant at a 0.05 level, ● = moderate significance (p-value = 0.05-0.1).
t-test applied to the logs of the data.

Previous studies have identified correlations between the location of eruptions at PdlF and the petrology of their lavas (Stieltjes and Moutou, 1989; Peltier et al., 2009). Peltier et al. (2009) grouped the lavas into three categories; poorly-phyric lavas (PP) with < 5 % phenocrysts, olivine-rich basalts (OR) with 10 - 20 % olivine crystals and oceanites (O) with > 20 % olivine crystals. They found that distal eruptions were often categorized by high volume eruptions of olivine-rich or oceanite lavas while the poorly-phyric lavas are more commonly associated with summit and proximal eruptions. This same relationship can be seen in Fig. 4.18. Given such a strong relationship between the petrology of erupted lavas and the source location of the eruption, analyses into variations in eruption duration with petrology would reflect the location analyses previously discussed and therefore additional analyses have not been conducted in this study.

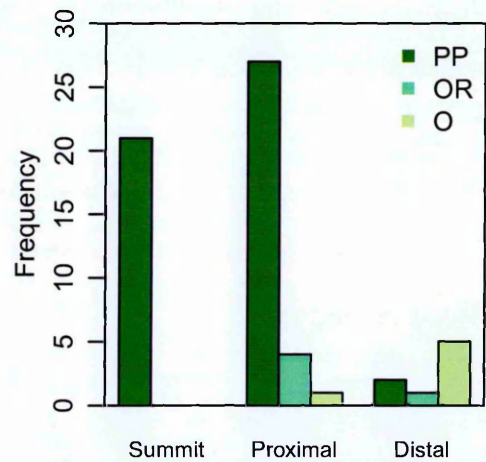


Fig. 4.18 Bar plot showing the frequency of eruptions with poorly-phyric (PP), Olivine rich (OR) and Oceanite (O) lavas from summit, proximal and distal regions of PdIF in the period 1972-2008 (data from Peltier et al. (2009) and summarised in Table 3.3)

4.5.4 Spatial variation on Iceland

The durations of single basaltic eruptions (d_6) from Icelandic volcanic systems (Table 3.5) are shown in Fig. 4.19, distinguished by source volcano and time period (1300-1899 and 1900-2011). The data are displayed such that the different volcanic systems are arranged in north to south order. Krafla and Askja lie in the Northern Volcanic Zone and the active axial rifting region of the plate boundary (Fig. 1.4). Grímsvötn lies close to the centre of the Iceland plume (Wolfe et al., 1997) and is the most frequently active volcanic system in Iceland (Thordarson and Larsen, 2007). It is located at the northern end of the Eastern Volcanic zone and has an associated fissure swarm extending to the south-west (Fig. 1.4). Hekla, Katla, Eyjafjallajökull and Vestmannaeyjar are found in the South Iceland Volcanic Zone which lacks well-developed fissure swarms and lies beyond the divergent plate boundary (Fig. 1.4), and is effectively in an intra-plate setting (Einarsson, 2008).

The 1996 Gjàlp eruption is either associated with Grímsvötn or Bárðarbunga, both of which are situated within the active rift zone of Iceland. For the purpose of Fig.

4.19 this eruption is placed in a separate category between Grímsvötn and Hekla and coloured according to inside rift zone eruptions. The volcanoes associated with active rifting (Krafla, Askja and Grímsvötn) erupt tholeiitic basalts whereas the volcanoes outside the active rifting region erupt transitional (Hekla, Eyjafjallajökull, Katla) to alkali (Vestmannaeyjar) basalts (Jakobsson, 1979).

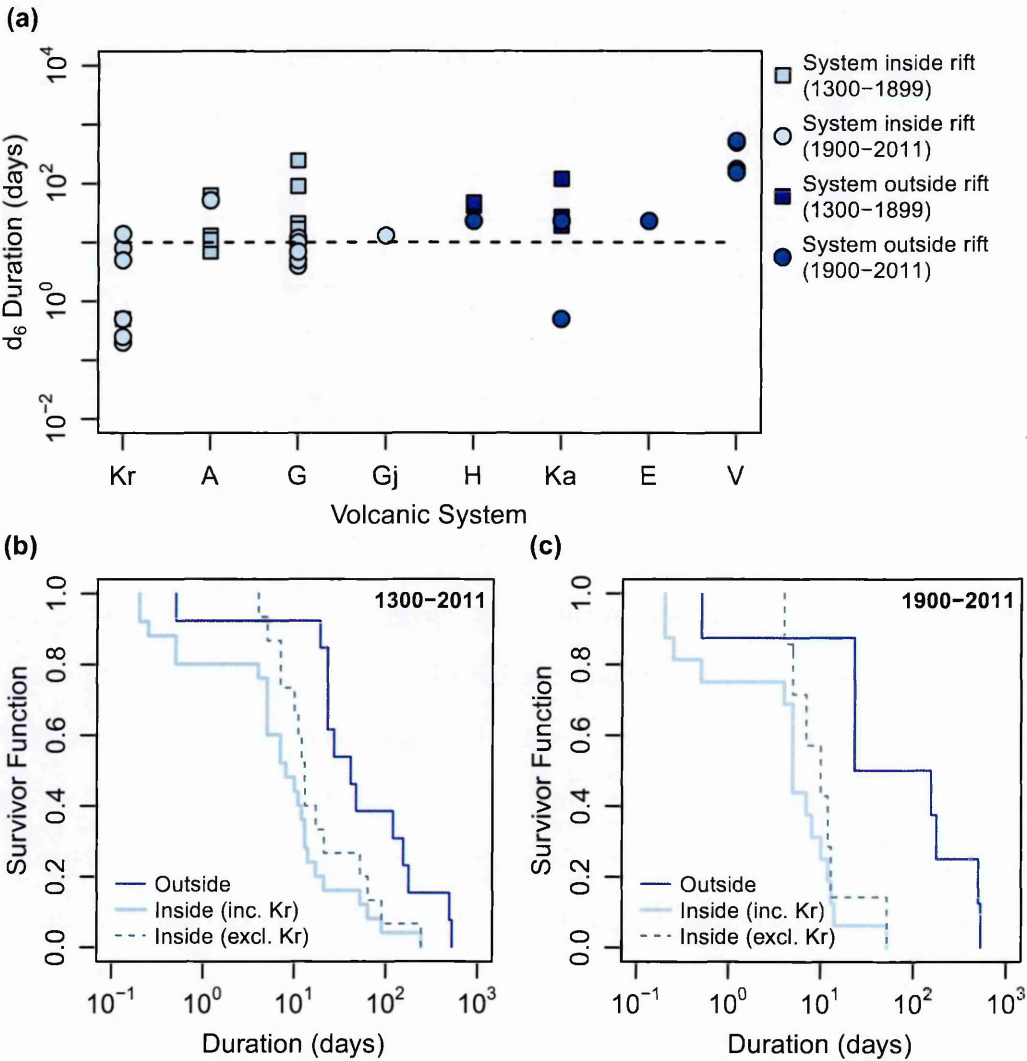


Fig. 4.19 (a) Plot of d_6 eruption duration at different Icelandic volcanic system separated by their location relative to the active rift. (b) and (c) empirical survivor function curves for d_6 eruption durations from volcanic systems situated inside (both including and excluding Krafla) and outside the activity rift zone on Iceland for the periods 1300-2011 and 1900-2011 respectively. Kr = Krafla, A = Askja, G = Grímsvötn, Gj = the Gjálpi 1996 eruption, H = Hekla, Ka = Katla, E = Eyjafjallajökull and V = Vestmannaeyjar

Fig. 4.19a reveals that only 1 of the 13 basaltic eruptions from volcanic systems sit-

uated outside the rift had a duration of < 10 days (this is the sub-glacial eruption of Katla in 1955 (#28, Table 3.5)), whereas 14 of the 25 eruptions from within the active rift lasted for 10 days or less. However, 9 of the short duration inside rift eruptions are from the Krafla volcanic system which has previously been shown to have a significantly different distribution of eruption durations to that of Askja, Grímsvötn and Katla.

Table 4.12: Significance test results for single basaltic eruption duration data from inside (both including and excluding data from Krafla (Kr)) and outside rift volcanoes on Iceland for the periods 1300-2011 and 1900-2011

Data		Logrank	Mann-Whitney	t-test
1300-2011	A (n=13) B (n=25)	p = 0.001 *	p = 0.001 *	p = 0.004 *
	A (n=13) C (n=15)	p = 0.027 *	p = 0.021 *	p = 0.120
1900-2011	A (n=8) B (n=16)	p = 0.000 *	p = 0.003 *	p = 0.015 *
	A (n=8) C (n=7)	p = 0.009 *	p = 0.042 *	p = 0.010 *

A = Outside rift eruptions, B = Inside rift eruptions (incl. Kr), C = Inside rift eruptions (excl. Kr).

* = significant at a 0.05 level, • = moderate significance (p-value = 0.05-0.1).

t-test applied to the logs of the data.

Fig. 4.19b shows empirical survivor function curves for inside (both including and excluding eruptions from Krafla) and outside rift eruption durations for the period 1300-2011. The greater proportion of < 10 day eruptions from inside rift volcanoes causes its curve to be offset from the outside rift curve. When the Krafla eruptions are excluded, this offset is still apparent, although less pronounced (Fig. 4.19b). Significance tests support these observations finding that in both cases the two distributions are statistically different at the 0.05 level (Table 4.12). The only exception to this is the t-test performed on the Krafla-excluded data (Table 4.12). To assess the effect of the general reporting bias towards longer eruptions in the early historical record the same analysis has been performed on data for the period 1900-2011 (Fig. 4.19c). Here the offset between the inside and outside empirical survivor function curves appear more pronounced and significance tests still indicate differences between the distribution of inside and outside rift eruptions that are significant at the 0.05 level.

These analyses imply that the short duration tail to the d_6 duration data (Fig. 4.6) is dominated by inside rift systems in general and is not just a result short eruptions from the Krafla volcanic system. In contrast the long duration tail to the distribution is dominated by eruptions from off-rift volcanic systems and in particular those from Vestmannaeyjar (Fig. 4.19a). However, there have been too few eruptions to assess whether this is a volcano specific effect or a function of outside rift volcanism.

4.6 Conclusions

The distribution of preferred eruption duration from Mt. Etna, Kilauea, PdlF and the datasets of Iceland have been described in this chapter and temporal or spatial variation within the data assessed. Very small datasets often lack long and short duration tails, producing an empirical survivor function curve which is relatively straight (Iceland (d_7) and Hekla (d_{3a} and d_4), Figs. 4.7 and 4.8, respectively). Where more data exists long and short duration tails to their distribution can be observed, although the degree of these vary depending on the dataset (Mt. Etna, Kilauea and Iceland (d_6), Figs. 4.3, 4.4 and 4.6, respectively). The exception to this is PdlF which shows a bimodal distribution to its duration data (Fig. 4.5).

The results of temporal analyses have identified a significant difference in the distribution of eruption durations at Mt. Etna following 1669 (Fig. 4.10), and Hekla following 1947 (Fig. 4.14) and a moderate change in duration distribution following 1959 was noted at Kilauea (Fig. 4.11). Spatial variations were found to have little effect on the distribution of eruption durations at Mt. Etna, Kilauea and PdlF (Figs. 4.15, 4.16, 4.17, respectively), however, the distribution of basaltic eruption durations from Iceland differs for volcanic systems situated inside and outside the active rift zone (Fig. 4.19).

Chapter 5

An empirical probabilistic approach to forecasting the duration of volcanic eruptions



Chapter 4 analysed the duration data for Mt. Etna, Kilauea, Piton de la Fournaise (PdlF) and Iceland identifying any changes related to temporal or spatial variations. This chapter summarises those results and uses the data to perform duration forecasts based on the empirical models outlined in Chapter 2. The model is based on historic eruption duration data, and therefore assumes that the past eruption record is a good representation of future volcanic activity. The forecasts produced can be considered to give useful insight into the typical eruptive behaviour of the volcanic system or type of volcanism being investigated. Here we present the likely and unlikely duration of

future eruptions using the likelihood scale devised by the Intergovernmental Panel on Climate Change (IPCC) which is summarised in Table 2.6.

For each dataset parameter values for the best fit exponential, Weibull, log-logistic and Burr type XII distribution have been found by maximum likelihood estimation. Kolmogorov-Smirnov (KS) goodness-of-fit tests and likelihood ratio (LR) tests are performed for each dataset to determine which theoretical distribution best describes the data and should be used in the empirical forecasting model (see section 2.3). Forecasts are then performed on the chosen datasets and their results compared.

5.1 Forecasting the duration of future flank eruptions at Mt. Etna

The completeness of the historical record of flank eruption durations from Mt. Etna was found to improve following 1600 AD (section 3.1) and data from the period 1600-2010 was used in the temporal and spatial analyses of Chapter 4. Results indicate that while eruption duration does not appear to be affected by the location of the eruptive vent or fissure, eruption durations changed after the year 1669, with the period 1600-1669 being dominated by longer duration eruptions. It is possible that these longer duration eruptions are a result of the shallow magma reservoir speculated by Hughes et al. (1990) and Behncke and Neri (2003) to have existed beneath Mt. Etna. Directly following the 1669 eruption Mt. Etna experienced a sharp decrease in productivity and a reduction in the phenocryst content of erupted lavas interpreted as a draining of this shallow magma reservoir which has not been re-established since (Hughes et al., 1990; Behncke and Neri, 2003).

Although evidence for a return to pre-1670 petrology is not yet found, a gradual increase in eruption frequency, output rate and magma accumulation has been identified

at Mt. Etna in recent years (Behncke and Neri, 2003). This may suggest that the plumbing system beneath Mt. Etna is gradually returning to the 1600-1670 physical state and if so, long duration eruptions akin to those of 1600-1670 may occur again in the future. Duration forecasts have therefore been made using the 1600-2010 and 1670-2010 datasets. The 1600-2010 dataset accounts for the possibility of very long future flank eruptions while the model based on the 1670-2010 data may provide more realistic forecasts of eruption durations that we can expect in the near future i.e. before the culminating phase of the current century-scale cycle.

5.1.1 Identifying the best fit distribution to the data of Mt. Etna

Parameter values for the best fit exponential, Weibull, log-logistic and Burr type XII distribution of each dataset are reported in Table 5.1. Fig. 5.1 plots the survivor function of each fitted distribution alongside the empirical survivor function curve of the corresponding observed data.

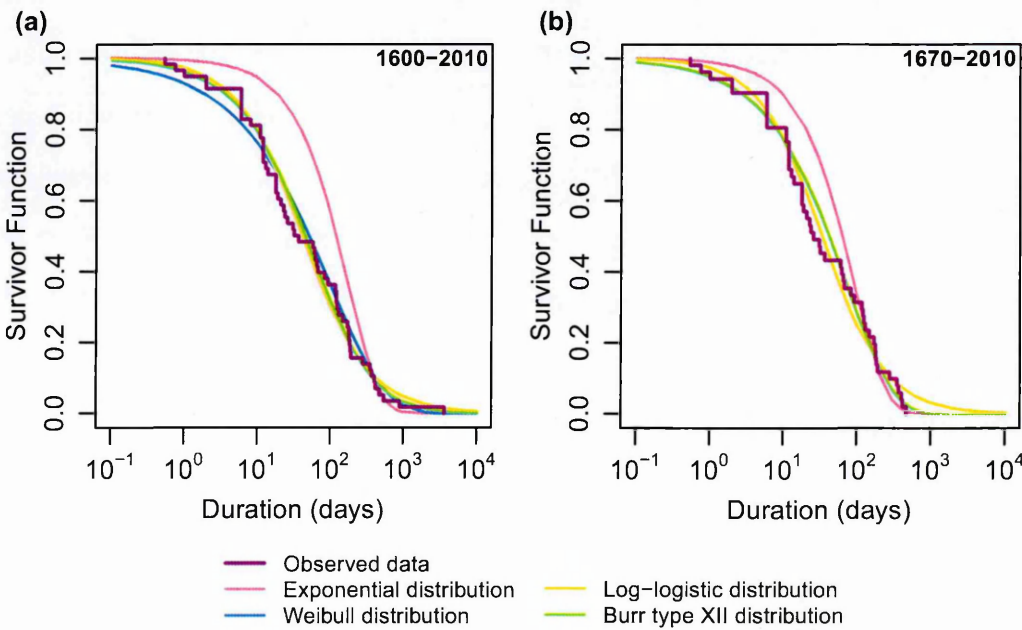


Fig. 5.1 Empirical survivor function curves and fitted theoretical distributions for flank eruption durations at Mt. Etna for the periods (a) 1600-2010 and (b) 1670-2010 (data from Table 3.1). Parameter values can be found in Table 5.1

KS goodness-of-fit tests indicate that both datasets could have derived from the Weibull, log-logistic or Burr type XII distributions (Table 5.1). Visually the Weibull distribution of the 1600-2010 data can be seen to give the poorest fit to the data diverging at durations < 10 days (Fig. 5.1a). In contrast, the shapes and positions of the 1670-2010 theoretical distributions show very little variation with the Weibull and Burr type XII distributions plotting almost identically (Fig. 5.1b). A *LR* test indicates that in both cases there is no benefit in employing the more complex Burr type XII distribution rather than the log-logistic distribution (Table 5.1). For these reasons, and our findings that a log-logistic distribution often provides an adequate fit to eruption duration data, the best fit log-logistic distribution of both datasets have been used to perform the following duration forecasts.

5.1.2 Forecasting results for Mt. Etna

Table 5.2 contains the results of seven forecasts performed on both the 1600-2010 and 1670-2010 flank eruption duration data of Mt. Etna. The primary difference between these two time periods is the longer durations associated with the 1600-1670 eruptions and as a result the probability of exceeding a given duration is consistently, but not considerably, lower for the 1670-2010 dataset which does not contain these eruptions (Table 5.2). For example, when the 1600-2010 data is considered, results show an 84 % (± 5 %) probability of exceeding 1 week (7 days) and a 57 % (± 7 %) probability of exceeding 1 month (30 days) which are reduced to 83 % and 52 % when only the 1670-2010 data is considered (Tables 5.2a and b). A similar trend is present in the results of the residual life function.

Quantile function results based on the 1600-2010 data suggest that a future flank eruption at Mt. Etna is likely to exceed 20 days (± 7 days) and unlikely to exceed 86 days (± 28 days) (Table 5.2a). When the dataset is restricted to the period 1670-2010 these

Table 5.1: Parameter values, Kolmogorov-Smirnov (KS) test and likelihood ratio (LR) test results for theoretical distributions fitted to the flank eruption duration data of Mt. Etna for (a) 1600-2010 and (b) 1670-2010

(a) 1600-2010

	Exponential	Weibull	Log-logistic	Burr type XII
	$\mu = 175.33$	$\beta = 0.57$	$\beta = 0.95$	$\alpha = 1.44$
		$\mu = 97.06$	$\sigma = 40.64$	$\beta = 0.81$
				$\sigma = 111.14$
D_{obs}	0.333	0.097	0.095	0.080
\hat{p}	0.000	0.177 \diamond	0.100 \diamond	0.199 \diamond
r	3000	2862	3000	2980
LR test statistic (log-logistic and Burr type XII):				0.726

(b) 1670-2010

	Exponential	Weibull	Log-logistic	Burr type XII
	$\mu = 92.12$	$\beta = 0.69$	$\beta = 1.01$	$\alpha = 65.96$
		$\mu = 71.01$	$\sigma = 33.07$	$\beta = 0.69$
				$\sigma = 52116.85$
D_{obs}	0.264	0.115	0.096	0.115
\hat{p}	0.000	0.077 \diamond	0.138 \diamond	0.055 \diamond
r	3000	2930	3000	2909
LR test statistic (log-logistic and Burr type XII):				3.282

In both tables:

\diamond not significant at the 0.05 level (p -value > 0.05).

D_{obs} = KS statistic, \hat{p} = estimated p -value and r = final bootstrap size.

durations are reduced to 17 days (± 6 days) and 67 days (± 22 days) respectively (Table 5.2b).

Mulargia et al. (1985) performed extreme value statistics on flank eruption duration data from Mt. Etna and concluded a 65 % probability of a 500 day eruption in the next 100 years. This highlights the difference between models designed to forecast ‘worse case scenarios’ (e.g. Mulargia et al. (1985)) and those designed to forecast

Table 5.2: Survivor function (SF), residual life function (R_{life}) and quantile function (Q) forecasts for flank eruption durations based on the (a) 1600-2010 and (b) 1670-2010 data of Mt. Etna. For the residual life function $t = 7$ days

(a) 1600-2010 (log-logistic)

	Input	Result	C/I	
			95 %	80 %
SF	7 d	84 %	$\pm 8 \%$	$\pm 5 \%$
	30 d	57 %	$\pm 11 \%$	$\pm 7 \%$
	365 d	11 %	$\pm 6 \%$	$\pm 4 \%$
R_{life}	21 d	77 %	$\pm 7 \%$	$\pm 4 \%$
	74 d	43 %	$\pm 11 \%$	$\pm 7 \%$
Q	0.34	20 d	$\pm 10 d$	$\pm 7 d$
	0.67	86 d	$\pm 43 d$	$\pm 28 d$

(b) 1670-2010 (log-logistic)

	Input	Result	C/I	
			95 %	80 %
SF	7 d	83 %	$\pm 9 \%$	$\pm 6 \%$
	30 d	52 %	$\pm 12 \%$	$\pm 8 \%$
	365 d	8 %	$\pm 5 \%$	$\pm 4 \%$
R_{life}	21 d	74 %	$\pm 8 \%$	$\pm 5 \%$
	74 d	37 %	$\pm 12 \%$	$\pm 8 \%$
Q	0.34	17 d	$\pm 9 d$	$\pm 6 d$
	0.67	67 d	$\pm 34 d$	$\pm 22 d$

In both tables:

d = days, C/I = confidence interval

typical eruptive behaviour (the current study). Both types of model have their uses, and a combined approach would best inform mitigation strategies highlighting not just what events are likely in the future but also what extreme events have the potential to occur.

5.2 Forecasting the duration of eruptions from Kilauea

The Kilauea dataset compiled for this study stops with the onset of the Pu'u'Ō'ō - Kūpaianaha eruption in January 1983. This eruption was still continuing on 19 July 2013 (Heliker and Mattox, 2003; Venzke et al., 2013). The forecasts made here do not necessarily refer to future eruptions at Kilauea but represent what would have been expected prior to the 1983 eruption.

Section 3.2 demonstrated improvement in the reporting of eruptive activity at Kilauea following the establishment of the Hawaiian Volcano Observatory in 1912. Temporal

and spatial analyses performed on durations reported for the period 1912-1983 identified a higher proportion of short duration eruptions following 1959, however, it is unclear whether these reflect an earlier reporting bias or a new eruption duration regime in response to a change in the physical properties of the volcano's plumbing system. Eruption duration forecasts have been made using both the 1912-1983 and 1960-1983 datasets.

5.2.1 Identifying the best fit distribution to the data of Kilauea

Parameter values for the best fit exponential, Weibull, log-logistic and Burr type XII distribution of each dataset are reported in Table 5.3. Fig. 5.2 plots the survivor function of each fitted distribution alongside the empirical survivor function curve of the corresponding observed data.

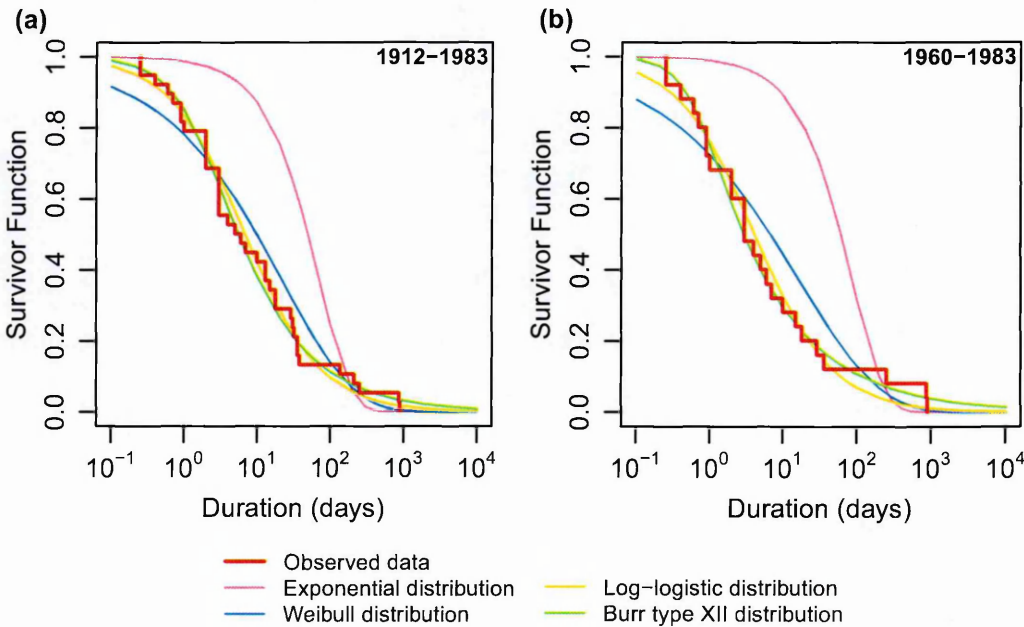


Fig. 5.2 Empirical survivor function curves and fitted theoretical distributions for the duration of eruptions at Kilauea for the periods (a) 1912-1983 and (b) 1960-1983 (data from Table 3.2). Parameter values can be found in Table 5.3

KS goodness-of-fit tests indicate that the log-logistic and Burr type XII distributions

provide adequate fits to the data (Table 5.3). For the 1912-1983 dataset, strong similarities exist between these two distributions (Fig. 5.2a) and a LR test indicates that there is no benefit in employing the Burr type XII distribution (Table 5.3a) and a log-logistic distribution forms the basis of the 1912-1983 forecasts of Kilauea. A LR test performed on the best fit log-logistic and Burr type XII distributions of the 1960-1983 data is also not significant at the 0.05 level, however, the test statistic (3.754) is very close to the critical value of 3.84. This, in conjunction with the visually poorer fit of the log-logistic distribution to the long and short duration tails of the data (Fig. 5.2b) has led to the best fit Burr type XII distribution being used to model the 1960-1983 data in the following forecasts.

5.2.2 Forecasting results for Kilauea

Table 5.4 contains the results of nine forecasts performed on both the 1912-1983 and 1960-1983 duration data of Kilauea. Forecasts of 0 % do not indicate that an event of this duration is impossible, but reflect probabilities of between 0 and 0.5 but have been rounded for presentation purposes in Table 5.4.

The primary difference between the 1912-1983 and 1960-1983 datasets exists in the short duration data (Fig. 5.2) and is reflected in the survivor function forecasts made where exceedance probabilities for $x = 3, 7$ and 30 days are lower when based on the 1960-1983 data than when based on the 1912-1983 data (Table 5.4). In contrast, forecasts performed for longer durations show the opposite relationship, with the probability of an eruption exceeding a duration of 1 year (365 days) increasing from 3 % (± 2 %) to 6 % (± 5 %) when the data is restricted to the period 1960-1983 (Table 5.4). A similar trend exists in the residual life function results (Table 5.4).

It is worth noting that although the difference between the forecasting results obtained from these two datasets is larger than those between the two versions of the Mt. Etna

Table 5.3: Parameter values, Kolmogorov-Smirnov (KS) test and likelihood ratio (LR) test results for theoretical distributions fitted to the duration data of Kilauea for (a) 1912-1983 and (b) 1960-1983

(a) 1912-1983

	Exponential	Weibull	Log-logistic	Burr type XII
	$\mu = 71.39$	$\beta = 0.45$	$\beta = 0.84$	$\alpha = 0.55$
		$\mu = 22.10$	$\sigma = 6.66$	$\beta = 1.25$
				$\sigma = 1.87$
D_{obs}	0.490	0.378	0.111	0.094
\hat{p}	0.000	0.000	0.126 \diamond	0.326 \diamond
r	3000	2851	3000	2958
LR test statistic (log-logistic and Burr type XII):				1.505

(b) 1960-1983

	Exponential	Weibull	Log-logistic	Burr type XII
	$\mu = 86.92$	$\beta = 0.40$	$\beta = 0.82$	$\alpha = 0.44$
		$\mu = 16.79$	$\sigma = 4.02$	$\beta = 7.88$
				$\sigma = 0.62$
D_{obs}	0.610	0.484	0.096	0.103
\hat{p}	0.000	0.000	0.679 \diamond	0.541 \diamond
r	3000	2971	3000	2905
LR test statistic (log-logistic and Burr type XII):				3.754

In both tables:

\diamond not significant at the 0.05 level (p -value > 0.05).

$D_{obs} = KS$ statistic, \hat{p} = estimated p -value and r = final bootstrap size.

dataset (section 5.1.2) they often fall within the range defined by 80 % confidence intervals. For example when the 1912-1983 data is used a future eruption has a 22 % (± 7 %) probability of exceeding 30 days, resulting in a probability range of 15-29 %. This therefore covers the probability calculated when the 1960-1983 data is used of 18 % (± 8 %) (Table 5.4).

The next eruption to occur at Kilauea was the January 1983 Pu'u'Ō'ō - Kūpaianaha

Table 5.4: Survivor function (SF), residual life function (R_{life}) and quantile function (Q) forecasts for eruption durations based on the (a) 1912-1983 and (b) 1960-1983 data of Kilauea. For the residual life function $t = 3$ days

(a) 1912-1983 (log-logistic)					(b) 1960-1983 (Burr type XII)				
	Input	Result	C/I			Input	Result	C/I	
			95 %	80 %				95 %	80 %
SF	3 d	66 %	± 13 %	± 8 %	SF	3 d	49 %	± 18 %	± 12 %
	7 d	49 %	± 14 %	± 9 %		7 d	34 %	± 15 %	± 10 %
	30 d	22 %	± 11 %	± 7 %		30 d	18 %	± 13 %	± 8 %
	365 d	3 %	± 3 %	± 2 %		365 d	6 %	± 8 %	± 5 %
	30 y	0 %	± 0 %	± 0 %		30 y	1 %	± 3 %	± 2 %
R_{life}	10 d	63 %	± 11 %	± 7 %	R_{life}	10 d	59 %	± 17 %	± 11 %
	33 d	31 %	± 14 %	± 9 %		33 d	35 %	± 21 %	± 14 %
Q	0.34	3 d	± 2 d	± 1 d	Q	0.34	1 d	± 1 d	± 1 d
	0.67	15 d	± 11 d	± 7 d		0.67	8 d	± 8 d	± 5 d

In both tables:
 d = days, y = years
C/I = confidence interval

eruption. The empirical forecasting model gives a very low probability of an eruption exceeding a 30 year duration at Kilauea, the highest result being 1 % (± 2 %) when the 1960-1983 dataset is used (Table 5.4). The 18th Century sustained summit eruption of Kilauea which was dominated by lava lake activity (# 1, Table 3.2) is arguably similar to the on-going Pu’u’Ō’ō - Kūpaianaha eruption, however due to the possible reporting biases discussed in Chapter 3 this eruption is not included in either of these datasets. The addition of this 36,890 day eruption to the 1960-1983 dataset has the effect of increasing the probability of an > 30 year duration eruption at Kilauea to only 3 % (± 3 %) (forecast obtained using a Burr type XII distribution with $\alpha = 0.35$, $\beta = 2.33$ and $\sigma = 0.46$).

Although events with such low probabilities do occur they are incredibly rare and it is reasonable to suppose that the physical properties of the plumbing system beneath Kilauea changed, allowing such an unusually long duration eruption to occur. Evi-

dence for a change in volcanic activity prior to the eruption includes a dominance of intrusions following the magnitude 7.2 earthquake in 1975 and Heliker and Mattox (2003) suggest that three intrusions that occurred in the upper ERZ from September to December 1982 may have primed the magmatic system for the eruption in January 1983. The idea of a change in the physical properties of Kilauea prior to the January 1983 Pu'u Ō'ō - Kūpaianaha eruption will be returned to in Chapter 7.

5.3 Forecasting the duration of future eruptions from Piton de la Fournaise (PdIF)

A good historical record exists for PdIF and in terms of reported durations the early eruption record was found to be less biased than the other datasets investigated in this study (subsection 3.3.4). The duration data from PdIF in the period 1911-2011 was found to be bimodal, and although this was visually more pronounced for data from the period 1972-1992 than that before or after it and least pronounced in distal eruptions from outside the Enclos Fouqué caldera, these variations were not found to be significant at the 0.05 level (Chapter 4). Therefore data from the 1911-2011 period forms the basis of the forecasting model presented in the following sections, however, modified versions of the data according to these visual findings are also used to reduce the bimodal nature of the observed data and improve the fit of theoretical distributions.

5.3.1 Identifying the best fit distribution to the data of PdIF

Parameter values for the best fit exponential, Weibull, log-logistic and Burr type XII distribution of the 1911-2011 dataset are reported in Table 5.5a. Fig. 5.3a plots the survivor function of each fitted distribution alongside the empirical survivor function

curve of the observed data. The shape of the 1911-2011 empirical survivor function curve (Fig. 5.3a) reflects the bimodal nature of the duration data for PdIF. Visually it is evident that all four theoretical distributions provide a poor fit to the data at durations < 10 days (Fig. 5.3a). *KS* goodness-of-fit tests support this observation with only the Burr type XII distribution having a *p*-value of > 0.05 (0.091) (Table 5.5a).

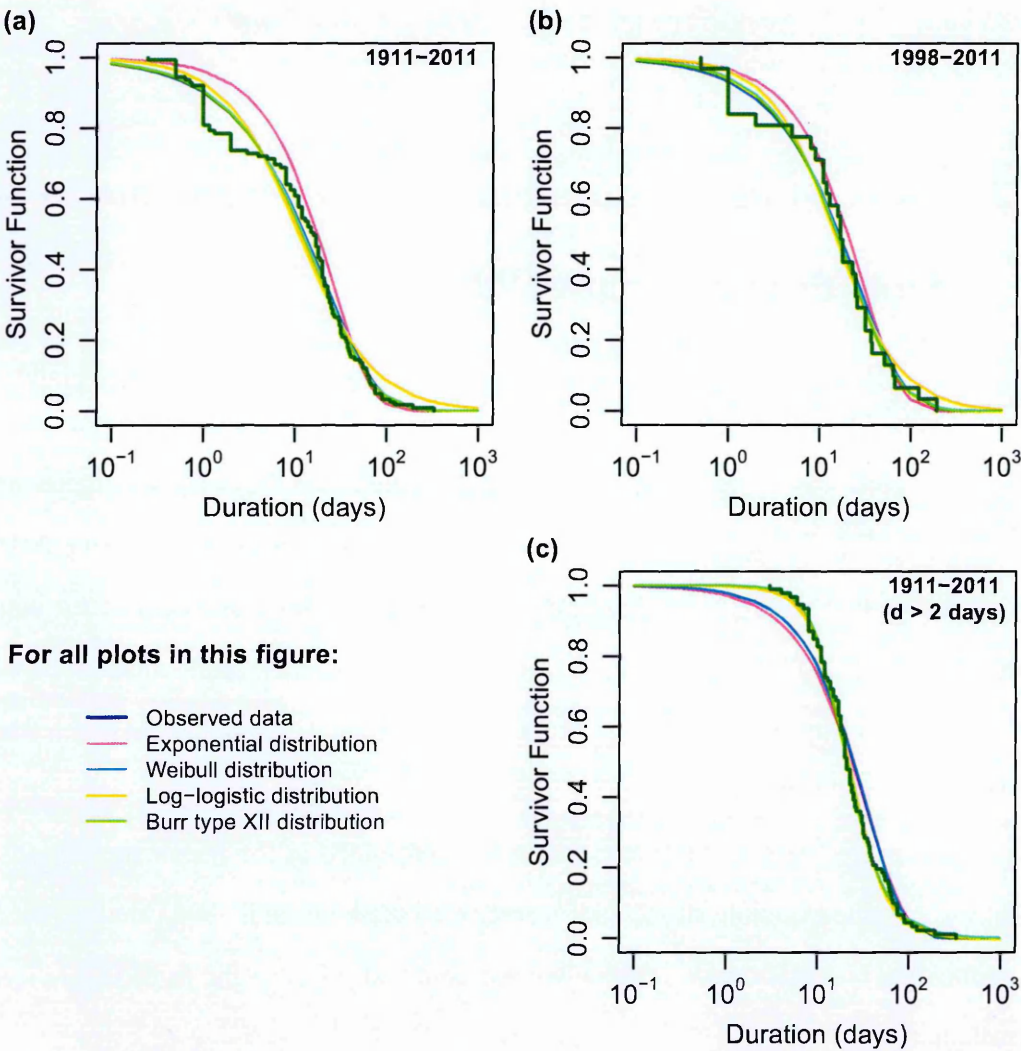


Fig. 5.3 Empirical survivor function curves and best fit theoretical distributions for the duration of eruptions at PdIF for the period (a) 1911-2011, (b) 1998-2011 and (c) 1911-2011 but restricted to eruptions > 2 days (data from Table 3.3). Parameter values can be found in Table 5.5

The temporal analyses of section 4.4 identified a reduced bimodal distribution in data from the periods 1911-1966 and 1998-2011. The empirical survivor function curve and its fitted exponential, Weibull, log-logistic and Burr type XII distributions for the

Table 5.5: Parameter values, Kolmogorov-Smirnov (KS) test and likelihood ratio (LR) test results for theoretical distributions fitted to the duration data of PdIF for (a) 1911-2011, (b) 1998-2011 and (c) 1911-2011 durations > 2 days

(a) All reported durations, 1911-2011

	Exponential	Weibull	Log-logistic	Burr type XII
	$\mu = 25.57$	$\beta = 0.74$	$\beta = 1.07$	$\alpha = 7.44$
		$\mu = 21.04$	$\sigma = 11.28$	$\beta = 0.79$
				$\sigma = 318.19$
D_{obs}	0.189	0.103	0.127	0.111
\hat{p}	0.000	0.002	0.000	0.091 \diamond
r	3000	3000	3000	2865
LR test statistic (log-logistic and Burr type XII):				14.510

(b) All reported durations, 1998-2011

	Exponential	Weibull	Log-logistic	Burr type XII
	$\mu = 29.18$	$\beta = 0.81$	$\beta = 1.21$	$\alpha = 4.90$
		$\mu = 25.81$	$\sigma = 14.93$	$\beta = 0.91$
				$\sigma = 139.15$
D_{obs}	0.128	0.104	0.125	0.106
\hat{p}	0.424 \diamond	0.514 \diamond	0.121 \diamond	0.874 \diamond
r	3000	2998	3000	2966
LR test statistic (log-logistic and Burr type XII):				2.948

(c) Durations > 2 days, 1911-2011

	Exponential	Weibull	Log-logistic	Burr type XII
	$\mu = 34.36$	$\beta = 1.07$	$\beta = 2.08$	$\alpha = 1.63$
		$\mu = 35.49$	$\sigma = 22.14$	$\beta = 2.48$
				$\sigma = 16.64$
D_{obs}	0.143	0.119	0.055	0.050
\hat{p}	0.005	0.003	0.594 \diamond	0.673 \diamond
r	3000	3000	3000	3000
LR test statistic (log-logistic and Burr type XII):				1.187

In all three tables: \diamond not significant at the 0.05 level (p -value > 0.05).
 D_{obs} = KS statistic, \hat{p} = estimated p -value and r = final bootstrap size.

most recent dataset (1998-2011) are displayed in Fig. 5.3b. Significance tests indicate that although the theoretical distributions are still poor descriptors of durations < 10 days it is conceivable that the observed data could have derived from any of the four distributions (Table 5.5b). Differences can be observed in the three best fit distributions, with the log-logistic distribution proving a poor fit the long duration tail of the observed data and the exponential distribution showing the greatest divergence at low durations (Table 5.5b). Despite a LR test indicating that there is little benefit in using the Burr type XII distribution in preference to the log-logistic distribution, the visually better fit of the Burr type XII distribution led to its use in forecasts performed from this dataset.

Eruption durations from distal vents at PdlF (outside the Enclos Fouqué caldera) also appear to have a reduced bimodal shape to their duration distribution. However, distal eruptions are rare and this result is based on only 8 known durations from the period 1911-2011 and therefore is considered inconclusive and forecasts have not been performed for these eruptions separately here.

As previously mentioned the duration data for PdlF in the period 1998-2011 is not entirely free of a bimodal distribution and theoretical distributions struggle to accurately describe the data at durations < 10 days. The bimodal nature of the PdlF data has one mode affects duration of ≤ 2 days, and the ability to forecast such short duration eruptions is considered unnecessary from a hazard perspective (longer duration eruptions are likely to have a greater impact of the lives of surrounding communities. Instead eruptions of ≤ 2 days have been excluded and this restricted dataset is used to perform forecasts for the duration of future eruptions (Fig. 5.3c). In this sense, the model is similar to the residual life function. Further applications of this model on data which is bimodal, with both modes affecting sufficiently long durations may require a combination of theoretical distributions to model the observed data more effectively.

KS goodness-of-fit test results indicate that the > 2 day data could have derived from

either the log-logistic or Burr type XII distribution and a LR test indicates that there is no benefit in employing the Burr type XII distribution rather than the log-logistic distribution (Table 5.5c). The log-logistic distribution is therefore used in the forecasts of the following section. Forecasts based on the complete 1911-2011 dataset and the temporally restricted 1998-2011 dataset using their best fit Burr type XII distributions (Table 5.5a and b) are also performed for comparative purposes.

5.3.2 Forecasting results for PdIF

Table 5.6 contains the results of eight forecasts based on data from 1911-2011, 1998-2011 and a restricted dataset of durations > 2 days. To simplify future discussion these datasets will be referred to as 1911-2011 (unrestricted), 1998-2011 and 1911-2011 (restricted) respectively.

For the 1911-2011 (unrestricted) data and the 1998-2011 data residual life functions have been performed for total durations of 7 and 30 days where $t = 2$ days (Table 5.6a and b). This scenario is comparable to the survivor function results for 7 and 30 days based on the 1911-2011 (restricted) data (Table 5.6c). The key difference between these two methods is that the restricted data has its own best fit theoretical distribution on which forecasts are based, however, the residual life function does not find a new best fit distribution to the data with duration $> t$ but uses the original distribution in its calculations. In response to this the probability of exceeding 7 or 30 days is highest when the survivor function is used on the restricted data and the difference between the results is reduced when longer durations are considered. For example the difference is 28 % for 7 days and 9 % for 30 days, Table 5.6.

Using the 1911-2011 (restricted) data the quantile function indicates that once a future eruption of PdIF has been on-going for 2 days its total duration is likely to exceed 16 days (± 2 days) but unlikely to exceed 31 days (± 4 days) (Table 5.6c).

Table 5.6: Survivor function (SF), residual life function (R_{life}) and quantile function (Q) forecasts for eruption durations based on the (a) 1911-2011 data, (b) 1998-2011 and (c) 1911-2011 data excluding eruptions ≤ 2 days. For the residual life function of table (a) and (b) $t = 2$ days and table (c) $t = 7$ days

(a) 1911-2011: All data (Burr type XII)

	Input	Result	C/I	
			95 %	80 %
SF	3 d	79 %	$\pm 6 \%$	$\pm 4 \%$
	7 d	64 %	$\pm 7 \%$	$\pm 5 \%$
	30 d	26 %	$\pm 6 \%$	$\pm 4 \%$
	180 d	1 %	$\pm 1 \%$	$\pm 1 \%$
R_{life}	7 d	76 %	$\pm 4 \%$	$\pm 3 \%$
	30 d	31 %	$\pm 7 \%$	$\pm 5 \%$
Q	0.34	6 d	$\pm 13 d$	$\pm 8 d$
	0.67	23 d	$\pm 38 d$	$\pm 25 d$

(b) 1998-2011: All data (Burr type XII)

	Input	Result	C/I	
			95 %	80 %
SF	3 d	85 %	$\pm 11 \%$	$\pm 7 \%$
	7 d	71 %	$\pm 13 \%$	$\pm 9 \%$
	30 d	30 %	$\pm 14 \%$	$\pm 9 \%$
	180 d	1 %	$\pm 3 \%$	$\pm 2 \%$
R_{life}	7 d	79 %	$\pm 8 \%$	$\pm 5 \%$
	30 d	34 %	$\pm 15 \%$	$\pm 10 \%$
Q	0.34	9 d	$\pm 30 d$	$\pm 19 d$
	0.67	27 d	$\pm 75 d$	$\pm 49 d$

(c) 1911-2011: Durations > 2 days
(log-logistic)

	Input	Result	C/I	
			95 %	80 %
SF	3 d	98 %	$\pm 1 \%$	$\pm 1 \%$
	7 d	92 %	$\pm 4 \%$	$\pm 3 \%$
	30 d	35 %	$\pm 8 \%$	$\pm 6 \%$
	180 d	1 %	$\pm 1 \%$	$\pm 1 \%$
R_{life}	14 d	73 %	$\pm 8 \%$	$\pm 5 \%$
	37 d	37 %	$\pm 8 \%$	$\pm 5 \%$
Q	0.34	16 d	$\pm 3 d$	$\pm 2 d$
	0.67	31 d	$\pm 6 d$	$\pm 4 d$

In all three tables tables:

d = days, C/I = confidence interval

Since the submission of this thesis a short, 1 day eruption has occurred at PdIF (21-22 June 2014 (Venzke et al., 2013)). For reasons previously discussed the model presented here poorly describes such short duration eruptions and therefore this eruption cannot

be used to validate the forecasting results obtained.

5.4 Forecasting the duration of volcanic eruptions on Iceland

5.4.1 Forecasting mixed eruption durations (d_{3a} and d_4) from Hekla

The unusually complete record of eruptions from Hekla in the period 1300-2000 has enabled volcano-specific forecasts of the total duration (d_4) and the duration of the initial explosive phase (d_{3a}) of mixed eruptions to be performed. Chapter 4 identified a decrease in the d_4 duration of these eruptions following 1947 which is unlikely to be related to reporting. Eruption duration forecasts have therefore been made on two datasets of d_4 durations for the periods 1300-2000 and 1948-2000. Temporal variations in the d_{3a} durations were not found and therefore the forecasts in the following sections are based on all available durations of this type in Table 4.2.

Identifying the best fit distribution to the d_{3a} and d_4 data of Hekla

Parameter values for the best fit exponential, Weibull, log-logistic and Burr type XII distribution of each dataset are reported in Table 5.7. Fig. 5.4 plots the survivor function of each fitted distribution alongside the empirical survivor function curve of the corresponding observed data.

KS goodness-of-fit tests indicate that the d_{3a} data could have derived from any of the tested distributions (Table 5.7). Visually there is very little difference between their survivor function curves and a LR test indicates that there is no benefit in employing the more complex Burr type XII distribution rather than the log-logistic distribution.

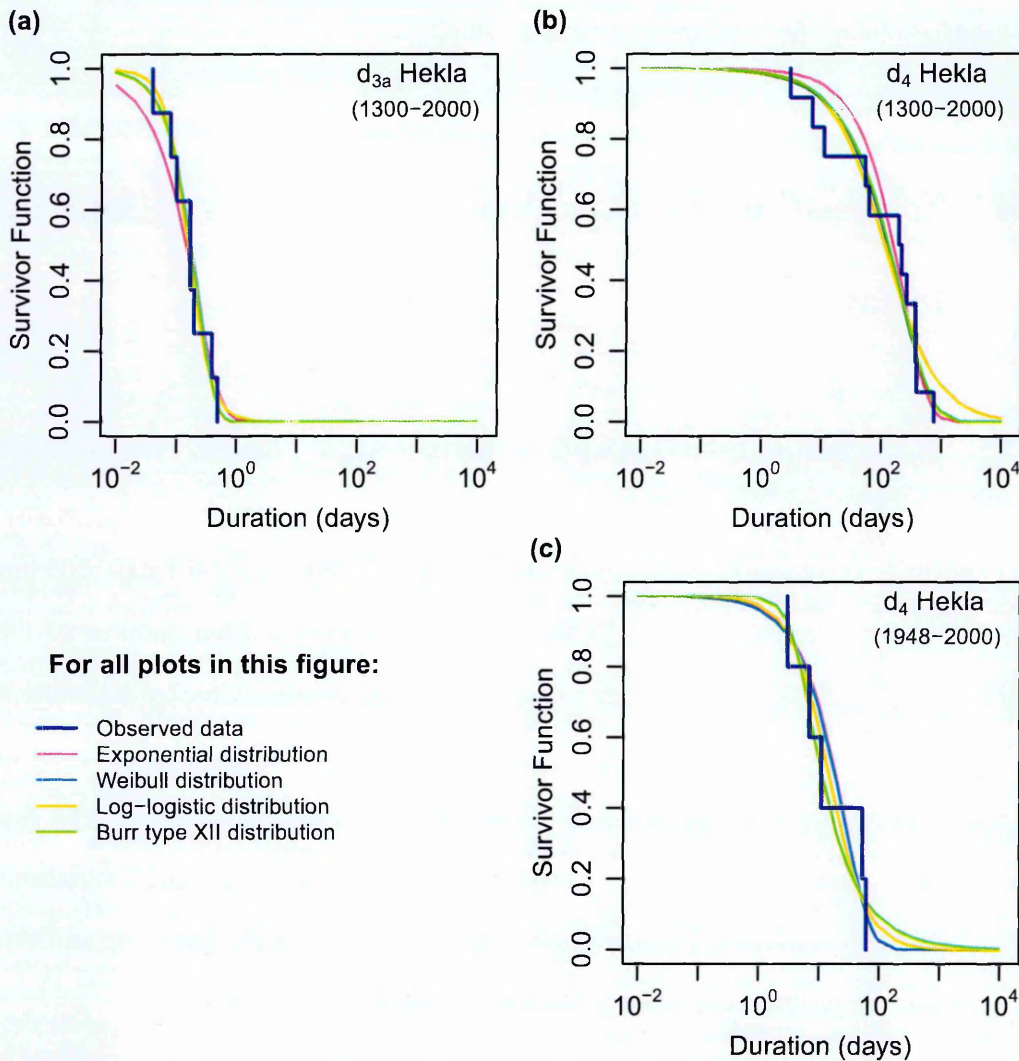


Fig. 5.4 Empirical survivor function curves and best fit theoretical distributions for the duration of mixed eruptions from Hekla, Iceland. (a) d_{3a} : 1300-2000, (b) d_4 : 1300-2000 and (c) d_4 : 1948-2000. Parameter values can be found in Table 5.5

The log-logistic distribution has been used to perform forecasts of this type of duration from Hekla.

For the 1300-2000 d_4 data of Hekla KS tests indicate that the data could have derived from the exponential, Weibull or Burr type XII distributions (Table 5.7b). The p -value obtained for the log-logistic distribution is 0.047 and although this implies that it is a poor fit to the observed data a LR test suggests that there is no benefit in using the Burr type XII distribution in preference to the log-logistic distribution. The LR test statistic (3.310) is close to the critical value (3.84) and given that the log-logistic distribution

Table 5.7: Parameter values, Kolmogorov-Smirnov (KS) test and likelihood ratio (LR) test results for theoretical distributions fitted to the mixed eruption duration data of Hekla, Iceland. (a) d_{3a} : 1300-2000, (b) d_4 : 1300-2000 and (c) d_4 : 1948-2000

(a) d_{3a} : 1300-2000

	Exponential	Weibull	Log-logistic	Burr type XII
	$\mu = 0.21$	$\beta = 1.44$	$\beta = 2.19$	$\alpha = 26.65$
		$\mu = 0.23$	$\sigma = 0.16$	$\beta = 1.48$
				$\sigma = 1.56$
D_{obs}	0.195	0.192	0.162	0.186
\hat{p}	0.074 \diamond	0.553 \diamond	0.697 \diamond	0.447 \diamond
r	3000	2877	3000	2901
LR test statistic (log-logistic and Burr type XII):				0.167

(b) d_4 : 1300-2000

	Exponential	Weibull	Log-logistic	Burr type XII
	$\mu = 224.33$	$\beta = 0.79$	$\beta = 0.98$	$\alpha = 139.37$
		$\mu = 200.85$	$\sigma = 112.73$	$\beta = 0.81$
				$\sigma = 119305.99$
D_{obs}	0.202	0.204	0.213	0.203
\hat{p}	0.413 \diamond	0.187 \diamond	0.047	0.109 \diamond
r	3000	2939	3000	2990
LR test statistic (log-logistic and Burr type XII):				3.301

(c) d_4 : 1948-2000

	Exponential	Weibull	Log-logistic	Burr type XII
	$\mu = 27.00$	$\beta = 0.98$	$\beta = 1.37$	$\alpha = 0.77$
		$\mu = 26.76$	$\sigma = 14.67$	$\beta = 2.67$
				$\sigma = 4.70$
D_{obs}	0.265	0.258	0.253	0.246
\hat{p}	0.614 \diamond	0.405 \diamond	0.271 \diamond	0.271 \diamond
r	3000	2999	3000	2997
LR test statistic (log-logistic and Burr type XII):				0.021

In all three tables: \diamond not significant at the 0.05 level (p -value > 0.05).
 D_{obs} = KS statistic, \hat{p} = estimated p -value and r = final bootstrap size.

has a KS test p -value of < 0.05 the Burr type XII distribution is used to perform the duration forecasts of the following section (Table 5.7b).

When only the most recent durations are considered (1948-2000) all four theoretical distributions have KS test results indicating that they adequately describe the observed data (Table 5.7c). The survivor function curves of the distributions plot with similar shapes and positions and this, combined with the small sample size, makes deciding which distribution to use in the forecasting model difficult. A log-logistic distribution often provides adequate fit to eruption duration data and therefore the best fit log-logistic distribution of the 1948-2000 d_4 data has been used to perform the following duration forecasts.

Forecasting results for mixed eruptions from Hekla

Table 5.8 contains the results of seven forecasts made from the best fit log-logistic distribution of the d_{3a} : 1300-2000 dataset. Due to the short duration of these eruptions input values for the survivor function (x) and the residual life function (x and t) are considerably smaller than they are for the other forecasts made in this study. Despite this, results indicate that the probability of the initial explosive phase of a future mixed eruption from Hekla exceeding 12 hours (0.5 day) is only 8 % (± 9 %) (Table 5.8). Furthermore quantile function results indicate that the d_{3a} duration of a future mixed eruption at Hekla is likely to exceed 3 hours (± 1 hour) but unlikely to exceed 5 hours (± 2 hours) (Table 5.8).

Nine forecasts have been made for the d_4 datasets of Hekla (1300-2000 and 1948-2000) and their results are displayed in Table 5.9. Eruptions during the period 1300-1947 were considerably longer than any mixed eruption of Hekla since and the absence of these long duration eruptions in the 1948-2000 dataset is reflected in the forecasting results obtained. For example when the 1300-2000 data is used the probability of an

Table 5.8: Survivor function (SF), residual life function (R_{life}) and quantile function (Q) forecasts for the initial explosive phase duration of mixed eruptions (d_{3a}) from Hekla for the period 1300-2000. For the residual life function $t = 0.25$ days

1300-2000: d_{3a} (log-logistic)				
	Input	Result	C/I	
			95 %	80 %
SF	0.25 d	27 %	± 26 %	± 17 %
	0.5 d	8 %	± 13 %	± 9 %
	1 d	2 %	± 5 %	± 3 %
R_{life}	0.75 d	12 %	± 18 %	± 12 %
	1.25 d	4 %	± 9 %	± 6 %
Q	0.34	0.12 d	± 0.07 d	± 0.04 d
	0.67	0.22 d	± 0.13 d	± 0.08 d

d = days, C/I = confidence interval

eruption duration exceeding 30 days is 81 % (± 12 %) and is reduced to 27 % (± 23 %) when the data is restricted to the period 1948-2000 (Table 5.9). Even when the 80 % confidence intervals are taken into account these probabilities do not overlap (Table 5.9).

The same relationship is true for the residual life function and quantile function forecasts (Table 5.9). Considering that the 1948-2000 period represents the most recent eruptions at Hekla it is probable that eruptions during this period best reflect the state of the plumbing system beneath Hekla today and therefore forecasts of future activity are based on the eruptions within this time period. Quantile functions performed on this data indicate that a future mixed eruption at Hekla is likely to exceed 9 days (± 7 days) but unlikely to exceed 25 days (± 20 days) (Table 5.9b).

Table 5.9: Survivor function (SF), residual life function (R_{life}) and quantile function (Q) forecasts for the total duration of mixed eruptions from Hekla based on data from the periods (a) 1300-2000 and (b) 1948-2000. For the residual life function $t = 7$ days

(a) d_4 , 1300-2000 (Burr type XII)					(b) d_4 , 1948-2000 (Log-logistic)				
	Input	Result	C/I			Input	Result	C/I	
			95 %	80 %				95 %	80 %
SF	7 d	94 %	$\pm 10 \%$	$\pm 6 \%$		7 d	73 %	$\pm 34 \%$	$\pm 22 \%$
	30 d	81 %	$\pm 18 \%$	$\pm 12 \%$		30 d	27 %	$\pm 35 \%$	$\pm 23 \%$
	365 d	21 %	$\pm 19 \%$	$\pm 12 \%$		365 d	1 %	$\pm 4 \%$	$\pm 3 \%$
	730 d	6 %	$\pm 12 \%$	$\pm 8 \%$		730 d	0 %	$\pm 2 \%$	$\pm 1 \%$
R_{life}	37 d	83 %	$\pm 13 \%$	$\pm 98 \%$		37 d	30 %	$\pm 36 \%$	$\pm 24 \%$
	187 d	43 %	$\pm 21 \%$	$\pm 14 \%$		187 d	4 %	$\pm 11 \%$	$\pm 7 \%$
	373 d	21 %	$\pm 19 \%$	$\pm 13 \%$		373 d	2 %	$\pm 6 \%$	$\pm 4 \%$
Q	0.34	70 d	$\pm 71 d$	$\pm 47 d$		0.34	9 d	$\pm 11 d$	$\pm 7 d$
	0.67	236 d	$\pm 169 d$	$\pm 111 d$		0.67	25 d	$\pm 30 d$	$\pm 20 d$

In both tables:
 d = days, C/I = confidence interval

5.4.2 Forecasting the duration of single basaltic eruptions (d_6) on Iceland

Single basaltic eruptions with reported durations have occurred from seven volcanic systems on Iceland since 1300 AD. Section 3.4 suggested that the severity of reporting bias varies for each volcanic system according to their geographical location and the different population densities surrounding them. As a result a unique point in time after which the historical record for this type of eruption can be considered complete has not been identified.

The general nature of reporting is such that with time increased human population and detection of small eruptions results in fewer short duration eruptions going unnoticed. In terms of forecasting this increased proportion of short duration eruptions reported in more recent years causes the probability of exceeding a given duration to decrease.

A forecast performed on a less biased dataset would then indicate that long durations are less likely than forecasts performed on the dataset that is currently available. The results here can therefore be considered a conservative forecast, i.e. probabilities are most probably over-estimates. To assess how different these results could be, forecasts are performed based on the d_6 duration data for the period 1300-2011 and also a smaller subset of most recent data (1900-2011).

The analyses of Chapter 4 identified a significant difference between the duration of eruptions from volcanic systems situated inside and outside the active rift zone on Iceland . Volcano specific investigations also found that eruptions from Krafla have a significantly different duration distribution to those of Grímsvötn, Askja and Katla. In the following sections the forecasting model has been performed on d_6 duration data from inside rift volcanic systems and outside rift volcanic systems. Durations from the Krafla volcanic system have been forecast separately and therefore its durations are excluded from the inside rift dataset.

Identifying the best fit distributions to the d_6 data of Iceland

Parameter values for the best fit exponential, Weibull, log-logistic and Burr type XII distribution for the d_6 duration data of Iceland from the periods 1300-2011 and 1900-2011 are reported in Table 5.10. Fig. 5.5 plots the survivor function of each fitted distribution alongside the empirical survivor function curve of the corresponding observed data.

KS goodness-of-fit tests indicate that the 1300-2011 dataset could have derived from the Weibull, log-logistic or Burr type XII distributions (Table 5.10a), whereas only the log-logistic and Burr type XII distributions of the 1900-2011 dataset yield p -values of > 0.05 (Table 5.10b). A LR test indicates that in both cases there is no benefit in employing the Burr type XII distribution in preference to the log-logistic distribution

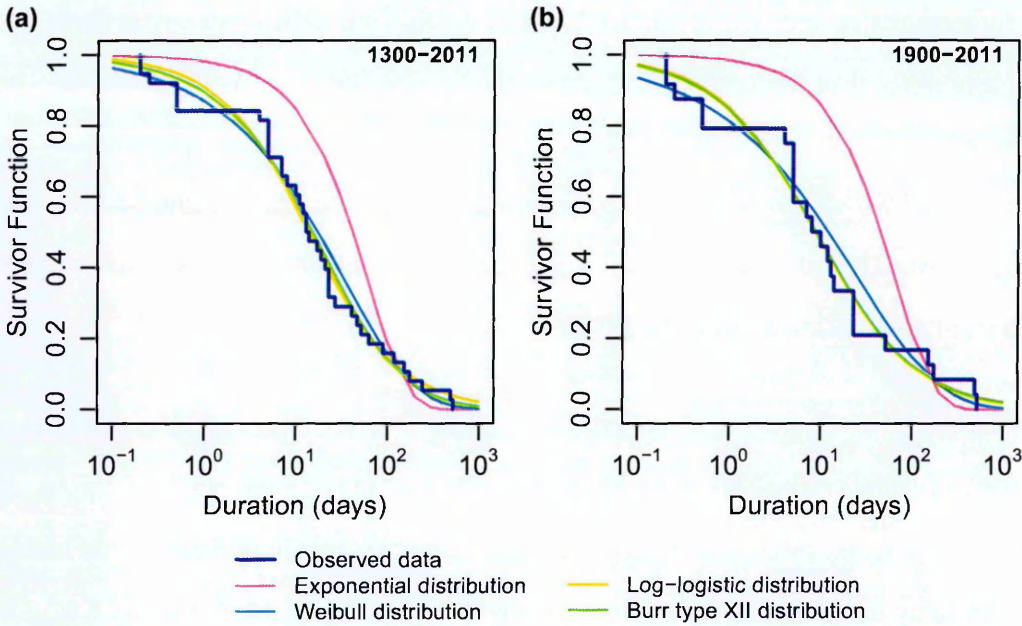


Fig. 5.5 Empirical survivor function curves and best fit theoretical distributions for the duration of single basaltic eruptions (d_6) for volcanic systems on Iceland for the periods (a) 1300-2011 and (b) 1900-2011. Parameter values can be found in Table 5.10

(Table 5.10). The poor fit of the exponential distribution is evident in Fig. 5.5, however, the Weibull, log-logistic and Burr type XII distributions plot with similar shapes and positions especially for the 1300-2011 dataset (Fig. 5.5). The best fit log-logistic distribution off each dataset will be used in the forecasts of the following section.

Maximum likelihood estimation has also been used to estimate the parameter values of these four theoretical distributions using data from the volcanic systems inside the axial rift, the volcanic systems outside the axial rift, and for Krafla. These are reported in Table 5.11 and displayed graphically in Fig. 5.6. *KS* goodness-of-fit tests indicate that the inside rift duration data could have derived from either the log-logistic or Burr type XII distribution (Table 5.11a). Visually the Burr type XII distribution appear to provide the best fit to the data, especially at low durations where the data lacks an obvious short duration tail (Fig. 5.6a). However, a *LR* test comparing the log-logistic and Burr type XII distribution results in a test statistic that is 0.4 less than the critical value suggesting that there is little benefit in employing the more complex

Table 5.10: Parameter values, Kolmogorov-Smirnov (KS) test and likelihood ratio (LR) test results for theoretical distributions fitted to the single basaltic eruption duration data (d_6) of Iceland for (a) 1300-2011 and (b) 1900-2011

(a) d_6 : 1300-2011

	Exponential	Weibull	Log-logistic	Burr type XII
	$\mu = 60.03$	$\beta = 0.56$	$\beta = 0.88$	$\alpha = 1.62$
		$\mu = 33.69$	$\sigma = 14.10$	$\beta = 0.72$
				$\sigma = 63.42$
D_{obs}	0.366	0.130	0.108	0.103
\hat{p}	0.000	0.098 \diamond	0.160 \diamond	0.213 \diamond
r	3000	2981	3000	2954
LR test statistic (log-logistic and Burr type XII):				1.095

(b) d_6 : 1900-2011

	Exponential	Weibull	Log-logistic	Burr type XII
	$\mu = 65.07$	$\beta = 0.48$	$\beta = 0.80$	$\alpha = 0.89$
		$\mu = 26.07$	$\sigma = 8.88$	$\beta = 0.75$
				$\sigma = 12.20$
D_{obs}	0.494	0.181	0.138	0.137
\hat{p}	0.000	0.034	0.124 \diamond	0.126 \diamond
r	3000	2978	3000	2927
LR test statistic (log-logistic and Burr type XII):				0.044

In both tables:

\diamond not significant at the 0.05 level (p -value > 0.05).

D_{obs} = KS statistic, \hat{p} = estimated p -value and r = final bootstrap size.

Burr type XII distribution instead of the log-logistic distribution (Table 5.11a). Due to the closeness of this result to the critical value and the visually better fit of the Burr type XII distribution to the observed data this distribution is used to forecast future d_6 durations from inside rift volcanic systems in the following section.

In contrast, KS goodness-of-fit tests performed on the outside rift duration data suggest that a log-logistic distribution does not provide an adequate fit to the data. Weibull

CHAPTER 5. DURATION FORECASTING

Table 5.11: Parameter values, Kolmogorov-Smirnov (KS) test and likelihood ratio (LR) test results for theoretical distributions fitted to the single basaltic eruption duration data (d_6) of Iceland for (a) inside rift (b) outside rift and (c) Krafla

(a) d_6 : Inside rift (excluding Krafla)

	Exponential	Weibull	Log-logistic	Burr type XII
	$\mu = 37.93$	$\beta = 0.80$	$\beta = 1.59$	$\alpha = 0.87$
		$\mu = 32.41$	$\sigma = 15.54$	$\beta = 4.27$
				$\sigma = 6.02$
D_{obs}	0.310	0.227	0.174	0.113
\hat{p}	0.016	0.025	0.178 \diamond	0.758 \diamond
r	3000	3000	3000	2859
LR test statistic (log-logistic and Burr type XII):				3.425

(b) d_6 : Outside rift

	Exponential	Weibull	Log-logistic	Burr type XII
	$\mu = 224.33$	$\beta = 0.79$	$\beta = 0.98$	$\alpha = 31.57$
		$\mu = 200.85$	$\sigma = 112.73$	$\beta = 0.72$
				$\sigma = 18614.26$
D_{obs}	0.310	0.181	0.213	0.181
\hat{p}	0.026	0.268 \diamond	0.047	0.211 \diamond
r	3000	2987	3000	2903
LR test statistic (log-logistic and Burr type XII):				0.685

(c) d_6 : Krafla (1975-1984)

	Exponential	Weibull	Log-logistic	Burr type XII
	$\mu = 4.24$	$\beta = 0.74$	$\beta = 0.95$	$\alpha = 848.38$
		$\mu = 3.58$	$\sigma = 1.72$	$\beta = 0.74$
				$\sigma = 490475.72$
D_{obs}	0.333	0.277	0.291	0.278
\hat{p}	0.063 \diamond	0.046	0.003	0.022
r	3000	2993	2992	2997
LR test statistic (log-logistic and Burr type XII):				1.671

In all three tables: \diamond not significant at the 0.05 level (p -value > 0.05).
 $D_{obs} = KS$ statistic, \hat{p} = estimated p -value and r = final bootstrap size.

and Burr type XII distributions result in p -values of > 0.05 (Table 5.11b) and plot in almost identical positions on Fig. 5.6b. Considering that the forecasting model has been applied to the best fit Burr type XII distribution of the inside rift data, the same distribution is used for the outside rift data.

With the exception of the 1724 eruptions the dataset of single basaltic eruptions from Krafla all represent individual eruptions during the longer basaltic eruption sequence of the 1975-1984 Krafla fires. The data is therefore restricted to this time period for forecasting purposes. Visually the Weibull and Burr type XII distributions plot with almost identical shapes and positions and all four distributions poorly describe the observed data at low durations (Fig. 5.6c). Interestingly the exponential distribution, which appears to give the worst fit to the data at short durations, is the only distribution that is considered adequate by a KS goodness-of-fit test (Table 5.11c).

The Weibull distribution has a p -value of 0.046 and is therefore close to 0.05 (Table 5.11c) and visually plots closer to the low duration portion of the data while maintaining the good fit of the exponential distribution at longer durations (Fig. 5.6c). The Weibull distribution with parameter values displayed in Table 5.11c is therefore used to perform the duration forecasts for the Krafla volcanic system in the following section.

Forecasting results for the duration of single basaltic eruptions (d_6) on Iceland

The same seven forecasts have been performed on the 1300-2011, 1900-2011 (Table 5.12), inside rift, outside rift and Krafla (Table 5.13) datasets of single basaltic eruption durations on Iceland. As expected the reduced reporting bias towards large eruptions for the period 1900-2011 generally results in forecasts with lower exceedance probabilities than the more biased 1300-2011 dataset (Table 5.12). Quantile functions based on the best fit log-logistic distribution of the 1300-2011 data indicate that the duration

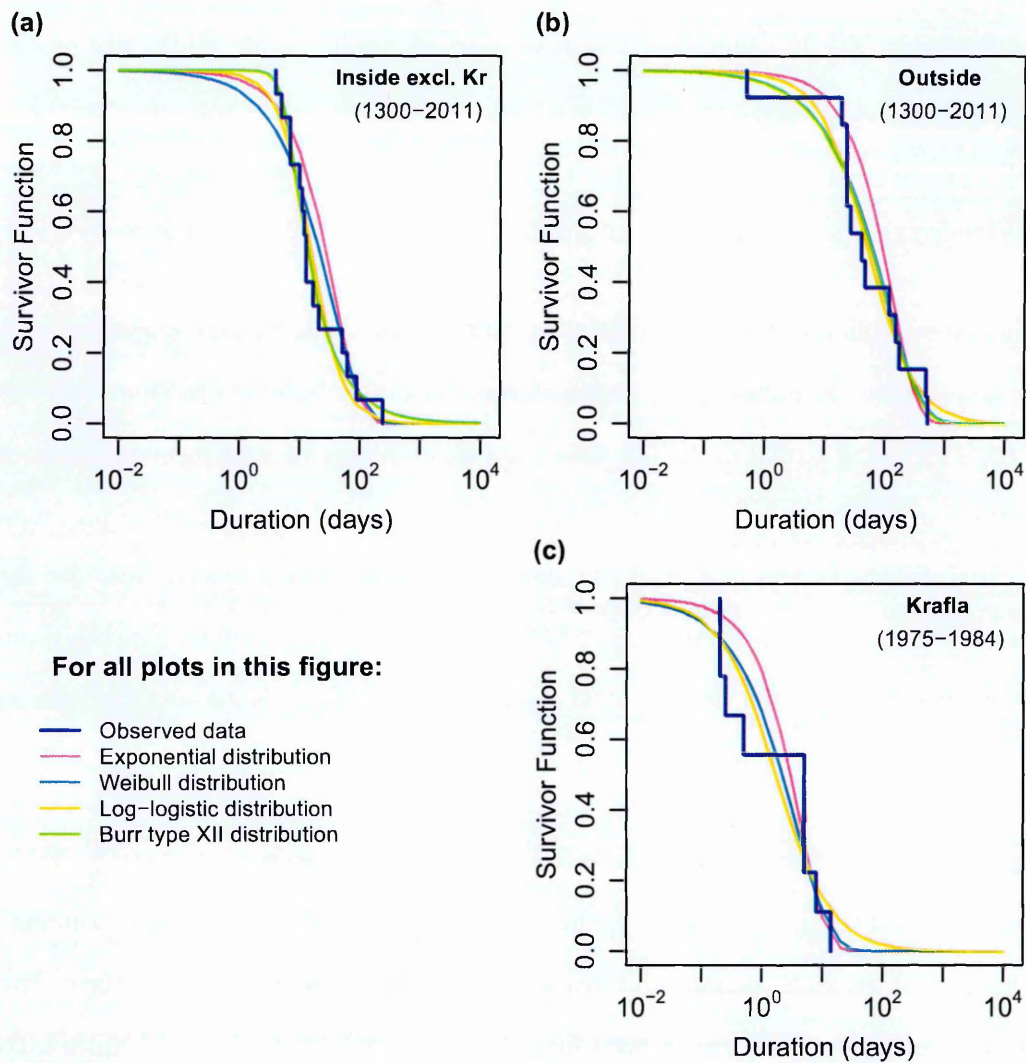


Fig. 5.6 Empirical survivor function curves and best fit theoretical distributions for the duration of single basaltic eruptions (d_6) from volcanic systems in different regions of Iceland. (a) d_6 : inside rift systems (excluding Krafla), (b) d_6 : outside rift systems and (c) d_6 : Krafla (1975-1984). Parameter values can be found in Table 5.5

of a future basaltic eruption on Iceland is likely to exceed 7 days (± 3 days) and unlikely to exceed 32 days (± 13 days) (Table 5.12a). These are reduced to 4 days (± 2 days) and 22 days (± 13 days) respectively when the 1900-2011 data is used (Table 5.12b).

Table 5.13a and b display the forecasting results for the d_6 1300-2011 data separated into eruptions from volcanic systems inside and outside the active rift zone on Iceland. The very low proportion of outside rift eruptions with durations < 10 days results in

Table 5.12: Survivor function (SF), residual life function (R_{life}) and quantile function (Q) forecasts for the duration of single basaltic eruptions (d_6) from volcanic systems on Iceland for the periods (a) 1300-2011 and (b) 1900-2011. For the residual life function $t = 7$ days

(a) d_6 , 1300-2011 (Log-logistic)					(b) d_6 , 1900-2011 (Log-logistic)				
	Input	Result	C/I			Input	Result	C/I	
			95 %	80 %				95 %	80 %
SF	7 d	65 %	± 13 %	± 9 %	SF	7 d	55 %	± 17 %	± 11 %
	30 d	34 %	± 13 %	± 8 %	SF	30 d	27 %	± 15 %	± 10 %
	365 d	5 %	± 5 %	± 3 %	SF	365 d	5 %	± 6 %	± 4 %
R_{life}	14 d	77 %	± 8 %	± 5 %	R_{life}	14 d	75 %	± 10 %	± 7 %
	37 d	46 %	± 13 %	± 9 %	R_{life}	37 d	44 %	± 17 %	± 11 %
Q	0.34	7 d	± 4 d	± 3 d	Q	0.34	4 d	± 4 d	± 2 d
	0.67	32 d	± 20 d	± 13 d	Q	0.67	22 d	± 20 d	± 13 d

In both tables:

d = days, C/I = confidence interval

higher exceedance probabilities for the same durations than for eruptions from inside rift volcanic systems (Table 5.13a and b). Quantile functions indicate that the duration of a future eruption of this type from an inside rift volcanic system (with the exception of Krafla) is likely to exceed 9 days (± 3 days) but unlikely to exceed 22 days (± 9 days) whereas those from outside rift systems are likely to exceed 29 days (± 21 days) but unlikely to exceed 115 days (± 6 days) (Table 5.13).

Despite being an inside rift volcanic system forecasts made for the duration of d_6 eruptions from Krafla are quite different from those for the other inside rift systems (Tables 5.13c and a respectively). Eruptions from Krafla are all very short and a quantile function implies that eruptions of this type from Krafla are likely to have durations in excess of 1 day (± 1 day) but are unlikely to exceed 4 days (± 2 days) (Table 5.13c). Although these forecasts are considered specific to the Krafla volcanic system they may actually provide insight into the duration of individual eruptive episodes during longer eruptive sequences on a more general level.

Table 5.13: Survivor function (SF), residual life function (R_{life}) and quantile function (Q) forecasts for the duration of single basaltic eruptions (d_6) from different regions of Iceland. (a) Inside rift zone systems (excluding Krafla), (b) Outside rift zone systems and (c) eruptions from Krafla for the period 1975-1984. For the residual life function of tables (a) and (b) $t = 7$ days and table (c) $t = 1$ day

(a) d_6 , Inside rift (Burr type XII)

	Input	Result	C/I	
			95 %	80 %
SF	7 d	80 %	$\pm 19 \%$	$\pm 13 \%$
	30 d	25 %	$\pm 18 \%$	$\pm 11 \%$
	365 d	3 %	$\pm 6 \%$	$\pm 4 \%$
R_{life}	14 d	59 %	$\pm 17 \%$	$\pm 11 \%$
	37 d	26 %	$\pm 20 \%$	$\pm 13 \%$
Q	0.34	9 d	$\pm 4 d$	$\pm 3 d$
	0.67	22 d	$\pm 14 d$	$\pm 9 d$

(b) d_6 , Outside rift (Burr type XII)

	Input	Result	C/I	
			95 %	80 %
SF	7 d	86 %	$\pm 15 \%$	$\pm 9 \%$
	30 d	65 %	$\pm 22 \%$	$\pm 14 \%$
	365 d	8 %	$\pm 12 \%$	$\pm 8 \%$
R_{life}	14 d	91 %	$\pm 6 \%$	$\pm 4 \%$
	37 d	71 %	$\pm 15 \%$	$\pm 10 \%$
Q	0.34	29 d	$\pm 32 d$	$\pm 21 d$
	0.67	115 d	$\pm 91 d$	$\pm 6 d$

(c) d_6 , Krafla (Weibull)

	Input	Result	C/I	
			95 %	80 %
SF	0.5 d	79 %	$\pm 22 \%$	$\pm 14 \%$
	1 d	68 %	$\pm 26 \%$	$\pm 17 \%$
	5 d	28 %	$\pm 23 \%$	$\pm 15 \%$
R_{life}	2 d	77 %	$\pm 13 \%$	$\pm 9 \%$
	5 d	41 %	$\pm 25 \%$	$\pm 16 \%$
Q	0.34	1 d	$\pm 1 d$	$\pm 1 d$
	0.67	4 d	$\pm 4 d$	$\pm 2 d$

In all three tables tables:

d = days, C/I = confidence interval

5.4.3 Forecasting the total duration of basaltic eruption sequences (d_7) on Iceland

Given the limited data available for basaltic eruption sequences on Iceland additional analyses into any temporal or spatial variations that the dataset may contain could not

be performed. Despite this duration forecasts are made based on the entire dataset of eight d_7 durations and their results discussed in the following sections.

Identifying the best fit distribution to the d_7 duration data on Iceland

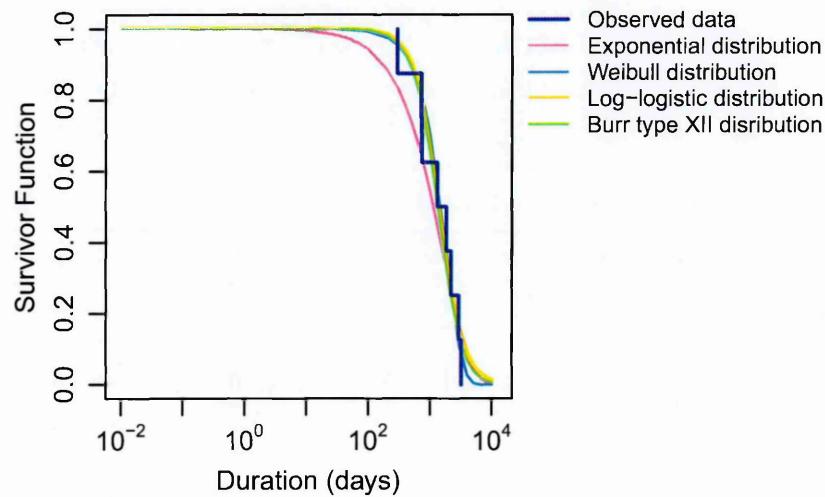


Fig. 5.7 Empirical survivor function curves and best fit theoretical distributions for the total duration of basaltic eruption sequences (d_7) on Iceland. Parameter values can be found in Table 5.14

Parameter values for the best fit exponential, Weibull, log-logistic and Burr type XII distribution of the d_7 duration dataset are reported in Table 5.14. Fig. 5.7 plots the survivor function of each fitted distribution alongside the empirical survivor function curve of the observed data.

KS test results indicate that the distribution of d_7 durations on Iceland could have derived from any of the four tested theoretical distributions (Table 5.14). Visually the exponential distribution provides a poor fit at lower durations, however, variations between the other distributions are slight (Fig. 5.7). A LR test indicates that there is no benefit in employing the Burr type XII distribution instead of the log-logistic distribution. This, in conjunction with our findings that a log-logistic distribution often provides adequate fit to eruption duration data, is reason to use the log-logistic distribution in the forecasts of the following section.

Table 5.14: Parameter values, Kolmogorov-Smirnov (*KS*) test and likelihood ratio (*LR*) test results for theoretical distributions fitted to data for basaltic eruption sequence duration (d_7) on Iceland

	Exponential	Weibull	Log-logistic	Burr type XII
	$\mu = 1647.88$	$\beta = 1.67$	$\beta = 2.19$	$\alpha = 2.71$
		$\mu = 1844.62$	$\sigma = 1368.91$	$\beta = 2.06$
				$\sigma = 1566.50$
D_{obs}	0.228	0.183	0.173	0.178
\hat{p}	0.571 \diamond	0.626 \diamond	0.582 \diamond	0.528 \diamond
r	3000	2914	2999	2969
<i>LR</i> test statistic (log-logistic and Burr type XII):				0.282

\diamond not significant at the 0.05 level (p -value > 0.05).
 D_{obs} = *KS* statistic, \hat{p} = estimated p -value and r = final bootstrap size.

Forecasting results for the duration of basaltic eruption sequences (d_7) on Iceland

Table 5.15 contains the results of seven forecasts based on the best fit log-logistic distribution of the d_7 duration data. These data represent very long periods of continuous eruptive activity at individual volcanic systems on Iceland and therefore the input durations for the survivor function (x) and the residual life function (x and t) are considerable longer than they are for the other forecasts made in this study and are reported in years instead of days (Table 5.15). Quantile function results indicate that a future basaltic sequence is likely to exceed 2.77 years (± 1.09 years) and unlikely to exceed 5.18 years (± 1.96 years) (Table 5.15).

5.5 Conclusions

The empirical probabilistic model outlined in Chapter 2 is used here to forecast the likely duration of future eruptions from the volcanic systems investigated in this study.

Table 5.15: Survivor function (SF), residual life function (R_{life}) and quantile function (Q) forecast results for the total duration of basaltic eruption sequences (d_7) (for the residual life function $t = 1$ year (365 days))

d_7 (log-logistic)				
	Input	Result	C/I	
			95 %	80 %
SF	3 y	62 %	± 30 %	± 20 %
	5 y	35 %	± 29 %	± 19 %
	7 y	20 %	± 23 %	± 15 %
R_{life}	3 y	65 %	± 31 %	± 20 %
	5 y	37 %	± 33 %	± 21 %
Q	0.34	2.77 y	± 1.66 y	± 1.09 y
	0.67	5.18 y	± 3.00 y	± 1.96 y

y = years, C/I = confidence interval

The empirical nature of this model relies on historical eruption data being unbiased and a good representation of future activity. Here the analyses of Chapters 3 and 4 have been used to restrict the available data such that it best fulfils this criteria. A marked effect on the forecasts generated could be observed when these results were compared to the same forecasts based on unrestricted datasets. For example forecasts made for Mt. Etna based on the 1600-2010 data compared to those based on the 1670-2010 data (Table 5.2) or for the basaltic eruption durations from volcanic systems on Iceland situated inside or outside the active rift zone (Table 5.13). This highlights the importance of data analyses prior to forecasting.

A modification of the forecasting model was presented to deal with data described by a bimodal distribution (e.g. PdIF eruption durations, section 5.3). The example of this study contained one mode with durations < 2 days, and as a result a restriction method was applied whereby input data was limited to historic eruption durations of ≥ 2 days. If a bimodal distribution were encountered with modes of longer durations, where forecasting both aspects of the data accurately would be beneficial then a means of fitting a theoretical distribution which can model bimodal data would need to be

developed. The method applied here is considered appropriate for the duration data of PdlF.

With the exception of Kilauea and PdlF, eruption durations since the end of the datasets compiled have not occurred and therefore verification of the accuracy of this forecasting model on eruption durations has not been possible. For Kilauea, a survivor function forecast where $x = 30$ years only resulted in a 1 % exceedance probability and it is concluded here that a fundamental change in the plumbing system occurred at Kilauea prior to this eruption, promoting its longer than expected duration. This is returned to in Chapter 7. For PdlF the most recent eruption was short, lasting only 1 day. Due to the bimodal nature of the PdlF dataset and the limitations of the forecasting model presented here, such short duration eruptions cannot be accurately forecast.

With time, not only can the forecasting results presented here be tested against future eruption durations from the investigated volcanic systems, but additional eruption duration data will become available and can be added to the model input data. This will allow better constraints on the fitted theoretical distributions and a subsequent reduction of the uncertainty behind the estimated parameter values. As such the currently large confidence intervals should decrease.

Chapter 6

An investigation of repose intervals



The focus of this PhD is to investigate volcanic eruption durations, however, with the exception of Kilauea and PdlF, it was not possible to compare the eruption duration forecasts presented in Chapter 5 with a subsequent eruption's duration as the last recorded eruption of each system is within the time period of the input data. The model itself is not limited to use on eruption durations, but can be applied to other types of data. Repose intervals refer to the periods of inactivity between eruptions, and are as such a type of duration data and the volcanic systems of this study are either currently within a period of repose or, in the case of Kilauea, have had a period of repose since the end of the compiled dataset. This allows comparison of forecasting results with real-life data, to obtain some insight into the validity of the results produced.

Furthermore, while previous investigations into eruption durations are rare, studies concentrated on repose interval data are more common and have involved the use of

survival analysis (Chapter 1). This allows the methods of this investigation to be compared with those used in the past. Differences between the probabilistic model developed here and the very similar models of Connor et al. (2003, 2006) and Dzierma and Wehrmann (2010) were discussed in Chapter 2, however, the key differences were the use of maximum likelihood estimation to obtain theoretical distribution parameter values, the addition of a fourth theoretical distribution (Burr type XII) and the three types of forecast that are made in each case (survivor function, residual life function and quantile function). Where previous authors have made forecasts of future repose intervals at the volcanic systems investigated here, their results are compared to the results of this investigation in the appropriate sections.

6.1 The definition and calculation of repose interval

The definition of a repose interval is the period of inactivity between two volcanic eruptions (Klein, 1982). As such true repose intervals are calculated between the end date of one eruption and the start date of the next, however, due to difficulties in defining eruption end dates (see section 2.1) many previous studies have used eruption recurrence intervals (Fig. 6.1), measured between the start date of two successive eruptions (Klein, 1982; Mulargia et al., 1985; Stieltjes and Moutou, 1989; De la Cruz-Reyna, 1991; Bebbington and Lai, 1996; Passarelli et al., 2010). In using recurrence interval as a proxy for repose interval the assumption that eruption duration represents a negligible proportion of a recurrence interval is made.

Considering the focus of eruption duration when compiling datasets for this study, eruption end dates have been uniformly defined. The datasets presented in Chapter 3 have enabled repose intervals to be calculated for the volcanic systems investigated here, and therefore recurrence intervals are not required. However, section 6.3 compares repose intervals and recurrence intervals for each dataset in order to assess the

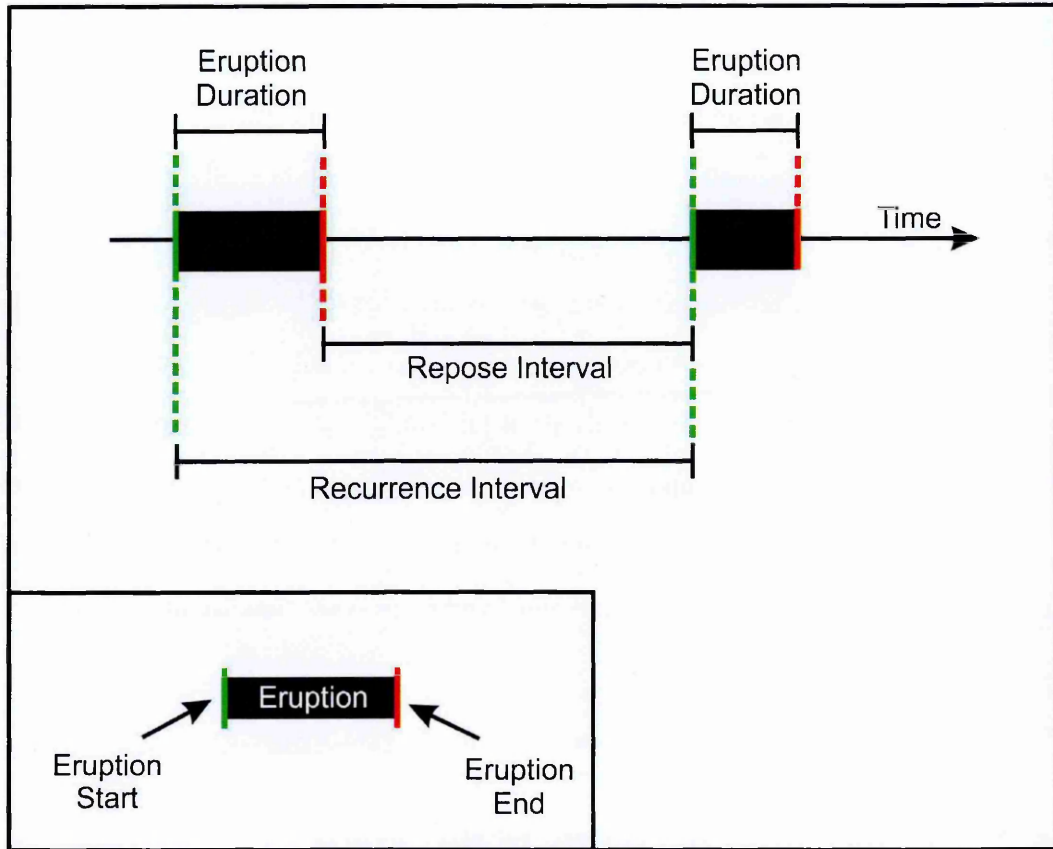


Fig. 6.1 Schematic diagram highlighting the difference between a repose interval and a recurrence interval

validity of using recurrence interval as a proxy for repose where eruption end dates are unavailable or unclear. Repose interval is however used in all other analyses within this chapter.

Accurate calculation of repose intervals relies on information about eruption start and end dates and are therefore prone to the same reporting biases and uncertainties that were encountered during the eruption duration calculations of this study. Unlike eruption duration data, any undocumented eruptions are of particular importance as they cannot be accounted for and thus apparently long repose intervals will exist as an artefact of the data. Analyses of repose period data performed in this study have therefore been restricted to the time periods identified as free from reporting biases in Chapter 3 and due to the likelihood that reporting biases still exist in most of the eruption record for Iceland, analyses are only performed on data for repose intervals between mixed

eruptions from Hekla, which is considered more complete.

The tables of repose presented here represent the repose interval and recurrence interval following each eruption, and as such the final eruption in each dataset does not have a known repose interval. The calculations themselves are based on the preferred start and end dates of eruptions and are all > 10 days due to the eruption duration definition given in Chapter 2. Eruptions with unknown or unreliable eruption durations were excluded from the duration analyses of this study, and not presented in the data tables of Chapter 3. These eruptions are also not considered in the repose interval and recurrence interval calculations here, and therefore are the major reason why repose intervals are missing in the following datasets. Where this is not the case specific reasons are given in the accompanying text.

6.2 Repose data available to this study

6.2.1 Repose intervals at Mt. Etna

The dataset of Mt. Etna flank eruptions enables 50 repose intervals to be calculated for the period 1600-2010 ranging from 22 days (0.06 years) to 52.87 years with an average of 5.73 years (Table 6.1).

Two eruptions were reported to start on 17 January 1651, however, the end date of only one of these eruptions is known, and it is this eruption which is included in the duration analyses of this study (#10, Table 3.1). The unknown end date of the other eruption creates ambiguity in the repose interval following eruptive activity at this time and therefore a true repose cannot be determined. A repose following eruption # 10 therefore cannot be calculated.

CHAPTER 6. AN INVESTIGATION OF REPOSE INTERVALS

Table 6.1: Repose intervals following flank eruptions at Mt. Etna for the period 1600-2011

#	Year	Interval (years)		#	Year	Interval (years)	
		Repose	Recurrence			Repose	Recurrence
5	1610	3.88	4.4	26	1865	-	-
6	1614	10.47	20.48	27	1879	3.79	3.82
7	1634	6.69	8.18	28	1883	3.16	3.16
8	1643	3.73	3.75	29	1886	6.09	6.15
9	1646	4	4.16	30	1892	15.34	15.81
10	1651	-	-	31	1908	1.9	1.9
11	1669	-	-	32	1910	1.4	1.47
12	1702	52.87	53.04	33	1911	-	-
13	1755	-	-	34	1923	5.3	5.38
14	1763	0.27	0.36	35	1928	13.62	13.67
15	1763	-	-	36	1942	4.66	4.66
16	1766	13.54	14.07	37	1947	3.72	3.75
17	1780	12	12.03	38	1950	4.25	5.27
18	1792	9.51	10.48	39	1956	7.92	7.93
19	1802	6.36	6.37	40	1964	3.87	3.93
20	1809	2.55	2.59	41	1968	-	-
21	1811	7.09	7.59	42	1971	2.64	2.82
22	1819	13.26	13.44	43	1974	0.06	0.11
23	1832	10.99	11.05	44	1974	0.91	0.96
24	1843	8.73	8.76	45	1975	0.25	0.76
25	1852	11.69	12.45	46	1975	1.3	2.42

Continued on next page...

Table 6.1 – Continued

Interval (years)				Interval(years)			
#	Year	Repose	Recurrence	#	Year	Repose	Recurrence
47	1978	0.22	0.32	55	1986	2.58	2.91
48	1978	0.22	0.24	56	1989	2.18	2.21
49	1978	0.67	0.71	57	1991	8.3	9.6
50	1979	1.61	1.62	58	2001	1.22	1.28
51	1981	2.01	2.03	59	2002	1.61	1.87
52	1983	1.59	1.95	60	2004	1.6	2.1
53	1985	0.45	0.79	61	2006	1.41	1.58
54	1985	0.83	0.85	62	2008	-	-

6.2.2 Repose intervals at Kilauea

The dataset of Kilauea eruptions from the period 1912-1983 is almost complete and most repose intervals can be calculated. However, due to the nature of the dataset some eruptions overlap in time and although for duration analyses these were treated as separate events based on location, the more general repose analyses of this chapter requires the overlapping eruptions to be disregarded. The most obvious example of this is the very long 1823 summit eruption (# 1 Table 3.2) which overlaps in time with three East Rift Zone (ERZ) and one South-West Rift Zone (SWRZ) eruption such that the first repose interval calculated at Kilauea follows the 1927 summit eruption (#6 Table 3.2).

Some complexity also exists surrounding the two very long East Rift Zone (ERZ) eruptions (# 30 and # 33 Table 3.2) which overlap with short periods of summit activity that were again treated as separate eruptions for the purpose of duration analysis. These

CHAPTER 6. AN INVESTIGATION OF REPOSE INTERVALS

summit eruptions are disregarded here and repose intervals are calculated between eruptions # 30 and # 33 (true repose is between 15 October 1971 and 5 February 1972) and between eruptions # 33 and # 35 (true repose is between 22 July 1974 and 19 September 1974).

Table 6.2: Repose intervals following eruptions at Kilauea for the period 1927-1983

#	Year	Interval (years)		#	Year	Interval (years)	
		Repose	Recurrence			Repose	Recurrence
6	1927	1.59	1.63	24	1965	0.78	0.81
7	1929	0.42	0.42	25	1965	1.86	1.87
8	1929	1.31	1.32	26	1967	0.11	0.80
9	1930	1.04	1.09	27	1968	0.12	0.13
10	1931	2.67	2.71	28	1968	0.34	0.38
11	1934	17.73	17.82	29	1969	0.23	0.25
12	1952	1.55	1.93	30	1969	0.30	2.70
13	1954	0.74	0.75	31	1971	-	-
14	1955	0.05	0.15	32	1971	-	-
15	1955	4.47	4.56	33	1972	0.16	2.63
16	1959	0.07	0.17	34	1974	-	-
17	1960	1.02	1.12	35	1974	0.27	0.28
18	1961	0.29	0.37	36	1974	0.91	0.91
19	1961	0.18	0.20	37	1975	1.79	1.79
20	1961	1.20	1.21	38	1977	2.13	2.18
21	1962	0.70	0.70	39	1979	2.45	2.45
22	1963	0.12	0.12	40	1982	0.40	0.41
23	1963	1.41	1.42	41	1982	-	-

Table 6.2 contains 32 repose intervals calculated for Kilauea alongside the number and start year of the eruption immediately preceding that repose interval. These range from 45 days (0.12 years) to 17.82 years with an average of 1.73 years.

6.2.3 Repose intervals at Piton de la Fournaise (PdIF)

The dataset of PdIF eruptions enables 109 repose intervals to be calculated for the period 1911-2011. These are reported in Table 6.3 alongside the number and start year of the eruption immediately preceding that repose interval. Repose intervals at PdIF range from 12 days (0.03 years) to 6.07 years with an average repose of 212 days (0.58 years).

Table 6.3: Repose intervals following eruptions at PdIF for the period 1911-2011

#	Year	Interval (years)		#	Year	Interval (years)	
		Repose	Recurrence			Repose	Recurrence
48	1913	-	-	59	1927	0.04	0.07
49	1915	0.08	0.08	60	1927	-	-
50	1915	0.05	0.09	61	1929	0.39	0.41
51	1915	1.44	1.47	62	1930	-	-
52	1917	3.17	3.17	63	1931	0.08	0.33
53	1920	0.27	0.28	64	1931	-	-
54	1920	-	-	65	1931	-	-
55	1924	1.3	1.32	66	1933	-	-
56	1925	-	-	67	1933	0.03	0.03
57	1926	0.13	0.13	68	1933	0.23	0.24
58	1926	0.18	0.18	69	1934	0.1	0.15

Continued on next page...

CHAPTER 6. AN INVESTIGATION OF REPOSE INTERVALS

Table 6.3 – Continued

#	Year	Interval (years)		#	Year	Interval (years)	
		Repose	Recurrence			Repose	Recurrence
70	1934	-	-	91	1957	0.12	0.13
71	1937	0.15	0.23	92	1957	0.53	0.61
72	1937	0.66	0.72	93	1958	0.18	0.19
73	1938	0.36	0.37	94	1958	0.47	0.59
74	1938	-	-	95	1959	0.29	0.4
75	1942	0.44	0.5	96	1959	0.43	0.44
76	1943	0.96	1.02	97	1960	0.07	0.08
77	1944	0.96	1.01	98	1960	1.07	1.16
78	1945	1.12	1.18	99	1961	2.54	2.59
79	1946	-	-	100	1963	0.44	0.48
80	1948	-	-	101	1964	0.62	0.64
81	1950	0.41	0.51	102	1964	1.08	1.23
82	1950	-	-	103	1966	6.07	6.24
83	1951	0.66	0.69	104	1972	0.12	0.13
84	1952	0.65	0.82	105	1972	0.06	0.12
85	1953	0.17	0.26	106	1972	0.03	0.08
86	1953	-	-	107	1972	0.08	0.25
87	1954	-	-	108	1973	0.31	0.33
88	1956	0.61	0.71	109	1973	0.27	0.32
89	1956	0.1	0.1	110	1973	2.16	2.17
90	1956	0.47	0.67	111	1975	0.08	0.12

Continued on next page...

CHAPTER 6. AN INVESTIGATION OF REPOSE INTERVALS

Table 6.3 – Continued

#	Year	Interval (years)		#	Year	Interval (years)	
		Repose	Recurrence			Repose	Recurrence
112	1975	0.58	0.88	133	1987	0.1	0.19
113	1976	0.39	0.39	134	1988	0.13	0.28
114	1977	0.03	0.03	135	1988	0.08	0.29
115	1977	0.52	0.55	136	1988	0.25	0.29
116	1977	1.53	1.59	137	1988	1.05	1.1
117	1979	0.12	0.13	138	1990	0.24	0.25
118	1979	1.56	1.56	139	1990	1.2	1.25
119	1981	2.58	2.83	140	1991	1.11	1.11
120	1983	1.32	1.53	141	1992	5.46	5.53
121	1985	0.14	0.14	142	1998	0.82	1.36
122	1985	0.15	0.33	143	1999	0.16	0.19
123	1985	0.07	0.07	144	1999	0.31	0.38
124	1985	0.11	0.22	145	2000	0.31	0.36
125	1986	0.27	0.32	146	2000	0.2	0.3
126	1986	0.33	0.33	147	2000	0.37	0.45
127	1986	0.04	0.04	148	2001	0.19	0.21
128	1986	0.02	0.03	149	2001	0.5	0.57
129	1986	0.42	0.51	150	2002	0.83	0.86
130	1987	0.05	0.11	151	2002	0.49	0.53
131	1987	0.3	0.3	152	2003	0.13	0.23
132	1987	0.06	0.07	153	2003	0.09	0.11

Continued on next page...

Table 6.3 – Continued

#	Year	Interval (years)		#	Year	Interval (years)	
		Repose	Recurrence			Repose	Recurrence
154	2003	0.18	0.19	164	2006	0.13	0.47
155	2003	0.04	0.09	165	2007	0.11	0.11
156	2004	0.31	0.32	166	2007	1.39	1.48
157	2004	0.24	0.28	167	2008	0.15	0.18
158	2004	0.34	0.52	168	2008	0.04	0.05
159	2005	0.6	0.63	169	2008	0.75	0.89
160	2005	0.12	0.15	170	2009	0.75	0.94
161	2005	0.07	0.07	171	2010	0.11	0.15
162	2005	0.5	0.56	172	2010	-	-
163	2006	0.04	0.11				

6.2.4 Repose intervals at Hekla, Iceland

The historic eruption record for Hekla is considerably better than that of other Icelandic volcanic systems and repose intervals between mixed eruptions for the period 1300-2000 have been investigated in this study. Volcanic activity at Hekla is not restricted to mixed eruptions. Basaltic eruptions from fissures outside the central volcano are reported in the years 1440, 1554, 1725, 1878 and 1913 and therefore these eruptions occur during the repose intervals that have been calculated for mixed eruptions. To ensure that any conclusions drawn from the repose analyses of this study are not a function of these eruptions not being accounted for, repose intervals have been calculated between both mixed eruptions only and all eruptions at Hekla irrespective of their type (columns Repose (d_4) and Repose (All) in Table 6.4 respectively).

Table 6.4: Repose intervals following eruptions at Hekla, Iceland for the period 1300-2000

#	Year	d-type	Interval (years)		
			Repose (All)	Repose (d_4)	Recurrence (d_4)
1	1300	d_4	-	-	-
2	1554	d_6	42.58	-	-
3	1597	d_4	38.84	38.84	39.37
4	1636	d_4	55.79	55.79	56.81
6	1693	d_4	-	72.47	73.19
10	1766	d_4	77.39	77.39	79.46
14	1845	d_4	31.92	101.05	101.64
22	1878	d_6	35.05	-	-
24	1913	d_6	33.88	-	-
27	1947	d_4	22.05	22.05	23.12
33	1970	d_4	10.13	10.13	10.29
40	1980	d_4	0.64	0.64	0.64
43	1981	d_4	9.76	9.76	9.78
47	1991	d_4	8.97	8.97	9.12
50	2000	d_4	-	-	-

Repose intervals between mixed eruptions at Hekla range from 234 days (0.64 years) to 101.05 years with an average of 39.71 years. When all reported eruptions are taken into account the maximum repose is reduced to 77.39 years and the average to 30.58 years.

6.3 A comparison of true and inferred repose

Fig. 6.2 plots repose interval against recurrence interval for the data from Mt. Etna, Kilauea, PdIF and Hekla. The dashed line in each plot represents the impossible scenario where repose interval is equal to recurrence interval (i.e. the eruption had no duration). Deviations from this line in an upwards and left direction represent the proportion of recurrence interval accounted for by eruption duration, and therefore provide an assessment of recurrence interval as a proxy for repose interval.

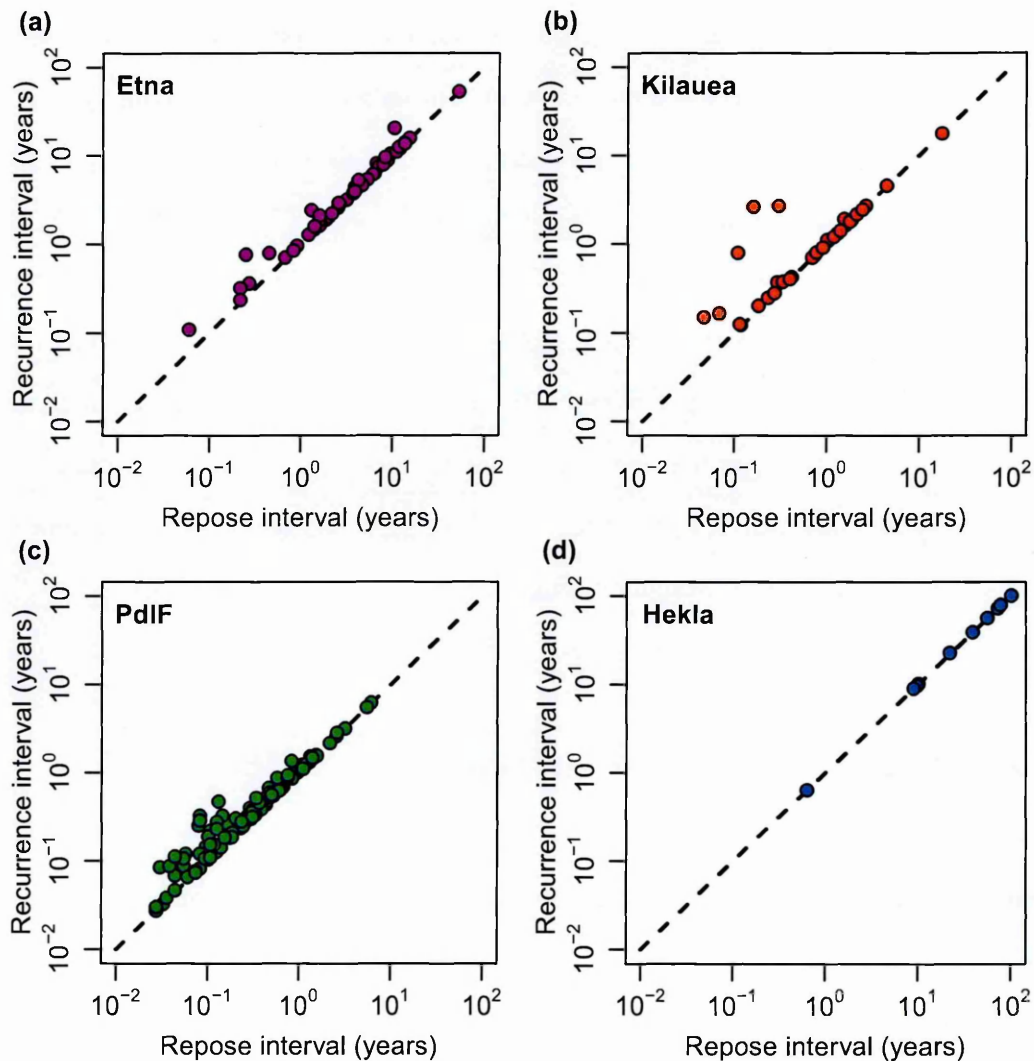


Fig. 6.2 Plots assessing the use of recurrence interval as a proxy for repose interval at (a) Mt. Etna, (b) Kilauea, (c) PdIF and (d) Hekla

Mt. Etna and Kilauea show similar patterns with most of the data plotting close to the

dashed line and 5 instances in each case where recurrence interval and repose interval differ more severely (Fig. 6.2a and b). In these cases eruption duration accounts for > 40 % of recurrence interval. These are most extreme for Kilauea (Fig. 6.2b). A comparison of the repose intervals for Kilauea calculated here and the recurrence intervals used in Klein (1982), indicate that 3 of these differ considerably (reposes following eruptions # 14, # 30 and # 33 Table 3.2). This is largely in response to how eruption durations are defined and the inclusion of intrusive events following the May 1969 and February 1972 eruptions in the calculations made by Klein (1982).

Data for PdlF shows a greater divergence from the dashed line, while the Hekla data plots close to it (Fig. 6.2c and d respectively). This is a function of the highly active nature of PdlF generating more frequent eruptions and thus shorter repose intervals whereas repose intervals at Hekla are generally much longer. These analyses suggest that using recurrence interval as a proxy for repose interval where eruption end dates are less readily available is often acceptable. However, care should be taken with volcanic systems known to erupt frequently (e.g. PdlF) where recurrence intervals may be considerably longer than the repose intervals they represent and therefore could sufficiently alter any analyses performed. This is of particular importance if the data is being used to forecast future eruption onsets.

6.4 Temporal variation in repose intervals

Temporal variation in repose interval may indicate fundamental changes in the physical properties of the volcanic system. For forecasting purposes, being aware of these temporal variations is important for restricting the data and ensuring that it best represents repose intervals derived from the current state of the volcanic system. This section investigates temporal variation in the repose data from Mt. Etna, Kilauea, PdlF and Hekla.

6.4.1 Temporal variation in repose intervals at Mt. Etna

Previous studies of historic eruptions at Mt. Etna have identified a general increase in flank eruption frequency with time and a more sudden increase following 1971 (Behncke and Neri, 2003; Behncke et al., 2005; Andronico and Lodato, 2005; Branca and Del Carlo, 2005; Smethurst et al., 2009; Cappello et al., 2013). Repose data at Mt. Etna clearly reflect this, with median repose intervals decreasing from 6.22 years (1600-1970) to 1.36 years (1971-2010) across the 1971 boundary (Fig. 6.3a). Previous investigations have suggested that the plumbing system beneath Mt. Etna was fundamentally different during the early 17th Century (Hughes et al., 1990; Behncke and Neri, 2003) and the analyses of Chapter 4 found significant difference in the duration of eruptions before and after 1670. For this reason the distribution of repose intervals during the period 1600-1669, 1670-1971 and 1972-2010 are compared here (Fig. 6.3).

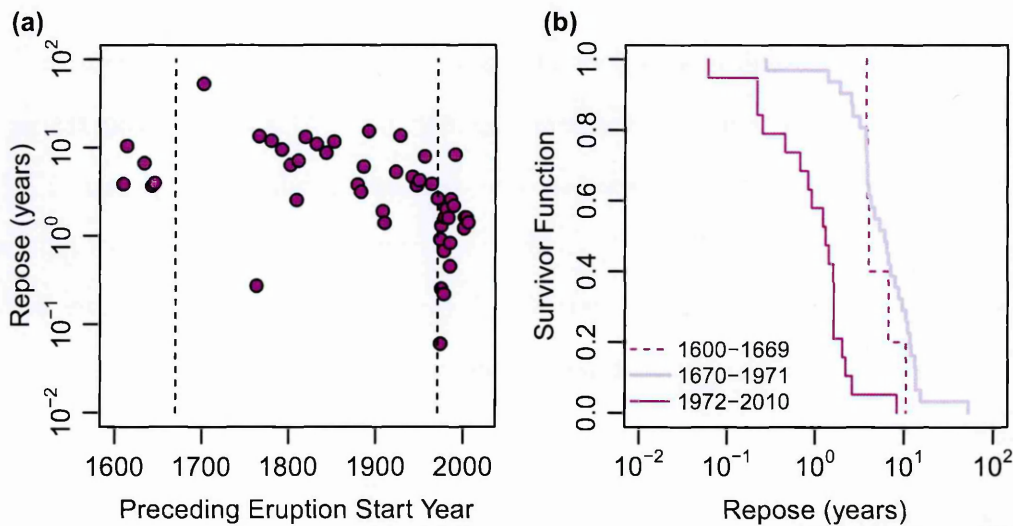


Fig. 6.3 (a) Plot of repose interval with time at Mt. Etna where dashed vertical lines represent the years 1670 and 1971. (b) Empirical survivor function curves for repose intervals during the periods 1600-1669 ($n = 5$), 1670-1971 ($n = 31$) and 1972-2010 ($n=19$) (data from Table 6.1)

While the data from 1600-1669 and 1670-1971 plot with similar shapes and positions, the dominantly shorter repose intervals of the period 1972-2010 cause its curve to be

completely offset (Fig. 6.3b). Significance tests verify this observation with data from the most recent period being significantly different from the 1600-1669 and 1670-2010 data at the 0.05 level (Table 6.5). This implies that Mt. Etna entered a new regime of volcanic activity following 1971 and that repose data restricted to the period 1972-2010 may provide a better representation of activity in the future.

Table 6.5: Significance test results comparing the distribution of flank eruption repose from Mt. Etna for the periods 1600-1669, 1670-1971 and 1972-2010.

Data		Logrank	Mann-Whitney	t-test
A (n=5)	B (n=31)	p = 0.366	p = 0.637	p = 0.729
A (n=5)	C (n=19)	p = 0.004 *	p = 0.002 *	p = 0.000 *
B (n=31)	C (n=19)	p = 0.000 *	p = 0.000 *	p = 0.000 *

A = 1600-1669, B = 1670-1971, C = 1972-2010.
 * = significant at a 0.05 level, • = moderate significance (p-value = 0.05-0.1).
 t-test applied to the logs of the data.

6.4.2 Temporal variation in repose at Kilauea

Klein (1982) recognised three periods of repose at Kilauea: 1918-1924, 1924-1959 and 1969-1979 characterised by mean reposes of 1.04, 3.23 and 0.72 years respectively. The repose interval data used here does not contain information prior to 1927 and therefore the period 1918-1924 cannot be investigated, however, a plot of repose interval against preceding eruption start year shows a general decrease in repose with time reflecting the previously observed reduction in repose interval following 1959 (Fig. 6.4a).

Median reposes for these two datasets are 1.31 years and 135 days (0.37 years) for the periods 1927-1959 and 1960-1983 respectively and their empirical survivor function curves are offset for reposes longer than ~ 3 months (Fig. 6.4b). Despite this, only moderately significant differences are found between the distributions of repose in the two time periods (Table 6.6). This may imply that repose intervals are changing with time, and that as more data becomes available these moderately significant differences

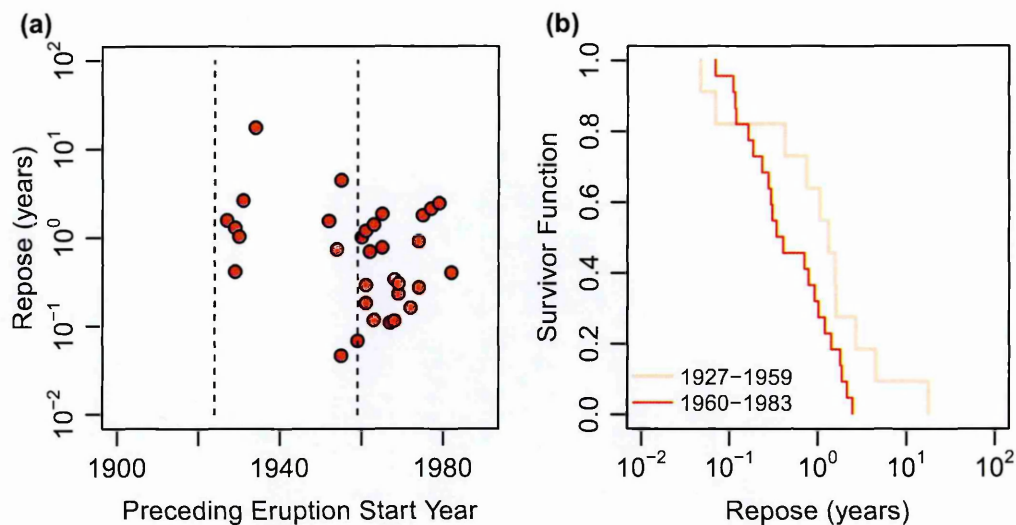


Fig. 6.4 (a) Plot of repose interval with time at Kilauea where dashed vertical lines represent the years 1959 and 1924. (b) Empirical survivor function curves for repose intervals during the periods 1927-1959 ($n = 11$) and 1960-1983 ($n=22$) (data from Table 6.2)

may become significant. Forecasts of repose interval at Kilauea have therefore been performed on both the 1927-1983 and a smaller subset restricted to more recent data (1960-1983) in section 6.5.

Table 6.6: Significance test results comparing the distribution of repose intervals from Kilauea for the periods 1927-1959 and 1960-1983.

Data		Logrank	Mann-Whitney	t -test
A ($n=11$)	B ($n=22$)	$p = 0.051$	• $p = 0.136$	$p = 0.207$
A = 1927-1959, B = 1960-1983.				
★ = significant at a 0.05 level, • = moderate significance (p -value = 0.05-0.1).				
t -test applied to the logs of the data.				

6.4.3 Temporal variation in repose at Piton de la Fournaise (PdIF)

The repose data from PdIF shows little systematic variation with time (Fig. 6.5a) and therefore the same time periods that were investigated for eruption durations (Chapter 4) have been used here (1911-1966, 1972-1992, 1998-2011). The median repose of these datasets are 0.43, 0.25 and 0.22 years respectively and the similarity between them causes the central portion of their empirical survivor function curves to plot close

together while greater variation exists in their long duration tails (Fig. 6.5b).

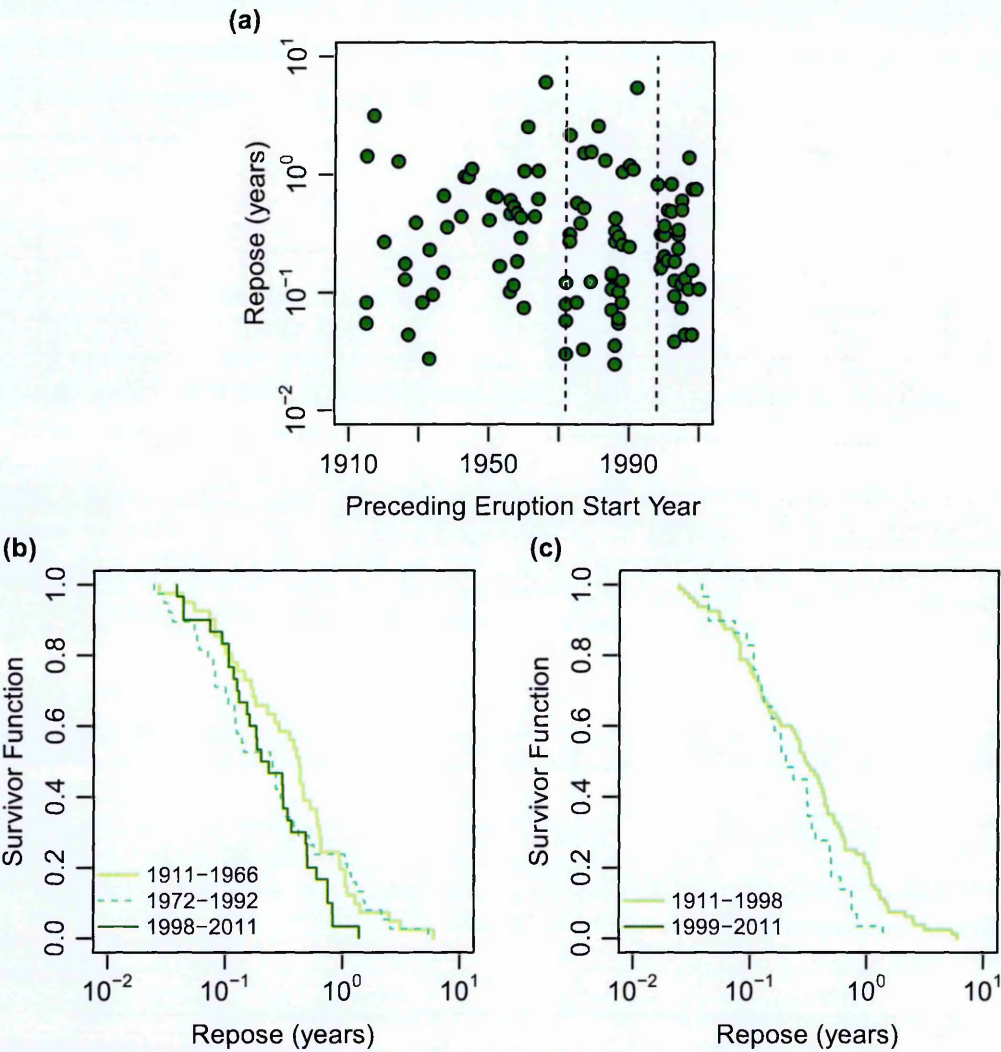


Fig. 6.5 (a) Plot of repose interval with time at PdlF where dashed vertical lines represent the years 1972 and 1998. (b) Empirical survivor function curves for repose intervals during the periods 1911-1966 ($n = 41$) 1972-1992 ($n = 38$) and 1998-2011 ($n=30$) and (c) for the periods 1911-1998 ($n = 80$) and 1999-2011 ($n = 29$) (data from Table 6.3)

Peltier et al. (2009) suggested that the plumbing system beneath PdlF may have changed following 1998 and therefore repose intervals for the periods 1911-1998 and 1999-2011 have also been investigated. Their empirical survivor function curves are displayed in Fig. 6.5c and show a clear divergence for repose intervals greater than ~ 0.8 years (~ 9.5 months).

Table 6.7: Significance test results comparing the distribution repose intervals from PdIF for the periods 1911-1966, 1972-1992 and 1998-2011 and also comparing the periods 1911-1998 and 1999-2011.

Data		Logrank	Mann-Whitney	t-test
A (n=41)	B (n=38)	p = 0.401	p = 0.137	p = 0.175
A (n=41)	C (n=30)	p = 0.041 *	p = 0.129	p = 0.089 •
B (n=38)	C (n=30)	p = 0.332	p = 0.839	p = 0.887
D (n=80)	E (n=29)	p = 0.059 •	p = 0.315	p = 0.182

A = 1911-1966, B = 1972-1992, C = 1998-2011, D = 1911-1998, E = 1999-2011.
* = significant at a 0.05 level, • = moderate significance (p-value = 0.05-0.1).
t-test applied to the logs of the data.

Significance tests performed on the distribution of repose within these datasets indicate that differences are largely not significant at the 0.05 level (Table 6.7). Significant and moderately significant differences are found between the 1911-1966 and 1998-2010 data and moderately significant differences are also found between the 1911-1998 and 1999-2011 data. This may imply that repose is changing with time and that as more data becomes available the moderate differences between older and more recent data may become significant. For these reasons forecasts of future repose intervals are performed using both the entire dataset (1911-2011) and a subset restricted to 1999-2011 in section 6.5.

6.4.4 Temporal variation in repose at Hekla, Iceland

An increase in eruption frequency at Hekla following 1947 was recognised by Thor-darson and Larsen (2007) and Fig. 6.6a demonstrates this feature of the data as a reduction in mixed eruption repose intervals following 1947. During the period 1300-1947 basaltic eruptions are also reported at Hekla. It is possible that the longer repose intervals of this period are due to these basaltic eruption not being accounted for. How-ever, Fig. 6.6b plots the repose interval between all eruptions from Hekla (mixed and basaltic) against preceding eruption start year and although the median repose for the period 1300-1947 is reduced from 64 years to 38 years the pattern of increased eruption

frequency following 1947 can still be observed.

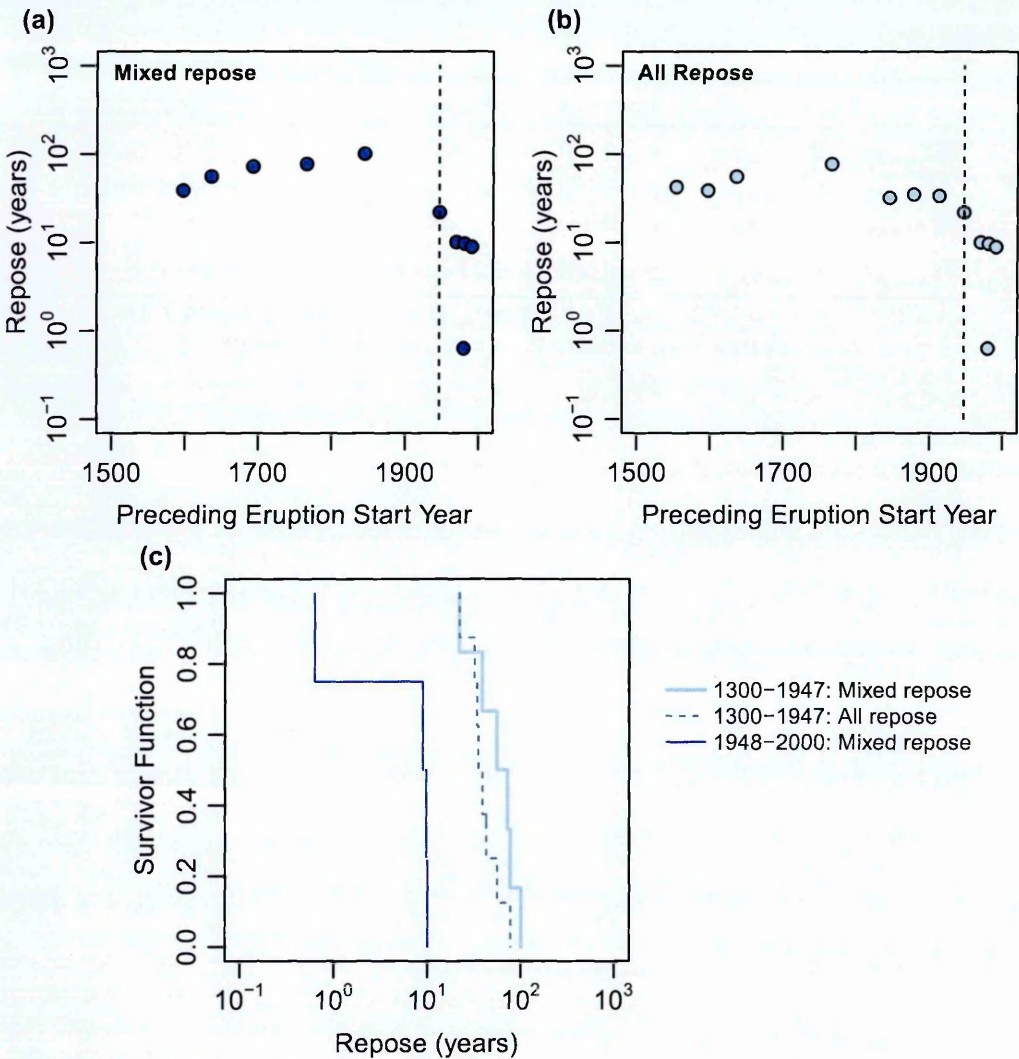


Fig. 6.6 (a) Repose interval between mixed eruptions and (b) between all eruptions from Hekla plotted against preceding eruption start year where the dashed vertical line represents the year 1947. (c) Empirical survivor function curves for repose intervals between mixed eruptions during the periods 1300-1947 ($n = 6$) 1948-2000 ($n = 4$) and and repose intervals between all eruptions types during the 1300-1947 ($n = 8$) (data from Table 6.4)

Empirical survivor function curves for repose intervals between mixed eruptions and all eruptions in the periods 1300-1947 have similar shapes and positions (Fig. 6.6c). Significance tests comparing both of these curves with the 1948-2000 data indicate that their distributions are significantly different at the 0.05 level (Table 6.8). This implies that the observed reduction in repose following 1947 is not a function of only the mixed eruptions being considered. For this reason forecasts of future repose following mixed

eruptions at Hekla will be performed on the 1948-2000 mixed eruption data.

Table 6.8: Significance test results comparing the distribution of repose intervals from Hekla for the periods 1300-1947 and 1947-2000.

Data		Logrank	Mann-Whitney	<i>t</i> -est
A _(n=6)	C _(n=4)	p = 0.001 *	p = 0.010 *	p = 0.032 *
B _(n=8)	C _(n=4)	p = 0.000 *	p = 0.004 *	p = 0.051 •

A = 1300-1947: mixed repose, B = 1300-1947: all repose, C = 1948-2000: mixed repose.

* = significant at a 0.05 level, • = moderate significance (p-value = 0.05-0.1).

t-test applied to the logs of the data.

6.5 Forecasting future repose intervals and the onset of future eruption

The following subsections use the datasets discussed above as the basis of the empirical probabilistic model (outlined in Chapter 2) in order to forecast the onset of future volcanic eruptions. For each dataset, parameter values for the best fit exponential, Weibull, log-logistic and Burr type XII distribution have been found by maximum likelihood estimation. Kolmogorov-Smirnov (*KS*) goodness-of-fit tests and likelihood ratio (*LR*) tests are then performed to determine which theoretical distribution best describes the observed data (see section 2.3). Forecasts are then performed and their results compared.

6.5.1 Forecasting repose intervals between flank eruptions at Mt. Etna

The temporal analyses of section 6.4 identified that the distribution of repose intervals between flank eruptions at Mt. Etna within the periods 1670-1971 and 1972-2010 is significantly different at the 0.05 level. This suggests a fundamental change across

the 1971 boundary and implies that forecasts should be performed on the more recent data which may provide a better representation of future activity. Forecasts of future repose intervals between flank eruptions at Mt. Etna have been made using both the 1600-2010 and 1972-2010 datasets.

Identifying the best fit distribution to the repose data of Mt. Etna

Parameter values for the best fit exponential, Weibull, log-logistic and Burr type XII distribution of each dataset are reported in Table 6.9. Fig. 6.7 plots the survivor function curve of each fitted distribution alongside the empirical survivor function curve of the corresponding observed data.

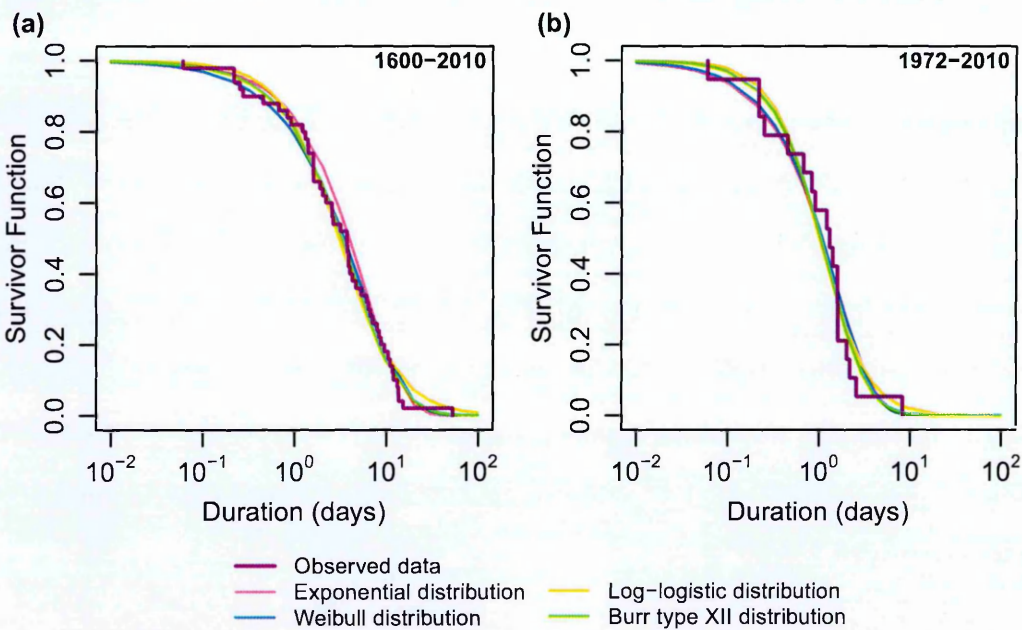


Fig. 6.7 Empirical survivor function curves and fitted theoretical distributions for repose intervals between flank eruptions at Mt. Etna for the periods (a) 1600-2010 and (b) 1972-2010 (data from Table 6.1). Parameter values can be found in Table 6.9

KS goodness-of-fit tests suggest that both datasets could have derived from any of the four distributions (Table 6.9) and visually the fitted distributions of each dataset plot with similar shapes and positions (Fig. 6.7). *LR* tests indicate that in both cases there is little benefit in employing the Burr type XII distribution in preference to the

log-logistic distribution.

Table 6.9: Parameter values, Kolmogorov-Smirnov (KS) test and likelihood ratio (LR) test results for theoretical distributions fitted to the repose interval data of Mt. Etna for (a) 1600-2010 and (b) 1972-2010

(a) 1600-2010

	Exponential	Weibull	Log-logistic	Burr type XII
	$\mu = 5.69$	$\beta = 0.87$	$\beta = 1.36$	$\alpha = 3.87$
		$\mu = 5.28$	$\sigma = 3.11$	$\beta = 1.05$
				$\sigma = 14.82$
D_{obs}	0.095	0.062	0.083	0.057
\hat{p}	0.762 \diamond	0.899 \diamond	0.367 \diamond	0.918 \diamond
r	3000	3000	3000	2962
LR test statistic (log-logistic and Burr type XII):				3.284

(b) 1972-2010

	Exponential	Weibull	Log-logistic	Burr type XII
	$\mu = 1.53$	$\beta = 1.03$	$\beta = 1.67$	$\alpha = 3.51$
		$\mu = 1.55$	$\sigma = 1.02$	$\beta = 1.37$
				$\sigma = 2.45$
D_{obs}	0.137	0.143	0.151	0.144
\hat{p}	0.652 \diamond	0.380 \diamond	0.154 \diamond	0.211 \diamond
r	3000	3000	3000	2876
LR test statistic (log-logistic and Burr type XII):				1.200

In both tables:

\diamond not significant at the 0.05 level (p -value > 0.05).

D_{obs} = KS statistic, \hat{p} = estimated p -value and r = final bootstrap size.

Given the visually poorer fit of the log-logistic distribution to the long repose tail of the 1600-2010 data (Fig. 6.7a) and the visually better fit of the Weibull distribution to the short repose tail of the 1972-2010 data (Fig. 6.7b) the best fit Weibull distribution of both datasets have been used to perform the following repose interval forecasts.

Forecasting results for Mt. Etna

Table 6.10 contains the results of eight forecasts performed on the 1600-2010 data and seven forecast performed on the 1972-2010 data of repose intervals between flank eruptions at Mt. Etna. Survivor function forecasts based on the 1972-2010 data have markedly lower exceedance probabilities than those resulting from from the 1600-2010 data (Table 6.10). The difference is sufficiently large that although the 1600-2010 data indicate a 4 % probability of a future repose period exceeding 20 years a forecast for this repose was not considered necessary for the 1972-2010 data which yield a very low probability of exceeding even 10 years (Table 6.10). It is worth noting that the 0 % probabilities presented here are actually between 0 and 0.5 % but presented as 0 % due to rounding for presentation purposes. A similar trend exists in the residual life function results (Table 6.10).

Table 6.10: Survivor function (SF), residual life function (R_{life}) and quantile function (Q) forecasts for repose intervals between flank eruptions at Mt. Etna based on the (a) 1600-2010 and (b) 1972-2010 data. For the residual life function $t = 5$ years

(a) 1600-2010 (Weibull)

	Input	Result	C/I	
			95 %	80 %
SF	1 y	79 %	$\pm 9 \%$	$\pm 6 \%$
	5 y	39 %	$\pm 11 \%$	$\pm 7 \%$
	10 y	17 %	$\pm 8 \%$	$\pm 6 \%$
	20 y	4 %	$\pm 4 \%$	$\pm 3 \%$
R_{life}	6 y	85 %	$\pm 4 \%$	$\pm 3 \%$
	10 y	45 %	$\pm 12 \%$	$\pm 8 \%$
Q	0.34	1.92 y	$\pm 0.86 y$	$\pm 0.56 y$
	0.67	5.94 y	$\pm 1.95 y$	$\pm 1.27 y$

(b) 1972-2010 (Weibull)

	Input	Result	C/I	
			95 %	80 %
SF	1 y	53 %	$\pm 18 \%$	$\pm 12 \%$
	5 y	4 %	$\pm 6 \%$	$\pm 4 \%$
	10 y	0 %	$\pm 0 \%$	$\pm 0 \%$
R_{life}	6 y	50 %	$\pm 26 \%$	$\pm 17 \%$
	10 y	3 %	$\pm 9 \%$	$\pm 6 \%$
Q	0.34	0.66 y	$\pm 0.40 y$	$\pm 0.26 y$
	0.67	1.71 y	$\pm 0.77 y$	$\pm 0.51 y$

In both tables:

y = years, C/I = confidence interval

Considering that the 1972-2010 period represents the most recent eruptive activity at Mt. Etna it is probable that repose intervals during this period best reflect the state

of the plumbing system beneath Mt. Etna today. Quantile functions performed on this data indicate that a future repose between flank eruptions at Mt. Etna is likely to exceed 0.66 years (241 days) (± 0.26 years) but unlikely to exceed 1.71 years (± 0.51 years) (Table 6.10b), however, the last flank eruption at Mt. Etna ended in July 2009 and thus almost 5 years of repose has passed to date (May 2014). A residual life function where $t = 5$ years yields a 50 % (± 26 %) probability that the repose will continue until at least July 2015 (Table 6.10b). If the temporal variation in repose is not taken into account and the 1600-2010 data is used a repose of 5 years falls between the likely and unlikely quantile function results (Table 6.10a) and residual life functions where $t = 5$ years give higher exceedance probabilities for the total repose intervals considered.

Wickman (1966) used an exponential distribution to forecast repose intervals at Mt. Etna and concluded an 86 % probability of repose intervals exceeding 1 year, a 46 % probability of repose intervals exceeding 5 years and a 21 % probability of repose intervals exceeding 10 years. These results are very similar to those obtained here when the model is based on the 1600-2010 input data (Table 6.10a). The current study, however, presents confidence intervals for these forecast.

6.5.2 Forecasting repose between eruptions at Kilauea

A general trend of increased eruption frequency and therefore reduced repose interval with time at Kilauea was observed in section 6.4 and may reflect improved monitoring during the late 1950's (Dzurisin et al., 1984). Moderately significant differences were found between the repose data of the periods 1927-1959 and 1960-1983 and forecasts have been performed based on the entire repose dataset (1927-1983) and a smaller subset of this for the period 1960-1983.

Identifying the best fit distribution to the repose data of Kilauea

Parameter values for the best fit exponential, Weibull, log-logistic and Burr type XII distribution of each dataset are reported in Table 6.11. Fig. 6.8 plots the survivor function curve of each fitted distribution alongside the empirical survivor function curve of the corresponding observed data.

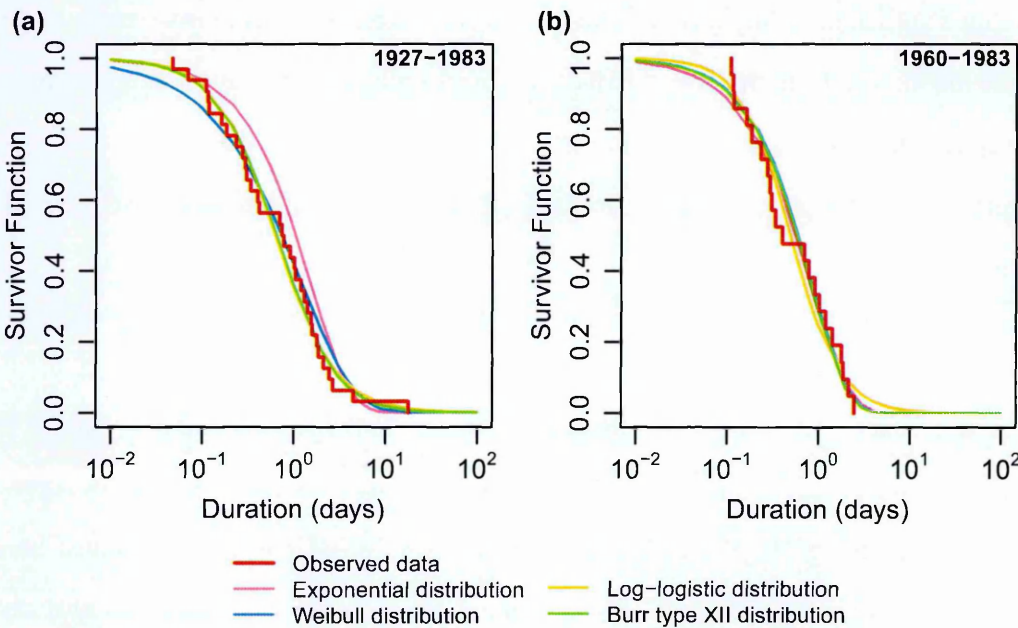


Fig. 6.8 Empirical survivor function curves and fitted theoretical distributions for repose intervals between eruptions at Kilauea for the periods (a) 1927-1983 and (b) 1960-1983 (data from Table 6.2). Parameter values can be found in Table 6.11

KS goodness-of-fit tests for the 1927-1983 data indicate that the Weibull, log-logistic and Burr type XII distributions provide adequate fits to the data (Table. 6.11a). While this is supported by the poor fit of the exponential distribution in Fig. 6.8a, the Weibull distribution also provides a poor visual fit to the observed data at durations $< \sim 4$ years (Fig. 6.8a). In contrast the survivor function curves fitted to the 1960-1983 data all plot with similar shapes and positions (Fig. 6.8b) and KS goodness-of-fit tests indicate that all four distributions provide adequate fit to the data.

In both cases LR tests indicate that there is little benefit in employing the more com-

Table 6.11: Parameter values, Kolmogorov-Smirnov (*KS*) test and likelihood ratio (*LR*) test results for theoretical distributions fitted to the repose interval data of Kilauea for (a) 1927-1983 and (b) 1960-1983

(a) 1927-1983

	Exponential	Weibull	Log-logistic	Burr type XII
	$\mu = 1.51$	$\beta = 0.75$	$\beta = 1.33$	$\alpha = 1.68$
		$\mu = 1.21$	$\sigma = 0.64$	$\beta = 1.21$
				$\sigma = 0.94$
D_{obs}	0.196	0.100	0.092	0.082
\hat{p}	0.037	0.548 \diamond	0.563 \diamond	0.720 \diamond
r	3000	2992	3000	2897
<i>LR</i> test statistic (log-logistic and Burr type XII):				0.206

(b) 1960-1983

	Exponential	Weibull	Log-logistic	Burr type XII
	$\mu = 0.80$	$\beta = 1.10$	$\beta = 1.61$	$\alpha = 7798.99$
		$\mu = 0.83$	$\sigma = 0.50$	$\beta = 1.10$
				$\sigma = 2580.85$
D_{obs}	0.132	0.167	0.128	0.167
\hat{p}	0.658 \diamond	0.115 \diamond	0.355 \diamond	0.076 \diamond
r	3000	2999	2993	2874
<i>LR</i> test statistic (log-logistic and Burr type XII):				0.999

In both tables:

\diamond not significant at the 0.05 level (p -value > 0.05).

D_{obs} = *KS* statistic, \hat{p} = estimated p -value and r = final bootstrap size.

plex Burr type XII distribution in preference to the log-logistic distribution and for these reasons the best fit log-logistic distributions are used to perform forecasts based on both sets of data.

Forecasting results for Kilauea

Table 6.12 contains the results of nine forecasts performed on both the 1927-1983 and 1960-1983 repose data of Kilauea. Despite the moderate differences in the distribution of repose intervals in the periods before and after 1959, point forecasting results obtained from both datasets are the same in all instances (Table 6.12a and b respectively). Differences only occur in the confidence intervals calculated for each forecast but these are slight.

Table 6.12: Survivor function (SF), residual life function (R_{life}) and quantile function (Q) forecasts for repose intervals between eruptions at Kilauea based on the (a) 1927-1983 and (b) 1960-1983 data. For the residual life function $t = 0.25$ years

(a) 1927-1983 (log-logistic)					(b) 1960-1983 (log-logistic)				
	Input	Result	C/I			Input	Result	C/I	
			95 %	80 %				95 %	80 %
SF	0.25 y	75 %	± 18 %	± 12 %	SF	0.25 y	75 %	± 16 %	± 10 %
	0.55 y	50 %	± 24 %	± 15 %		0.55 y	50 %	± 19 %	± 13 %
	10y	25 %	± 18 %	± 12 %		10y	25 %	± 16 %	± 10 %
	5 y	2 %	± 3 %	± 2 %		5 y	2 %	± 3 %	± 2 %
R_{life}	0.75 y	45 %	± 16 %	± 11 %	R_{life}	0.75 y	45 %	± 16 %	± 11 %
	1.75 y	16 %	± 11 %	± 7 %		1.75 y	16 %	± 13 %	± 8 %
	3.25 y	6 %	± 6 %	± 4 %		3.25 y	6 %	± 7 %	± 5 %
Q	0.34	0.33 y	± 0.20 y	± 0.13 y	Q	0.34	0.33 y	± 0.16 y	± 0.11 y
	0.67	0.78 y	± 0.46 y	± 0.30 y		0.67	0.78 y	± 0.39 y	± 0.26 y

In both tables:
 y = years, C/I = confidence interval

This suggests that there is little benefit in restricting the data based on observed differences that are not statistically significant and that it is acceptable to use all available repose data to perform forecasts for Kilauea. Quantile functions indicate that repose intervals at Kilauea are likely to exceed 120 days (± 48 days) but unlikely to exceed 284 days (± 109 days) (0.33 years (± 0.13 years) and 0.78 years (± 0.30 years) respectively in Table 6.12). The Kilauea data of this study does not include the Pu'u'Ō'ō -

Kūpaianaha eruption which started in January 1983. This was ~ 4 months (0.33 years) after the end of the final eruption considered in this study (# 41, Table 3.2) and falls on the lower boundary of this forecast. This implies that the repose interval prior to the 1983 eruption was not deviation from typical and expected behaviour at Kilauea, despite the eruption itself having a duration considerably longer than expected (section 5.2).

6.5.3 Forecasting repose between eruptions at PdIF

Moderately significant differences were found between the most recent repose data of PdIF (1999-2011) and the data prior to it (1911-1998) indicating potentially changing repose intervals with time (section 6.4). For this reason separate forecasts of repose intervals at PdIF have been made using both the 1911-2011 and 1999-2011 datasets.

Identifying the best fit distribution to the repose data of PdIF

Parameter values for the best fit exponential, Weibull, log-logistic and Burr type XII distribution of each dataset are reported in Table 6.13. Fig. 6.9 plots the survivor function of each fitted distribution alongside the empirical survivor function curve of the corresponding observed data.

KS goodness-of-fit tests for the 1911-2011 data yield p -values > 0.05 for the Weibull, log-logistic and Burr type XII distributions (Table 6.13a). These are still low but imply that these distributions provide a reasonable fit to the observed repose data. All four distributions of the 1999-2011 data have higher KS tests p -values and therefore all adequately describe the data (Table 6.13b). In both cases the log-logistic and Burr type XII distributions plot with similar shapes and positions (Fig. 6.9) and LR tests

Table 6.13: Parameter values, Kolmogorov-Smirnov (KS) test and likelihood ratio (LR) test results for theoretical distributions fitted to the repose interval data of PdIF for (a) 1911-2011 and (b) 1999-2011

(a) 1911-2011

	Exponential	Weibull	Log-logistic	Burr type XII
	$\mu = 0.58$	$\beta = 0.82$	$\beta = 1.41$	$\alpha = 1.39$
		$\mu = 0.51$	$\sigma = 0.27$	$\beta = 1.42$
				$\sigma = 0.26$
D_{obs}	0.146	0.079	0.065	0.065
\hat{p}	0.001	0.083 \diamond	0.188 \diamond	0.124 \diamond
r	3000	3000	2995	2986
LR test statistic (log-logistic and Burr type XII):				0.002

(b) 1999-2011

	Exponential	Weibull	Log-logistic	Burr type XII
	$\mu = 0.33$	$\beta = 1.17$	$\beta = 1.85$	$\alpha = 2.89$
		$\mu = 0.35$	$\sigma = 0.22$	$\beta = 1.56$
				$\sigma = 0.39$
D_{obs}	0.111	0.104	0.096	0.084
\hat{p}	0.680 \diamond	0.570 \diamond	0.573 \diamond	0.750 \diamond
r	3000	2861	2999	2898
LR test statistic (log-logistic and Burr type XII):				0.288

In both tables:

\diamond not significant at the 0.05 level (p -value > 0.05).

D_{obs} = KS statistic, \hat{p} = estimated p -value and r = final bootstrap size.

indicating that there is little benefit in employing the Burr type XII distribution in preference to the log-logistic distribution (Table 6.13).

Visually the exponential and Weibull distributions of both datasets provide the poorest fit to the data (Fig. 6.9) and the best fit log-logistic distributions have therefore been used to perform the following forecasts of repose intervals at PdIF.

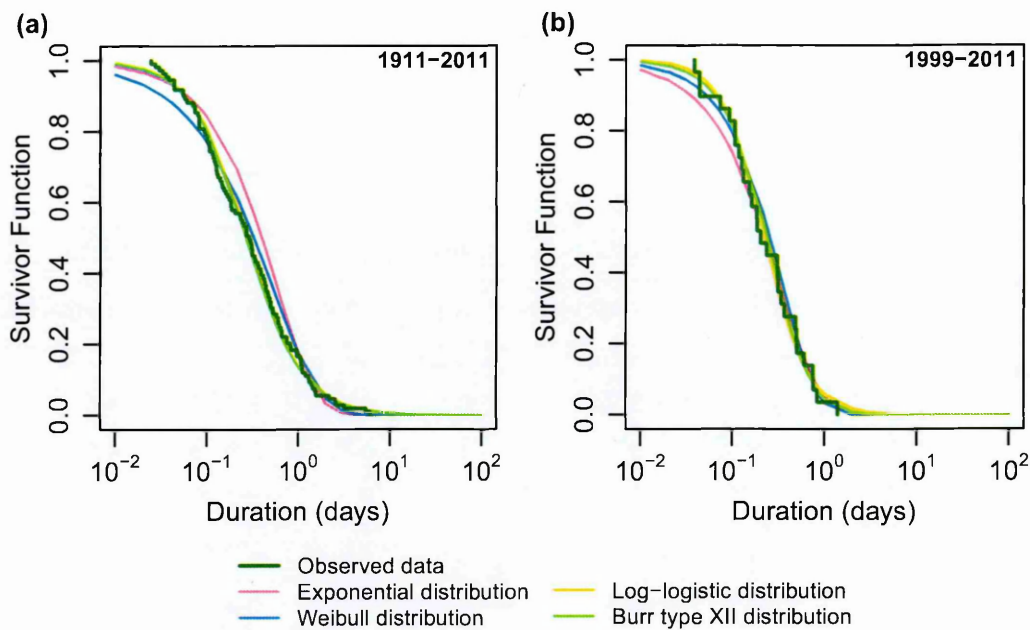


Fig. 6.9 Empirical survivor function curves and fitted theoretical distributions for repose intervals between eruptions at PdlF for the periods (a) 1911-2011 and (b) 1999-2011 (data from Table 6.3). Parameter values can be found in Table 6.13

Forecasting results for PdlF

Table 6.14 contains the results of nine forecasts performed on both the 1911-2011 and 1999-2011 repose data of PdlF. The higher proportion of short repose in the 1999-2011 dataset causes its survivor function results to have slightly lower exceedance probabilities than those based on the 1911-2011 data for the same x values. This difference is sufficiently small that the two forecasts often fall within the repose range when confidence intervals are taken into account.

These results imply that it is not necessary to restrict the data to more recent years for forecasting purposes. Quantile functions performed on the 1911-2011 data indicate that a future repose interval at PdlF is likely to exceed 62 days (± 11 days) but unlikely to exceed 164 days (± 26 days) (0.17 years (± 0.03 years) and 0.45 years (± 0.07 years) respectively in Table 6.14a). Residual life functions have been performed to incorporate this data ($t = 3$) and results give a 67 % (± 3 %) probability of the repose

Table 6.14: Survivor function (SF), residual life function (R_{life}) and quantile function (Q) forecasts for repose intervals eruptions at PdIF based on the (a) 1911-2011 and (b) 1999-2011 data. For the residual life function $t = 3$ years

(a) 1911-2011 (log-logistic)					(b) 1999-2011 (log-logistic)				
	Input	Result	C/I			Input	Result	C/I	
			95 %	80 %				95 %	80 %
SF	0.17 y	66 %	± 8 %	± 5 %		0.17 y	62 %	± 16 %	± 10 %
	0.25 y	53 %	± 8 %	± 5 %	SF	0.25 y	44 %	± 16 %	± 10 %
	0.5 y	30 %	± 7 %	± 5 %		0.5 y	18 %	± 12 %	± 8 %
	1 y	14 %	± 5 %	± 3 %		1 y	6 %	± 6 %	± 4 %
	5 y	2 %	± 1 %	± 1 %		5 y	0 %	± 1 %	± 0 %
R_{life}	3.5 y	81 %	± 3 %	± 2 %	R_{life}	3.5 y	75 %	± 7 %	± 4 %
	4 y	67 %	± 4 %	± 3 %		4 y	59 %	± 10 %	± 6 %
	5 y	49 %	± 6 %	± 4 %		5 y	39 %	± 11 %	± 7 %
Q	0.34	0.17 y	± 0.04 y ± 0.03 y		Q	0.34	0.15 y	± 0.06 y ± 0.04 y	
	0.67	0.45 y	± 0.11 y ± 0.07 y			0.67	0.32 y	± 0.12 y ± 0.08 y	

In both tables:
 y = years, C/I = confidence interval

continuing for at least another year (December 2014) (Table 6.14a).

6.5.4 Forecasting repose between mixed eruptions at Hekla, Iceland

Previous investigations have identified increased eruption frequency at Hekla with time. This is apparent in the mixed eruption data of this study as a reduction in repose interval following 1947 (section 6.4). As such, forecasting models based on the data in the period 1948-2000 may be more appropriate than one containing data in the period 1300-2011. Forecasts are performed here on both the 1300-2000 and 1948-2000 data.

Identifying the best fit distribution to the mixed eruption repose data of Hekla

Parameter values for the best fit exponential, Weibull, log-logistic and Burr type XII distributions of each dataset are reported in Table 6.15. Fig. 6.10 plots the survivor function of each fitted distribution alongside the empirical survivor function curve of the corresponding observed data.

Table 6.15: Parameter values, Kolmogorov-Smirnov (*KS*) test and likelihood ratio (*LR*) test results for theoretical distributions fitted to the repose interval data of mixed eruptions from Hekla for (a) 1300-2000 and (b) 1948-2000

(a) 1911-2011

	Exponential	Weibull	Log-logistic	Burr type XII
	$\mu = 39.71$	$\beta = 0.98$	$\beta = 1.26$	$\alpha = 2777.22$
		$\mu = 39.43$	$\sigma = 27.79$	$\beta = 1.00$
				$\sigma = 111181.01$
D_{obs}	0.175	0.169	0.155	0.174
\hat{p}	0.738 \diamond	0.595 \diamond	0.591 \diamond	0.417 \diamond
r	3000	3000	3000	2855
LR test statistic (log-logistic and Burr type XII):				2.581

(b) 1999-2011

	Exponential	Weibull	Log-logistic	Burr type XII
	$\mu = 7.37$	$\beta = 1.50$	$\beta = 1.56$	$\alpha = 12078.54$
		$\mu = 7.97$	$\sigma = 6.31$	$\beta = 1.50$
				$\sigma = 3229.53$
D_{obs}	0.454	0.447	0.383	0.446
\hat{p}	0.080 \diamond	0.003	0.004	0.006
r	3000	2997	3000	3000
LR test statistic (log-logistic and Burr type XII):				2.00

In both tables:

\diamond not significant at the 0.05 level (p -value > 0.05).

D_{obs} = *KS* statistic, \hat{p} = estimated p -value and r = final bootstrap size.

KS goodness-of-fit tests for the 1300-2000 data indicate that all four tested distribu-

tions provide an adequate fit to the data (Table 6.15). Visually the Exponential, Weibull and Burr type XII distributions plot with almost identical shapes and positions, however, the log-logistic distribution diverges from these curves at repose intervals > 80 years suggesting a poorer fit to the data (Fig. 6.10a). Despite this a LR test indicates that it is not beneficial to employ the Burr type XII distribution in preference to the log-logistic distribution (Table 6.15a). For these reasons the best fit Weibull distribution has been used to perform repose forecasts based on this dataset in the following section.

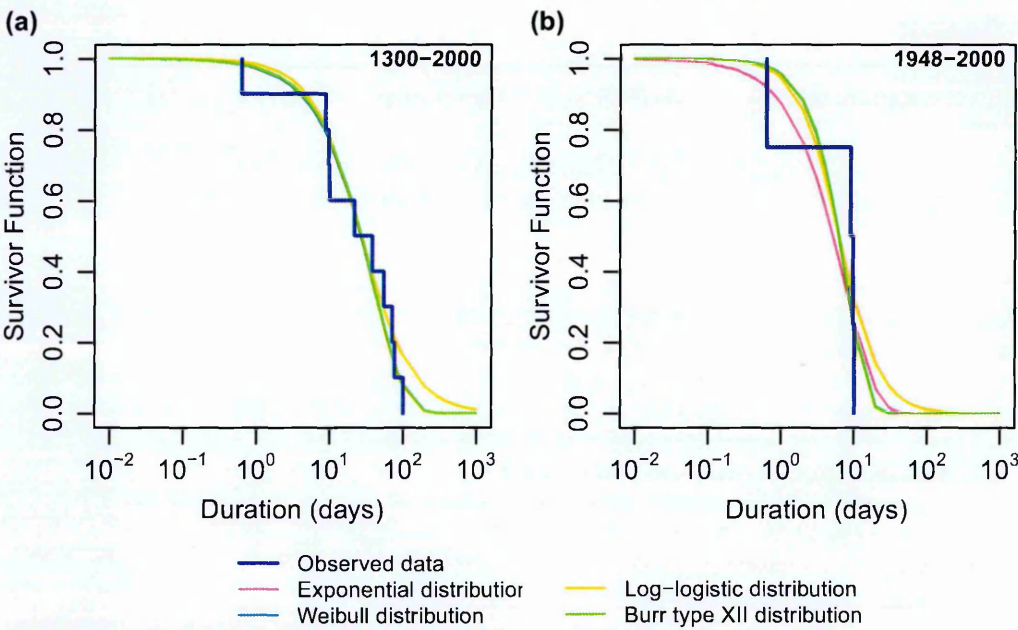


Fig. 6.10 Empirical survivor function curves and fitted theoretical distributions for repose intervals between mixed eruptions at Hekla for the periods (a) 1300-2000 and (b) 1948-2000 (data from Table 6.4). Parameter values can be found in Table 6.15

Fig. 6.10b highlights the difficulty in assessing the fit of a theoretical distribution when sample sizes are small, i.e the four data points of the 1948-2000 dataset of repose at Hekla. KS goodness-of-fit tests reveal that only the exponential distribution gives a p -value of > 0.05 (Table 6.15b) and therefore this distribution has been used to provide forecasts on the data in the following section. Given the weakness of the distributions fit to the data and the very small sample size of the observed dataset the author suggests that this should be considered for comparative purposes only and not used as a sensible

forecast of future repose at Hekla.

Forecasting results for Hekla

Table 6.16 contains the results of ten forecasts performed on the 1300-2000 data and eight forecasts performed on the 1948-2000 data of repose intervals between mixed eruptions from Hekla. Survivor function forecasts based on the 1300-2000 data yield higher exceedance probabilities than those based on the restricted dataset containing only the shorter repose intervals of the 1948-2000 time period (Tables 6.16a and b respectively).

Table 6.16: Survivor function (SF), residual life function (R_{life}) and quantile function (Q) forecasts for repose intervals between mixed eruptions at Hekla, Iceland based on the (a) 1300-2000 and (b) 1947-2000 data. For the residual life function $t = 14$ years

(a) 1300-2000 (Weibull)					(b) 1948-2000 (Exponential)				
	Input	Result	C/I			Input	Result	C/I	
			95 %	80 %				95 %	80 %
SF	1 y	97 %	± 6 %	± 4 %	SF	1 y	87 %	± 12 %	± 8 %
	5 y	88 %	± 16 %	± 11 %		5 y	51 %	± 34 %	± 22 %
	10 y	77 %	± 22 %	± 14 %		10 y	26 %	± 34 %	± 22 %
	50 y	28 %	± 22 %	± 15 %		50 y	0 %	± 1 %	± 0 %
	100 y	8 %	± 14 %	± 9 %					
R_{life}	15 y	97 %	± 2 %	± 1 %	R_{life}	15 y	6 %	± 3 %	± 2 %
	20 y	86 %	± 8 %	± 5 %		20 y	3 %	± 8 %	± 5 %
	50 y	41 %	± 24 %	± 15 %	Q	0.34	3.1 y	± 3.0 y	± 2.0 y
Q	0.34	16.1 y	± 14.7 y	± 9.6 y		0.67	8.2 y	± 8.0 y	± 5.2 y
	0.67	43.8 y	± 28.4 y	± 18.5 y					

In both tables:

y = years, C/I = confidence interval

The data from the period 1948-2000 should better reflect the plumbing system beneath Hekla today and thus give a better indication of its future activity. The last mixed eruption from Hekla was in 2000 and thus 14 years of repose have passed to date.

Quantile functions performed on this dataset indicate that a future repose is likely to exceed 3.1 years but unlikely to exceed 8.2 years and a residual life function where $t = 14$ years suggest only a 6 % and 3 % probability of exceeding 1 and 6 more years respectively (Table 6.16b). These same forecasts performed on the 1300-2000 dataset are more reasonable, indicating that future repose intervals are likely to exceed 16.1 years and unlikely to exceed 43.8 years (Table 6.16a). Although this may indicate that eruptive behaviour at Hekla is changing and returning to a regime similar to that prior to 1948, this cannot be concluded definitively due to the forecasts derived from the 1948-2000 data being based on a poorly fitting exponential distribution constrained by very few data points.

6.6 Conclusions

This chapter applied the empirical probabilistic model outlined in Chapter 2 to repose interval data at Mt. Etna, Kilauea, PdlF and Hekla. Previous investigations have focussed on repose intervals more frequently than eruption durations and they have formed the basis of survival analysis style probabilistic models in the past. This has enabled more comparisons of our work with the existing literature and also a chance to highlight the key differences between the model developed here and those used by previous authors.

Firstly, recurrence intervals are often used as a proxy for repose due to insufficient information regarding eruption ends (Fig. 6.1) (Klein, 1982; Mulargia et al., 1985; Stieltjes and Moutou, 1989; De la Cruz-Reyna, 1991; Bebbington and Lai, 1996; Passarelli et al., 2010). Here we are able to demonstrate while recurrence interval is often a good estimate of repose interval, biases become important when used at volcanic systems which erupt frequently (e.g. PdlF, section 6.3). Despite the slightly different repose data used in this study compared to these other studies, the results obtained are

similar, even when the forecasts performed for Mt. Etna here are compared to those made when Wickman (1966) first suggested the potential use of repose interval data to forecast future eruption onsets (subsection 6.5.1).

Despite these similarities, the forecasting results themselves are less promising than one would hope. By still using 66 % and 33 % probabilities to correspond to likely and unlikely events respectively, the on-going repose intervals at the volcanic systems investigated often do not fall within these expected values (for example results from Mt. Etna and PdIF, Tables 6.10 and 6.14 respectively). To some extent this may suggest that the arbitrary probabilities assigned to these qualitative terms are unrealistic and perhaps need modifying to better suit the data. However, it is also possible that the physical properties controlling repose are more complicated than represented by this model and perhaps a better dataset of repose which also considers intrusive events and any relationships between adjacent volcanic systems or other types of volcanism may improve these results.

Unlike the models of previous investigations (Connor et al., 2003, 2006; Dzierma and Wehrmann, 2010), a residual life function forecast is included here and when performed with t equal to the time currently passed since the last eruption, results become more promising. While survivor function forecasts gave results indicating that a repose interval of the current length is unlikely, residual life function results suggest that once a repose interval of the current length has been reached the probability of it continuing further is high enough to be reasonable.

Furthermore, the analyses presented here are volcano specific and the repose datasets themselves subjected to temporal analyses prior to their use in the empirical probabilistic model, allowing the input data to be sensibly split such that it best represents future activity. With the exception of Mt. Etna, temporal variations identified in the repose data corresponded with changes observed in the eruption duration data in Chapter 4. This may indicate that some relationship exists between the physical parameters con-

trolling eruption duration and those controlling repose interval. However, the repose data for PdlF may suggest otherwise, as although both its repose and eruption duration data show marginal temporal variations, the bimodal nature of the eruption duration data (section 4.2.3) is not reflected in its repose intervals. This possible link between eruption durations and repose intervals will be returned to in Chapter 7.

Chapter 7

Conclusions: possible controls on eruption duration and further work



Whilst empirical probabilistic forecasts provide useful information about the likely duration of future eruptions when other information is unknown or unavailable, they could be improved with increased understanding of the processes physically controlling an eruption's duration (Decker, 1986). The current chapter considers some of these potential factors. It notes correlations between varying distributions of eruption durations and the physical properties of the volcanic systems to which they pertain. Although this enables some hypotheses to be made regarding which parameters are important in controlling eruption duration at the volcanic systems investigated it is not a complete study, and additional work is required before conclusive results can be made.

The second half of the current chapter outlines the conclusions of this PhD and discusses the additional work required to make definitive conclusions on the leading controls on eruption duration as well as possible refinement of the empirical forecasting model and its application to other types of duration data within the field of volcanic hazards.

7.1 A brief summary of the duration regimes identified in this thesis

Chapter 4 analysed the duration data of Mt. Etna (flank eruptions), Kilauea, Piton de la Fournaise (PdIF) and Iceland with the aim of identifying temporal and spatial variations in their distributions. Spatial variations were found to be slight, however, variations in the distribution of eruption duration with time were often found to be significant. These subsets are therefore described by different duration regimes resulting from differences in the physical properties of the volcanic system at the time. This chapter considers each duration regime and its corresponding physical properties separately in order to assess the possible leading controls on eruption duration.

For Mt. Etna two duration regimes are identified: 1600-1669 and 1670-2010. For Kilauea evidence of a reporting bias affecting data prior to 1959 has been found leading to its exclusion here and only one duration regime is considered here (for the period 1960-1983). Although significant differences were not found in the duration data of PdIF, the period 1972-1992 has a strongly bimodal distribution which is less evident in the period 1998-2011. These two periods are considered as different duration regimes here and are investigated independently.

Data from Iceland are largely restricted to mixed eruptions from Hekla due to their good documentation and near complete record. Data for the total duration of these

eruptions (d_4) are separated into two subgroups (1300-1947 and 1948-2000), however it is not considered necessary to split the data for the initial explosive phase (with duration d_{3a}) in the same way.

7.2 The relationship between repose interval and eruption duration

Chapter 6 investigated the period of inactivity (repose interval) between eruptions from Mt. Etna (flank eruptions), Kilauea, PdlF and Hekla (mixed eruptions) and found that the time periods described by different duration regimes (identified in Chapter 4) often also have different distributions of repose intervals. This suggests that a relationship may exist between eruption duration and repose interval at the volcanoes studied.

7.2.1 Repose interval as a control on eruption duration

Fig. 7.1 plots eruption duration against preceding repose interval to investigate whether a relationship exists between the duration of a period of inactivity and the duration of the eruption immediately succeeding it. Linear regressions performed on the logs of the data indicate little to no relationship between these parameters (Fig. 7.1). This is reflected in the very small values of the ‘coefficient of determination’ presented here as a squared correlation coefficient (R^2). These results imply that in general, the period of repose prior to an eruption has little effect on the duration of the following eruption. In terms of a potential forecasting tool, this suggests that the duration of a period of repose is a poor predictor of future eruption duration.

The temporal subsets of Mt. Etna and PdlF investigated also do not show evidence of clustering implying that changes in repose interval, and thus eruption frequency, are

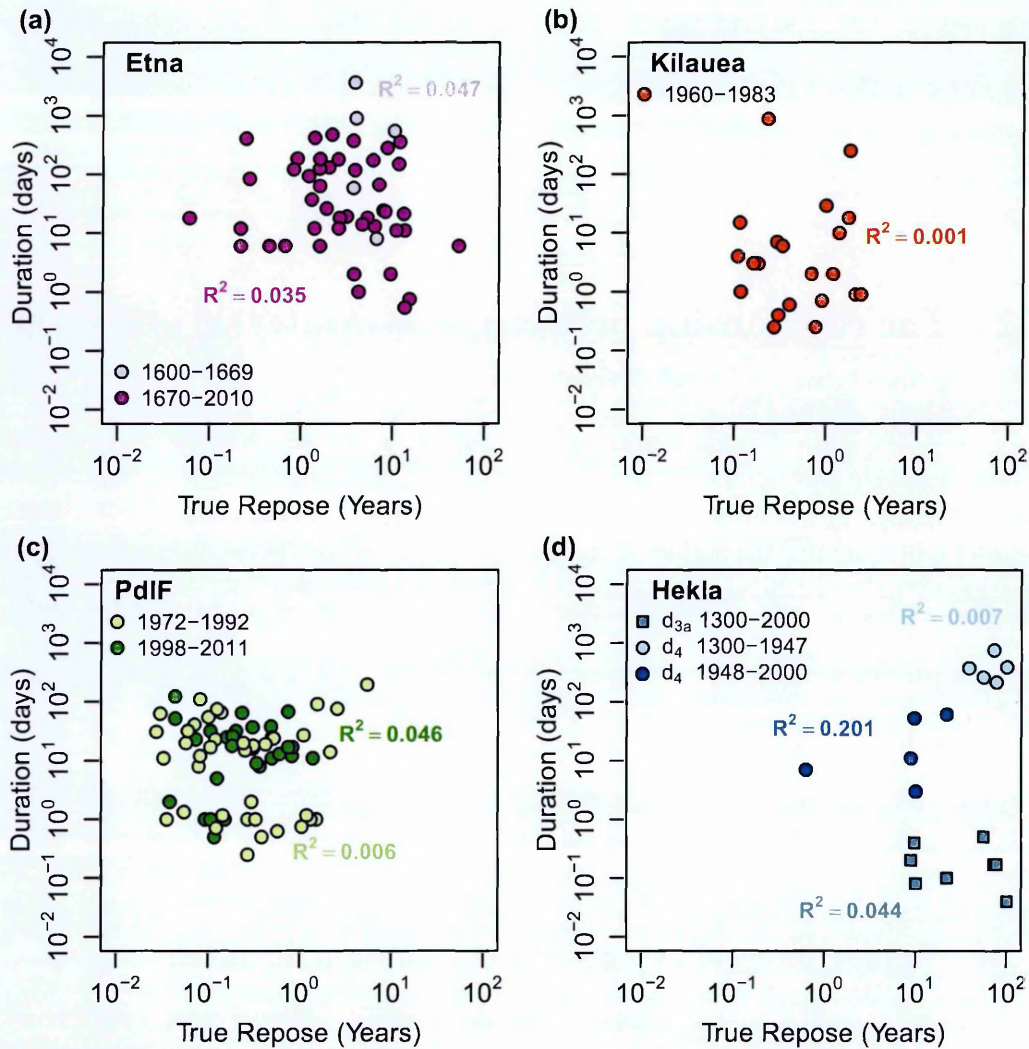


Fig. 7.1 Plots assessing the effect of repose interval on succeeding eruption duration at (a) Mt. Etna (flank eruptions), (b) Kilauea, (c) PdIF and (d) Hekla (flank eruptions) for the stated time periods. (d) d_{3a} represents the duration on the initial eruptive phase and d_4 the total eruption duration. R^2 values correspond to linear regressions performed on the logs of the data

not responsible for the observed variations in eruption duration (Fig. 7.1a and c). In contrast, Fig. 7.1d shows how d_4 data of Hekla in the periods 1300-1947 and 1948-2000 segregate into two clusters. Furthermore, this data shows the strongest correlation between repose and succeeding eruption duration ($R^2 = 0.201$), although it is worth noting that this is based on few data values. This implies that repose interval at Hekla may provide some information about the duration of a following eruption, such that if a repose interval were to exceed $\sim 10,000$ days (27.4 years) we might expect the

following eruption to have a long duration in excess of 150 days, alternatively repose intervals of < 27.4 years may imply a following eruption duration of between 2 and 150 days. (Fig. 7.1d).

7.2.2 Eruption duration as a control on repose interval

The other possibility for different eruption duration regimes correlating with changes in repose interval is that the duration of an eruption influences the duration of the period of inactivity immediately following it. Such a possibility has been alluded to in the past. Stieltjes and Moutou (1989) performed analyses on repose intervals at PdIF and identified a relationship between eruption duration and succeeding repose interval where, with the exception of very short eruptions, most short periods of repose (< 2 months) followed eruptions lasting < 1 month. Furthermore, Klein (1982) suggested that longer periods of repose tended to follow eruptions with high erupted volumes at Kilauea and concluded that it is unrealistic to expect two voluminous eruptions to occur in close succession. Although this is not directly related to eruption duration, a correlation between eruption duration and erupted volume, whereby larger volume eruptions generally have longer durations has been proposed in the past (Mulargia et al., 1985; Stieltjes and Moutou, 1989). If this relationship is correct it could imply that longer periods of repose could be expected to follow longer duration eruptions.

To assess this relationship Fig. 7.2 plots eruption duration against succeeding repose interval for the volcanic systems studied. Interestingly, despite the claims of Stieltjes and Moutou (1989) and Klein (1982) our data gives only a weak correlation between eruption duration and following repose interval in most instances (Fig. 7.2). For Kilauea there is generally a weak negative correlation, although this weak trend is mainly due to the three very long duration eruptions having been followed by relatively short repose intervals (#27, #31 and #34, Table 3.2). Conversely a relatively strong

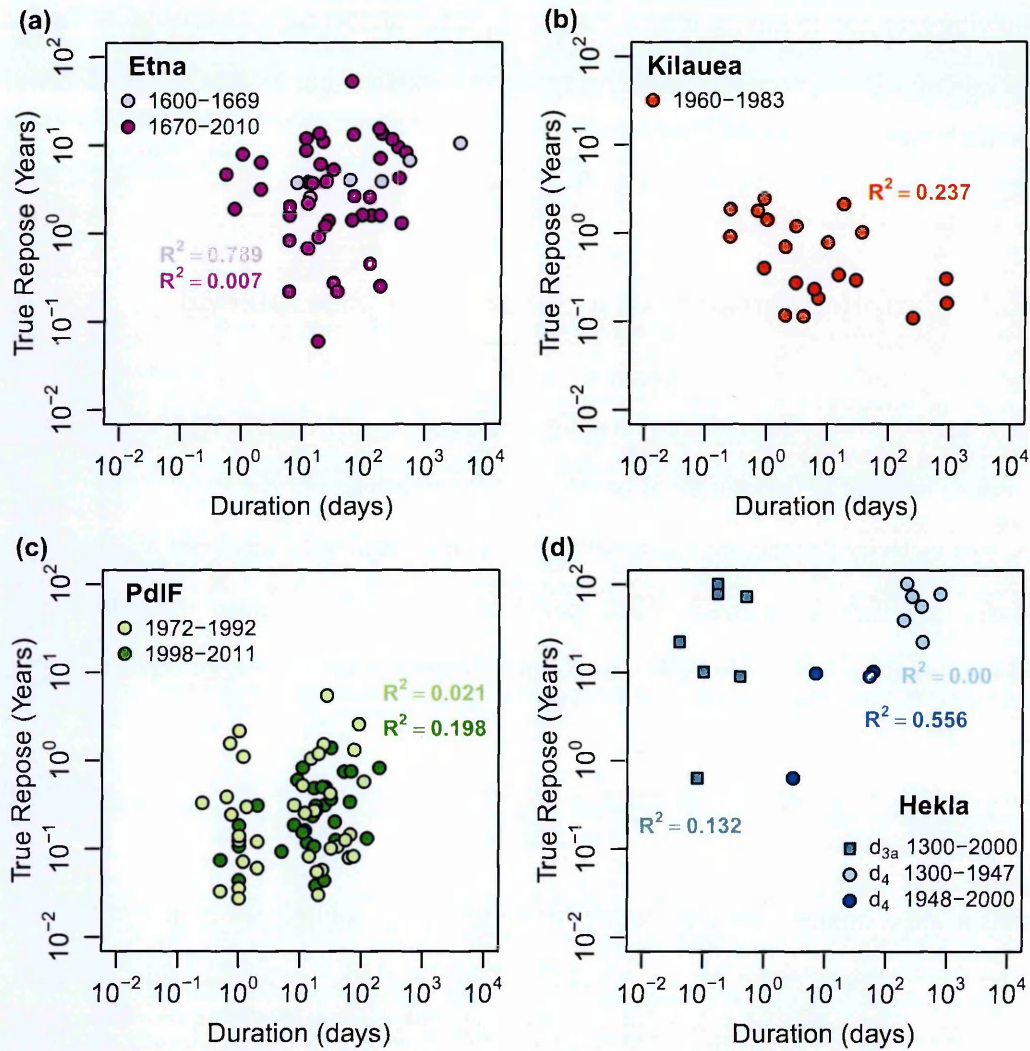


Fig. 7.2 Plots assessing the effect of eruption duration on succeeding repose interval at (a) Mt. Etna (flank eruptions), (b) Kilauea, (c) PdIF and (d) Hekla (mixed eruptions) for the stated time periods. (d) d_{3a} represents the duration on the initial eruptive phase and d_4 the total eruption duration. R^2 values correspond to linear regressions performed on the logs of the data

positive correlation is found for the Mt. Etna subset 1600-1669 and for the d_4 data of Hekla with R^2 values of 0.789 and 0.556 respectively, however, in both cases the sample size is small.

7.3 Eruption duration as a function of erupted volume and average eruption rate

In its simplest form the final duration of an eruption can be considered a function of the volume of material available and the average rate at which it is erupted (Eq.7.1).

$$Duration = \frac{Volume}{Eruption\ Rate} \quad (7.1)$$

The following section considers the role of volume and average eruption rate in controlling the final duration of eruptions at the volcanic systems investigated in this study. Throughout this chapter, the term eruption rate refers to the mean output rate as defined by Harris et al. (2007) i.e. it represents the average eruption rate over the entire eruption duration and is calculated by dividing the total erupted volume by the final eruption duration.

7.3.1 Volume data for Mt. Etna, Kilauea, PdlF and Hekla

Eruptions from Mt Etna (flank), Kilauea and PdlF are generally effusive and are dominated by basaltic lava flows. For the purpose of this investigation tephra production during these eruptions is considered negligible and erupted volume equates to the total volume of lava erupted. For each volcanic system.

Many methods for measuring and calculating lava flow volumes exist within the literature. In many cases these methods use an average thickness for the lava flow, which is then multiplied by the surface area of the flow field, however other methods base they calculations on a series of effusion rate estimations over the duration of the eruption (Murray and Stevens, 2000). It is clear that these methods suffer from huge uncertain-

ties and inaccuracies, especially when eruptions further back in the historical record are concerned. Murray and Stevens (2000) present a new method for calculating lava flow volumes at Mt. Etna. While this method of lava volume calculation results yields very accurate results, it has only been successful on 25 lava flows from Mt. Etna, and has not been applied to the other volcanoes investigated in this study. Furthermore, this study requires detailed information about which eruption each volume relates to, ensuring that the eruption duration and eruption volumes correspond well.

Despite the aforementioned inaccuracies in lava volume calculations, this study uses previously published erupted volumes for the historic eruptions of Mt. Etna, Kilauea and PdlF that are investigated in this study. For this reason the results found here are based on the available data and would benefit from a more thorough assessment of individual erupted volumes before any definitive conclusions are drawn. However, this investigation still provides valuable insight into the importance of volume in controlling eruption durations.

To try and maintain a degree of internal consistency a single source is used to obtain the volume for each volcanic system. The sources themselves are discussed, along with any volcano specific considerations that were made, in the appropriate sections of Chapter 3 and the volume data for Mt. Etna, Kilauea and PdlF are presented in Tables 3.1, 3.2 and 3.3 respectively. It is worth noting that the Hawaii volume data following 1970 has the most consistently accurate flow volume data. Unfortunately the range of historic eruptions with reported volumes depends on the range investigated by the chosen source and for Mt. Etna, Kilauea and PdlF volume data stops with eruptions in 2004, 1979 and 2007 respectively. Average eruption rates are calculated from these volumes and therefore this data also stop with eruptions in these years.

The eruptions from Hekla considered here are typified by an initial explosive phase which transitions into an effusive phase with time. As such, the tephra content of these eruptions is higher than those of Mt. Etna, Kilauea and PdlF and the volume

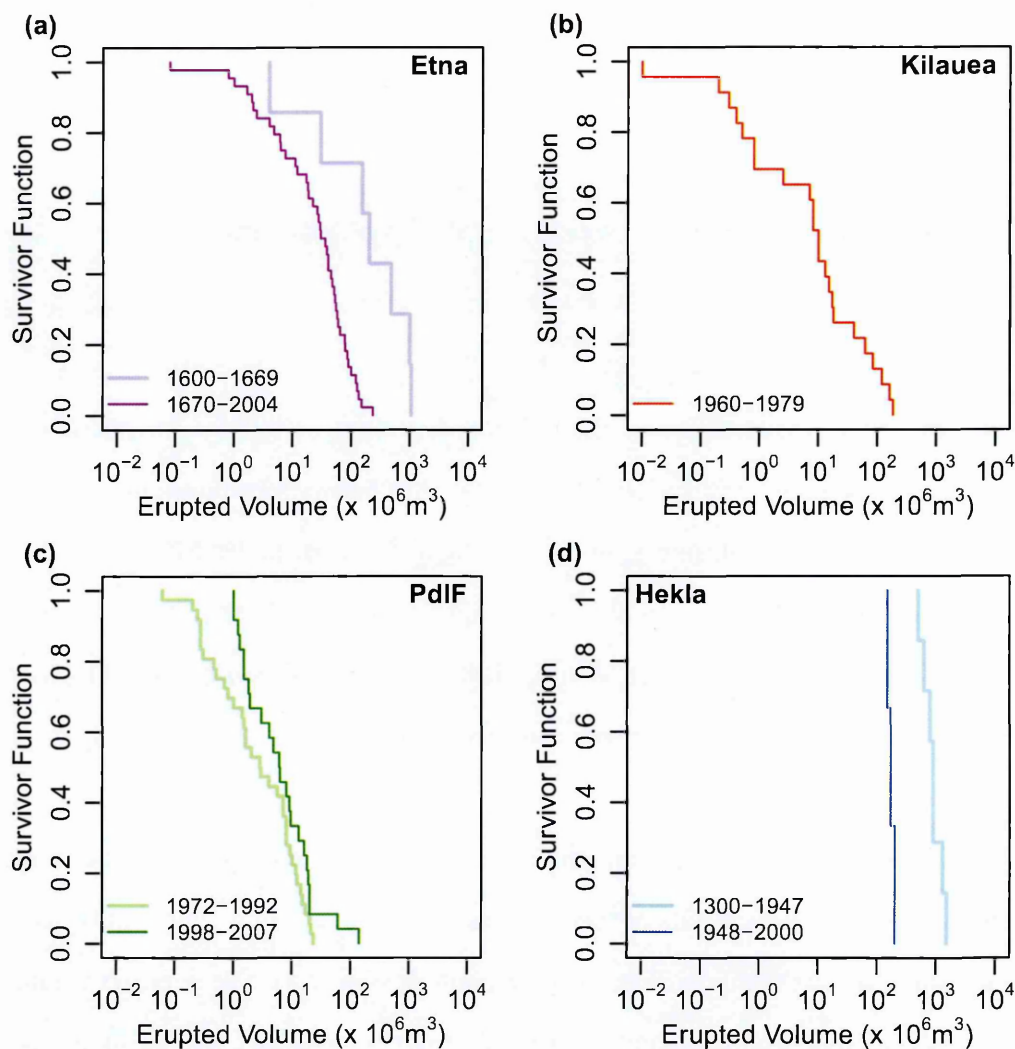


Fig. 7.3 Empirical survivor function plots of erupted volumes at (a) Mt. Etna (flank eruptions), (b) Kilauea, (c) PdIF and (d) Hekla (mixed eruptions, lava volume)

of both the tephra (dense rock equivalent, DRE) and lava are combined to give total erupted volumes for each of these eruptions (sourced from Thordarson and Larsen (2007) and presented in Table 4.2). Due to their eruptive style, the tephra deposits can be considered to have formed mostly during the eruption’s initial Plinian phase (with duration d_{3a}), while the volume of lava largely relates to the following effusive phase (with duration d_{3b}). Average eruption rates are also calculated using this same distinction providing data for both explosive and effusive phases.

Fig. 7.3 plots empirical survivor function curves for the erupted volume data of Mt.

Etna, Kilauea, PdlF and Hekla (lava volume). In each case data is separated into the time periods described by different duration regimes.

7.3.2 The relationship between erupted volume and eruption duration

Despite the likely inaccuracies of the volume data used in this investigation, Fig. 7.4 shows the expected positive correlation (Eq. 7.1) between eruption duration and erupted volume at the volcanic systems investigated (in particular Mt. Etna, PdlF (1972-1992) and Hekla (1300-1947)). Such correlations have been noted in the past (Mulargia et al., 1985; Stieltjes and Moutou, 1989) and Aki and Ferrazzini (2001) tried to simulate this relationship using physical models of the volcano plumbing systems. Wadge (1981) noted that volcanic systems show large variations in their eruption durations, erupted volumes and eruption rates. The broad range of eruption durations and erupted volumes within the data of this study is demonstrated here, with both types of data spanning similar numbers of orders of magnitude (Fig. 7.4). The duration-volume data, however, plots in narrow bands suggesting that a more restricted range of average eruption rates exists at these volcanic systems (Fig. 7.4).

The strength of the correlation is reduced when the d_{3a} (1300-2000) data and d_{3b} (1948-2000) data of Hekla is considered (R^2 values of 0.023 and 0.025 respectively, Fig. 7.4d). While the first reflects the low sample size involved, the latter indicates a poor correlation between the volume of tephra erupted and the duration of the initial explosive phase from which it was produced, implying that average eruption rate may have a more important role in controlling the duration of this phase. Factors controlling average eruption rate and the effect they have on final eruption duration are discussed in subsections 7.3.3 and 7.3.4.

The positive correlation between lava volume and total eruption duration causes the

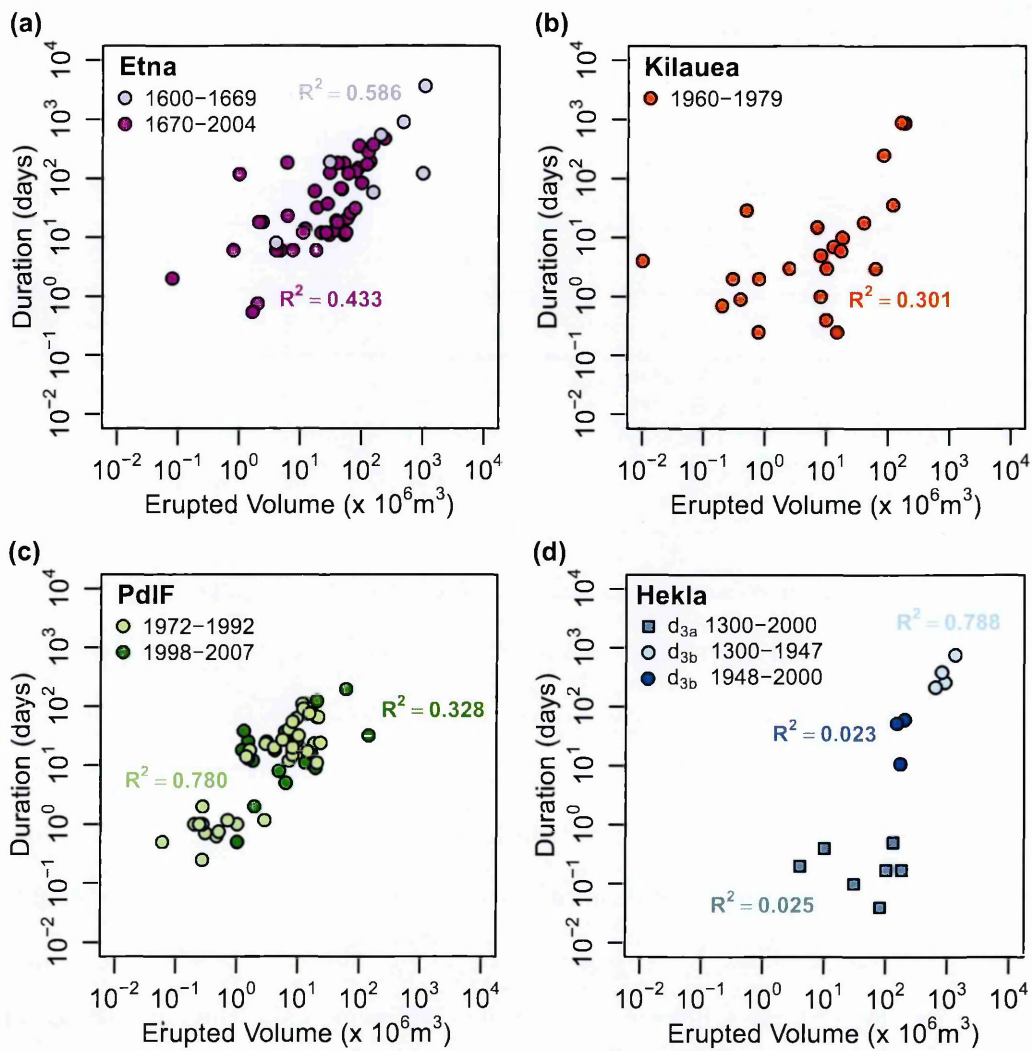


Fig. 7.4 Plots of eruption duration against erupted volume for (a) Mt. Etna (flank eruptions), (b) Kilauea, (c) PdIF and (d) Hekla (mixed eruptions) for the time periods stated. For (d) d_{3a} and d_{3b} duration data are plotted against erupted tephra volume and lava volume respectively. R^2 values are linear regressions performed on the logs of the data

identified time periods defined by different duration regimes to also have different erupted volumes. For example the Mt. Etna data of 1600–1669 is typified by longer duration eruptions than those for the period 1670–2010, and the mean erupted volume is reduced from $418.8 \times 10^6 \text{ m}^3$ to $46.4 \times 10^6 \text{ m}^3$ across this temporal boundary. Similarly the data for d_{3b} durations at Hekla plot in two discrete clusters in Fig. 7.4d, with the 1300–1947 data having higher durations and lava volumes than the 1948–2000 data. These variations are more evident in Figs. 7.3a and d. The volume data of PdIF reflects

Table 7.1: Significance test results comparing the distribution of erupted lava volumes at Mt. Etna (1600-1669, 1670-2004), PdIF (1972-1992 and 1998-2007) and Hekla (1300-1947 and 1948-2000)

Data			Logrank	Mann-Whitney	<i>t</i> -test
Etna	A (<i>n</i> =7)	B (<i>n</i> =44)	<i>p</i> = 0.001 *	<i>p</i> = 0.012 *	<i>p</i> = 0.039 *
PdIF	A (<i>n</i> =36)	B (<i>n</i> =24)	<i>p</i> = 0.090 •	<i>p</i> = 0.072 •	<i>p</i> = 0.022 *
Hekla	A (<i>n</i> =7)	B (<i>n</i> =3)	<i>p</i> = 0.001 *	<i>p</i> = 0.022 *	<i>p</i> = 0.000 *

Etna: A = 1600-1669, B = 1670-2004

PdIF: A = 1972-1992, B = 1998-2007

Hekla: A = 1300-1947, B = 1948-2000

* = significant at a 0.05 level, • = moderate significance (*p*-value = 0.05-0.1).

t-test applied to the logs of the data.

the bimodal nature of its eruption durations, plotting in two distinct clusters in Fig. 7.4c. The two time periods identified here are not described by significantly different duration distributions, but eruption durations from the 1972-1992 period were found to be more bimodal than the 1998-2011 data. The same is true for erupted volumes with a greater proportion of the low volume cluster of Fig. 7.4c comprising of eruptions from the 1972-1992 period, and their empirical survivor function curves diverging at volumes $< 7 \times 10^6 \text{m}^3$ (Fig. 7.3c). Significance tests performed on these volume data indicate that the observed differences are either significant (Mt. Etna and Hekla) or moderately significant (PdIF) at the 0.05 level (Table 7.1).

The results presented here suggest that volume most probably is an important control on eruption duration and that eruptions with higher volumes often have longer durations. This relationship could work both ways, and it is possible that longer duration eruptions have higher erupted volumes if the output rate is similar or less than the supply rate of magma to the volcanic system. It is also worth noting that these conclusions are currently based on volume data that carries large errors and should be revised before the strength of this relationship is investigated further.

7.3.3 The role of eruption rate in controlling eruption duration

Simple models of volcanic conduits consider viscous flow through a circular pipe, where volumetric flow rate, or in this case, eruption rate (Q) can be considered a function of viscosity (μ), conduit radius (R) and the pressure gradient from depth. Eq. 7.2 gives this relationship for the flow of magma through volcanic conduits of nearly circular cross section where ρ_s is the rock density, ρ_l is the magma density and $(\rho_s - \rho_l)g$ the pressure gradient available to drive the magma from depth to the surface (Turcotte and Schubert, 1982).

$$Q = \frac{\pi}{8} \frac{(\rho_s - \rho_l)gR^4}{\mu} \quad (7.2)$$

In reality a volcano's plumbing system is more likely to consist of dykes rather than circular pipes and therefore a model of flow rate through a slot (with width W and along-strike length S) may be more appropriate (Eq. 7.3) (Turcotte and Schubert, 1982; Mouginiis-mark et al., 1982).

$$Q = \frac{(\rho_s - \rho_l)gSW^3}{12\mu} \quad (7.3)$$

Each volcanic system will have a unique range of possible values for each of the parameters in Eq. 7.2 or 7.3. For a single volcanic eruption the configuration of these values will vary, such that often eruption rates will be similar and around an average, however occasional extremely high or low eruption rates could occur. While the potential range of these parameter values may be relatively small at a single volcanic system, they may vary more dramatically between volcanic systems with different plumbing systems, volcanic architecture and style of volcanic activity.

In terms of importance it is difficult to identify the leading control on eruption rate,

however, the relationship expressed in Eq. 7.2 can be used to hypothesise some ranking. For example, both equations show eruption rate to be inversely proportional to magma viscosity. With the exception of mixed eruptions from Hekla, the eruptions considered in this Chapter (Mt. Etna (flank eruptions), Kilauea and PdlF) are all basaltic effusive eruptions. Previous investigations have shown that despite their broadly similar chemistry, erupted lavas from Mt. Etna behave differently to those of Hawaii and PdlF, having a Bingham plastic nature as opposed to a Newtonian fluid nature (Robson, 1967). This, however, is more probably more strongly developed in the degassed lava following eruption, than in the less-degassed magma in the conduit. Considering it is the rheology of the magma in the conduit that will have an effect on eruption rate, the viscosity variation between the lavas of these three volcanic systems is most probably slight. In contrast, R is shown to the power of four in Eq. 7.2 and W to the power of three in Eq. 7.3, indicating that a small change in conduit radius or dyke width could have a large effect on the overall eruption rate of an eruption.

Dyke widths in nature vary considerably, ranging from centimetres to hundreds of meters Krumbholz et al. (2014). Although these measurements are post emplacement and may not equate directly with the dyke widths during emplacement, it is entirely possible that a similarly broad range of dyke widths exist during eruptions. This implies that conduit radius or dyke width has the potential to vary considerably. Furthermore, Krumbholz et al. (2014) demonstrated that Weibull distributions are consistently able to describe dyke width data from individual volcanic systems, although the parameter values of these distributions vary for different volcanic systems. The similarity between the shape of this theoretical distribution and those that were used to model eruption duration data in this study (Chapter 5) suggest that dyke width may be an important control on eruption duration. The following section will consider dyke widths in terms of volcano spreading rate, drawing evidence from variations in the volcanic systems investigated throughout this thesis.

7.3.4 Hypothesised link between volcano spreading rate and eruption duration

It is reasonable to assume that volcanic systems subjected to extensional stresses are likely to have larger dyke widths (or wider volcanic conduits) than systems in a intra-plate setting with minimal extension taking place. Variable volcano spreading rate (either due to gravitational spreading or rift-type extension driven by tectonic forces) could therefore be an important factor controlling conduit width at volcanic systems, and thus an important control on eruption rate and consequently eruption duration for a given erupted volume. Both Kilauea and PdlF represent ocean island volcanism which have been subjected to gravitational mass wasting and have developed rift zones (Walter et al., 2006). Walter et al. (2006) noted how the geometry and expression of these rift zones are very different, with those on Kilauea being narrow and well defined while those on PdlF being broad and more diffuse. Mechanisms for this variation include volcano spreading, which has been described as short and intermittent at PdlF (Le Corvec and Walter, 2009) while maximum spreading rates of 25 cm y^{-1} were recorded for Kilauea for the period 1960-1983 (Delaney et al., 1993).

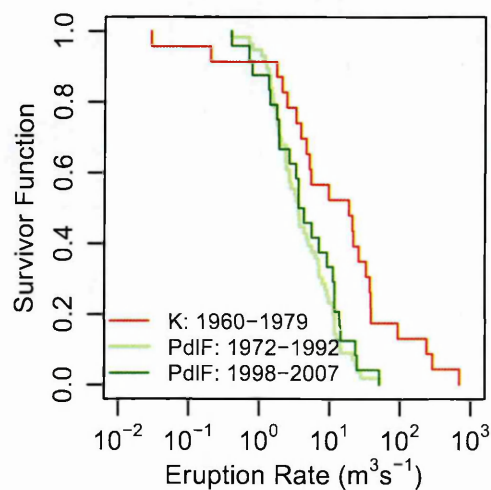


Fig. 7.5 Empirical survivor function plot of average eruption rates from PdlF (1972-1992 and 1998-2007) and Kilauea (1960-1979)

Table 7.2: Significance test results comparing the distribution of average eruption rate from Kilauea (1960-1983) to that of PdIF (1972-1992 and 1998-2007)

Data		Logrank	Mann-Whitney	<i>t</i> -test
K (<i>n</i> =23)	F₁ (<i>n</i> =36)	<i>p</i> = 0.000 *	<i>p</i> = 0.004 *	<i>p</i> = 0.035 *
K (<i>n</i> =23)	F₂ (<i>n</i> =24)	<i>p</i> = 0.001 *	<i>p</i> = 0.041 *	<i>p</i> = 0.093 •

K = Kilauea (1960-1979), **F₁** = PdIF (1972-1992), **F₂** = PdIF (1998-2007)
* = significant at a 0.05 level, • = moderate significance (*p*-value = 0.05-0.1).
t-test applied to the logs of the data.

Mean average eruption rate for Kilauea is $69.01 \text{ m}^3\text{s}^{-1}$ whereas for PdIF it is only $6.93 \text{ m}^3\text{s}^{-1}$. The higher eruption rates of Kilauea are consistent with the theory that higher spreading rates encourage wider conduits and thus higher eruption rates. Fig. 7.5 plots empirical survivor function curves for average eruption rates at PdIF (1972-1992 and 1998-2007) and Kilauea (1960-1983) and Table 7.2 reports significance test results indicating that the distribution of eruption rates at Kilauea is significantly different from that of PdIF at the 0.05 level, regardless of which time period data for PdIF is taken.

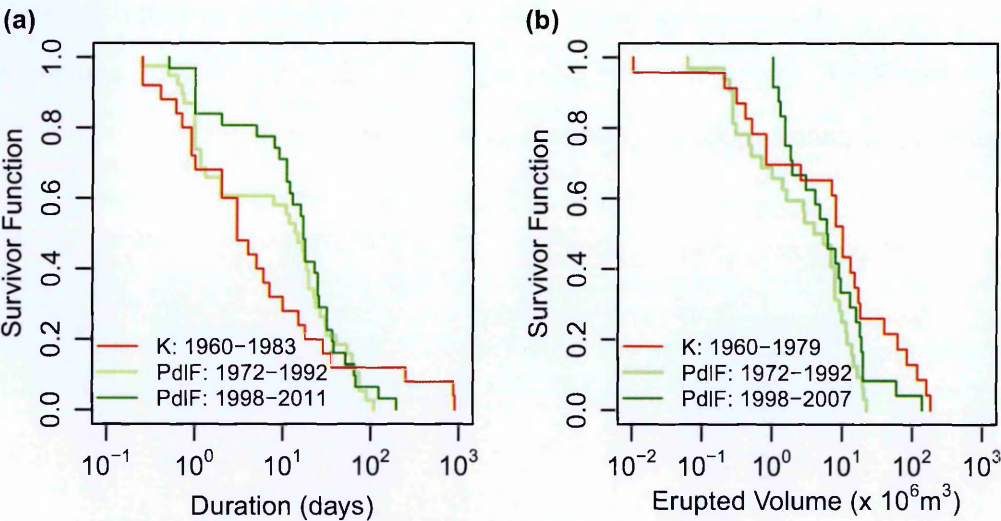


Fig. 7.6 Empirical survivor function curves of (a) eruption durations (previously seen in Figs. 4.11 and 4.13a) and (b) erupted volumes (previously seen in Fig. 7.3b and c) at Kilauea and PdIF for the periods stated. Note that the periods covered by volume data are not the same as the duration data for reasons mentioned in subsection 7.3.1

It is worth noting that despite this result, only eruption durations from the period 1998-2011 at PdIF are found to be significant to moderately significantly different to Kilauea

Table 7.3: Significance test results comparing the distribution of eruption durations and erupted lava volumes at PdIF (1972-1992 and 1998-2011) and Kilauea (1960-1983)

Data			Logrank	Mann-Whitney	t-test
Duration	K (n=25)	F ₁ (n=38)	p = 0.761	p = 0.216	p = 0.485
	K (n=25)	F ₂ (n=31)	p = 0.307	p = 0.016 *	p = 0.083 •
Volume	K (n=23)	F ₁ (n=36)	p = 0.008 •	p = 0.071 •	p = 0.140
	K (n=23)	F ₂ (n=24)	p = 0.284	p = 0.790	p = 0.963

K = Kilauea (1960-1983), F₁ = PdIF (1972-1992), F₂ = PdIF (1998-2007)
* = significant at a 0.05 level, • = moderate significance (p-value = 0.05-0.1).
t-test applied to the logs of the data.

(Fig. 7.6a and Table 7.3). This reflects interplay between volume and eruption rate in controlling eruption duration. According to Eq. 7.1 scenarios described by high volumes and high rates (i.e. Kilauea) could result in similar eruption durations to those described by lower volumes and lower rates (i.e. PdIF). Fig. 7.6b plots empirical survivor function curves for the volumes erupted at PdIF (1972-1992 and 1998-2007) and Kilauea (1960-1979). While the curves are similar it is clear that volumes erupted by Kilauea are generally higher than those erupted at PdIF. Significance tests performed on these data indicate that the distribution of erupted volumes from Kilauea are moderately significantly different from those erupted during the period 1972-1992 (Table 7.3). This corresponds well with the theory outlined above.

Furthermore, eruption duration forecasts presented in Chapter 5 implied that since 1983 eruptive behaviour at Kilauea has changed. This has been noted before with decelerations in ground surface deformation and extension following the onset of the January 1983 Pu’u’Ō’ō - Kūpaianaha eruption (Delaney et al., 1993, 1998). It is possible that this very long duration eruption is a direct result of this reduced spreading rate (from 25 cm yr⁻¹ before 1983 to < 5 cm yr⁻¹ since (Delaney et al., 1998)) restricting conduit width and thus eruption rate.

Finally Chapter 4 found that volcanic systems situated within the active rift zone of Iceland tended to produced shorter basaltic effusive eruptions than volcanic systems

situated outside this zone (Fig. 4.19). The occurrence of periods of intense rifting at inside rift volcanic systems (i.e. Krafla fires) has been used in the past to indicate that axial rift volcanism is controlled by the spreading and subsequent rifting of the crust (Thordarson and Larsen, 2007). This close association between volcanism and spreading may extend further and also control the duration of these eruptions. For example the extensional setting of inside rift volcanic systems (Björnsson, 1985) may promote wider conduits and thus higher eruption rates than the volcanic systems situated outside this rift zone and this relationship may be driving the observed differences in the distribution of eruption durations at these two regional settings. Unfortunately, accurate estimates of the volume of material involved in these eruptions on Iceland are rare and thus it is unclear how much volume variation occurs between the individual volcanic systems themselves or their regional setting.

Wadge and Burt (2011) investigated the relationship between dyke orientation and eruption duration at Nyamuragira, Democratic Republic of Congo and found that eruptions from dykes orientated parallel to the rift are often longer lived than those from dykes in other orientations. This is attributed to the lower magma over pressure that must be sustained for eruptions from these dykes to continue. This is perhaps inconsistent with the theory proposed above, whereby greater extensional stresses (rift parallel dykes) results in wider dykes with shorter duration eruptions. However, the dykes of Wadge and Burt (2011) are all within a rift zone (extensional setting) and it is the spatially variable interplay of the radial and linear stress fields that is important there. The fact that changes in the stress field of eruptive dykes/vents have the potential to alter the dynamics of eruptions on a local scale implies that the larger scale hypothesis outlined here is conceivable.

7.4 Conclusions

The following section outlines the main conclusions of this thesis:

1. Datasets of historic eruption durations have been compiled from the existing literature for Mt. Etna (flank eruptions only), Kilauea, Piton de la Fournaise (PdIF) and Iceland (presented in Chapter 3), using a clearly stated definition of eruption duration and method of qualitative uncertainty assessment (outlined in section 2.1). This thorough approach means that the datasets are both consistent and reliable allowing comparisons to be made both within the datasets of individual volcanic systems and between the different volcanic systems.
2. A broad range of eruption durations exists even when only eruptions of similar type or from the same volcanic system are considered (Chapter 4). Durations are generally uni-modal with heavy long and short duration tails, however, eruption durations from Piton de la Fournaise (PdIF) are bi-modally distributed (section 4.2).
3. Similarities can be drawn between the empirical forecasting model developed in this study and those used on repose interval or recurrence interval data in the past. The model presented here differs from these other model by:
 - (a) Considering the fit of four theoretical distributions: exponential, Weibull, log-logistic and Burr type XII.
 - (b) Estimating the parameter values of theoretical distributions by maximum likelihood. This also allows confidence intervals to be calculated for the forecasting results obtained.
 - (c) Allowing three types of forecast to be made: The probability of a future eruption exceeding a specified duration (survivor function), the minimum

duration associated with a given probability (quantile function) and the probability of an eruption which has been on-going for t days exceeding a specified total duration (residual life function) (section 2.4).

4. A log-logistic model is often found to provide the best fit to the duration and repose data of this study (Chapters 5 and 6).
5. If 66 % and 33 % probabilities are used to represent likely and unlikely events respectively (Table 2.6), quantile function forecasts reveal that:
 - (a) A flank eruption at Mt. Etna is likely to exceed 17 days (± 6 days) but unlikely to exceed 67 days (± 22 days). This is based on historic duration data from the period 1600-2010 and therefore assumes that a return to eruptive activity akin to that of 1600-1669 may occur again in the future.
 - (b) An eruption at Kilauea is likely to exceed 3 days (± 1 days) but unlikely to exceed 15 days (± 7 days) This is based on historic duration data from the period 1912-1983. The current eruption at Kilauea have been on-going for > 30 years and it is suspected that the physical properties of the plumbing system beneath Kilauea changed in 1983, allowing such an unusually long duration eruption to occur.
 - (c) An eruption at PdlF is likely to exceed 16 days (± 2 days) but unlikely to exceed 31 days (± 4 days). Due to the bimodal nature of duration data at PdlF this is based on historic eruptions from the period 1911-2011 with durations > 2 days. These results are therefore only appropriate for eruptions with durations exceeding 2 days. Note that a shorter eruption of only 1 day occurred on 21 June 2014 (following thesis submission).
 - (d) A mixed eruption at Hekla is likely to have an initial explosive phase in excess of 0.12 days (± 0.04 days) but this phase is unlikely to exceed 0.22

days (± 0.08 days). The total duration of a future mixed eruption from Hekla is likely to exceed 9 days (± 7 days) but unlikely to exceed 25 days (± 20 days). The forecast for total duration is based on historic duration data from 1948-2000.

(e) A basaltic eruption from an inside rift volcanic system on Iceland is likely to exceed 9 days (± 3 days) but unlikely to exceed 22 days (± 9 days). This excludes the Krafla volcanic system for which a future basaltic eruption is likely to exceed 1 day (± 1 day) but unlikely to exceed 4 days (± 2 days).

(f) A basaltic eruption from an outside rift volcanic system on Iceland is likely to exceed 29 days (± 21 days) but unlikely to exceed 115 days (± 6 days).

(g) A fire event on Iceland is likely to have a total duration in excess of 2.77 years (± 1.09 years) but is unlikely to exceed 5.18 years (± 1.96 years).

6. When the residual life function of the forecasting model is applied to current repose intervals at Mt. Etna and PdIF results indicate:

(a) A 50 % (± 17 %) probability that the current flank eruption repose at Mt. Etna will continue beyond July 2015.

(b) A 67 % (± 3 %) probability that the current repose between eruptions at PdIF will continue beyond December 2014.

7. Systematic variations in eruption duration and repose interval often occur over the same temporal boundaries, however, the two parameters themselves are not related (i.e. repose interval does not affect the following eruption duration and eruption duration does not affect the following repose interval).

8. Spatial variations in eruption duration at individual volcanic systems are minimal. However, regional variations in eruption durations were found on Iceland,

where the distribution of basaltic eruption durations from inside and outside rift volcanic systems were found to be different.

9. Within the limits of the data available, a strong correlation exists between eruption duration and erupted volume indicating that volume of magma available prior to and during an eruption may be an important control on eruption duration.
10. Small variations in the widths of volcanic conduits or dykes could have a marked effect on average eruption rate. Volcano spreading rate is hypothesised to be an important factor controlling these widths and, considering eruption rate influences eruption duration, volcano spreading rate may be considered a controlling factor on eruption duration.

7.5 Suggestions for further work

The following section outlines potential future work related to eruption durations and the forecasting model developed in this study. The ideas are separated into three subsection, the first and second concentrate on possible refinements that could be made to the empirical probabilistic model itself and potential other applications of the model in the field of volcanic hazards. The third subsection lists further work required to improve current understandings on the factors controlling eruption durations before a more sensitive forecasting model can be developed which incorporates other features of the volcanic systems instead of being based entirely on the historical eruption record.

7.5.1 Possible model refinements

1. In statistics censoring occurs when the value of a measurement or observation is only partially known. For medical applications of survival analyses censored data is used to represent patients for which the event of interest has not been reached or who left the survey for some other reason. Here a minimum survival time is known and right censoring is applied. Sometimes a minimum eruption duration (i.e. the last date the eruption was observed) is reported along with a date sometime after the eruption had ended, but the precise date that the eruption ended is not.

Where these scenarios are encountered within this study a sensible end date and appropriate uncertainty is assigned and, so long as the uncertainty is not considered too high, the eruption is used in the analyses. This is a rare occurrence affecting $< 5\%$ of the data in this study. However, if future analyses were to apply the model to volcanic systems with poorer historical records or without a thorough critical assessment of the data this scenario may become more frequent and the model may benefit from treating this data as a type of interval censoring (Machin et al., 2006).

2. Eruption durations at PdlF were found to have a bi-modal distribution (Chapter 4). For the purpose of this study a refinement to the model was made such that eruptions with durations < 2 days were excluded from the study therefore forcing the data to be uni-modal. Although this was considered acceptable for a bimodal distribution with one mode being of very low duration, if a dataset were to be investigated with two modes, both of longer durations then a model refinement which fitted a theoretical distribution to both parts of the distribution would be beneficial.

7.5.2 Possible other applications for the empirical probabilistic model

1. Forecast the duration of eruptions from other well documented, highly active volcanic systems (e.g. Mauna Loa, Nyamuragira, Kliuchevskoi). This would allow additional comparisons to be made which might highlight correlations between the tectonic setting of the volcanic system and the duration of its eruptions.
2. Similarly the duration of eruptions from a greater variety of eruption styles or magma compositions could be investigated. For example intermediate and felsic magma compositions and Plinian eruptions or a more general VEI based assessment.
3. Forecast the duration of volcanic ash plumes which are considered a flight hazard. This would provide flight companies with information about the likely duration of flight disruption during a volcanic eruption.

7.5.3 Further assessment of the factors controlling eruption duration

1. A more thorough assessment of the physical properties relating to each duration regime identified in this study is required so that in-depth comparisons can be made. This process would highlight which parameters of Eqs. 7.1, 7.2 and 7.3 are the most variable and which variations correlated with the observed duration changes. This would need to include eruption driver variables such as reservoir overpressure, buoyancy, degassing and fracture toughness which define to the $(\rho_s - \rho_l)$ term of equations 7.2 and 7.3. This work would greatly increase current understanding on the factors controlling eruption durations and be a useful step towards developing a more physical probabilistic model.

2. Considering that eruption durations and repose intervals were found to vary across the same temporal boundaries some investigation into the relationship between repose interval and preceding or succeeding erupted volume and average eruption rate might show some interesting results.

References

- Acocella, V. and Neri, M. (2003). What makes flank eruptions? The 2001 Etna eruption and its possible triggering mechanisms. *Bulletin of Volcanology*, 65(7):517–529.
- Aki, K. and Ferrazzini, V. (2001). Comparison of Mount Etna, Kilauea, and Piton de la Fournaise by a quantitative modeling of their eruption histories. *Journal of Geophysical Research*, 106(B3):4091–4102.
- Albarède, F., Luais, B., Fitton, G., Semet, M., Kaminski, E., Upton, B. G. J., Bachélery, P., and Cheminée, J.-L. (1997). The geochemical regimes of Piton de la Fournaise Volcano (Réunion) during the last 530 000 years. *Journal of Petrology*, 38(2):171–201.
- Allard, P., Behncke, B., D’Amico, S., Neri, M., and Gambino, S. (2006). Mount Etna 1993-2005: Anatomy of an evolving eruptive cycle. *Earth-Science Reviews*, 78(1-2):85–114.
- Andronico, D. and Lodato, L. (2005). Effusive activity at Mount Etna volcano (Italy) during the 20th Century: A contribution to volcanic hazard assesment. *Natural Hazards*, 36:407–443.
- Arason, T., Björnsson, H., and Petersen, G. N. (2011). Plume-top altitudes during the Eyjafjallajökull 2010 eruption. In *EGU General Assembly 2011*.
- Armienti, P., Innocenti, F., and Petrini, R. (1989). Petrology and Sr-Nd isotope geochemistry of recent lavas from Mt. Etna: bearing on the volcano feeding system. *Journal of Volcanology and Geothermal Research*, 39(4):315–327.
- Bebbington, M. S. (2007). Identifying volcanic regimes using Hidden Markov Models.

REFERENCES

- Geophysical Journal International*, 171(2):921–942.
- Bebbington, M. S. (2012). Models for temporal volcanic hazard. *Statistics in Volcanology*, 1:1–24.
- Bebbington, M. S. (2013). Assessing probabilistic forecasts of volcanic eruption onsets. *Bulletin of Volcanology*, 75(12):783.
- Bebbington, M. S. and Lai, C. D. (1996). Statistical analysis of New Zealand volcanic occurrence data. *Journal of Volcanology and Geothermal Research*, 74(1-2):101–110.
- Behncke, B., Falsaperla, S., and Pecora, E. (2009). Complex magma dynamics at Mount Etna revealed by seismic, thermal, and volcanological data. *Journal of Geophysical Research*, 114:1–17.
- Behncke, B. and Neri, M. (2003). Cycles and trends in the recent eruptive behaviour of Mount Etna (Italy). *Canadian Journal of Earth Sciences*, 40(10):1405–1411.
- Behncke, B., Neri, M., and Nagay, A. (2005). Lava flow hazard at Mount Etna (Italy): New data from a GIS-based study. In Manga, M. and Ventura, G., editors, *Kinematics and Dynamics of Lava Flows*, pages 189–208. Geological Society of America Special Paper 369, Boulder, Colorado.
- Benoit, J. P. and McNutt, S. R. (1996). Global volcanic earthquake swarm database and preliminary analysis of volcanic earthquake swarm duration. *Annali di Geofisica*, 39:221–229.
- Bisson, M., Behncke, B., Fornaciai, A., and Neri, M. (2009). LiDAR-based digital terrain analysis of an area exposed to the risk of lava flow invasion: the Zafferana Etnea territory, Mt. Etna (Italy). *Natural Hazards*, 50(2):321–334.

- Björnsson, A. (1977). Current rifting episode in north Iceland. *Nature*, 266:318–321.
- Björnsson, A. (1985). Dynamics of crustal rifting in NE Iceland. *Journal of Geophysical Research*, 90(B12):10151–10162.
- Björnsson, A. (2008). Temperature of the Icelandic crust: Inferred from electrical conductivity, temperature surface gradient, and maximum depth of earthquakes. *Tectonophysics*, 447(1-4):136–141.
- Björnsson, A., Johnsen, G. V., Sigurdsson, S., and Thorbergsson, G. (1979). Rifting of the plate boundary in North Iceland 1975-1978. *Journal of Geophysical Research*, 84(B6):3029–3038.
- Boivin, P. and Bachélery, P. (2009). Petrology of 1977 to 1998 eruptions of Piton de la Fournaise, La Réunion Island. *Journal of Volcanology and Geothermal Research*, 184(1-2):109–125.
- Bonaccorso, A., Bonforte, A., Calvari, S., Del Negro, C., Di Grazia, G., Ganci, G., Neri, M., Vicari, A., and Boschi, E. (2011a). The initial phases of the 2008 - 2009 Mount Etna eruption: A multidisciplinary approach for hazard assessment. *Journal of Geophysical Research*, 116:1–19.
- Bonaccorso, A., Cannata, A., Corsaro, R. A., Di Grazia, G., Gambino, S., Greco, F., Miraglia, L., and Pistorio, A. (2011b). Multidisciplinary investigation on a lava fountain preceding a flank eruption: The 10 May 2008 Etna case. *Geochemistry, Geophysics, Geosystems*, 12(7):1–21.
- Bonadonna, C. (2006). Probabilistic modelling of tephra dispersion. In Mader, H. M., Coles, S. G., Connor, C. B., and Connor, L. J., editors, *Statistics in Volcanology*, pages 243–257. Special publications of the geological society.
- Branca, S., Coltelli, M., De Beni, E., and Wijbrans, J. (2008). Geological evolution of

REFERENCES

- Mount Etna volcano (Italy) from earliest products until the first central volcanism (between 500 and 100 ka ago) inferred from geochronological and stratigraphic data. *International Journal of Earth Sciences*, 97(1):135–152.
- Branca, S., Coltelli, M., Groppelli, G., and Lentini, F. (2011). Geological map of Etna volcano, 1 : 50, 000 scale. *Italian Journal of Geoscience*, 130(3):265–291.
- Branca, S. and Del Carlo, P. (2004). Eruptions of Mt. Etna during the past 3200 years: A revised compilation integrating the historical and stratigraphical records. In Bonaccorso, A., Calvari, S., Coltelli, M., Negro, C. D., and Falsaperla, S., editors, *Mt. Etna: Volcano Laboratory*, pages 1–22. American Geophysical Union, Washington, United States.
- Branca, S. and Del Carlo, P. (2005). Types of eruptions of Etna volcano AD 1670-2003: implications for short-term eruptive behaviour. *Bulletin of Volcanology*, 67(8):732–742.
- Brandsdóttir, B. and Einarsson, P. (1979). Seismic activity associated with the September 1977 deflation of the Krafla central volcano in Northeastern Iceland. *Journal of Volcanology and Geothermal Research*, 6(3-4):197–212.
- Budescu, D. V., Broomell, S., and Por, H. H. (2009). Improving communication of uncertainty in the reports of the Intergovernmental Panel on Climate Change. *Psychological Science*, 20(3):299–308.
- Burton, M. R., Neri, M., Andronico, D., Branca, S., Caltabiano, T., Calvari, S., Corsaro, R. A., Del Carlo, P., Lanzafame, G., Lodato, L., Miraglia, L., Salerno, G., and Spampinato, L. (2005). Etna 2004-2005: An archetype for geodynamically-controlled effusive eruptions. *Geophysical Research Letters*, 32(9):1–4.
- Cappello, A., Bilotta, G., Neri, M., and Negro, C. D. (2013). Probabilistic modeling

- of future volcanic eruptions at Mount Etna. *Journal of Geophysical Research: Solid Earth*, 118(5):1925–1935.
- Cappello, A., Neri, M., Acocella, V., Gallo, G., Vicari, A., and Del Negro, C. (2012). Spatial vent opening probability map of Etna volcano (Sicily, Italy). *Bulletin of Volcanology*, 74(9):2083–2094.
- Carey, R., Houghton, B., and Thordarson, T. (2010). Tephra dispersal and eruption dynamics of wet and dry phases of the 1875 eruption of Askja Volcano, Iceland. *Bulletin of Volcanology*, 72(3):259–278.
- Casadevall, T. J. and Hazlett, R. (1983). Thermal areas on Kilauea and Mauna Loa volcanoes, Hawaii. *Journal of Volcanology and Geothermal Research*, 16:173–188.
- Cayol, V., Dieterich, J. H., Okamura, A. T., and Miklius, A. (2000). High magma storage rates before the 1983 Eruption of Kilauea, Hawaii. *Science*, 288(5475):2343–2346.
- Chester, D. K., Duncan, A. M., Dikken, C., Guest, J. E., and Lister, P. H. (1999). Mascali, Mount Etna region Sicily: An example of fascist planning during the 1928 eruption and its continuing legacy. *Natural Hazards*, 19(1):29–46.
- Chester, D. K., Duncan, A. M., Guest, J. E., and Kilburn, C. R. J. (1985). *Mount Etna The anatomy of a volcano*. Chapman and Hall, London.
- Chester, D. K., Duncan, A. M., and Sangster, H. (2012). Human responses to eruptions of Etna (Sicily) during the late-pre-industrial era and their implications for present-day disaster planning. *Journal of Volcanology and Geothermal Research*, 225-226:65–80.
- Coles, S. and Sparks, R. (2006). Extreme value methods for modelling historical series of large volcanic magnitudes. In Mader, H. M., Coles, S., Connor, C. B., and

REFERENCES

- Connor, L., editors, *Statistics in Volcanology*, pages 47–57. Special Publication of the Geological Society, London.
- Coltelli, M., Proietti, C., Branca, S., Marsella, M., Andronico, D., and Lodato, L. (2007). Analysis of the 2001 lava flow eruption of Mt. Etna from three-dimensional mapping. *Journal of Geophysical Research*, 112:1–18.
- Connor, C. B., McBirney, A. R., and Furlan, C. (2006). What is the probability of explosive eruption at a long-dormant volcano. In Mader, H. M., Coles, S. G., Connor, C. B., and Connor, L. J., editors, *Statistics in Volcanology*, volume 1, pages 39–46. Special Publications of the Geological Society, London.
- Connor, C. B., Sparks, R. S. J., Mason, R. M., Bonadonna, C., and Young, S. R. (2003). Exploring links between physical and probabilistic models of volcanic eruptions: The Soufriere Hills Volcano, Montserrat. *Geophysical Research Letters*, 30(13):1–4.
- Coppola, D., Piscopo, D., Staudacher, T., and Cigolini, C. (2009). Lava discharge rate and effusive pattern at Piton de la Fournaise from MODIS data. *Journal of Volcanology and Geothermal Research*, 184(1-2):174–192.
- Corsaro, R. and Miraglia, L. (2009). Dynamics of magma in the plumbing system of Mt. Etna volcano, Sicily, Italy: A contribution from petrologic data of volcanics erupted from 2007 to 2009. In *American Geophysical Union, Fall Meeting, abstract # V51C-1690*.
- Crisci, G. M., Avolio, M. V., Behncke, B., D'Ambrosio, D., Di Gregorio, S., Lupiano, V., Neri, M., Rongo, R., and Spataro, W. (2010). Predicting the impact of lava flows at Mount Etna, Italy. *Journal of Geophysical Research*, 115(B4):B04203.
- De la Cruz-Reyna, S. (1991). Poisson distributed patterns of explosive activity. *Bul-*

- letin of Volcanology*, 54:57–67.
- De la Cruz-Reyna, S. (1993). Random patterns of occurrence of explosive eruptions at Colima Volcano, Mexico. *Journal of Volcanology and Geothermal Research*, 55(1-2):51–68.
- Decker, R. W. (1986). Forecasting volcanic eruptions. *Annual Review Earth and Planetary Science*, 14:267–297.
- Delaney, P. T., Denlinger, R. P., Lisowski, M., Miklius, A., Okubo, P. G., and Okamura, A. T. (1998). Volcanic spreading at Kilauea, 1976-1996. *Journal of Geophysical Research*, 103(B8):18003–18023.
- Delaney, P. T., Miklius, A., Arnadottir, T., and Sako, M. K. (1993). Motion of Kilauea volcano during sustained eruption from the Puu Oo and Kupaianaha vents , 1983-1991. *Journal of Geophysical Research*, 98:17801–17820.
- Donovan, A. R. and Oppenheimer, C. (2011). The 2010 Eyjafjallajökull eruption and the reconstruction of geography. *The Geographical Journal*, 177(1):4–11.
- Druitt, T. H., Young, S. R., Baptie, B., Bonadonna, C., Calder, E. S., Clarke, A. B., Cole, P. D., Harford, C. L., Herd, R. A., Luckett, R., Ryan, G., and Voight, B. (2002). Episodes of cyclic Vulcanian explosive activity with fountain collapse at Soufrière Hills Volcano, Montserrat. In Druitt, T. H. and Kokelaar, B. P., editors, *The eruption of Soufrière Hills Volcano, Montserrat, from 1995 to 1999*, pages 281–306. Geological Society, London, Memoirs No. 21.
- Duffield, W. A., Christiansen, R. L., Koyanagi, R. Y., and Peterson, D. W. (1982). Storage, migration and eruption of magma at Kilauea Volcano, Hawaii, 1971-1872. *Journal of Volcanology and Geothermal Research*, 13.
- Dugmore, A. J., Newton, A. J., Smith, K. T., and Mairs, K.-A. (2013). Tephrochronol-

REFERENCES

- ogy and the late Holocene volcanic and flood history of Eyjafjallajökull, Iceland. *Journal of Quaternary Science*, 28(3):237–247.
- Duncan, A. M., Chester, D. K., and Guest, J. E. (1981). Mount Etna volcano: Environmental impact and problems of volcanic prediction. *The Geographical Journal*, 147(2):164–178.
- Dvorak, J. J. (1990). Geometry of the September 1971 eruptive fissure at Kilauea volcano, Hawaii. *Bulletin of Volcanology*, 52(7):507–514.
- Dzierma, Y. and Wehrmann, H. (2010). Eruption time series statistically examined: Probabilities of future eruptions at Villarrica and Llaima Volcanoes, Southern Volcanic Zone, Chile. *Journal of Volcanology and Geothermal Research*, 193:82–92.
- Dzurisin, D., Anderson, L. A., Eaton, G. P., Koyanagi, R. Y., Lipman, P. W., Lockwood, J. P., Okamura, R. T., Puniwai, G. S., Sako, M. K., and Yamashita, K. M. (1980). Geophysical observations of Kilauea Volcano, Hawaii, 2. Constraints on the magma supply during November 1975– September 1977. *Journal of Volcanology and Geothermal Research*, 7:241–296.
- Dzurisin, D., Koyanagi, R. Y., and English, T. T. (1984). Magma supply and storage at Kilauea volcano, Hawaii, 1956–1983. *Journal of Volcanology and Geothermal Research*, 21:177–206.
- Eaton, J. P. (1962). Crustal structure and volcanism in Hawaii. In *Crust of the Pacific Basin*, pages 13–29. American Geophysical Union.
- Edwards, B., Magnússon, E., Thordarson, T., Gudmundsson, M. T., Höskuldsson, A., Oddsson, B., and Haklar, J. (2012). Interactions between lava and snow/ice during the 2010 Fimmvörðuháls eruption, south-central Iceland. *Journal of Geophysical Research*, 117(B4):B04302.

-
- Einarsson, P. (1991). Umbrotin við Kröflu 1975-1989 (The magmato-tectonic events at Krafla 1975-1989, in Icelandic). In Einarsson, A. and Garðarsson, A., editors, *Náttúra Mývatns*, chapter 97-139. Hið Íslenska Náttúrufræðifélag.
- Einarsson, P. (2008). Plate Boundaries, rifts and transform zones in Iceland. *Jökull*, 58:25–58.
- Einarsson, P. and Boucher, A. (1974). *The Heimaey-eruption in words and pictures*.
- Einarsson, P. and Brandsdóttir, B. (1984). Seismic activity preceding and during the 1983 volcanic eruption in Grímsvötn, Iceland. *Jökull*, 34:13–23.
- Einarsson, P., Brandsdóttir, B., Guðmundsson, G., Björnsson, H., Grönvold, K., and Sigmarsson, F. (1997). Center of the Iceland hotspot experiences volcanic unrest. *EOS, Transactions of the American Geophysical Union*, 78:369–375.
- Einarsson, T. (1949). The rate of production of material during the eruption. In Einarsson, T., Kjartansson, G., and Pórarinnsson, S., editors, *The Eruption of Hekla 1947-1948*, chapter 2, page IV. Societas Scientiarum Islandica, Reykjavík.
- Eliasson, J., Larsen, G., Tumi Gudmundsson, M., and Sigmundsson, F. (2006). Probabilistic model for eruptions and associated flood events in the Katla caldera, Iceland. *Computational Geosciences*, 10(2):179–200.
- Fiske, R. S. and Koyanagi, R. Y. (1968). The December 1965 Eruption of Kilauea Volcano, Hawaii. *U.S. Geological Survey Professional Paper*, 607.
- Fiske, R. S., Simkin, T., and Nielsen, E. A. (1987). *The volcano letter*. Smithsonian Institution Press for the National Museum of Natural History, Washington D.C.
- Frazzetta, G. and Romano, R. (1978). Approccio di studio per la stesura di una carta del rischio vulcanico (Etna-Sicilia). *Memorie della Società Geologica Italiana*, 19:691–
-

REFERENCES

697.

Froger, J. L., Fukushima, Y., Briole, P., Staudacher, T., Souriot, T., and Villeneuve, N. (2004). The deformation field of the August 2003 eruption at Piton de la Fournaise, Reunion Island, mapped by ASAR interferometry. *Geophysical Research Letters*, 31(14):L14601.

Fukushima, Y., Cayol, V., and Durand, P. (2005). Finding realistic dike models from interferometric synthetic aperture radar data: The February 2000 eruption at Piton de la Fournaise. *Journal of Geophysical Research*, 110(B3):B03206.

Fukushima, Y., Cayol, V., Durand, P., and Massonnet, D. (2010). Evolution of magma conduits during the 1998-2000 eruptions of Piton de la Fournaise volcano, Réunion Island. *Journal of Geophysical Research*, 115(B10):B10204.

Furman, T., Frey, F. A., and Park, K. (1991). Chemical constraints on the petrogenesis of mildly alkaline lavas from Vestmannaeyjar, Iceland: the Eldfell (1973) and Surtsey (1963-1967) eruptions. *Contributions to Mineralogy and Petrology*, 109(1):19–37.

Grasso, J. R. and Bachélery, P. (1995). Hierarchical organization as a diagnostic approach to volcano mechanics: Validation on Piton de la Fournaise. *Geophysical Research Letters*, 22(21):2897–2900.

Grímsstaðir, G. (1875). *Norðanfari*, volume 14.

Grönvold, K. (1984). Mývatn fires 1724-1729. Chemical composition of the lava. Technical report, University of Iceland.

Grönvold, K. and Jóhannesson, H. (1984). Eruption in Grímsvötn 1983; course of events and chemical studies of the tephra. *Jökull*, 34:1–11.

-
- Grönvold, K., Larsen, G., Einarsson, P., Thorarinsson, S., and S
aemundsson, K. (1983). The Hekla eruption 1980-1981. *Bulletin of Volcanology*,
46(4):349–363.
- Gudmundsson, A. (1987). Lateral magma flow, caldera collapse, and a mechanism
of large eruptions in Iceland. *Journal of Volcanology and Geothermal Research*,
34(1-2):65–78.
- Gudmundsson, A. (2000). Dynamics of volcanic systems in Iceland: Example of tec-
tonism and volcanism at juxtaposed hot spot and mid-ocean ridge systems. *Annual
Review Earth and Planetary Science*, 28(1):107–140.
- Gudmundsson, A., Oskarsson, N., Grönvold, K., S
aemundsson, K., Sigurdsson, O., Stefansson, R., Gislason, S. R., Einarsson, P.,
Brandsdóttir, B., Larsen, G., Johannesson, H., and Thordarson, T. (1992). The 1991
eruption of Hekla, Iceland. *Bulletin of Volcanology*, 54(3):238–246.
- Gudmundsson, M., Sigmundsson, F., Björnsson, H., and Högnadóttir, T. (2004). The
1996 eruption at Gjálp, Vatnajökull ice cap, Iceland: Efficiency of heat transfer, ice
deformation and subglacial water pressure. *Bulletin of Volcanology*, 66(1):46–65.
- Gudmundsson, M. T. (2005). Subglacial volcanic activity in Iceland. In Caseldine,
C. J., Russell, A., Hardardóttir, J., and Knudsen, O., editors, *Developments in Qua-
ternary Science 5. Iceland: Modern processes, Past Environments*, volume 5, chap-
ter 6, pages 127–151. Elsevier.
- Gudmundsson, M. T., Pedersen, R., Vogfjörð, K., Thorbjarnardóttir, B., Jakobsdóttir,
S., and Roberts, M. J. (2010). Eruptions of Eyjafjallajökull volcano, Iceland. *EOS,
Transactions of the American Geophysical Union*, 91(21).
- Gudmundsson, M. T., Sigmundsson, F., and Björnsson, H. (1997). Ice-volcano in-
-

REFERENCES

- teraction of the 1996 Gjalp subglacial eruption, Vatnajökull, Iceland. *Nature*, 389(6654):954–957.
- Gudmundsson, M. T., Thordarson, T., Höskuldsson, A., Larsen, G., Björnsson, H., Prata, F. J., Oddsson, B., Magnússon, E., Högnadóttir, T., Petersen, G. N., Hayward, C. L., Stevenson, J. A., and Jónsdóttir, I. (2012). Ash generation and distribution from the April-May 2010 eruption of Eyjafjallajökull, Iceland. *Scientific Reports*, 2.
- Guerra, I., Lo Bascio, A., Luongo, G., and Scarpa, R. (1976). Seismic activity accompanying the 1974 eruption of Mt. Etna. *Journal of Volcanology and Geothermal Research*, 1(4):347–362.
- Guest, J. E., Chester, D. K., and Duncan, A. M. (1984). The Valle del Bove Mount Etna: Its origin and relation to the stratigraphy and structure of the volcano. *Journal of Volcanology and Geothermal Research*, 21:1–23.
- Guest, J. E. and Murray, J. B. (1979). An analysis of hazard from Mount Etna volcano. *Journal of the Geological Society, London*, 136:347–354.
- Haraldsson, K., Árnason, S., Larsen, G., and Eiríksson, J. (2002). The Hekla eruption of 2000 - The tephra fall (abstract). In *25th Nordic Geological Winter Meeting*, Reykjavík.
- Haraldsson, K. and Ólafsdóttir, R. (2002). Pyroclastic flows formed in the eruption of Hekla 2000 (abstract). In *25th Nordic Geological Winter Meeting*, Reykjavík.
- Harris, A. J. L., Dehn, J., and Calvari, S. (2007). Lava effusion rate definition and measurement : a review. *Bulletin of Volcanology*, 70:1–22.
- Harris, A. J. L., Favalli, M., Wright, R., and Garbeil, H. (2011). Hazard assessment at Mount Etna using a hybrid lava flow inundation model and satellite-based land classification. *Natural Hazards*, 58(3):1001–1027.

- Harris, A. J. L., Murray, J. B., Aries, S. E., Davies, M. A., Flynn, L. P., Wooster, M. J., Wright, R., and Rothery, D. A. (2000). Effusion rate trends at Etna and Krafla and their implications for eruptive mechanisms. *Journal of Volcanology and Geothermal Research*, 102:237–269.
- Hartley, M. E. and Thordarson, T. (2013). The 1874-1876 volcano-tectonic episode at Askja, North Iceland: Lateral flow revisited. *Geochemistry, Geophysics, Geosystems*, 14(7):2286–2309.
- Heliker, C. and Mattox, T. N. (2003). The first two decades of the Pu'u 'O'o-Kupaianaha eruption: Chronology and selected bibliography. In Heliker, C., Swanson, D. A., and Takahashi, T. J., editors, *The Pu'u 'O'o-Kupaianaha eruption of Kilauea volcano, Hawai'i: The first 20 years*, volume 1676, pages 1–27. U. S. Geological Survey Professional Paper.
- Hill, D. P. and Zucca, J. J. (1987). Geophysical constraints on the structure of Kilauea and Mauna Loa volcanoes and some implications for seismomagmatic processes. In Decker, R. W., Wright, T. L., and Stauffer, P. H., editors, *Volcanism in Hawaii, U.S. Geological Survey Professional Paper 1350*, volume 2. United States Government Printing Office, Washington.
- Holcomb, R. T. (1987). Eruptive history and long-term behaviour of Kilauea Volcano. In Decker, R. W., Wright, T. L., and Stauffer, P. H., editors, *Volcanism in Hawaii, U.S. Geological Survey Professional Paper 1350*, volume 1, chapter 12. United States Government Printing Office, Washington.
- Höskuldsson, A., Óskarsson, N., Pedersen, R., Grönvold, K., Vogfjörð, K., and Ólafsdóttir, R. (2007). The millennium eruption of Hekla in February 2000. *Bulletin of Volcanology*, 70(2):169–182.
- Hughes, J. W., Guest, J. E., and Duncan, A. M. (1990). Changing styles of effusive

REFERENCES

- eruption on Mount Etna since AD 1600. In *Magma Transport and Storage*, pages 385–406. Wiley, New York.
- Imbò (1928). Sistemi eruttivi etnei. *Bulletin Volcanologique*, 5(Series 1):89–119.
- Jackson, D. B., Swanson, D. A., Koyanagi, R. Y., and Wright, T. L. (1975). The August and October 1968 East Rift eruptions of Kilauea Volcano, Hawaii. *U.S. Geological Survey Professional Paper*, 890.
- Jakobsson, S., Leonardsen, E., Balic-Zunic, T., and Jónsson, S. (2008). Encrustations from three recent volcanic eruptions in iceland: the 1963-1967 Surtsey, the 1973 Eldfell and the 1991 Hekla eruptions. Technical report, Fjölrit Náttúrufræðistofnunar.
- Jakobsson, S. P. (1979). *Petrology of recent basalts of Eastern Volcanic Zone, Iceland*, volume 26. Acta Naturalia Islandica.
- Jónsson, S., Einarsson, P., and Sigmundsson, F. (1997). Extension across a divergent plate bounday, the Eastern Volcanic Rift Zone, south Iceland, 1967-1994, observed with GPS and electronic distance measurements. *Journal of Geophysical Research*, 102:11913–11929.
- Jude-Eton, T. C., Thordarson, T., Gudmundsson, M. T., and Oddsson, B. (2012). Dynamics, stratigraphy and proximal dispersal of supraglacial tephra during the ice-confined 2004 eruption at Grímsvötn Volcano, Iceland. *Bulletin of Volcanology*, 74(5):1057–1082.
- Karlsdóttir, S., Gylfason, A., Höskuldsson, A., Brandsdóttir, B., Ilyinskaya, E., Gudmundsson, M., Högnadóttir, T., and Þorkelsson, B. (2012). The 2010 Eyjafjallajökull eruption, Iceland. Technical report.
- Keller, G. V., Jackson, D. B., Rapolla, A., Abbot, S., Andreasen, G., Basalamah, A., Brewer, P., Fournier, R., and Hackett, J. (1972). Magnetic noise preceding the Au-

- gust 1971 summit eruption of Kilauea Volcano. *Science*, 175(4029):1457–1458.
- Kinoshita, W. T., Koyanagi, R. Y., Wright, T. L., and Fiske, R. S. (1969). Kilauea volcano: the 1967-68 summit eruption. *Science*, 166(3904):459–68.
- Klein, F. W. (1982). Patterns of historical eruptions at Hawaiian volcanoes. *Journal of Volcanology and Geothermal Research*, 12:1–35.
- Krumbholz, M., Hieronymus, C. F., Burchardt, S., Troll, V. R., Tanner, D. C., and Friese, N. (2014). Weibull-distributed dyke thickness reflects probabilistic character of host-rock strength. *Nature communications*, 5:1–7.
- Larsen, G. (1999). The eruption of the Eyjafallajökull volcano in 1821-1823 (in Icelandic). Technical Report RH-28-99, Reykjavik: Science Institute, Reykjavík.
- Larsen, G. (2002). A brief overview of eruptions from ice-covered and ice-capped volcanic systems in Iceland during the past 11 centuries: Frequency, periodicity and implications. *Geological Society, London, Special Publications*, 202(1):81–90.
- Larsen, G., Dugmore, A., and Newton, A. (1999). Geochemistry of historical-age silica tephras in Iceland. *Holocene*, 9(4):463–471.
- Larsen, G., Vilmundardóttir, E. G., and Thorkelsson, B. (1992). The Hekla eruption of 1991 - The tephra fall. *Náttúrufræðingurinn*, 61:176.
- Le Corvec, N. and Walter, T. R. (2009). Volcano spreading and fault interaction influenced by rift zone intrusions: Insights from analogue experiments analyzed with digital image correlation technique. *Journal of Volcanology and Geothermal Research*, 183(3-4):170–182.
- Le Guern, F. (1972). Etudes dynamiques sur la phase gazeuse éruptive. Technical report, Commissariat à l’Energie Atomique, France.

REFERENCES

- Lénat, J.-F., Bachèlery, P., and Merle, O. (2012). Anatomy of Piton de la Fournaise volcano (La Réunion, Indian Ocean). *Bulletin of Volcanology*, 74(9):1945–1961.
- Lockwood, J. P., Tilling, R. I., Holcomb, R. T., Klein, F. W., Okamura, A. T., and Peterson, D. W. (1999). Magma migration and resupply during the 1974 summit eruptions of Kilauea Volcano, Hawaii. *U.S. Geological Survey Professional Paper*, 1613:1–47.
- Ludden, J. N. (1977). Eruptive patterns for the volcano piton de la fournaise, Réunion Island. *Journal of Volcanology and Geothermal Research*, 2(4):385–395.
- Lupi, M., Geiger, S., Carey, R. J., Thordarson, T., and Houghton, B. F. (2011). A model for syn-eruptive groundwater flow during the phreatoplinian phase of the 28-29 March 1875 Askja volcano eruption, Iceland. *Journal of Volcanology and Geothermal Research*, 203(3-4):146–157.
- Macdonald, G. A. (1962). The 1959 and 1960 eruptions of Kilauea volcano, Hawaii, and the construction of walls to restrict the spread of lava flows. *Bulletin Volcanologique*, 24(1):249–294.
- Macdonald, G. A. and Eaton, J. P. (1957). Hawaiian Volcanoes During 1954. *U.S. Geological Survey Bulletin*, 1061-B.
- Machin, D., Cheung, Y., and Parmar, M. K. B. (2006). *Survival analysis: A practical approach*. Wiley, second edition.
- Marzocchi, W. and Bebbington, M. (2012). Probabilistic eruption forecasting at short and long time scales. *Bulletin of Volcanology*, 74(8):1777–1805.
- Marzocchi, W. and Zaccarelli, L. (2006). A quantitative model for the time-size distribution of eruptions. *Journal of Geophysical Research*, 111(B4).

- Mastin, L., Guffanti, M., Servranckx, R., Webley, P., Barsotti, S., Dean, K., Durant, A., Ewert, J., Neri, A., Rose, W., Schneider, D., Siebert, L., Stunder, B., Swanson, G., Tupper, A., Volentik, A., and Waythomas, C. (2009). A multidisciplinary effort to assign realistic source parameters to models of volcanic ash-cloud transport and dispersion during eruptions. *Journal of Volcanology and Geothermal Research*, 186(1-2):10–21.
- Mastrandrea, M. D., Field, C. B., Stocker, T. F., Edenhofer, O., Ebi, K., Frame, D., Held, H., Kriegler, E., Mach, K., Matschoss, P., Plattner, G., Yohe, G., and Zwiers, F. (2010). Guidance note for lead authors of the IPCC fifth assessment report on consistent treatment of uncertainties. Technical report, Intergovernmental Panel on Climate Change (IPCC).
- Moore, J. G. and Koyanagi, R. (1969). The October 1963 eruption of Kilauea Volcano Hawaii. *U.S. Geological Survey Professional Paper*, 614 - C.
- Moore, J. G. and Krivoy, H. L. (1964). The 1962 flank eruption of Kilauea Volcano and struction of the East Rift Zone. *Journal of Geophysical Research*, 69(10):2033–2045.
- Moore, R. B., Helz, R. T., Dzurisin, D., Eaton, G. P., Koyanagi, R. Y., Lipman, P. W., Lockwood, J. P., and Puniwai, G. S. (1980). The 1977 eruption of Kilauea volcano, Hawaii. *Journal of Volcanology and Geothermal Research*, 7(3-4):189–210.
- Mouginis-mark, P. J., Wilson, L., and Iii, W. H. (1982). Explosive volcanism on Hecates Tholus, Mars: Investigation of eruption conditions. *Journal of Geophysical Research*, 87(2):9890–9904.
- Mulargia, F., Tinti, S., and Boschi, E. (1985). A statistical analysis of flank eruptions on Etna volcano. *Journal of Volcanology and Geothermal Research*, 23(3-4):263–272.

REFERENCES

- Murray, J. B. and Stevens, N. F. (2000). New formulae for estimating lava flow volumes at Mt. Etna Volcano, Sicily. *Bulletin of Volcanology*, 61(8):515–526.
- Neri, M. and Acocella, V. (2006). The 2004-2005 Etna eruption: Implications for flank deformation and structural behaviour of the volcano. *Journal of Volcanology and Geothermal Research*, 158(1):195–206.
- Neri, M., Acocella, V., Behncke, B., Giammanco, S., Mazzarini, F., and Rust, D. (2011). Structural analysis of the eruptive fissures at Mount Etna (Italy). *Annals of Geophysics*, 65(5):464–479.
- Nicholls, J. and Stout, M. Z. (1988). Picritic Melts in Kilauea - Evidence from the 1967-1968 Halemaumau and Hiiaka Eruptions. *Journal of Petrology*, 29:1031–1057.
- Nordic Volcanological Center (2013). <http://www2.norvol.hi.is/>. Last Accessed: 13-11-2013.
- Ofeigsson, B., Hreinsdottir, S., Sigmundsson, F., Spaans, K., Vogfjord, K., Hooper, A., Sturkell, E., Roberts, M., Gudmundsson, G., Einarsson, P., Arnadottir, T., Jakobsdottir, S., Sigurdsson, G., Gudmundsson, M., Geirsson, H., and Bennett, R. A. (2011). Increased volcanic unrest at Katla volcano, Iceland? In *American Geophysical Union, Fall Meeting, abstract # V53E-2690*.
- Öladóttir, B., Larsen, G., and Sigmarsson, O. (2011). Holocene volcanic activity at Grímsvötn, Bárðarbunga and Kverkfjöll subglacial centres beneath Vatnajökull, Iceland. *Bulletin of Volcanology*, 73(9):1187–1208.
- Óladóttir, B., Sigmarsson, O., Larsen, G., and Thordarson, T. (2008). Katla volcano, Iceland: Magma composition, dynamics and eruption frequency as recorded by Holocene tephra layers. *Bulletin of Volcanology*, 70(4):475–493.

-
- Ólafsdóttir, R., Höskuldsson, A., and Grönvöld, K. (2002). The evolution of the lava flow from Hekla eruption 2000 (abstract).
- Ólafsson, J. (1975). Volcanic influence on seawater at Heimaey. *Nature*, 255:138–141.
- Pagli, C., Sigmundsson, F., Lund, B., Sturkell, E., Geirsson, H., Einarsson, P., Árnadóttir, T., and Hreinsdóttir, S. (2007). Glacio-isostatic deformation around the Vatnajökull ice cap, Iceland, induced by recent climate warming: GPS observations and finite element modelling. *Journal of Geophysical Research*, 112:1–12.
- Passarelli, L., Sansò, B., Sandri, L., and Marzocchi, W. (2010). Testing forecasts of a new Bayesian time-predictable model of eruption occurrence. *Journal of Volcanology and Geothermal Research*, 198(1-2):57–75.
- Patané, D., Gori, P. D., Chiarabba, C., and Bonaccorso, A. (2003). Magma ascent and the pressurization of Mount Etna's volcanic system. *Science*, 299(5615):2061–2063.
- Peck, D. L., Moore, J. G., and Kojima, G. (1964). Temperatures in the crust and melt of Alae Lava Lake, Hawaii, after the August 1963 eruptions of Kilauea Volcano- A preliminary report. *Geological Survey Research*.
- Peltier, A., Bachèlery, P., and Staudacher, T. (2009). Magma transport and storage at Piton de La Fournaise (La Réunion) between 1972 and 2007: A review of geophysical and geochemical data. *Journal of Volcanology and Geothermal Research*, 184(1-2):93–108.
- Peltier, A., Bachèlery, P., and Staudacher, T. (2011). Early detection of large eruptions at Piton de La Fournaise volcano (La Réunion Island): Contribution of a distant tiltmeter station. *Journal of Volcanology and Geothermal Research*, 199(1-2):96–104.
- Peltier, A., Famin, V., Bachèlery, P., Cayol, V., Fukushima, Y., and Staudacher, T.
-

REFERENCES

- (2008). Cyclic magma storages and transfers at Piton de La Fournaise volcano (La Réunion hotspot) inferred from deformation and geochemical data. *Earth and Planetary Science Letters*, 270(3-4):180–188.
- Peterson, D. W. and Moore, R. B. (1987). Geologic history and evolution of geologic concepts, Island of Hawaii. In Decker, R. W., Wright, T. L., and Stauffer, P. H., editors, *Volcanism in Hawaii*, U.S. Geological Survey Professional Paper 1350, volume 1, chapter 7, pages 149–207. United States Government Printing Office, Washington.
- Pinkerton, H. and Sparks, R. S. J. (1976). The 1975 sub-terminal lavas, Mount Etna: a case history of the formation of a compound lava field. *Journal of Volcanology and Geothermal Research*, 1(2):167–182.
- Prestvik, T., Goldberg, S., Karlsson, H., and Gr onvold, K. (2001). Anomalous strontium and lead isotope signatures in the Öræfajökull central volcano in south-east Iceland. Evidence for enriched endmember(s) of the Iceland mantle plume? *Earth and Planetary Science Letters*, 190:211–220.
- Proietti, C., De Beni, E., Coltelli, M., and Branca, S. (2011). The flank eruption history of Etna (1610-2006) as a constraint on lava flow hazard. *Annals of Geophysics*, 54(5):480–490.
- Pyle (1998). Forecasting sizes and repose times of future extreme volcanic events. *Geology*, 26(4):367–370.
- R Development Core Team (2011). R: A language and environment for statistical computing. R Foundation for Statistical Computing. Vienna, Austria.
- Richter, D. H., Ault, W. U., Eaton, J. P., and Moore, J. G. (1964). The 1961 eruption of Kilauea Volcano Hawaii. *U.S. Geological Survey Professional Paper*, 474-D.

-
- Richter, D. H., Eaton, J. P., Murata, K., Ault, W., and Krivoy, H. (1970). *Chronological narrative of the 1959-60 eruption of Kilauea volcano, Hawaii*. U.S. Geological Survey Professional Paper.
- Robson, G. R. (1967). Thickness of Etnean Lavas. *Nature*, 216:251–252.
- Romano, R., Sturiale, C., and Lentini, F. (1979). *Geological Map of Mt. Etna*. CNR, Progetto Finalizzato Geodinamica, Istituto Internazionale di Vulcanologia (Catania). 1:50.000 scale.
- Rossi, M. J. (1997). Morphology of the 1984 open-channel lava flow at Krafla volcano, Northern Iceland. *Geomorphology*, 20(1-2):95–112.
- Salvi, F., Scandone, R., and Palma, C. (2006). Statistical analysis of the historical activity of Mount Etna, aimed at the evaluation of volcanic hazard. *Journal of Volcanology and Geothermal Research*, 154:159–168.
- Sammonds, P., McGuire, B., and Edwards, S. (2010). Volcanic hazard from Iceland: Analysis and implications of the Eyjafjallajökull eruption. Technical report, UCL Institute for Risk and Disaster Reduction.
- Schmid, A., Grasso, J. R., Clarke, D., Ferrazzini, V., Bachèlery, P., and Staudacher, T. (2012). Eruption forerunners from multiparameter monitoring and application for eruptions time predictability (Piton de la Fournaise). *Journal of Geophysical Research: Solid Earth*, 117(B11).
- Selbekk, R. S. and Trønnes, R. G. (2007). The 1362 AD plinian Öräfajökull eruption, Iceland: Petrology and geochemistry of large-volume homogeneous rhyolitic eruption. *Journal of Volcanology and Geothermal Research*, 160:42–58.
- Siebert, L., Simkin, T., and Kimberley, P. (2010). *Volcanoes of the World*. Smithsonian Institution, Washington, D.C., 3rd edition.
-

REFERENCES

- Sigmarsson, O., Hémond, C., Condomines, M., Fourcade, S., and Oskarsson, N. (1991). Origin of Silicic magma in Iceland revealed by Th isotopes. *Geology*, 19:621–624.
- Sigmarsson, O., Karlsson, H. R., and Larsen, G. (2000). The 1996 and 1998 subglacial eruptions beneath the Vatnajökull ice sheet in Iceland: contrasting geochemical and geophysical inferences on magma migration. *Bulletin of Volcanology*, 61(7):468–476.
- Sigmarsson, O., Vlastelic, I., Andreassen, R., Bindeman, I., Devidal, J.-L., Moune, S., Keiding, J. K., Larsen, G., Höskuldsson, A., and Thordarson, T. (2011). Remobilization of silicic intrusion by mafic magmas during the 2010 Eyjafjallajökull eruption. *Solid Earth Discussions*, pages 271–281.
- Sigmundsson, F., Hreinsdottir, S., Hooper, A., Arnadóttir, T., Pedersen, R., Roberts, M. J., Oskarsson, N., Auriac, A., Decriem, J., Einarsson, P., Geirsson, H., Hensch, M., Ofeigsson, B. G., Sturkell, E., Sveinbjörnsson, H., and Feigl, K. L. (2010). Intrusion triggering of the 2010 Eyjafjallajökull explosive eruption. *Nature*, 468(7322):426–430.
- Sigurdsson, H. and Sparks, R. (1978). Rifting episode in North Iceland in 1874–1875 and the eruptions of Askja and Sveinagja. *Bulletin of Volcanology*, 41(3):149–167.
- Sigurdsson, H. and Sparks, R. S. J. (1981). Petrology of rhyolitic and mixed magma ejecta from the 1875 eruption of Askja, Iceland. *Journal of Petrology*, 22(58).
- Simkin, T. (1993). Terrestrial volcanism in space and time. *Earth and Planetary Science Letters*, 21:427–452.
- Smethurst, L., James, M. R., Pinkerton, H., and Tawn, J. A. (2009). A statistical analysis of eruptive activity on Mount Etna, Sicily. *GJI*, 179(1):655–666.

- Soosalu, H., Einarsson, P., and Jakobsdóttir, S. (2003). Volcanic tremor related to the 1991 eruption of the Hekla volcano, Iceland. *Bulletin of Volcanology*, 65(8):562–577.
- Sparks, R. S. J. and Aspinall, W. P. (2004). Volcanic activity : Frontiers and challenges in forecasting, prediction and risk assessment. In Sparks, R. S. J. and Hawkesworth, C. J., editors, *The state of the planet: Frontiers and Challenges in Geophysics*, pages 359–373. IUGG/AGU.
- Sparks, R. S. J., Wilson, L., and Sigurdsson, H. (1981). The pyroclastic deposits of the 1875 eruption of Askja, Iceland. *Philosophical Transactions of the Royal Society of London. Series A, Mathematical and Physical Sciences*, 299(1447):241–273.
- Statistics Iceland (2013). <http://www.statice.is/Statistics/Population>.
- Staudacher, T. (2010). Field observations of the 2008 summit eruption at Piton de la Fournaise (Isle de La Réunion) and implications for the 2007 Dolomieu collapse. *Journal of Volcanology and Geothermal Research*, 191(1-2):60–68.
- Staudacher, T., Ferrazzini, V. A., Peltier, A., Kowalski, P., Boissier, P., Catherine, P., Lauret, F. A., and Massin, F. A. (2009). The April 2007 eruption and the Dolomieu crater collapse, two major events at Piton de la Fournaise (La Réunion Island, Indian Ocean). *Journal of Volcanology and Geothermal Research*, 184:126–137.
- Stein, S. and Geller, R. J. (2012). Communicating uncertainties in natural hazard forecasts. *EOS, Transactions of the American Geophysical Union*, 93(38):361–372.
- Steinthorsson, S., Hardarson, B. S., Ellam, R. M., and Larsen, G. (2000). Petrochemistry of the Gjálp-1996 subglacial eruption, Vatnajökull, SE Iceland. *Journal of Volcanology and Geothermal Research*, 98(1-4):79–90.
- Stevenson, J. A., Loughlin, S., Rae, C., Thordarson, T., Milodowski, A. E., Gilbert,

REFERENCES

- J. S., Harangi, S., Lukács, R., Højgaard, B., Ártíng, U., Pyne-O'Donnell, S., MacLeod, A., Whitney, B., and Cassidy, M. (2012). Distal deposition of tephra from the Eyjafjallajökull 2010 summit eruption. *Journal of Geophysical Research*, 117:B00C10.
- Stieltjes, L. and Moutou, P. (1989). A statistical and probabilistic study of the historic activity of Piton de la Fournaise, Reunion Island, Indian Ocean. *Journal of Volcanology and Geothermal Research*, 36(1-3):67–86.
- Sturkell, E. (2003). Recent unrest and magma movements at Eyjafjallajökull and Katla volcanoes, Iceland. *Journal of Geophysical Research*, 108(B8):2369.
- Sturkell, E., Einarsson, P., Geirsson, H., Tryggvason, E., Moore, J. G., and Ólafsdóttir, K. (2009). Precision levelling and geodetic GPS observations performed on Surtsey between 1967 and 2002. *Surtsey Research*.
- Swanson, D. A., Duffield, W. A., Jackson, D. B., and Peterson, D. W. (1979). Chronological narrative of the 1969-71 Mauna Ulu eruption of Kilauea Volcano , Hawaii. *U.S. Geological Survey Professional Paper*, 1056.
- Swanson, D. A., Jackson, D. B., Koyanagi, R. Y., and Wright, T. L. (1976). The February 1969 East Rift Eruption of Kilauea Volcano, Hawaii. *U.S. Geological Survey Professional Paper*, 891.
- Tanguy, J. (1981). Les éruptions historiques de l'Etna: chronologie et localisation. *Bulletin Volcanologique*, 44(3):585–640.
- Tanguy, J.-C., Condomines, M., Le Goff, M., Chillemi, V., La Delfa, S., and Patanè, G. (2007). Mount Etna eruptions of the last 2,750 years: revised chronology and location through archeomagnetic and ^{226}Ra - ^{230}Th dating. *Bulletin of Volcanology*, 70(1):55–83.

- Tanguy, J. C., Tazieff, H., and Cristofolini, R. (1973). The 1971 Etna Eruption: Petrography of the Lavas. *Philosophical Transactions of the Royal Society of London. Series A, Mathematical and Physical Sciences*, 274(1238):45–53.
- Tesche, M., Glantz, P., Johansson, C., Norman, M., Hiebsch, A., Ansmann, A., Althausen, D., Engelmann, R., and Seifert, P. (2012). Volcanic ash over Scandinavia originating from the Grímsvötn eruptions in May 2011. *Journal of Geophysical Research*, 117(D9):D09201.
- Thelen, W. A., Malone, S. D., and West, M. E. (2010). Repose time and cumulative moment magnitude: A new tool for forecasting eruptions? *Geophysical Research Letters*, 37:1–5.
- Pórarinsson, S. (1950). The approach and beginning of the Hekla eruption eyewitness accounts. In Einarsson, T., Kjartansson, G., and Pórarinsson, S., editors, *The Eruption of Hekla 1947-1948*. Societas Scientiarum Islandica, Reykjavík.
- Pórarinsson, S. (1954). The Tephra-fall from Hekla on March 29th 1947. In Einarsson, T., Kjartansson, G., and Pórarinsson, S., editors, *The Eruption of Hekla 1947-1948*. Societas Scientiarum Islandica, Reykjavík.
- Thorarinsson, S. (1958). The Öräfajökull eruption of 1362. *Acta Naturalia Islandica*, 2(2):1–99.
- Thorarinsson, S. (1965). The Surtsey Eruption: Course of events and the development of the new island. Technical report, Museum of Natural History, Reykjavík, Iceland.
- Thorarinsson, S. (1966). The Surtsey Eruption: Course of events and the development of Surtsey and other new islands. Technical report, Museum of Natural History, Reykjavík, Iceland.
- Thorarinsson, S. (1967a). *The eruptions of Hekla in historical times: A tephrochronology*. Societas Scientiarum Islandica, Reykjavík.

REFERENCES

- logical study*. Societas Scientiarum Islandica, Reykjavík.
- Thorarinsson, S. (1967b). The Surtsey eruption and related scientific work. *Polar record*, 13:571–578.
- Thorarinsson, S. (1967c). The Surtsey eruption: Course of events during the year 1966. Technical report, Museum of Natural History, Reykjavík, Iceland.
- Thorarinsson, S. (1968). The Surtsey Eruption: Course of events during the year 1967. Technical report, Museum of Natural History, Reykjavík, Iceland.
- Pórarinnsson, S. (1974). *The swift flowing waters. The history of Jökulhauks and eruptions of Grímsötn (Vötnin stríð Skeiðarárhlaupa og Grímsvatnagosa, in Icelandic)*. Meiningarsjóður Publishers, Reykjavík.
- Pórarinnsson, S. (1975). Katla and an annal of its eruptions (Katla og annáll Kötlugosa, in Icelandic). In *Icelandic Travel Club Yearbook*, pages 125–149. Heimskringla, Reykjavík.
- Pórarinnsson, S. (1976). Course of events. In *The Eruption of Hekla 1947 to 1948*. Societas Scientiarum Islandica, Reykjavík.
- Thorarinsson, S. (1979). The postglacial history of the Mývatn area. *Oikos*, 32(1/2):17–28.
- Thorarinsson, S., Hannesson, J., and Karlsson, P. (1970). *Hekla: A notorious volcano*. almenna Bókafélagid.
- Thorarinsson, S. and Sigvaldason, G. (1962). The eruption in Askja, 1961: A preliminary report. *American Journal of Science*, 260:641–651.
- Thorarinsson, S., Steinthorsson, S., Einarsson, T. H., Kristmannsdóttir, H., and Os-

- karsson, N. (1973). The eruption on Heimaey, Iceland. *Nature*, 241(5389):372–375.
- Thordarson, T. and Höskuldsson, A. (2008). Postglacial volcanism in Iceland. *Jökull*, 58:197–228.
- Thordarson, T. and Larsen, G. (2007). Volcanism in Iceland in historical time: Volcano types, eruption styles and eruptive history. *Journal of Geodynamics*, 43(1):118–152.
- Thordarson, T., Larsen, G., Steinthorsson, S., and Self, S. (2003). The 1783-1785 A.D. Laki-Grímsvötn eruptions. II. Appraisal based on contemporary accounts. *Jökull*, 53:11–48.
- Thordarson, T., Miller, D. J., Larsen, G., Self, S., and Sigurdsson, H. (2001). New estimates of sulfur degassing and atmospheric mass-loading by the 934 AD Eldgjá eruption, Iceland. *Journal of Volcanology and Geothermal Research*, 108:33–54.
- Thordarson, T. and Self, S. (1993). The Laki (Skaftár Fires) and Grímsvötn eruptions in 1783-1785. *Bulletin of Volcanology*, 55(4):233–263.
- Thordarson, T. and Self, S. (2003). Atmospheric and environmental effects of the 1783-1784 Laki eruption: A review and reassessment. *Journal of Geophysical Research*, 108(D1):4011.
- Thordarson, T. and Sigmarsson, O. (2009). Effusive activity in the 1963-1967 Surtsey eruption, Iceland: Flow emplacement and growth of small lava shields. In Thordarson, T., Self, S., Larsen, G., Rowland, S. K., and Höskuldsson, A., editors, *Studies in Volcanology: The Legacy of George Walker*, pages 53–84. Special publications of IAVCEI, 2. Geological Society, London.
- Thoroddsen, T. (1925). *Die Geschichte der Isländischen Vulkane*. The Royal Danish Society, Copenhagen.

REFERENCES

- Tilling, R. I., Christiansen, R. L., Duffield, W. A., Endo, E. T., Holcomb, R. T., Koyanagi, R. Y., Peterson, D. W., and Unger, J. D. (1987). The 1972-1974 Mauna Ulu eruption, Kilauea Volcano: An example of quasi-steady-state magma transfer. In Decker, R. W., Wright, T. L., and Stauffer, P. H., editors, *Volcanism in Hawaii, U.S. Geological Survey Professional Paper 1350*, volume 1, chapter 16, pages 405–469. United States Government Printing Office, Washington.
- Tilling, R. I. and Dvorak, J. J. (1993). Anatomy of a basaltic volcano. *Nature*, 363(6425):125–133.
- Tryggvason, E. (1980). Observed ground deformation during the Krafla eruption of March 16, 1980. Technical Report NVI Research Report 8005, University of Iceland.
- Tryggvason, E. (1984). Widening of the Krafla fissure swarm during the 1975-1981 volcano-tectonic episode. *Bulletin of Volcanology*, 47(1):47–69.
- Tryggvason, E. (1994). Observed ground deformation at Hekla, Iceland prior to and during the eruptions of 1970, 1980-1981 and 1991. *Journal of Volcanology and Geothermal Research*, 61(3-4):281–291.
- Turcotte, D. and Schubert, G. (1982). *Geodynamics: Applications of continuum physics to geological problems*. Cambridge University Press, second edition.
- Varley, N., Johnson, J., Ruiz, M., Reyes, G., and Martin, K. (2006). Applying statistical analysis to understanding the dynamics of volcanic explosions. In Mader, H. M., Coles, S. G., Connor, C. B., and Connor, L. J., editors, *Statistics in Volcanology*, volume 1, pages 57–76. Special Publication of the Geological Society, London.
- Venzke, E., Wuderman, R. W., McClelland, L., Simkin, T., Luhr, J. F., Siebert, L., Mayberry, G., and Sennert, S. (2013). Global Volcanism Program Digital Infor-

- mation Series. <http://www.volcano.si.edu/reports/>. Last Accessed: 01-05-2014.
- Vogfjörð, K., Jakobsdóttir, S., Gudmundsson, G., Roberts, M., Ágústsson, K., Arason, T., Geirsson, H., Karlsdóttir, S., Hjaltadóttir, B., Skaftadóttir, T., Sturkell, E., Jónasdóttir, E., Hafsteinsson, G., Sveinbjörnsson, H., Stefánsson, R., and Jónsson, T. (2005). Forecasting and monitoring a subglacial eruption in Iceland. *EOS, Transactions of the American Geophysical Union*, 86(26):245–252.
- Wadge, G. (1976). Deformation of Mount Etna, 1971-1974. *Journal of Volcanology and Geothermal Research*, 1(3):237–263.
- Wadge, G. (1981). The variation of magma discharge during basaltic eruptions. *Journal of Volcanology and Geothermal Research*, 11:139–168.
- Wadge, G. and Burt, L. (2011). Stress field control of eruption dynamics at a rift volcano: Nyamuragira, D.R.Congo. *Journal of Volcanology and Geothermal Research*, 207:1–15.
- Wadge, G. and Guest, J. E. (1981). Steady-state magma discharge at Etna 1971-81. *Nature*, 294(5841):548–550.
- Wadge, G., Walker, G. P. L., and Guest, J. E. (1975). The output of the Etna volcano. *Nature*, 255(5507):385–387.
- Walter, T. R., Klugel, A., and Munn, S. (2006). Gravitational spreading and formation of new rift zones on overlapping volcanoes. *Terra Nova*, 18(1):26–33.
- Wang, T. and Bebbington, M. (2013). Robust estimation for the Weibull Process applied to eruption records. *Mathematical Geosciences*, 45(7):851–872.
- Watt, S. F. L., Mather, T. A., and Pyle, D. M. (2007). Vulcanian explosion cycles:

REFERENCES

- Patterns and predictability. *Geology*, 35(9):839–842.
- Wickman, F. E. (1966). Repose-period patterns of volcanoes. *Arkiv for Mineralogi och Geologi*, 4:291–367.
- Witham, C. S., Hort, M. C., Potts, R., Servranckx, R., Husson, P., and Bonnardot, F. (2007). Comparison of VAAC atmospheric dispersion models using the 1 November 2004 Grimsvötn eruption. *Meteorological Applications*, 14(1):27–38.
- Wolfe, C. J., Th. Bjarnason, I., VanDecar, J. C., and Solomon, S. C. (1997). Seismic structure of the Iceland mantle plume. *Nature*, 385(6613):245–247.
- Wolfe, E. W., Garcia, M. O., Jackson, D. B., Koyanagi, R. Y., Neal, C. A., and Okamura, A. T. (1987). The Pu'u'Ō'ō eruption of Kilauea Volcano, episodes 1 - 20, January 3, 1983 to June 8, 1984. In Decker, R. W., Wright, T. L., and Stauffer, P. H., editors, *Volcanism in Hawaii, U.S. Geological Survey Professional Paper 1350*, volume 1, chapter 17, pages 470–508. United States Government Printing Office, Washington.
- Woodhouse, M. J., Hogg, a. J., Phillips, J. C., and Sparks, R. S. J. (2013). Interaction between volcanic plumes and wind during the 2010 Eyjafjallajökull eruption, Iceland. *Journal of Geophysical Research: Solid Earth*, 118(1):92–109.
- Wright, T. L. (2008). Dynamics of magma supply to Kilauea volcano, Hawai'i: integrating seismic, geodetic and eruption data. *Special publication - Geological Society of London*, 304(1):83.
- Wright, T. L., Kinoshita, W. T., and Peck, D. L. (1968). March 1965 eruption of Kilauea Volcano and the formation of Makaopuhi lava lake. *Journal of Geophysical Research*, 73(10):3181–3205.

Appendix A

Additional information regarding the Mt. Etna dataset

The following section contains information about the reported start dates, end dates and durations of historic flank eruptions from Mt. Etna for the period 1300 to 2010. In each case any discrepancies in the reported dates are discussed and the duration uncertainty assigned in this study explained.

Table A.1 summarises the available information for the reported flank eruptions from Mt. Etna. Those with eruption durations that are considered reliable and thus used in this study have numbers in column one which correspond to the eruption numbers of Table 3.1. These numbers are also referred to in the following text. Three eruptions were originally thought to be flank eruptions but are not best described as summit eruptions. These are reported in Table A.2 and in the text below but are not included in any of the analyses of this study.

APPENDIX A. MT. ETNA FLANK ERUPTIONS

Table A.1: Table containing the 76 flank eruptions from Mt. Etna reported for the period 1300-2010

#	Location	Start Year	Preferred Date		Duration	Duration U/C	
			Start	End		+	-
1	VDB	1329	28-06-1329	25-08-1329	58	5.5	5.5
		1333					
		1381	05-08-1381			0.5	1
2	S-Rift	1408	09-11-1408	21-11-1408	12	1	1
		1444					
		1446	25-09-1446			0.5	0.5
3	S-Rift	1536	22-03-1536	05-04-1536	14	5.5	5.5
4	S-Rift	1537	11-05-1537	29-05-1537	18	1.5	1.5
		1566	15-11-1566	15-12-1566	30	30	30
		1579	09-09-1579			0.5	365
		1607	28-06-1607	01-07-1608	369	183	183
5	SW flank	1610	06-02-1610	15-08-1610	190	1	1
6	NE-Rift	1614	01-07-1614	01-07-1624	3653	183	183
7	S-Rift	1634	19-12-1634	15-06-1636	544	16	16
8	NE-Rift	1643	20-02-1643	28-02-1643	8	1	1
9	NE-Rift	1646	20-11-1646	17-01-1647	58	1	1
10	W-Rift	1651	17-01-1651	01-07-1653	896	183.5	212.5
11	S-Rift	1669	11-03-1669	11-07-1669	122	1	1
		1682	15-09-1682	15-10-1682	44	30	30
		1689	14-03-1689				
12	VDB	1702	08-03-1702	08-05-1702	61	1	1
13	VDB	1755	09-03-1755	15-03-1755	6	1.5	1
		1759	01-05-1759	02-08-1759	93	1	1
14	W-Rift	1763	06-02-1763	10-03-1763	32	6	1
15	S-Rift	1763	18-06-1763	10-09-1763	84	1.5	2.5
		1764	01-07-1764	01-07-1765	365	365	365
16	S-Rift	1766	28-04-1766	07-11-1766	193	1.5	1.5
17	S-Rift	1780	18-05-1780	29-05-1780	11	2.5	1.5
18	S-Rift	1792	26-05-1792	15-05-1793	354	18	32
19	VDB	1802	15-11-1802	17-11-1802	2	1.5	1.5

Continued on next page...

APPENDIX A. MT. ETNA FLANK ERUPTIONS

Table A.1 – Continued

#	Location	Start Year	Preferred Date		Duration	Duration U/C	
			Start	End		+	-
20	NE-Rift	1809	27-03-1809	09-04-1809	13	1	1.5
21	VDB	1811	27-10-1811	24-04-1812	180	1	1.5
22	VDB	1819	27-05-1819	01-08-1819	66	5	1
23	W-Rift	1832	01-11-1832	22-11-1832	21	2	1
24	W-Rift	1843	17-11-1843	28-11-1843	11	1	1
25	VDB	1852	20-08-1852	27-05-1853	280	1	1
26	NE flank	1865	30-01-1865	28-06-1865	149	1	1
	NE-Rift	1874	29-08-1874	31-08-1874	2	1	2
27	NE-Rift	1879	26-05-1879	07-06-1879	12	1	1.5
28	S-Rift	1883	22-03-1883	24-03-1883	2	1	1
29	S-Rift	1886	19-05-1886	07-06-1886	19	1	1
30	S-Rift	1892	09-07-1892	29-12-1892	173	20.5	3
31	VDB	1908	29-04-1908	30-04-1908	0.75	0.04	0.04
32	S-Rift	1910	23-03-1910	18-04-1910	26	1	1
33	NE-Rift	1911	10-09-1911	22-09-1911	12	2	1.5
		1918	30-11-1918	01-12-1918	1	1	1.5
34	NE-Rift	1923	17-06-1923	18-07-1923	31	1.5	1
35	NE flank	1928	02-11-1928	20-11-1928	18	1	1.5
36	SW flank	1942	30-06-1942	30-06-1942	0.54	0.04	0.04
37	NE-Rift	1947	24-02-1947	10-03-1947	14	3.5	1
		1949	02-12-1949	05-12-1949	3	1.5	1.5
38	VDB	1950	25-11-1950	02-12-1951	372	1	1.5
39	VDB	1956	01-03-1956	02-03-1956	1	1	1
40	VDB	1964	01-02-1964	25-02-1964	24	5.5	5.5
41	VDB	1968	07-01-1968	04-05-1968	118	1	1
42	VDB	1971	05-04-1971	12-06-1971	68	1	1
43	W-Rift	1974	30-01-1974	17-02-1974	18	1.5	1
44	W-Rift	1974	11-03-1974	29-03-1974	18	1	1
45	NE-Rift	1975	24-02-1975	29-08-1975	186	14.5	1
46	NW flank	1975	29-11-1975	08-01-1977	406	1	1
47	VDB	1978	29-04-1978	05-06-1978	37	1	1

Continued on next page...

APPENDIX A. MT. ETNA FLANK ERUPTIONS

Table A.1 – Continued

#	Location	Start Year	Preferred Date		Duration	Duration U/C	
			Start	End		+	-
48	VDB	1978	24-08-1978	30-08-1978	6	1.5	2
49	VDB	1978	18-11-1978	30-11-1978	12	1	6
50	VDB	1979	03-08-1979	09-08-1979	6	1	1
51	N flank	1981	17-03-1981	23-03-1981	6	1	1.5
52	S-Rift	1983	28-03-1983	06-08-1983	131	1	1
53	S-Rift	1985	10-03-1985	13-07-1985	125	1	2.5
54	VDB	1985	25-12-1985	31-12-1985	6	1	1
55	VDB	1986	30-10-1986	01-03-1987	122	1	4.5
56	VDL	1989	27-09-1989	09-10-1989	12	1	1
57	VDB	1991	14-12-1991	31-03-1993	473	1	1.5
58	S-Rift	2001	17-07-2001	09-08-2001	23	1	1
59	S-Rift	2002	27-10-2002	28-01-2003	93	1.5	1
60	SE flank	2004	07-09-2004	08-03-2005	182	1	1
61	E flank	2006	13-10-2006	15-12-2006	63	1	1
62	E flank	2008	13-05-2008	06-07-2009	419	1	2.5

U/C = uncertainty. Units: durations and duration uncertainties = days.

Table A.2: Potential flank eruptions for the period 1300-2010 which are excluded from the study due to their close association with summit vents

Start Year	Preferred Date		Duration	Duration U/C	
	Start	End		+	-
1759	01-05-1759	02-08-1759	93	1	1
1869	26-09-1869	26-09-1869	0.4	0.04	0.04
1999	04-02-1999	05-11-1999	274	1	1
2006	14-07-2006	24-07-2006	10	1	1

U/C = Uncertainty. Units: durations and duration uncertainties = days.

1. June 1329. For this eruption we use the start date 28 June 1329 reported by Tanguy (1981), Branca and Del Carlo (2004) and Tanguy et al. (2007). The end date of this eruption is reported by Tanguy (1981) and Tanguy et al. (2007) as the end of August 1329 and it is treated according to the ‘late month’ category of Table 2.1.

The principle vent for this eruption was within the Valle del Bove, however, a second vent opened at a lower altitude on the south-east flank later in the eruption (Mt. Rosso near the Fleri village) (Tanguy, 1981; Tanguy et al., 2007). The eruption is attributed to sector B of Fig. 3.1, however, the lava flows from both vents are included in Fig. 3.1.

1333: Excluded. An eruption in the year 1333 is reported by Tanguy (1981) and Tanguy et al. (2007), however, precise start and end dates of this eruption are unknown.

August 1381: Excluded. An eruption starting on either 5 or 6 August is reported by Tanguy (1981), Branca and Del Carlo (2004) and Tanguy et al. (2007), however, the end date of this eruption is unknown.

2. November 1408. For this eruption we use the start date 9 November 1408 reported by Tanguy (1981), Branca and Del Carlo (2004) and Tanguy et al. (2007) and the end date 21 November 1408 as reported by Branca and Del Carlo (2004). Reported end dates later than this can be found in the literature (Tanguy, 1981; Tanguy et al., 2007), however, these dates relate to the end of the summit activity which began on 8 November from the central crater and continued throughout this flank eruption (Tanguy, 1981; Tanguy et al., 2007).

The eruption was from a series of vents in the area of Mt. Albero (South flank) (Tanguy, 1981; Branca and Del Carlo, 2004; Tanguy et al., 2007) and is attributed to sector B of Fig. 3.1.

1444: Excluded. An eruption in the year 1444 is reported by Tanguy et al. (2007),

however, precise start and end dates are unknown. Tanguy et al. (2007) also suggest that the eruptions certainty is questionable.

1446: Excluded. An eruption starting on 25 September is reported by Tanguy (1981), Branca and Del Carlo (2004) and Tanguy et al. (2007), however, the end date of this eruption is unknown.

3. March 1536. For this eruption we use the start date 22 March 1536 reported by Tanguy (1981), Branca and Del Carlo (2004) and Tanguy et al. (2007). Although this eruption was accompanied by summit activity lasting until the end of the year, the flank eruption is reported to end in April 1536 (Branca and Del Carlo, 2004). Tanguy et al. (2007) consider the eruption most likely to have ended on 8 April 1536. To account for the uncertainty in this statement this end date is treated according to the 'early month' category of Table 2.1.

The flank component of this eruption was from a vent located somewhere between Mt. Vetore and Mt. Sona on the South flank of Mt. Etna (Tanguy, 1981; Branca and Del Carlo, 2004; Tanguy et al., 2007). It is worth noting that large lava flows from this year on the North flank are visible on both the 1979 and 2010 geological maps of Mt. Etna (Romano et al., 1979; Branca et al., 2011) and have been attributed to summit overflows so are not included on Fig. 3.1. The eruption is attributed to sector B of Fig. 3.1.

4. May 1537. This eruption is reported as starting between 10 and 12 May 1537 (Tanguy, 1981; Branca and Del Carlo, 2004; Tanguy et al., 2007). Here we use the end date 11 May 1537 and a duration uncertainty of ± 1 day is assigned to account for this literature-derived uncertainty. The end date 29 May 1537 is used here as reported by Branca and Del Carlo (2004), however, some catalogues report this activity as ending in June or July. This later date most probably relates to the end of summit activity which was concurrent with the flank eruption.

Tanguy et al. (2007) describe the vent location of this eruption as being at approximately 1700 m elevation below the Sapienza refuge and therefore it is attributed to sector B of Fig. 3.1.

November 1566: Excluded. An eruption between November and December 1566 is reported for Mt. Etna, however, the precise dates are unknown (Tanguy, 1981; Branca and Del Carlo, 2004; Tanguy et al., 2007). Treating both dates according to the ‘nearest month’ category of Table 2.1 would result in a duration uncertainty of > 50 % and therefore it is excluded from the analyses of this study.

September 1578/79: Excluded. An eruption is reported by Branca and Del Carlo (2004) and Tanguy (1981) as starting on 9 September of either 1578 or 1579. Tanguy et al. (2007) suggest that there may have been one or several eruptions on the flanks of Mt. Etna at this time. Further information is unknown and the eruption is excluded from the analyses of this study.

June 1607: Excluded. An eruption starting on 28 June 1607 and ending the following year has been speculated in the literature (Tanguy, 1981; Branca and Del Carlo, 2004; Behncke et al., 2005; Tanguy et al., 2007). Although treating the end date according to the ‘nearest year’ category of Table 2.1 would result in an acceptable duration uncertainty this eruption has been confused in the past with the 1610 eruption and is therefore excluded from the analyses of this study.

5. February 1610. The catalogues of eruptions within Tanguy et al. (2007) and Behncke et al. (2005) split this eruption into two separate flank eruptions (6 February 1610 to 3 May 1610 and 3 May 1610 to 15 August 1610). The similar location of these eruptions and the < 10 day pause in activity between them results in a single eruption being reported here.

This eruption is attributed to sector B of Fig. 3.1.

6. July 1614. For this eruption we use the start date of 1 July 1614 reported by Tanguy (1981), Branca and Del Carlo (2004), Behncke et al. (2005) and Tanguy et al. 2007. Tanguy (1981), Branca and Del Carlo (2004), Behncke et al. (2005) and Tanguy et al. (2007) report the eruption as ending in the year 1624 and it is treated according to the ‘nearest year’ category of Table 2.1.

The eruption formed the Due Pizzi super hornitos on the volcano’s North flank and it is attributed to sector A of Fig. 3.1.

7. December 1634. For this eruption we use the start date 19 December 1634 reported by Tanguy (1981), Branca and Del Carlo (2004) and Behncke et al. (2005). Mulargia et al. (1985) and Tanguy et al. (2007) report this eruption starting the previous day and a duration uncertainty of + 1 day has been assigned to account for this literature-derived uncertainty. The end date of this eruption is reported as June 1636 by Tanguy (1981), Branca and Del Carlo (2004), Behncke et al. (2005) and Tanguy et al. (2007) and it has been treated according to the ‘nearest month’ category of Table 2.1.

This eruption is attributed to sector B of Fig. 3.1.

8. February 1643. For this eruption we use the start date 20 February 1643 and end date 28 February 1643 reported by Tanguy (1981) and Behncke et al. (2005). Tanguy et al. (2007) exclude this eruption from their catalogue due to some confusion in the literature between its vent location and that of the 1646-7 eruption. Close inspection of the descriptions within Tanguy (1981) suggests that this eruption generated lava flows towards Castiglione di Sicillia and although the precise location of this eruption is uncertain, the position of its erupted material is used here to conclude that it should be attributed to sector A of of Fig. 3.1.

9. November 1646. For this eruption we use the start date 20 November 1646 re-

ported by Tanguy (1981), Mulargia et al. (1985), Branca and Del Carlo (2004), Behncke et al. (2005) and Tanguy et al. (2007) and end date 17 January 1647 reported by Tanguy (1981), Branca and Del Carlo (2004), Behncke et al. (2005) and Tanguy et al. (2007). The duration given by Mulargia et al. (1985) supports this end date.

The source location of this eruption is reported as the Mt. Nero cinder cone (Tanguy, 1981; Branca and Del Carlo, 2004; Tanguy et al., 2007) and it is attributed to sector A of Fig. 3.1.

10. January 1651. For this eruption we use the start date 17 January 1651 reported by Tanguy (1981), Behncke et al. (2005) and Tanguy et al. (2007). Mulargia et al. (1985) report this eruption starting on 16 January 1651 and Branca and Del Carlo (2004) report it starting 17 February 1651. A duration uncertainty of + 1 day and - 30 days is assigned to the start date of this eruption to account for this literature-derived uncertainty. The end date is also uncertain with both Tanguy et al. (2007) and Behncke et al. (2005) reporting a questionable end date of July 1653 while Tanguy (1981) and Branca and Del Carlo (2004) report only the year 1653. Here the end date is treated according to the ‘nearest year’ category of Table 2.1.

Two eruptions are reported for Mt. Etna in 1651, both with the same start date. The dates here reflect the eruption on the West flank and therefore it is attributed to sector C of Fig. 3.1. The other eruption was on the volcano’s East flank, however, little information about this eruption has been found.

11. March 1669. For this eruption we use the start date 11 March 1669 reported by Tanguy (1981), Mulargia et al. (1985), Branca and Del Carlo (2004), Behncke et al. (2005) and Tanguy et al. (2007) and end date 11 July 1669 reported by Tanguy (1981), Branca and Del Carlo (2004), Behncke et al. (2005) and Tanguy et al. (2007). The duration given by Mulargia et al. (1985) supports this end date.

The vent location of this eruption is reported as the Mt. Rossi cinder cone (Tanguy, 1981; Branca and Del Carlo, 2004; Tanguy et al., 2007) and it is attributed to sector B of Fig. 3.1.

September 1682: Excluded. This eruption is reported by Tanguy (1981), Branca and Del Carlo (2004, 2005), Behncke et al. (2005) and Tanguy et al. (2007) starting in September 1682 and The Smithsonian Institution's Global Volcanism program (Siebert et al., 2010; Venzke et al., 2013) reports it ending in October 1682. Both the start and end date of this eruption need to be treated according to the 'nearest month' category of Table 2.1, however, this would result in a duration uncertainty of > 50 % and therefore the eruption is excluded from the analyses of this study.

March 1689: Excluded. This eruption is reported by Tanguy (1981), Mulargia et al. (1985) and Branca and Del Carlo (2004) starting on 14 March 1689, however, the end date of this eruption is unknown.

12. March 1702. For this eruption we use the start date 8 March 1702 reported by Tanguy (1981), Mulargia et al. (1985), Branca and Del Carlo (2004), Behncke et al. (2005) and Tanguy et al. (2007) and the end date 8 May 1702 reported by Tanguy (1981), Branca and Del Carlo (2004), Behncke et al. (2005) and Tanguy et al. (2007). Mulargia et al. (1985) give a 5 day duration for this eruption which is considerably shorter than the 61 days obtained from other sources. Given the limited information included within Mulargia et al. (1985) and the wealth of other sources reporting an end date of 8 May 1702 this short duration is not used in this study.

This eruption is attributed to sector B of Fig. 3.1.

13. March 1755. For this eruption we use the start date 9 March 1755 reported by Tanguy (1981), Mulargia et al. (1985), Branca and Del Carlo (2004, 2005) and Behncke et al. (2005) and end date 15 March 1755 reported by Tanguy (1981), Branca

and Del Carlo (2004, 2005), Behncke et al. (2005) and Tanguy et al. (2007). The duration given by Mulargia et al. (1985) supports this end date. Tanguy et al. (2007) report this eruption as starting one day earlier and a + 1 day duration uncertainty has been assigned to account for this literature-derived uncertainty.

This eruption occurred within the Valle del Bove and has been attributed to sector A of Fig. 3.1.

May 1759: Excluded. A 93 day duration flank eruption starting on 1 May 1759 is reported by Mulargia et al. (1985). Other records of historic eruptions on Mt. Etna recognise summit activity beginning in April 1759 and ending in 1763, however, they do not provide separate dates for the flank component of this activity. This eruption is therefore excluded from this study.

14. February 1763. For this eruption we use the start date 6 February 1763 reported by Tanguy (1981), Branca and Del Carlo (2004, 2005), Behncke et al. (2005) and Tanguy et al. (2007), however, Mulargia et al. (1985) report this eruption starting 1 day earlier and a + 1 day duration uncertainty has been assigned to the eruption start date account for this literature-derived uncertainty. The end date of this eruption is also uncertain. Here we use the end date 10 March 1763 reported by Branca and Del Carlo (2004, 2005) and Behncke et al. (2005), however, Tanguy (1981) and Tanguy et al. (2007) report an end date of 5 days later and a + 5 day duration uncertainty has been assigned to the eruption end date to account for this literature-derived uncertainty.

This eruption occurred from two vents on the West flank of Mt. Etna (Mt. Nuovo and Mt. Mezza Luna) and it is attributed to sector C of Fig. 3.1.

15. June 1763. For this eruption we use the start date 18 June 1763 reported by Branca and Del Carlo (2004, 2005) and Behncke et al. (2005) and the end date 10

September 1763 reported by Tanguy (1981), Branca and Del Carlo (2004, 2005), Behncke et al. (2005) and Tanguy et al. (2007). Tanguy et al. (2007) reports the start date 17 June 1763, Tanguy (1981) reports 19 June 1763 and Mulargia et al. (1985) reports 20 June 1763. A duration uncertainty of +1 day and -2 days is assigned to account for this literature-derived uncertainty.

The La Montagnola scoria cone on the South flank of Mt. Etna was formed by the proximal deposits of this eruption (Tanguy, 1981; Branca and Del Carlo, 2004; Tanguy et al., 2007) and it is attributed to sector B of Fig. 3.1.

1764: Excluded. Branca and Del Carlo (2004, 2005) report an eruption in the year 1764, however, the precise start and end dates of this eruption are unknown.

16. April 1766. For this eruption we use the start date 28 April 1766 and end date 7 November 1766 reported by Tanguy (1981) and Tanguy et al. (2007). Some catalogues report the eruption starting one day earlier (Mulargia et al., 1985; Branca and Del Carlo, 2004, 2005; Behncke et al., 2005) and/or ending one day earlier (Behncke et al., 2005; Branca and Del Carlo, 2004). We have assigned a ± 1 day duration uncertainty to account for this literature derived uncertainty.

The eruption formed the Mt. Calcarazzi cinder cones (Branca and Del Carlo, 2004, 2005; Behncke et al., 2005; Tanguy et al., 2007) and it is attributed to sector B of Fig. 3.1.

17. May 1780. For this eruption we use the start date 18 May 1780 as reported by Tanguy (1981), Mulargia et al. (1985), Branca and Del Carlo (2004), Behncke et al. (2005) and Tanguy et al. (2007) and the end date 29 May 1780 as reported by Branca and Del Carlo (2004). Behncke et al. (2005) reports the end date 28 May 1780, Tanguy et al. (2007) reports 30 May 1780 and the duration given by Mulargia et al. (1985) implies an end date in July. The later of these relates to the end of periodic summit

activity and can therefore be ignored. A duration uncertainty of +2 days and - 1 day is assigned to account for the other literature-derived uncertainty.

This eruption has been attributed to sector B of Fig. 3.1.

18. May 1792. For this eruption we use the start date 26 May 1792 reported by Branca and Del Carlo (2004, 2005) and Behncke et al. (2005). Chester et al. (2012) reports the start date 23 May 1792 and Tanguy (1981) reports the 12 June 1792. A duration uncertainty of + 3 days and - 17 days has been assigned to the start date of this eruption to account for this literature-derived uncertainty. Tanguy (1981), Branca and Del Carlo (2004, 2005), Behncke et al. (2005), and Tanguy et al. (2007) report this eruption ending in May and it is treated according to the ‘nearest month’ category of Table 2.1.

Four vents were responsible for this eruption. The majority of these produced small flows along the South-West wall of the Valle del Bove, however, the main vent was at an altitude of 1900 m and produced the large lava flow which headed towards Zafferana (Tanguy, 1981; Branca and Del Carlo, 2004). This eruption is attributed to sector B of Fig. 3.1.

19. November 1802. For this eruption we use the start date 15 November 1802 reported by Tanguy (1981), Mulargia et al. (1985), Branca and Del Carlo (2004, 2005), Behncke et al. (2005), and Tanguy et al. (2007) and the end date 17 November 1802 reported by Branca and Del Carlo (2004). Tanguy (1981) report the end date 16 November 1802 and Behncke et al. (2005) report 18 November 1802. A duration uncertainty of ± 1 day has been assigned to the eruption end date to account for this literature-derived uncertainty.

This eruption is attributed to sector A of Fig. 3.1.

20. March 1809. For this eruption we use the start date 27 March 1809 and the end

date 9 April 1809 reported by Tanguy (1981), Branca and Del Carlo (2004, 2005), Behncke et al. (2005), Tanguy et al. (2007) and Chester et al. (2012). Mulargia et al. (1985) reports this eruption starting on 28 March 1809 and a duration uncertainty of - 1 day is assigned to account for this literature-derived uncertainty. This eruption was accompanied by an explosion at the central crater (Branca and Del Carlo, 2004; Behncke et al., 2005; Proietti et al., 2011).

The flank eruption formed a chain of craters along the NE rift zone (Branca and Del Carlo, 2004; Tanguy et al., 2007) and it is attributed to sector A of Fig. 3.1.

21. October 1811. For this eruption we use to start date 27 October 1811 and end date 24 April 1812 reported by Tanguy (1981), Branca and Del Carlo (2004, 2005), Behncke et al. (2005) and Tanguy et al. (2007). Mulargia et al. (1985) report this eruption starting on 28 October 1811 and a duration uncertainty of - 1 day is assigned to account for this literature-derived uncertainty. This eruption was accompanied by an explosion at the central crater (Branca and Del Carlo, 2004; Behncke et al., 2005; Proietti et al., 2011).

The eruption produced the Mt. Simone scoria cone within the Valle del Bove (Tanguy, 1981; Branca and Del Carlo, 2004, 2005; Tanguy et al., 2007) and it is attributed to sector A of Fig. 3.1.

22. May 1819. For this eruption we use the start date 27 May 1819 reported by Tanguy (1981), Mulargia et al. (1985), Branca and Del Carlo (2004), Branca and Del Carlo (2005) and Tanguy et al. (2007) and the end date 1 August 1819 reported by Tanguy (1981) and Tanguy et al. (2007). The duration given by Mulargia et al. (1985) supports this end date. However, Behncke et al. (2005) reports the eruption starting on 26 May 1819 and a duration uncertainty of + 1 day is assigned to the eruption start date to account for this literature-derived uncertainty. Branca and Del Carlo (2004, 2005) and Behncke et al. (2005) report the eruption ending on 5 August 1819 and a

duration uncertainty of + 5 days is assigned to the eruption end date to account for this literature-derived uncertainty.

The vent location for this eruption was on the upper wall of the Valle del Bove (Behncke et al., 2005; Tanguy et al., 2007) and it is attributed to sector B of Fig. 3.1.

23. October 1832.

This eruption can be separated into two components. The initial phase reportedly began on either 30 (Chester et al., 2012) or 31 October (Branca and Del Carlo, 2004, 2005; Behncke et al., 2005) from a vent high on the South-South-East flank of the volcano. Following this, the main phase took place from a fissure on the volcano's West flank. This is reported to have started on 1 November 1832 (Tanguy, 1981; Mulargia et al., 1985; Tanguy et al., 2007) and ended on 22 November 1832 (Tanguy, 1981; Branca and Del Carlo, 2004, 2005; Behncke et al., 2005; Tanguy et al., 2007). For this eruption we use the dates associated with the West flank component of the eruption (1 November - 22 November 1832). However, a duration uncertainty of + 2 days has been assigned to account for the earlier initial phase of the eruption.

The main activity from the vent on the W flank formed the Mt. Nunziata scoria cone (Tanguy, 1981; Branca and Del Carlo, 2004; Behncke et al., 2005; Tanguy et al., 2007) and it is attributed to sector C of Fig. 3.1.

24. November 1843. For this eruption we use the start date 17 November 1843 as reported by Tanguy (1981), Mulargia et al. (1985), Branca and Del Carlo (2004, 2005), Behncke et al. (2005), Tanguy et al. (2007) and Chester et al. (2012), and the end date 28 November 1843 as reported by Tanguy (1981), Branca and Del Carlo (2004, 2005), Behncke et al. (2005) and Tanguy et al. (2007). The duration given by Chester et al. (2012) supports this end date. Volcanic activity from summit craters continued at Mt. Etna until December 1843 (Branca and Del Carlo, 2004; Chester et al., 2012).

This eruption formed coalescent scoria cones on the West flank (Branca and Del Carlo, 2004) and it is attributed to sector C of Fig. 3.1.

25. August 1852. For this eruption we use the start date 20 August 1852 reported by Tanguy (1981), Mulargia et al. (1985), Branca and Del Carlo (2004), Behncke et al. (2005), Branca and Del Carlo (2005), Tanguy et al. (2007) and Chester et al. (2012) and the end date 27 May 1853 reported by Tanguy (1981), Branca and Del Carlo (2004), Behncke et al. (2005) Branca and Del Carlo (2005) and Tanguy et al. (2007). The durations given by Mulargia et al. (1985) and Chester et al. (2012) support this end date.

This eruption formed the Mt. Centenari scoria cones (Tanguy, 1981; Branca and Del Carlo, 2004, 2005; Behncke et al., 2005; Tanguy et al., 2007) and it is attributed to sector B of Fig. 3.1.

26. January 1865. For this eruption we use the start date 30 January 1865 reported by Tanguy (1981), Branca and Del Carlo (2004), Branca and Del Carlo (2005), Behncke et al. (2005), Tanguy et al. (2007) and Chester et al. (2012) and the end date 28 June 1865 reported by Tanguy (1981), Branca and Del Carlo (2004), Behncke et al. (2005) Branca and Del Carlo (2005) and Tanguy et al. (2007). In contrast, Mulargia et al. (1985) give the start date 30 May 1865 and the duration 28 days (implying an end date of 28 June 1865). Given the wealth of evidence for a start date of this eruption in January and therefore a far longer duration we have discounted this Mulargia et al. (1985)'s start date for this eruption and do not account for the discrepancy in the uncertainty allocated to this eruption.

This eruption formed the Mt. Satorius scoria cones along the eruptive fissure (Tanguy, 1981; Branca and Del Carlo, 2004, 2005; Behncke et al., 2005; Tanguy et al., 2007) and it is attributed to sector A of Fig. 3.1.

September 1869: Excluded. A 9 hour eruption is reported for 26 November 1869 by Tanguy (1981), Branca and Del Carlo (2004, 2005) and Behncke et al. (2005). The location of this eruption is reported to be on the East flank, close to the base of the central crater (Tanguy, 1981; Branca and Del Carlo, 2004, 2005), however, Behncke et al. (2005) consider this a summit eruption. Given the close association with the summit crater it has been excluded from this study.

August 1874: Excluded An eruption starting on 29 August 1874 is reported by Tanguy (1981), Mulargia et al. (1985), Behncke and Neri (2003); Behncke et al. (2005), Branca and Del Carlo (2004), Branca and Del Carlo (2005) and Tanguy et al. (2007). Behncke and Neri (2003); Behncke et al. (2005) and Branca and Del Carlo (2004, 2005) report it ending on 31 August 1874, however, Tanguy (1981) and Tanguy et al. (2007) report that it lasted only 7 hours. This would result in a duration uncertainty of > 50 % and therefore it is excluded from the analyses of this study.

27. May 1879. The May 1879 eruption can be separated into two components with an eruption on the North flank and an eruption on the South-West flank both beginning on 26 May 1879 (Tanguy, 1981; Branca and Del Carlo, 2004, 2005; Behncke et al., 2005; Tanguy et al., 2007; Chester et al., 2012). The eruption on the South-West flank is reported to have ended on 27 May 1879 (Tanguy, 1981; Tanguy et al., 2007), while that on the North flank is reported to have ended on either 6 (Tanguy, 1981) or 7 June 1879 (Branca and Del Carlo, 2004, 2005; Behncke et al., 2005; Tanguy et al., 2007; Chester et al., 2012). We use the dates of the North flank eruption in this study as it is the principle activity that was ongoing for the entire duration. The end date chosen is 7 June 1879 and a duration uncertainty of - 1 day is assigned to account for the literature-derived uncertainty.

This eruption is attributed to sector A of Fig. 3.1.

28. March 1883. For this eruption we use the start date 22 March 1883 reported by

Tanguy (1981), Mulargia et al. (1985), Branca and Del Carlo (2004, 2005), Behncke et al. (2005), Tanguy et al. (2007) and Chester et al. (2012) and the end date 24 March 1883 reported by Tanguy (1981), Branca and Del Carlo (2004, 2005), Behncke et al. (2005) and Tanguy et al. (2007).

The Mt. Leone scoria cone formed during this eruption (Branca and Del Carlo, 2004, 2005) and it is attributed to sector B of Fig. 3.1.

29. May 1886. For this eruption we use the start date 19 May 1886 reported by Tanguy (1981), Branca and Del Carlo (2004, 2005), Behncke et al. (2005) and Chester et al. (2012) and the end date 7 June 1886 reported by Tanguy (1981), Behncke and Neri (2003); Behncke et al. (2005), Branca and Del Carlo (2004, 2005), Tanguy et al. (2007) and Chester et al. (2012). Mulargia et al. (1985) and Tanguy et al. (2007) report this eruption starting on 18 May 1886, however, Chester et al. (2012) suggest that this marked the start of summit activity which preceded the flank eruption and it therefore does not need to be accounted for in the duration uncertainty.

This eruption formed the Mt. Gemmellaro scoria cone (Branca and Del Carlo, 2004, 2005; Behncke et al., 2005; Tanguy et al., 2007) and it is attributed to sector B of Fig. 3.1.

30. July 1892. For this eruption we use the start date 9 July 1892 reported by Tanguy (1981), Behncke and Neri (2003), Branca and Del Carlo (2004, 2005), Behncke et al. (2005), Tanguy et al. (2007) and Chester et al. (2012) and the end date 29 December 1892 reported by Behncke and Neri (2003), Branca and Del Carlo (2004, 2005), Behncke et al. (2005) and Tanguy et al. (2007). Mulargia et al. (1985) give the start date 11 July 1892 and a duration uncertainty of - 2 days is assigned to the eruption start date to account for this literature-derived uncertainty. Tanguy (1981) report the end date 28 December 1892 and Chester et al. (2012) give a duration of 193 days implying the end date 18 January 1893. A duration uncertainty of -1 and + 20 days has been assigned to

the eruption end date to account for this literature-derived uncertainty.

This eruption formed the Mt. Silvestri scoria cones (Branca and Del Carlo, 2004, 2005; Behncke et al., 2005; Tanguy et al., 2007) and it is attributed to sector B of Fig. 3.1.

31. April 1908. For this eruption we use the start date 29 April 1908 and end date 30 April 1908 reported by Tanguy (1981), Acocella and Neri (2003), Behncke and Neri (2003), Branca and Del Carlo (2004, 2005), Andronico and Lodato (2005), Behncke et al. (2005), Tanguy et al. (2007) and Neri et al. (2011). Whilst normally these dates would give a duration of 1 day, here we use the duration reported in Acocella and Neri (2003), Andronico and Lodato (2005), Behncke et al. (2005) and Neri et al. (2011) of 0.75 days (18 hours).

This eruption is attributed to sector B of Fig. 3.1.

32. March 1910. For this eruption we use the start date 23 March 1910 reported by Tanguy (1981), Mulargia et al. (1985), Acocella and Neri (2003), Behncke and Neri (2003), Branca and Del Carlo (2004, 2005), Andronico and Lodato (2005), Behncke et al. (2005), Tanguy et al. (2007) and Neri et al. (2011) and the end date 18 April 1910 reported by Tanguy (1981), Acocella and Neri (2003), Behncke and Neri (2003), Branca and Del Carlo (2004, 2005), Andronico and Lodato (2005), Behncke et al. (2005), Tanguy et al. (2007) and Neri et al. (2011).

The eruption formed the Ricco scoria cones (Branca and Del Carlo, 2004, 2005; Behncke et al., 2005; Tanguy et al., 2007; Neri et al., 2011) and it is attributed to sector B of Fig. 3.1.

33. September 1911. For this eruption we use the start date 10 September 1911 reported by Tanguy (1981), Acocella and Neri (2003), Behncke and Neri (2003), Branca and Del Carlo (2004, 2005), Andronico and Lodato (2005), Behncke et al. (2005),

Tanguy et al. (2007), Neri et al. (2011) and Chester et al. (2012) and the end date 22 September 1911 reported by Acocella and Neri (2003), Behncke and Neri (2003), Andronico and Lodato (2005), Behncke et al. (2005) and Neri et al. (2011). Mulargia et al. (1985) report the start date 9 September 1911 and a duration uncertainty of + 1 day is assigned to the start date to account for this literature-derived uncertainty. Tanguy (1981) and Tanguy et al. (2007) report the end date 21 September 1911 while Branca and Del Carlo (2004, 2005) report 23 September 1911 and a duration uncertainty of + 1 days and - 1 day is assigned to the eruption end date to account for this literature-derived uncertainty.

The vent location for this eruption is a long fracture system on the NE rift zone (Branca and Del Carlo, 2004, 2005) and it is attributed to sector A of Fig. 3.1.

November 1918: Excluded. An eruption is reported starting on either 29 November 1918 (Tanguy, 1981; Mulargia et al., 1985; Tanguy et al., 2007) or 30 November 1918 (Acocella and Neri, 2003; Behncke and Neri, 2003; Branca and Del Carlo, 2004, 2005; Andronico and Lodato, 2005; Behncke et al., 2005; Neri et al., 2011) and ending on 1 December 1918 (Acocella and Neri, 2003; Branca and Del Carlo, 2004, 2005; Andronico and Lodato, 2005; Behncke et al., 2005; Neri et al., 2011). Tanguy (1981) and Tanguy et al. (2007) state that the eruption occurred during poor weather conditions and that it was not actually observed. Due to these uncertainties the eruption is excluded from the analyses within this study.

34. June 1923. For this eruption we use the start date 17 June 1923 reported by Tanguy (1981), Acocella and Neri (2003), Behncke and Neri (2003), Branca and Del Carlo (2004, 2005), Andronico and Lodato (2005), Behncke et al. (2005), Tanguy et al. (2007) and Neri et al. (2011) and the end date 18 July 1923 reported by Tanguy (1981), Acocella and Neri (2003), Behncke and Neri (2003), Branca and Del Carlo (2004, 2005), Andronico and Lodato (2005), Behncke et al. (2005), Tanguy et al. (2007), Neri et al. (2011) and Chester et al. (2012). Mulargia et al. (1985) report this eruption

starting on 16 June 1923 and Chester et al. (2012) states that "on June 16 the eruption started early on June 17". A duration uncertainty of + 1 day is assigned to account for this confusion and literature-derived uncertainty.

This eruption was from several vents along the NE rift zone (Branca and Del Carlo, 2004) and it is attributed to sector A of Fig. 3.1.

35. November 1928. For this eruption we use the start date of 2 November 1928 and the end date 20 November 1928 reported by Tanguy (1981), Chester et al. (1999), Acocella and Neri (2003), Behncke and Neri (2003), Branca and Del Carlo (2004, 2005), Andronico and Lodato (2005), Behncke et al. (2005), Tanguy et al. (2007) and Neri et al. (2011). Mulargia et al. (1985) report two eruptions at this time, starting on 3 and 4 November 1928. It is probable that this reflects eruptions at different vent sites and are therefore not considered separately here. The earliest start date is one day later than that reported by other sources and therefore a duration uncertainty of - 1 day is assigned to account for this literature-derived uncertainty.

There are three vent locations for this eruption, a small lava flow in the Valle del Leone, followed by two fissures at a higher altitude on the NE flank (Branca and Del Carlo, 2004, 2005) and it is attributed to sector A of Fig. 3.1.

36. June 1942. A short eruption on 30 June 1842 is reported by Tanguy (1981), Acocella and Neri (2003), Behncke and Neri (2003), Branca and Del Carlo (2004, 2005), Andronico and Lodato (2005), Behncke et al. (2005), Tanguy et al. (2007) and Neri et al. (2011). The duration of this eruption is reported by Acocella and Neri (2003), Andronico and Lodato (2005) and Neri et al. (2011) as 0.54 days which is the duration used in this study. Mulargia et al. (1985) report the same start date and a duration of 2 days, however, this could be a calculation issue and it is therefore not accounted for in the assigned uncertainty.

This eruption is attributed to sector B of Fig. 3.1.

37. February 1947. For this eruption we use the start date 24 February 1947 and the end date 10 March 1947 reported by Tanguy (1981), Acocella and Neri (2003), Behncke and Neri (2003), Branca and Del Carlo (2004, 2005), Andronico and Lodato (2005), Behncke et al. (2005), Tanguy et al. (2007) and Neri et al. (2011). Mulargia et al. (1985) report this eruption as starting on 21 February 1947 and a duration uncertainty of + 3 days is assigned to account for this literature derived uncertainty.

This eruption is attributed to sector A of Fig. 3.1.

December 1949: Excluded. An eruption is reported starting on either the 1 (Tanguy et al., 2007) or 2 December 1949 (Tanguy, 1981; Mulargia et al., 1985; Acocella and Neri, 2003; Behncke and Neri, 2003; Branca and Del Carlo, 2004, 2005; Andronico and Lodato, 2005; Behncke et al., 2005; Neri et al., 2011) and ending on either 4 (Tanguy, 1981; Behncke and Neri, 2003; Tanguy et al., 2007) or 5 December 1949 (Acocella and Neri, 2003; Andronico and Lodato, 2005; Behncke et al., 2005; Neri et al., 2011). If the shortest eruption duration is considered (2-4 December 1949) then the duration uncertainty associated with it would be > 50 %. Although it could be argued that using alternative dates results in an acceptable duration uncertainty, the range of possible dates and the short duration of this eruption has led us to exclude it from this analysis.

38. November 1950. For this eruption we use the start date 25 November 1950 reported by Tanguy (1981), Mulargia et al. (1985), Acocella and Neri (2003), Behncke and Neri (2003), Branca and Del Carlo (2004, 2005), Behncke et al. (2005), Andronico and Lodato (2005), Tanguy et al. (2007) and Neri et al. (2011) and the end date 2 December 1951 reported by Tanguy (1981), Behncke and Neri (2003), Branca and Del Carlo (2004, 2005) and Tanguy et al. (2007). The duration given by Mulargia et al. (1985) supports this end date. Acocella and Neri (2003), Andronico and Lodato

(2005), Behncke et al. (2005) and Neri et al. (2011) report the end date 1 December 1951 and a duration uncertainty of - 1 day has been assigned to account for this literature-derived uncertainty.

This eruption is attributed to sector A of Fig. 3.1.

39. March 1956. For this eruption we use the start date 1 March 1956 and end date 2 March 1956 as reported by Tanguy (1981), Branca and Del Carlo (2004, 2005) and Andronico and Lodato (2005). This eruption coincided with a period of summit activity and Acocella and Neri (2003), Behncke and Neri (2003) and Neri et al. (2011) report this eruption with a longer duration due to this addition summit component.

This eruption is attributed to sector A of Fig. 3.1.

40. February 1964. For this eruption we use the start date 1 February 1964 reported by Tanguy (1981), Branca and Del Carlo (2004, 2005). They report the eruption ending at the end of February 1984 and this is treated according to the 'late month' category of Table 2.1. This flank eruption coincided with a period of longer summit activity and the end date reported in Acocella and Neri (2003), Andronico and Lodato (2005), Behncke and Neri (2003) and Neri et al. (2011) include this summit component and the discrepancy is not accounted for in the duration uncertainty allocated here.

This eruption is attributed to sector A of Fig. 3.1.

41. January 1968. For this eruption we use the start date 7 January 1968 reported by Tanguy (1981), Acocella and Neri (2003), Branca and Del Carlo (2004, 2005), Andronico and Lodato (2005), Behncke et al. (2005) and Neri et al. (2011) and the end date 4 May 1968 reported by Tanguy (1981), Branca and Del Carlo (2004, 2005), Andronico and Lodato (2005), Behncke et al. (2005) and Neri et al. (2011). Acocella and Neri (2003) report a longer duration for this eruption, however, they also include summit activity in their entry and it is probably this which continued into June and

a duration uncertainty has not been allocated. It is worth noting that this eruption is missing from the catalogue within Tanguy et al. (2007), however this is possibly an oversight on their part with the eruption being included within the earlier catalogue of Tanguy (1981).

This eruption is attributed to sector B of Fig. 3.1.

June 1968: Excluded. An eruption is reported starting on 9 June 1968 (Tanguy, 1981; Branca and Del Carlo, 2004, 2005) and ending on 15 July 1968 (Branca and Del Carlo, 2004, 2005). This eruption led to the formation of the Bocca Nuova summit crater and is therefore best described as a summit eruption so is excluded from this study.

42. April 1971. For this eruption we use the start date 5 April 1971 and end date 12 June 1971 reported by Le Guern (1972), Tanguy et al. (1973), Wadge (1976), Tanguy (1981), Wadge and Guest (1981), Acocella and Neri (2003), Behncke and Neri (2003) Branca and Del Carlo (2004, 2005), Andronico and Lodato (2005), Behncke et al. (2005), Tanguy et al. (2007) and Neri et al. (2011).

There were several vents active during this eruption many of which were within the Valle del Bove and this eruption is attributed to sector A of Fig. 3.1.

43. January 1974. For this eruption we use the start date 30 January 1974 reported by Guerra et al. (1976), Tanguy (1981), Mulargia et al. (1985), Acocella and Neri (2003), Branca and Del Carlo (2004, 2005), Andronico and Lodato (2005), Behncke et al. (2005), Tanguy et al. (2007) and Neri et al. (2011) and the end date 17 February 1974 reported by Guerra et al. (1976), Tanguy (1981), Acocella and Neri (2003); Andronico and Lodato (2005), Behncke et al. (2005), Tanguy et al. (2007) and Neri et al. (2011). Branca and Del Carlo (2004, 2005) report the eruption ending on 18 February 1974 and a + 1 day duration uncertainty is assigned to account for this literature-derived uncertainty.

The Mt. De Foire I scoria cone formed during this eruption and it is attributed to sector C of Fig. 3.1.

44. March 1974. For this eruption we use the start date 11 March 1974 reported by Guerra et al. (1976), Tanguy (1981), Mulargia et al. (1985), Acocella and Neri (2003), Branca and Del Carlo (2004, 2005), Andronico and Lodato (2005), Behncke et al. (2005), Tanguy et al. (2007) and Neri et al. (2011) and the end date 29 March 1974 reported by Guerra et al. (1976), Tanguy (1981), Acocella and Neri (2003), Branca and Del Carlo (2004, 2005), Andronico and Lodato (2005), Behncke et al. (2005), Tanguy et al. (2007) and Neri et al. (2011). The duration given Mulargia et al. (1985) supports this end date.

The Mt. De Foire II scorio cone formed during this eruption and it is attributed to sector C of Fig. 3.1.

45. February 1975. For this eruption we use the start date 24 February 1975 reported by Pinkerton and Sparks (1976), Tanguy (1981), Acocella and Neri (2003), Branca and Del Carlo (2004, 2005), Andronico and Lodato (2005), Behncke et al. (2005) and Neri et al. (2011) and the end date 29 August 1975 reported by Acocella and Neri (2003), Branca and Del Carlo (2004, 2005), Andronico and Lodato (2005), Behncke et al. (2005), Branca and Del Carlo (2005), Neri et al. (2011). It has been suggested that the eruption ended on 12 September (J. Murray pers.comm.) and a duration uncertainty of + 14 days is assigned to account for this literature-derived uncertainty.

The eruption produced a series of hornitos within the N rift zone (Behncke et al., 2005) and it is attributed to sector A of Fig. 3.1.

46. November 1975. For this eruption we use the start date 29 November 1975 reported by Tanguy (1981), Acocella and Neri (2003), Branca and Del Carlo (2004, 2005), Andronico and Lodato (2005), Behncke et al. (2005) and Neri et al. (2011) and

the end date 8 January 1977 reported by Acocella and Neri (2003), Branca and Del Carlo (2004, 2005), Andronico and Lodato (2005), Behncke et al. (2005) and Neri et al. (2011).

The Mt. Cumin scoria cone was formed during this eruption (Branca and Del Carlo, 2004, 2005) and it is attributed to sector A of Fig. 3.1.

47. April 1978. For this eruption we use the start date 29 April 1978 reported by Tanguy (1981), Mulargia et al. (1985), Acocella and Neri (2003), Behncke and Neri (2003), Branca and Del Carlo (2004, 2005), Andronico and Lodato (2005), Branca and Del Carlo (2005), Tanguy et al. (2007) and Neri et al. (2011) and the end date 5 June 1978 reported by Acocella and Neri (2003), Behncke and Neri (2003), Branca and Del Carlo (2004, 2005), Andronico and Lodato (2005), Behncke et al. (2005), Tanguy et al. (2007) and Neri et al. (2011). The duration given by Mulargia et al. (1985) supports this end date.

This eruption is attributed to sector B of Fig. 3.1.

48. August 1978. For this eruption we use the start date 24 August 1978 reported by Mulargia et al. (1985), Behncke and Neri (2003) and Branca and Del Carlo (2004, 2005) and the end date 30 August 1978 reported by Acocella and Neri (2003), Behncke and Neri (2003), Branca and Del Carlo (2004, 2005), Andronico and Lodato (2005), Behncke et al. (2005) and Neri et al. (2011). Tanguy et al. (2007) and Neri et al. (2011) report the start date 23 August 1978 while Acocella and Neri (2003) and Behncke et al. (2005) report 25 August 1978. A ± 1 day duration uncertainty is assigned to the start date to account for this literature-derived uncertainty. Tanguy et al. (2007) report the end date 29 August and a duration uncertainty of - 1 day is assigned to the end date to account for this literature-derived uncertainty.

This eruption is attributed to sector B of Fig. 3.1.

49. November 1978. For this eruption we use the start date 18 November 1978 reported by Mulargia et al. (1985), Behncke and Neri (2003) and Branca and Del Carlo (2004, 2005) and the end date 30 November 1978 reported by Acocella and Neri (2003), Branca and Del Carlo (2004, 2005), Andronico and Lodato (2005), Behncke et al. (2005) and Neri et al. (2011). Acocella and Neri (2003), Andronico and Lodato (2005), Behncke et al. (2005), Tanguy et al. (2007) and Neri et al. (2011) report the start date 23 November 1978, however, The Smithsonian Institution's monthly report (SEAN 03:11) indicates that this was when the eruption became more pronounced. Despite this a duration uncertainty of - 5 days has been assigned to the start date to account for this literature-derived uncertainty. Behncke et al. (2005) and Tanguy et al. (2007) report the eruption end date 29 November 1978 and a duration uncertainty of - 1 day is assigned to the end date to account for this literature-derived uncertainty.

This eruption is attributed to sector B of Fig. 3.1.

50. August 1979. For this eruption we have used the start 3 August 1979 and end date 9 August 1979 reported by Tanguy (1981), Acocella and Neri (2003), Behncke and Neri (2003), Branca and Del Carlo (2004, 2005), Andronico and Lodato (2005), Behncke et al. (2005) Tanguy et al. (2007) and Neri et al. (2011).

This eruption is attributed to sector A of Fig. 3.1.

51. March 1981. For this eruption we have used the start date 17 March 1981 reported by Acocella and Neri (2003), Behncke and Neri (2003) Branca and Del Carlo (2004, 2005), Andronico and Lodato (2005), Behncke et al. (2005), Tanguy et al. (2007) and Neri et al. (2011) and the end date 23 March 1981 reported by Acocella and Neri (2003), Behncke and Neri (2003), Branca and Del Carlo (2004, 2005), Andronico and Lodato (2005), Behncke et al. (2005) and Neri et al. (2011). Tanguy et al. (2007) report the end date 22 March 1981 and a duration uncertainty of - 1 day is assigned to account for this literature-derived uncertainty.

This eruption was from a long eruptive fissure on the volcano's N flank and it is attributed to sector A of Fig. 3.1.

52. March 1983. For this eruption we have used the start date 28 March 1983 and end date 6 August 1983 reported by Acocella and Neri (2003), Behncke and Neri (2003), Branca and Del Carlo (2004, 2005), Andronico and Lodato (2005), Behncke et al. (2005), Tanguy et al. (2007) and Neri et al. (2011).

Reports indicate that this eruption was on the S-rift zone and it is attributed to sector B of Fig. 3.1.

53. March 1985. For this eruption we use the start date 10 March 1985 reported by Acocella and Neri (2003), Andronico and Lodato (2005), Behncke et al. (2005), Tanguy et al. (2007) and Neri et al. (2011) and the end date 13 July 1985 reported by Acocella and Neri (2003), Branca and Del Carlo (2004, 2005), Andronico and Lodato (2005), Behncke et al. (2005), Tanguy et al. (2007) and Neri et al. (2011). Branca and Del Carlo (2004, 2005) report the start date 12 March 1985 and a duration uncertainty of - 2 days is assigned to account for this literature-derived uncertainty.

This eruption affected the same area as the 1983 eruption (Tanguy et al., 2007) and it is therefore attributed to sector B of Fig. 3.1.

54. December 1985. For this eruption we use the start date 25 December 1985 and end date 31 December 1985 reported by Harris et al. (2000), Acocella and Neri (2003), Andronico and Lodato (2005), Behncke et al. (2005), Branca and Del Carlo (2005), Tanguy et al. (2007) and Neri et al. (2011). Branca and Del Carlo (2004) report this eruption into two phases (25 December 1985 and 28 - 31 December 1985). These are separated by < 10 days and therefore are not treated separately in this study.

This eruption is attributed to sector B of Fig. 3.1.

55. October 1986. For this eruption we use the start date 30 October 1986 reported by Acocella and Neri (2003), Behncke and Neri (2003) Branca and Del Carlo (2004, 2005), Andronico and Lodato (2005), Behncke et al. (2005), Tanguy et al. (2007) and Neri et al. (2011) and the end date 1 March 1987 reported by Acocella and Neri (2003), Branca and Del Carlo (2004, 2005), Andronico and Lodato (2005), Behncke et al. (2005) and Neri et al. (2011). Tanguy et al. (2007) report the end date 25 February 1987 and Behncke and Neri (2003) report 27 February 1987 and a - 4 day duration uncertainty is assigned to account for this literature-derived uncertainty.

This eruption is attributed to sector A of Fig. 3.1.

56. September 1989. For this eruption we use the start date 27 September 1989 reported by Behncke and Neri (2003), Branca and Del Carlo (2004, 2005), Behncke et al. (2005), Tanguy et al. (2007) and Neri et al. (2011) and the end date 9 October 1989 as reported by Acocella and Neri (2003), Behncke and Neri (2003), Branca and Del Carlo (2004, 2005), Andronico and Lodato (2005), Behncke et al. (2005), Tanguy et al. (2007) and Neri et al. (2011). Acocella and Neri (2003) and Andronico and Lodato (2005) report the start date 11 September 1989, however, The Smithsonian Institution's monthly report (SEAN 14:09) indicates that this early activity is most probably related to the summit SE crater and therefore this earlier start date is not accounted for in the duration uncertainty of this eruption.

This eruption is attributed to sector A of Fig. 3.1.

57. December 1991. For this eruption we use the start date 14 December 1991 reported by Acocella and Neri (2003), Behncke and Neri (2003), Branca and Del Carlo (2004, 2005), Andronico and Lodato (2005), Behncke et al. (2005), Tanguy et al. (2007) and Neri et al. (2011) and the end date 31 March 1993 reported by Acocella and Neri (2003), Branca and Del Carlo (2004, 2005), Andronico and Lodato (2005), Behncke et al. (2005), Tanguy et al. (2007) and Neri et al. (2011). Behncke and Neri

(2003) report the end date 30 March 1993 and a duration uncertainty of - 1 day is assigned to account for this literature-derived uncertainty.

This eruption is attributed to sector B of Fig. 3.1.

February 1999: Excluded. Although some flank activity is suggested during the summit eruption of 1999, it is described as being down slope of the central SE crater (Tanguy et al., 2007) and is therefore most probably a summit eruption. For this reason it is excluded from this study.

58. July 2001. For this eruption we use the start date 17 July 2001 and end date 9 August 2001 reported by Harris et al. (2000), Acocella and Neri (2003), Branca and Del Carlo (2004, 2005), Coltelli et al. (2007), Tanguy et al. (2007), Corsaro and Miraglia (2009) and Neri et al. (2011) .

Two eruptions with the same durations occurred at different locations during this eruption (Valle del Leone and South flank) (Behncke et al., 2005). Here we use the S flank eruption for the location due to its larger volume of lava and tephra (Neri et al., 2011) and therefore it is attributed to sector B of Fig. 3.1.

59. October 2002. Previous catalogues report two separate eruptions both starting on 27 October 2002 then ending on 3 November 2002 and 28 January 2003 respectively (Branca and Del Carlo, 2004, 2005; Behncke et al., 2005; Tanguy et al., 2007; Neri et al., 2011). These eruptions overlap and therefore we use the start date 27 October 2002 and end date 28 January 2003. Corsaro and Miraglia (2009) report the first eruptions starting on 26 October 2002 and a duration uncertainty of +1 day is assigned to the eruption start date to account for this literature-derived uncertainty.

The location of these two phases of activity are the North-North-East and South flanks. The South flank activity was on-going throughout the time period used in this study and therefore the eruption is attributed to sector B of Fig. 3.1.

60 September 2004. For this eruption we use the start date 7 September 2004 as reported by Behncke et al. (2005), Burton et al. (2005), Neri and Acocella (2006), Corsaro and Miraglia (2009) and Neri et al. (2011) and the end date 8 March 2005 as reported by Behncke et al. (2005) Neri and Acocella (2006), and Neri et al. (2011).

Based on the information within Corsaro and Miraglia (2009) this eruption is attributed to sector B of Fig. 3.1.

July 2006: Excluded. An eruption between 14 and 24 July 2006 is reported by Neri and Acocella (2006), Behncke et al. (2009) and Neri et al. (2011). Behncke et al. (2009) describe this eruption as summit activity and therefore it is excluded from the analyses of this study.

61. October 2006. For this eruption we use the start date 13 October 2006 and end date 15 December 2006 as reported by Behncke et al. (2009).

The vent location for this eruption is identified based on the descriptions and maps within Behncke et al. (2009) and it is attributed to sector B of Fig. 3.1.

62. May 2008. For this eruption we use the start date 13 May 2008 and end date 6 July 2009 as reported by Branca et al. (2008) and Bonaccorso et al. (2011b,a). The Smithsonian Institution's monthly report (BGVN 36:05) indicate that the end of this eruption may have been 4 July 2009 and a duration uncertainty of - 2 days is assigned to account for this literature-derived uncertainty.

The vent location for this eruption is identified based on the descriptions and maps within Behncke et al. (2009) and it is attributed to sector B of Fig. 3.1.

Appendix B

Additional information regarding the Kilauea dataset

The following section contains information about the reported start dates, end dates and eruption durations of historical eruptions from Kilauea, Hawaii. The Smithsonian Institution's Global Volcanism Program first reports historical records of volcanic activity in 1750 (Siebert et al., 2010; Venzke et al., 2013), and this is used as the starting point for the Kilauea dataset compiled for this study. The dataset ends with the onset of the Pu'u'Ō'ō - Kūpaianaha eruption in January 1983 (Heliker and Mattox, 2003), which was still continuing on 19 July 2013 (Venzke et al., 2013).

For each eruption, any discrepancies in the reported dates are discussed and the duration uncertainty assigned in this study explained. Each section is prefixed by its start date and source location where S = summit (Kilauea caldera or Halemaumau crater), ERZ = east rift zone and SWRZ = south west rift zone. A summary of this information is included within Table B.1. Eruptions with numbers in the first column are those with reliable eruption durations and correspond with the eruption numbers reported in Table 3.2.

APPENDIX B. KILAUEA ERUPTIONS

Table B.1: Table containing the 53 historic eruptions reported for Kilauea in the period 1750-1983

#	Location	Start Year	Preferred Date		Duration	Duration U/C	
			Start	End		+	-
	ERZ	1750	01-07-1750			182.5	182.5
	ERZ	1790	01-07-1790			182.5	182.5
	S	1790	15-11-1790			15	15
	S	1820	01-07-1820			182.5	182.5
	SWRZ	1823	15-02-1823	15-07-1823	150	30	30
1	S	1823	01-07-1823	01-07-1924	36890	365	365
2	ERZ	1840	30-05-1840	25-06-1840	26	1	1
	SWRZ	1868	02-04-1868			0.5	0.5
	ERZ	1877	21-05-1877			0.5	0.5
3	ERZ	1884	22-01-1884	23-01-1884	1	1	1
4	SWRZ	1919	15-12-1919	15-07-1920	213	15.5	21
5	ERZ	1922	28-05-1922	30-05-1922	2	1	1
	ERZ	1923	25-08-1923	01-09-1923	7	1	6.5
6	S	1927	07-07-1927	20-07-1927	13	1	1
7	S	1929	20-02-1929	22-02-1929	2	1	1.5
8	S	1929	25-07-1929	28-07-1929	3	1.5	1
9	S	1930	19-11-1930	07-12-1930	18	1.5	1
10	S	1931	23-12-1931	05-01-1932	13	1.5	1
11	S	1934	06-09-1934	07-10-1934	31	2.5	1
12	S	1952	27-06-1952	10-11-1952	136	1	1
13	S	1954	31-05-1954	03-06-1954	3	1	1
14	ERZ	1955	28-02-1955	07-04-1955	38	1.5	1
15	ERZ	1955	24-04-1955	26-05-1955	32	1	1
16	ERZ	1959	14-11-1959	20-12-1959	36	1	1
17	ERZ	1960	14-01-1960	19-02-1960	36	1	1.5
18	S	1961	24-02-1961	25-03-1961	29	1	1
19	S	1961	10-07-1961	17-07-1961	7	1	1
20	ERZ	1961	22-09-1961	25-09-1961	3	1	1
21	ERZ	1962	07-12-1962	09-12-1962	2	1	1
22	ERZ	1963	21-08-1963	23-08-1963	2	1	1

Continued on next page...

Table B.1 – Continued

#	Location	Start Year	Preferred Date		Duration	Duration U/C	
			Start	End		+	-
23	ERZ	1963	05-10-1963	06-10-1963	1	1	1
24	ERZ	1965	05-03-1965	15-03-1965	10	1	1
25	ERZ	1965	24-12-1965	25-12-1965	0.25	0.04	0.04
26	S	1967	05-11-1967	13-07-1968	251	1	1
27	ERZ	1968	22-08-1968	26-08-1968	4	1	1
28	ERZ	1968	07-10-1968	22-10-1968	15	1	1
29	ERZ	1969	22-02-1969	28-02-1969	6	2.5	1
30	ERZ	1969	24-05-1969	15-10-1971	874	1	1
31	S	1971	14-08-1971	14-08-1971	0.4	0.04	0.04
32	S	1971	24-09-1971	29-09-1971	5	1	1
33	ERZ	1972	05-02-1972	22-07-1974	900	5.5	5.5
34	S	1974	19-07-1974	22-07-1974	3	1	1
35	ERZ	1974	19-09-1974	22-09-1974	3	0.5	0.5
36	SWRZ	1974	31-12-1974	31-12-1974	0.25	0.04	0.04
37	S	1975	29-11-1975	29-11-1975	0.7	0.04	0.04
38	ERZ	1977	13-09-1977	01-10-1977	18	2	1
39	ERZ	1979	16-11-1979	17-11-1979	0.9	0.04	0.04
	ERZ	1980	11-03-1980				
40	S	1982	30-04-1982	01-05-1982	0.9	0.04	0.04
41	S	1982	25-09-1982	26-09-1982	0.6	0.04	0.04
	ERZ	1983	03-01-1983	Continuing			

U/C = uncertainty. Units: durations and duration uncertainties = days.

ERZ: 1750. Peterson and Moore (1987) report this eruption as starting in the year 1750 and it is treated according to the ‘nearest year’ category of Table 2.1, however, the end date of this eruption is unknown.

ERZ: 1790. Peterson and Moore (1987) report this eruption as starting in the year 1790 and it is treated according to the ‘nearest year’ category of Table 2.1, however, the end date of this eruption is unknown.

APPENDIX B. KILAUEA ERUPTIONS

S: 1790. Peterson and Moore (1987) report this eruption as starting in November 1790 and it is treated according to the ‘nearest month’ category of Table 2.1, however, the end date of this eruption is unknown.

S: 1820. The Smithsonian Institution’s Global Volcanism Program (Siebert et al., 2010; Venzke et al., 2013) reports this eruption as starting in the year 1820 and it is treated according to the ‘nearest year’ category of Table 2.1, however, the end date of this eruption is unknown.

SWRZ: February 1823. The Smithsonian Institution’s Global Volcanism Program (Siebert et al., 2010; Venzke et al., 2013) reports this eruption as starting in February 1823 and ending in July 1823. Both of these dates are treated according to the ‘nearest month’ category of table 2.1, however, alternative sources for these dates have not been found.

S: #1. August 1823 A sustained summit eruption dominated by lava lake activity is reported starting in 1823 and ending in 1924 (Dzurisin et al., 1984; Holcomb, 1987; Peterson and Moore, 1987). Both dates are treated according to the ‘nearest year’ category of Table 2.1.

ERZ: #2. May 1840 For this eruption we use the start date 30 May 1840 and end date 26 June 1840 reported by Wadge (1981) and Peterson and Moore (1987).

SWRZ: April 1868 Two eruptions are reported by Peterson and Moore (1987) as starting on 2 April 1868. Here we include this as one event, however, their end dates are unknown.

ERZ: May 1877 This eruption is reported by Peterson and Moore (1987) as starting on 21 May 1877, however, the end date of this eruption is unknown.

ERZ: #3 January 1884 A one day eruption is reported by Peterson and Moore (1987)

as starting on 22 January 1884. The eruption is therefore reported here with an end date of 23 January 1884.

SWRZ: #4. December 1919 For this eruption we use the start date 15 December 1919 reported by Peterson and Moore (1987). Wadge (1981) and Klein (1982) report this eruption starting on 21 December 1919 a duration uncertainty of - 6 days is assigned to the eruption start date to account for this literature-derived uncertainty. The duration of this eruption is reported as either 221 (Wadge, 1981) or 222 (Klein, 1982; Peterson and Moore, 1987) days, which depending on the start date used results in different end dates within July 1920. Here we treat the end date of this eruption according to the ‘nearest month’ category of Table 2.1.

ERZ: #5. May 1922 For this eruption we use the start date 28 May 1922 reported by Klein (1982) and Peterson and Moore (1987). These references report the eruption as lasting for 2 days, resulting in the end date 30 May 1922.

ERZ: August 1923 Both Klein (1982) and Peterson and Moore (1987) report this eruption as starting on 25 August 1923, however, each report a different eruption duration (1 and 7 days respectively). This results in a duration uncertainty > 50 % of the preferred eruption duration and therefore the eruption is excluded from this study.

S: #6. July 1927 For this eruption we use the start date 7 July 1927 reported by Wadge (1981), Klein (1982), Fiske et al. (1987) and Peterson and Moore (1987) and the end date 20 July 1927 reported by Wadge (1981) and Fiske et al. (1987). The durations given by Klein (1982) and Peterson and Moore (1987) also support this end date.

S: #7. February 1929 For this eruption we use the start date 20 February 1929 reported by Wadge (1981), Klein (1982), Fiske et al. (1987) and Peterson and Moore (1987). Some uncertainty surrounds the end date of this eruption. Fiske et al. (1987) suggest that the fire fountaining of this eruption ended on 21 February 1929 and that Hale-

maumau crater appeared clear on 22 February 1929. This implies that the eruption probably ended on 21 February 1929 and is in accordance with Wadge (1981), however, eruptive activity may have been continuing after the fire fountaining ended. To be conservative we use the end date 22 February 1929 resulting in a 2 day eruption duration (also reported by Klein (1982) and Peterson and Moore (1987)) and assign a duration uncertainty of -1 day to the eruption end date to account for this literature-derived uncertainty.

S: #8. July 1929 For this eruption we use the start date 25 July 1929 reported by Wadge (1981), Klein (1982), Fiske et al. (1987) and Peterson and Moore (1987) and the end date 28 July 1929 reported by Wadge (1981) and Fiske et al. (1987). Klein (1982) and Peterson and Moore (1987) report a duration of 4 days which results in an end date of 29 July 1929 and a duration uncertainty of +1 days is assigned to the eruption end date to account for this literature-derived uncertainty.

S: #9. November 1930 For this eruption we use the start date 19 November 1930 reported by Wadge (1981), Klein (1982), Fiske et al. (1987) and Peterson and Moore (1987) and the end date 7 December 1930 reported by Wadge (1981) and Fiske et al. (1987). Klein (1982) and Peterson and Moore (1987) report a duration of 19 days which results in an end date of 8 December 1930. Interestingly, Wadge (1981) also reports a duration of 19 days indicating that the varying dates here are most probably a calculation issue, however, a duration uncertainty of +1 days has been assigned to the eruption end date to account for the possible literature-derived uncertainty.

S: #10. December 1931 For this eruption we use the start date 23 December 1931 reported by Wadge (1981), Klein (1982), Fiske et al. (1987) and Peterson and Moore (1987) and the end date 5 January 1932 reported by Wadge (1981) and Fiske et al. (1987). Klein (1982) and Peterson and Moore (1987) report a duration of 14 days which results in an end date of 6 January 1932 and a duration uncertainty of +1 days is assigned to the eruption end date to account for this literature-derived uncer-

tainty.

S: #11. September 1934 For this eruption we use the start date 6 September 1934 reported by Wadge (1981), Klein (1982), Fiske et al. (1987) and Peterson and Moore (1987) and the end date 7 October 1934 reported by Wadge (1981) and Fiske et al. (1987). Klein (1982) and Peterson and Moore (1987) report a duration of 33 days which results in an end date of 9 October 1934. Interestingly, Wadge (1981) also reports a duration of 33 days indicating that the varying dates here are most probably a calculation issue. Fiske et al. (1987) state that lava was last seen moving on 7 October 1934, but that the eruption ended on either 8 or 9 October 1934. Here a duration uncertainty of + 2 days has been assigned to the eruption end date to account for this literature-derived uncertainty.

S: #12. June 1952 For this eruption we use the start date 27 June 1952 reported by Wadge (1981), Klein (1982), Fiske et al. (1987) and Peterson and Moore (1987) and the end date 10 November 1952 reported by Wadge (1981) and Fiske et al. (1987). The durations given by Klein (1982) and Peterson and Moore (1987) also support this end date.

S: #13. May 1954 For this eruption we use the start date 31 May 1954 reported by Macdonald and Eaton (1957), Wadge (1981), Klein (1982), Fiske et al. (1987) and Peterson and Moore (1987) and the end date 3 June 1954 reported by Macdonald and Eaton (1957), Wadge (1981) and Fiske et al. (1987). The durations given by Klein (1982) and Peterson and Moore (1987) also support this end date.

ERZ: #14. February 1955 For this eruption we use the start date 28 February 1955 reported by Wadge (1981), Klein (1982), Fiske et al. (1987) and Peterson and Moore (1987) and the end date 7 April 1955 reported by Wadge (1981). Tilling et al. (1987) report this eruption as ending on the 8 April 1955 and a duration uncertainty of +1 days is assigned to the eruption end date to account for this literature-derived uncer-

tainty.

ERZ: #15. April 1955 For this eruption we use the start date 24 April 1955 and the end date 26 May 1955 reported by Wadge (1981) and Fiske et al. (1987).

S: #16. November 1959 For this eruption we use the start date 14 November 1959 reported by Macdonald (1962), Richter et al. (1970), Wadge (1981), Klein (1982) and Peterson and Moore (1987) and the end date 20 December 1959 reported by Macdonald (1962), Richter et al. (1970), Wadge (1981). The durations given by Klein (1982) and Peterson and Moore (1987) also support this end date. The duration reported within Wadge (1981) is only 14 days, however, the periods of repose between the eruptive phases of this eruption are all < 10 days and are not taken into account in this study (Richter et al., 1970).

ERZ: #17. January 1960 For this eruption we use the start date of 13 January 1962 reported by Macdonald (1962), Klein (1982) and Peterson and Moore (1987) and the end date 19 February reported by Macdonald (1962) and Wadge (1981). The durations within Klein (1982) and Peterson and Moore (1987) also support this end date. Wadge (1981) report the alternative start date 14 January 1962 for this eruption and a duration uncertainty of -1 day is assigned to the eruption start date to account for this literature-derived uncertainty.

S: #18. February 1961 A short eruption on 24 February 1961 is reported by Richter et al. (1964), Wadge (1981), Klein (1982) Peterson and Moore (1987). While Klein (1982) and Peterson and Moore (1987) give the duration 1 day, Wadge (1981) report the more precise duration 0.3 days. However, close inspection of the descriptions within Richter et al. (1964) implies that the eruption started at approximately 07:00 on 24 February 1961 and was virtually over by the 25 February 1961. Here the longer duration of 1 day is used along with the start and end dates of Richter et al. (1964).

The following eruption started on 3 March 1961 (Richter et al., 1964; Wadge, 1981; Klein, 1982; Peterson and Moore, 1987) and end on 25 March 1961 (Richter et al., 1964; Wadge, 1981) period of inactivity between these two eruptions is < 10 days and therefore here we have grouped the two eruptions and treated them as a single event starting on 24 February 1961 and ending on 25 March 1961 with a total duration of 29 days.

S: #19. July 1961 For this eruption we use the start date 10 July 1961 reported by Richter et al. (1964), Wadge (1981), Klein (1982) and Peterson and Moore (1987) and the end date 17 July 1961 reported by Richter et al. (1964); Wadge (1981). The durations given by Klein (1982) and Peterson and Moore (1987) also supports this end date.

ERZ: #20. September 1961 For this eruption we use the start date 22 September 1961 reported by Wadge (1981), Klein (1982) and Peterson and Moore (1987). Descriptions within Richter et al. (1964) do not give a definitive start date but indicate that a visual glow in the area was noted before sunrise on 23 September 1961. This possible later start is covered by the resolution-derived uncertainty assigned to the eruption start date and is not commented on further. The end date 25 September 1961 is used here reported by Richter et al. (1964), Wadge (1981). The duration given by Peterson and Moore (1987) also supports this end date, however, Klein (1982) reports a 4 day duration for this eruption implying an end date of 26 September 1961. The descriptive and detailed nature of Richter et al. (1964) means we have discounted this discrepancy on the grounds that it is most probably a calculation issue.

ERZ: #21. December 1962 For this eruption we use the start date 7 December 1962 reported by Moore and Krivoy (1964), Wadge (1981), Klein (1982) and Peterson and Moore (1987) and the end date 9 December 1961 reported by Moore and Krivoy (1964), Wadge (1981). The duration given by Peterson and Moore (1987) also supports this end date, however, Klein (1982) reports a 3 day duration for this eruption imply-

ing an end date of 10 December 1962. The descriptive and detailed nature of Moore and Krivoy (1964) (including times for the start and end of the eruption) means we have discounted this discrepancy on the grounds that it is most probably a calculation issue.

ERZ: #22 August 1963 For this eruptions we use the start date 21 August 1963 reported by Peck et al. (1964), Wadge (1981), Klein (1982) and Peterson and Moore (1987) and the end date 23 August 1963 reported by Peck et al. (1964). Klein (1982) gives a 3 day duration for this eruption implying an end date of 24 August 1963. The descriptive and detailed nature of Peck et al. (1964) (including times for the start and end of the eruption) means we have discounted this discrepancy on the grounds that it is most probably a calculation issue. Furthermore, Wadge (1981) gives a far shorter duration on only 0.5 days, however, this seems unlikely and it is also discounted.

ERZ: #23 October 1963 For this eruption we use the start date 5 October 1963 reported by Moore and Koyanagi (1969), Wadge (1981), Klein (1982) and Peterson and Moore (1987) and the end date 6 October 1963 reported by Moore and Koyanagi (1969), and Wadge (1981) and also supported by the duration given by Peterson and Moore (1987). Klein (1982) give a 2 day duration for this eruption implying an end date of 7 October 1963. The descriptive and detailed nature of Moore and Koyanagi (1969) (including times for the start and end of the eruption) means we have discounted this discrepancy on the grounds that it is most probably a calculation issue.

ERZ: #24. March 1965 For this eruption we use the start date 5 March 1965 reported by Wright et al. (1968), Wadge (1981), Klein (1982) and Peterson and Moore (1987) and the end date 15 March 1965 reported by Wright et al. (1968), Wadge (1981). Peterson and Moore (1987) gives a duration supporting this end date, however, Klein (1982) gives a duration of 11 days for this eruption implying an end date of 16 March 1965. The descriptive and detailed nature of Wright et al. (1968) (including times for the start and end of the eruption) means we have discounted this discrepancy on the

grounds that it is most probably a calculation issue.

ERZ: #25 December 1965 For this eruption we use the start date 24 December 1965 reported by Fiske and Koyanagi (1968), Wadge (1981), Klein (1982) and Peterson and Moore (1987) and the end date 25 December 1965 reported by Fiske and Koyanagi (1968) and Wadge (1981). Fiske and Koyanagi (1968) gives start and end times for this eruption implying that the eruption started at 23:00 on 24 December and lasted only 6 hours and this is used for the duration of this eruption. Klein (1982) give a 2 day duration for this eruption, however, the descriptive and detailed nature of Fiske and Koyanagi (1968) (including times for the start and end of the eruption) means we have discounted this discrepancy on the grounds that it is most probably a calculation issue.

S: #26 November 1967 For this eruption we use the start date 5 November 1967 reported by Kinoshita et al. (1969), Wadge (1981), Klein (1982), Peterson and Moore (1987) and Nicholls and Stout (1988) and the end date 13 July 1968 reported by Kinoshita et al. (1969), Wadge (1981) and Nicholls and Stout (1988). The durations given by Klein (1982) and Peterson and Moore (1987) also support this end date. The duration reported within Wadge (1981) is only 204 days, however, an active lava lake was still present during the inactive periods between the recognised eruptive phases and are not taken into account in this study (Kinoshita et al., 1969; Nicholls and Stout, 1988).

ERZ: #27 August 1968 For this eruption we use the start date 22 August 1968 reported by Jackson et al. (1975), Wadge (1981), Klein (1982) and Peterson and Moore (1987) and the end date 26 August 1968 reported by Jackson et al. (1975), Wadge (1981). Peterson and Moore (1987) gives a duration supporting this end date, however, Klein (1982) gives a duration of 5 days for this eruption implying an end date of 27 August 1968. The descriptive and detailed nature of Jackson et al. (1975) means we have discounted this discrepancy on the grounds that it is most probably a calculation

issue.

ERZ: #28 October 1968 For this eruption we use the start date 7 October 1968 reported by Jackson et al. (1975), Wadge (1981), Klein (1982) and Peterson and Moore (1987) and the end date 22 October 1968 reported by Jackson et al. (1975) and Wadge (1981). Peterson and Moore (1987) gives a duration supporting this end date, however, Klein (1982) gives a duration of 16 days for this eruption implying an end date of 23 October 1968. The descriptive and detailed nature of Jackson et al. (1975) means we have discounted this discrepancy on the grounds that it is most probably a calculation issue.

ERZ: #29 February 1969 For this eruption we use the start date 22 February 1969 reported by Swanson et al. (1976), Wadge (1981), Klein (1982) and Peterson and Moore (1987) and the end date 28 February 1969 reported by Swanson et al. (1976) and Wadge (1981). Peterson and Moore (1987) gives a duration supporting this end date however, Klein (1982) gives a duration of 7 days for this eruption implying an end date of 1 March 1969. Descriptions within Swanson et al. (1976) suggest that foundering of the lava lake crust continued until the 1 or 2 March and therefore this possible longer duration cannot be discounted as a calculation issue. A duration uncertainty of + 2 days is therefore assigned to the eruption end date to account for this.

ERZ: #30 May 1969 For this eruption we use the start date 24 May 1969 reported by Swanson et al. (1979), Wadge (1981), Klein (1982) and Peterson and Moore (1987) and the end date 15 October 1971 reported by Swanson et al. (1979), Wadge (1981) and Tilling et al. (1987). Klein (1982) and Peterson and Moore (1987) give a duration of 875 days for this eruption implying an end date of 16 October 1971. The descriptive and detailed nature of Swanson et al. (1979) means we have discounted this discrepancy on the grounds that it is most probably a calculation issue.

S: #31 August 1971 A short eruption is reported for 14 August 1971 by Keller et al.

(1972), Wadge (1981), Duffield et al. (1982), Klein (1982) and Peterson and Moore (1987). Although both Klein (1982) and Peterson and Moore (1987) give a 1 day duration for this eruption Wadge (1981) give a more precise duration of 0.4 days which corresponds with the information within The Smithsonian Institution's monthly report (CSLP 81_71) indicating that the eruption started at 08:55 and ended at 19:00 Hawaiian Standard Time. This duration is therefore used in the analyses of this study.

S #32 September 1971 For this eruption we use the start date 24 September 1971 reported by Wadge (1981), Duffield et al. (1982), Klein (1982), Peterson and Moore (1987) and Dvorak (1990) and the end date 29 September 1971 reported by Wadge (1981), Duffield et al. (1982) and Dvorak (1990). Klein (1982) and Peterson and Moore (1987) give a durations supporting this end date.

ERZ: #33 February 1972 The start date of this eruption is uncertain. The Smithsonian Institution's Global Volcanism monthly report (CSLP 09_72) state that a lava lake was discovered in Mauna Ulu summit caldera at 09:00 on 5 February 1972 implying that the eruption started between 2 and 4 February 1972. Duffield et al. (1982) report that the eruption started early in February while Tilling et al. (1987) state the 2 February as the eruption start date. Here we treat the eruption according to the 'early month' category of Table 2.1. The end date of 22 July 1972 is used as reported by Tilling et al. (1987).

S: #34 July 1974 For this eruption we use the start date 19 July 1974 reported by Wadge (1981), Klein (1982), Peterson and Moore (1987) and Lockwood et al. (1999) and the end date 22 July 1974 reported by Wadge (1981) and Lockwood et al. (1999). Klein (1982) and Peterson and Moore (1987) give a durations supporting this end date.

S: #35 September 1974 A short eruption on 19 September 1974 is reported by Wadge (1981), Klein (1982), Peterson and Moore (1987) and Lockwood et al. (1999). Wadge

(1981) give a duration of 0.5 days to this eruption while Klein (1982) and Peterson and Moore (1987) give durations of 1 day implying an end date of 20 September 1974. Lockwood et al. (1999) describe active fountaining ending mid afternoon on 19 September 1974 and irregular overturning of the lava lake crust stopping of 22 September 1974. Given that this still implies some activity beneath the lava lake until the 22 September 1974, this is the data chosen as the end of the eruption.

SWRZ: #36 December 1974 A short eruption is reported for 31 December 1974 by Wadge (1981), Klein (1982), Peterson and Moore (1987) and Lockwood et al. (1999). Although both Klein (1982) and Peterson and Moore (1987) give a 1 day duration for this eruption Wadge (1981) give a more precise duration of 0.25 days which corresponds with the information within Lockwood et al. (1999) indicating that the eruption started at 02:56 and ended at 08:50 on 31 December 1974. This duration is therefore used in the analyses of this study.

S: #37 November 1975 A 7.2 earthquake and minor eruption is reported for 29 November 1975 by Dzurisin et al. (1980), Wadge (1981), Klein (1982) and Peterson and Moore (1987). Although both Klein (1982) and Peterson and Moore (1987) give a 1 day duration for this eruption Wadge (1981) give a more precise duration of 0.35 days. However, descriptions within The Smithsonian Institution's monthly report (SEAN 01:02) indicate that there were two phases of activity with a total duration of 16 hours/0.7 days (05:32 to 22:00 on 29 November 1975) and this is the duration used in the analyses of this study.

ERZ: #38 September 1977 For this eruption we use the start date 13 September 1977 and end date 1 October 1977 reported by Dzurisin et al. (1980), Moore et al. (1980) and Wadge (1981) and the end date 1 October 1977 and reported by Dzurisin et al. (1980) and Moore et al. (1980). Klein (1982) and Peterson and Moore (1987) report this eruption starting on 12 September 1977 with a duration of 20 days implying an end date of 2 October 1977. A duration uncertainty of + 1 day has been assigned to both

the eruption start and end date to account for this literature-derived uncertainty.

ERZ: #39 November 1979 A 1 day eruption is reported by Klein (1982) and Peterson and Moore (1987) starting on 16 November 1979 implying an end date of 17 November 1979. The Smithsonian Institution's monthly report (SEAN 04:11) states that the eruption started at 08:21 on 16 November 1979 and ended at 06:30 on 17 November 1979 giving a duration of 22 hours/0.9 days that is used in the analyses of this study.

ERZ: March 1980: Excluded Peterson and Moore (1987) report a 1 day eruption starting on 11 March 1980, however, The Smithsonian Institution's month report (SEAN 05:03) suggests that while volcanic tremor and summit deflation was detected no eruption took place and it was most probably an intrusion. It is therefore discounted from this study.

S: #40 April 1982 A 1 day eruption is reported by Peterson and Moore (1987) starting on 30 April 1982 implying an end date of 1 May 1982. The Smithsonian Institution's monthly report (SEAN 07:04) states that the eruption started at 11:37 on 30 April 1982 and ended 19 hours later on 1 May 1982. A duration of 0.9 days is therefore used in the analyses of this study.

S: #41 September 1982 A 1 day eruption is reported by Peterson and Moore (1987) starting on 23 September 1982 implying an end date of 24 September 1982. The Smithsonian Institution's monthly report (SEAN 07:09) also report this eruption, however, they state that it started at 18:44 on 25 September 1982 and lasted 15 hours. Casadevall and Hazlett (1983) also refer an eruption on 25 to 26 September 1982 and these are the dates used here with a duration of 0.6 days.

ERZ: January 1983 This is the Pu'u'Ō'ō - Kūpaianaha eruption starting in January 1983 (Heliker and Mattox, 2003), and still continuing on 19 July 2013 (Venzke et al.,

APPENDIX B. KILAUEA ERUPTIONS

2013). Due to the ongoing nature of this eruption, it is not used in this study.

Appendix C

Additional information regarding the Piton de la Fournaise dataset

The following section contains information about the reported start dates, end dates and durations of the 267 historical eruptions from Piton de la Fournaise, Réunion, Indian Ocean(PdlF) for the period 1644-2010. For each eruption, any discrepancies in the reported dates are discussed and the duration uncertainty assigned in this study explained. A summary of this information is included within Table C.1. Eruptions with numbers in the first column are those with reliable eruption durations and correspond with the eruption numbers reported in Table 3.3.

APPENDIX C. PITON DE LA FOURNAISE ERUPTIONS

Table C.1: Table containing the 267 historic eruptions reported for PdIF in the period 1644-2011

#	Location	Start Year	Preferred Date		Duration	U/C	
			Start	End		+	-
		1649					
		1669					
		1671					
		1672					
		1703	01-07-1703	01-07-1705	730	365	365
		1708	15-04-1708	29-04-1708	14	29	29
		1709					
		1721	15-06-1721			15	15
		1733					
		1733					
		1734	15-01-1734	15-03-1734	60	30	30
		1734	15-12-1734	29-12-1734	14	29	29
		1751	15-06-1751	29-06-1751	14	29	29
		1753					
		1759					
1		1760	15-12-1760	29-12-1760	14	1	1
		1766	15-03-1766			15	15
2		1766	14-05-1766	31-05-1766	17	1	1
		1768					
		1771					
		1772	15-02-1772			15	15
		1772	15-11-1772			15	15
		1774					
		1775					
		1776					
		1784					
		1785					
		1786	04-08-1786			0.5	0.5
3		1787	14-06-1787	01-08-1787	48	1	1
		1789	15-06-1789	15-07-1789	30	30	30

Continued on next page...

APPENDIX C. PITON DE LA FOURNAISE ERUPTIONS

Table C.1 – Continued

#	Location	Start Year	Preferred Date		Duration	U/C	
			Start	End		+	-
4		1791	26-06-1791	17-07-1791	21	1	1
		1791	15-10-1791			15	15
		1792	15-12-1792			15	15
		1794	15-01-1794			15	15
		1795					
		1797					
5		1800	02-11-1800	08-11-1800	6	1	1
		1801	15-10-1801	15-11-1801	31	30	30
6		1802	17-01-1802	30-01-1802	13	1	1
		1802	14-04-1802	28-04-1802	14	7.5	7.5
		1802	15-12-1802	14-01-1803	28	36	36
7		1807	23-03-1807	27-05-1807	65	1	1
8		1807	10-06-1807	13-06-1807	3	1	1
9		1809	17-07-1809	08-08-1809	22	1	1
10		1810	20-11-1810	28-11-1810	8	1	1
		1812	15-08-1812			15	15
11		1812	03-09-1812	30-09-1812	27	1	1
		1812	15-11-1812	30-11-1812	15	15.5	15.5
		1812	15-12-1812			15	15
12		1813	16-09-1813	16-09-1813	0.5	0.04	0.04
13		1813	18-11-1813	26-11-1813	8	1	1
14		1814	10-09-1814	12-09-1814	2	1	1
15		1814	13-10-1814	13-10-1814	0.5	0.04	0.04
16		1815	21-01-1815	27-01-1815	6	1	1
17		1815	15-08-1815	16-08-1815	1	1	1
18		1816	15-12-1816	15-12-1816	0.5	0.04	0.04
		1817	15-01-1817	15-04-1817	90	30	30
		1820	15-01-1820	15-02-1820	31	30	30
19		1821	27-02-1821	10-04-1821	42	1	1
		1824	15-02-1824			15	15
		1824	15-12-1824			15	15

Continued on next page...

APPENDIX C. PITON DE LA FOURNAISE ERUPTIONS

Table C.1 – Continued

#	Location	Start Year	Preferred Date		Duration	U/C	
			Start	End		+	-
20		1830	15-10-1830	12-11-1830	28	29	29
		1832	15-03-1832	05-04-1832	21	29	29
		1842	15-04-1842	13-05-1842	28	29	29
		1843					
		1844	19-03-1844	11-05-1844	53	1	1
		1844	15-12-1844			15	15
		1845					
		1846					
		1847					
		1848					
21		1849					
		1850	03-11-1850	12-11-1850	9	1	1
		1851					
		1852					
		1858	03-11-1858			0.5	0.5
22		1859	08-05-1859	08-05-1859	0.5	0.04	0.04
		1859	23-05-1859			0.5	0.5
23		1860	22-01-1860	24-02-1860	33	1	1
24		1860	11-03-1860	20-03-1860	9	1	1
25		1861	19-03-1861	19-03-1861	0.5	0.04	0.04
26		1863	20-12-1863	29-01-1864	40	1	1
27		1865	05-02-1865	10-02-1865	5	1	1
		1868	15-03-1868	12-04-1868	28	29	29
		1869					
		1870					
		1871	21-06-1871	05-07-1871	14	1	1
28		1872					
		1874					
		1874	29-06-1874	24-07-1874	25	1	1
29		1874	05-11-1874				
		1874	20-12-1874	20-12-1874	0.5	0.04	0.04
30		1874					

Continued on next page...

APPENDIX C. PITON DE LA FOURNAISE ERUPTIONS

Table C.1 – Continued

#	Location	Start Year	Preferred Date		Duration	U/C	
			Start	End		+	-
31		1875	26-11-1875	26-11-1875	0.5	0.04	0.04
32		1875	11-12-1875	11-12-1875	0.5	0.04	0.04
33		1876	11-12-1876	11-12-1876	0.5	0.04	0.04
34		1878	14-03-1878	30-03-1878	16	1	1
35		1880	24-11-1880	25-11-1880	1	1	1
36		1884	04-02-1884	05-02-1884	1	1	1
37		1889	15-06-1889	15-08-1889	61	30	30
		1890	15-02-1890	01-03-1890	14	29	29
		1890	15-06-1890			15	15
		1890	15-09-1890			15	15
38		1890	21-10-1890	20-11-1890	30	1	1
		1890	15-12-1890			15	15
		1891		04-02-1891		0.5	0.5
		1894	15-08-1894			15	15
		1897	05-01-1897	02-02-1897	28	19	19
39		1898	14-01-1898	20-01-1898	6	1	1
		1898	26-11-1898			0.5	0.5
		1899	13-02-1899			0.5	0.5
		1899	14-03-1899			0.5	0.5
		1899	08-07-1899			0.5	0.5
40		1900	11-05-1900	30-05-1900	19	1	1
41		1901	21-02-1901	25-02-1901	4	1	1
42		1901	04-07-1901	06-07-1901	2	1	1
43		1902	13-08-1902	18-08-1902	5	1	1
		1903					
44		1904	19-08-1904	20-08-1904	1	1	1
45		1904	04-10-1904	17-10-1904	13	1	1
46		1905	15-02-1905	16-02-1905	1	1	1
		1907	29-11-1907	05-12-1907	6	5	5
		1909	15-04-1909			15	15
47		1910	16-11-1910	12-12-1910	26	1	1

Continued on next page...

APPENDIX C. PITON DE LA FOURNAISE ERUPTIONS

Table C.1 – Continued

#	Location	Start Year	Preferred Date		Duration	U/C	
			Start	End		+	-
48		1913	10-07-1913	03-08-1913	24	1	1
		1915	22-07-1915			0.5	0.5
49		1915	08-09-1915	08-09-1915	0.5	0.04	0.04
50		1915	08-10-1915	20-10-1915	12	1	1
51		1915	09-11-1915	21-11-1915	12	1	1
52		1917	29-04-1917	29-04-1917	0.5	0.04	0.04
53		1920	28-06-1920	04-07-1920	6	1	1
54		1920	10-10-1920	18-10-1920	8	1	1
		1921	27-11-1921			0.5	0.5
		1924	19-05-1924			0.5	0.5
55		1924	03-09-1924	13-09-1924	10	1	1
56		1925	30-12-1925	30-12-1925	0.5	0.04	0.04
		1926	15-01-1926	15-04-1926	90	30	30
57		1926	18-09-1926	19-09-1926	1	1	1
58		1926	05-11-1926	08-11-1926	3	1	1
59		1927	11-01-1927	20-01-1927	9	1	1
60		1927	05-02-1927	20-02-1927	15	5.5	5.5
		1927	28-04-1927				
		1927	05-06-1927			5	5
61		1929	23-12-1929	31-12-1929	8	1	1
62		1930	23-05-1930	24-05-1930	1	1	1
		1931	15-01-1931			15	15
63		1931	15-02-1931	15-05-1931	89	30	30
64		1931	14-06-1931	25-06-1931	11	5.5	5.5
		1931	15-07-1931	25-07-1931	10	5.5	5.5
65		1931	04-08-1931	25-08-1931	21	5.5	5.5
		1932	15-11-1932	15-11-1932	0.5	30	30
66		1933	07-06-1933	15-06-1933	8	1	1
		1933	19-09-1933			0.5	0.5
67		1933	01-11-1933	01-11-1933	0.5	0.04	0.04
68		1933	11-11-1933	13-11-1933	2	1	1

Continued on next page...

APPENDIX C. PITON DE LA FOURNAISE ERUPTIONS

Table C.1 – Continued

#	Location	Start Year	Preferred Date		Duration	U/C	
			Start	End		+	-
69		1934	05-02-1934	23-02-1934	18	1	1
70		1934	30-03-1934	01-04-1934	2	1	1
		1935					
		1936	15-09-1936			0.5	0.5
71		1937	13-08-1937	12-09-1937	30	1	1
72		1937	05-11-1937	25-11-1937	20	1	1
73		1938	25-07-1938	29-07-1938	4	1	1
74		1938	07-12-1938	15-01-1939	39	1	1
		1941					
75		1942	05-10-1942	25-10-1942	20	1	1
76		1943	04-04-1943	25-04-1943	21	1	1
77		1944	11-04-1944	01-05-1944	20	1	1
78		1945	15-04-1945	06-05-1945	21	1	1
79		1946	18-06-1946	05-07-1946	17	1	1
		1947					
80		1948	14-02-1948	08-03-1948	23	1	1
		1949	15-10-1949			15	15
81		1950	25-02-1950	02-04-1950	36	1	1
82		1950	30-08-1950	05-09-1950	6	1	1
		1951	15-06-1951			15	15
83		1951	10-09-1951	20-09-1951	10	1	1
84		1952	19-05-1952	20-07-1952	62	1	1
85		1953	13-03-1953	15-04-1953	33	1	1
86		1953	15-06-1953	08-07-1953	23	1	1
		1953	15-12-1953			15	15
87		1954	15-01-1954	15-12-1954	334	30	30
		1955	15-07-1955			15	15
		1955	15-10-1955			15	15
88		1956	08-03-1956	15-04-1956	38	1	1
89		1956	22-11-1956	23-11-1956	1	1	1
90		1956	30-12-1956	16-03-1957	76	1	1

Continued on next page...

APPENDIX C. PITON DE LA FOURNAISE ERUPTIONS

Table C.1 – Continued

#	Location	Start Year	Preferred Date		Duration	U/C	
			Start	End		+	-
91		1957	02-09-1957	09-09-1957	7	1	1
92		1957	21-10-1957	16-11-1957	26	1	1
93		1958	30-05-1958	31-05-1958	1	1	1
94		1958	06-08-1958	20-09-1958	45	1	1
95		1959	11-03-1959	20-04-1959	40	1	1
96		1959	04-08-1959	06-08-1959	2	1	1
97		1960	11-01-1960	12-01-1960	1	1	1
98		1960	08-02-1960	10-03-1960	31	1	1
99		1961	05-04-1961	25-04-1961	20	1	1
100		1963	07-11-1963	21-11-1963	14	1	1
101		1964	30-04-1964	08-05-1964	8	1	1
102		1964	21-12-1964	15-02-1965	56	1	1
103		1966	15-03-1966	15-05-1966	61	1	1
104	Proximal	1972	09-06-1972	11-06-1972	2	1	1
105	Proximal	1972	25-07-1972	17-08-1972	23	1	1
106	Proximal	1972	07-09-1972	27-09-1972	20	1	1.5
107	Proximal	1972	08-10-1972	10-12-1972	63	1	1
108		1973	08-01-1973	16-01-1973	8	1	1
109	Summit	1973	10-05-1973	28-05-1973	18	7.5	1
110		1973	04-09-1973	05-09-1973	1	1	1
111	Summit	1975	04-11-1975	18-11-1975	14	1	1
112	Summit	1975	18-12-1975	06-04-1976	110	1	1
113	Proximal	1976	02-11-1976	03-11-1976	0.63	0.04	0.04
114	Proximal	1977	24-03-1977	24-03-1977	0.5	0.04	0.04
115	Distal	1977	05-04-1977	16-04-1977	11	1	1
116	Proximal	1977	24-10-1977	17-11-1977	24	1	1
117	Proximal	1979	28-05-1979	29-05-1979	1	1	1
118	Proximal	1979	13-07-1979	14-07-1979	0.71	0.04	0.04
119	Proximal	1981	03-02-1981	05-05-1981	91	1	1
120	Proximal	1983	04-12-1983	18-02-1984	76	1	1
121	Proximal	1985	14-06-1985	15-06-1985	1	0.04	0.04

Continued on next page...

APPENDIX C. PITON DE LA FOURNAISE ERUPTIONS

Table C.1 – Continued

#	Location	Start Year	Preferred Date		Duration	U/C	
			Start	End		+	-
122	Summit	1985	05-08-1985	10-10-1985	66	6.5	1
123	Proximal	1985	02-12-1985	03-12-1985	1.17	0.04	0.04
124	Summit	1985	29-12-1985	08-02-1986	41	10.5	1.5
125	Distal	1986	19-03-1986	05-04-1986	17	1	4
126	Summit	1986	13-07-1986	14-07-1986	0.25	0.04	0.04
127	Summit	1986	12-11-1986	13-11-1986	1	1	1
128	Summit	1986	26-11-1986	27-11-1986	1	1	1
129	Summit	1986	06-12-1986	06-01-1987	31	1.5	1
130	Summit	1987	10-06-1987	29-06-1987	19	1	1
131	Proximal	1987	19-07-1987	20-07-1987	1.33	0.04	0.04
132	Proximal	1987	06-11-1987	08-11-1987	2	1	1
133	Proximal	1987	30-11-1987	01-01-1988	32	1	1
134	Proximal	1988	07-02-1988	02-04-1988	55	1	1
135	Proximal	1988	18-05-1988	01-08-1988	75	1	1
136	Proximal	1988	31-08-1988	12-09-1988	12	1	1
137	Proximal	1988	14-12-1988	29-12-1988	15	1	1
138	Summit	1990	18-01-1990	19-01-1990	0.75	0.04	0.04
139	Proximal	1990	18-04-1990	08-05-1990	20	1	1
140	Summit	1991	19-07-1991	20-07-1991	1.17	0.04	0.04
141	Summit	1992	27-08-1992	23-09-1992	27	1	1
142	Distal	1998	09-03-1998	21-09-1998	196	1	1
143	Summit	1999	19-07-1999	31-07-1999	12	1	1
144	Summit	1999	28-09-1999	23-10-1999	25	1	1
145	Proximal	2000	14-02-2000	03-03-2000	18	2	1
146	Proximal	2000	23-06-2000	30-07-2000	37	1	1
147	Proximal	2000	12-10-2000	13-11-2000	32	1	1
148	Proximal	2001	27-03-2001	04-04-2001	8	1	1
149	Proximal	2001	11-06-2001	07-07-2001	26	1	1
150	Distal	2002	05-01-2002	16-01-2002	11	1.5	1
151	Proximal	2002	16-11-2002	03-12-2002	17	1.5	1
152	Summit	2003	30-05-2003	07-07-2003	38	1	1

Continued on next page...

APPENDIX C. PITON DE LA FOURNAISE ERUPTIONS

Table C.1 – Continued

#	Location	Start Year	Preferred Date		Duration	U/C	
			Start	End		+	-
153	Proximal	2003	22-08-2003	27-08-2003	5	1.5	1.5
154	Proximal	2003	30-09-2003	01-10-2003	1	1	1
155	Proximal	2003	07-12-2003	25-12-2003	18	1	1
156	Distal	2004	08-01-2004	10-01-2004	2	1	1
157	Proximal	2004	02-05-2004	18-05-2004	16	1	1
158	Summit	2004	12-08-2004	16-10-2004	65	1	13
159	Distal	2005	17-02-2005	26-02-2005	9	1	1
160	Summit	2005	04-10-2005	17-10-2005	13	1.5	1
161	Summit	2005	29-11-2005	29-11-2005	0.5	0.04	0.04
162	Distal	2005	26-12-2005	18-01-2006	23	1	1.5
163	Proximal	2006	20-07-2006	14-08-2006	25	1.5	1
164	Summit	2006	30-08-2006	01-01-2007	124	1	1
165	Summit	2007	18-02-2007	19-02-2007	1	1	1
166	Distal	2007	30-03-2007	01-05-2007	32	1	1
167	Summit	2008	21-09-2008	02-10-2008	11	1	1
168	Summit	2008	27-11-2008	28-11-2008	1	1	1
169	Summit	2008	14-12-2008	04-02-2009	52	1	1.5
170	Summit	2009	05-11-2009	12-01-2010	68	1	1
171	Proximal	2010	14-10-2010	31-10-2010	17	1	1
172	Proximal	2010	09-12-2010	10-12-2010	1	1	1

U/C = uncertainty. Units: durations and duration uncertainties = days

Eruptions with numbers in column one have reported eruption duration which are considered reliable and thus used in the duration analyses of this study. These numbers refer to the eruption numbers of Table 3.3.

1649: Excluded. An eruption in the year 1649 is reported by Stieltjes and Moutou (1989), however, precise start and end dates are unknown.

1669: Excluded. An eruption in the year 1669 is reported by Stieltjes and Moutou (1989), however, precise start and end dates are unknown.

1671: Excluded. An eruption in the year 1671 is reported by Stieltjes and Moutou (1989), however, precise start and end dates are unknown.

1672: Excluded. An eruption in the year 1672 is reported by Stieltjes and Moutou (1989), however, precise start and end dates are unknown.

1703: Excluded. An eruption is reported by The Smithsonian Institution's Global Volcanism Program (Siebert et al., 2010; Venzke et al., 2013) as starting on or before 1703 and ending in 1705, however, alternative sources for these dates have not been found.

April 1708: Excluded. An eruption starting in April 1708 is reported by Stieltjes and Moutou (1989), and is treated according to the 'nearest month' category of Table 2.1. A precise end date for this eruption is unknown, however, Stieltjes and Moutou (1989) report volcanic activity lasting 2 weeks \pm 2 weeks. This would result in a total duration uncertainty of > 50 % and the eruption is excluded from the analyses of this study.

1709: Excluded. An eruption in the year 1709 is reported by Stieltjes and Moutou (1989), however, precise start and end dates are unknown.

June 1721: Excluded. An eruption starting in June 1721 is reported by Stieltjes and Moutou (1989), and is treated according to the 'nearest month' category of Table 2.1, however, the end date is unknown.

1733 (two eruptions): Excluded Two eruptions are reported for the year 1733 by Stieltjes and Moutou (1989), however, precise start and end dates of these eruptions are unknown. Some uncertainty also surrounds the year of these eruptions.

January 1734: Excluded An eruption starting in January and ending in March 1734 is reported by Stieltjes and Moutou (1989). Although The Smithsonian Institution's

Global Volcanism Program (Siebert et al., 2010; Venzke et al., 2013) provide more precise dates for the start and end of this eruption (1 January 1734 and 6 March 1734, respectively) other sources reporting these dates have not been found. The dates are therefore treated according to the ‘nearest month’ category of Table 2.1, however, this results in a duration uncertainty of $> 50 \%$ and the eruption is excluded from the analyses of this study.

December 1734: Excluded. An eruption starting in December 1734 is reported by Stieltjes and Moutou (1989), and is treated according to the ‘nearest month’ category of Table 2.1. A precise end date for this eruption is unknown, however, Stieltjes and Moutou (1989) report volcanic activity lasting $2 \text{ weeks} \pm 2 \text{ weeks}$. This would result in a total duration uncertainty of $> 50 \%$ and the eruption is excluded from the analyses of this study.

June 1751: Excluded. An eruption starting in June 1751 is reported by Stieltjes and Moutou (1989), and is treated according to the ‘nearest month’ category of Table 2.1. A precise end date for this eruption is unknown, however, Stieltjes and Moutou (1989) report volcanic activity lasting $2 \text{ weeks} \pm 2 \text{ weeks}$. This would in a total duration uncertainty of $> 50 \%$ and the eruption is excluded from the analyses of this study.

1753: Excluded. An eruption in the year 1753 is reported by Stieltjes and Moutou (1989), however, precise start and end dates are unknown.

1759: Excluded. An eruption in the year 1759 is reported by Stieltjes and Moutou (1989), however, precise start and end dates are unknown.

#1. December 1760. For this eruption we use the start date 15 December 1760 and end date 29 December 1760 reported by Stieltjes and Moutou (1989).

March 1766: Excluded. An eruption starting in March 1766 is reported by Stieltjes and Moutou (1989), and is treated according to the ‘nearest month’ category of Table

2.1, however, the end date is unknown.

#2. May 1766. For this eruption we use the start date 14 May 1766 and end date 31 May 1766 reported by Stieltjes and Moutou (1989).

1768: Excluded. An eruption in the year 1768 is reported by Stieltjes and Moutou (1989), however, precise start and end dates are unknown.

1771: Excluded. An eruption in the year 1771 is reported by Stieltjes and Moutou (1989), however, precise start and end dates are unknown.

February 1772: Excluded The Smithsonian Institution's Global Volcanism Program (Siebert et al., 2010; Venzke et al., 2013) reports this eruption as starting in February 1772 and it is treated according to the 'nearest month' category of Table 2.1, however, the end date is unknown.

November 1772: Excluded. This eruption is reported by Stieltjes and Moutou (1989) as starting in November 1772 and it is treated according to the 'nearest month' category of Table 2.1, however, the end date is unknown.

1774: Excluded. An eruption in the year 1774 is reported by Stieltjes and Moutou (1989), however, precise start and end dates are unknown.

1775: Excluded. An eruption in the year 1775 is reported by Stieltjes and Moutou (1989), however, precise start and end dates are unknown.

1776: Excluded. An eruption in the year 1776 is reported by Stieltjes and Moutou (1989), however, precise start and end dates are unknown.

1784: Excluded. An eruption in the year 1784 is reported by Stieltjes and Moutou (1989), however, precise start and end dates are unknown.

1785: Excluded. An eruption in the year 1785 is reported by Stieltjes and Moutou (1989), however, precise start and end dates are unknown.

August 1786: Excluded. This eruption is reported by Stieltjes and Moutou (1989) as starting on 4 August 1786, however, the end date of this eruption is unknown.

#3. June 1787. For this eruption we use the start date 14 June 1787 and end date 1 August 1787 reported by Stieltjes and Moutou (1989).

June 1789: Excluded. Stieltjes and Moutou (1989) report this eruption as starting in June and ending in July 1789. These are treated according to the ‘nearest month’ category of Table 2.1, however, this results in a duration uncertainty of > 50 % and the eruption is excluded from the analyses of this study.

#4. June 1791. For this eruption we use the start date 26 June 1791 and end date 17 July 1791 reported by Stieltjes and Moutou (1989).

October 1791: Excluded. An eruption starting in October 1785 is reported by Stieltjes and Moutou (1989), and is treated according to the ‘nearest month’ category of Table 2.1, however, the end date is unknown.

December 1792: Excluded. An eruption starting in December 1792 is reported by Stieltjes and Moutou (1989), and is treated according to the ‘nearest month’ category of Table 2.1, however, the end date is unknown.

January 1794: Excluded. An eruption starting in January 1794 is reported by Stieltjes and Moutou (1989), and is treated according to the ‘nearest month’ category of Table 2.1. A precise end date for this eruption is unknown, however, Stieltjes and Moutou (1989) report volcanic activity lasting 2 weeks \pm 2 weeks. This would result in a total duration uncertainty of > 50 % and the eruption is excluded from the analyses of this study.

1795: Excluded. An eruption in the year 1795 is reported by Stieltjes and Moutou (1989), however, precise start and end dates are unknown.

1797: Excluded. An eruption in the year 1797 is reported by Stieltjes and Moutou (1989), however, precise start and end dates of this eruption are unknown. The start year of this eruption is also uncertain.

#5. November 1800. For this eruption we use the start date 2 November 1800 and end date 8 November 1800 reported by Stieltjes and Moutou (1989).

October 1801: Excluded. Stieltjes and Moutou (1989) report this eruption as starting in October and ending in November 1801. These are treated according to the ‘nearest month’ category of Table 2.1, however, this results in a duration uncertainty of > 50 % and the eruption is excluded from the analyses of this study.

#6. January 1802. For this eruption we use the start date 17 January 1802 and end date 30 January 1802 reported by Stieltjes and Moutou (1989).

April 1802: Excluded. This eruption is reported by Stieltjes and Moutou (1989) as starting on 14 April 1802, however the end date is unknown.

December 1802: Excluded. Stieltjes and Moutou (1989) report an eruption starting in December 1802 and it is treated according to the ‘nearest month’ category of Table 2.1. A precise end date for this eruption is unknown, however, Stieltjes and Moutou (1989) report volcanic activity lasting 4 weeks \pm 3 weeks. This would result in a total duration uncertainty of > 50 % and the eruption is excluded from the analyses of this study.

#7. March 1807. For this eruption we use the start date 23 March 1807 and end date 27 May 1807 reported by Stieltjes and Moutou (1989).

#8. June 1807. For this eruption we use the start date 10 June 1807 and end date 13

June 1807 reported by Stieltjes and Moutou (1989).

#9. July 1809. For this eruption we use the start date 17 July 1809 and end date 8 August 1809 reported by Stieltjes and Moutou (1989).

#10. November 1810. Stieltjes and Moutou (1989) report two eruptions in November 1810 (20-22 November 1810 and 24-28 November 1810). The period of inactivity between the two eruptions is < 10 days and they are reported here as a single eruptions starting on 20 November and ending on 28 November.

August 1812. An eruption starting in August 1812 is reported by Stieltjes and Moutou (1989), and is treated according to the ‘nearest month’ category of Table 2.1, however, the end date is unknown.

#11. September 1812. For this eruption we use the start date 3 September 1812 and end date 30 September 1812 reported by Stieltjes and Moutou (1989).

November 1812: Excluded. Stieltjes and Moutou (1989) report an eruption starting in November 1812 and ending on 30 November 1812. The start date is treated according to the ‘nearest month’ category of Table 2.1, however, this results in a duration uncertainty of > 50 % and the eruption is excluded from the analyses of this study.

December 1812: Excluded. An eruption starting in December 1812 is reported by Stieltjes and Moutou (1989), and is treated according to the ‘nearest month’ category of Table 2.1, however, the end date is unknown.

#12. September 1813: Excluded. A less than 1 day eruption on 16 September 1813 is reported by Stieltjes and Moutou (1989).

#13. November 1813. For this eruption we use the start date 18 November 1813 and end date 26 November 1813 reported by Stieltjes and Moutou (1989).

#14. September 1814. For this eruption we use the start date 10 September 1814 and end date 12 September 1814 reported by Stieltjes and Moutou (1989).

#15. October 1814. A less than 1 day eruption on 13 October 1814 is reported by Stieltjes and Moutou (1989).

#16. January 1815. For this eruption we use the start date 21 January 1815 and end date 27 January 1815 reported by Stieltjes and Moutou (1989).

#17. August 1815. For this eruption we use the start date 15 August 1815 and end date 16 August 1815 reported by Stieltjes and Moutou (1989).

#18. December 1816. A less than 1 day eruption on 15 December 1816 is reported by Stieltjes and Moutou (1989).

January 1817: Excluded. Several short eruptions are reported by Stieltjes and Moutou (1989) as starting in January 1817 and ending in April 1817. This is not one individual eruption and therefore it is excluded from any analysis within this study.

January 1820: Excluded. Stieltjes and Moutou (1989) report this eruption as starting in January and ending in February 1820. These are treated according to the ‘nearest month’ category of Table 2.1, however, this results in a duration uncertainty of > 50 % and the eruption is excluded from the analyses of this study.

#19. February 1821. For this eruption we use the start date 27 February 1821 and end date 10 April 1821 reported by Stieltjes and Moutou (1989).

February 1824: Excluded. An eruption starting in February 1824 is reported by Stieltjes and Moutou (1989), and is treated according to the ‘nearest month’ category of Table 2.1, however, the end date is unknown.

December 1824: Excluded. An eruption starting in December 1824 is reported by Stielt-

jes and Moutou (1989), and is treated according to the ‘nearest month’ category of Table 2.1, however, the end date is unknown.

October 1830: Excluded An eruption starting in October 1830 is reported by Stieltjes and Moutou (1989), and is treated according to the ‘nearest month’ category of Table 2.1. A precise end date for this eruption is unknown, however, Stieltjes and Moutou (1989) report volcanic activity lasting $4 \text{ weeks} \pm 2 \text{ weeks}$. This would result in a total duration uncertainty of $> 50 \%$ and the eruption is excluded from the analyses of this study.

March 1832: Excluded An eruption starting in March 1832 is reported by Stieltjes and Moutou (1989), and is treated according to the ‘nearest month’ category of Table 2.1. A precise end date for this eruption is unknown, however, Stieltjes and Moutou (1989) report volcanic activity lasting $3 \text{ weeks} \pm 2 \text{ weeks}$. This would result in a total duration uncertainty of $> 50 \%$ and the eruption is excluded from the analyses of this study.

April 1842: Excluded An eruption starting in April 1842 is reported by Stieltjes and Moutou (1989), and is treated according to the ‘nearest month’ category of Table 2.1. A precise end date for this eruption is unknown, however, Stieltjes and Moutou (1989) report volcanic activity lasting $4 \text{ weeks} \pm 2 \text{ weeks}$. This would result in a total duration uncertainty of $> 50 \%$ and the eruption is excluded from the analyses of this study.

1843: Excluded An eruption in the year 1843 is reported by Stieltjes and Moutou (1989), however, precise start and end dates of this eruption are unknown. The start year of this eruption is also uncertain.

#20. March 1844 For this eruption we use the start date 19 March 1844 and end date 11 May 1844 reported by Stieltjes and Moutou (1989).

December 1844: Excluded. An eruption starting in December 1844 is reported by Stieltjes and Moutou (1989), and is treated according to the ‘nearest month’ category of Table 2.1, however, the end date is unknown.

1845: Excluded. An eruption in the year 1845 is reported by Stieltjes and Moutou (1989), however, precise start and end dates are unknown.

1846: Excluded. An eruption in the year 1846 is reported by Stieltjes and Moutou (1989), however, precise start and end dates are unknown.

1847: Excluded. An eruption in the year 1847 is reported by Stieltjes and Moutou (1989), however, precise start and end dates are unknown.

1848: Excluded. An eruption in the year 1848 is reported by Stieltjes and Moutou (1989), however, precise start and end dates are unknown.

1849: Excluded. An eruption in the year 1849 is reported by Stieltjes and Moutou (1989), however, precise start and end dates of this eruption are unknown.

#21. November 1850. For this eruption we use the start date 3 November 1850 and end date 12 November 1850 reported by Stieltjes and Moutou (1989).

1851: Excluded. The Smithsonian Institution’s Global Volcanism Program (Siebert et al., 2010; Venzke et al., 2013) reports an eruption in the year 1851, however, alternative sources for this eruption have not been found.

1852: Excluded. The Smithsonian Institution’s Global Volcanism Program (Siebert et al., 2010; Venzke et al., 2013) reports an eruption in the year 1852, however, alternative sources for this eruption have not been found.

November 1858: Excluded. Stieltjes and Moutou (1989) report an eruption starting on 3 November 1858 and ending 14 December 1858. The following eruption in their

APPENDIX C. PITON DE LA FOURNAISE ERUPTIONS

catalogue is reported as starting January 1859, however, it's activity is described as a continuation of that of December 1858. Given that an end date is not provided for the January 1858 eruption a total duration cannot be determined.

#22 May 1859_i. A less than 1 day eruption on 8 May 1859 is reported by Stieltjes and Moutou (1989).

May 1859_{ii}: Excluded. Stieltjes and Moutou (1989) report an eruption starting on 23 May 1859, however, the end date is unknown.

#23. January 1860. For this eruption we use the start date 22 January 1860 and the end date 24 February 1860 reported by Stieltjes and Moutou (1989).

#24. March 1860. For this eruption we use the start date 11 March 1860 and end date 20 March 1860 reported by Stieltjes and Moutou (1989).

#25. March 1861. A less than 1 day eruption on 19 March 1861 is reported by Stieltjes and Moutou (1989).

#26. December 1863. For this eruption we use the start date 20 December 1863 and end date 29 January 1864 reported by Stieltjes and Moutou (1989).

#27. February 1865. For this eruption we use the start date 5 February 1865 and end date 10 February 1865 reported by Stieltjes and Moutou (1989).

March 1868: Excluded. An eruption starting in March 1868 is reported by Stieltjes and Moutou (1989), and is treated according to the 'nearest month' category of Table 2.1. A precise end date for this eruption is unknown, however, Stieltjes and Moutou (1989) report volcanic activity lasting 4 weeks \pm 2 weeks. This would result in a total duration uncertainty of > 50 % and the eruption is excluded from the analyses of this study.

1869: Excluded. An eruption in the year 1869 is reported by Stieltjes and Moutou (1989), however, precise start and end dates of this eruption are unknown. The start year of this eruption is also uncertain.

1870: Excluded. An eruption starting early in the year 1870 is reported by Stieltjes and Moutou (1989), however, precise start and end dates of this eruption are unknown.

#28. June 1871. For this eruption we use the start date 21 June 1871 and end date 5 July 1871 reported by Stieltjes and Moutou (1989).

1872: Excluded. An eruption starting early in the year 1872 is reported by Stieltjes and Moutou (1989), however, precise start and end dates of this eruption are unknown.

1874: Excluded. An eruption starting early in the year 1874 is reported by Stieltjes and Moutou (1989), however, precise start and end dates of this eruption are unknown.

#29. June 1874. For this eruption we use the start date 29 June 1874 and end date 24 July 1874 reported by Stieltjes and Moutou (1989).

November 1874: Excluded. An eruption starting on 5 November 1874 is reported by Stieltjes and Moutou (1989), however the end date of this eruption is unknown.

#30. December 1874. A less than 1 day eruption on 20 December 1874 is reported by Stieltjes and Moutou (1989).

#31. November 1875. A less than 1 day eruption on 26 November 1875 is reported by Stieltjes and Moutou (1989).

#32. December 1875. A less than 1 day eruption on 11 December 1875 is reported by

Stieltjes and Moutou (1989).

#33. December 1876. A less than 1 day eruption on 11 December 1876 is reported by Stieltjes and Moutou (1989).

#34. March 1878. For this eruption we use the start date 14 March 1878 and end date 30 March 1878 reported by Stieltjes and Moutou (1989).

#35. November 1880. For this eruption we use the start date 24 November 1880 and end date 25 November 1880 reported by Stieltjes and Moutou (1989).

#36. February 1884. For this eruption we use the start date 4 February 1884 and end date 5 March 1884 reported by Stieltjes and Moutou (1989).

#37. June 1889. An eruption is reported by Stieltjes and Moutou (1989) as starting in June and ending in August 1889 and are both treated according to the ‘nearest month’ category of Table 2.1.

February 1890: Excluded. An eruption starting in February 1890 is reported by Stieltjes and Moutou (1989), and is treated according to the ‘nearest month’ category of Table 2.1. A precise end date for this eruption is unknown, however, Stieltjes and Moutou (1989) report volcanic activity lasting $2 \text{ weeks} \pm 2 \text{ weeks}$. This would result in a total duration uncertainty of $> 50 \%$ and the eruption is excluded from the analyses of this study.

June 1890: Excluded. An eruption starting in June 1890 is reported by Stieltjes and Moutou (1989), and is treated according to the ‘nearest month’ category of Table 2.1, however, the end date is unknown.

September 1890: Excluded. An eruption starting in September 1890 is reported by Stieltjes and Moutou (1989), and is treated according to the ‘nearest month’ category of Table 2.1, however, the end date is unknown.

#38. October 1890. For this eruption we use the start date 21 October 1890 and end date 20 November 1890 reported by Stieltjes and Moutou (1989).

December 1890: Excluded. An eruption starting in December 1890 is reported by Stieltjes and Moutou (1989), and is treated according to the ‘nearest month’ category of Table 2.1, however, the end date is unknown.

1891: Excluded. An eruption ending in February 1891 is reported by Stieltjes and Moutou (1989), and is treated according to the ‘nearest month’ category of Table 2.1, however, the start date is unknown.

August 1894: Excluded. An eruption starting in August 1894 is reported by Stieltjes and Moutou (1989), and is treated according to the ‘nearest month’ category of Table 2.1, however, the end date is unknown.

January 1897: Excluded. An eruption starting at the beginning of January 1894 is reported by Stieltjes and Moutou (1989), and is treated according to the ‘early month’ category of Table 2.1. A precise end date for this eruption is unknown, however, Stieltjes and Moutou (1989) report volcanic activity lasting $4 \text{ weeks} \pm 2 \text{ weeks}$. This would result in a total duration uncertainty of $> 50 \%$ and the eruption is excluded from the analyses of this study.

#39. January 1898. For this eruption we use the start date 14 January 1898 and end date 20 January 1898 reported by Stieltjes and Moutou (1989).

November 1898: Excluded. Stieltjes and Moutou (1989) report an eruption starting on 26 November 1898, however, the end date of this eruption is unknown.

February 1899: Excluded. Stieltjes and Moutou (1989) report an eruption starting on 13 February 1899 and ending after the 19 February 1899. The uncertain end date of this eruption has led us to exclude it from the study.

APPENDIX C. PITON DE LA FOURNAISE ERUPTIONS

March 1899: Excluded. Stieltjes and Moutou (1989) report an eruption starting on 14 March 1899, however, the end date of this eruption is unknown.

July 1899: Excluded. Stieltjes and Moutou (1989) report an eruption starting on 8 July 1899 and ending after the 18 July 1899. The uncertain end date of this eruption has led us to exclude it from the study.

#40. May 1900. For this eruption we use the start date 11 May 1900 and end date 30 May 1900 reported by Stieltjes and Moutou (1989).

#41. February 1901. For this eruption we use the start date 21 February 1901 and end date 25 February 1901 reported by Stieltjes and Moutou (1989).

#42. July 1901. For this eruption we use the start date 4 July 1901 and end date 6 July 1901 reported by Stieltjes and Moutou (1989).

#43. August 1902. For this eruption we use the start date 13 August 1902 and end date 18 August 1902 reported by Stieltjes and Moutou (1989).

1903: Excluded. An eruption in the year 1903 is reported by Stieltjes and Moutou (1989), however, the start and end dates of this eruption are unknown and the year is uncertain.

#44. August 1904. For this eruption we use the start date 19 August 1904 and end date 20 August 1904 reported by Stieltjes and Moutou (1989).

#45. October 1904. For this eruption we use the start date 4 October 1904 and end date 17 October 1904 reported by Stieltjes and Moutou (1989).

#46. February 1905. For this eruption we use the start date of 15 February 1905 and end date of 16 February 1905 reported by Stieltjes and Moutou (1989).

November 1907: Excluded. An eruption is reported by Stieltjes and Moutou (1989) as starting on 29 November 1907 and ending in the beginning of December 1907. The end date of this eruption is treated according to the ‘early month’ category of Table 2.1, however, this results in a duration uncertainty of > 50 % and the eruption is excluded from the analyses of this study.

April 1909: Excluded. An eruption starting in April 1909 is reported by Stieltjes and Moutou (1989), and is treated according to the ‘nearest month’ category of Table 2.1, however the end date is unknown.

#47. November 1910. For this eruption we use the start date 16 November 1910 and end date 12 December 1910 reported by Stieltjes and Moutou (1989).

#48. July 1913. For this eruption we use the start date 10 July 1913 and end date 3 August 1913 reported by Stieltjes and Moutou (1989).

July 1915: Excluded. Stieltjes and Moutou (1989) report an eruption starting on 22 July 1915 and ending after the 27 July 1915. The uncertain end date of this eruption has led us to exclude it from the study.

#49. September 1915. A less than 1 day eruption on 8 September 1915 is reported by Stieltjes and Moutou (1989).

#50. October 1915. For this eruption we use the start date 8 October 1915 and end date 20 October 1915 reported by Stieltjes and Moutou (1989).

#51. November 1915. For this eruption we use the start date 9 November 1915 and end date 21 November 1915 reported by Stieltjes and Moutou (1989).

#52. April 1917. A less than 1 day eruption on 29 April 1917 is reported by Stieltjes and Moutou (1989).

#53. June 1920. For this eruption we use the start date 28 June 1920 and end date 4 July 1920 reported by Stieltjes and Moutou (1989).

#54. October 1920. For this eruption we use the start date 10 October 1920 and end date 18 October 1920 reported by Stieltjes and Moutou (1989).

November 1921: Excluded. Stieltjes and Moutou (1989) report an eruption starting on 27 November 1921 and ending on 3 December 1921. However, activity is described as 'continuing afterwards' so this date cannot be considered the true end of the eruption and therefore the eruption is excluded from this study.

May 1924: Excluded. An eruption is reported to have started on 19 May 1924 by Stieltjes and Moutou (1989) with a duration of > 4 days, however the precise end date is unknown.

#55. September 1924. For this eruption we use the start date 3 September 1924 and end date 13 September 1924 reported by Stieltjes and Moutou (1989).

#56. December 1925. A less than 1 day eruption on 30 December 1925 is reported by Stieltjes and Moutou (1989).

January 1926: Excluded. Many small lava flows are reported by Stieltjes and Moutou (1989) between January and April 1926. It is unclear whether these are several short eruptions or one longer eruption with many lava flows and therefore it is excluded from this study.

#57. September 1926. For this eruption we use the start date 18 September 1926 and end date 19 September 1926 reported by Stieltjes and Moutou (1989).

#58. November 1926. For this eruption we use the start date 5 November 1926 and end date 8 November 1926 reported by Stieltjes and Moutou (1989).

#59. January 1927. For this eruption we use the start date 11 January 1927 and end date 20 January 1927 reported by Stieltjes and Moutou (1989).

#60. February 1927. Stieltjes and Moutou (1989) report an eruption starting in the beginning of February 1927 and ending on 20 February 1927. The start date of this eruption is treated according to the ‘early month’ category of Table 2.1.

April 1927: Excluded. Stieltjes and Moutou (1989) report an eruption starting on 28 April 1927, however, the end date is unknown.

June 1927: Excluded. Stieltjes and Moutou (1989) report an eruption starting in the beginning of June 1927 and is treated according to the ‘early month’ category of Table 2.1, however, the end date is unknown.

#61. December 1929. For this eruption we use the start date 23 December 1929 and end date 31 December 1929 reported by Stieltjes and Moutou (1989).

#62. May 1930. For this eruption we use the start date 23 May 1930 and end date 24 May 1930 reported by Stieltjes and Moutou (1989).

January 1931: Excluded. Stieltjes and Moutou (1989) report an eruption starting in January 1931 and is treated according to the ‘nearest month’ category of Table 2.1, however, the end date is unknown.

#63. February 1931. Stieltjes and Moutou (1989) report an eruption starting in February and ending in May 1931 and have both been treated according to the ‘nearest month’ category of Table 2.1.

#64. June 1931. This eruption is reported by Stieltjes and Moutou (1989) as starting on 14 June 1931 and ending at the end of June 1931. The end date of this eruption is treated according to the ‘late month’ category of Table 2.1.

July 1931: Excluded. Stieltjes and Moutou (1989) report an eruption starting on 15 July 1931 and ending at the end of July 1931. The end date of this eruption is treated according to the ‘late month’ category of Table 2.1. Stieltjes and Moutou (1989) state that the start date of this eruption is uncertain and therefore this eruption is excluded from this study.

#65. August 1931. This eruption is reported by Stieltjes and Moutou (1989) as starting on 4 August 1931 and ending at the end of August 1931. The end date of this eruption is treated according to the ‘late month’ category of Table 2.1.

November 1932: Excluded. Stieltjes and Moutou (1989) report an eruption starting and ending in November 1932 and both dates are treated according to the ‘nearest month’ category of Table 2.1, however, this results in a duration uncertainty of > 50 % and the eruption is excluded from the analyses of this study.

#66. June 1933. For this eruption we use the start date 7 June 1933 and end date 15 December 1933 reported by Stieltjes and Moutou (1989).

September 1933: Excluded. Stieltjes and Moutou (1989) report an eruption starting on 19 September 1933, however the end date is unknown.

#67. November 1933_i. A less than 1 day eruption on 1 November 1933 is reported by Stieltjes and Moutou (1989).

#68. November 1933_{ii}. For this eruption we use the start date of 11 November 1933 and end date 13 November 1933 reported by Stieltjes and Moutou (1989).

#69. February 1934. For this eruption we use the start date 5 February 1934 and end date 23 February 1934 reported by Stieltjes and Moutou (1989).

#70. March 1934. For this eruption we use the start date 30 March 1934 and end date 1 April 1934 reported by Stieltjes and Moutou (1989).

1935: Excluded. An eruption in the year 1935 is reported by Stieltjes and Moutou (1989), however, the end date is unknown and the start year is uncertain.

September 1936: Excluded. The Smithsonian Institution's Global Volcanism Program (Siebert et al., 2010; Venzke et al., 2013) reports an eruption starting in September 1936 and it is treated according to the 'nearest month' category of Table 2.1. However, the end date is unknown and alternative sources for this eruption have not been found.

#71. August 1937. For this eruption we use the start date 13 August 1937 and end date 12 September 1937 reported by Stieltjes and Moutou (1989).

#72. November 1937. For this eruption we use the start date 5 November 1937 and end date 25 November 1937 reported by Stieltjes and Moutou (1989).

#73. July 1938. For this eruption we use the start date 25 July 1938 and end date 29 July 1938 reported by Stieltjes and Moutou (1989).

#74. December 1938. Stieltjes and Moutou (1989) report two eruptions between December 1938 and January 1939 (7 December-25 December 1938 and 2 January-15 January 1939). The period of inactivity between these two eruptions is < 10 days and therefore a single eruption starting on 7 December 1938 and ending on 15 January 1939 is used in this study.

1941: Excluded. An eruption in the year 1941 is reported by Stieltjes and Moutou (1989), however, the end date is unknown and the start year is uncertain.

#75. October 1942. For this eruption we use the start date 5 October 1942 and end date 25 October 1942 reported by Stieltjes and Moutou (1989).

#76. April 1943. For this eruption we use the start date 4 April 1943 and end date 25 April 1943 reported by Stieltjes and Moutou (1989).

APPENDIX C. PITON DE LA FOURNAISE ERUPTIONS

#77. April 1944. For this eruption we use the start date 11 April 1944 and end date 1 May 1944 reported by Stieltjes and Moutou (1989).

#78. April 1945. For this eruption we use the start date 15 April 1945 and end date 6 May 1945 reported by Stieltjes and Moutou (1989).

#79. June 1946. For this eruption we use the start date 18 June 1946 and end date 5 July 1946 reported by Stieltjes and Moutou (1989).

1947: Excluded. An eruption in the year 1947 is reported by Stieltjes and Moutou (1989), however, the end date is unknown and the start year is uncertain.

#80. February 1948. For this 1948 eruption we use the start date 14 February 1948 and end date 8 March 1948 reported by Stieltjes and Moutou (1989).

October 1949: Excluded. The Smithsonian Institution's Global Volcanism Program (Siebert et al., 2010; Venzke et al., 2013) reports an eruption starting in October 1949 and it is treated according to the 'nearest month' category of Table 2.1. However, the end date is unknown and alternative sources for this eruption have not been found.

#81. February 1950. For this eruption we use the start date 25 February 1950 and end date 2 April 1950 reported by Stieltjes and Moutou (1989).

#82. August 1950. For this eruption we use the start date 30 August 1950 and end date 5 September 1950 reported by Stieltjes and Moutou (1989).

June 1951: Excluded. The Smithsonian Institution's Global Volcanism Program (Siebert et al., 2010; Venzke et al., 2013) reports an eruption starting in June 1951 and it is treated according to the 'nearest month' category of Table 2.1. However, the end date is unknown and alternative sources for this eruption have not been found.

#83. September 1951. For this eruption we use the start date 10 September 1951 and

end date 20 September 1951 reported by Stieltjes and Moutou (1989).

#84. May 1952. For this eruption we use the start date 19 May 1952 and end date 20 July 1952 reported by Stieltjes and Moutou (1989).

#85. March 1953. For this eruption we use the start date 13 March 1953 and end date 15 April 1953 reported by Stieltjes and Moutou (1989).

#86. June 1953. For this eruption we use the start date 15 June 1953 and end date 8 July 1953 reported by Stieltjes and Moutou (1989).

December 1953: Excluded. Stieltjes and Moutou (1989) report an eruption starting in December 1953 and it is treated according to the 'nearest month' category of Table 2.1, however, the end date is unknown.

#87. January 1954. Stieltjes and Moutou (1989) report an eruption starting in January and ending in December 1954. Both of these dates are treated according to the 'nearest month' category of Table 2.1.

July 1955: Excluded. Stieltjes and Moutou (1989) report an eruption starting in July 1955 and it is treated according to the 'nearest month' category of Table 2.1, however, the end date is unknown.

October 1955: Excluded. Stieltjes and Moutou (1989) report an eruption starting in October 1955 and it is treated according to the 'nearest month' category of Table 2.1, however, the end date is unknown.

#88. March 1956. For this eruption we use the start date 8 March 1956 and end date 15 April 1956 reported by Stieltjes and Moutou (1989).

#89. November 1956. For this eruption we use the start date 22 November 1956 and end date 23 November 1956 reported by Stieltjes and Moutou (1989).

APPENDIX C. PITON DE LA FOURNAISE ERUPTIONS

#90. December 1956. For this eruption we use the start date 30 December 1956 and end date 16 March 1957 reported by Stieltjes and Moutou (1989).

#91. September 1957. For this eruption we use the start date 2 September 1957 and end date 9 September 1957 reported by Stieltjes and Moutou (1989).

#92. October 1957. For this eruption we use the start date 21 October 1957 and end date 16 November 1957 reported by Stieltjes and Moutou (1989).

#93. May 1958. For this eruption we use the start date 30 May 1958 and end date 31 May 1958 reported by Stieltjes and Moutou (1989).

#94. August 1958. For this eruption we use the start date 6 August 1958 and end date 20 September 1958 reported by Stieltjes and Moutou (1989).

#95. March 1959. For this eruption we use the start date 11 March 1959 and end date 20 April 1959 reported by Stieltjes and Moutou (1989).

#96. August 1959. For this eruption we use the start date 4 August 1959 and end date 6 August 1959 reported by Stieltjes and Moutou (1989).

#97. January 1960. For this eruption we use the start date 11 January 1960 and end date 12 January 1960 reported by Stieltjes and Moutou (1989).

#98. February 1960. For this eruption we use the start date 8 February 1960 and end date 10 March 1960 reported by Stieltjes and Moutou (1989).

#99. April 1961. For this eruption we use the start date 5 April 1961 and end date 25 April 1961 reported by Stieltjes and Moutou (1989).

#100. November 1963. For this eruption we use the start date 7 November 1963 and end date 21 November 1963 reported by Stieltjes and Moutou (1989).

#101. April 1964. For this eruption we use the start date 30 April 1964 and end date 8 May 1964 reported by Stieltjes and Moutou (1989).

#102. December 1964. For this eruption we use the start date 21 December 1964 and end date 15 February 1965 reported by Stieltjes and Moutou (1989).

#103. March 1966. For this eruption we use the start date 15 March 1966 and end date 15 May 1966 reported by Stieltjes and Moutou (1989).

#104. June 1972. For this eruption we use the start date 9 June 1972 and end date 11 June 1972 reported by Stieltjes and Moutou (1989) and Peltier et al. (2009).

#105. July 1972. For this eruption we use the start date 25 July 1972 and end date 17 August 1972 reported by Stieltjes and Moutou (1989) and Peltier et al. (2009).

#106. September 1972. For this eruption we use the start date 7 September 1972 reported by Stieltjes and Moutou (1989) and Peltier et al. (2009) and end date of 27 September 1972 reported by Stieltjes and Moutou (1989). Peltier et al. (2009) report an end date of 26 September 1972 and a duration uncertainty of - 1 day is assigned to account for this literature-derived uncertainty.

#107. October 1972. For this eruption we use the start date 8 October 1972 and end date 10 December 1972 reported by Stieltjes and Moutou (1989) and Peltier et al. (2009). Both of these sources report numerous eruptive phases during this eruption, however, these either overlap in time or the periods of inactivity between these phases are < 10 days.

#108. January 1973. For this eruption we use the start date 8 January 1973 and end date 16 January 1973 reported by Stieltjes and Moutou (1989).

#109. May 1973. For this eruption we use the start date 10 May 1973 reported by Stieltjes and Moutou (1989) and Peltier et al. (2009) and end date of 28 May 1973

reported by Peltier et al. (2009). Stieltjes and Moutou (1989) report the end date 4 June 1973 and a duration uncertainty of + 7 days is assigned to account for this literature-derived uncertainty.

#110. September 1973. For this eruption we use the start date 4 September 1973 and end date 5 September 1973 reported by Stieltjes and Moutou (1989).

#111. November 1975. For this eruption we use the start date 4 November 1975 and end date 18 November 1975 reported by Stieltjes and Moutou (1989) and Peltier et al. (2009).

#112. December 1975. For this eruption we use the start date 18 December 1975 and end date 6 April 1976 reported by Stieltjes and Moutou (1989) and Peltier et al. (2009).

#113. November 1976. For this eruption we use the start date 2 November 1976 reported by Stieltjes and Moutou (1989) and Peltier et al. (2009) and end date of 3 November 1976 reported by Peltier et al. (2009). Stieltjes and Moutou (1989) report an end date of 4 November 1976, however, The Smithsonian Institution's monthly report (SEAN 01:04) indicates that the eruption started at 13:00 on 2 November and ended at 04:00 on 3 November resulting in the 15 hour (0.63 day) duration used here.

#114. March 1977. A less than 1 day eruption on 24 March 1977 is reported by Boivin and Bachélery (2009) and Peltier et al. (2009).

#115. April 1977. For this eruption we use the start date 5 April 1977 and end date 16 April 1977 reported by Boivin and Bachélery (2009) and Peltier et al. (2009).

#116. October 1977. For this eruption we use the start date 24 October 1977 and end date 17 November 1977 reported by Stieltjes and Moutou (1989), Boivin and Bachélery (2009) and Peltier et al. (2009).

#117. May 1979. For this eruption we use the start date 28 May 1979 and end date 29 May 1979 reported by Stieltjes and Moutou (1989), Boivin and Bachélery (2009) and Peltier et al. (2009).

#118. July 1979. For this eruption we use the start date 13 July 1979 reported by Stieltjes and Moutou (1989), Boivin and Bachélery (2009) and Peltier et al. (2009) and end date of 14 July 1979 reported by Peltier et al. (2009) and Boivin and Bachélery (2009). Stieltjes and Moutou (1989) report the end date 15 July 1979, however, The Smithsonian Institution's monthly report (SEAN 04:07) indicates that the eruption started at 18:45 on 13 July 1989 and ended at 11:30 on 14 July 1989 resulting in the 17 hour (0.71 days) duration used here.

#119. February 1981. For this eruption we use the start date 3 February 1981 and end date 5 May 1981 reported by Stieltjes and Moutou (1989), Boivin and Bachélery (2009) and Peltier et al. (2009).

#120. December 1983 For this eruption we use the start date 4 December 1983 and end date 18 February 1984 reported by Stieltjes and Moutou (1989), Boivin and Bachélery (2009) and Peltier et al. (2009).

#121. June 1985. For this eruption we use the start date 14 June 1985 and end date 15 June 1985 reported by Stieltjes and Moutou (1989), Boivin and Bachélery (2009) and Peltier et al. (2009). The Smithsonian Institution's monthly report (SEAN 10:06) indicates that the eruption started at 16:00 and ended as 16:04 on these days, and therefore the eruption lasted approximately 24 hours. The assigned uncertainty is therefore attributed according to the 'nearest hour' category of Table 2.1.

#122. August 1985. For this eruption we use the start date 5 August reported by Stieltjes and Moutou (1989), Boivin and Bachélery (2009) and Peltier et al. (2009) and the end date 10 October 1985 reported by Boivin and Bachélery (2009) and Peltier

et al. (2009). Stieltjes and Moutou (1989) report the end date 16 October 1985 and a duration uncertainty of + 6 days is assigned to account for this literature-derived uncertainty.

#123. December 1985_i. For this eruption we use the start date 2 December 1985 reported by Stieltjes and Moutou (1989) and Boivin and Bachélery (2009) and the end date 3 December 1985 reported by Stieltjes and Moutou (1989), Boivin and Bachélery (2009) and Peltier et al. (2009). Peltier et al. (2009) report the start date 1 December 1985, however, descriptions within The Smithsonian Institution's monthly report (SEAN 10:12) indicates that the eruption started on 2 December 1985 with a duration of 28 hours (1.17 days). This duration is used here.

#124. December 1985_{ii}. For this eruption we use the start date 29 December 1985 reported by Stieltjes and Moutou (1989), Boivin and Bachélery (2009) and Peltier et al. (2009). The end date of this eruption is reported by Peltier et al. (2009) as 7 February 1986, by Boivin and Bachélery (2009) as 8 February 1986 and by Stieltjes and Moutou (1989) as 18 February 1986. Here the end date of Boivin and Bachélery (2009) is used and duration uncertainties of + 10 days and - 1 day are assigned to account for this literature-derived uncertainty.

#125. March 1986. For this eruption we use the start date 19 March 1986 reported by Stieltjes and Moutou (1989), Boivin and Bachélery (2009) and Peltier et al. (2009) and end date 5 April 1986 reported by Boivin and Bachélery (2009) and Peltier et al. (2009). Stieltjes and Moutou (1989) report the end date 1 April and a duration uncertainty of - 4 days has been assigned to account for this literature-derived uncertainty.

#126. July 1986. A short, less than 1 day duration eruption is reported between the 13 and 14 July 1986 (Boivin and Bachélery, 2009; Peltier et al., 2009). The Smithsonian Institution's monthly report (SEAN 10:12) states that this eruption started at 18:10 on

13 July and ended at 00:10 on 14 July, resulting in the 6 hour (0.25 days) duration used here.

#127. November 1986_i. For this eruption we use the start date 12 November 1986 and end date 13 November 1986 reported by Boivin and Bachélery (2009) and Peltier et al. (2009).

#128. November 1986_{ii}. For this eruption we use the start date 26 November 1986 and end date 27 November 1986 reported by Stieltjes and Moutou (1989), Boivin and Bachélery (2009) and Peltier et al. (2009).

#129. December 1986. For this eruption we use the start date 6 December 1986 reported by Stieltjes and Moutou (1989), Boivin and Bachélery (2009) and Peltier et al. (2009) and the end date 6 January 1987 reported by Boivin and Bachélery (2009) and Peltier et al. (2009). Stieltjes and Moutou (1989) report an end date of 7 January 1987 and a duration uncertainty of + 1 day is assigned to the eruption end date to account for this literature-derived uncertainty.

#130. June 1987. For this eruption we use the start date 10 June 1987 and end date 29 June 1987 reported by Stieltjes and Moutou (1989), Boivin and Bachélery (2009) and Peltier et al. (2009).

#131. July 1987. For this eruption we use the start date 19 July 1987 and end date 20 July 1987 reported by Stieltjes and Moutou (1989), Boivin and Bachélery (2009) and Peltier et al. (2009). The Smithsonian Institution's monthly report (SEAN 08/1987) states that this eruption lasted approximately 37 hours and a duration of 1.33 days is used here.

#132. November 1987_i. For this eruption we use the start date 6 November 1987 and end date 8 November 1987 reported by Stieltjes and Moutou (1989), Boivin and Bachélery (2009) and Peltier et al. (2009).

#133. November 1987ⁱⁱ. For this eruption we use the start date 30 November 1987 and end date 1 January 1988 reported by Boivin and Bachélery (2009) and Peltier et al. (2009).

#134. February 1988. For this eruption we use the start date 7 February 1988 and end date 2 April 1988 reported by Boivin and Bachélery (2009) and Peltier et al. (2009).

#135. May 1988. For this eruption we use the start date 18 May 1988 and end date 1 August 1988 reported by Boivin and Bachélery (2009) and Peltier et al. (2009).

#136. August 1988. For this eruption we use the start date 31 August 1988 reported by Boivin and Bachélery (2009) and Peltier et al. (2009) and the end date 12 September 1988 reported by Peltier et al. (2009). Boivin and Bachélery (2009) report this eruption lasting far longer and ending on 26 October 1988, however, The Smithsonian Institution's monthly report (SEAN 13:09) indicates that strong degassing followed the eruptions end in September and it was this that continued into October. Here we have chosen to exclude the end date of Boivin and Bachélery (2009) and use the dates reported by Peltier et al. (2009).

#137. December 1988. For this eruption we use the start date 14 December 1988 and end date 29 December 1988 reported by Boivin and Bachélery (2009) and Peltier et al. (2009).

#138. January 1990. For this eruption we use the start date 18 January 1990 and end date 19 January 1990 reported by Boivin and Bachélery (2009) and Peltier et al. (2009). The Smithsonian Institution's monthly report (SEAN 15:01 and 15:02) document this eruption as starting at 11:24 on 18 January and ending at 06:30 the following morning resulting in the 18 hour (0.75 day) duration used here

#139. April 1990. For this eruption we use the start date 18 April 1990 and end date 8

May 1990 reported by Boivin and Bachélery (2009) and Peltier et al. (2009).

#140. July 1991. For this eruption we use the start date 19 July 1991 and end date 20 July 1991 reported by Boivin and Bachélery (2009) and Peltier et al. (2009). The Smithsonian Institution's monthly report (SEAN 15:01 and 15:02) reports this eruption starting at 03:50 on 19 July and ending at 20:00 on 20 July resulting in the 28 hour (1.17 day) duration used here.

#141. August 1992. For this eruption we use the start date 27 August 1992 and end date 23 September 1992 reported by Boivin and Bachélery (2009) and Peltier et al. (2009).

#142. March 1998. For this eruption we use the start date 9 March 1998 reported by Boivin and Bachélery (2009), Coppola et al. (2009) and Peltier et al. (2009) and end date 21 September 1998 reported by Boivin and Bachélery (2009) and Peltier et al. (2009). The duration given by Coppola et al. (2009) also supports this end date.

#143. July 1999. For this eruption we use the start date 19 July 1999 reported by Coppola et al. (2009), Peltier et al. (2009) and Fukushima et al. (2010) and end date 31 July 1999 reported by Peltier et al. (2009) and Fukushima et al. (2010). The duration given by Coppola et al. (2009) also supports this end date.

#144. September 1999. For this eruption we use the start date 28 September 1999 reported by Coppola et al. (2009), Peltier et al. (2009) and Fukushima et al. (2010) and end date 23 October 1999 reported by Peltier et al. (2009) and Fukushima et al. (2010). The duration given by Coppola et al. (2009) also supports this end date.

#145. February 2000. For this eruption we use the start date 14 February 2000 reported by Fukushima et al. (2005) and end date 3 March 2000 reported by Peltier et al. (2009). Coppola et al. (2009) and Peltier et al. (2009) report the start date 13 February 2000 and Fukushima et al. (2005) report the end date 4 March 2000. The Smithsonian

Institution's monthly report (BGVN 25:07) indicates that the earlier start date was the beginning of a seismic crisis and the later end date refers to gas piston events before the seismic activity ended. We have therefore chosen the dates which best relate to the volcanic activity, however, a + 1 day duration uncertainty is assigned to both the eruptions start and end date to account for this literature-derived uncertainty.

#146. June 2000. For this eruption we use the start date 23 June 2000 reported by Coppola et al. (2009), Peltier et al. (2009) and Fukushima et al. (2010) and the end date 30 July 2000 reported by Peltier et al. (2009) and Fukushima et al. (2010). The duration given by Coppola et al. (2009) also supports this end date.

#147. October 2000. For this eruption we use the start date 12 October 2000 reported by Coppola et al. (2009) and Peltier et al. (2009) and the end date 13 November 2000 reported by Peltier et al. (2009). The duration given by Coppola et al. (2009) also supports this end date.

#148. March 2001. For this eruption we use the start date 27 March 2001 reported by Coppola et al. (2009) and Peltier et al. (2009) and the end date 4 April 2001 reported by Peltier et al. (2009). The duration given by Coppola et al. (2009) also supports this end date.

#149. June 2001. For this eruption we use the start date 11 June 2001 reported by Coppola et al. (2009) and Peltier et al. (2009, 2011) and the end date 7 July 2001 reported by Peltier et al. (2009). The duration given by Coppola et al. (2009) also supports this end date.

#150. January 2002. For this eruption we use the start date 5 January 2002 reported by Coppola et al. (2009) and Peltier et al. (2009) and the end date 16 January 2002 reported by Peltier et al. (2009). Coppola et al. (2009) give a duration of 12 days and a + 1 day duration uncertainty is assigned to the eruption end date to account for this

literature-derived uncertainty.

#151. November 2002. For this eruption we use the start date 16 November 2002 reported by Coppola et al. (2009) and Peltier et al. (2009, 2011) and the end date 3 December 2002 reported by Peltier et al. (2009). Coppola et al. (2009) give a duration of 18 days and a + 1 day duration uncertainty is assigned to the eruption end date to account for this literature-derived uncertainty.

#152. May 2003. For this eruption we use the start date 30 May 2003 reported by Coppola et al. (2009) and Peltier et al. (2009, 2011) and the end date 7 July 2003 reported by Peltier et al. (2009). Coppola et al. (2009) give a far shorter duration of 24 days which may stem from the numerous eruptive phases within this eruption reported by Boivin and Bachélery (2009) and Peltier et al. (2009). These phases either overlap in time or are separated by periods of inactivity of < 10 days and therefore a single eruption with a 38 day duration is reported here.

#153. August 2003. For this eruption we use the start date 22 August 2003 reported by Coppola et al. (2009) and Peltier et al. (2009, 2011) and end date 27 August 2003 reported by Peltier et al. (2009). Froger et al. (2004) report the start date 23 August 2003 and a duration uncertainty of - 1 day is assigned to account for this literature-derived uncertainty. Furthermore, Coppola et al. (2009) give a duration of 6 days and a + 1 day duration uncertainty is assigned to the eruption end date.

#154. September 2003. For this eruption we use the start date 30 September 2003 reported by Coppola et al. (2009) and Peltier et al. (2009, 2011) and the end date 1 October 2003 reported by Peltier et al. (2009). Coppola et al. (2009) give a duration of 0.5 days which is covered in the duration uncertainty of this eruption.

#155. December 2003. For this eruption we use the start date 7 December 2003 reported by Coppola et al. (2009) and Peltier et al. (2009, 2011) and the end date 25

December 2003 reported by Peltier et al. (2009). The duration given by Coppola et al. (2009) also supports this end date.

#156. January 2004. For this eruption we use the start date 8 January 2004 reported by Coppola et al. (2009) and Peltier et al. (2009) and the end date 10 January 2004 reported by Peltier et al. (2009). The duration given by Coppola et al. (2009) also supports this end date.

#157. May 2004. For this eruption we use the start date 2 May 2004 reported by Coppola et al. (2009) and Peltier et al. (2008, 2009) and the end date 18 May 2004 reported by Peltier et al. (2008, 2009). The duration given by Coppola et al. (2009) also supports this end date.

#158 August 2004. For this eruption we use the start date 12 August 2004 reported by Coppola et al. (2009) and Peltier et al. (2009, 2011) and the end date 16 October 2004 reported by Peltier et al. (2008, 2009). The duration given by Coppola et al. (2009) also supports this end date, however, information within The Smithsonian Institution's monthly reports (BGVN 29:12 and 30:11) indicate that the eruption started on 13 August 2004 and ended on 4 October 2004. A duration uncertainty of - 1 day is assigned to the eruption start date and -12 days to the eruption end date to account for this literature-derived uncertainty.

#159. February 2005. For this eruption we use the start date 17 February 2005 reported by Coppola et al. (2009) and Peltier et al. (2008, 2009, 2011) and the end date 26 February 2005 reported by Peltier et al. (2008, 2009). The duration given by Coppola et al. (2009) also supports this end date.

#160. October 2005. For this eruption we use the start date 4 October 2005 reported by Coppola et al. (2009) and Peltier et al. (2008, 2009, 2011) and the end date 17 October 2005 reported by Peltier et al. (2008, 2009). Coppola et al. (2009) give a duration of 14

days and a + 1 day duration uncertainty is assigned to the eruption end date to account for this literature-derived uncertainty.

#161. November 2005. A less than 1 day eruption on the 29 November 2005 is reported by Peltier et al. (2008, 2009, 2011) and Coppola et al. (2009).

#162. December 2005. For this eruption we use the start date 26 December 2005 reported by Coppola et al. (2009) and Peltier et al. (2008, 2009, 2011) and the end date 18 January 2005 reported by Peltier et al. (2009). The duration given by Coppola et al. (2009) also supports this end date, however, Peltier et al. (2008) reports the end date 17 January 2005 and a duration uncertainty of - 1 day is assigned to account for this literature-derived uncertainty.

#163. July 2006. For this eruption we use the start date 20 July 2006 reported by Coppola et al. (2009) and Peltier et al. (2009, 2011) and the end date 14 August 2006 reported by Peltier et al. (2009). Coppola et al. (2009) give a duration of 26 days and a + 1 day duration uncertainty is assigned to the eruption end date to account for this literature-derived uncertainty.

#164. August 2006. For this eruption we use the start date 30 August 2006 reported by Coppola et al. (2009) and Peltier et al. (2009, 2011) and the end date 1 January 2007 reported by Peltier et al. (2009). The duration given by Coppola et al. (2009) also supports this end date.

#165. February 2007. For this eruption we use the start date 18 February 2007 reported by Coppola et al. (2009) and Peltier et al. (2009, 2011) and the end date 19 February 2007 reported by Staudacher et al. (2009) and Peltier et al. (2009). Coppola et al. (2009) give a duration of 0.38 days for this eruption which is covered in the duration uncertainty of this eruption.

#166. March 2007. For this eruption we use the start date 30 March 2007 reported

by Coppola et al. (2009) and Peltier et al. (2009, 2011) and the end date 1 May 2007 reported by Staudacher et al. (2009) and Peltier et al. (2009). Coppola et al. (2009) give a far shorter duration of 0.38 days which may either be a repeat of the previous duration (which is reported as the same) or stem from the numerous eruptive phases within this eruption reported by Peltier et al. (2009). These phases either overlap in time or are separated by periods of inactivity of < 10 days and therefore a single eruption with a 32 day duration is reported here.

#167. September 2008. For this eruption we use the start date 21 September 2008 and the end date 2 October 2008 reported by Staudacher (2010).

#168. November 2008. For this eruption we use the start date 27 November 2008 and the end date 28 November 2008 reported by Staudacher (2010).

#169. December 2008. For this eruption we use the start date 14 December 2008 and the end date 4 February 2009 reported by Staudacher (2010). The Smithsonian Institution's monthly report (BGVN 34:02) contains information about this eruption indicating that although the seismic activity began on this date the eruption started on 15 December 2008. A duration uncertainty of - 1 day is assigned to the eruption start date to account for this literature-derived uncertainty.

#170. November 2009. The Smithsonian Institution's monthly reports (BGVN 34:03 and 37:03) document an eruption starting on 5 November 2009 and ending on 12 January 2010. These dates are used here.

#171. October 2010. The Smithsonian Institution's monthly report (BGVN 37:03) documents an eruption starting on 14 October 2010 and ending on 31 October 2010. These dates are used here.

#172. December 2010. The Smithsonian Institution's monthly report (BGVN 37:03) documents an eruption starting on 9 December 2010 and ending on 10 December 2010.

These dates are used here.

Appendix D

Additional information regarding the Icelandic dataset

The following section contains information about the reported start dates, end dates and eruption durations of the 163 historical Icelandic eruptions from Askja, Brennisteinfjöll, Eyjafjallajökull, Grímsvötn, Hekla, Katla, Krafla, Krýsuvík, Kverkfjöll, Örfajökull, Torfajökull and Vestmannaeyjar reported between the years 1300 AD and 2011 inclusive. In each case any discrepancies in the reported dates are discussed and the duration uncertainty assigned in this study explained. A summary of this information is included within Table D.1. Many eruptions only have start years associated with them and unless otherwise stated this year is sourced from catalogue compiled by The Smithsonian Institution's Global Volcanism Program (Siebert et al., 2010; Venzke et al., 2013). Eruptions with durations used in this study are numbered in Table 3.5; these numbers are reported in column one of Table D.1 and precede the eruption paragraph in the following section.

Section D.14 provides the same information for the fire events documented for Iceland. Each of these is given an identification letter which refers to the ID column in Table 3.6.

APPENDIX D. ICELANDIC ERUPTIONS

Table D.1: Table containing the 163 historical Icelandic eruptions from Askja, Brennisteinfjöll, Eyjafjallajökull, Grímsvötn, Hekla, Katla, Krafla, Krýsuvík, Kverkfjöll, Öraefajökull, Torfajökull and Vestmannaeyjar reported for the period 1300-2011

#	System	Start	Preferred Date		Duration	Duration U/C	
		Year	Start	End		+	-
	Askja	1300					
	Krafla	1300					
1	Hekla	1300	11-07-1300	15-07-1301	369	15.5	15.5
	Grímsvötn	1310	15-11-1310			15	15
	Katla	1311	18-01-1311			0.5	0.5
	Krýsuvík	1325					
	Grímsvötn	1332	15-11-1332			15	15
	Krýsuvík	1340					
	Brennisteinfjöll	1341					
	Grímsvötn	1341	15-05-1341			15	15
	Hekla	1341	19-05-1341			0.5	0.5
	Grímsvötn	1350					
	Grímsvötn	1354					
	Katla	1357					
	Öraefajökull	1362	15-06-1362	15-10-1362	122	60	60
	Grímsvötn	1369					
	Grímsvötn	1370					
	Hekla	1389	01-12-1389	01-07-1390	212	212.5	212.5
	Grímsvötn	1390					
	Katla	1416					
	Grímsvötn	1430					
	Hekla	1440					
	Katla	1440					
	Grímsvötn	1450					
	Katla	1450					
	Grímsvötn	1469					
	Grímsvötn	1470					
	Grímsvötn	1471					
	Torfajökull	1477	15-03-1477			15	15

Continued on next page...

Table D.1 – Continued

#	System	Start Year	Preferred Date		Duration	Duration U/C	
			Start	End		+	-
	Katla	1485					
	Grímsvötn	1490					
	Grímsvötn	1500					
	Katla	1500					
	Grímsvötn	1509					
	Hekla	1510	25-07-1510			0.5	0.5
	Grímsvötn	1521					
	Grímsvötn	1530					
	Katla	1550					
2	Hekla	1554	05-05-1554	15-06-1554	41	20	20
	Katla	1580	11-08-1580				
3	Hekla	1597	03-01-1597	15-07-1597	193	15.5	15.5
	Grímsvötn	1598	07-11-1598				
	Grímsvötn	1603	31-10-1603	15-11-1603	15	15.5	15.5
	Grímsvötn	1610					
	Katla	1612	12-10-1612			0.5	0.5
	Eyjafjallajökull	1613					
	Hekla (?)	1619	29-07-1619			0.5	0.5
	Grímsvötn	1622					
	Katla	1625	02-09-1625	14-09-1625	12	1	1
	Grímsvötn	1629					
	Grímsvötn	1632					
4	Hekla	1636	08-05-1636	15-05-1637	372	15.5	15.5
	Vestmannaeyjar	1637	15-10-1637	28-02-1638	136	75	75
	Grímsvötn	1638	24-02-1638			4	4
	Kverkfjöll	1655	15-04-1655			45	45
	Grímsvötn	1659	15-11-1659			15	15
	Katla	1660	03-11-1660	01-07-1661	240	183	183
	Grímsvötn	1665					
	Grímsvötn	1681	10-04-1681			0.5	0.5
5	Grímsvötn	1684	20-12-1684	10-01-1685	21	1	1

Continued on next page...

APPENDIX D. ICELANDIC ERUPTIONS

Table D.1 – Continued

#	System	Start Year	Preferred Date		Duration	Duration U/C	
			Start	End		+	-
6	Hekla	1693	13-02-1693	01-11-1693	261	45.5	75
	Grìmsvötn	1697					
	Grìmsvötn	1706	15-10-1706			45	45
	Grìmsvötn	1716	06-10-1716			0.5	0.5
	Katla	1721	11-05-1721	15-10-1721	157	45.5	45.5
	Krafla	1724	17-05-1724	18-05-1724	1	1	1
	Grìmsvötn	1725	15-02-1725			15	15
	Hekla	1725	02-04-1725			0.5	0.5
7	Öræfajökull	1727	05-08-1727	15-04-1728	254	20	20
	Krafla	1727	21-08-1727			0.5	0.5
	Krafla	1728	18-04-1728			0.5	0.5
	Krafla	1728	18-12-1728			0.5	0.5
	Krafla	1729	30-06-1729	25-09-1729	87	5.5	5.5
	Kverkfjöll	1729	15-02-1729			45	45
	Kverkfjöll	1729	15-08-1729			15	15
	Grìmsvötn	1730					
8	Krafla	1746	10-07-1746	10-07-1746	0.5	0.04	0.04
	Grìmsvötn	1753	15-10-1753			45	45
9	Katla	1755	17-10-1755	13-02-1756	119	1	1
10	Hekla	1766	05-04-1766	01-05-1768	757	30.5	30.5
11	Grìmsvötn	1783	08-06-1783	07-02-1784	244	1	1
	Grìmsvötn	1785		26-05-1785		0.5	0.5
	Grìmsvötn	1794	15-07-1794			45	45
	Askja	1797					
	Grìmsvötn	1816	15-05-1816	15-06-1816	31	30	30
12	Eyjafjallajökull	1821	15-12-1821	01-02-1823	427	75	75
	Grìmsvötn	1823	04-02-1823			4.5	4.5
13	Katla	1823	26-06-1823	23-07-1823	27	1	1
	Grìmsvötn	1838	15-06-1838			15	15
14	Hekla	1845	02-09-1845	05-04-1846	215	5.5	2.5
	Grìmsvötn	1854					

Continued on next page...

Table D.1 – Continued

#	System	Start Year	Preferred Date		Duration	Duration U/C	
			Start	End		+	-
15	Katla	1860	08-05-1860	27-05-1860	19	1	1
	Grímsvötn	1861	15-05-1861			15	15
	Grímsvötn	1867	26-08-1867			0.5	0.5
16	Grímsvötn	1873	08-01-1873	25-01-1873	17	1	1
17	Askja	1875	18-02-1875	25-02-1875	7	1	1
18	Askja	1875	10-03-1875	23-03-1875	13	1.5	1
19	Askja	1875	28-03-1875	29-03-1875	0.6	0.04	0.04
20	Askja	1875	04-04-1875	15-04-1875	11	5.5	4.5
21	Askja	1875	15-08-1875	17-10-1875	63	1	1
22	Hekla	1878	27-02-1878	15-04-1878	47	15.5	15.5
23	Grímsvötn	1883	15-01-1883	15-04-1883	90	5.5	5.5
	Grímsvötn	1887	15-08-1887	01-07-1889	686	183	183
	Grímsvötn	1891	15-11-1891	16-03-1892	122	15.5	15.5
	Grímsvötn	1897					
	Vestmannaeyjar	1896	15-09-1896			15	15
	Grímsvötn (?)	1903	28-05-1903	12-01-1904	229	15.5	15.5
	Grímsvötn	1910					
24	Hekla	1913	25-04-1913	18-05-1903	23	1	1
25	Katla	1918	12-10-1918	04-11-1918	23	1	1
	Askja	1919					
	Grímsvötn	1919					
	Askja	1921	15-03-1921			0.5	0.5
	Grímsvötn	1922	29-09-1922	23-10-1922	24	1	1
	Askja	1922	15-11-1922			0.5	0.5
	Askja	1923					
	Askja	1923					
	Askja	1924					
	Askja	1926	15-07-1926			45	45
	Kverkfjöll	1929	15-01-1929	15-02-1929	31	30	30
	Grímsvötn	1933	29-11-1933	09-12-1933	10	1	1
26	Grímsvötn	1934	30-03-1934	11-04-1934	12	4.5	4.5

Continued on next page...

APPENDIX D. ICELANDIC ERUPTIONS

Table D.1 – Continued

#	System	Start Year	Preferred Date		Duration	Duration U/C	
			Start	End		+	-
	Askja	1938	19-12-1938			0.5	0.5
	Grímsvötn	1938	15-05-1938			15	15
	Grímsvötn	1939	15-06-1939			15	15
	Grímsvötn	1941	15-04-1941	15-08-1941	122	30	30
	Grímsvötn	1945	25-07-1945			0.5	0.5
27	Hekla	1947	29-03-1947	22-04-1948	390	3.5	1.5
	Grímsvötn	1948	15-02-1948			15	15
	Grímsvötn	1954	15-01-1954			45	45
	Grímsvötn	1954	15-07-1954			15	15
28	Katla	1955	25-06-1955	25-06-1955	0.5	0.04	0.04
	Kverkfjöll	1959					
29	Askja	1961	26-10-1961	17-12-1961	52	1	12.5
30	Vestmannaeyjar	1963	06-11-1963	30-04-1964	176	1	1
31	Vestmannaeyjar	1964	09-06-1964	17-10-1965	495	1	1
32	Vestmannaeyjar	1965	26-12-1965	05-06-1967	526	1	1
	Kverkfjöll	1968	23-05-1968	15-06-1967	23	15.5	15.5
33	Hekla	1970	05-05-1970	05-07-1970	61	5.5	5.5
	Grímsvötn	1972	15-03-1972	15-04-1972	31	30	30
34	Vestmannaeyjar	1973	23-01-1973	26-06-1973	154	1	1
35	Krafla	1975	20-12-1975	20-12-1975	0.2	0.04	0.04
36	Krafla	1977	27-04-1977	27-04-1977	0.5	0.04	0.04
37	Kralfa	1977	08-09-1977	08-09-1977	0.2	0.04	0.04
38	Krafla	1980	16-03-1980	16-03-1980	0.25	0.04	0.04
39	Krafla	1980	10-07-1980	18-07-1980	8	1	1
40	Hekla	1980	17-08-1980	20-08-1980	3	1	1
41	Krafla	1980	18-10-1980	23-10-1980	5	1	1
42	Krafla	1981	30-01-1981	04-02-1981	5	1	1
43	Hekla	1981	09-04-1981	16-04-1981	7	1	1
44	Krafla	1981	18-11-1981	23-11-1981	5	1	1
45	Grímsvötn	1983	28-05-1983	01-06-1983	4	1.5	1.5
	Grímsvötn	1984	20-08-1984			0.5	0.5

Continued on next page...

Table D.1 – Continued

#	System	Start Year	Preferred Date		Duration	Duration U/C	
			Start	End		+	-
46	Krafla	1984	04-09-1984	18-09-1984	14	1	1
47	Hekla	1991	17-01-1991	11-03-1991	53	1	1
48	Gjálp	1996	30-09-1996	13-10-1996	13	1	1
49	Grímsvötn	1998	18-12-1998	28-12-1998	10	1	1
	Katla	1999	18-07-1999	18-07-1999	0.5	0.04	0.04
50	Hekla	2000	26-02-2000	08-03-2000	11	1	1
51	Grímsvötn	2004	01-11-2004	06-11-2004	5	1	1
52	Eyjafjallajökull	2010	20-03-2010	12-04-2010	23	1	1
53	Eyjafjallajökull	2010	14-04-2010	22-05-2010	38	2.5	1.5
54	Grímsvötn	2011	21-05-2011	28-05-2011	7	1	1

U/C = uncertainty. Units: durations and duration uncertainties = days.

D.1 Askja

A: 1300: Excluded. Precise start and end dates of this eruption are unknown.

A: 1797: Excluded. Precise start and end dates of this eruption are unknown.

#17. A: February 1875 (d_6). For this eruption we use the start date 18 February 1875 as reported by Sigurdsson and Sparks (1978) and Sparks et al. (1981) and the end date 25 February 1875 as reported by Sparks et al. (1981).

#18. A: March_(i) 1875 (d_6). For this eruption we use the start date 10 March 1875 reported by Sigurdsson and Sparks (1978), Sigurdsson and Sparks (1981), and Sparks et al. (1981). The end date of this eruption is reported as 23 March 1875 by Sparks et al. (1981) and 24 March 1875 by Sigurdsson and Sparks (1978). Here we use the end date 23 March 1875 and assign a +1 day duration uncertainty to account for this

literature-derived uncertainty.

#19. A: *March_(ii) 1875 (d_1)*. For this eruption we use the start date 28 March 1875 and the end date 29 March 1875 reported by Thorarinsson (1958), Thorarinsson and Sigvaldason (1962), Sigurdsson and Sparks (1978), Sigurdsson and Sparks (1981), Sparks et al. (1981), Carey et al. (2010) and Lupi et al. (2011). Sigurdsson and Sparks (1981) also provides the time of day that the eruption started and ended on these dates (21:00 and noon respectively) and the duration 0.6 days (15 hours) is used as the duration of this eruption.

#20. A: *April 1875 (d_6)*. For this eruption we use the start date 4 April 1875 reported by Sigurdsson and Sparks (1978) and Sparks et al. (1981). The end date of this eruption is reported as 11 April 1875 by Sparks et al. (1981) and 20 April 1875 by Sigurdsson and Sparks (1978). Here we use the end date 15 April 1875 and assign a +5 and -4 day duration uncertainty to account for this literature-derived uncertainty.

#21. A: *August 1875 (d_6)*. For this eruption we use the start date 15 August 1875 reported by Thoroddsen (1925) and the end date 17 October 1875 according to the newspaper Norðanfari (Grímsstaðir, 1875) who report that the eruption ended on the ‘last Sunday of the summer’ (P. Einarsson pers.comm.).

A: *1919: Excluded.* Precise start and end dates of this eruption are unknown.

A: *March 1921: Excluded.* This eruption is reported by Thorarinsson and Sigvaldason (1962) as starting on 15 March 1921, however, the end date is unknown.

A: *November 1922: Excluded.* This is reported by Thorarinsson and Sigvaldason (1962) as starting on 15 November 1922, however, the end date is unknown.

A: *1923_(i): Excluded.* Precise start and end dates of this eruption are unknown.

A: *1923_(ii): Excluded.* Precise start and end dates of this eruption are unknown.

A: 1924: Excluded. Precise start and end dates of this eruption are unknown.

A: July 1926: Excluded. The Smithsonian Institution's Global Volcanism program (Siebert et al., 2010; Venzke et al., 2013) reports this eruption as starting on 15 July 1926 (\pm 45 days), however, the end date is unknown.

A: December 1938: Excluded. The Smithsonian Institution's Global Volcanism program (Siebert et al., 2010; Venzke et al., 2013) reports this eruption as starting on 19 December 1938, however, the end date is unknown.

#29. A: October 1961 (d_6). For this eruption we use the start date 26 October 1961 reported by Thorarinsson and Sigvaldason (1962). The end of this eruption is reported by Thorarinsson and Sigvaldason (1962) as being about a week after 28 November 1961 and they state an end date of 17 December 1961. Here we use the end date of 17 December 1961 and assign a - 12 day duration uncertainty to account for this literature-derived uncertainty.

Chemical composition and duration type classification of Askja eruptions

With the exception of the 28 March 1875 eruption, the other eruptions with reliable durations were all effusive basaltic eruptions (Thorarinsson and Sigvaldason, 1962; Sigurdsson and Sparks, 1981) classified here as single basaltic eruptions with durations d_6 (Fig. 3.7). The 28 March 1875 eruption was an explosive Plinian eruption with produced rhyolitic ejecta (Thorarinsson and Sigvaldason, 1962) and is therefore best described as a single explosive eruption with duration d_1 (Fig. 3.7).

D.2 Brennisteinfjöll

Br: 1341: Excluded. Precise start and end dates of this eruption are unknown.

D.3 Eyjafjallajökull

E: 1613: Excluded. An eruption in the year 1613 is reported by Thordarson and Höskuldsson (2008) and Edwards et al. (2012), however precise start and end dates are unknown.

#12. E: December 1821 (d_2). The start and end date of this eruptive sequence is poorly constrained. Although Larsen (1999) report a start date of 19 December 1821, no other reference to this date have been found. The Smithsonian Institution’s Global Volcanism program (Siebert et al., 2010; Venzke et al., 2013) reports the eruption ending on 1 January 1821, however, alternative sources for this date have not been found. Sammonds et al. (2010) state that eruptive period lasted for 14 months, while Edwards et al. (2012) suggest it lasted 13 months. We have combined the available information to assign a ‘nearest month’ start date of December 1821 and have assumed an end date of 1 February 1823 \pm 30 days.

#52. E: March 2010 (d_6). For this eruption we use the start date 20 March 2010 reported by Sigmundsson et al. (2010), Donovan and Oppenheimer (2011), Sigmarsson et al. (2011), Edwards et al. (2012), Gudmundsson et al. (2012) and Karlsdóttir et al. (2012) and the end date 12 April 2010 reported by Sigmundsson et al. (2010), Edwards et al. (2012), Gudmundsson et al. (2012) and Karlsdóttir et al. (2012).

#53. E: April 2010 (d_5). For this eruption we use the start date 14 April 2010 reported by Sigmundsson et al. (2010), Gudmundsson et al. (2010), Arason et al. (2011), Sigmarsson et al. (2011), Edwards et al. (2012), Gudmundsson et al. (2012), Karlsdóttir

et al. (2012), Stevenson et al. (2012) and Woodhouse et al. (2013). The end date of this eruption is reported as 22 May 2010 by Gudmundsson et al. (2010), Edwards et al. (2012), Gudmundsson et al. (2012), Karlsdóttir et al. (2012), Stevenson et al. (2012), Woodhouse et al. (2013) and 24 May 2010 by Sigmundsson et al. (2010). Here we use the end date 22 May 2010 and assign a duration uncertainty of + 2 days is to account for this literature-derived uncertainty.

Chemical composition and duration type classification of Eyjafjallajökull eruptions

The three eruption of Eyjafjallajökull have been been classified as different duration types according to Fig. 3.7. The 1821-1823 eruption represents a sequence of explosive rhyolitic eruptions and is therefore described here as a d_2 eruption. In contrast the March 2010 flank eruption was not explosive but is described as a basaltic effusive fissure eruption by Edwards et al. (2012) and Gudmundsson et al. (2010) and is therefore described by the d_6 category of Fig. 3.7.

The April 2010 summit eruption was non-basaltic with erupted products having SiO_2 contents of 61-58 wt % (Gudmundsson et al., 2012). Gudmundsson et al. (2012), Karlsdóttir et al. (2012) and Woodhouse et al. (2013) recognise phases within the eruption and indicate that it consisted of an initial explosive phase, followed by a dominantly effusive phase before becoming explosive once again. During the effusive phase explosive activity was weak but sustained, producing 2-4 km high plumes. The return to explosive activity during the eruption suggests that its total duration is best described by the d_5 category of Fig. 3.7.

These eruptions and their classification are discussed in greater detail in subsection 3.4.3.

D.4 Grímsvötn

G: 1310: Excluded. The Smithsonian Institution's Global Volcanism program (Siebert et al., 2010; Venzke et al., 2013) reports this eruption as starting in November and it is treated according to the 'nearest month' category of Table 2.1, however, the end date is unknown.

G: 1332: Excluded. The Smithsonian Institution's Global Volcanism program (Siebert et al., 2010; Venzke et al., 2013) reports this eruption as starting in November and it is treated according to the 'nearest month' category of Table 2.1, however, the end date is unknown.

G: 1341: Excluded. The Smithsonian Institution's Global Volcanism program (Siebert et al., 2010; Venzke et al., 2013) reports this eruption as starting in May and it is treated according to the 'nearest month' category of Table 2.1, however, the end date is unknown.

G: 1350: Excluded. Precise start and end dates of this eruption are unknown.

G: 1354: Excluded. Precise start and end dates of this eruption are unknown.

G: 1369: Excluded. Precise start and end dates of this eruption are unknown.

G: 1370: Excluded. Precise start and end dates of this eruption are unknown..

G: 1390: Excluded. Precise start and end dates of this eruption are unknown.

G: 1430: Excluded. Precise start and end dates of this eruption are unknown.

G: 1450: Excluded. Precise start and end dates of this eruption are unknown.

G: 1469: Excluded. Precise start and end dates of this eruption are unknown.

G: 1470: Excluded. Precise start and end dates of this eruption are unknown.

G: 1471: Excluded. Precise start and end dates of this eruption are unknown.

G: 1490: Excluded. Precise start and end dates of this eruption are unknown.

G: 1500: Excluded. Precise start and end dates of this eruption are unknown.

G: 1509: Excluded. Precise start and end dates of this eruption are unknown.

G: 1521: Excluded. Precise start and end dates of this eruption are unknown.

G: 1530: Excluded. Precise start and end dates of this eruption are unknown.

G: 1598: Excluded. The Smithsonian Institution's Global Volcanism program (Siebert et al., 2010; Venzke et al., 2013) reports this eruption as starting on 7 November 1598, however, the end date is unknown.

G: October 1603: Excluded. The Smithsonian Institution's Global Volcanism program (Siebert et al., 2010; Venzke et al., 2013) reports this eruption as starting on 31 October 1603 and ending in November 1603. The end date is treated according to the 'nearest month' category of Table 2.1, however, this results in a total duration uncertainty of > 50 % of the preferred eruption duration. Also alternative sources for these dates have not been found.

G: 1610: Excluded. Precise start and end dates of this eruption are unknown.

G: 1622: Excluded. Precise start and end dates of this eruption are unknown.

G: 1629: Excluded. Precise start and end dates of this eruption are unknown.

G: 1632: Excluded. Precise start and end dates of this eruption are unknown.

APPENDIX D. ICELANDIC ERUPTIONS

G: February 1638: Excluded. The Smithsonian Institution's Global Volcanism program (Siebert et al., 2010; Venzke et al., 2013) reports this eruption as starting on 24 February 1638 (± 4 days), however, the end date is unknown.

G: November 1659: Excluded. The Smithsonian Institution's Global Volcanism program (Siebert et al., 2010; Venzke et al., 2013) reports this eruption as starting in November 1659 and it is treated according to the 'nearest month' category of Table 2.1, however, the end date is unknown.

G: 1665: Excluded. Precise start and end dates of this eruption are unknown.

G: April 1681: Excluded. The Smithsonian Institution's Global Volcanism program (Siebert et al., 2010; Venzke et al., 2013) reports this eruption as starting on 10 April 1681, however, the end date is unknown.

#5. G: December 1684 (d_6). For this eruption we use the start date 20 December 1684 and end date 10 January 1685 as reported by Þórarinnsson (1974).

G: 1697: Excluded. Precise start and end dates of this eruption are unknown.

G: October 1706: Excluded. The Smithsonian Institution's Global Volcanism program (Siebert et al., 2010; Venzke et al., 2013) reports this eruption as starting on 15 October 1706 (± 45 days), however, the end date is unknown.

G: October 1716: Excluded The Smithsonian Institution's Global Volcanism program (Siebert et al., 2010; Venzke et al., 2013) reports this eruption as starting on 6 October 1716, however, the end date is unknown.

G: February 1725: Excluded The Smithsonian Institution's Global Volcanism program (Siebert et al., 2010; Venzke et al., 2013) reports this eruption starting in February 1725 and it is treated according to the 'nearest month' category of Table 2.1, however, the end date is unknown.

G: 1730: Excluded. Precise start and end dates of this eruption are unknown.

G: October 1753: Excluded. The Smithsonian Institution's Global Volcanism program (Siebert et al., 2010; Venzke et al., 2013) reports this eruption as starting on 15 October 1753 (± 45 days), however, the end date of this eruption is unknown.

#11. G: June 1783 (d_6). For this eruption we use the start date 8 June 1783 and the end date 7 February 1784 reported by Thordarson and Self (1993), Thordarson and Self (2003) and Thordarson et al. (2003).

G: 1785: Excluded. A start date is not reported for this eruption, however, its end date is reported as 26 May 1785 by Thordarson and Self (1993), Thordarson and Self (2003) and Thordarson et al. (2003).

G: July 1794: Excluded. The Smithsonian Institution's Global Volcanism program (Siebert et al., 2010; Venzke et al., 2013) reports this eruption as starting on 15 July 1794 (± 45 days), however, the end date is unknown.

G: May 1816: Excluded. The Smithsonian Institution's Global Volcanism program (Siebert et al., 2010; Venzke et al., 2013) reports this eruption as starting in May 1816 and ending in June 1816. If these are treated according to the 'nearest month' category of Table 2.1 the duration uncertainty would be $> 50\%$ of the preferred eruption duration. Also alternative sources for these dates have not been found.

G: July 1823: Excluded. The Smithsonian Institution's Global Volcanism program (Siebert et al., 2010; Venzke et al., 2013) reports this eruption as starting on 4 February 1823 (± 4 days), however, the end date is unknown.

G: June 1838: Excluded. The Smithsonian Institution's Global Volcanism program (Siebert et al., 2010; Venzke et al., 2013) reports this eruption as starting in June 1838 and it is treated according to the 'nearest month' category of Table 2.1, however, the end date

is unknown.

G: 1854: Excluded. Precise start and end dates of this eruption are unknown.

G: May 1861: Excluded. The Smithsonian Institution's Global Volcanism program (Siebert et al., 2010; Venzke et al., 2013) reports this eruption as starting in May 1861 and it is treated according to the 'nearest month' category of Table 2.1, however, the end date is unknown.

G: August 1867: Excluded. The Smithsonian Institution's Global Volcanism program (Siebert et al., 2010; Venzke et al., 2013) reports this eruption as starting on 26 August 1867, however, the end date is unknown.

#16. G: January 1873 (d_6). For this eruption we use the start date 8 January 1873 and the end date 25 January 1873 as reported by Þórarinnsson (1974).

#23. G: January 1883 (d_6). For this eruption we use the start date 15 January 1883 and the end date 15 April 1883 (± 5 days) as reported by Þórarinnsson (1974).

G: August 1887: Excluded. The Smithsonian Institution's Global Volcanism program (Siebert et al., 2010; Venzke et al., 2013) reports this eruption as starting on 15 August 1887 and ending in the year 1889. The end date of this eruption is treated according to the 'nearest year' category of Table 2.1, however, alternative sources for these dates have not been found.

G: November 1891: Excluded. The Smithsonian Institution's Global Volcanism program (Siebert et al., 2010; Venzke et al., 2013) reports this eruption as starting in November 1891 and ending on 16 March 1891. The start date of this eruption is treated according to the 'nearest month' category of Table 2.1, however, alternative sources for these dates have not been found.

G: 1897: Excluded. Precise start and end dates of this eruption are unknown.

G: 1910: Excluded. Precise start and end dates of this eruption are unknown.

G: 1919: Excluded. Precise start and end dates of this eruption are unknown.

G: September 1922: Excluded. The Smithsonian Institution's Global Volcanism program (Siebert et al., 2010; Venzke et al., 2013) reports this eruption as starting on 29 September 1922 and ending on 23 October 1923, however, alternative sources for these dates have not been found.

G: November 1933: Excluded. The Smithsonian Institution's Global Volcanism program (Siebert et al., 2010; Venzke et al., 2013) reports this eruption as starting on 29 November 1933 and ending on 9 December 1933, however, however, alternative sources for these dates have not been found.

#26. G: March 1934 (d_6). For this eruption we use the start date 30 March 1934 reported by Þórarinnsson (1974) and Gudmundsson (2005). Reported end dates for this eruption range from 7 April 1934 to 15 April 1934 (P. Einarsson pers. comm.). Here we use the end date 11 April 1934 reported by Þórarinnsson (1974) and a duration uncertainty of ± 4 days has been assigned to account for this literature-derived uncertainty.

G: May 1938: Excluded. This eruption is reported by Gudmundsson (2005) as starting in May 1938 and is treated according to the 'nearest month' category of Table 2.1, however, the end date is unknown.

G: June 1939: Excluded. The Smithsonian Institution's Global Volcanism program (Siebert et al., 2010; Venzke et al., 2013) reports this eruption as starting in June 1939 and it is treated according to the 'nearest month' category of Table 2.1, however, the end date is unknown.

G: April 1941: Excluded. The Smithsonian Institution's Global Volcanism program

(Siebert et al., 2010; Venzke et al., 2013) reports this eruption as starting in April 1941 and ending in August 1941. Both the start and end date of this eruption have been treated according to the ‘nearest month’ category of Table 2.1, however, alternative sources for these dates have not been found.

G: July 1945: Excluded. The Smithsonian Institution’s Global Volcanism program (Siebert et al., 2010; Venzke et al., 2013) reports this eruption as starting on 25 July 1945, however, the end date is unknown.

G: February 1948. The Smithsonian Institution’s Global Volcanism program (Siebert et al., 2010; Venzke et al., 2013) reports this eruption as starting in February 1948 and it is treated according to the ‘nearest month’ category of Table 2.1, however, the end date is unknown.

G: January 1954: Excluded. The Smithsonian Institution’s Global Volcanism program (Siebert et al., 2010; Venzke et al., 2013) reports this eruption as starting on 15 January 1954 (± 45 days), however, the end date is unknown.

G: July 1954: Excluded. The Smithsonian Institution’s Global Volcanism program (Siebert et al., 2010; Venzke et al., 2013) reports this eruption as starting in July 1954 and it is treated according to the ‘nearest month’ category of Table 2.1, however, the end date of this eruption is unknown.

G: March 1972: Excluded. The Smithsonian Institution’s Global Volcanism program (Siebert et al., 2010; Venzke et al., 2013) reports this eruption as starting in March 1972 and ending in April 1972. Both the start and end date of this eruption is treated according to the ‘nearest month’ category of Table 2.1, however, this results in a duration uncertainty that is $> 50\%$ of the preferred eruption duration. Also alternative sources for these dates have not been found.

#45. G: May 1983 (d_6). For this eruption we use the start date 28 May 1983 according

to Grönvold and Jóhannesson (1984) who state that although the eruption was first observed on 29 May 1983, intense seismic activity and volcanic tremor began the day before and most likely represents the start of the eruption. Here we assign a -1 day duration uncertainty to account for this literature derived uncertainty. Similarly, activity was last observed on 1 June 1983 (Einarsson and Brandsdóttir, 1984; Grönvold and Jóhannesson, 1984), however seismic activity finished the following day. Here we use an end date of 1 June 1983 and assign a duration uncertainty of +1 day to account for this literature derived uncertainty. Einarsson and Brandsdóttir (1984) state that the eruption lasted for 3.5 days, which is covered within the uncertainty of this eruption.

G: August 1984: Excluded. The Smithsonian Institution's Global Volcanism program (Siebert et al., 2010; Venzke et al., 2013) reports this eruption as starting on 20 August 1984, however, the end date is unknown.

#49. G: December 1998 (d_6). For this eruption we use the start date 18 December 1998 reported by Sigmarsson et al. (2000). The Smithsonian Institution's Global Volcanism program (Siebert et al., 2010; Venzke et al., 2013) reports this eruption as ending on 28 December 1998, however, other sources reporting a specific end date for this eruption have not been found. Sigmarsson et al. (2000) report that the eruption had a total duration of 10 days which supports this end date and it is therefore used in this study.

#51. G: November 2004 (d_6). For this eruption we use the start date 1 November 2004 reported by Vogfjörð et al. (2005), Witham et al. (2007) and Jude-Eton et al. (2012) and the end date 6 November 2004 reported by Vogfjörð et al. (2005) and Jude-Eton et al. (2012).

#54. G: May 2011 (d_6). For this eruption we use the start date 21 May 2011 and the end date 28 May reported by Nordic Volcanological Center (2013) and Tesche et al. (2012).

Chemical composition and duration type classification of Grimsvötn eruptions

The sub-glacial nature of the Grimsvötn volcanic system makes defining the type of eruption difficult. Where known (eruption #11, #26, #45, #49 and #48, Table D.1) these eruptions are all basaltic in composition and display largely effusive activity with any explosive phases being phreatomagmatic or surtseyan due to their interaction with ice (Thordarson and Self, 1993; Jakobsson, 1979; Sigmarsson et al., 2000; Gudmundsson, 2005). The other eruptions here are assumed to be similar and therefore all eruptions from Grimsvötn used in this study are attributed to the d_6 category of Fig. 3.7.

D.5 Hekla

#1 H: December 1300 (d_4). For this eruption we use the start date 11 July 1300 as reported by Thorarinsson (1967a). The precise end date of this eruption is unknown, however, Thorarinsson (1967a) states that the eruption lasted “approximately 12 months”. Here we use the end date 15 July 1301 and have assigned a duration uncertainty of + 15 and - 15 days to account for this information. The presence of an associated tephra layer has been used to infer that the eruption had an explosive initial phase, however, its precise time of emplacement and thus its duration is unknown (Thorarinsson, 1967a).

H: 1341: Excluded. This eruption is reported by Thorarinsson (1967a) and Thorarinsson et al. (1970) to have started on 19 May 1341, however, the end date is unknown.

H: 1389: Excluded. The Smithsonian Institution’s Global Volcanism Program reports this eruption as starting on 1 December 1389 (± 30 days) and ending in 1390. The end date of this eruption is treated according to the ‘nearest year’ category of Table 2.1,

however, this results in a duration uncertainty that is $> 50\%$ of the preferred eruption duration. Also alternative sources for this eruption have not been found.

H:1440: Excluded. Precise start and end dates of this eruption are unknown.

H: July 1510: Excluded. This eruption is reported by Thorarinsson (1967a) and Thorarinsson et al. (1970) as starting on 25 July 1510, however, the end date is unknown.

#2. H: May 1554 (d_6). This eruption is reported by Thorarinsson (1967a) as starting in early May or June and lasting for nearly 6 weeks. Here we use the start date 5 May 1554 (± 5 days) according to the ‘early month’ category of Table 2.1 and the end date 15 June 1554 according to the ‘nearest month’ category of Table 2.1 and as reported by the Smithsonian Institution’s Global Volcanism Program Siebert et al. (2010); Venzke et al. (2013). This results in a preferred eruption duration of 41 days (slightly less than 6 weeks) and a maximum duration uncertainty of ± 20 days.

#3. H: January 1597 (d_4). For this eruption we use the start date 3 January 1597 reported by Thorarinsson (1967a) and Thorarinsson et al. (1970). Thorarinsson (1967a) and Thorarinsson et al. (1970) report that it lasted for greater than 6 months. Here we use the end date 15 July 1597 (± 15 days) which results in a preferred eruption duration of 193 days and a maximum duration uncertainty of ± 15 days.

#4. H: May 1636 (d_{3a} , d_{3b} and d_4). For this eruption we use the start date 8 May 1636 reported by Thorarinsson (1967a). The precise end date for this eruption is unknown, however, the eruption is reported as lasting ‘a good 12 months’ by Thorarinsson (1967a) and Thorarinsson et al. (1970) and therefore the end date 15 May 1637 (± 15 days) is assigned and used in this study.

#6 H: February 1693 (d_{3a} , d_{3b} and d_4). For this eruption we use the start date 13 February 1693 reported by Thorarinsson (1967a), however, Thorarinsson et al. (1970) report

this eruption as starting on 13 January 1693 so a duration uncertainty of - 30 days has been assigned to the eruption start date to account for this literature-derived uncertainty. The precise end date of this eruption is unknown, however, Thorarinsson (1967a) state that the eruption lasted ‘more than 7 month and possibly 10.5 months’. Here we use the end date 1 November 1693 and assign a duration uncertainty of ± 45 days to the end date of this eruption to account for this information. The duration of the initial explosive phase of this eruption is reported by Thorarinsson (1967a) as lasting for 12 hours.

H: April 1725: Excluded. This eruption is reported by Thorarinsson (1967a) as starting on 2 April 1725. Thorarinsson et al. (1970) report that the eruption lasted ‘well into that spring’, however, the precise end date is unknown.

#10. H: April 1766 (d_{3a} , d_{3b} and d_4). For this eruption we use the start date 5 April 1766 reported by Thorarinsson (1967a) and Thorarinsson et al. (1970). The precise end date of this eruption is unknown, however, descriptions within Thorarinsson (1967a) suggest that the eruption ended in April 1768 and that explosions continued into May. Here we use the end date 1 May 1768 ± 30 days to account for this information. It is worth noting that the eruption may have experienced some quiet periods between August 1767 and March 1768, however, the exact nature of these phases is unknown (Thorarinsson, 1967a). The duration of the initial explosive phase of this eruption is reported by Thorarinsson (1967a) as lasting approximately 4 hours.

#14. H: September 1845 (d_{3a} , d_{3b} and d_4). For this eruption we use the start date 2 September 1845 reported by Thorarinsson (1967a), Thorarinsson et al. (1970), Grönvold et al. (1983) and Thorarinsson et al. (1973). The end of this eruption is reported by Grönvold et al. (1983) as 3 April 1846 and by Thorarinsson (1967a) as either 5 or 10 April 1846. Here we use the end date 5 April 1846 and assign a duration uncertainty of + 5 days and - 2 days to account for this literature-derived uncertainty. The duration of the initial explosive phase of this eruption is reported by Thorarinsson (1967a)

and Thorarinsson et al. (1970) as lasting approximately 4 hours.

A small recurrence of activity at Hekla is reported on the 13th-16th August, however, its status as an eruption is uncertain (Thorarinsson, 1967a).

#22. H: February 1878 (d_6). For this eruption we use the start date 27 February 1878 reported by Thorarinsson et al. (1970). Thorarinsson et al. (1970) report the eruption was over within about 2 months and therefore the end date 15 April 1878 is used here and treated according to the ‘nearest month’ category of Table 2.1.

#24. H: April 1913 (d_6). For this eruption we use the start date 25 April 1913 and the end date 18 May 1913 as reported by Thorarinsson et al. (1970).

#27. H: March 1947 (d_{3a} , d_{3b} and d_4). For this eruption we use the start date 29 March 1947 reported by Þórarinnsson (1950), Þórarinnsson (1954), Thorarinsson (1967a), Thorarinsson et al. (1970) and Þórarinnsson (1974). Thorarinsson et al. (1970) report that lava was last seen at Hekla on 21 April 1948 and Jakobsson et al. (2008) report this as the end date, however, Einarsson (1949) report this eruption as ending between 22 and 25 April 1948. Here we use the end date 22 April 1948 and assign a duration uncertainty of + 3 days and - 1 day to account for this literature-derived uncertainty. The duration of the initial explosive phase of this eruption is reported by Thorarinsson (1967a) and Þórarinnsson (1974) as lasting approximately 1 hour.

#33. H: May 1970 (d_{3a} , d_{3b} and d_4). For this eruption we use the start date 5 May 1970 reported by Thorarinsson et al. (1970) and Tryggvason (1994). The end date of this eruption is reported by Thorarinsson et al. (1970) as 5 July 1970 and Tryggvason (1994) states that the eruption lasted for two months, while Grönvold et al. (1983) report that the eruption lasted for 64 days. It can be inferred from this that the eruption ended early in July and therefore we have treated this according to the ‘early month’ category of Table 2.1. The duration of the initial explosive phase of this eruption can

be inferred from information within the monthly report Card 0936 (The Smithsonian Institution's Global Volcanism Program) as lasting approximately 2.5 hours.

#40. H: August 1980 (d_{3a} , d_{3b} and d_4) For this eruption we use the start date 17 August 1980 and the end date 20 August 1980 reported by Grönvold et al. (1983) and Tryggvason (1994). The duration of the initial explosive phase of this eruption is inferred from the main ash fall period as having a duration of 2 hours (Grönvold et al., 1983).

#43. H: April 1981 (d_4) For this eruption we use the start date 9 April 1981 and the end date 16 April 1981 reported by Grönvold et al. (1983) and Tryggvason (1994). The duration of the initial explosive phase of this eruption is unknown.

#47. H: January 1991 (d_{3a} , d_{3b} and d_4) For this eruption we use the start date 17 January 1991 reported by Gudmundsson et al. (1992), Larsen et al. (1992), Tryggvason (1994), Haraldsson and Ólafsdóttir (2002) and Soosalu et al. (2003) and the end date 11 March 1991 reported by Gudmundsson et al. (1992), Haraldsson and Ólafsdóttir (2002) and Soosalu et al. (2003). The duration of the initial explosive phase of this eruption can be inferred from information within the monthly report Cards BGVN 15:12 and 16:01 (The Smithsonian Institution's Global Volcanism Program) as lasting approximately 10 hours.

#50. H: February 2000 (d_{3a} , d_{3b} and d_4). For this eruption we use the start date 26 February 2000 and the end date 8 March 2000 reported by Haraldsson and Ólafsdóttir (2002), Haraldsson et al. (2002) and Ólafsdóttir et al. (2002). The start date and duration reported by Höskuldsson et al. (2007) also support this information. The duration of the initial explosive phase of this eruption can be inferred from information within Höskuldsson et al. (2007) as lasting approximately 4 hours.

Chemical composition and duration type classification of Hekla eruptions

15 eruptions from Hekla have reported eruption durations that are considered reliable and used in this study. 12 of these are from Hekla's central volcano and 3 are from its associated fissure swarm. Eruptions from the central volcano are either known or inferred to have been mixed eruptions (Fig. 3.7.), with a high silica content initial explosive phase followed by lower silica effusive phase (Thorarinsson, 1967a; Thordarson and Larsen, 2007). Each of these eruptions have a total duration d_4 , however the duration of the initial explosive phase d_{3a} is not always available. Information about the explosive phase of each eruption is discussed below. The fissure swarm produces basaltic eruptions (Thorarinsson, 1967a; Thordarson and Larsen, 2007) and therefore these three eruptions fall into the single basaltic eruption category of Fig. 3.7.

D.6 Katla

Ka: 1311: Excluded. The Smithsonian Institution's Global Volcanism program (Siebert et al., 2010; Venzke et al., 2013) reports this eruption as starting on 18 January 1311, however, the end date is unknown.

Ka: 1357: Excluded. Precise start and end dates of this eruption are unknown.

Ka: 1416: Excluded. Precise start and end dates of this eruption are unknown.

Ka: 1440: Excluded. Precise start and end dates of this eruption are unknown.

Ka: 1450: Excluded. Precise start and end dates of this eruption are unknown.

Ka: 1485: Excluded. Precise start and end dates of this eruption are unknown.

Ka: 1500: Excluded. Precise start and end dates of this eruption are unknown.

Ka: 1550: Excluded. Precise start and end dates of this eruption are unknown.

Ka: August 1580: Excluded. This eruption is reported by Eliasson et al. (2006) as starting on 11 August 1580, however, the end date of this eruption is unknown.

Ka: October 1612: Excluded. This eruption is reported by Eliasson et al. (2006) as starting on 12 October 1612, however, the end date is unknown.

Ka: September 1625: Excluded. This eruption is reported by Thorarinsson (1958) and Eliasson et al. (2006) as starting on 2 September 1625. The Smithsonian Institution's Global Volcanism program (Siebert et al., 2010; Venzke et al., 2013) reports this eruption as ending on 14 September 1625, however, alternative sources for these dates have not been found.

Ka: November 1660: Excluded. This eruption is reported by Thorarinsson (1958) and Eliasson et al. (2006) as starting on 3 November 1660. The end date of this eruption is reported as the year 1661 by the Smithsonian Institution's Global Volcanism program (Siebert et al., 2010; Venzke et al., 2013) and is treated according to the 'nearest year' category of Table 2.1, however, alternative sources for these dates have not been found.

Ka: May 1721: Excluded. This eruption is reported by Þórarinnsson (1975) and Eliasson et al. (2006) as starting on 11 May 1721. The Smithsonian Institution's Global Volcanism program (Siebert et al., 2010; Venzke et al., 2013) reports this eruption as ending on 15 October 1721 (± 45 days), however, alternative sources for these dates or additional information about this eruption have not been found.

#9. Ka: October 1755 (d_6). For this eruption we use the start date 17 October reported by Thorarinsson (1958), Þórarinnsson (1975) and Eliasson et al. (2006) and the end date

13 February 1756 reported by Þórarinnsson (1975).

#13. Ka: June 1823 (d_6). For this eruption we use the start date 26 June 1823 reported by Þórarinnsson (1975) and Eliasson et al. (2006) and the end date 23 July 1823 reported by Þórarinnsson (1975).

#15. Ka: May 1860 (d_6). For this eruption we use the start date 8 May 1860 reported by Þórarinnsson (1975) and Eliasson et al. (2006) and the end date 27 May 1860 reported by Þórarinnsson (1975).

#25. Ka: October 1918 (d_6). For this eruption we use the start date 12 October 1918 as reported by Þórarinnsson (1975), Gudmundsson (2005) and Eliasson et al. (2006) and the end date 4 November 1918 as reported by Þórarinnsson (1975). Although Gudmundsson (2005) did not state a specific end date for this eruption, he reported that the eruption lasted approximately 3 weeks which is in accordance with the dates used here.

#28. Ka: June 1955 (d_6). A less than one day eruption is reported on 25 June 1955 by Gudmundsson (2005). Some debate existed about whether this was an actual eruption, due to it not breaking through the ice, however, it is now largely accepted (P. Einarsson pers. comm.) and is therefore included in the analyses of this study.

Ka: July 1999: Excluded. 20 minutes of volcanic tremor is reported on 17 July 1999 followed by a Jokullhauþ on 18 July 1999 lasting less than 24 hours by the BVGN 24:09 monthly report (The Smithsonian Institution's Global Volcanism Program). However, its status as an eruption is debated (P. Einarsson pers. comm.) and it is therefore excluded from the analyses of this study.

Chemical composition and duration type classification of Katla eruptions

Given the ice covered nature of Katla the chemistry of erupted products for its individual eruptions are difficult to find. Jakobsson (1979) analysed 34 samples from different eruptive units from the ice-free portion of the system and found that they were all transitional alkali basalts with a narrow chemical range. This and the lack of any intermediate or acid rocks attributed to Katla by previous authors (Jakobsson, 1979) has led to all eruptions from Katla being considered as single basaltic eruptions in the d_6 category of Fig. 3.7

D.7 Krafla

Kr: 1300: Excluded. Precise start and end dates of this eruption are unknown.

Kr: May 1724: Excluded. This eruption is reported by Thorarinsson (1979) and Thorarson and Höskuldsson (2008) as starting on 17 May 1724. The Smithsonian Institution's Global Volcanism program (Siebert et al., 2010; Venzke et al., 2013) reports this eruption as ending on 18 May 1724, however, alternative sources for this date has not been found.

Kr: August 1727: Excluded This is reported by the Smithsonian Institution's Global Volcanism program (Siebert et al., 2010; Venzke et al., 2013) as starting on 21 August 1727, however, the end date is unknown.

Kr: April 1728: Excluded. This eruption is reported by Thorarinsson (1979) as starting on 18 April 1728, however, the end date is unknown.

Kr: August 1728: Excluded This eruption is reported by the Smithsonian Institution's

Global Volcanism program (Siebert et al., 2010; Venzke et al., 2013) as starting on 18 December 1728, however, the end date is unknown.

Kr: June 1729: Excluded. This eruption is reported by the Smithsonian Institution's Global Volcanism program (Siebert et al., 2010; Venzke et al., 2013) as starting on 30 June 1729 and is assumed to be the final eruptive episode of the 1724-1729 Krafla fires, which ended in late September. When treated according to the 'late month' category of Table 2.1 this results in an end date of 25 September 1729 \pm 5 days which is in accordance with the end date reported by the Smithsonian Institution's Global Volcanism program (Siebert et al., 2010; Venzke et al., 2013). However, alternative sources for these dates have not been found.

#8. Kr: July 1746 (d_6). A less than one day eruption on 10 July 1746 is reported by Thorarinsson (1979).

#35. Kr: December 1975 (d_6). A less than one day eruption on 20 December 1975 is reported by Thorarinsson (1979), Einarsson (1991) and Harris et al. (2000). The SEAN 01:03 monthly report (The Smithsonian Institution's Global Volcanism Program) record this eruption as starting at 11:20 and ending at 17:00 on this day, giving a more precise eruption duration of 5.5 hours which is used in this study.

#36. Kr: April 1977 (d_6). A less than one day eruption on 27 April 1977 is reported by Björnsson et al. (1979), Einarsson (1991) and Harris et al. (2000).

#37. Kr: September 1977 (d_6). A less than one day eruption on 8 September 1977 is reported by Björnsson et al. (1979), Brandsdóttir and Einarsson (1979), Einarsson (1991) and Sturkell et al. (2009). The SEAN 02:09 monthly report (The Smithsonian Institution's Global Volcanism Program) and Brandsdóttir and Einarsson (1979) report this eruption as starting at 18:00 and ending by 22:30 on this day, giving a more precise eruption duration of 4.5 hours which is used in this study.

#38. Kr: March 1980 (d_6). A less than one day eruption on 16 March 1980 is reported by Tryggvason (1980) and Sturkell et al. (2009). The SEAN 05:03 monthly report (The Smithsonian Institution's Global Volcanism Program) report this eruption as starting at 16:20 and ending by 22:30 on this day, giving a more precise eruption duration of 6 hours which is used in this study.

#39. Kr: July 1980 (d_6). For this eruption we use the start date 10 July 1980 and the end date 18 July 1980 reported by Sturkell et al. (2009).

#41. Kr: October 1980 (d_6). For this eruption we use the start date 18 October 1980 and the end date 23 October 1980 reported by Einarsson (1991) and Sturkell et al. (2009).

#42. Kr: January 1981 (d_6). For this eruption we use the start date 30 January 1981 and the end date 4 February 1981 reported by Tryggvason (1984), Einarsson (1991) and Sturkell et al. (2009).

#44. Kr: November 1981 (d_6). For this eruption we use the start date 18 November 1981 and the end date 23 November 1981 reported by Einarsson (1991) and Sturkell et al. (2009).

#46. Kr: September 1984 (d_6). For this eruption we use the start date 4 September 1984 and the end date 18 September 1984 reported by Einarsson (1991), Rossi (1997) and Sturkell et al. (2009).

Chemical composition and duration type classification of the Krafla eruptions used in this study

The eruptions from Krafla with reported durations that are considered reliable and used in this study are individual episodes from either the 1724-1729 Mývatn fires (#

8, Table 3.5) or the 1975-1884 Krafla fires (#36, #36, #37, #38, #39, #41, #42, #44 and #46, Table 3.5). These episodes of periodic rifting and faulting are characterised by small effusive eruptions with outpourings of basaltic lava (Björnsson et al., 1979; Thordarson and Larsen, 2007). For this reason these eruptions are all characterised as single basaltic eruptions d_6 eruption durations (Fig. 3.7). The first eruption of the Mývatn fires in 1724 would be an exception to this if its duration were used. It was an explosive eruption ejecting a small quantity of rhyolite pumice and is the most recent example of explosive silicic volcanism at Krafla (Grönvold, 1984).

D.8 Krýsuvík

Krý: 1325: Excluded. Precise start and end dates of this eruption are unknown.

Krý: 1340: Excluded. Precise start and end dates of this eruption are unknown.

D.9 Kverkfjöll

Kv: April 1655: Excluded. The Smithsonian Institution's Global Volcanism program (Siebert et al., 2010; Venzke et al., 2013) reports this eruption as starting on 15 April 1655 (± 45 days), however, the end date is unknown.

Kv: February 1729: Excluded. The Smithsonian Institution's Global Volcanism program (Siebert et al., 2010; Venzke et al., 2013) reports this eruption as starting on 15 February 1729 (± 45 days), however, the end date is unknown.

Kv: August 1729: Excluded. The Smithsonian Institution's Global Volcanism Program (Siebert et al., 2010; Venzke et al., 2013) reports this eruption as starting in August 1729 and is treated according to the 'nearest month' category of Table 2.1, however,

the end date is unknown.

Kv: August 1929: Excluded. The Smithsonian Institution's Global Volcanism Program reports this eruption as starting in January 1929 and ending in February 1929. Both the start and end date of this eruption is treated according to the 'nearest month' category of Table 2.1, however, alternative sources for these dates have not been found.

Kv: 1959: Excluded. Precise start and end dates of this eruption are unknown.

Kv: August 1968: Excluded. The Smithsonian Institution's Global Volcanism Program reports this eruption as starting on 23 May 1968 and ending in June 1968. The eruptions end date is treated according to the 'nearest month' category of Table 2.1, however, alternative sources for these dates have not been found.

D.10 Öraefajökull

O: 1362: Excluded. This eruption is reported by Thorarinsson (1958) and Selbekk and Trønnnes (2007) as starting in June 1362 and has been treated according to the 'nearest month' category of Table 2.1. The end date of this eruption is reported as 15 October 1362 (± 45 days) by the Smithsonian Institution's Global Volcanism program (Siebert et al., 2010; Venzke et al., 2013), however, alternative sources for this date have not been found.

#7. O: August 1727 (d_4). Dates for this eruption have been inferred from eye witness descriptions included within Thorarinsson (1958). The start date of this eruption is not specifically mentioned, however, accounts indicate that the associated Jökulhlaup began on 8 August 1727 when 'fires' could also been seen. We use this to assume that the eruption must have begun in early August, and therefore report a start date for this eruption of 5 August 1727 according to the 'early month' category of Table

2.1. Eyewitness accounts within Thorarinsson (1958) indicate that the eruption ended in April 1728 and here an end date of 15 April 1728 is used according to the ‘nearest month’ category of Table 2.1.

Chemical composition and duration type classification of eruptions

Öræfajökull

The August 1727 eruption is the only Öræfajökull eruption used in this study. The erupted products of this eruption are non-basaltic (57 wt% SiO₂, (Prestvik et al., 2001)) and is described by Larsen et al. (1999) and Selbekk and Trønnnes (2007) as a minor explosive eruption of benmoreitic composition. Due to this eruption's weak explosivity and relatively long eruption duration it is described here as a mixed eruption with total duration d_4 . It is worth noting that this eruption is not included in the detailed analyses of this study.

D.11 Torfajökull

T: March 1477: Excluded. The Smithsonian Institution's Global Volcanism Program reports this eruption as starting in March 1477 and it is treated according to the ‘nearest month’ category of Table 2.1, however, the end date is unknown.

D.12 Vestmannaeyjar

V: October 1637: Excluded. This eruption is reported by the Smithsonian Institution's Global Volcanism program (Siebert et al., 2010; Venzke et al., 2013) as starting in October 1637 and ending on 28 February 1638 (± 60 days). The start date is treated

APPENDIX D. ICELANDIC ERUPTIONS

according to the ‘early month’ category of Table 2.1, however, alternative sources for these dates have not been found.

V: September 1896: Excluded. This eruption is reported by the Smithsonian Institution’s Global Volcanism program (Siebert et al., 2010; Venzke et al., 2013) as starting in September 1896 and has been treated according to the ‘nearest month’ category of Table 2.1, however, the end date is unknown.

#30. V: November 1963. (Surtsey p1) (d_6). For this eruption we use the start date 6 November 1963 reported by Thorarinsson (1967c) and Thordarson and Sigmarsson (2009) and the end date 30 April 1964 reported by Thorarinsson (1965), Thorarinsson (1967c) and Sturkell et al. (2009).

#31. V: June 1964. (Surtsey p2) (d_6). For this eruption we use the start date 9 June 1964 reported by Thorarinsson (1965), Thorarinsson (1966) and Thorarinsson (1967c) and the end date 17 October 1965 reported by Thorarinsson (1966), Thorarinsson (1967b), Thorarinsson (1967c) and Sturkell et al. (2009).

#32. V: December 1965. (Surtsey p3) (d_6). For this eruption we use the start date 26 December 1965 reported by Thorarinsson (1967c) and Thorarinsson (1967b) and the end date 5 June 1967 reported by Thorarinsson (1967b), Thorarinsson (1967c) and Thorarinsson (1968).

#34. V: January 1973 (Heimaey) (d_6). For this eruption we use the start date 23 January 1973 reported by Thorarinsson et al. (1973). Einarsson and Boucher (1974) and Olafsson (1975) and the end date 26 June 1973 reported by Jakobsson et al. (2008).

Chemical composition and duration type classification of eruptions

Vestmannaeyjar

The three phases of the Surtsey eruption are classified here as single basaltic eruptions with duration d_6 due to the effusive, Hawaiian type activity displayed during its effusive phases when access to the sea was restricted (Thorarinsson, 1967c).

The Heimaey eruption of 1973 produced hawaiite, trachybasalt and basalt (Thorarinsson et al., 1973; Jakobsson, 1979; Furman et al., 1991) and while Thordarson and Larsen (2007) suggest that this eruption is best described as a mixed eruption, here we classify it as a single basaltic eruption with duration d_6 (Fig. 3.7. Precise details about the reasoning behind this is discussed in subsection 3.4.3.

D.13 Miscellaneous

Hekla/Grímsvötn: July 1619: Excluded. An eruption is reported in the year 1619 as occurring to the East of Hekla and it is unknown whether this belongs to the Hekla or Grímsvötn volcanic systems (Thorarinsson, 1967a). It is reported as starting on 29 July 1619 (Thorarinsson, 1967a), however, the end date is unknown.

Grímsvötn/Thordarhyna: May 1903: Excluded. An eruption from either Grímsvötn or Thordarhyna is reported by Þórarinnsson (1974) as starting on 28 May 1903 and ending on 12 January 1904. However, some suggest that this eruption ended in 1905, and the location of the eruption is also uncertain (P. Einarsson pers. comm.) We have therefore excluded this eruption from any analysis in the study.

#48. Gjálp: September 1996. For this eruption we use the start date 30 September 1996 reported by Einarsson et al. (1997), Gudmundsson et al. (1997), Sigmarsson et al.

(2000), Steinthorsson et al. (2000) and Gudmundsson et al. (2004) and the end date 13 October 1996 reported by Einarsson et al. (1997), Gudmundsson et al. (1997), Sigmarsson et al. (2000), Steinthorsson et al. (2000), Gudmundsson et al. (2004) and Gudmundsson (2005).

D.14 Fire Events

A. Eldjá This basaltic flood lava eruption was sourced from the Eldj' 'a vent system belonging to the Katla volcanic system (Thordarson et al., 2001). The eruptive sequence consisted of at least eight distinct eruptive episodes (Thordarson et al., 2001) starting in the year 934 (Thordarson et al., 2001; Thordarson and Larsen, 2007) and ending in the year 940 (Thordarson et al., 2001). Both of these dates are treated according to the year only category of Table 2.1 resulting in a maximum duration uncertainty of ± 365 days.

B. Mývatnseldar This episode of fires belongs to the Krafla volcanic system. The eruptive sequence consisted of six to seven distinct eruptive episodes (Thordarson and Larsen, 2007) starting in the year 1724 and ending in the year 1729 (Thordarson and Larsen, 2007). Both of these dates are treated according to the year only category of Table 2.1 resulting in a maximum duration uncertainty of ± 365 days.

C. Laki This episode of fires belongs to the Grímsvötn volcanic system. The main rifting event can be separated into ten eruption episodes, however, magma discharge appears to have been continuous throughout (Thordarson et al., 2003) and therefore this is included in our dataset of individual eruption durations. Two eruptions occurred shortly after the main rifting episode at the Grímsvötn central volcano, and these are included in the duration of the Laki fires here. Therefore, here we use the start date 8 June 1783 as reported by Thordarson and Self (1993) and the end date 26 May 1785

as reported by Thordarson and Self (1993) and Thordarson and Larsen (2007).

D. Tröllahraun This episode of fires most probably belongs to the Bàrðarbunga volcanic system (Jónsson et al., 1997) while Hartley and Thordarson (2013) claim Veðivötn. The eruptive sequence consisted of two to three distinct eruptive episodes (Thordarson and Larsen, 2007) starting in the year 1862 and ending in the year 1864 (Jónsson et al., 1997; Thordarson and Larsen, 2007). Both of these dates are treated according to the year only category of Table 2.1 resulting in a maximum duration uncertainty of ± 365 days.

E. Askja This rifting episode from the Askja volcanic system is not included in the list of fires within Thordarson and Larsen (2007), however, here we feel that the total duration of this episode is best described within the d_7 category and therefore it is included as such within this study. Here we use the start date 1 January 1875 and the end date 20 October 1875 as reported by Sparks et al. (1981).

F. Askja The Askja fires consisted of five to six distinct eruptive episodes (Thordarson and Larsen, 2007) starting in the year 1921 and ending in the year 1929 (Thordarson and Larsen, 2007). Both of these dates are treated according to the year only category of Table 2.1 resulting in a maximum duration uncertainty of ± 365 days.

G. Surtsey This episode of fires belongs to the Vestmannaeyjar volcanic system. The eruptive sequence consisted of at least 3 distinct eruptive episodes starting on 6 November 1963 (Thorarinsson, 1967a; Thordarson and Sigmarsson, 2009) and ending on 5 November 1967 (Thorarinsson, 1967b,c, 1968)).

H. Krafla fires The Krafla fires consisted of nine distinct eruptive episodes (Thordarson and Larsen, 2007). Here we use the start date 20 December 1975 and the end date 18 September 1984 as reported by Thordarson and Larsen (2007).